Universidade de Aveiro
2021

DANIEL TORRÃO PIO

GASIFICAÇÃO DIRETA DE BIOMASSA PARA PRODUÇÃO DE GÁS COMBUSTÍVEL

DIRECT GASIFICATION OF BIOMASS FOR FUEL GAS PRODUCTION

Universidade de Aveiro
2021

DANIEL TORRÃO PIO

GASIFICAÇÃO DIRETA DE BIOMASSA PARA PRODUÇÃO DE GÁS COMBUSTÍVEL

DIRECT GASIFICATION OF BIOMASS FOR FUEL GAS PRODUCTION

Tese apresentada à Universidade de Aveiro para cumprimento dos requisitos necessários à obtenção do grau de Doutor em Engenharia da Refinação, Petroquímica e Química, realizada sob a orientação científica do Doutor Luís António da Cruz Tarelho, Professor associado da Universidade de Aveiro, co-orientação do Doutor Francisco Manuel da Silva Lemos, Professor Catedrático do Instituto Superior Técnico, e co-orientação empresarial da Doutora Paula Cristina de Oliveira Rodrigues Pinto da The Navigator Company.

Este trabalho foi financiado pela The Navigator Company e por Fundos Nacionais através da Fundação para a Ciência e a Tecnologia (FCT).

This work was funded by The Navigator Company and by the Portuguese Foundation for Science and Technology (FCT).

THE NAVIGATOR COMPANY

PD-F FCT PhD PROGRAMMES

FCT Fundação para a Ciência e a Tecnologia
MINISTÉRIO DA CIÊNCIA, TECNOLOGIA E ENSINO SUPERIOR

“We are facing nothing less than the collapse of the living world. The very thing that gave birth to our civilization”
David Attenborough

o júri

presidente

Doutor **Fernando Manuel dos Santos Ramos**
Professor Catedrático, Universidade de Aveiro

Doutor **Klas Engvall**
Professor Catedrático, KTH - Royal Institute of Technology

Doutor **Carlos Fernandes Teixeira**
Professor Catedrático, Universidade do Minho

Doutora **Maria Amélia Nortadas Duarte de Almeida Lemos**
Professora Associada, Universidade de Lisboa

Doutor **Carlos Manuel Coutinho Tavares de Pinho**
Professor Associado, Universidade do Porto

Doutor **Luís António da Cruz Tarelho**
Professor Associado, Universidade de Aveiro

Doutor **Edgar Caetano Fernandes**
Professor Auxiliar, Universidade de Lisboa

Doutor **Manuel Arlindo Amador de Matos**
Professor Auxiliar, Universidade de Aveiro

agradecimentos

A tese de doutoramento, apesar de ser um trabalho individual, envolve o contributo de diversas pessoas. No decorrer da minha investigação estes contributos revelaram-se essenciais e influenciaram este trabalho de diferentes formas. Posto isto, apresento os meus sinceros agradecimentos aos meus orientadores, colegas de trabalho, família, amigos e, de uma forma geral, a todos os que contribuíram para a realização deste trabalho.

palavras-chave Biomassa, Gasificação, Gás produto, Leito fluidizado borbulhante

resumo

O consumo excessivo de combustíveis fósseis para garantir as necessidades e interesses da sociedade conduziu à emissão de elevadas quantidades de gases com efeito de estufa nas últimas décadas, contribuindo significativamente para a maior ameaça ambiental do século XXI: Alterações Climáticas. A solução para este desastre de origem humana é de caráter complexo e só pode ser atingida através da cooperação de todos os governos e partes interessadas. Para isto, é obrigatória a criação de uma bioeconomia como base de um futuro mais sustentável, cujas necessidades energéticas e materiais sejam garantidas pelas eternas energias da natureza (e.g., vento, sol). Neste sentido, a biomassa pode ter um papel principal como uma matéria-prima ajustável e renovável que permite a substituição de combustíveis fósseis num variado número de aplicações, e a sua conversão através da gasificação pode ser a chave para este propósito. Afinal, na prática, os combustíveis fósseis são apenas biomassa sujeita a elevada temperatura e pressão durante milhões de anos. Além do mais, a gestão eficaz da biomassa é fundamental para a redução dos riscos de incêndio florestal e, como tal, temos o dever de utilizar e valorizar este recurso.

Neste trabalho, foi obtido novo conhecimento científico para suporte do desenvolvimento das tecnologias de gasificação direta (ar) de biomassa em leitos fluidizados borbulhantes para produção de gás combustível, com o objetivo da substituição de gás natural em queimadores industriais. Este é o primeiro passo para o desenvolvimento de biorrefinarias de gasificação, uma potencial futura indústria que irá providenciar um variado número de produtos de valor acrescentado através da biomassa e competir com a atual indústria petroquímica. Neste sentido, foram analisadas várias medidas para a melhoria da qualidade do gás produto bruto e dos parâmetros de eficiência do processo. Em primeiro, a adição de vapor sobreaquecido como medida primária permitiu o aumento da concentração de H_2 e da razão molar H_2/CO no gás produto sem comprometer a estabilidade do processo. No entanto, esta medida somente revelou potencial para a gasificação direta (ar) de biomassa de alta densidade (e.g., pellets) devido à necessidade da acumulação de carbonizados no leito do reator para a ocorrência de reações de reforma com vapor. Em segundo, a mistura de combustíveis derivados de resíduos e biomassa residual florestal permitiu a melhoria dos produtos de gasificação, constituindo desta forma uma estratégia bastante promissora a nível económico e ambiental, devido à elevada abundância e baixo custo dos resíduos urbanos. Contudo, devem ser efetuadas análises técnico-económicas e de ciclo de vida para a completa caraterização do processo. Em terceiro, a aplicação de catalisadores de baixo custo como medida primária demonstrou elevado potencial para a melhoria do gás produto (e.g., concentração de H_2 e CO, poder calorífico inferior) e para o incremento dos parâmetros de eficiência do processo; em particular, a aplicação de betão, faialite sintética e carbonizados de pellets de madeira, demonstrou resultados promissores. Finalmente, foi demonstrada a viabilidade económica da integração do processo de gasificação direta (ar) de biomassa na indústria da pasta e papel, apesar dos parâmetros determinados não serem atrativos para potenciais investidores. Neste contexto, a intervenção dos governos e o desenvolvimento de instrumentos de apoio económico é de grande relevância para a implementação destes projetos.

keywords Biomass, Gasification, Producer gas, Bubbling fluidized bed

abstract

The excessive consumption of fossil fuels to satisfy the world necessities of energy and commodities led to the emission of large amounts of greenhouse gases in the last decades, contributing significantly to the greatest environmental threat of the 21st century: Climate Change. The answer to this man-made disaster is not simple and can only be made if distinct stakeholders and governments are brought to cooperate and work together. This is mandatory if we want to change our economy to one more sustainable and based in renewable materials, and whose energy is provided by the eternal nature energies (e.g., wind, solar). In this regard, biomass can have a main role as an adjustable and renewable feedstock that allows the replacement of fossil fuels in various applications, and the conversion by gasification allows the necessary flexibility for that purpose. In fact, fossil fuels are just biomass that underwent extreme pressures and heat for millions of years. Furthermore, biomass is a resource that, if not used or managed, increases wildfire risks. Consequently, we also have the obligation of valorizing and using this resource.

In this work, it was obtained new scientific knowledge to support the development of direct (air) gasification of biomass in bubbling fluidized bed reactors to obtain a fuel gas with suitable properties to replace natural gas in industrial gas burners. This is the first step for the integration and development of gasification-based biorefineries, which will produce a diverse number of value-added products from biomass and compete with current petrochemical refineries in the future. In this regard, solutions for the improvement of the raw producer gas quality and process efficiency parameters were defined and analyzed. First, addition of superheated steam as primary measure allowed the increase of H_2 concentration and H_2/CO molar ratio in the producer gas without compromising the stability of the process. However, the measure mainly showed potential for the direct (air) gasification of high-density biomass (e.g., pellets), due to the necessity of having char accumulation in the reactor bottom bed for char-steam reforming reactions. Secondly, addition of refused derived fuel to the biomass feedstock led to enhanced gasification products, revealing itself as a highly promising strategy in terms of economic viability and environmental benefits of future gasification-based biorefineries, due to the high availability and low costs of wastes. Nevertheless, integrated techno-economic and life cycle analyses must be performed to fully characterize the process. Thirdly, application of low-cost catalyst as primary measure revealed potential by allowing the improvement of the producer gas quality (e.g., H_2 and CO concentration, lower heating value) and process efficiency parameters with distinct solid materials; particularly, the application of concrete, synthetic fayalite and wood pellets chars, showed promising results. Finally, the economic viability of the integration of direct (air) biomass gasification processes in the pulp and paper industry was also shown, despite still lacking interest to potential investors. In this context, the role of government policies and appropriate economic instruments are of major relevance to increase the implementation of these projects.

TABLE OF CONTENTS

Table of contents ..... **I**

List of Figures ..... **V**

List of Tables ..... **XII**

List of publications ..... **XV**

Nomenclature and abbreviations ..... **XVII**

1 Introduction **1**

1.1 Objectives *1*

1.2 Layout *2*

1.3 Experimental infrastructures *5*
1.3.1 DAO-UA 80 kW_{th} pilot-scale BFB gasifier (Portugal) 5
1.3.2 DAO-UA 3 kW_{th} bench-scale BFB gasifier (Portugal) 9
1.3.3 KTH 5 kW_{th} bench-scale BFB gasifier (Sweden) 11

1.4 Methodologies *13*

2 State-of-the-art of biomass gasification technologies **15**

2.1 Article I - Gasification-based biorefinery integration in the PP industry: A critical review *15*
2.1.1 Abstract 15
2.1.2 Introduction 15
2.1.3 Gasification 17
2.1.3.1 Reactions and stages 17
2.1.3.2 Regime concepts and designs 20
2.1.3.3 Tar formation and removal strategies 24
2.1.4 Biorefinery opportunities and challenges 26
2.1.5 Gasification-based biorefineries in the PP industry 30
2.1.5.1 Drivers and barriers 30
2.1.5.2 PP byproducts gasification 32
2.1.5.3 PG as gas/oil substitute in the PP industry 38
2.1.6 Future perspectives 41
2.1.7 Conclusions 42

2.2 Article II - Industrial gasification systems (>3 MW_{th}) for bioenergy in Europe: Current status and future perspectives *43*
2.2.1 Abstract 43
2.2.2 Introduction 43
2.2.3 Conventional gasification technologies 46
2.2.3.1 Fixed bed 48
2.2.3.2 Fluidized bed 49
2.2.3.3 Entrained-flow 51
2.2.4 Status in Europe 52
2.2.4.1 Sweden 58
2.2.4.2 Finland 59
2.2.4.3 Germany 60
2.2.4.4 The Netherlands 60
2.2.4.5 Austria 61
2.2.4.6 Denmark 62
2.2.4.7 Italy 62
2.2.5 Future trends and perspectives 62
2.2.6 Conclusions 65

3 Numerical tools to predict PG composition during biomass gasification 67

3.1 Article III - Empirical and chemical equilibrium modelling for prediction of biomass gasification in an autothermal pilot-scale bubbling fluidized bed reactor 67
3.1.1 Abstract 67
3.1.2 Introduction 67
3.1.3 Methods and literature data collection 69
3.1.4 Experimental and CEM results comparison 76
3.1.4.1 Properties of the PG 77
3.1.4.1.1 Combustible gases yield (H_2, CO and CH_4) 77
3.1.4.1.2 Gas phase products yield ratios 81
3.1.4.2 Process efficiency parameters 83
3.1.4.2.1 LHV and Y_{gas} 83
3.1.4.2.2 CGE and CCE 86
3.1.5 Empirical and CEM correlations evaluation 89
3.1.6 Conclusions 90

4 Characterization of the PG from direct biomass gasification 92

4.1 Article IV - Characteristics of the gas produced during direct gasification of biomass in an autothermal pilot-scale bubbling fluidized bed reactor 93
4.1.1 Abstract 93
4.1.2 Introduction 93
4.1.3 Materials and methods 94
4.1.3.1 Feedstock characterization 94
4.1.3.2 Operating conditions 95
4.1.4 Results and discussion 96
4.1.4.1 Steady-state operation of the gasifier 96
4.1.4.2 Influence of the ER 99
4.1.4.3 Influence of the temperature 101
4.1.4.4 Comparison with literature data 102
4.1.5 Conclusions 114

4.2 Article V - Superheated steam injection as primary measure to improve PG quality from biomass air gasification in an autothermal pilot-scale gasifier 115
4.2.1 Abstract 115
4.2.2 Introduction 115
4.2.3 Materials and methods 117
4.2.3.1 Feedstock characterization 117
4.2.3.2 Operating conditions 118
4.2.4 Results and discussion 119
4.2.4.1 Influence of S/B on temperature and gas composition profiles along time 119
4.2.4.2 Influence of S/B on PG composition 122
4.2.4.3 Influence of steam on process efficiency parameters 126
4.2.4.3.1 LHV and Y_{gas} 126
4.2.4.3.2 CGE and CCE 128
4.2.5 Conclusions 131

4.3 Article VI - Co-gasification of refused derived fuel and biomass in a bubbling fluidized bed reactor 132
4.3.1 Abstract 132
4.3.2 Introduction 132
4.3.3 Materials and methods 134
4.3.3.1 Feedstock characterization 134
4.3.3.2 Operating conditions 137
4.3.4 Results and discussion 137
4.3.4.1 Operating conditions of the gasifier 138
4.3.4.2 Characteristics of the PG 141
4.3.4.2.1 Gas composition 141
4.3.4.2.2 Gaseous products ratios 145

4.3.4.3 Process efficiency parameters 147
4.3.4.3.1 LHV and Y_{gas} 147
4.3.4.3.2 CGE and CCE 149
4.3.5 Conclusions 151

4.4 Article VII - Tar formation during eucalyptus gasification in a bubbling fluidized bed reactor: Effect of feedstock and reactor bed composition 153
4.4.1 Abstract 153
4.4.2 Introduction 153
4.4.3 Materials and methods 154
4.4.3.1 Feedstock characterization 154
4.4.3.2 Operating conditions 156
4.4.4 Results and discussion 157
4.4.4.1 Gas composition and gasification efficiency parameters 157
4.4.4.2 Tar composition and concentration 159
4.4.4.2.1 Influence of gasification operation time 162
4.4.4.2.2 Influence of feedstock chemical composition 172
4.4.5 Conclusions 175

4.5 Integrated results discussion 177

5 Low-cost catalysts as primary methods to improve the PG quality 178

5.1 Article VIII - Low-cost catalysts for in-situ improvement of PG quality during direct gasification of biomass 179
5.1.1 Abstract 179
5.1.2 Introduction 179
5.1.3 Materials and methods 182
5.1.3.1 Feedstock characterization 182
5.1.3.2 Low-cost catalysts characterization 182
5.1.3.1 Operating conditions 184
5.1.4 Results and discussion 185
5.1.4.1 Steady-state operation of the gasifier 186
5.1.4.2 Characteristics of the PG at the exhaust of the BFB gasifier 190
5.1.4.3 Influence of the tested catalysts on the PG composition 192
5.1.5 Conclusions 197

5.2 Articles IX and X - Concrete and Ilmenite as low-cost catalysts to improve gas quality during biomass gasification in a pilot-scale gasifier 199
5.2.1 Abstract 199
5.2.2 Introduction 199
5.2.3 Materials and methods 201
5.2.3.1 Feedstock characterization 201
5.2.3.2 Concrete and ilmenite characterization 202
5.2.3.3 Operating conditions 204
5.2.4 Results and discussion 204
5.2.4.1 Influence of the tested catalysts on the PG composition 204
5.2.4.2 Influence of the tested catalysts on the gasification efficiency parameters 211
5.2.5 Conclusions 213

5.3 Integrated results discussion 215

6 Combustion of PP byproducts as a co-integrable biorefinery process 216

6.1 Article XI - Co-combustion of residual forest biomass and sludge in a pilot-scale bubbling fluidized bed 216
6.1.1 Abstract 216
6.1.2 Introduction 216
6.1.3 Materials and methods 218
6.1.3.1 Feedstock characterization 221
6.1.3.2 Operating conditions 222

6.1.4 Results and discussion 223
6.1.4.1 Temperature profiles 223
6.1.4.2 Gas composition profiles 225
6.1.4.2.1 CO_2 and H_2O 225
6.1.4.2.2 HCl 226
6.1.4.2.3 NO 228
6.1.4.2.4 CO 231
6.1.4.2.5 SO_2 232
6.1.4.3 Particulate matter analysis 233
6.1.4.3.1 Fly ashes in the exhaust gases 233
6.1.4.3.2 Bottom bed ashes and fly ashes deposited along the combustion system 237
6.1.5 Conclusions 238

7 Techno-economic analysis of direct biomass gasification 240

7.1 Article XII - Biomass direct gasification for electricity generation and natural gas replacement in the lime kilns of the pulp and paper industry: A techno-economic analysis 240
7.1.1 Abstract 240
7.1.2 Nomenclature 241
7.1.3 Introduction 242
7.1.4 Materials and methods 243
7.1.4.1 Feedstock characterization 243
7.1.4.2 Technologies and PG characteristics 244
7.1.4.3 Cases definition 245
7.1.4.3.1 Case I: Direct (air) gasification of eucalyptus RFB for electricity generation in CC . 246
7.1.4.3.2 Case II: Direct (air) gasification of eucalyptus RFB for natural gas replacement in the lime kiln 249
7.1.4.3.3 Case III: Direct (air) gasification of eucalyptus RFB for electricity generation in CC and natural gas replacement in the lime kiln 251
7.1.4.4 Methodology for the economic and sensitivity analysis 253
7.1.5 Results and discussion 256
7.1.5.1 Energy analysis results 256
7.1.5.2 Economic analysis results 257
7.1.5.3 Sensitivity analysis results 261
7.1.6 Conclusions 265

8 Discussion 266

9 Conclusions 268

10 Future work 269

11 Acknowledgments 271

12 Bibliography 272

LIST OF FIGURES

Figure 1.1– Diagram of the thesis layout 4

Figure 1.2 – Schematic layout of the 80 kWth autothermal BFB pilot-scale gasification facility (steam injection mode) 6

Figure 1.3 – Schematic layout of the 80 kWth autothermal BFB pilot-scale gasification facility (in-situ catalyst mode) 7

Figure 1.4 – DAO-UA pilot-scale 80kW_{th} BFB reactor 8

Figure 1.5 – Schematic layout of the 3 kW_{th} allothermal BFB bench-scale gasification facility. 10

Figure 1.6 – DAO-UA 3 kW_{th} allothermal BFB bench-scale infrastructure 11

Figure 1.7 – Schematic view of the experimental infrastructure. Adapted from [2] 12

Figure 1.8 – KTH 5 kW_{th} allothermal BFB bench-scale infrastructure 12

Figure 2.1 – Schematics of a typical biomass gasification process, including stages, inputs and outputs 18

Figure 2.2 – Schematics of direct and indirect gasification processes, including inputs and outputs 20

Figure 2.3 – Schematic of the conventional Güssing type (a) [101] and SilvaGas (b) [109] DFB gasification processes 23

Figure 2.4 – Schematic of the indirect MILENA gasifier [110]. S1 – Sampling point 1; S2 – Sampling point 2; Ne and Ar – Tracer gases. 23

Figure 2.5 – Example of mass composition of biomass tars (excluding benzene, values highly dependent on the gasification operating conditions). Adapted from Ref. [116]. 24

Figure 2.6 – Schematic example of integrated biomass conversion processes in a biorefinery design, including distinct conversion routes, middle platform compounds and obtainable products. 27

Figure 2.7 – Products obtainable in petrochemical refineries and biorefineries 28

Figure 2.8 – Chemrec entrained-flow gasifier with quenching section for green liquor recovery [168]. 34

Figure 2.9 – Gasification history and milestones 44

Figure 2.10 – General characteristics of conventional gasification technologies 47

Figure 2.11 – Schematic representation of an updraft (left) and downdraft (right) gasifier 48

Figure 2.12 – Schematic representation of a BFB and CFB gasifier 49

Figure 2.13 – Schematic representation of a DFB gasifier 51

Figure 2.14 – Schematic representation of an entrained-flow gasifier 52

Figure 2.15 – Industrial-scale (>3MW_{th}) gasification plants in Europe, countries participating on IEA Task 33. Green – Operational; Yellow – On hold; Red – Cancelled; Blue – Planned. 58

Figure 3.1 – Influence of the ER (a) and bed temperature (b) on the H_2 concentration in the PG for the experimental results reported in the literature and CEM results. 77

Figure 3.2 – Influence of the ER (a) and bed temperature (b) on the CO concentration in the PG for the experimental results reported in the literature and CEM results. 79

Figure 3.3 – Influence of the ER (a) and bed temperature (b) on the CH_4 concentration in the PG for the experimental results reported in the literature and CEM results. 80

Figure 3.4 – Influence of the ER (a) and bed temperature (b) on the H_2:CO molar ratio in the PG for the experimental results reported in the literature and CEM results. 82

Figure 3.5 – Influence of the ER (a) and bed temperature (b) on the CO:CO_2 molar ratio in the PG for the experimental results reported in the literature and CEM results. 83

Figure 3.6 – Influence of the ER (a) and bed temperature (b) on the LHV of the PG for the experimental results reported in the literature and CEM results. 84

Figure 3.7 – Influence of the ER (a) and bed temperature (b) on the Y_{gas} for the experimental results reported in the literature and CEM results. 85

Figure 3.8 – Influence of the ER (a) and bed temperature (b) on the CGE for the experimental results reported in the literature and CEM results. 87

Figure 3.9 – Influence of the ER (a) and bed temperature (b) on the CCE for the experimental results reported in the literature and CEM results. 88

Figure 4.1 – Example of the typical evolution of the temperature along time at different locations along the reactor height during the gasification of: (a) wood pellets and (b) eucalyptus RFB type A. 97

Figure 4.2 – Longitudinal temperature profile in the BFB reactor during the biomass gasification experiments performed. Legend according to experiments references in Table 4.2. 98

Figure 4.3 – Example of the typical dry gas composition (CO_2, CO, CH_4, C_2H_4) progress along time during the gasification of: (a) wood pellets and (b) eucalyptus RFB type B2. 99

Figure 4.4 – Influence of ER on the average dry gas composition (CO_2, CO, H_2, CH_4 and C_2H_4) and LHV during the gasification experiments in the pilot-scale BFB with (a) pine RFB, (b) wood pellets and (c) eucalyptus RFB. Legend according to experiments reference in Table 4.2. 101

Figure 4.5 – Comparison between the composition of the PG from this work and the composition reported in the literature regarding direct (air) biomass gasification studies in BFB gasifiers. Experiments reference according to Table 4.2 (this work) and Table 4.3 (literature survey). 107

Figure 4.6 – Comparison between the LHV of the PG from the experiments performed in this work and the LHV reported in the literature regarding direct (air) biomass gasification studies in BFB gasifiers. Experiments reference according to Table 4.2 (this work) and Table 4.3 (literature survey). 108

Figure 4.7 – Influence of ER on the Y_{gas} during the experiments performed in this work and reported in the literature regarding direct (air) biomass gasification in BFB reactors. Experiments reference according to Table 4.2 (this work) and Table 4.3 (literature survey). 109

Figure 4.8 – Influence of ER on the CGE during the experiments performed in this work and reported in the literature regarding direct (air) biomass gasification in BFB reactors. Experiments reference according to Table 4.2 (this work) and Table 4.3 (literature survey). 110

Figure 4.9 – Influence of ER on the CCE during the experiments performed in this work and reported in the literature regarding direct (air) biomass gasification in BFB reactors. Experiments reference according to Table 4.2 (this work) and Table 4.3 (literature survey). 110

Figure 4.10 – Composition (CO_2, CH_4, CO and H_2) and LHV of the PG reported in the literature regarding biomass direct (air) gasification studies in downdraft/updraft fixed bed and CFB reactors. Experiments reference according to Table 4.3. 111

Figure 4.11 – Composition (CO_2, CH_4, CO and H_2) of the PG reported in the literature regarding biomass indirect (steam) gasification studies in different types of reactors. Experiments reference according to Table 4.3. 113

Figure 4.12 – Typical temperature profile along time at different locations of the pilot-scale BFB reactor for the experiment (a) PP-0.5 (Pine pellets, 6.2 kg/h steam) and (b) PE-0.4 (Eucalyptus RFB, 5.7 kg/h steam).120

Figure 4.13 – Typical PG composition profile along time at different locations of the pilot-scale BFB reactor for the experiment (a) PP-0.5 (Pine pellets, 6.2 kg/h steam) and (b) PE-0.4 (Eucalyptus RFB, 5.7 kg/h steam). 121

Figure 4.14 – Influence of the S/B on the composition of the dry PG (H_2, CO, CO_2, CH_4 and H_2/CO molar ratio) for the gasification experiments in the autothermal pilot-scale and allothermal bench-scale BFB reactors, and comparison with thermodynamic predictions for the same operating parameters. Operating parameters detailed in Table 4.6. 126

Figure 4.15 – Influence of the S/B on the LHV of the PG and Y_{gas} for the gasification experiments in the autothermal pilot-scale and allothermal bench-scale BFB reactors, and comparison with thermodynamic predictions for equal operating parameters. Operating parameters detailed in Table 4.6. 127

Figure 4.16 – Influence of the S/B on the CGE and CCE for the gasification experiments in the autothermal pilot-scale and allothermal bench-scale BFB reactors, and comparison with thermodynamic predictions for equal operating parameters. Operating parameters detailed in Table 4.6. 129

Figure 4.17 – Relation between CGE, CCE and the LHV of the PG for the gasification experiments performed in the autothermal pilot-scale and allothermal bench-scale BFB reactors and for the thermodynamic predictions (Paper V). Operating parameters detailed in Table 4.6. 130

Figure 4.18 – Feedstocks used in the G-CG experiments, namely (a) RDF pellets, (b) pine pellets and (c) pine chips, over millimeter paper. 135

Figure 4.19 – Typical temperature profile along time at different locations of the pilot-scale BFB reactor . 138

Figure 4.20 – Longitudinal temperature profile in the pilot-scale BFB reactor during the G-CG experiments performed. Legend according to experiments reference in Table 4.9. 139

Figure 4.21 – Typical PG composition (CO_2, CO, CH_4 and C_2H_4) profiles along time for the G-CG experiments with: (a) 100 %wt pine pellets, (b) 50 %wt pine pellets - 50 %wt RDF, (c) 50 %wt pine chips - 50 %wt RDF and (d) 100 %wt RDF. 140

Figure 4.22 – Influence of the RDF weight percentage on the average PG composition (H_2, CO and CO_2) for the G-CG experiments 142

Figure 4.23 – Influence of the RDF weight percentage on the average PG composition (CH_4, C_2H_4, C_2H_6 and C_3H_8) for the G-CG experiments. 145

Figure 4.24 – Influence of the RDF weight percentage on the H_2:CO and CO:CO_2 molar ratios for the G-CG experiments. 147

Figure 4.25 – Influence of the RDF weight percentage on the LHV and Y_{gas} for the G-CG experiments.....149

Figure 4.26 – Influence of the RDF weight percentage on the CGE and CCE for the G-CG experiments....151

Figure 4.27 – Average dry gas composition for the gasification experiments performed with different eucalyptus pellets. Legend according to experiments reference in Table 4.11. 159

Figure 4.28 – Tar production values for the different gasification experiments. Legend according to experiments reference in Table 4.11. 161

Figure 4.29 – Decay of the total tar (a), BTX (b), naphthalene (c) and indene (d) concentration in the raw PG with operation time. Experiments information in Table 4.11.....163

Figure 4.30 – Equilibrium thermodynamic prediction of the reactor bed composition along time for the experiments LTS – Pellets 1 (a), LTS – Pellets 2 (b), ETS – Pellets 3 (c) and ETS – Pellets 4 (d). Experiments information in Table 4.11.....168

Figure 4.31 – SEM micrographs of a representative ash particle from Pellets 1 (a) and Pellets 3 (b), and respective Ca, Cl, Na and K elemental intensity maps.....169

Figure 4.32 – Relation between the solid carbon and inorganic species content in the reactor bed (predicted by thermodynamic equilibrium) and the tar concentration in the PG for the different gasification experiments performed. Experiments information in Table 4.11. 170

Figure 4.33 – Variation of the LHV of the dry and clean PG with (a) operation time and (b) total tar concentration in the raw PG. Experiments information in Table 4.11. 171

Figure 4.34 – Variation of total tar, BTX and naphthalene concentration in the raw PG with the chemical properties of the eucalyptus RFB pellets used in the gasification experiments: ash (a), volatile matter (b), fixed carbon (c), carbon concentration (d) and oxygen concentration (e). Feedstock characteristics in Table 4.10 and experiments reference in Table 4.11.....175

Figure 5.1 – Thermodynamic predictions of redox phase stability conditions for the Fe-Si-O system at 1373 K superimposed on CO:CO_2 equilibrium in the gas phase. 184

Figure 5.2 – SEM of SiC precursor powders (a) and one representative single phase Fe_2SiO_4 (b) sample prepared by solid state reaction of stoichiometric SiC+Fe_2O_3 powder mixtures, in CO_2 atmosphere, with optimized firing cycle. 184

Figure 5.3 – Typical evolution of the temperature along time at different locations along the reactor height during the gasification of: (a) wood pellets and (b) RFB from pine. 187

Figure 5.4 – Average vertical temperature profile in the BFB reactor for the biomass gasification experiments performed. Legend according to experiments references in Table 5.3. 188

Figure 5.5 – Typical composition (CO_2, CO, CH_4, C_2H_4) along time of the dry gas produced at the exhaust (GE) during the gasification of: (a) wood pellets and (b) RFB from pine. 189

Figure 5.6 – Composition (CH_4, CO, CO_2, C_2H_4 and H_2) of the dry gas sampled at the exhaust (GE). Experiments reference according to Table 5.3.....190

Figure 5.7 – LHV and Y_{gas} of the dry gas sampled at the exhaust (GE). Experiments reference according to Table 5.3. 191

Figure 5.8 – CGE and CCE for experiments regarding the dry gas sampled at the exhaust (GE). Experiments reference according to Table 5.3.....192

Figure 5.9 – Composition (CH_4, CO, CO_2, C_2H_4 and H_2) of the dry gas sampled above the surface of the bed (GB) and above the surface of the bed passing through a fixed bed of catalytic materials (GBC). Experiments reference according to Table 5.3. 193

Figure 5.10 – Influence of the different catalytic materials tested in this work on the composition (CH_4, CO and H_2) of the PG sampled above the surface of the fluidized bed. Experiments reference according to Table 5.3. 194

Figure 5.11 – LHV and Y_{gas} for the experiments regarding the PG sampled above the surface of the bed (GB) and above the surface of the bed after passing through a fixed bed of catalytic materials (GBC). Experiments reference according to Table 5.3. 195

Figure 5.12 – CGE and CCE for the experiments regarding the PG sampled above the surface of the bed (GB) and above the surface of the bed after passing through a fixed bed of catalytic materials (GBC). Experiments reference according to Table 5.3. 196

Figure 5.13 – Influence of the different catalytic materials tested on this work on LHV, Ygas, CGE and CCE. Experiments reference according to Table 5.3. 196

Figure 5.14 – Normalized XRD patterns of the fresh ilmenite and concrete samples. 203

Figure 5.15 – PG composition and LHV for the distinct gasification experiments performed in the pilot and bench-scale fluidized bed reactors. Experiments reference according to Table 5.7. 206

Figure 5.16 – Influence of the distinct low-cost catalytic materials on the composition and LHV of the PG for the different gasification experiments performed. Experiments reference according to in Table 5.7. 207

Figure 5.17 – CO_2, CO and H_2 yield for the distinct gasification experiments performed in the pilot and bench-scale fluidized bed reactors. Experiments reference according to Table 5.7 208

Figure 5.18 – Average vertical temperature profile in the allothermal bench-scale BFB reactor. Experiments reference according to Table 5.7. 210

Figure 5.19 – Average vertical temperature profiles for the distinct gasification experiments performed in the autothermal pilot-scale BFB reactor. Experiments reference according to Table 5.7. 210

Figure 5.20 – Y_{gas}, CGE and CCE for the distinct gasification experiments performed in the pilot and bench-scale BFB reactors. Experiments reference according to Table 5.7. 212

Figure 5.21 – Influence of the distinct low-cost catalytic materials on Y_{gas}, CGE and CCE for the different gasification experiments made. Experiments reference according to Table 5.7. 213

Figure 6.1 – Layout of the experimental infrastructure with the pilot-scale BFB reactor (combustion mode). 220

Figure 6.2 – Typical evolution of the temperature with time at different locations along the reactor height during the combustion experiments: (a) EL-O, (b) EL-10 and (c) ELP-5. Experiments reference according to Table 6.3. 224

Figure 6.3 – Longitudinal temperature profile in the BFB reactor during the biomass combustion experiments performed. Legend according to experiments references in Table 6.3. 225

Figure 6.4 – Typical CO_2 and H_2O concentration with time in the exhaust gases for (a) EL-10 #7 and (b) ELP-5 #3. 226

Figure 6.5 – Typical HCl concentration with time in the exhaust gases for (a) EL-10 #7 and (b) ELP-5 #3. Experiments reference according to Table 6.3. 227

Figure 6.6 – HCl concentration with time (30 minutes moving average) for the distinct combustion experiments performed. Experiments reference according to Table 6.3. 228

Figure 6.7 – Typical NO concentration with time in the exhaust gases for (a) EL-10, (b) EL-10 #6, (c) EL-10 #7 and (d) ELP-5 #3. Experiments reference according to Table 6.3. 230

Figure 6.8 – NO concentration with time (30 minutes moving average) for the distinct combustion experiments performed and comparison with the limit value referred on the BAT reference document for Large Combustion Plants [504]. Experiments reference according to Table 6.3. 231

Figure 6.9 – CO concentration with time (30 minutes moving average) for the distinct combustion experiments performed and comparison with the limit value referred to biomass boilers in the Portuguese legislation, in Portaria 677/2009 [505]: (a) experiments with lower CO concentration values and (b) experiments with higher CO concentration values. Experiments reference according to Table 6.3. 232

Figure 6.10 – SO_2 concentration along time (30 minutes moving average) for the distinct combustion experiments performed and comparison with the limit value referred to biomass boilers in the Portuguese legislation, in Portaria 677/2009 [505]. Experiments reference according to Table 6.3. 232

Figure 6.11 – Average particle (fly ash) concentration in the exhaust gases during the combustion experiments. The gas sampling was performed after the cyclone, except for references with FM, where the gas sampling was downstream of the bag filter. Experiments reference according to Table 6.3. 233

Figure 6.12 – Average Cl, K, Ca and Na concentration emitted associated with the fly ashes present in the exhaust gases during the combustion experiments. These elements were measured as ion Cl^-, K^+, Ca^{2+} and Na^+, and expressed as mg chemical element/Nm^3 dry gas, corrected to 6%v O_2. Sampling was performed downstream of the cyclone (Figure 6.1). Experiments reference according to Table 6.3. 234

Figure 6.13 – Relation between the content of K, Ca and Na with Cl in the fly ashes present in the exhaust gas during the combustion experiments: (a) K and Cl, (b) Ca and Cl and (c) Na and Cl. 235

Figure 6.14 – Average Cl concentration in the solid phase, measured as ion Cl^- in fly ashes (denoted as Cl-particles), and expressed as mg Cl/Nm^3 dry gas corrected to 6%v O_2, and in gaseous phase (denoted as Cl-HCl), measured as HCl in the flue gas and expressed as mg Cl/Nm^3 dry gas corrected to 6%v O_2, in the exhaust gases during the combustion experiments. Sampling was performed downstream of the cyclone (Figure 6.1). Experiments reference according to Table 6.3. 236

Figure 6.15 – Average composition (Ca, K, Mg, P, Na, Al, Mn and Cl) (and respective standard deviation) of the ashes deposited or settled in different locations of the combustion system. 237

Figure 7.1 – OLGA syngas cleaning system [523]. 245

Figure 7.2 – Integrated schematics of Case I 246

Figure 7.3 – Integrated schematics of Case II 250

Figure 7.4 – Integrated schematics of Case III (combination of Cases I and II). 252

Figure 7.5 – Sankey diagram for the main energy flows in the system configurations studied: a) Case I, b) Case II and c) Case III. 257

Figure 7.6 – Cash-flows through the useful lifetime of the plant for (a) Case I, (b) Case II and (c) Case III. 258

Figure 7.7 – Financial indicators (NPV, IRR and PBP) throughout the useful lifetime of the plant, for (a) Case I, (b) Case II and (c) Case III. 260

Figure 7.8 – Probability distribution for NPV for (a) Case I, (b) Case II and (c) Case III. 262

Figure 7.9 – Impact of changes in selected input variables on the NPV for (a) Case I, (b) Case II and (c) Case III. 264

LIST OF TABLES

Table 2.1 – Suggested upper limits of tar concentration for using the PG in distinct applications [26,50,113,120–122] 25

Table 2.2 – Feedstock characteristics, types of conversion processes and range of end-products for petrochemical refineries and biorefineries 29

Table 2.3 – Published studies regarding gasification-based biorefinery processes for integration in the PP industry. 32

Table 2.4 – Typical characteristics of different byproducts from the PP industry with potential to be used in gasification processes. 33

Table 2.5 – Composition (CO_2, CH_4, CO and H_2), molar ratios ($Y_{CH4/H2}$, $Y_{CO/CO2}$ and $Y_{H2/CO}$) and LHV of the PG obtained by wood direct (air) gasification and BLG. 37

Table 2.6 – Average composition (CO_2, CH_4, CO and H_2, and tar) and LHV of the PG from different industrial gasification plants. 40

Table 2.7 – Industrial-scale (>3 MW_{th}) gasification plants in Europe. 53

Table 2.8 – Average composition (H_2, CO, CO_2, CH_4, N_2, C_xH_y and tar) and LHV of the PG from different commercial gasifiers (>3 MW_{th}) in Europe 57

Table 2.9 – Investment costs of different industrial-scale (>3 MW_{th}) gasification plants in Europe 63

Table 3.1 – Experiment references and operating conditions of the studies reported in the literature. 70

Table 3.2 – Proximate and ultimate analysis of the biomass used for the models development 74

Table 3.3 – PCC values for the correlation between operating conditions (temperature (T) and ER) and the PG composition (H_2, CO and CH_4), LHV, Y_{gas}, CGE and CCE, for the experimental results reported in the literature and CEM predictions. 78

Table 3.4 – Operating conditions during the biomass gasification experiments performed in the pilot-scale BFB 89

Table 3.5 – Comparison between obtained results in direct (air) gasification of biomass experiments in a BFB reactor and predicted by the empirical correlations and CEM correlations for the same operating conditions (Table 3.4). 90

Table 4.1 – Characteristics of the different types of biomass used as fuel in the gasification experiments performed in Paper IV 95

Table 4.2 – Operating conditions during the gasification experiments performed in Paper IV. 96

Table 4.3 – Survey of some published works in the literature regarding direct and indirect biomass gasification in distinct reactors 103

Table 4.4 – Range of CO and H_2 concentration in the PG, LHV of the PG, Y_{gas}, CGE and CCE during the biomass gasification experiments. Comparison of data from this study with other studies of direct and indirect gasification, including BFB and other types of reactors (Table 4.3). 113

Table 4.5 – Proximate and elemental analysis of the biomass types used as feedstock in the gasification experiments and as input for the thermodynamic equilibrium model (Paper V) 118

Table 4.6 – Gasification experiments reference and respective operating conditions (Paper V) 119

Table 4.7 – Proximate and elemental analysis of RDF and biomass types used as feedstock in the G-CG experiments in the pilot-scale BFB. 136

Table 4.8 – Ash fusibility temperature for the different feedstocks used in the G-CG experiments. 137

Table 4.9 – G-CG experiments reference and respective operating conditions (Paper VI). 137

Table 4.10 – Characteristics of the different types of eucalyptus pellets used as feedstock in the gasification experiments performed in the BFB (Paper VII) 155

Table 4.11 – Operating conditions during the gasification experiments in the BFB reactor 156

Table 5.1 – Characteristics of the different types of biomass used as feedstock in the gasification experiments in the pilot-scale BFB (Paper VIII). 182

Table 5.2 – Characteristics of the different types of low-cost catalysts tested in gasification experiments in the pilot-scale BFB (Paper VIII). 183

Table 5.3 – Pilot-scale BFB gasification experiments reference and respective operating conditions (Paper VIII)..... 185

Table 5.4 – Parameters of the experiments performed for testing the catalysts in direct (air) gasification regime in the pilot-scale BFB (Paper VIII). 185

Table 5.5 – Proximate and elemental analysis of the pine pellets used as feedstock in the gasification experiments. 202

Table 5.6 – Physical-chemical characteristics of the low-cost solid materials used as catalysts in the gasification experiments performed. 203

Table 5.7 – Gasification experiments reference and respective operating conditions. 204

Table 6.1 – Characteristics of the different types of biomass used as feedstock in the combustion experiments in the pilot-scale BFB. 222

Table 6.2 – Concentration of Ca, Na, K, Mg, Al, Mn and P in the ashes from the different types of biomass used as feedstock in the combustion experiments in the pilot-scale BFB 222

Table 6.3 – Combustion experiments reference and respective operating parameters. 223

Table 7.1 – Characteristics of the eucalyptus RFB considered as feedstock in this work 244

Table 7.2 – Operating conditions of the gasifier and characteristics of the PG 244

Table 7.3 – Predetermined data of the PP industry 246

Table 7.4 – Assumed concentration for the main compounds present in the tar in the raw PG, and its LHV [530–532]. 247

Table 7.5 – Operating parameters for the plant designed in Case I 249

Table 7.6 – Operating parameters for the plant designed in Case II 251

Table 7.7 – Operating parameters for the plant designed in Case III 253

Table 7.8 – Initial input financial data and cost factors considered to model the plant configurations preconized in the developed Cases (I, II and III). 254

Table 7.9 – Eucalyptus RFB consumption, total electricity generated, CaO production and the global efficiency of electricity generation for the three configurations studied. 256

Table 7.10 – Summary of the results of the economic evaluation 261

Table 7.11 – Parameters of the probability distributions for IRR and PBP, considering Cases I, II and III .. 263

LIST OF PUBLICATIONS

The following articles are part of this thesis:

- **Article I:** D.T. Pio, L.A.C. Tarelho. Gasification-based biorefinery integration in the pulp and paper industry: A critical review. Renewable & Sustainable Energy Reviews 2020:133.
- **Article II:** D.T. Pio, L.A.C. Tarelho. Industrial gasification systems (>3 MW_{th}) for bioenergy in Europe: Current status and future perspectives. In submission in the Renewable and Sustainable Energy Review Journal, currently under review.
- **Article III:** D.T. Pio, L.A.C. Tarelho. Empirical and chemical equilibrium modelling for prediction of biomass gasification products in bubbling fluidized beds. Energy 2020:202
- **Article IV:** D.T. Pio, L.A.C. Tarelho, M.A.A. Matos, Characteristics of the gas produced during biomass direct gasification in an autothermal pilot-scale bubbling fluidized bed reactor. Energy 2017:120.
- **Article V:** D.T. Pio, H.G.M.F. Gomes, L.A.C. Tarelho, A.C.M Vilas-Boas, M.A.A. Matos, F.M.S. Lemos. Superheated steam injection as primary measure to improve producer gas quality from biomass air gasification in an autothermal pilot-scale gasifier. In submission in the Renewable Energy Journal, currently under review.
- **Article VI:** D.T. Pio, L.A.C. Tarelho, A.M.A. Tavares, M.A.A. Matos, V. Silva. Co-gasification of refused derived fuel and biomass in a pilot-scale bubbling fluidized bed reactor. Energy Conversion and Management 2020:206.
- **Article VII:** D.T. Pio, L.C.M. Ruivo, L.A.C Tarelho, J.R. Frade, E. Kantarelis, K. Engball. Tar formation during eucalyptus gasification in a bubbling fluidized bed reactor: Effect of feedstock and reactor bed composition. In submission in the Energy Conversion and Management Journal, currently under review.
- **Article VIII:** D.T. Pio, L.A.C. Tarelho, R.G. Pinto, M.A.A. Matos, J.R. Frade, A. Yaremchenko, G.S. Mishra, P.C.R. Pinto. Low-cost catalysts for in-situ improvement of producer gas quality during direct gasification of biomass. Energy 2018:165
- **Article IX:** D.T. Pio, H.G.M.F Gomes, L.A.C. Tarelho, L.C.M. Ruivo, M.A.A. Matos, R.G. Pinto, J.R. Frade, F.M.S. Lemos. Ilmenite as low-cost catalyst for producer gas quality improvement from a biomass pilot-scale gasifier. Energy Reports 2020:6
- **Article X:** D.T. Pio, H.G.M.F. Gomes, L.C.M. Ruivo, L.A.C. Tarelho, M.A.A. Matos, J.R. Frade. Concrete and ilmenite as low-cost catalysts to improve direct (air) biomass gasification in a pilot-scale gasifier. In submission in the Energy & Fuels Journal, currently under review.
- **Article XI:** D.T. Pio, L.A.C. Tarelho, T.F.V. Nunes, M.F. Baptista, M.A.A Matos. Co-combustion of residual forest biomass and sludge in a pilot-scale bubbling fluidized bed. Journal of Cleaner Production 2020:249.
- **Article XII:** J.R.C Rey, D.T. Pio, L.A.C Tarelho. Biomass direct gasification for electricity generation and natural gas replacement in the lime kilns of the pulp and paper industry: A techno-economic analysis. In submission in the Energy Journal, currently under review.

Daniel Torrão Pio (D.T. Pio) is the main author of Articles I to XI. In Article XII, D.T. Pio acted as co-author and the major part of the economic and sensitivity analysis was led by José Ramón Copa Rey (J.R.C Rey).

The following articles were performed during this thesis, but are not directly related to this document:

- **D.T. Pio**, L.A.C. Tarelho. Predicting producer gas composition in bubbling fluidized beds using chemical equilibrium and empirical correlations. European Biomass Conference & Exhibition Proceedings 2019.

- **D.T. Pio**, L.A.C. Tarelho, T.F.V. Nunes, M.F. Baptista, M.A.A Matos. Co-combustion of residual forest biomass and sludge in a pilot-scale bubbling fluidized bed. European Biomass Conference & Exhibition Proceedings 2019.

- F.R. Charvet, F. Silva, **D.T. Pio**, L.A.C Tarelho, M.A.A. Matos, J.J.F. Silva, D. Neves. Production from alternative agroforestry woody residues typical of southern Europe charcoal. European Biomass Conference & Exhibition Proceedings 2020.

- L.C.M Ruivo, **D.T. Pio**, A.A. Yaremchenko, L.A.C Tarelho, J.R. Frade, E. Kantarelis, K. Engvall. Iron-based catalyst ($Fe_{2-x}Ni_xTiO_5$) for tar decomposition in biomass gasification. In the final phase of preparation for submission.

- M. Puig-Gamero, **D.T. Pio**, LA.C. Tarelho, P. Sánchez, L. Sanchez-Silva. Simulation of autothermal pilot-scale bubbling fluidized bed reactor using Aspen Plus. In submission in the Energy Conversion and Management Journal, currently with the Editor.

- L.C.M. Ruivo, R.M.B. Lourenço, M.A.A. Russo, **D.T. Pio**. Energy efficiency of the Portuguese ceramic industry. In submission in the Applied Energy Journal, currently under review.

- M.P. González-Vázquez, F. Rubiera, C. Pevida, **D.T. Pio**, L.A.C. Tarelho. Comparison of two thermodynamic models for fluidized bed gasification using Aspen Plus. Under reformulation after rejection in the Chemical Engineering Journal.

- N. Daniel, H.G.M.F. Gomes, **D.T. Pio**, L.C.M. Ruivo, M.A.A. Matos, J.R. Frade, L.A.C. Tarelho. Relevance of O_2/steam addition during biomass air gasification in bubbling fluidized bed. In the final phase of preparation for submission.

- A.C.M. Vilas-Boas, L.A.C. Tarelho, M. Kamali, Hauschild, **D.T. Pio**, D. Jahanianfard, A.P. Gomes, M.A.A. Matos. Biochar produced by biological sludge pyrolysis from wastewater treatment from PP industry. In submission in the BioFPR Journal, currently with the Editor.

- V.A.F Costa, L.A.C Tarelho, **D.T. Pio**. Mass, energy and exergy analysis of biomass direct gasification in an autothermal pilot-scale bubbling fluidized bed reactor. Under preparation.

- L.C.M. Ruivo, H.S.M. Oliveira, H.G.M.F. Gomes, **D.T. Pio**, L.A.C. Tarelho, J.R. Frade. Improvement of catalytic properties of olivine in fluidized bed gasifiers by microwave dielectric calcination. Under preparation.

- J. R. Copa-Rey, **D. T. Pio**, A. Briones-Hidrovo, V. Silva, L.A.C. Tarelho. Cleaning technologies for biomass-derived PG: A critical review. Under preparation.

NOMENCLATURE AND ABBREVIATIONS

AAEM	Alkali and Alkaline Earth Metals (Ca, K, Mg, Na and Ba)
ANN	Artificial neural network
ASU	Air separation unit
BAT	Best Available Technologies
BFB	Bubbling fluidized bed
BIGCC	Biomass integrated gasification combined cycle
BLG	Black liquor gasification
BLGCC	Black liquor gasification combined cycle
BtL	Biomass to liquid
BTX	Benzene, toluene and xylene
$C_{(s)}$	Unconverted solid carbon
CC	Combined cycle
CCE	Carbon conversion efficiency [%]
CCS	Carbon capture and storage
CEM	Chemical equilibrium model
CFB	Circulating fluidized bed
CFD	Computational fluid dynamic
CGE	Cold gas efficiency [%]
CHP	Combined heat and power
$CO_{2,eq}$	Carbon dioxide equivalent
daf	Dry ash free
db	Dry basis
DFB	Dual fluidized bed
DME	Dimethyl ether
EDS	Energy Dispersive X-ray Spectroscopy
EL	Experiments with secondary sludge
ELP	Experiments with primary sludge
ELV	Emission Limit Value
ER	Equivalence ratio
ETS	Gasification experiments with a tar sampling start between 17 and 32 minutes
EU	European Union
FID	Flame Ionization Detector
FT	Fischer-Tropsch
FTIR	Fourier Transform Infrared Spectroscopy
G-CG	Gasification and co-gasification
GCC	Gasification combined cycle
GC-TCD	Gas chromatography coupled with thermal conductivity detector
GHG	Greenhouse gas

GIFBR	Green Integrated Forest Biorefinery
GT	Gas turbine
H_2/CO	Molar ratio between hydrogen and carbon monoxide (mol H_2.mol CO^{-1})
HPLC	High performance liquid chromatography
HTSU	High Temperature Sampling Unit
i	Gaseous compound CO_2, CO, CH_4, C_2H_4, C_2H_6 and C_3H_8
ICE	Internal combustion engine
ICP-MS	Induced Coupled Plasma Mass Spectrometry
ICP-SFMS	Induced Coupled Plasma Mass Sector Field Mass Spectrometry
IEA	International Energy Agency
IFBR	Integrated Forest Biorefinery
IGCC	Integrated Gasification Combined Cycle
IRR	Internal rate of return
LHV	Lower heating value [MJ/Nm^3]
LHV_F	Lower heating value of the biomass [MJ/kg db]
LHV_G	Lower heating value of the dry gas produced [MJ/Nm^3]
LTS	Gasification experiments with a tar sampling start between 119 and 129 minutes
M_C	Molar mass of Carbon [kg/mol]
m_F	Biomass (dry basis) mass flow rate [kg db/s]
MSW	Municipal solid waste
NDIR	Nondispersive infrared
NG	Natural gas
NL	Refers to L at normal pressure (1.013×10^5 Pa) and temperature (0 ºC)
Nm^3	Refers to m^3 at normal pressure (1.013×10^5 Pa) and temperature (0 ºC)
NPT	Normal pressure (1.013×10^5 Pa) and temperature (0 ºC)
NPV	Net present value
OLGA	Dutch acronym for oil based gas washer
PBP	Payback period
PCC	Pearson-R correlation coefficient
P_G	Absolute pressure of the dry gas [Pa]
PG	Producer gas
PP	Pulp and paper
PS	Primary sludge
ppmv	parts per million by volume
PSA	Pressure Swing Adsorption
Q_{air}	Air flow rate [NL/min]
$Q_{biomass}$	Biomass flow rate [kg/h]
Q_{steam}	Water steam flow rate [kg/h]
R	Ideal gas constant [8.314 $J.mol^{-1}.K^{-1}$]

RDF	Refused derived fuel
RFB	Residual forest biomass
S/B	Steam to biomass [kg steam/kg biomass]
SEM	Scanning Electron Microscopy
SNG	Synthetic natural gas
SOFC	Solid oxide fuel cell
SPA	Solid Phase Adsorption
SPE	Solid Phase Extraction
SRF	Solid recovered fuel
SS	Secondary sludge
ST	Steam turbine
T_{bed}	Temperature of the reactor bed [ºC]
TC	Thermal conductivity
TCD	Thermal conductivity detector
$T_{freeboard}$	Temperature of the reactor freeboard [ºC]
T_G	Absolute temperature of the dry gas [T]
TGA	Thermogravimetric analysis
V_G	Dry gas volumetric flow rate [Nm^3/s]
W_{CF}	Mass fraction of Carbon in the biomass [kg C/kg biomass db]
WGS	Water-gas shift
WtE	Waste-to-energy
Y_{gas}	Dry gas specific production [Nm^3 dry gas/kg dry biomass]
y_i	Molar fraction of CO_2, CO, CH_4, C_2H_4, C_2H_6 and C_3H_8 in the dry gas
%v	Volume percentage [%]
wb	Wet basis
WI	Wobbe Index
%wt	Weight percentage [%]
ΔG	Gibbs free energy of reaction
ΔH	Enthalpy of reaction
$\varepsilon_{C,I}$	Molar fraction of Carbon in i [mol C/mol i]

1 INTRODUCTION

The foundation of the current society production of services and materials is largely based on finite feedstocks extracted from earth, which are being depleted at an unsustainable rate. Current world population is growing and developing countries demands are increasing, leading to higher materials and services necessities. Environmental and economic issues associated to these feedstocks urge the transition to a more sustainable production system. To answer these issues, a partial or complete adjustment of the current economy to one based on renewable raw materials, denominated by bioeconomy, must happen. These renewable solutions must be introduced into our existing production chain and must be acknowledged not as immediate solutions, but as long-term solutions, which must be employed as soon as possible and improved and perfected along time. Nonetheless, a complete transition of the current production system to a more sustainable one is an enormous and difficult challenge. This will require technologies development and significant scientific advancements, as well as innovative thinking and research approaches and proper support from governments and stakeholders.

Lignocellulosic biomass is a key material for the transition to a sustainable bioeconomy by being a non-intermittent renewable source of energy capable of fitting into the current carbon-based (fossil) fuel infrastructure. Biomass can be used for CHP and the production of gaseous/liquid fuels, chemicals and other bioproducts, using thermochemical conversion processes. These processes include biomass gasification to produce a fuel gas with diverse applications, pyrolysis for production of biochar and bio-oils or combustion for direct production of energy. In the bioeconomy context, the gasification process is extremely relevant due to: i) the recognition that gaseous fuels have practical advantages over solid fuels, such as handling and application, ii) the necessity of renewable fuels that can replace gaseous fossil fuels in distinct applications and iii) the flexibility of gasification processes, due to the various bioproducts that can be obtained from the produced fuel gas. Thus, biomass gasification technologies are expected to have a major role in this future bioeconomy and in future biorefineries that will produce a diverse number of value-added products from biomass and compete with current petrochemical refineries.

1.1 OBJECTIVES

The objectives of this work revolve around obtaining new scientific knowledge to support the development of direct gasification of biomass in bubbling fluidized bed (BFB) reactors to produce a gaseous fuel with suitable properties to replace natural gas in industrial gas burners, such as the burners installed at kiln ovens and boilers of the pulp and paper (PP) industry. This is the first step for the integration and development of gasification-based biorefineries in the PP industry. These objectives include:

- Characterization of the state-of-the-art of gasification technologies, including commercial and technical barriers, potential gasification-based biorefinery designs and current status and implementation in Europe.

- Development and evaluation of numerical tools to predict and support gasification processes.

- Characterization of the direct gasification process of distinct low-cost feedstocks in BFB reactors, including byproducts from the PP industry and refused derived fuel, focusing on the influence of the process operating parameters (e.g., bed temperature and ER) and feedstock chemical composition, on the combustible gases concentration in the clean and

dry PG, tar concentration in the raw PG and efficiency parameters (e.g., carbon conversion efficiency).

- Evaluation of primary measures for the improvement of the PG quality from direct biomass gasification:
    - Steam injection in the bottom bed of the reactor.
    - Low-cost catalysts in-situ application above the bottom bed of the reactor.
- Evaluation of the co-combustion process of byproducts from the PP industry to consider as a co-integrable process in a future gasification-based biorefinery design.
- Development of a technical-economical pre-feasibility analysis for the replacement of the natural gas used in the lime kilns of the PP industry by PG from direct gasification of biomass wastes. This is the first step for the integration of gasification-based biorefinery processes in the PP industry.

1.2 LAYOUT

The thesis is composed by 10 Chapters and is based on 12 Articles (Figure 1.1). A short description of each Chapter is given below.

Chapter 1 states the objectives and layout of this thesis, and describes the experimental infrastructures and methodologies used in the studies performed.

Chapter 2 explains the theory behind the biomass gasification process and shows the current status of biomass gasification technologies, their future potential and current technical and commercial barriers, as well as potential key findings that must be achieved to promote their market breakthrough. This chapter is composed by Articles I and II. Article I reviews the integration of gasification technologies in the PP industry, focusing on the current technological and commercial drivers and barriers and Article II evaluates the current state, progress and utilization of large-scale (>3 MW_{th}) gasification plants in Europe.

Chapter 3 is composed by Article III, which includes the development, comparison and evaluation of two models to predict PG composition from direct (air) biomass gasification processes in BFBs, namely a non-stoichiometric chemical equilibrium model and an empirical model. These prediction tools were developed to support and validate the experimental research and techno-economic analysis performed in this work.

Chapter 4 demonstrates and evaluates distinct direct gasification processes performed in different experimental infrastructures and is composed by Articles IV, V, VI and VII. Article IV performed the demonstration of the direct (air) gasification process of distinct types of residual forest biomass (RFB) in an autothermal pilot-scale 80 kW_{th} BFB, focusing on the composition of the PG and process efficiency parameters. An extensive comparison with literature results was also performed. For similar operating conditions, Paper V evaluated the effect of superheated steam addition on the reactor bottom bed, focusing on the effect of the S/B ratio, and Article VI evaluated the impact of using distinct mixtures of RDF with RFB as feedstock. The main objective of steam addition was the improvement of H_2 concentration and H_2/CO molar ratio in the PG, while the main objective of mixing RDF with RFB was to seek synergistic effects for the improvement of the PG quality. Article VII investigated tar formation and evolution during direct gasification of distinct types of RFB from eucalyptus (*Eucalyptus Globulus*) in a 5 kW_{th} bench-scale BFB reactor. The main objective was the

analysis of the effect of the composition of distinct eucalyptus parts, and respective ash and char accumulation in the reactor during the gasification process, on the tar concentration in the PG.

Chapter 5 evaluates the application of low-cost catalysts as primary catalysts, i.e., inserted in a high-temperature zone of the gasifier, to improve the quality of the PG and gasification process efficiency parameters. This chapter is composed by Articles VIII, IX and X. Article VIII tested three distinct types of low-cost catalysts, namely synthesized Fe_2SiO_4, bottom bed eucalyptus ashes and pine pellets char particles, in an alternative configuration inserted in an 80 kW_{th} BFB reactor. The Article focused on the increment of combustible gases concentration in the PG and efficiency parameters. Article IX continued the work performed in Article VIII by analyzing the application of natural occurring iron-titanium mineral ($FeTiO_3$, ilmenite) under the same process conditions and in the same configuration. Article X further continued this work by performing a more in-depth analysis of the application of ilmenite and comparing its results to the application of synthetic concrete. As Article X is an extension and more in-depth analysis of the results presented in Article IX, only the content of the prior was discussed in this Chapter.

Chapter 6 is composed by Article XI, which evaluates the co-combustion process of distinct types of byproducts from the PP industry in a pilot-scale BFB reactor. This process was evaluated as a valid energetic solution, focusing on HCl and NOx emission, because it can potentially constitute a co-integrable process in future gasification-based biorefinery designs in the PP industry.

Chapter 7 is composed by Article XII, which performs a comparative techno-economic analysis of the integration of eucalyptus RFB direct gasification in the PP industry. For this purpose, three possible configurations using BFB gasifiers were considered and analyzed, including natural gas replacement in the lime kilns and electricity generation.

Chapter 8 performs a comprehensive integrated discussion based on the previous Chapters.

Chapter 9 performs the conclusion of the work.

Chapter 10 proposes future studies of major relevance.

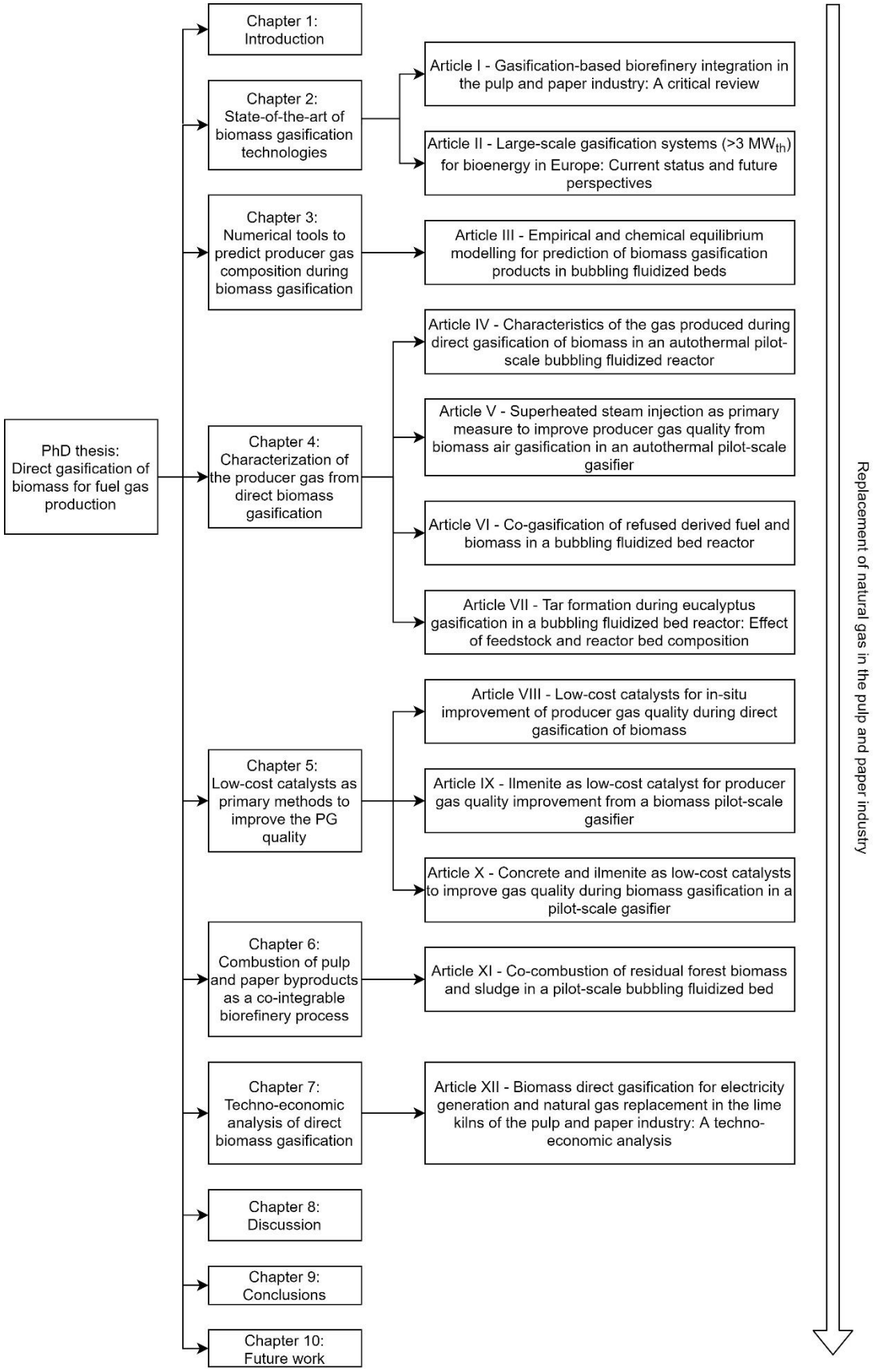

Figure 1.1– Diagram of the thesis layout.

1.3 EXPERIMENTAL INFRASTRUCTURES

1.3.1 DAO-UA 80 kW_{TH} PILOT-SCALE BFB GASIFIER (PORTUGAL)

The 80 kW_{th} pilot-scale BFB gasifier experimental infrastructure is located at the Department of Environmental Planning of the University of Aveiro in Portugal, and is the main infrastructure supporting this work. The infrastructure was developed/updated during the course of this PhD and the final version offers the following functionalities:

- Direct (air) gasification of distinct types of biomass and wastes feedstocks.
- Steam insertion at the bottom bed of the reactor for converting residual char.
- Combustion of the PG before release to the atmosphere.
- In-situ application of catalytic materials for improvement of the gas quality.

The layout of the experimental facility is shown in Figure 1.2 (steam injection mode) and Figure 1.3 (in-situ catalysts mode).

The experimental facility includes a thermally insulated pilot-scale 80 kW_{th} BFB reactor made of AISI 310 SS with a reaction chamber of 0.25 m internal diameter and 2.3 m height (Figure 1.4). The bottom bed of the reactor has a (static) height of 0.23 m and is composed by sand (high quartz content; particles with size in range 355 mm to 1000 mm); 17 kg of sand composed the bottom bed. The biomass is fed at the bed surface, namely 0.30 m above the distributor plate, by means of a screw feeder.

The primary air flow is fed through a distributor plate. The distributor is composed by 19 injectors, each one with 3 holes (1.25 mm diameter) placed perpendicularly to the direction of the gas flow in the reactor, thus providing an uniform distribution of the primary air to the bottom bed of the reactor. The fluidized bed is operated at bubbling regime and atmospheric pressure, with superficial gas velocity of around 0.27 and 0.30 m/s (depending on the operating conditions, namely bed temperature), which is two times higher than the determined minimum fluidization velocity (0.14 m/s, for bottom bed particles with an average granulometry of 700 μm). The temperature along the reactor height is monitored by 9 thermocouples located above the distributor plate: T1 – 0.05 m, T2 - 0.18 m, T3 - 0.29 m, T4 - 0.44 m, T5 - 0.66 m, T6 - 0.84 m, T7 - 1.19 m, T8 - 1.66 m and T9 - 2.88 m. The temperature monitored by the thermocouples T2 to T9 are used for the temperature profiles in Articles IV to XI. The bed temperature is assumed to be the value given by thermocouple T2 and is maintained at the desired level by regulating the insertion of a set of eight water-cooled probes located at the bed level.

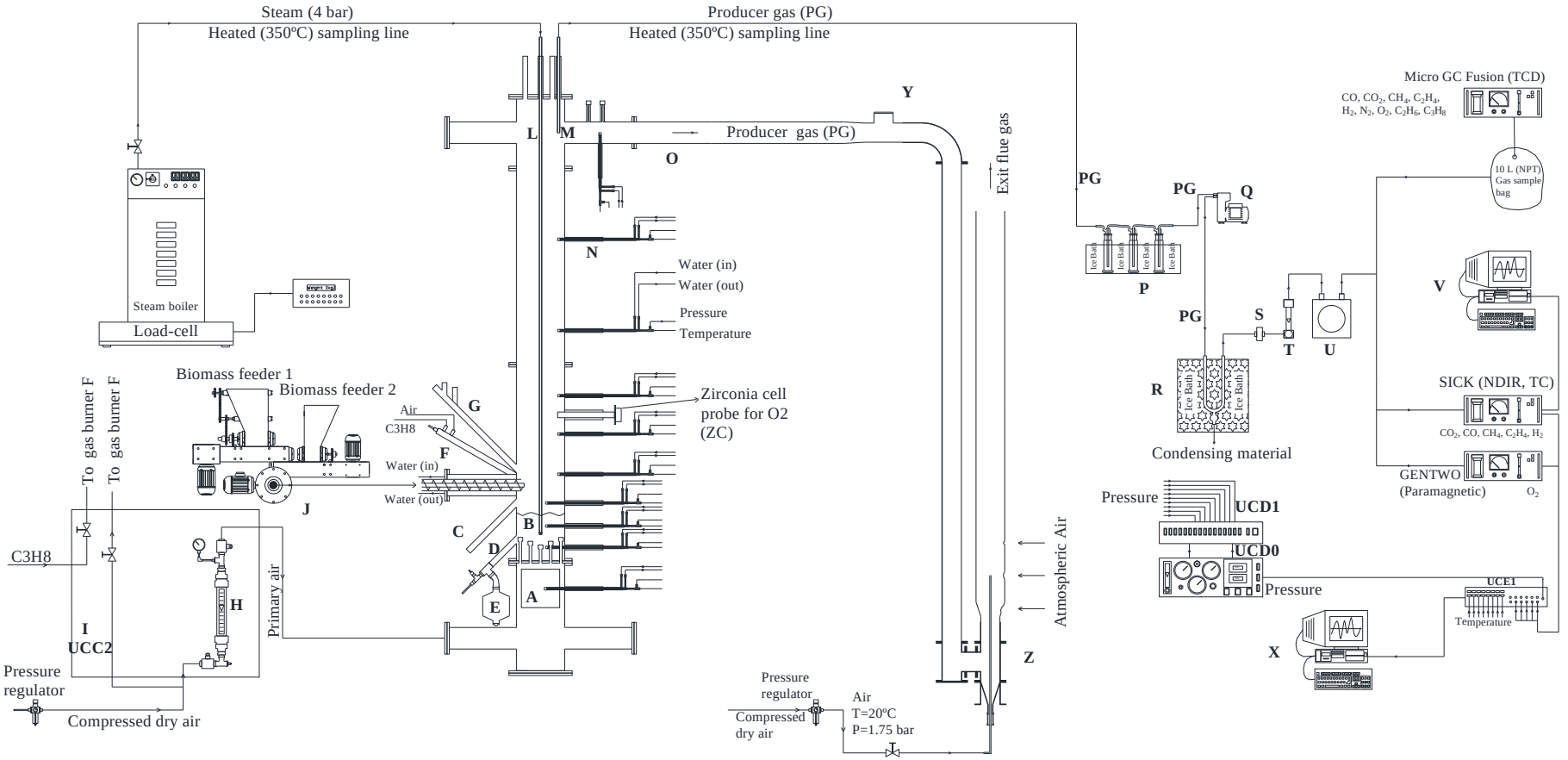

Figure 1.2 - Schematic layout of the 80 kWth autothermal BFB pilot-scale gasification facility (steam injection mode). Dashed line - Electric circuit, Continuous line - Pneumatic circuit, A - Primary air heating system, B - Sand bed, C - Bed solids level control, D - Bed solids discharge, E - Bed solids discharge silo, F - Propane burner for preheating, G - Port for visual inspection of bed surface, H - Air flow meter (primary air), I - Control and command unit (UCC2), J - Biomass feeder, L – Steam injection probe, M1 - Probe for sampling the raw exhaust gas, N - Water-cooled probe for pressure and temperature monitoring, O - Gas exhaust, P - Gas condensation unit with impingers for condensable gases (water, tars) removal, Q - Gas sampling pump, R - Gas condensation unit for moisture and other condensable gases removal, S - Filter for particle matter/aerosol removal, T - Gas flow meter, U - Dry gas meter, V - Computer for data acquisition from the SICK analyzer, X - Computer for data acquisition, Y - Security exhaust pipe, Z - Raw gas burner, GENTWO – Paramagnetic online gas analyzer for O_2, UCD0, UCD1 - Electro-pneumatic command and gas distribution units, UCE1 - Electronic command unit, Micro GC Fusion - Gas chromatograph with TCD, SICK – NDIR and TC online gas analyzer for CO_2, CO, CH_4, C_2H_4 and H_2.

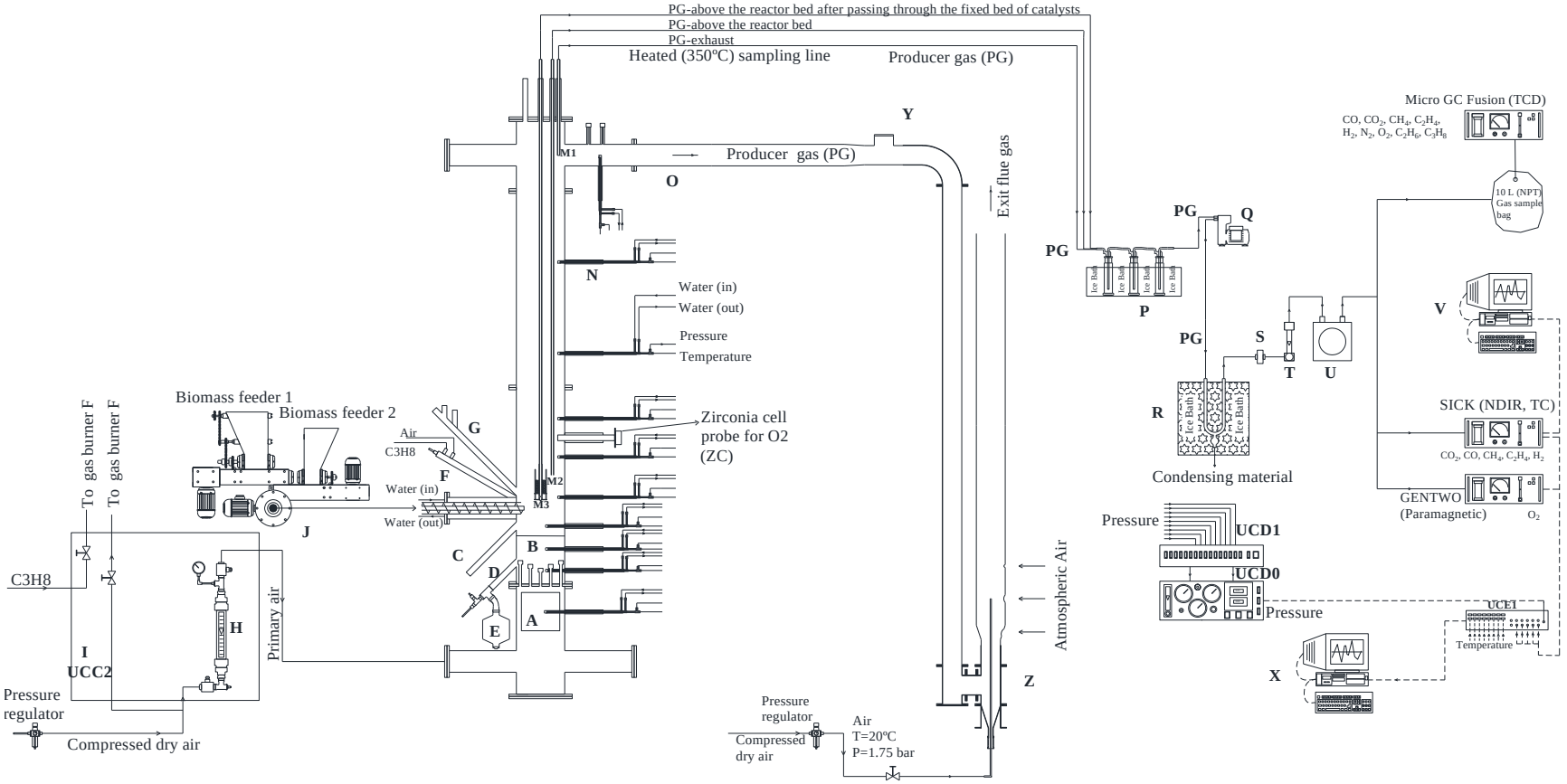

Figure 1.3 - Schematic layout of the 80 kWth autothermal BFB pilot-scale gasification facility (in-situ catalyst mode). Dashed line - Electric circuit, Continuous line - Pneumatic circuit, A - Primary air heating system, B - Sand bed, C - Bed solids level control, D - Bed solids discharge, E - Bed solids discharge silo, F - Propane burner for preheating, G - Port for visual inspection of bed surface, H - Air flow meter (primary air), I - Control and command unit (UCC2), J - Biomass feeder, M1 - Probe for sampling the raw exhaust gas, M2 - Probe for sampling the raw gas present above the reactor bed, M3 - Fixed bed reactor with catalyst particles, coupled to a gas sampling probe, N - Water-cooled probe for pressure and temperature monitoring, O - Gas exhaust, P - Gas condensation unit with impingers for condensable gases (water, tars) removal, Q - Gas sampling pump, R - Gas condensation unit for moisture and other condensable gases removal, S - Filter for particle matter/aerosol removal, T - Gas flow meter, U - Dry gas meter, V - Computer for data acquisition from the SICK analyzer, X - Computer for data acquisition, Y - Security exhaust pipe, Z - Raw gas burner, GENTWO – Paramagnetic online gas analyzer for O_2, UCD0, UCD1 - Electro-pneumatic command and gas distribution units, UCE1 - Electronic command unit, Micro GC Fusion - Gas chromatograph with TCD, SICK – NDIR and TC online gas analyzer for CO_2, CO, CH_4, C_2H_4 and H_2.

Figure 1.4 – DAO-UA pilot-scale 80kW$_{th}$ BFB reactor.

The start-up of the reactor until an operating bed temperature of around 500 ºC is done by a propane burner (F, Figure 1.2 and Figure 1.3) and by pre-heating (A, Figure 1.2 and Figure 1.3) the primary air. After reaching a bed temperature of around 500 ºC, the biomass feeding is started, and the gas burner and primary air pre-heating system are switched off. Afterwards, the biomass combustion allows the delivery of the necessary heat to achieve the desired operating bed temperature and the equivalence ratio (ER) is controlled by adjusting the biomass feeding rate while keeping the primary air gas flow rate constant. Then, the direct gasifier is operated under autothermal and steady-state conditions without any external auxiliary heating systems being used, thus, with the necessary heat for the gasification process delivered from the partial combustion of the biomass fuel in the reactor.

Steam injection (120 to 135 ºC, 4 bar) in the reactor bottom bed can be performed by using a 6.6 kW steam boiler and an AISI 316 SS steel probe (L, Figure 1.2) installed in the reactor. The mass flow rate of steam is controlled and monitored indirectly by continuous measuring of the consumption of water in the boiler along the operation time, namely by using a platform weight scale placed below the steam boiler. A heated sampling line (at ~350 ºC) is used to transport the steam to the top of the injection steel probe (L, Figure 1.2). The steam is then transported from the top of the BFB gasifier to the inside of the bottom bed through the steel probe, thus absorbing

heat (mainly from the reactor freeboard) and increasing its temperature. During this process, heat from the freeboard of the gasifier is absorbed to generate superheated steam, thus avoiding a sharp drop in the bed temperature upon the steam release, and boosting water-gas shift (WGS) and char-steam reforming reactions (explained in Chapter 2) [1]. The bottom point of the injection steel probe (L, Figure 1.2) has 4 holes (4 mm diameter) disposed in radial configuration to perform an uniform steam injection in the bottom bed of the reactor.

Insertion of catalysts in the freeboard of the reactor can be performed by placing the solid materials in a fixed bed reactor (M3, Figure 1.3) installed in the freeboard of the BFB gasifier, just above the bottom bed and biomass feeding location. The effect of the low-cost catalysts in the PG and gasification efficiency parameters is evaluated upon a comparison between the composition of the gas sampled after passing the fixed bed (M3, Figure 1.3) and sampled without passing the fixed bed (M2, Figure 1.3); this methodology is explained in Section 1.4.

The sampling and analysis of the PG is performed by two heated hoses, thermally isolated and heated at 350ºC to avoid tar condensation, three probes for sampling the gas at different locations, namely at the exhaust (M1, Figure 1.2 and Figure 1.3) and above the surface of the bed (M2 and M3, Figure 1.3), a gas conditioning unit and a set of gas analyzers. This latter is composed by the following equipment:

- GMS-810 SICK – Online non-dispersive infrared and thermal conductivity analyzer (CO, CO_2, CH_4, C_2H_4 and H_2).
- GENTWO – Paramagnetic analyzer (O_2).
- SRI 8610C – Gas cromatograph with FID and TCD detector.
- INFICON Micro GC Fusion – Gas cromatograph with TCD detector.

The PG is continuously combusted in an atmospheric gas burner located downstream of the gasifier, before being released to the atmosphere. The objective is the elimination of the major pollutants present in the produced gas, that endanger the local human and environmental health, namely CO, CH_4, C_2H_4, C_2H_6, C_3H_8 and other heavier hydrocarbons. The elimination is performed through the gas burning, thus converting most of the aforementioned gases to CO_2 and H_2O and increasing the safety of the gas release.

For this purpose, compressed air at 1.7 barg is injected at the bottom of the burner to aspirate the produced gas from the reactor and release it from the burner. The aspired produced gas is ignited in a pilot flame, sustained by and external propane blowtorch, located at the burner. The compressed air flow is 40 NL/min, which only represents roughly 10 % of the stochiometric necessities, thus, the burner contains three circular openings close to the pilot flame to allow the admission of atmospheric air to contribute to the complete burning of the PG. As a safety measure to prevent flame flashback to the BFB reactor, the connection between the reactor and the burner is performed by a T-shaped tube.

1.3.2 DAO-UA 3 kW_{TH} BENCH-SCALE BFB GASIFIER (PORTUGAL)

The 3 kW_{th} bench-scale BFB gasifier experimental infrastructure (Figure 1.5 and Figure 1.6) is located at the Department of Environmental Planning of the University of Aveiro, Portugal. The infrastructure is analogous to the 80 kW_{th} BFB autothermal pilot-scale infrastructure and uses the same gas conditioning and analysis system (previously described in Section 1.3.1.). However, the 3 kW_{th} BFB reactor (approximately 49 mm internal diameter and a reaction chamber of 340 mm) is operated under allothermal regime, i.e., heat is continuously supplied by an electrical furnace (4.2. kW_e). The bed material consists of silica sand with particle sizes in the range of 180 to 250 μm. Nearly 150 g of bed material are placed into the inner cylindrical tube of the reactor

leading to a static bed height of ≈50 mm. Considering the bed material and the distributor plate performance, the fluidization velocity is ≈ 0.14 m/s at 800 ºC, equivalent to a fluidization gas flowrate of ≈ 4 NL/min of air. In-situ testing of low-cost catalyst materials can be performed by using a fixed bed reactor (K, Figure 1.5) placed in the freeboard of the bench-scale BFB reactor. The fixed bed reactor consists in a cerablanket bed involved in wire and placed at the bottom of a sampling probe with 8 mm internal diameter (K, Figure 1.5). The effect of the low-cost catalysts on the PG and gasification efficiency parameters is evaluated based on a comparison between the composition of the following PGs:

i) Gas sampled after passing through the sampling probe with a fixed bed of catalyst materials.

ii) Gas sampled after passing through the sampling probe with an equal amount of inert material (e.g., sand).

Steam injection and flow rate is based on the continuous monitoring and supply of liquid water by a high performance liquid chromatography (HPLC) pump to an electrically heated evaporator; the superheated steam is mixed with the fluidization agent and introduced in the bottom of reactor bed at a temperature between 160 and 180 ºC and pressure of 1 barg.

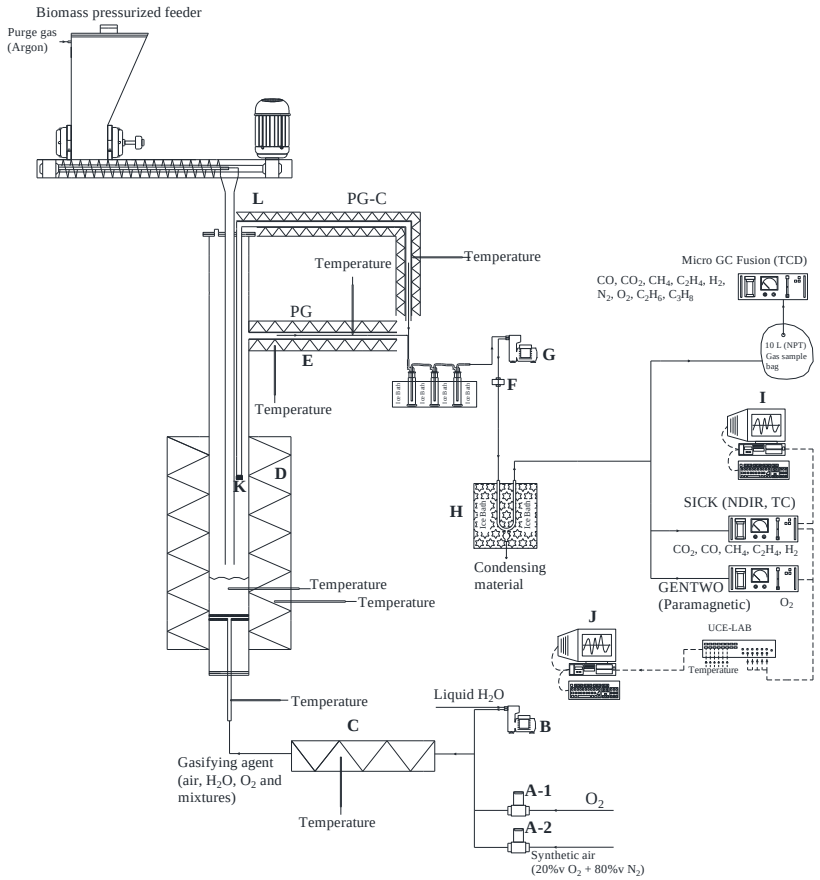

Figure 1.5 - Schematic layout of the 3 kW_{th} allothermal BFB bench-scale gasification facility. Dashed line - Electric circuit, Continuous line - Pneumatic circuit, A-1, A-2 – Mass-flow controllers, B – HPLC pump, C – Electrical furnace to produce steam from liquid water and preheat air, D – Electrical furnace to supply heat to the BFB reactor, E – Raw PG exhaust involved by an electrical furnace to maintain the PG above 400 ºC and avoid tar condensation, F – Filter for particle matter/aerosol removal, G – Gas sampling pump, H - Gas condensation unit for moisture and other condensable gases removal, I - Computer for data acquisition from SICK analyzer, J - Computer for data acquisition, K – Fixed bed of catalysts, L - Probe involved by an electrical furnace to maintain the PG above 400 ºC and avoid tar condensation, PG – Raw PG, PG-C - PG that passed through the fixed bed of catalysts, GENTWO – Paramagnetic online gas analyzer for O_2, UCE-LAB - Electronic command unit, Micro GC Fusion - Gas chromatograph with TCD, SICK – NDIR and TC online gas analyzer for CO_2, CO, CH_4, C_2H_4 and H_2.

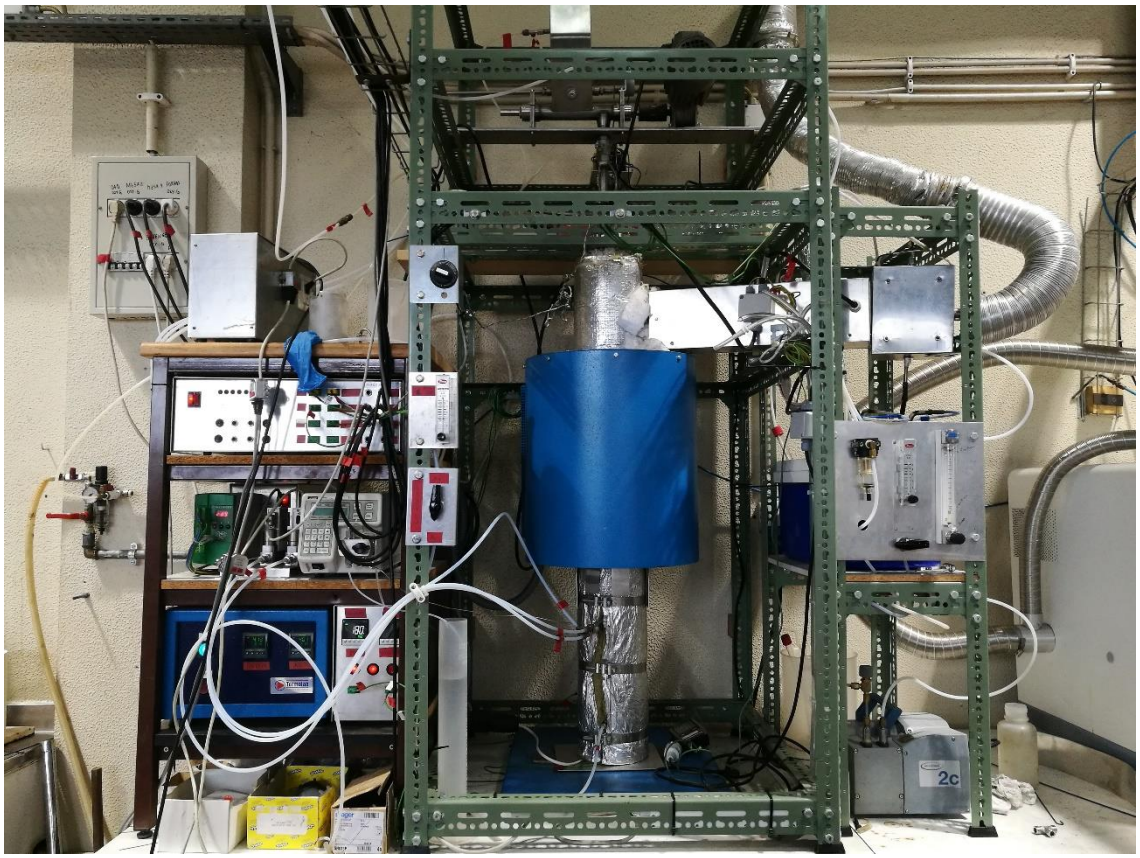

Figure 1.6 – DAO-UA 3 kW_{th} allothermal BFB bench-scale infrastructure.

1.3.3 KTH 5 kW_{TH} BENCH-SCALE BFB GASIFIER (SWEDEN)

The 5 kW_{th} bench-scale BFB gasifier is located at the KTH Royal Institute of Technology in Stockholm, Sweden. The experimental facility (Figure 1.7 and Figure 1.8) includes a 5 kW_{th} BFB composed of a bottom bed (50 mm inner diameter, 300 mm height) and a freeboard (104 mm inner diameter, 450 m height). The larger diameter of the freeboard, in comparison to the fluidized bed, allows for a reduction of the gas velocity, thus decreasing the entrainment of particles from the bottom bed.

The bottom bed of the reactor is composed by Al_2O_3 (approximately 3960 kg/m^3 bulk density) with a particle size between 63 and 125 µm. For the fluidization of the bed, 8.6 NL/min of a synthetic mixture of O_2 and N_2 (5.8 %v and 94.2 %v, respectively) is used, representing a fluidization velocity of 29 cm/s. This is higher than the determined minimum fluidization velocity (0.5 cm/s) for these bed material particles. This synthetic mixture has a significantly lower O_2/N_2 molar ratio (0.06 $mol \cdot mol^{-1}$) than atmospheric air (0.27 $mol \cdot mol^{-1}$) to promote a higher dilution of the PG in N_2 and consequently reduce tar partial pressure and condensation. A flow of 2 NL/min of N_2 is added to the fuel hopper to prevent hot gases from escaping from the reactor through the water-cooled feeding screw, which could cause undesired biomass pyrolysis and consequent clogging and blockage in the feeding system.

The non-condensable gases of the PG (after drying and cleaning) are analyzed with a micro gas chromatograph (Thermo Scientific, C2V-200). The tar concentration in the PG (before drying and cleaning) is determined according to the Solid Phase Adsorption (SPA) method (explained in the next Section).

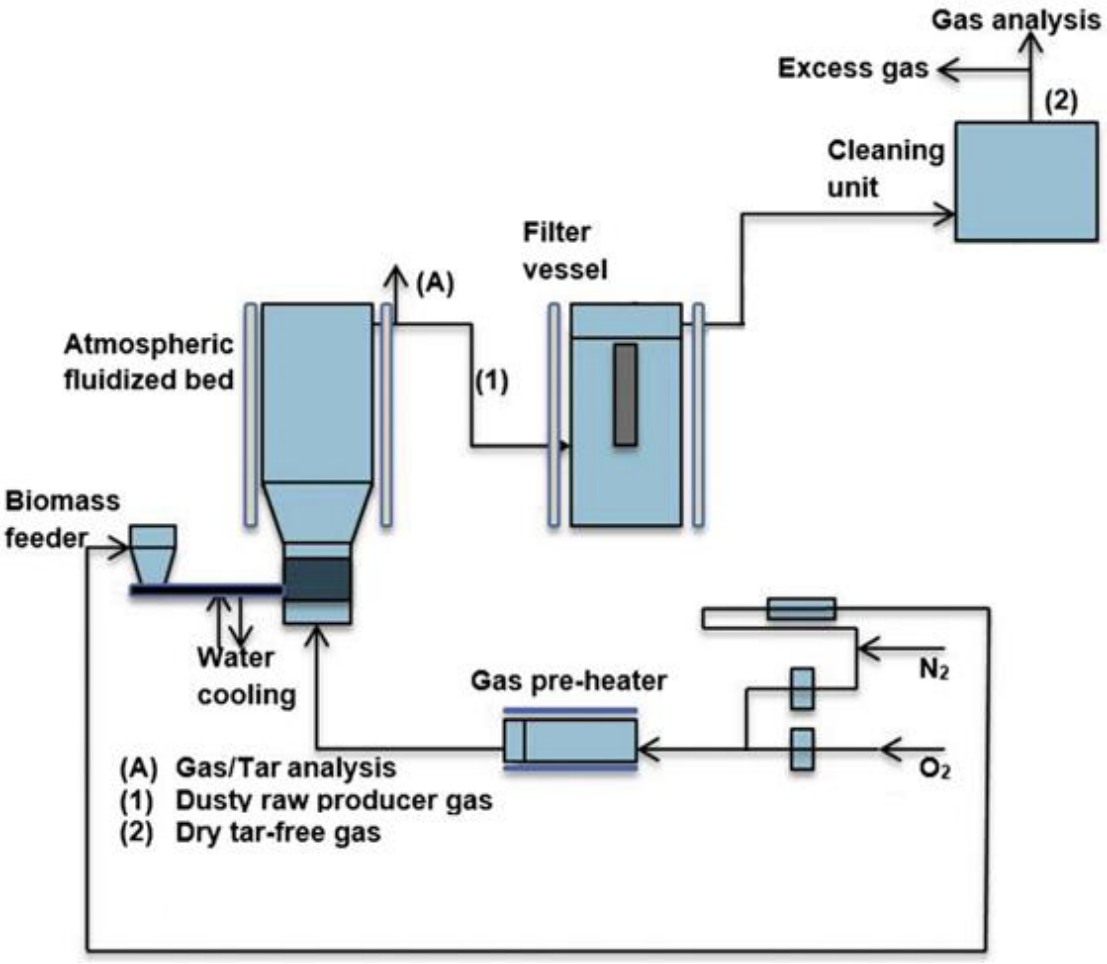

Figure 1.7 - Schematic view of the experimental infrastructure. Adapted from [2].

Figure 1.8 – KTH 5 kW_{th} allothermal BFB bench-scale infrastructure.

1.4 METHODOLOGIES

The gasification process was evaluated based on the composition of the PG and four efficiency parameters determined from the experimental data, namely lower heating value of the dry gas produced (LHV), specific dry gas production (Y_{gas}), cold gas efficiency (CGE) and carbon conversion efficiency (CCE). CGE is the ratio between chemical energy present in the PG in relation to the chemical energy present in the feedstock fed [3,4]. The CCE is the ratio between the carbon present in the PG in terms of gaseous compounds (e.g., CO, CO_2, CH_4, C_2H_4, C_2H_6, C_3H_8) and the carbon present in the feedstock fed [3,4]. This is a common procedure in the literature for characterizing gasification processes [5].

The ER was determined as the ratio between the O_2 added to the gasifier and the stoichiometric O_2 required for the complete oxidation of each biomass feedstock. The stoichiometric O_2 was determined based on the elemental analysis of the feedstocks used for the gasification experiments. The O_2 present in the steam injections (H_2O) was not considered for this calculation, and it was not expressed a specific ER parameter for water-oxidation (flow of H_2O in the steam injection in relation to the necessary flow of H_2O for the complete oxidation of each biomass feedstock), as suggested in other works [6]. Instead, the steam injection effect was evaluated based on the variation of the S/B parameter (steam flow rate in relation to biomass flow rate). The LHV of the PG for the distinct gasification experiments was determined based on the concentration of the combustible gases (H_2, CO, CH_4, C_2H_4, C_2H_6 and C_3H_8) and their respective LHV (at reference conditions, 273 K and 101.3 kPa) [7]. The efficiency parameters Y_{gas}, CGE and CCE, were determined through Equations 1.1 to 1.3.

$$Y_{gas} = \frac{V_G}{m_F} \quad \text{(Equation 1.1)}$$

$$CGE\ [\%] = \frac{V_G \times LHV_G}{m_F \times LHV_F} \times 100 \quad \text{(Equation 1.2)}$$

$$CCE\ [\%] = \frac{V_G \times \frac{P_G}{R \times T_G} \times M_C \times \sum_i \varepsilon_{C,i} \times y_i}{m_F \times w_{CF}} \times 100 \quad \text{(Equation 1.3)}$$

The tar concentration in the PG (before drying and cleaning) was determined according to the Solid Phase Adsorption (SPA) method [8]. In this regard, a solid phase extraction (SPE) 3 mL tube containing 500 mg of amino radical (NH_2) was coupled with a gastight syringe, which was then used to extract 100 mL gas samples from the exhaust pipe of the reactor in 1-minute procedures. Afterwards, the SPE tube was eluted with tert-butylcyclohexane and dichloromethane to obtain an aromatic fraction and a phenolic fraction, which were then analyzed by GC-FID. Tar sampling was conducted during two distinct times in each experiment, separated by 45 minutes. Three tar samples were taken at each time, representing approximately 10 minutes of operation time. This tar sampling procedure was only performed in the 5 kW_{th} KTH bench-scale BFB gasifier and is still under employment in the DAO-UA infrastructures.

Feedstock proximate analysis (moisture, volatile matter, ash) was made based on CEN/TS norms [9–11] and elemental analysis was performed by external laboratories. The chemical composition of the biomass ashes was determined by Induced Coupled Plasma Mass Sector Field Mass Spectrometry (ICP-SFMS) analysis in an external laboratory. The surface morphology and surface elemental composition of the feedstock ashes were characterized by Scanning Electron Microscopy (SEM, Hitachi SU-70) and Energy Dispersive X-ray Spectroscopy (EDS, Bruker Quantax 400 detector). The LHV of the feedstocks was determined based on the correlation made by Parikh et al., [12]. The crystalline phases of the fresh solid materials were assessed by powder X-ray diffraction (XRD) (BrukerD8 Advance DaVinci). Diffraction patterns were analyzed using ICDD (International Centre of Diffraction Data, PDF 4). Brunauer–Emmett–Teller (BET) and

Barrett–Joyner–Halenda (BJH) measurements were performed to determine the specific surface area and average pore diameter of the particles.

Chemical equilibrium modelling, based on the minimization of Gibbs free energy in the system, was performed to predict and support the gasification experiments. For this purpose, it was considered the molar input (biomass, gasifying agent and fresh reactor bed) and the predicted outputs (most abundant predicted gaseous and solid products) for distinct gasification processes. All products were assumed to act as ideals gases, except for solid products. Steady state conditions of operation were assumed. Tar formation was neglected and ash was assumed as inert. All the reactants were assumed to enter and leave the reactor at process temperature. The process temperature was assumed as homogeneous inside the gasifier, which is a common procedure in other non-stoichiometric thermodynamic models [13]. Hydrodynamics and kinetics were not considered. The chemical equilibrium model was applied to calculate the composition of the PG for distinct gasification operating parameters. Then, the respective efficiency parameters were calculated based on the obtained compositions. The software tool used for the model development was GASEQ (http://www.gaseq.co.uk/).

This modelling technique was also used to support the evaluation of tar composition and concentration in the PG from distinct gasification processes, namely for the determination of the reactor bottom bed composition along time and respective influence on tar formation. In this regard, the modelled compounds were assumed to reach equilibrium faster than the tar sampling start time. Quasi equilibrium conditions in the reactor bed were also assumed during the tar sampling interval due to the low quantities of ash fed to the reactor along time, in comparison to the bed material. In this case, the ash compounds of the biomass were not assumed as inert and the software tool used to implement the model was NASA Chemical Equilibrium with Applications (https://www.grc.nasa.gov/www/CEAWeb/).

Multiple regression tools in Microsoft Excel were used to analyze extensive databases containing experimental data from the literature, experimental data obtained by the authors and chemical equilibrium predictions results; this allowed the development of linear empirical and chemical equilibrium correlations. Pearson's correlation test was also used to measure the strength of the correlation between two variables. In this regard, it is important to note that correlation does not imply causation [14].

2 STATE-OF-THE-ART OF BIOMASS GASIFICATION TECHNOLOGIES

This chapter is composed by Articles I and II.

Article I, named "Gasification-based biorefinery integration in the PP industry: A critical review", reviews the integration of gasification technologies in the PP industry, focusing on the current technological and commercial drivers and barriers. The Article was published in the Renewable and Sustainable Energy Reviews Journal in 2020 (https://doi.org/10.1016/j.rser.2020.110210).

Article II, named "Industrial gasification systems (>3 MW_{th}) for bioenergy in Europe: Current status and future perspectives", evaluates the current state, progress and utilization of large-scale (>3 MW_{th}) gasification plants in Europe. The Article is currently under submission and review in the Renewable and Sustainable Energy Reviews Journal.

2.1 ARTICLE I - GASIFICATION-BASED BIOREFINERY INTEGRATION IN THE PP INDUSTRY: A CRITICAL REVIEW

2.1.1 ABSTRACT

The biorefinery design has attracted interest from the industry and scientific community due to its main role in a future transition to a sustainable bioeconomy. This Article provides a critical review of the integration of biorefinery concepts in the PP industry, focusing on gasification-based biorefineries, including technological and commercial drivers and barriers, and biorefinery general opportunities and challenges.

The PP industry is commonly recognized as highly suitable to integrate biorefinery concepts. For this purpose, various integrable biorefinery designs composed of distinct conversion processes are proposed in the literature. However, key technologies and biorefinery concepts must firstly be improved and proven at a market level to increase stakeholders confidence. Gasification can be a driving force for this integration and efficient replacement of natural gas by PG in burners is the first and most immediate step. Nonetheless, drawbacks associated with the contaminants present in the PG (e.g., tars) must be addressed. Research rarely focus on this first step and is more centered on sophisticated gasification applications (e.g., methanol synthesis), without considering associated technological and commercial barriers. Furthermore, supporting policies are generally required to make the integration of biomass gasification technologies in the PP industry profitable and to avoid the interruption of operation of fully functioning large-scale gasification plants.

Keywords: Biorefinery; Producer gas; Biomass; Gasification.

2.1.2 INTRODUCTION

The main driving force for energy from biomass has been the search for a non-intermittent renewable energy source alternative to fossil fuels which can guarantee security in energy supply. The interest in biomass is supported by several reasons:

1. Biomass can be used to complement the intermittence of other renewable energy sources, because it can be supplied in increased amounts when the production of intermittent renewable energies (e.g., solar, wind) is low [15].

2. A wide range of energy vectors and products can be obtained from biomass, such as heat, electricity, biofuels, biochemicals and biomaterials [16].

3. Biomass provides the necessary flexibility to reduce the reliance on fossil fuels (oil, coal and natural gas) in distinct applications [17–19]. In fact, fossil fuels are derivatives of decomposed biomass [20].

4. Biomass is a carbon neutral fuel that can fit in the existing carbon-based (fossil) fuel infrastructure [21].

5. Unlike fossil fuels, biomass is a global and widely distributed natural resource, which transcends sectors and borders and, consequently, is difficult to be monopolized [21,22].

Despite these recognized potentialities, sustainable use of biomass must be assured to avoid biodiversity and ecosystem endangerment [23], increased food prices and GHG emissions increase [24]. For example, to meet future bioenergy expectations and comply with higher biomass demands, significant areas of suitable land to grow biomass are required; this may lead to the displacement of food crops to unused lands, which can cause the conversion of forests to arable lands and, consequently, harm biodiversity and increase GHG emissions [24,25]. In this respect, several potential scenarios have been proposed in the literature to integrate food and bioenergy cropping systems within farmlands, without adversely affecting food production or the environment [25]. In fact, proper allocation of perennial cropping systems has been found to have positive impacts on the environment and biodiversity [25]. Thus, it has been argued that bioenergy can have positive and negative environmental impacts, and that the overall net impact can be positive or negative depending on the strategies followed [24].

Therefore, before establishing large-scale processes for production of multiple products from biomass, that can represent an alternative to conventional petrochemical refineries [26–28], food security and sustainable biomass growth must be safeguarded [22,24]. Accordingly, to compete with current petrochemical refineries, biomass must also be able to provide transports fuels, chemicals, fibers and energy for heat and power production, among other products, in an economic and environmentally sustainable way. The manufacturing process of modern petrochemical refineries is based on separating and converting each component (even residues) from crude oil to different products using distinct conversion technologies [27]. Lignocellulosic biomass can have analogous conversion process chains [26,27], due to its complex components and its potential to yield multiple usable products.

Biomass can be converted to gaseous [29–31] or liquid fuels [32,33], chemicals and other bioproducts [34,35], using biochemical [36] and thermochemical processes [37–39]. The former involves the use of bacteria, microorganisms and enzymes to breakdown biomass; a process design example may involve an enzymatic pretreatment step of the feedstock [40–42] and consequent anaerobic digestion to biogas [43] or fermentation to fuels (bioethanol [43–45] and biobutanol [46,47]) and chemicals (e.g., acetone [48]). In thermochemical conversion processes, the biomass is broken down by applying heat and through chemical interactions; it mainly includes combustion to obtain thermal energy in the form of hot gases, pyrolysis to obtain biochar, fuel gases and bio-oil [49,50] and gasification to obtain PG. Regarding combustion, the obtained hot gases can be used in process heat applications or electricity production [51]. For electricity production, a Rankine Cycle or Organic Rankine Cycle is required to convert heat into work [52]. Regarding pyrolysis, the obtained chars can be used as barbecue charcoal [53], fuel in the metallurgical industry [49], upgraded to activated carbon for adsorbent processes [49] and applied as soil amendment [54], while the bio-oil can be directly used as fuel for heat or power generation [49], refined for suitable application in power engines and petrochemical refineries [52,55] and reformed with steam for hydrogen production [30]. The fuel gas from gasification can be burnt in boilers and kiln ovens for thermal energy production or be used in more advanced applications such as the synthesis of chemicals and biofuels (in-depth analysis in Section 2.1.3.).

In the bioeconomy context, the gasification process is highly promising due to: i) the practical advantages that gaseous fuels have over solid fuels, such as handling, transport, storage and supply, ii) the necessity of replacing gaseous fossil fuels in various applications and iii) the integration potential of the gasification process as a biorefinery concept, due to the various

bioproducts that can be obtained from the PG. Thus, biomass gasification technologies are expected to have a major role in the transition to a sustainable bioeconomy and in future biorefineries for the production of multiple products from biomass [56,57]. However, these technologies still face economic and technical drawbacks that may turn the process unprofitable in various scenarios [58–60]. For example, high-end catalytic synthesis applications require a very clean fuel gas (e.g., low tar and particles concentration), consequently obligating the implementation of costly cleaning processes and equipment with high investment and operating costs [15]. Another relevant issue is the biomass availability for large-scale gasification processes, resulting from biomass seasonality, heterogeneity and potential local shortage, and the necessity to safeguard sustainable biomass feedstocks, as previously discussed. The biomass quality variability (e.g., moisture content, physical properties), and consequent potentially necessary expensive pretreatment processes, is also a major issue than can affect the gasification process efficiency and competitiveness. These aspects need to be considered upon the planning, construction and operation of gasification plants.

The PP industry is amongst the world largest biomass consumers and a significant producer of bioenergy and biomaterials [61]. In the transition to a bioeconomy, the PP industry must cope with declining markets and low-cost competition by adapting its processes and products to become more environmentally friendly [62,63]. Nowadays, this is the main challenge that the PP industry must face [62]. Accordingly, the PP industry has been giving significant attention to integrated biorefinery concepts [63]. Integrating biorefinery concepts in the PP industry can contribute to reduce the fossil fuel needs of the manufacturing process while allowing the generation of revenue from new bioproducts. Furthermore, the PP industry is highly suited to integrate future biorefineries, due to the current infrastructures characteristics and capacity to process large volumes of biomass. In this context, the integration of gasification processes in the PP industry is particularly relevant due to the potential of the various end-products that can be obtained from the PG [64] and because it can serve as a first step for the transformation of this industry into complete biorefineries, particularly by replacing the natural gas used in the boilers and kiln burners by PG.

The purpose of this work is to provide an overview and critical review of the integration of gasification technologies in the PP industry, focusing on the gasification process specificities, including current technological and commercial drivers and barriers, and biorefinery general opportunities and challenges. Finally, key technologies and relevant biorefinery concepts for the development of gasification-based biorefineries in the PP industry are discussed. This work will aid the research and development of gasification key technologies, and their scale-up, and consequent integration in future biorefineries, specifically in the PP industry.

2.1.3 GASIFICATION

2.1.3.1 REACTIONS AND STAGES

Gasification is the thermochemical conversion of a solid or liquid feedstock into a mixture of combustible gases by using a gasification agent (e.g., air, O_2, H_2O, CO_2) at high temperatures. Gasification is a complex process composed of distinct thermochemical phenomena without evident boundaries, which often overlap, and whose principal chemical reactions are those involving solid carbon, CO, CO_2, H_2, H_2O and CH_4 [50,65] (Figure 2.1).

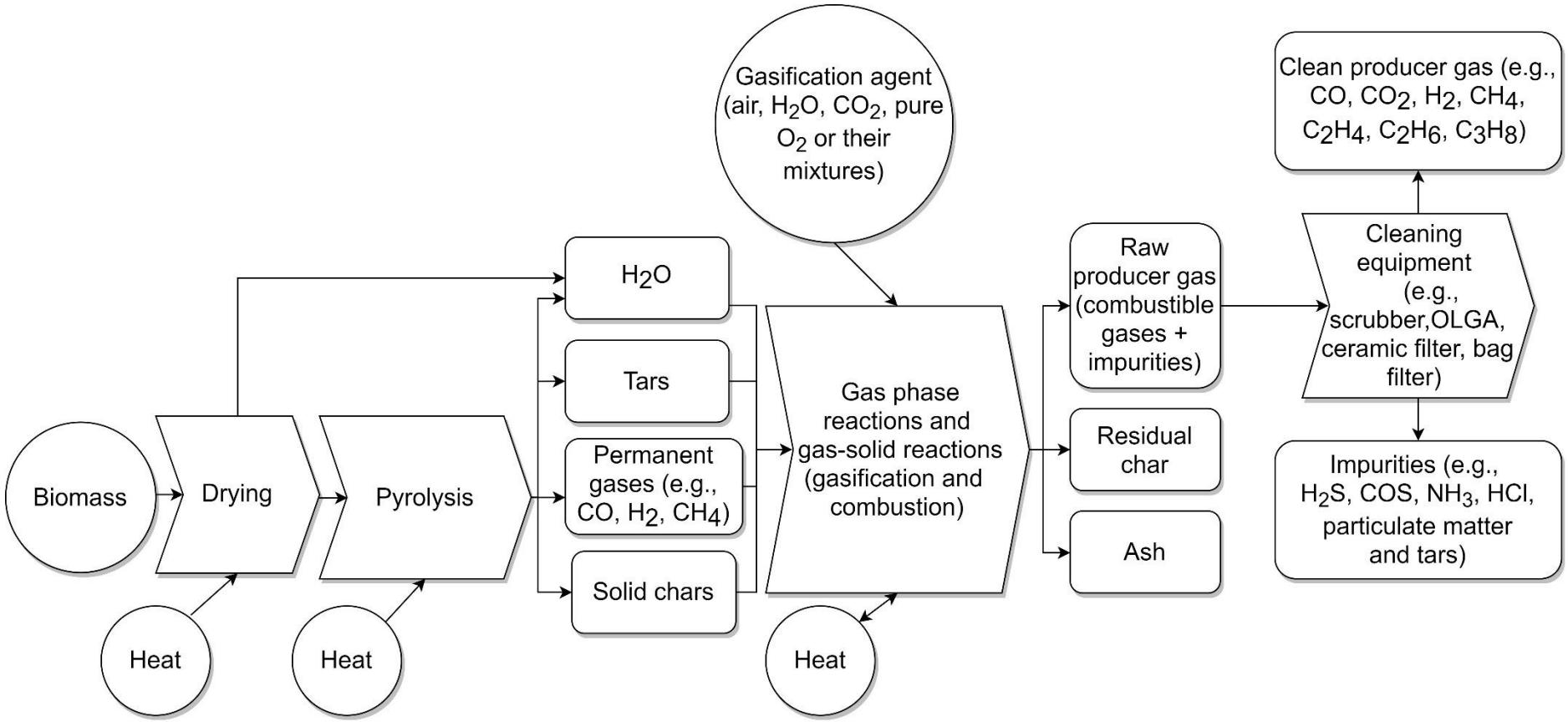

Figure 2.1 – Schematics of a typical biomass gasification process, including stages, inputs and outputs.

In a typical biomass gasification process, the biomass is firstly dried and then undergoes through pyrolysis (thermal decomposition). The resulting products from the pyrolysis step react among themselves and with the gasification agent, forming the final gaseous product [50]. The energy requirements for the main gasification reactions can be supplied externally (indirect gasification) or, if air or pure O_2 is used as gasification agent, by a limited amount of exothermic combustion reactions occurring in the gasifier (direct gasification) [50].

The first stage of the gasification process is the evaporation of water from the feedstock, which occurs immediately after the biomass enters the reactor and during its heating. Afterwards, as the temperature of the solid fuel rises above 150 ºC [50], the pyrolysis of the solid fuel begins (Reaction 2.1). This step occurs mainly between 300 and 600 ºC [66] and is particularly important in biomass gasification processes due to the large mass fraction of volatile matter present in biomass feedstocks [67]. Thus, the main organic constituents (e.g., extractives, cellulose, hemicellulose, lignin) of biomass are thermally decomposed and several chemical species, such as H_2O, H_2, CO, CO_2, CH_4, several light hydrocarbons (C_mH_n), tars (e.g., toluene, naphthalene, oxygenated compounds) and other impurities (e.g., H_2S, COS, HCl, NH_3 and alkali compounds), are formed and released to the gas phase [50,66,68]. Resulting from this stage, the biomass is reduced to a carbonaceous material (char) that is mainly composed of carbon [69] and inorganic elements [70], with residual amounts of hydrogen and oxygen [68].

$$\text{Biomass} + \text{Heat} \rightarrow H_2O + \text{Char} + \text{Tar} + \text{Permanent gases (e.g., CO}, H_2, CH_4) \qquad \text{Reaction 2.1}$$

The gases formed during the pyrolysis step take part in gas-phase reactions (between them and with the gasification agent) and gas-solid reactions with the char. The char is also involved in several reactions with the gasification agent [50]. The conversion of the remaining carbon and hydrogen present in the chars into gases is the main objective of the gasification process. If the energy required for the endothermic reactions is to be supplied by exothermic reactions inside the reactor, O_2 must be present in the gasification agent, and the chars and released gases will partially react with O_2, resulting in CO_2, H_2O and CO (Reactions 2.2, 2.3 and 2.4).

The carbon present in the chars is also converted into CO and H_2 according to endothermic reactions, e.g., *Boudouard reaction* and water-gas reaction (Reactions 2.5 and 2.6). The latter is often considered as the most relevant char gasification reaction occurring during typical gasification processes [50]. Solid carbon can also be converted to CH_4 according to the hydrogasification reaction (Reaction 2.7), however, this reaction is less relevant in biomass gasification processes due to a slower rate in comparison with other gasification reactions [50]. Nonetheless, it is an important reaction when the production of SNG is desired [50].

Apart from volatile matter combustion (Reaction 2.2), the gas-phase reactions in the gasification reactor are often summarized by the WGS reaction and methanation (Reactions 2.8 and 2.9) [71]. Methanation is favored by lower temperatures while WGS is favored by high temperatures [71]. Depending on the employed temperature, the water-gas shift reaction may be driven towards products or reactants, therefore allowing the conversion of CO to H_2 or H_2 to CO. This is critical due to the importance of the H_2/CO molar ratio in the fuel gas [50,72]. Accordingly, the following homogeneous and heterogeneous reactions are often cited as the most relevant to describe a typical gasification process [66,67]:

Volatile matter combustion:	$[C_xH_y,\ CO, H_2, CH_4, etc.,] + O_2 \rightarrow CO_2 + H_2O + \text{heat}$		Reaction 2.2 [73]
Char combustion:	$C\,(s) + O_2 \rightarrow CO_2$	$\Delta H^{\circ}_{298K} = -394\ \text{kJ/mol}$	Reaction 2.3 [59]
Char partial combustion:	$C\,(s) + 0.5O_2 \rightarrow CO$	$\Delta H^{\circ}_{298K} = -111\ \text{kJ/mol}$	Reaction 2.4 [59]
Boudouard reaction:	$C\,(s) + CO_2 \leftrightarrow 2CO$	$\Delta H^{\circ}_{298K} = +172\ \text{kJ/mol}$	Reaction 2.5 [59]
Water-gas reaction:	$C\,(s) + H_2O \leftrightarrow CO + H_2$	$\Delta H^{\circ}_{298K} = +131\ \text{kJ/mol}$	Reaction 2.6 [59]

Hydrogasification reaction:	$C\,(s) + 2H_2 \leftrightarrow CH_4$	$\Delta H^{\circ}_{298K} = -74.8\ kJ/mol$	Reaction 2.7 [59]
WGS reaction:	$CO + H_2O \leftrightarrow CO_2 + H_2$	$\Delta H^{\circ}_{298K} = -41.2\ kJ/mol$	Reaction 2.8 [59]
Methanation:	$CO + 3H_2 \leftrightarrow CH_4 + H_2O$	$\Delta H^{\circ}_{298K} = -206\ kJ/mol$	Reaction 2.9 [59]

The fuel gas resulting from these reactive processes is commonly denominated by PG and is a mixture of the products shown in Reactions 2.1 to 2.9, light hydrocarbons (e.g., C_2H_2, C_2H_4, C_2H_6 and C_3H_8) and impurities, such as H_2S, NH_3, tars and particles. H_2S and NH_3 are a consequence of the sulfur and nitrogen present in the biomass, respectively, while the heavier hydrocarbons and tars result mainly from the thermochemical decomposition of the biomass and practical gasification processes not attaining chemical equilibrium. Accordingly, this gas is mainly suited for heat production and power generation applications, for example burning in boilers and kiln furnaces. The PG can also be cleaned and refined (removal of impurities) to be suited for more sophisticated applications. After upgrading, if the obtained fuel gas is mainly composed of CO and H_2, it is denominated by syngas, and can be used to obtain diverse products as long as certain specifications are met (e.g., H_2/CO molar ratio, tar concentration), such as Fischer-Tropsch (FT) diesel [72], methanol [74], DME [75], methyl tertiary butyl ether, formaldehyde, acetic acid [26], among other products [26].

2.1.3.2 REGIME CONCEPTS AND DESIGNS

In order to supply the necessary heat for the gasification process, two main routes are commonly used [15,69,76]: the direct process and the indirect process (Figure 2.2).

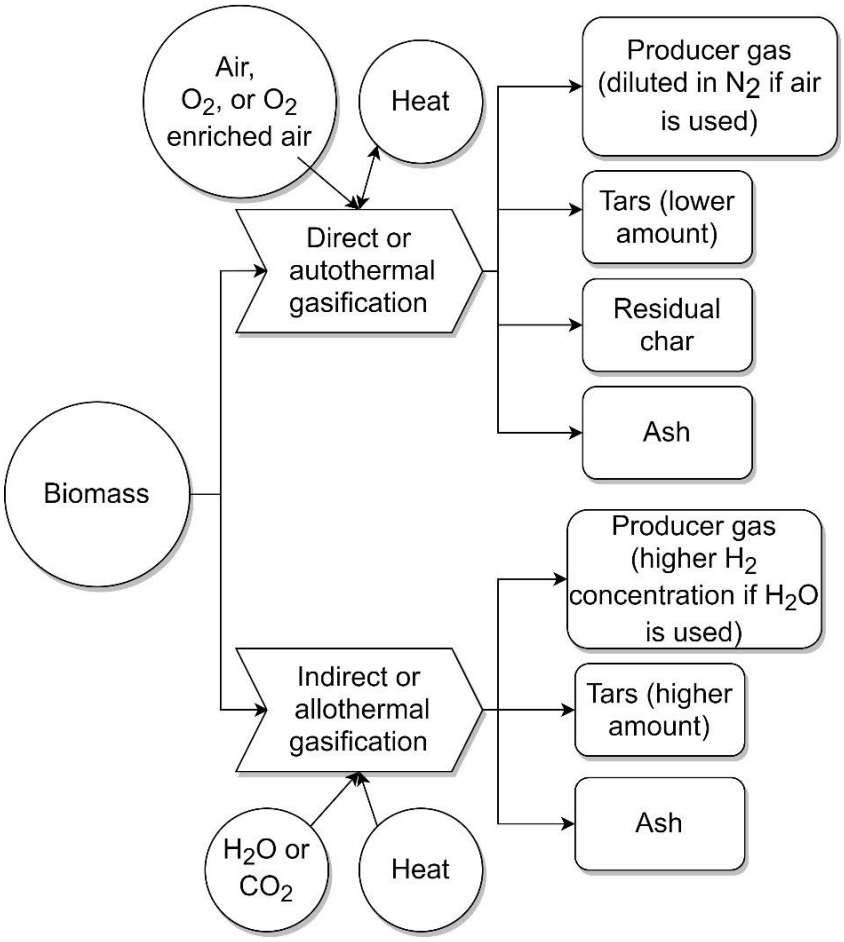

Figure 2.2 – Schematics of direct and indirect gasification processes, including inputs and outputs.

In the direct process, part of the biomass is oxidized (combustion) to generate the heat required for the endothermic gasification reactions. The gasification agent can be air or pure O_2, or, in order to produce a gaseous fuel with higher H_2 content, a mixture of these gases with H_2O. Under these conditions, the reactor should be autothermal and operated under very low ER, for example between 0.20 and 0.30 [4,15,69]. Adding H_2O can potentially lead to an increase of the H_2 concentration in the PG and be used as a measure to control the temperature of the reactor due to the lower temperature of the steam, in comparison with the gasifier reactor bed and freeboard, and the promotion of the endothermic water-gas reaction [66].

When using air as gasification agent, the PG will be diluted in N_2 and consequently have LHV (3 to 7 MJ/Nm^3) [4,77–79]. To avoid N_2 dilution during direct gasification, enriched air with O_2 or pure O_2 can be used as gasification agents, leading to LHV as high as 15 MJ/Nm^3 [77,78]. The major drawback associated with this type of gasification is the need of an ASU [66] to produce O_2. This separation process is currently performed by PSA, cryogenic distillation or membrane separation, which are technologies that consume large quantities of energy [80]. At small/medium scale biomass gasification plants operating at ambient pressure, air separation is mainly performed by N_2-O_2 sorption systems, such as PSA [66]. These technologies typically consume about 20% of the power generated by the biomass to energy conversion plant due to the necessary air feed compression, thus causing a significant decrease in energy efficiency [66]. Accordingly, PSA present higher economic viability for large-scale oxygen gasification plants (>100 MW_{th}) [66].

To increase the economic feasibility of O_2 separation, research has been focused on improving the design of ASUs [81,82], finding efficient uses for the resulting N_2 [83] or performing O_2 separation by conducting membranes [80]. This latter is argued to be a profitable, clean and efficient process to supply pure O_2 [80]. Membranes also present advantages for small to medium scale systems and can potentially be integrated into biomass gasification processes [66,84], including application inside the gasification reactor [85,86]. In this respect, Liu et al., [87] argued that using air enriched with O_2 (30 %, obtained by membrane separation) as gasification agent is more desirable than using air or pure O_2, because it allows a potential optimized balance between operating costs and the quality of the PG.

The conventional biomass gasification technologies for direct gasification can be divided in three main types of reactor designs, namely fixed beds, fluidized beds and entrained-flow. Gasification efficiency is dependent on various distinct operating parameters and can roughly be placed between 60 and 80 % for optimized gasification processes in this type of reactors [4,50,88,89]. Fixed bed gasifiers are mainly suited for small-scale operation (up 10 MW_{th}) and can be divided in updraft and downdraft configuration, which differs in terms of the PG flow direction and the zone where the gasification agent is introduced, consequently influencing the PG quality [50,66]. The updraft design is capable of processing feedstocks with high moisture content (up to 60 %wt) [90], however, this configuration promotes a significantly higher tar concentration (10 to 150 g/Nm^3) in the PG than the downdraft design (0.01 to 6 g/Nm^3) [50,66,78,91].

Fluidized beds are suited for larger-scale operation (5 to 100 MW_{th}) and are mainly divided in BFB and CFB gasifiers [50]. These designs are characterized by having enhanced mass and heat transfer characteristics and homogeneous temperature at the cross-section of the gasifier, in comparison with fixed bed gasifiers. The CFB design employs high temperature cyclones and particle separators to capture and recycle solids back into the gasifier, consequently increasing solids residence time and carbon conversion efficiency [78,90,92]. Tar concentration in fluidized beds can be placed between 1 to 30 g/Nm^3, thus being between the values reported for downdraft and updraft gasifiers [50,66,70,78].

The entrained-flow design is characterized by operating with O_2 as oxidant, employing very high temperatures (up to 1600 ºC), requiring the preprocessing of the feedstocks in very fine particles (less than 100 μm), having high complexity and investment costs, and, consequently, being more suited for extremely large applications (>100 MW_{th}) [66,90,93,94].

The indirect gasification process is allothermal, which means that a supplementary external heat source is needed to drive the process, for example a heated fluid or inert solid, such as sand.

Accordingly, the gasification agent can be CO_2 or H_2O because partial oxidation of the feedstock is not necessary to supply the thermal energy for the process. This contributes to a PG with higher H_2/CO molar ratio (up to 8 mol/mol [95,96]) when using H_2O as gasifying agent, and also with higher LHV (between 10 and 20 MJ/Nm^3 [4,77,95,96]), in part because it is not diluted in N_2, in comparison with the one resulting from direct (air) gasification processes [4,66,97]. Thus, the gas produced by indirect gasification is usually suited for more advanced applications (e.g., FT diesel synthesis, fuel cells) [98,99]. However, the application of this process at industrial scale is more challenging and complex due to the necessity of circulating elevated amounts of thermal energy between reactors [86].

The most common design for indirect gasification is the fast internal circulating fluidized bed reactor [66], often cited as DFB technology [100]. This design is composed of two interconnected fluidized beds: one BFB reactor typically operated under H_2O gasification regime and one CFB reactor operated under combustion regime to supply the necessary thermal energy for the endothermic gasification reactions [66]. The biomass is fed into the BFB gasification reactor along with H_2O [66], where common reactions of the gasification process, such as drying, devolatilization, steam reforming and partial char gasification take place [98]. Afterwards, the resulting residual char is transported with the bed material to the CFB combustion reactor where the char is burnt with air [66]. Then, after gas-solid separation, the heated bed material is recirculated from the CFB combustion reactor to the BFB gasification reactor, transporting the necessary thermal energy for the endothermic gasification reactions [66,98]. In this configuration, using a bed material with catalytic properties is a promising route, since the bed can easily be regenerated during its circulation between the gasification and combustion reactor [66].

DFB designs are under development since 1952, when Rayner proposed an indirectly heated gasifier with a separate CFB for combustion and a BFB for gasification [101]. Since then, several distinct DFB designs have been developed worldwide, including the Güssing gasifier in Austria (similar to the design described above), Trisaia gasifer in Italy, Battelle Columbus Laboratories gasifier in the United States of America and the CAPE FICFB Gasifier in New Zealand [102]. Currently, two DFB designs have been implemented at demonstration and industrial scales, namely the Güssing type DFB gasification process and the SilvaGas gasification process, initially developed by Battelle, which comprises two CFBs [66,101] (Figure 2.3). The Güssing type DFB was installed in some commercial plants in Europe (8 to 20 MW_{th}), namely Austria (Oberwart and Güssing), Germany (Stadtwerke Ulm/Neu) and Sweden (GoBiGas) [66,101]. With the exception of the Stadtwerke Ulm/Neu gasification plant, all the other Güssing DFB type plants stopped operation after governmental subsidies finished [103,104]. The SilvaGas process has no commercial unit installed so far [66]. Accordingly, the Güssing concept is recognized as the most successful and commercial indirect gasification system [101].

Further development of the indirect gasification process aims to use innovative methods for heat circulation, for example by using heat pipes containing liquid fluids that evaporate in the combustion reactor and condense in the gasifier reactor (e.g., Biomass Heatpipe Reformer) [101], and by combining the gasification and combustion zones in one reactor by having the gasification zone surrounded by the combustion zone [66], with heat circulating internally [101]. Examples of this latter development include the ECNs MILENA gasifier [105] (Figure 2.4), among others [106–108]. Another promising indirect gasification concept is the hydrothermal gasification, which can be divided in subcritical and supercritical water gasification, and involves biomass gasification in an aqueous medium at a temperature and pressure exceeding or close to water critical point [50]. This process can achieve high thermal efficiency for very wet biomass and has low tar production [50]. This type of technology is still in a research phase and under development [101].

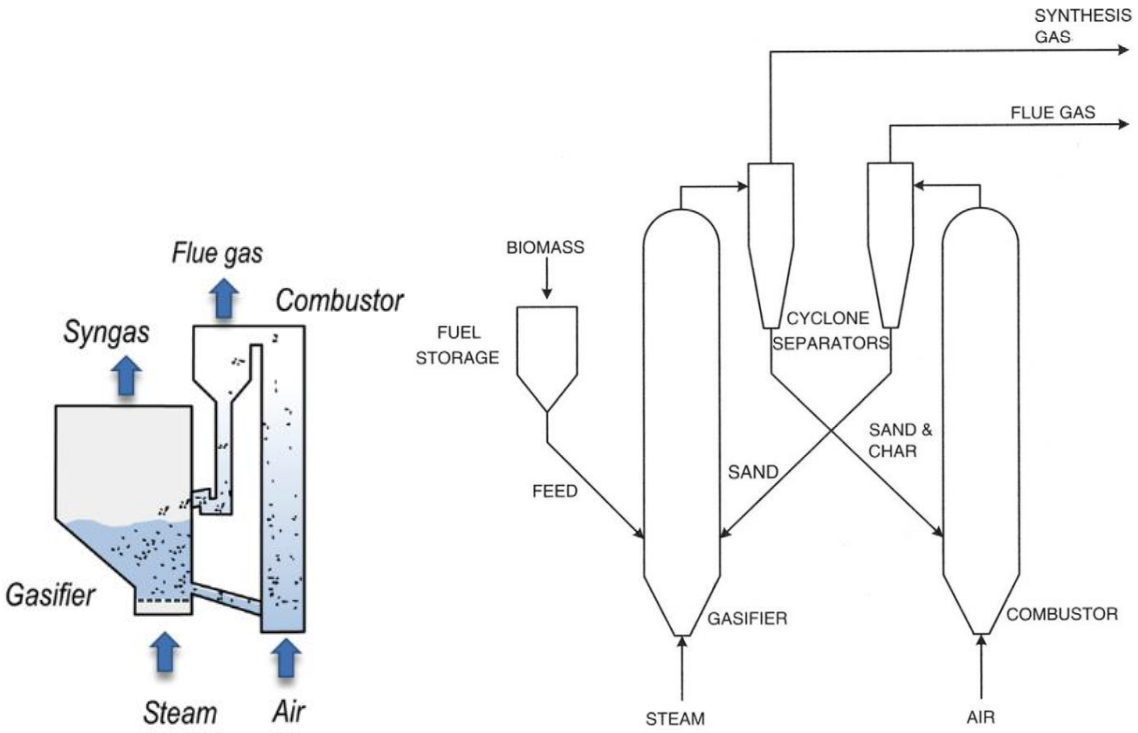

(a) **(b)**

Figure 2.3 – Schematic of the conventional Güssing type (a) [101] and SilvaGas (b) [109] DFB gasification processes.

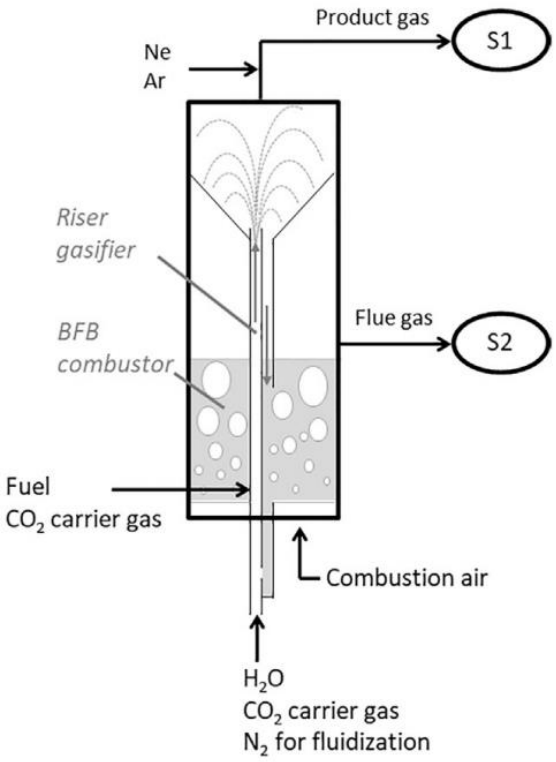

Figure 2.4 – Schematic of the indirect MILENA gasifier [110]. S1 – Sampling point 1; S2 – Sampling point 2; Ne and Ar – Tracer gases.

2.1.3.3 TAR FORMATION AND REMOVAL STRATEGIES

Tars in the PG are a common occurrence in biomass gasification processes and are recognized as the main technological barrier for the development and implementation of gasification technologies at industrial scale [15,59,111–113]. Tars are a mixture of highly aromatic organic condensable compounds (Figure 2.5) formed during thermal or partial-oxidation (gasification) regimes of any organic material [114]. The composition of tars is highly dependent on the thermal conversion process temperature and can be divided in primary (e.g., phenol), secondary (e.g., benzene, toluene, xylene) and tertiary (e.g., pyrene, indene, naphthalene) products, roughly placed at 200 to 500 ºC, 500 to 1000 ºC and over 700 ºC, respectively [114,115]; primary and tertiary tars are mutually exclusive, being that primary products are destroyed before tertiary products appear [114].

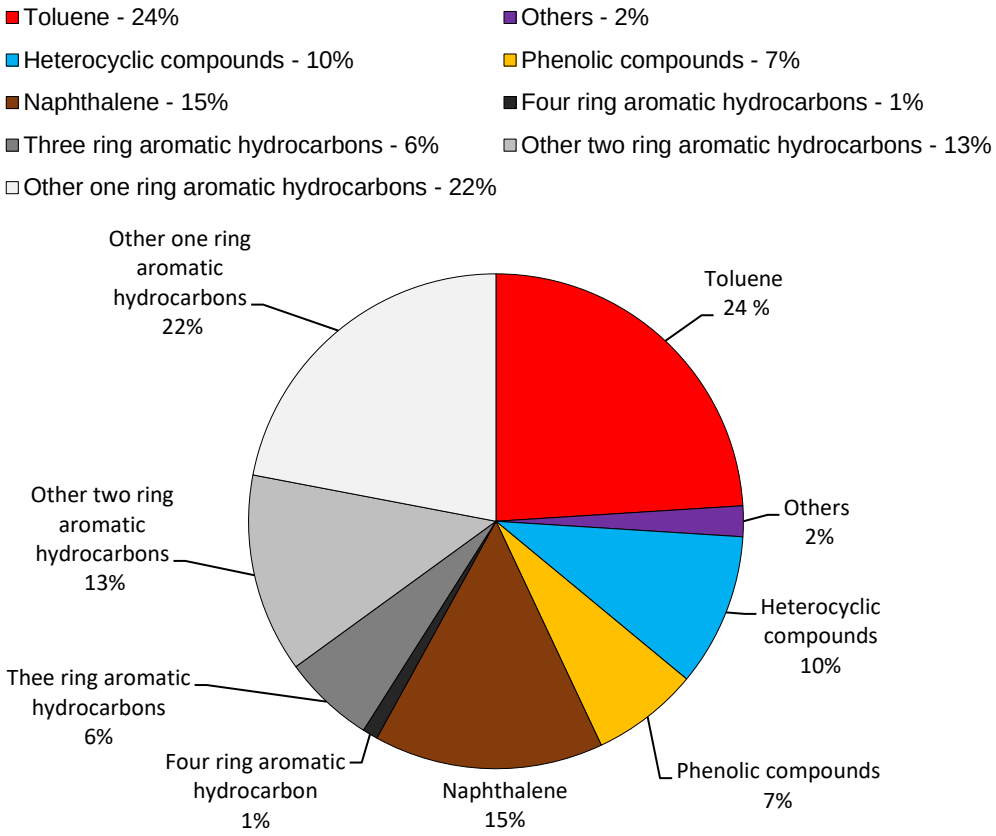

Figure 2.5 – Example of mass composition of biomass tars (excluding benzene, values highly dependent on the gasification operating conditions). Adapted from Ref. [116].

Tars start to condense downstream of the gasifier when the PG temperature decreases below 400 ºC (depending on the tar concentration), causing diverse problems in the equipment, such as fouling, corrosion, catalyst deactivation, clogging and general malfunction [113,117]. Thus, the use of raw PG with high tar concentration in some applications (e.g., fuels and chemicals catalytic synthesis) is technically unviable before significant cleaning and refining steps. Tar condensation in ducts, heat exchangers and filters also reduce the process efficiency and increase the system operation costs [113]. Furthermore, these compounds can evolve into more complex molecular arrangements through polymerization, increasing the difficulty of their removal [113]. Tar compounds may also contain a significant part of the biomass feedstock energy (up to 10 % in updraft gasifiers [118]), which is lost upon their removal from the PG [119].

Accordingly, tar concentration in the PG must be reduced to values compatible with the desired downstream applications (Table 2.1). This may require expensive gas conditioning processes and

equipment, which can turn the process economically unattractive. For direct use as fuel in combustion processes in furnaces and boilers, tars do not represent an issue if condensation is avoided in the transporting ducts that feed the burners. In this case, the energy content of the tars can be used and is not lost. However, more advanced applications such as combustion in internal combustion engines or synthesis of secondary fuels, present strict limits for tar concentration in the PG. Thus, for biomass gasification technologies to perform a commercial breakthrough and be available for integration in distinct biorefinery designs, it is important to develop cost-efficient processes to remove or minimize tar formation in the PG from distinct gasification processes [119]. In fact, tar compounds may even be converted to lighter gas species, such as CH_4, CO and H_2 [119], thus allowing PG to meet strict tar concentration limits, while converting the energy present in the tars into more useful gaseous energy vectors.

Table 2.1 – Suggested upper limits of tar concentration for using the PG in distinct applications [26,50,113,120–122].

Application	Tar concentration upper limit [mg/Nm^3]
Direct combustion in burners	No specified limit
Internal combustion engine	50
Gas turbine	5
Methanol	0.1
DME	10
FT diesel	Below dew point at FT pressure Heterocyclic aromatic tars with S or N hetero atoms must be removed below ppmv level
Compressors	50-500
Fuel cells	1

In this respect, several processes and technologies are under research for tar removal [15,67,113,123]. These can be broadly divided in primary measures, which are applied inside the reactor to minimize tar formation, and secondary measures, which are applied downstream of the gasification reactor to remove tar from the PG [123,124].

Primary measures for tar reduction are promising because they promote more efficient industrial applications by preserving and using the thermal energy of the PG and by reducing the necessity of downstream cleaning and refining [15,113,124]. In-situ reduction of tar formation can be attained by optimizing the reactor design and the process parameters, such as the ER, using active bottom bed materials (e.g., dolomite, limestone and olivine) and applying catalytic materials in an integrated second section of the gasifier freeboard [15,113,123,124]. Regarding the latter, natural minerals and gasification byproducts (e.g., ashes and chars) are under research due to their low-cost and abundance [123,125]. Several studies show that primary measures have the potential to reduce tar formation and improve the PG quality, however, these are still not fully understood and further research and technological development is required [113,123,124].

Secondary measures do not interfere with the gasifier operation and consist of tar removal by processes located downstream of the gasifier, such as physical processes (e.g., cyclones, scrubbers, electrostatic precipitators) and chemical processes (thermal or catalytic tar cracking) [113,124]. In fact, in existing gasification plants, removal of tar from the PG is mainly performed by physical processes [66,113]. These physical-mechanical treatments can attain high tar removal efficiencies, however, they may significantly reduce the energetic efficiency of the process (e.g. in result of additional energy consumption), generate hazardous wastes and reduce the gas yield, consequently reducing the process economic viability [66,113,124]. Nonetheless, some authors argue that secondary measures for tar reduction are more efficient, economical and easier to control than primary measures [126]. In this respect, the oil-based OLGA system shows high tar

removal efficiencies (~98 %), while generating a waste stream that can be used as feedstock in gasification processes [113,127–129]. Other recent studies for tar removal by secondary measures include mop fans (multifunctional fiber filters) to remove and retain tar directly from the PG [130], the use of gasification solid products as catalysts for tar reforming [123,131], oxidative filtration [132] and the combination of tar absorption and adsorption techniques to remove heavy and light tar, respectively [126,133].

Nevertheless, implementation of economic and environmentally friendly cleaning methods for the PG at an industrial level is still a complex and costly task [113]. It seems that the development of cost-efficient primary measures for in-situ high temperature gas cleaning and catalytic conditioning is mandatory to avoid excessive plant operating costs [15]. However, the application of primary measures may also not be sufficient to achieve complete tar removal [134]. In these cases, a combination of primary and secondary measures for tar removal, with primary measures having the role of removing the majority of tar compounds, can be a promising strategy [113,134].

2.1.4 BIOREFINERY OPPORTUNITIES AND CHALLENGES

Petroleum refining is a method of producing fuels, plastics, chemicals and pesticides [135]. In the transition to a bioeconomy, biorefining is gradually becoming a new method to produce energy vectors and chemical products, which can replace modern petrochemical refineries [135]. In general, biorefineries can be defined as a combination of processes to convert biomass into different middle platform compounds (e.g., PG, biogas), which are then used in distinct applications or further processed into bioproducts, such as biochemicals, biofuels and biomaterials [135,136] (Figure 2.6). The concept seeks the sustainable production of added-value biofuels and biochemicals to meet the society energy and material requirements [26].

The biorefinery concept is defined by the International Energy Agency (IEA) as “the sustainable processing of biomass into a spectrum of bio-based products (food, feed, chemicals, and materials) and bioenergy (biofuels, power and/or heat)” [137]. IEA Task 42 has classified biorefineries according to four main features: feedstocks, platforms, conversion processes and products [138]. For example, a biorefinery can be composed of biochemical platforms and thermochemical platforms (Figure 2.6). Nonetheless, any infrastructure that uses biomass for producing more than one product can be considered a biorefinery [139]. Accordingly, the concept implies that the conventional process of obtaining one product from biomass is replaced (e.g., heat production), so that biomass is seen as a natural feedstock for multiple bioproducts [27].

In the bioeconomy context, the biorefinery design is recognized as a highly promising concept in terms of economics and the environment [140]. Regarding economics, it can potentially allow different types of industries to significantly increase their productivity and profitability by accessing new markets for bioenergy and bioproducts and generating revenue from new products, while improving the industry efficiency [141]. For example, in a conventional sugar factory, sugar beet is used as feedstock to produce human and animal food, while in a sugar factory that integrates biorefinery concepts, the same sugar beet feedstock can be used for human and animal food while being used for energy, biofuels, biochemicals and biomaterials [142]. Furthermore, with fossil fuels depletion, increasing environmental restrictions and price rising, implementation of biorefineries is becoming more economically viable [139].

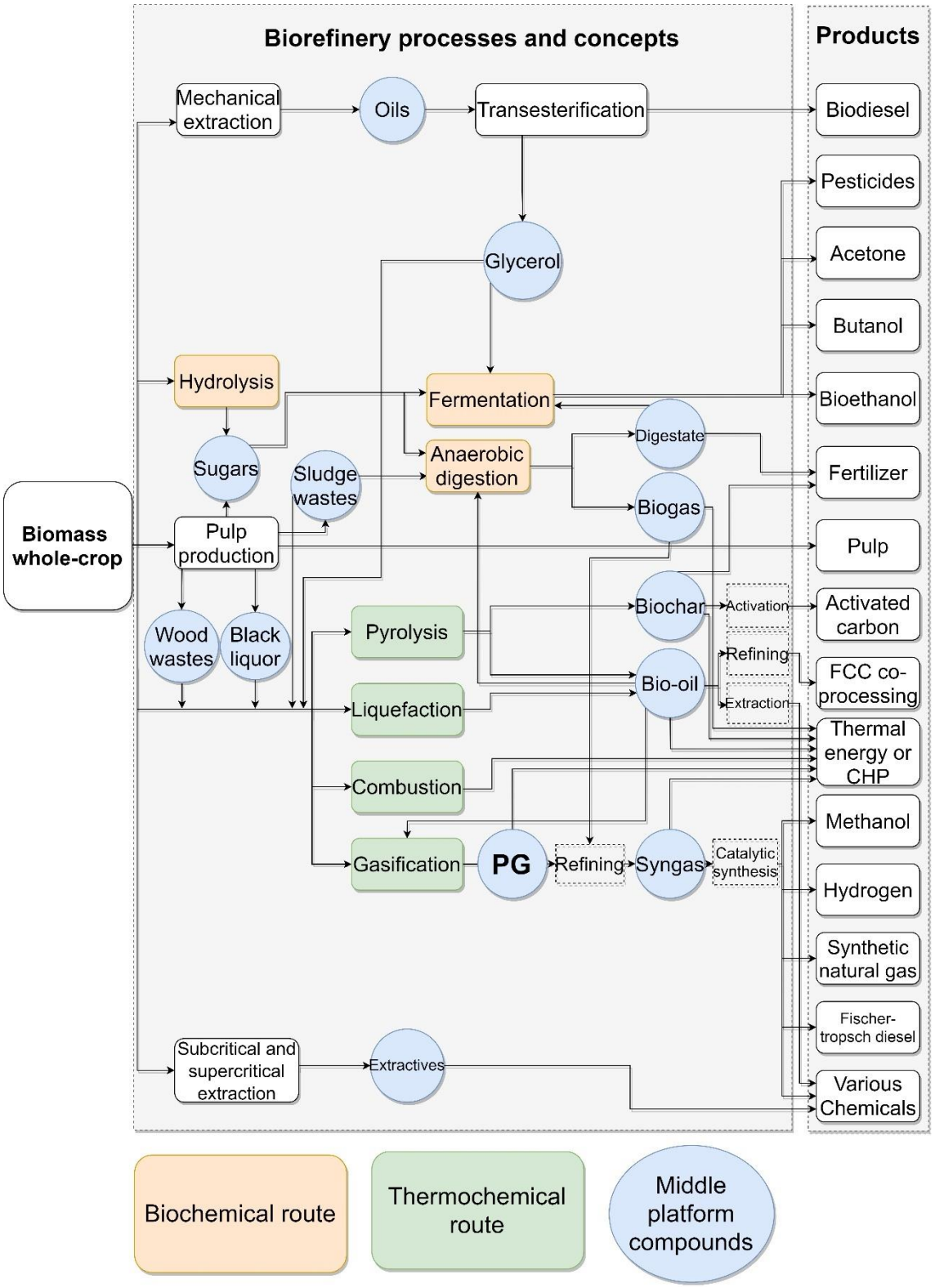

Figure 2.6 – Schematic example of integrated biomass conversion processes in a biorefinery design, including distinct conversion routes, middle platform compounds and obtainable products.

Regarding the impact on the environment, the concept of biorefinery is widely accepted as a potential cost-competitive way of lowering GHG emissions [136], as long as an adequate implementation is performed; this needs to be assessed for each specific case. The biorefinery design can also reduce the reliance on fossil fuel consumption and, consequently, increase energy supply security and contribute to the transition to a more sustainable material utilization. Thus, this concept is in line with circular economy principles and with the Agenda for Sustainable Development established by the United Nations [143], constituting a strategic mechanism for their realization [144]. However, sustainable production and utilization of "green" feedstocks must be safeguarded, environmental impact assessment must be performed for each scenario and further research is required to fully ascertain the environmental benefits of the biorefinery concept.

The concept design is analogous to current petrochemical refineries (Figure 2.7), in which multiple processes and technologies are used to obtain multiple products from crude oil [139,141,142,145]. The main differences are the feedstock used (biomass), conversion technologies and range of end-products (Table 2.2) [28,140]. Accordingly, the basis beneath a potential biorefinery manufacturing process chain includes: handling and preprocessing feedstocks for isolating its components, processing these components and separating the products formed [142]. For this purpose, a biorefinery should be composed of equipment to perform the pretreatment and separation/extraction of biomass components, thermochemical and biochemical conversion technologies, and a set of refining/upgrading processes. Thus, the components of biomass are separated and isolated, by using different pre-processing technologies, and processed to distinct bioproducts [139]. Future biorefineries may also attain energy efficiency values comparable to those of modern petrochemical refineries, due to energy integration and co-product development [139,140]. For example, heat released from distinct conversion processes in the biorefinery can be used to meet the heat requirements of distinct manufacturing processes [139,140].

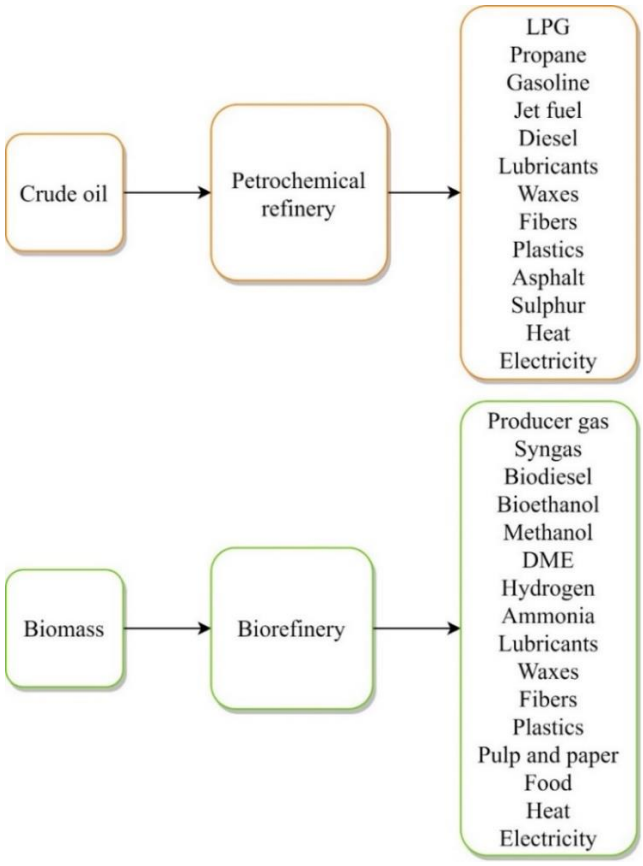

Figure 2.7 – Products obtainable in petrochemical refineries and biorefineries.

Table 2.2 – Feedstock characteristics, types of conversion processes and range of end-products for petrochemical refineries and biorefineries.

	Petrochemical refinery	Biorefinery
Feedstock	Relatively homogeneous	Heterogeneous
	Low oxygen content	High oxygen content
	Low inorganic content	Can have high inorganic content
	Can have high sulfur content	Low sulfur content
Conversion processes	Chemical processes (e.g., Hydrocracking and fluid catalytic cracking)	Biochemical processes (e.g., anaerobic digestion, fermentation), thermochemical processes (e.g., combustion, pyrolysis and gasification) and chemical processes (e.g., transesterification)
End-products	Narrower range of products	Wider range of products (e.g., pharmaceutics, food, fuels, PP)

Based on the aforementioned aspects, there is significant potential for biorefineries deployment, however, the practical potential is restricted by current technical and economic barriers [146]. Nowadays, development and employment of economically sustainable biorefineries is challenging due to low economic margins and significant technological restraints, in comparison with petrochemical refineries [140]. Thus, to successfully implement sustainable and profitable biorefineries, several weaknesses and threats must be addressed, for example [138]:

1. Proper definition of biomass value chains, including current and future market volumes and prices.
2. Definition and evaluation of the most promising biorefinery processes and concepts.
3. Determination of the variability of the quality, availability and energy density of the biomass types to use as feedstock.
4. Stakeholders operating in distinct market sectors (e.g., agriculture and forestry, transportation fuels, chemicals, energy, etc.,) must cooperate and work together.
5. Sustainability of biomass production must be assured, while avoiding competition with land for food production.
6. Governmental policies and subsidies must provide support for the building and operation of biorefineries.
7. Biorefinery concepts must be proven at a commercial market level.

Furthermore, key technologies must be fully developed and have higher profitability potential [27]. In fact, various biochemical, thermochemical and chemical processes (e.g., fermentation, gasification, liquefaction, catalytic synthesis, reforming, supercritical extraction) are suggested to obtain an immense number of products from biomass, however, the majority of these processes are not proven at a competitive market level. Stafford et al., [147] identified a total of 129 chemical, thermochemical, biological and mechanical process pathways that can be used to obtain up to 78 different bioproducts in distinct forestry biorefinery designs, with variable levels of technology readiness and market potentials. For example, biomass gasification, which is expected to have a main role in future biorefineries and is the basis of gasification-based biorefineries [123], is still in research and demonstration level and there exists an evident lack of reliable and commercial technologies [4], with several industrial gasification plants interrupting operation after the end of governmental subsidies [103]. In the same vein, biofuel production from the biochemical route face several economic barriers, such as costs of production, available markets, taxation policies and legislation, among others [139]. In fact, using agricultural wastes is too expensive to produce biofuels at a competitive price, while biochemical processes using lignocellulosic wastes still require technological advancements [139].

Another aspect that must be considered is the impact of the variation of the composition and quality of the biomass feedstock throughout the year [148]. For example, an annual biorefinery feedstock cycle might consist of agricultural wastes in the fall, wood residues or crops in the winter, cover crops in the spring and energy crops in the summer, leading to distinct technical and economic challenges [148]. Aspects of collection, transport and storage must be addressed in future sustainability studies as they have a direct impact on the sustainable utilization of the feedstock [144]. Separation of biomass components (lignin, hemicellulose and cellulose) must also be perfected for appropriate conversion to multiple bioproducts [27]. As argued by Waldron [27], if the components of the biomass feedstock cannot be effectively separated, it is impossible to control the quality of the products. Furthermore, if only one component is desired, as occurs with cellulose in the PP industry, and the other components are considered as wastes, the biorefinery potential is hindered. In this regard, the usage of the organosolv pretreatment method for the separation of lignocellulosic polymers into separate high-quality streams is sharing wide interest in the research community, with various distinct organosolv systems being developed for the pretreatment of different lignocellulosic feedstocks [149]. Specific analysis of this subject falls out of the scope of the current work.

In spite of significant challenges and barriers, the biorefinery concept shows potential to meet the interests of the society, environment and industry, and it seems that stakeholders are finally perceiving the vital role that biorefineries can have in a future transition to a sustainable bioeconomy [141], albeit their specific role still being largely undefined [144]. Available information regarding actual biorefinery plants is scarce, however, further investigation concerning actual practice is expected in the future, which will contribute to fully determine the potential of biorefineries in the circular bioeconomy context and to tackle all the aforementioned challenges [144]. In this respect, PG from biomass gasification can act as a major promoter of biorefinery designs and have a main role in gasification-based biorefineries, by being a middle platform compound to provide process heat and for the synthesis of multiple bioproducts.

2.1.5 GASIFICATION-BASED BIOREFINERIES IN THE PP INDUSTRY

2.1.5.1 DRIVERS AND BARRIERS

The PP industry is considered as highly suitable to integrate biorefinery processes, due to the large scale of industry, experience with biomass handling, process integration opportunities (sharing of raw materials, byproducts, utilities and infrastructures) and existence of partly processed byproducts [64,141,150,151]. Furthermore, integrating biorefinery processes in a production chain where fractioning is already performed can potentially allow significant cost reductions for the biorefinery [136]. In fact, conventional PP industries can already be considered as operating with biorefinery concepts, because distinct products are obtained from biomass, such as pulp, paper, electricity and process heat [150]. Accordingly, integrating additional biorefinery processes in the PP industry can be feasible and a potential pathway towards long-term sustainable growth by transforming this industrial sector into a multiple marketable bioproduct production design [61,63,151,152]. Thus, there are various drivers for implementing biorefinery processes in the PP industry [136,141]:

1. Current infrastructures located near sources of biomass and capable of processing large volumes of this resource.

2. Current knowledge and experience on managing and processing biomass using mechanical, chemical and thermochemical processes.

3. Reduction of the industry dependence on fossil fuels.

4. Increase of the efficiency of the utilization of biomass feedstocks. Currently, about 50 % of the harvested tree can end up as waste [147].

5. Providing of chemicals recovery, process heat (e.g., steam) and electricity for the manufacturing processes while allowing exportation of liquid fuels, electricity and other added-value bioproducts, such as DME and ammonia [44,61,153]. This allows the generation of revenue from new products.

6. Potential increase of annual profits, energy security and rural economic development and potential reduction of GHG emissions [44].

Nonetheless, for proper implementation of biorefinery concepts in the PP industry, several aspects must be considered, such as feedstocks and byproducts logistics, key technologies development and improvement, technical and commercial barriers, and uncertain market economics [136,152]. In this respect, Daya and Nourelfath [63] performed a sustainability assessment of the integration of biorefineries in the Canadian PP industry and found that the integration allows the PP industry to generate new revenues and reduce emissions, however, the following main challenges were identified:

1. Complexity of the integration due to the various types of biomass feedstocks and conversion technologies that can be used, which leads to the production of different bioproducts and distinct efficiency.
2. Uncertainty regarding the quantification of potential economic and environmental impacts.
3. Optimizing the balance between the economic and environmental impacts.

Amongst the potential biorefinery concepts to be integrated in the PP industry, the integration of biomass gasification technologies can represent a first and main step to upgrade PP mills into complete biorefineries. The most immediate integrable biorefinery configuration is based on the replacement of the natural gas used in the burners of the PP industry by PG (specifically discussed in Section 2.1.5.3). More advanced gasification designs to obtain distinct bioproducts, such as methanol and DME, are also under research to be integrated in the PP industry (Table 2.3). The integration of gasification technologies in the PP industry is supported by several specific reasons, for example:

1. PG can be obtained from the gasification of PP manufacturing process byproducts, such as wood wastes, sludges and black liquor [150].
2. PG can be used to obtain various biofuels and biochemicals or to provide steam, electricity and heat for the PP manufacturing process, according to the process needs [154,155].

The use of wood wastes or black liquor in GCC technologies is argued to allow the production of steam and electricity at higher efficiencies, in comparison with other conventional technologies (e.g., Rankine cycle) typically used in the PP industry [156,157].

In this regard, Rafione et al., [151] developed a biorefinery concept denominated by GIFBR, which contains a gasification unit to produce PG for the replacement of the natural gas used in the boilers and lime kilns of the PP industry. The study indicates that the concept is technically and economically feasible, being characterized by low GHG emissions, reduced water consumption and effluents production. The main challenges found were related to reaching a balanced level of integration between the receptor pulp mill and the biorefinery unit, attaining self-sufficiency in terms of energy consumption, and producing excess steam for the manufacturing process.

Table 2.3 – Published studies regarding gasification-based biorefinery processes for integration in the PP industry.

Product	Feedstock	References
Electricity (BIGCC)	Wood wastes	[154,155,158]
	Wood chips	[159,160]
Electricity (BLGCC)	Black liquor	[61,160,161]
Hydrogen	Black liquor	[162,163]
SNG	Wood wastes	[154,158]
	Black liquor	[164]
FT diesel	Wood wastes	[154,155,158]
	Black liquor	[44]
	Black liquor with wood wastes	[44]
Methanol	Wood wastes	[154,155,158]
	Black liquor	[165,166]
	Black liquor with pyrolysis liquids	[165,166]
	Black liquor with crude glycerol	[165]
	Black liquor with fermentation residues	[165]
DME	Wood chips	[159,160]
	Black liquor	[44,61,160]
Ammonia	Black liquor	[153]
	Black liquor with pulp sludge	[153]
	Black liquor with waste sludge	[153]
Mixed alcohols (ethanol, etc.,)	Black liquor with wood wastes	[44]

2.1.5.2 PP BYPRODUCTS GASIFICATION

The PP manufacturing process has several byproducts that can be converted by gasification to PG, for example black liquor, wood wastes and sludges. Black liquor is the spent liquor that results from the kraft pulping process after lignin and hemicellulose are removed from the cellulose fibers [153,167]. Wood wastes include residual forest biomass (RFB), e.g., tops and branches that are usually left in the forest after wood harvesting, and bark from the wood debarking process. Sludges (e.g. primary and biological) result from wastewater treatment processes in the PP industry. The typical properties of some of these byproducts (proximate and ultimate analysis, and heating value) are shown in Table 2.4.

Black liquor gasification (BLG) is considered as an alternative technology for energy and chemical recovery, that can be integrated in various biorefinery designs [150,168]. In the current PP industry, black liquor is mainly used as fuel in boilers to recover the inorganic chemicals and to produce process steam and electricity, with excess electricity being sold to the grid [153]. These recovery boilers are argued to be the bottleneck of pulp productivity [61]. Furthermore, some small pulp mills do not employ chemical recovery cycle, thus considering black liquor as a waste stream that must be disposed [164], which leads to additional costs. Despite its high ash and moisture content, which is a recognized drawback in several gasification technologies [16], black liquor has properties that make it a suitable feedstock for some gasification processes in specific scenarios [153], such as its liquid nature, which eases its feeding into pressurized gasifiers, and its high reactivity due to its high sodium and potassium content (Table 2.4) [141]. In fact, it is argued that the gasification of black liquor can attain faster reaction rates than many other biomass feedstocks [28,141].

Table 2.4 - Typical characteristics of different byproducts from the PP industry with potential to be used in gasification processes.

	Eucalyptus globulus RFB	*Eucalyptus globulus* bark [169]	Primary sludge	Biological sludge	Black liquor [170]
Proximate analysis [%wt, db]					
Volatile matter	80.5	77.9	na	na	55.6
Fixed carbon	16.6	17.1	na	na	8.8
Ash	1.1	5.0	61.5	26.5	35.6
Ultimate analysis [%wt, db]					
C	48.2	45.8	32.4	36.7	35.7
H	6.2	5.7	4.2	5.0	3.7
N	<0.2	0.8	0.5	2.2	na
S	0.03	na	na	0.4	4.4
O	42.7	42.3	1.4	29.0	35.8
Cl	0.05	na	0.02	0.19	0.30
Na	na	na	na	na	19.0
K	na	na	na	na	1.1
LHV [MJ/kg db]	18.4	17.2	15.3	14.7	12.3

na – not available.

Accordingly, BLG has been under development since 1960 and is currently designed as an alternative chemical recovery process for the replacement of conventional boilers [61]. This process allows the possibility of obtaining distinct bioproducts from black liquor and can potentially improve the energy efficiency of the plant [161]. For example, it has been argued that integrating BLG in a combined cycle can potentially result in higher thermal efficiency than the conventional black liquor combustion process integrated with a Rankine cycle [161]. BLG, including co-gasification processes of black liquor with wood wastes, sludges, pyrolysis liquids or fermentation residues, has also been under research for the production of DME, methanol, FT diesel, SNG, hydrogen and ammonia, constituting several possible pathways in various potential biorefinery designs (Table 2.3).

In addition, recovery boilers have been in operation in conventional PP industries for a long time and are becoming technically and economically obsolete due to low energy efficiency and competitive pressure for biofuels production, thus requiring replacement in the near future [153,168]. In these cases, implementing a BLG plant seems to have higher future profit potential than installing a new recovery boiler [153].

Despite these potential advantages, BLG technologies are still at a demonstration phase [161] and require further development. The most commercially advanced BLG technology is the Chemrec (Figure 2.8), which typically involves the gasification of black liquor in an entrained flow gasifier at high pressures [153,167,168]. In these systems, the black liquor is atomized with O_2, forming very small particles (~100 µm), and the gasification takes place at significantly higher temperatures (~1050 ºC) and pressures (~30 bar) [171,172] than in conventional wood gasifiers [4], leading to significantly distinct PG composition [31]. This design was developed by a company in Sweden [171] and was employed at the BioDME plant [173,174]. This plant operated under 3 MW_{th} capacity and outputted 4 tonne/day of DME, before being placed on hold [173,174]. The DME was tested as vehicle fuel and over 80000 km of truck operation were attained [103]. However, when governmental subsidies finished, the plant revenues could not support the process costs and operation was interrupted [103]. In 2013, the ownership of the plant was transferred to Luleå University of Technology to continue with more research-oriented activities [103].

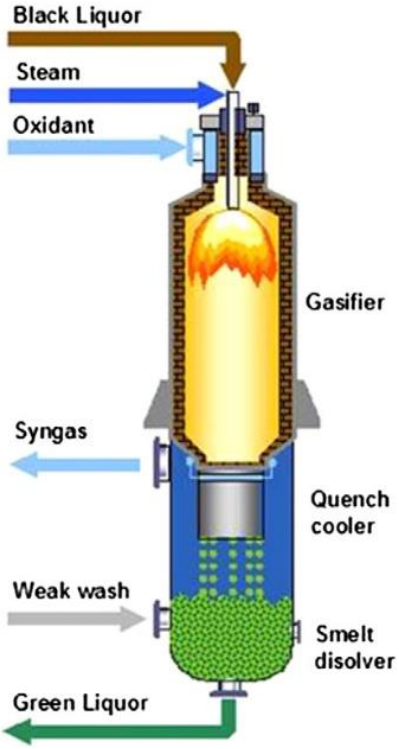

Figure 2.8 - Chemrec entrained-flow gasifier with quenching section for green liquor recovery [168].

Pettersson et al., [160] analyzed the integration of a BLG plant for the production of DME or electricity in pulp mills and PP mills, focusing on the economic performance and CO_2 emissions impact. The study showed that BLG coupled with DME production was the most profitable biorefinery concept amongst all scenarios considered, being profitable for both pulp mills and PP mills. From an economic point of view, the BLG plant for DME production in pulp mills should be complemented by a biomass gasification plant to produce DME and electricity. In PP mills, the BLG plant for DME production should be complemented by a bark boiler to cover steam deficits or to produce electricity. BLG to produce electricity also had good economic performance in pulp mills, however, this might change if policies and incentives to produce "green" electricity are reduced in the future. Furthermore, almost all biorefinery concepts had lower economic performance in PP mills than in pulp mills, which is mainly related to the highest steam demand considered for PP mills [160]. The authors also showed that carbon capture and storage (CCS) technology implementation turned several concepts profitable and led to the reduction of global CO_2 emissions. In fact, without CCS, several scenarios showed net increase of CO_2 emissions.

Naqvi et al., [164] analyzed the potential of SNG production by integrating BLG in small pulp mills without chemical recovery. The work results show that significant production of SNG is possible without external biomass import, as well as significant abatement potential of CO_2 emissions by combining SNG production with CCS. Nevertheless, the following main challenges were identified:

1. Improving the understanding of black liquor characteristics as feedstock for gasification processes.
2. Defining a process temperature that avoids inorganics agglomeration without significantly diminishing gas production and quality.
3. Improving the understanding of different gasification configurations to identify the most efficient routes to produce specific biofuels.

Mongkhonsiri et al., [175] analyzed the integration of biorefinery concepts into an existing pulp mill for the production of distinct bioproducts, including BLG and bagasse pith gasification for DME synthesis. The authors found the integration of succinic acid and DME synthesis into soda pulping process as the most profitable scenario, allowing a net CO_2 emissions abatement of up to 42 % and a maximum profit per year of 48 million dollars.

Regarding the wood wastes from the PP industry, the bark resulting from the wood debarking process is typically used in boilers for power generation, while the RFB resulting from harvest processes at the forest is usually left on site. The latter results in an unhealthy management of forest residues, which increases wildfire risks and the costs of fire suppression [176]. Accordingly, the gasification of these types of biomass has been intensively researched in the literature in the last years, and these resources are a proven feedstock to obtain PG from various types of gasification technologies [3,4]. Regarding the integration in the PP industry, wood wastes gasification has been considered for distinct gasification-based biorefinery concepts, such as the production of electricity, SNG, FT diesel, DME and alcohols (Table 2.3).

Isaksson et al., [155] evaluated the integration of wood wastes gasification in the Scandinavian PP industry, considering three distinct gasification-based biorefinery concepts, namely methanol production, FT diesel production and BIGCC for electricity production. The study concludes that the integration was feasible and presented good potential because the mill has continuous need of process heat. Isaksson et al., [154,158] also evaluated the heat integration, economic performance and GHG emissions of these concepts in the PP industry, while also considering the possibility of producing SNG. It was found that the end-product efficiency has a significant impact on the heat integration potential in the PP mill, i.e., higher production efficiency generates less excess heat per unit of end-product, and, consequently, less excess heat is available to meet the mill heating demands. The authors also show that the net annual profits were positive for all biofuels production scenarios, however, the results are highly sensitive to biofuel market prices and $CO_{2,eq}$ prices. In terms of GHG emissions, if a CCS process is not in place, the CHP production via BIGCC performs better or equal to the biofuel routes. It must be noted that the authors considered CCS as unavailable for BIGCC. The authors also show that CCS has an important role to play in terms of GHG emissions and process economics.

Wetterlund et al., [159] evaluated the integration of the gasification of wood wastes and purchased wood in the PP industry, namely biomass integrated gasification for DME production and BIGCC for electricity production. It was found that the integration of biomass gasification in the PP industry can be economically feasible. Nonetheless, it was also stated that the economic results obtained in this study were highly dependent on energy market parameters, particularly biofuel policy support, thus having a high degree of uncertainty. Furthermore, the potential for CO_2 emissions reduction was low.

Regarding the sludges resulting from wastewater treatment processes in the PP industry, this byproduct is usually disposed by incineration and landfill, and it is argued that it presents potential to be valorized as a biorefinery feedstock [177]. Specifically, research on the gasification of this feedstock is scarce, which may be related to the high ash content typically present in this type of biomass (Table 2.4), and consequent potential occurrence of fouling, corrosion and catalyst deactivation during thermochemical conversion processes. Accordingly, other biorefinery processes may be more suitable for the conversion of PP sludges (e.g., fermentation). Nonetheless, co-gasification with other byproducts (e.g., black liquor and wood wastes), may allow the valorization of this feedstock, while also providing technical and logistical benefits. In this respect, Akbari et al., [153] analyzed the economic feasibility of synthesizing ammonia from syngas resulting from the gasification of three different byproducts from PP mills, namely black liquor, and mixtures of black liquor with different types of sludge from wastewater treatment. The analyzed process consisted in the following steps:

1. N_2 removal from air in an ASU:
    a. To use the resulting N_2 in the ammonia synthesis plant.
    b. To use the resulting O_2 as gasifying agent in the BLG reactor.

2. Cleaning and refining the syngas obtained from the BLG reactor, so that it is mostly comprised of H_2. Specifically, acid gases such as COS, H_2S and CO_2, must be removed to avoid poisoning the ammonia synthesis catalyst.
3. H_2 and N_2 are used in the synthesis plant to produce ammonia.

The results of the study [153] showed that ammonia can be produced with competitive market prices in PP mills for all cases considered, thus indicating the suitability of PP sludges to be integrated in co-gasification processes.

In terms of the PG composition from the gasification of some of these byproducts, namely wood wastes and black liquor, the comparison cannot be made directly because wood wastes gasification and BLG are inherently different processes. For example, the conventional atmospheric bubbling fluidized beds used for direct (air) wood gasification, that typically operate at around 800 ºC and atmospheric pressure [4], are not suited for BLG due to the high ash content present in this feedstock, which would cause sintering and defluidization of the reactor bed. Thus, BLG is typically conducted in entrained-flow gasifiers (e.g., Chemrec) that operate at higher temperature and pressure than conventional wood gasifiers, as previously discussed. Furthermore, research regarding woody biomass gasification in entrained-flows is extremely scarce and mostly confined to laboratorial scales [178]. This may be related to the non-suitable properties of raw woody biomass for this reactor design, such as high particle size, and consequent required expensive and energy intensive feedstock pretreatment procedures (e.g., torrefaction and pulverization [26,31,179]).

Nonetheless, typical PG composition reported in the literature for wood direct (air) gasification in conventional fixed and fluidized beds and BLG is shown in Table 2.5. It can be observed that BLG typically leads to the production of a PG with higher CO_2 and H_2 concentration, similar CO concentration and lower CH_4 concentration, in comparison with wood direct (air) gasification. In terms of molar ratios in the PG, it can be seen that BLG produces a PG with very high H_2:CO molar ratio, while wood direct (air) gasification produces PG with higher CO:CO_2 and CH_4:H_2 molar ratios. It must be noted that high H_2:CO molar ratios are desired for advanced PG applications, such as the production of FT Diesel (0.6 mol/mol), DME (1 mol/mol) and methanol (2 mol/mol) [72,180–182]. Furthermore, as a consequence of the PG composition, the LHV of the PG from BLG is higher than the LHV of the PG typically reported in the literature regarding wood direct (air) gasification. In this respect, Dahlquist et al., [170] compared BLG and wood pellets gasification using numerical simulation and experimental research in similar pilot-scale reactive systems using similar operating conditions, and concluded that black liquor was a more suitable feedstock for the production of H_2, while the wood pellets were more suitable for the production of CH_4 and CO.

Thus, the results from these studies show that the integration of gasification to convert distinct byproducts from the PP industry into value-added products and energy vectors can be technically and economically feasible. Currently, various bioproducts are under research and potentially available, and this can serve as a major promoter for the integration of biorefinery concepts in this industry. This will allow the generation of revenue from new products (energy and materials) and will simultaneously promote the sustainability of the waste management and energy supply of this industry, thus acting in accordance with circular economy strategies. It also seems that positive net profits can be attained in distinct gasification scenarios for the production of different bioproducts. However, CCS systems are mandatory to attain significant CO_2 emissions abatement and this needs to be further quantified by life cycle assessment and cost-benefit analysis. Furthermore, for several distinct scenarios, the economic viability of the processes is highly sensitive to biofuel market and $CO_{2,eq}$ prices, which means that supporting policies are required to improve stakeholders confidence and to assure that gasification technologies are cost-competitive with conventional fossil fuel technologies. This highlights that a strong sense of concern will be required from governments to support biorefinery competition with conventional petrochemical refineries and to avoid the interruption of fully operating biorefineries and gasification plants.

Table 2.5 – Composition (CO_2, CH_4, CO and H_2), molar ratios ($Y_{CH4/H2}$, $Y_{CO/CO2}$ and $Y_{H2/CO}$) and LHV of the PG obtained by wood direct (air) gasification and BLG.

			%v, dry gas				mol/mol			MJ/Nm^3
Process	References	Ranges	CO_2	CH_4	CO	H_2	$Y_{CH4/H2}$	$Y_{CO/CO2}$	$Y_{H2/CO}$	LHV
Wood direct (air) gasification	[4,92,190,111,183–189]	Min	4.7	1.2	6.9	1.2	0.2	0.4	0.1	2.4
		Max	18.3	6.9	29.9	16.5	5.6	6.4	1.3	7.0
		Average	14.0	3.7	17.6	7.8	0.6	1.5	0.5	5.1
BLG	[170,172,191,192]	Min	29.8	0.5	9.8	33.0	0.0	0.3	1.1	5.9
		Max	48.5	4.8	31.0	42.0	0.1	1.0	4.1	8.3
		Average	35.7	1.5	25.2	36.2	0.0	0.7	1.6	7.5

2.1.5.3 PG AS GAS/OIL SUBSTITUTE IN THE PP INDUSTRY

Combustion for thermal energy is the most immediate application for the PG from biomass gasification and the first step for the development of PP gasification-based biorefineries. Although biomass gasification can be seen as a lower efficiency process for thermal energy generation when compared to biomass combustion, the PG has several practical advantages in comparison with solid biomass, such as handling, application and transport [4]. Furthermore, in certain industrial processes, solid biomass cannot be used as fuel; in these cases, the PG can have a particularly important role when integrated in industrial strategies to attain neutral carbon footprint. In the PP industry, PG can be obtained from several byproducts (e.g., black liquor, wood wastes, sludges) and serve as a middle platform compound to replace the natural gas in burners and kiln furnaces or to produce distinct bioproducts (e.g., Methanol, DME, etc.,). The application of PG can be interchangeable, according to necessity, i.e., when lower amounts of fuel gas are required for the PP manufacturing process, a higher export of bioproducts can be performed.

In this respect, before considering advanced applications for the PG, partial or complete replacement of natural gas in industrial burners must be considered. In fact, replacing part of the natural gas with PG may even improve the combustion behavior of the boilers and kiln furnaces burners [193]. From the combustion process point of view, PG is attractive for use in burners due to the following aspects:

1. Natural gas and PG mixtures present higher laminar burning velocity, allowing combustion at leaner conditions and, consequently, leading to lower NO_x emissions [193].
2. Natural gas and PG mixtures have slightly lower adiabatic flame temperature for any air/fuel ratio, which leads to lower thermal NO_x emissions and lower equipment abrasion [193–195].
3. Mixing PG with natural gas has been argued as a promising method to increase flame stability during lean combustion, consequently contributing to reduce the risk of blowout (reactants velocity exceeding the laminar burning velocity) [193].
4. The relatively high H_2 content present in the PG may reduce particulate and unburnt hydrocarbon emissions [195].

Despite these advantages, the typical natural gas burner design, and respective operating parameters, must be adjusted and optimized for the PG composition and properties [195]. Relevant combustion properties to characterize PG combustion include laminar flame speed, adiabatic flame temperature, Wobbe Index, flame stability, and extinction limits [194]. The most common parameter evaluated in PG combustion studies is the laminar flame speed, which has significant influence on the flame spatial distribution and the propensity for flame flashback, and reflects the general behavior of the combustion process of a fuel [195,196]. This parameter is important to characterize the reactivity, diffusivity and exothermicity of a combustion process, to develop predictive models and to estimate the performance and emissions of a combustion equipment [195]. Generally, higher temperature and laminar flame speed is observed with higher H_2 and CO concentration in the fuel mixture [194,196,197]. Flame instability and flashback problems have also been associated with higher H_2 concentration values [194]. According to the review performed by Chanphavong et al., [194], regarding the characterization and challenges of the development of PG combustors, similar laminar flame speeds were found for the combustion of PG in various numerical and experimental studies.

The low calorific value of the PG may also become a challenge to its utilization in combustion systems [194]. In consequence, larger volumetric flowrates of PG are necessary to replace other conventional gaseous fuels in distinct applications (e.g., 5 to 7 times the volumetric flowrate of natural gas, under similar conditions of pressure and temperature), which may require equipment modifications [194,198]. Furthermore, the low calorific value of the PG may lead to narrow

flammability limits, as well as lack of flame stability, during combustion [194]. Derived from these aspects, for a first step integration of gasification processes in the PP industry, partial replacement of natural gas by PG may be the most suitable pathway, instead of a complete replacement, as suggested in distinct works [193,194,199]. In fact, Hernandez et al., [193] analyzed laminar premixed flames derived from the combustion of natural gas and PG (25 and 50 %v) mixtures in a combustion pilot plant, composed of an atmospheric burner and a chemiluminescence camera, and suggested 37 %v as the optimum amount of PG to be mixed with natural gas.

Additionally, the PG is composed of various components and impurities (e.g., H_2S, NH_3, particulate matter and tars) and has significantly different composition for different gasification operating conditions [4], which leads to complex combustion reaction mechanisms, derived from different gaseous mixtures having different thermochemical properties [194], and operational problems. For example, the tar content present in the PG may condensate at the fuel inlet of the burner and block the fuel gas flow, causing the general malfunction of the equipment. Thus, previous gas cleaning may be required. Unpredicted changes in operating parameters of the gasifier (e.g., biomass feed ratio and ER) influences the PG composition, which may also lead to unpredicted impacts on the burner performance [196]. In fact, current demonstration and industrial biomass gasification plants present significantly different PG composition (Table 2.6). Thus, to use PG in gas burners, it may be required to adjust the operating parameters of the burner according to the PG characteristics.

Table 2.6 – Average composition (CO_2, CH_4, CO and H_2, and tar) and LHV of the PG from different industrial gasification plants.

Ref	Plant	Reactor type	Capacity [MW_{th}]	Gas composition [%v, dry gas]				LHV [MJ/Nm^3]	Tar [g/Nm^3]
				H_2	CO	CO_2	CH_4		
[66,174,198]	Harboøre	Updraft	4	19	29	9	4	7	nr
[200]	Oberwart	DFB	9	39	25	22	10	11	nr
[174,198,201]	Güssing	DFB	8	37	31	17	9	11	3
[174,201,202]	GoBiGas	DFB	32	40	24	20	9	10	1
[66,174]	Skive	BFB	26	16	20	12	4	6	nr
[66,203,204]	Värnamo	CFB	18	11	18	16	7	6	10
[205]	Lahti Energia Kymijärvi I	CFB	70	11	15	18	5	4	10
[206]	LTU Green Fuels DP1+DME pilot	Chemrec (entrained-flow)	3	38	26	33	1	8	nr
[207]	Stadtwerke Ulm/Neu	DFB	15	38	23	22	11	13	14
[208]	Metsä Fibre Oy, Äänekoski Mill	CFB	87	6	9	12	3	5	24

Nm^3 refers to a m^3 at standard conditions of temperature (0 ºC) and pressure (1.013×105 Pa); nr – not referred.

Therefore, experimental research regarding PG combustion is extremely relevant to serve as a tool to support biomass gasification related projects decisions, specifically those that seek to use PG in combustion systems or as a middle platform compound in a biorefinery design. Nonetheless, reported experimental research on PG combustion is mostly performed in small equipment [193,209–212]. There exists some pioneer large-scale gasification plants producing PG to replace oil/gas in lime kilns (e.g., Varkaus Stora Enso, OKI, Huangang, Metsä Fibre Oy at Joutseno Mill and Äänekoski Mill [173,174,208]), however, specific process information regarding these plants was not found. In this respect, Dattarajan [212] developed a combustor to burn raw PG in a 38 kW_e Stirling engine, with large fuel and air inlets to avoid blockage by particulate matter or tar adherence. The developed combustor showed good fuel-air mixing, stable flame over a range of operating conditions and complete fuel combustion, including combustion of the tar present in the PG. Sutar et al., [211] designed a partially aerated naturally aspirated burner for PG from a downdraft gasifier cookstove. The authors found that the burner increased the thermal efficiency of the cookstove. Ahrenfeldt [198] evaluated long term gas engine CHP operation with PG from three biomass gasification plants (Harboøre, Güssing and Viking), and concluded that PG is an excellent fuel for lean burn engines. The study shows that although the calorific value of PG is lower than that of natural gas, the first needs a lower stoichiometric air/fuel ratio, and, consequently, the energy density of the two fuel-air mixtures and power output can be similar. Regarding tar content, no problems were found during the combustion of the three distinct PGs.

Thus, despite some research being conducted for the development of PG burners [194], and the existing knowledge regarding PG combustion characteristics, new concepts and equipment must be developed to face the challenges of introducing PG as an effective and sustainable replacement for natural gas in industrial combustion systems. In this regard, efficient burners for PG must be conceived and developed to be applied in large industrial applications, e.g., to replace the existing furnaces and boilers at the PP industry. Furthermore, research must be performed, and knowledge produced, to support the techno-economic analysis of integrating PG in the PP industry as a middle platform compound that can be used to replace natural gas in the manufacturing process. These are considered as the main starting steps for the development of complete gasification-based biorefineries, which may also act as significant promoters for the implementation of other biorefinery concepts or advanced gasification processes for more sophisticated applications (e.g., DME production).

2.1.6 FUTURE PERSPECTIVES

Biorefineries are already a reality and are expected to fulfill a very important role in the combat against climate change, but it is necessary to determine its evolution in the following years. In theory, the potential of the concept is immense, however, current implementation of sustainable biorefineries is challenging due to debatable environmental benefits and significant technological and market limitations, in comparison with petrochemical refineries. On one hand, development and implementation of biorefineries will require increased biomass crop growing and harvest to use as feedstock. The land to grow biomass must not compete with land for food growth and the biomass must be sustainably provided to avoid negative environmental impacts. In this respect, using industry byproducts and wastes is extremely relevant to reduce biomass crops necessity and attain higher economic and environmental benefits; a shift towards this pathway is already ongoing and is expected to be continued in the future. This contributes to the sustainability of energy supply and waste management, and is in accordance with circular economy principles. On the other hand, biorefinery concepts and key technologies must be improved and proven at a competitive market level. These aspects will help stakeholders perceive the biorefineries economic potential and vital role in a future transition to a sustainable bioeconomy, leading them to cooperate and work together.

To answer the concerns of the PP industry regarding the integration of biomass gasification processes, industrial gas burners adjusted for specific PG compositions must be developed and integrated analyses that consider the economic, environmental and technical aspects of replacing natural gas by PG in the burners of the boilers and kiln furnaces of the PP industry, must be performed. This will allow the determination of the advantages and disadvantages of using PG for thermal energy generation in the industry, which is the first step for its transformation into complete gasification-based biorefineries. These are relevant drivers to ease the integration of gasification processes in the PP industry.

2.1.7 CONCLUSIONS

The PP industry is highly suitable to integrate biorefinery concepts and this can be considered as a potential pathway to attain economic and environmental sustainability, allowing the industry to generate revenues from several new bioproducts (fuels, chemicals and materials) and overcome a continuously declining paper market. The use of PG as a middle platform compound that can provide heat and electricity for the PP manufacturing process while allowing the export of bioproducts, according to necessity, is a key factor for the integration of biorefinery concepts in the PP industry. In this context, BLG and wood wastes gasification for the production of electricity, hydrogen, SNG, FT diesel, DME, ammonia and alcohols have been proposed and researched in the literature. Drivers for the integration of gasification processes in the PP industry include revenues from new products, reduced fossil fuel dependence, GHG emission reductions and higher energy efficiency. However, gasification technologies are still unreliable and must overcome several technological and market barriers associated with scaling-up, tar reduction and PG cleaning/refining, in order to be able to play their expected role in the transition to a future bioeconomy; this seldom is considered by gasification-based biorefineries proponents. In this respect, the development and integration of gas cleaning processes in the gasifier to use and preserve the thermal energy of the PG seems to be mandatory to avoid excessive plant investment and operation costs.

Replacement of natural gas by PG in boilers and kiln furnaces is the first and most immediate step for the integration of biomass gasification processes in the PP industry, and should be considered and evaluated before the implementation of more complex and expensive solutions. However, research regarding gasification integration in this industry is often focused on advanced applications (e.g., FT diesel production) and rarely considers this first step or the existing technological and market barriers associated with these sophisticated gasification processes. In fact, research on the development of PG combustors is mostly confined to laboratorial or pilot scales and information from existing pioneer gasification processes in the PP industry is extremely scarce. It also seems that CCS systems have a main role in terms of the economic and environmental impacts of the implemented gasification solutions, being that carbon sequestration must be performed to attain significant CO_2 emissions abatement, despite biomass gasification being typically profiled as CO_2 neutral; this needs to be further quantified by life cycle assessment and cost-benefit analysis. These are critical aspects that significantly hinder the integration of gasification processes in the PP industry.

The economic viability of various biorefinery projects is highly sensitive to biofuels and $CO_{2,eq}$ prices variation, which means that supporting policies are required to reduce the investment risks of the integration of gasification processes in the PP industry and to allow biorefineries to compete with conventional petrochemical refineries. Accordingly, a stronger commitment from governments is required to avoid the interruption of operation of fully functioning gasification-based biorefineries, as recently has occurred for various large-scale gasification plants in Europe (e.g., Oberwart, Güssing, GoBiGas). Thus, technology roadmaps, market-driven research, political goals and policy frameworks, are fundamental to reduce the risks and uncertainties associated with biorefineries implementation and give stakeholders confidence to invest in this industry. Particularly, the first years of biorefinery operation, and development towards market maturity and production stability, should be supported by suitable economic and financial tools.

2.2 ARTICLE II - INDUSTRIAL GASIFICATION SYSTEMS (>3 MW_{TH}) FOR BIOENERGY IN EUROPE: CURRENT STATUS AND FUTURE PERSPECTIVES

2.2.1 ABSTRACT

Gasification is a key technology for the use of biomass as a renewable energy source. This work provides a detailed survey of the current state, progress and utilization of industrial-scale gasification systems (>3 MW_{th}) in Europe, and identifies current challenges and future trends.

Europe has been active in the implementation and development of large-scale gasification processes, with various trends occurring that reflect the need of new knowledge and cost-competitive technologies. Large-scale gasification processes are becoming increasingly considered for biofuels and biochemicals synthesis and the economy of generating renewable bioproducts from biomass is becoming more attractive than power, because it creates a new value chain. However, large-scale gasification plants still entail significant issues (e.g., biomass collection and processing, PG cleaning costs) that decrease the projects economic viability and may cause the interruption of operation of existing plants. Identified measures currently occurring in Europe that must be further pressed to assure the commercial breakthrough of large-scale biomass gasification processes include: replacement of high quality wood by low-cost waste feedstocks, development of cost-efficient gas upgrading processes, analysis and integration of available information from demonstration and industrial-scale plants, and improvement of governmental policies. This will allow biomass gasification to present a stronger answer to climate-neutrality concerns.

Keywords: Industrial; Gasification; Bioenergy; Europe; Biomass.

2.2.2 INTRODUCTION

The gasification process history dates over 300 years (Figure 2.9). The earliest investigation recorded regarding gasification was performed by Thomas Shirley in 1659, which consisted in experiments for methane production [50]. The gasification of coal was then demonstrated in 1733, but the first real use of this gas, denominated by town gas at the time, was only performed in 1798 by William Murdoch for lighting purposes [50]. The first gasification technologies were based on a two-step gasification process, consisting of thermal cracking of the coal and consequent steam blowing of the remaining char in a fixed bed reactor [213]. Afterwards, Siemens developed the first continuous gasification fixed bed reactor, where the combustion and gasification sections were physically separated [213,214]. During this time, town gas obtained through these gasification technologies was mainly used for lighting and heating purposes [67,215]; In fact, various towns and cities in Britain used town gas (also called coal-gas) for street lighting [50]. Using this gas for street lighting was significantly cheaper than using oil lamps, which intensively promoted the development of gasification technologies [50] and led to the constitution of the relevant town gas industry [216]. All gasifiers in operation during this time were air-blown fixed bed reactors [213]. Afterwards, the invention of the electric bulb (after 1879) led to a significant decline of the town gas industry and gasification was confined to heating and cooking applications [50]. During this period, the concept of continuous gasification using cryogenic separation of air was demonstrated by Carl Linde [217] and three major commercial gasification technologies were developed, namely the Winkler air-blown fluidized bed gasifier in 1926, the Lurgis pressurized oxygen-blow gasifier in 1931 and the Koppers-Totzek entrained flow gasifier in 1938 [67,213,214]. Later, the widespread of natural gas further confined gasification technologies to niche applications [50,216].

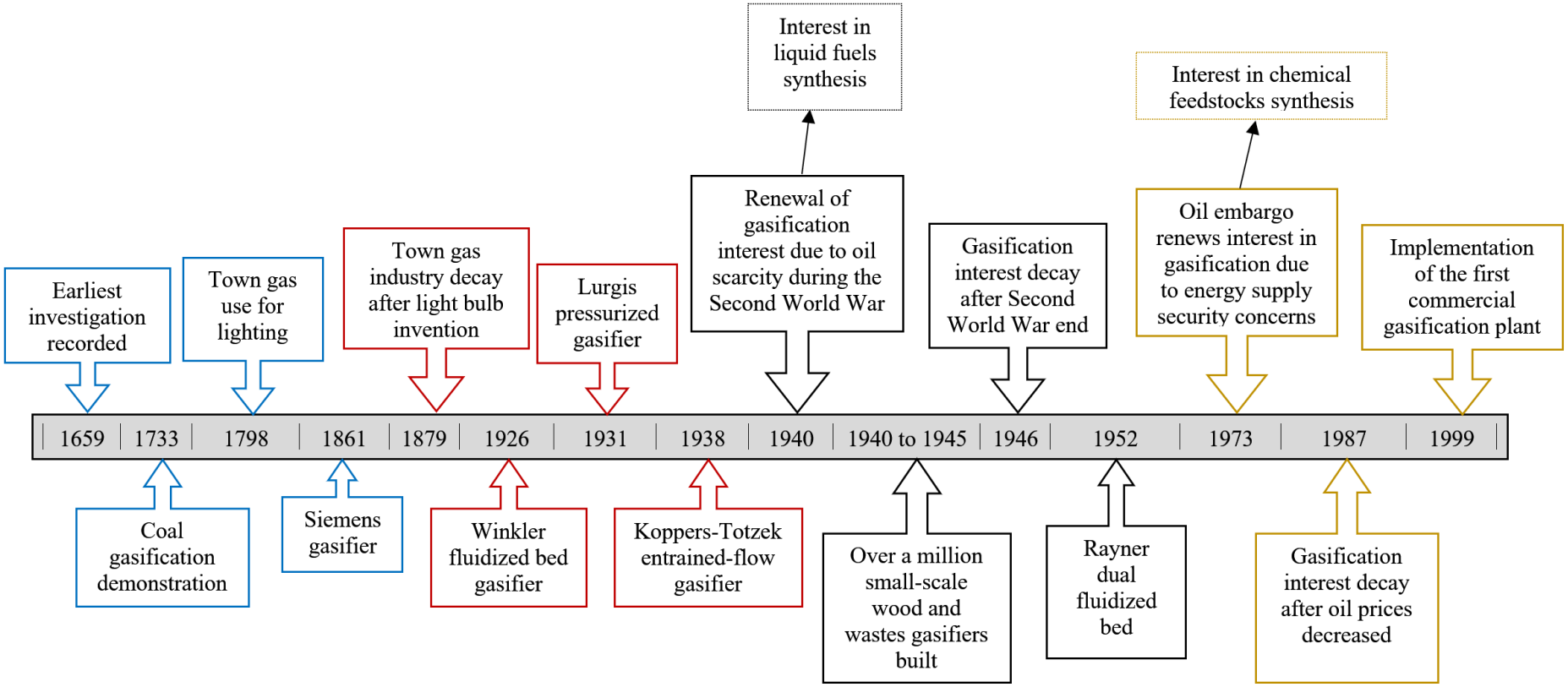

Figure 2.9 – Gasification history and milestones.

The interest in gasification was renewed during the Second World War due to the Allied bombing of Nazi oil refineries and oil supply routes and consequent oil scarcity; This forced Germany to synthesize oil from syngas ($CO + H_2$) by using the Fischer-Tropsch process [50]. For this purpose, over a million small-scale fixed bed reactors were built for the gasification of wood and wastes and the concept of producing biofuels from gasification processes was developed [50,213]. After the war, interest in gasification technologies declined again due to the availability of cheap crude oil [213]. Nevertheless, in 1952, Rayner developed an indirectly heated gasifier with a separate circulating fluidized bed (CFB) for combustion and a bubbling fluidized bed (BFB) for gasification, constituting the first dual fluidized bed (DFB) design [101]. After the oil embargo in 1973, Western countries were forced to develop alternative technologies to reduce their dependence on imported oil from the Middle East, and interest in gasification technologies resurged [50]; In this phase, gasification found major commercial interest as a process for chemical feedstock production, which was provided by petrochemical refineries [50]. This led to a development phase that went from 1973 to 1987, mainly led by developments in the USA [218]. After the oil crisis, a subsequent drop in oil price damped this gasification development and confined the technologies back to niche applications. Thus, the first commercial gasification plant was only implemented in 1999 in the United States [217].

Nowadays, the interest in biomass gasification technologies mainly results from concerns associated to global warming and fossil fuels depletion, and consequent search for an affordable, renewable and clean energy source [67,90]. In comparison with other renewable energy sources, biomass has the major advantages of being a non-intermittent source of energy [4,219] and its gasification allowing the production of a fuel gas that can fit in the current carbon-based energy infrastructure through diverse thermal, power and synthesis applications [26,123,220], for example production of hydrogen [221,222], FT-liquids [216], DME [75] and methanol [74], and application in IGCC technologies [223,224] with CO_2 capture [216], SOFCs [225,226] or ICEs [227].

Despite these advantageous aspects, gasification technologies commercial breakthrough has been hindered by various technical and economic aspects that turned the process unprofitable in diverse scenarios [58–60] and, consequently, gasification implementation has not been as prominent as expected in the last decades [90,103,218]. Currently, CHP from gasification is mainly applied at small-scales due to biomass feedstock collection representing a barrier for the establishment of large-scale gasification plants, and small-scale decentralized gasification systems showing advantages for the effective use of locally produced biomass [90,228,229]. In the future, it is expected that CHP remains dominant at a small-scale while biofuels and biochemicals synthesis become more relevant for large-scale gasification plants [103]. In fact, large-scale gasification processes are argued to be more suitable for efficient biofuels and biochemicals production due to its efficiency to investment ratio [90] and scaling-down issues of advanced catalytic synthesis processes. Accordingly, it is expected that large-scale gasification technologies represent a main role in various biorefinery designs, that are currently under development, for the production of high quantities of high-value biofuels and biochemicals with viable process economics [26,150,153,158,159]. For this purpose, development and implementation of reliable large-scale gasification systems are required.

In this work, the current state, progress and utilization of industrial-scale (>3 MW_{th}) gasification plants in Europe is analyzed. For this purpose, conventional gasification technologies were determined and evaluated, and large-scale gasification plants implemented in Europe were summarized according to various parameters, including state of operation, location, technology type, installed power and investment costs. Thus, the degree of large-scale gasification plants implementation in various European countries was determined. Based on this, current challenges, potential breakthroughs and future trends for large-scale gasification processes implementation in Europe are discussed.

2.2.3 CONVENTIONAL GASIFICATION TECHNOLOGIES

Gasification is the thermochemical conversion of a carbonaceous feedstock into a mixture of combustible gases with various potential applications [230]. This complex process is composed by various thermochemical phenomena without clear boundaries, which often overlap, and whose principal chemical reactions are those involving solid carbon, H_2O, CO, CO_2, H_2, H_2O, light hydrocarbons and tar compounds (e.g., naphthalene, indene, BTX) [50,65]. In a typical biomass gasification process, the biomass is firstly dried and then undergoes through thermal decomposition. Afterwards, the resulting products react among themselves and with the gasification agent, forming the final gaseous product [50]. This product is commonly denominated by PG and is a mixture of various components, such as CO, CO_2, H_2, light hydrocarbons (e.g., C_2H_2, C_2H_4, C_2H_6 and C_3H_8), unconverted tars and particles. The raw PG is only suited to be used as fuel in thermochemical applications but can be cleaned and refined to be suitable for the catalytic synthesis of liquid fuels and chemicals or other appliances [26,75,225].The current commercially available gasification technologies are classified according to various parameters, including the heat supply method, gasifying agent used and reactor design [66]; The choice of these parameters has a major influence on the quality of PG and the efficiency of the process.

The gasification process can be autothermal or allothermal depending on the necessity of an external heat source to support the endothermic gasification reactions. In the autothermal regime, also know as direct process, the gasifying agent contains O_2 to promote a controlled partial oxidation of the biomass inside the gasifier for heat generation. In the allothermal regime, also known as indirect process, the gasifying agent does not contain O_2, which means that heat must be provided by an external source [50]. Direct gasification is technically easier to perform than indirect gasification and has lower investment costs [86], thus being more suitable for lower-scale implementation [90]; However, when using air as gasification agent, the resulting PG will be diluted in N_2 and consequently have lower calorific value [4,227]. The heat supply method has significant impact on the process and will influence the desired reactor design, further impacting the obtainable products.

The conventional biomass gasification technologies can be divided in three main types of reactor designs, namely fixed bed, fluidized bed and entrained flow, which are currently the most common options for biomass gasification implementation at demonstration and large-scale in Europe (Section 2.3). All these designs present advantages and disadvantages and the selection is dependent on the scale of operation, feedstock characteristics and desired downstream PG application (Figure 2.10).

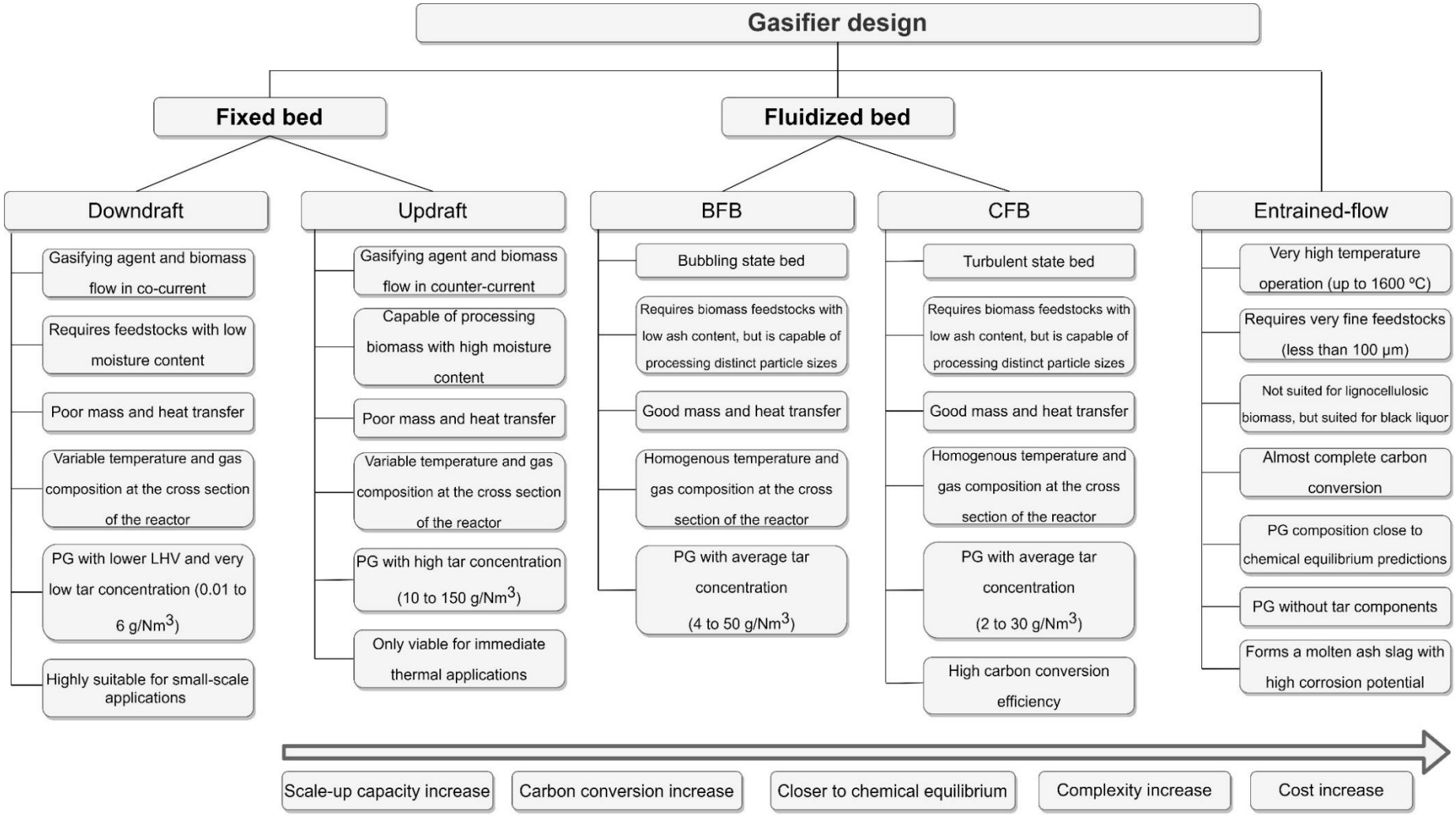

Figure 2.10 – General characteristics of conventional gasification technologies.

2.2.3.1 FIXED BED

The fixed bed gasifiers are the pioneer reactor design for gasification (Figure 2.11) [90]. Fixed bed gasifiers are mainly suited for small-scale operation, up to some MW_{th}, and are mainly divided in updraft and downdraft configurations [50,66]. These reactors are characterized by having the gasification process taking place in a fixed bed, in which different reactions occur in different zones [50,66]. Both updraft and downdraft types of reactors allow the attainment of high temperatures and efficiency but present poor mass and heat transfer characteristics, making it difficult to achieve uniform temperature and gas composition at the cross sections of the reactor [113]. Updraft and downdraft configuration differ in terms of the product gas flow direction and the zone where the gasification agent is introduced, thus influencing the contact between the gasifying agent and the biomass fed and consequently changing the order and location of the reaction zones (Figure 2.11), and the quality of the PG [50,66,70].

In the updraft design (Figure 2.11, (a)), the gasifier agent is introduced at the bottom of the reactor, and the PG is released at the top, where the biomass is fed. Therefore, the biomass and gasifying agent move in counter-current. This leads to two main factors that highly influence the impact of this design on the process efficiency and PG quality. On one hand, the PG will be in contact with the biomass in the drying zone, leading to its sensible heat being used to dry the biomass. On the other hand, the PG immediately flows to the cooler part of the reactor after formation, leading to low tar cracking into gases and low pyrolysis gases oxidation [90]. Accordingly, this design is capable of using biomass feedstocks with high moisture content (up to 60 %wt) [90], but is becoming obsolete and considered only viable in immediate thermal applications due to the high tar concentration present in the PG (10-150 g/Nm^3) [78,91]. In fact, updraft gasifiers are the simplest and were the first type of gasifier developed [231].

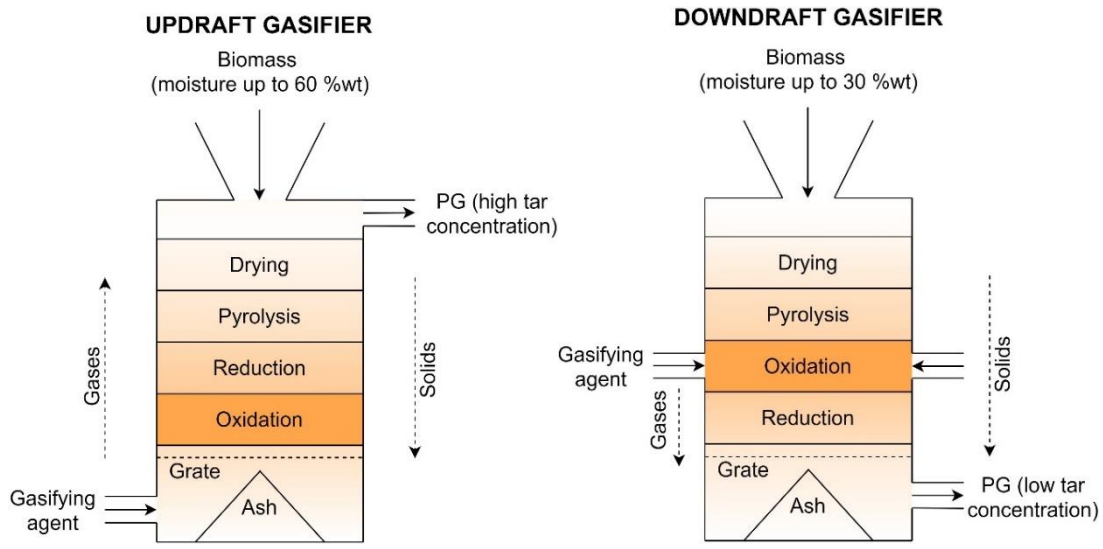

Figure 2.11 – Schematic representation of an updraft (left) and downdraft (right) gasifier.

In the downdraft design (Figure 2.11 (b)), the biomass is also fed on the top of the gasifier, however, the gasification agent is introduced at the sides or at the top, and the PG exits at the bottom. Thus, the biomass and the gasifying agent move in co-current flow [90], leading the pyrolysis gases to flow through a high temperature oxidation zone, which causes the cracking and oxidation of tars [50,66]. Consequently, the tar concentration in the PG will be low (0.01-6 g/Nm^3) [50,66]. On the other hand, this also causes the oxidation of the pyrolysis gases, consequently decreasing the heating value of the PG. Furthermore, in this design, the heat transfer between the hot and cold zones is poor, restricting the usage of biomass feedstocks with moisture content over 30 %wt, and the residence time of biomass is low, due to the drag force of the gasifying agent being aligned with gravity, which promotes lower carbon conversion efficiency. The low tar

content present in the PG simplifies the gasification process and turns this gasifier configuration highly suitable for small-scale CHP applications (10 to 1 MW_{th}) [50,90,232], however, its capacity is limited to a feed rate of approximately 500 kg/h due to physical limitations of the reactor diameter in relation to the particle size [213].

2.2.3.2 FLUIDIZED BED

Fluidized bed gasifiers (Figure 2.12) are divided in BFBs and CFBs and can have installed power over 100 MW_{th} [66]. The principle of gas-solid fluidization is the basis of these reactors, in which the fuel together with the inert bed material behaves like a fluid when interacting with the upward gasifying agent flow [70]. By adopting the fluidization mechanism, the fluidized beds offer enhanced mass and heat transfer characteristics and more homogenous temperature distribution at the cross section of the gasifier, leading to higher gas yield and carbon conversion efficiency, in comparison with fixed bed gasifiers. Thus, these designs are more suited for large-scale applications [90,113,218]. The fresh reactor bed is constituted by nonfuel granular solids that act as heat carriers and the gasifying agent is inserted at the bottom of the reactor at a velocity that induces the desired level of fluidization [50]. Silica sand is the most common option for bed material due to its abundancy and price, however, using other solids, particularly those that exhibit some catalytic activity, such as olivine, limestone and dolomite, can improve tar cracking and consequently increase the quality of the PG [66,70,100]. Tar concentration in fluidized beds typically revolves between 1 to 30 g/Nm^3, thus being between the values reported for downdraft and updraft gasifiers (Section 2.1.3.3) [50,66,70,78]. These designs are also suited to be pressurized, which can be an interesting strategy when the downstream application for the PG requires a pressurized input, and may lead to higher throughput capacity [70].

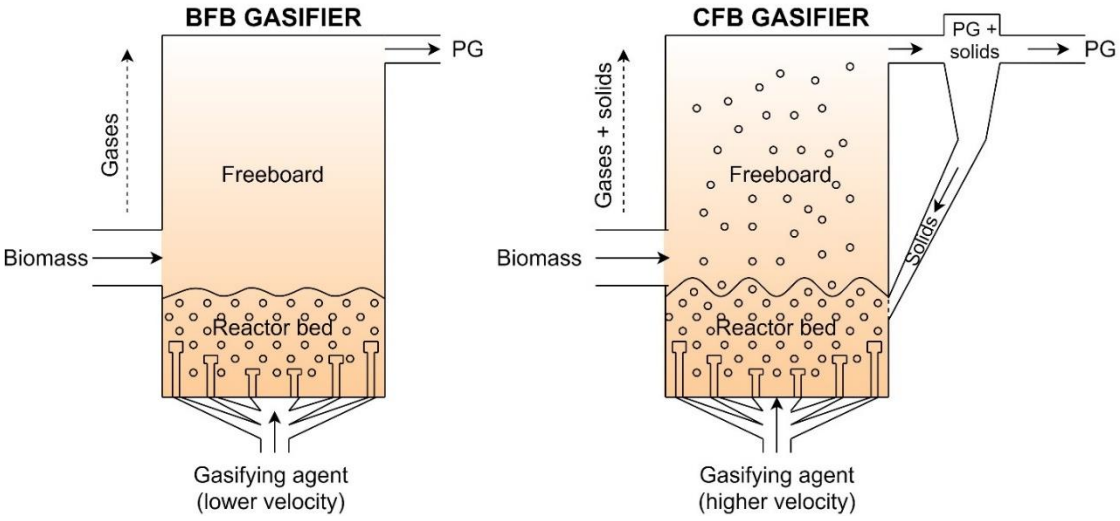

Figure 2.12 – Schematic representation of a BFB and CFB gasifier.

The BFBs operates with a fluidization velocity three to five times lower than CFBs, thus working in a bubbling regime in contrast with a turbulent state [90]. Furthermore, in BFBs there is always incomplete carbon conversion due to small char particles entrainment and elutriation [68]. When the particle terminal velocity becomes lower or equal to the superficial gas velocity in the reactor (resulting from devolatilization and gasification), the char is entrained and elutriated with the exhaust gas, contributing to lower carbon conversion efficiency [68]. The CFB design minimizes this issue by recirculating elutriated char particles back to the reactor bed. For this purpose, CFBs designs integrate high temperature cyclones and particle separators to capture and recycle solids

back into the gasifier [92]. This increases the solid residence time and carbon conversion efficiency, and may also promote lower tar concentration in the PG, in comparison with BFB gasifiers [78,90,92]. However, this is achieved at the expense of a much more complex operation and higher investment and operation costs [90].

The hydrodynamics characteristics of these fluidized bed reactors, such as the heat and mass transfer characteristics and the possibility for solid circulation between different reaction zones of even between different gasifiers [101], turn this type of reactors suitable for specific regimes of operation. For example, the dual fluidized bed (DFB) configuration (Figure 2.13), which typically consists in the combination of a BFB and a CFB, is the most common technology to perform indirect gasification [101,233]. The principle beneath this design is the physical separation of the endothermic gasification reactions and exothermic combustion reactions [233].

In a typical DFB design, one BFB reactor is operated in indirect gasification regime and one CFB reactor under combustion regime to supply the necessary thermal energy for the endothermic gasification reactions [66]. Thus, biomass is fed into the BFB gasifier along with the gasifying agent (e.g., steam), where endothermic gasification reactions occur [66,98]. The resulting residual char is transported with the bed material to the CFB combustor where it is burnt with air [66]. After gas-solid separation in the high temperature cyclone, the hot bed material is recirculated from the CFB combustor to the BFB gasifier, transporting the required thermal energy for the endothermic gasification reactions [66,98]. The contact between the gas streams of each reactor is avoided by using loop seals fluidized with inert gases [101]. The BFB gasifier employs a higher thermal load than the CFB combustor, for example a thermal load ratio of 3:2 [202]; the CFB combustor can stand alone operation dedicated to CHP production and chars from the BFB gasifier can sustain the process as main fuel, with recirculated byproducts from the downstream processes serving as supplementary fuels [202].

Under this typical configuration, it may be required to combust part of the PG or natural gas to sustain the process under certain conditions (e.g., start-up), therefore adding external biomass feeding to the CFB combustor may simplify the process and reduce operational costs [202]. The PG quality can also be improved by using a bed material in the BFB gasifier with catalytic properties [234], since the bed can easily be regenerated during its circulation between the gasification and combustion reactor [66]. To avoid the complexity of circulating bed material, heat pipes connecting the two reactors can be integrated for heat transportation [101]. In this case, the heat pipes are closed and contain a liquid acting as heat carrier that evaporates in the combustion reactor and condenses in the gasifier reactor (e.g., Biomass Heatpipe Reformer) [101].

In the DFB configuration, the gasifying agent does not contain N_2 and, consequently, the PG will present higher combustible gases concentration and higher heating value, in comparison with PG obtained from direct (air) gasification in a single BFB or single CFB. However, the addition of a second fluidized bed significantly increases the costs and complexity of the system [94]. In theory, the DFB design generates a PG with a composition comparable to that obtained in direct gasification with steam/oxygen used as gasifying agent [101], thus it also represents a trade-off between the additional fluidized bed and the employment of an air separation unit. Currently, two DFB designs have been implemented at demonstration and industrial scales, namely the Güssing DFB gasification process, which is analogous to the DFB design described above, and the SilvaGas gasification process, initially developed by Battelle, which comprises two CFBs [66,101]. Further development of the indirect gasification process aims to combine the gasification and combustion zones in one reactor, by having the gasification zone surrounded by the combustion zone [66], and the heat circulated internally [101]. Examples of these designs include the ECNs MILENA gasifier [105], among others [106–108], which are still under development [101].

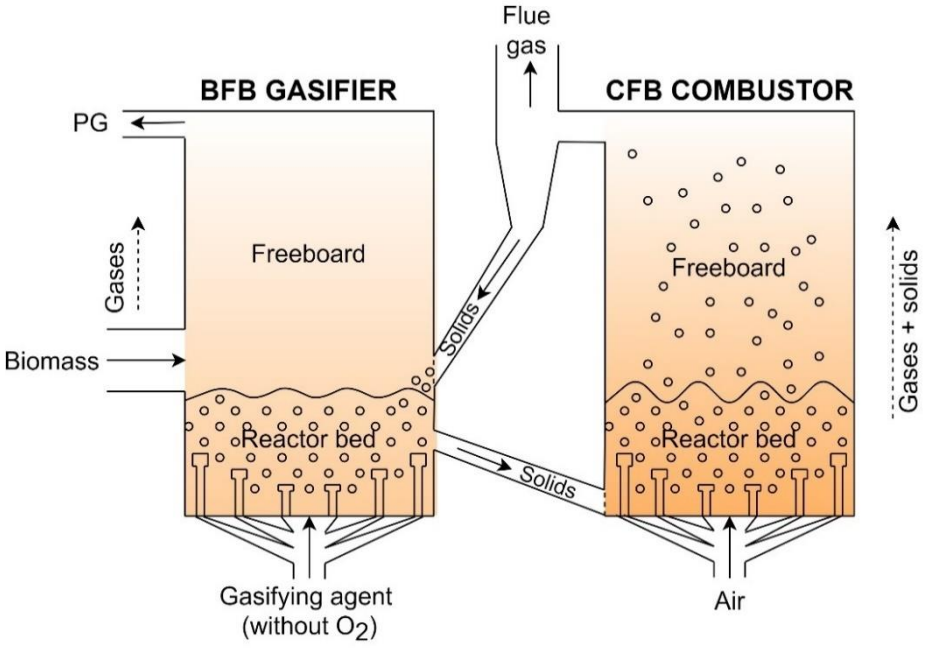

Figure 2.13 – Schematic representation of a DFB gasifier.

2.2.3.3 ENTRAINED-FLOW

Entrained-flow reactors are characterized by operating in direct gasification regime with O_2 as oxidant, employing very high temperatures (up to 1600 ºC), requiring the preprocessing of the feedstocks in very fine particles (less than 100 μm), having high complexity and investment costs, and, consequently, being more suited for extremely large applications (>100 MW_{th}) [66,90,93,94]. The high temperature employed promotes the thermal conversion of tar, light hydrocarbons (including CH_4) and solid carbon, with carbon conversion efficiency attaining values close to 100 % [50]. Thus, in comparison with other gasifier designs, the composition of the obtained PG is significantly closer to chemical equilibrium [70]. In conventional entrained-flow reactors (Figure 2.14) the feedstock is inserted by a high-velocity gasifying agent jet that forms a recirculation zone near the entry point [50]. Thus, as it is observed in downdraft gasifiers, this type of reactor operates in co-current flow. Fuel particles are rapidly heated by radiative heat from the hot walls of the reactor and downstream hot gases, and start burning with the available O_2. Therefore, the majority of the fuel is consumed near the entrance zone through devolatilization and partial oxidation [50]. Afterwards, downstream of the devolatilization/combustion zone, O_2 is no longer available and the residual char undergoes gasification reactions in a reduction environment [50]. This type of reactor has been highly applied for large-scale gasification of coal, petroleum coke and refinery residues, however, biomass has significant distinct properties than these materials, including ash behavior, feeding and pressurizing properties [50,235]. In fact, the suitability of this kind of reactor for lignocellulosic biomass gasification is debatable [50] due to a number of factors:

1. Woody biomass has non-suitable properties for this process and consequently require expensive and energy intensive feedstock pre-treatments (e.g., torrefaction and grinding [26,31,179]). In fact, grinding fibrous biomass to a particle size below 100 μm needs significant energy consumption and is highly difficult [50].
2. The high temperature employed in this reactor causes the melting of biomass ash, whose melting point is significantly lower than coal ash due to its alkali content [50]. This biomass molten ash is highly aggressive and can cause significant fouling in the reactor, consequently decreasing the gasifier life span [50].

Thus, regarding biomass feedstocks, this type of reactor is being considered mainly for the gasification of black liquor in the PP industry. The specific developed reactor design is denominated by Chemreq and was developed by a company in Sweden [171]. In this entrained-flow reactor, the black liquor is atomized with O_2, forming very small particles (~100 µm), and the gasification takes place at significantly higher temperatures (~1050 ºC) and pressures (~30 bar) [171,172] than in conventional biomass gasifiers [4].

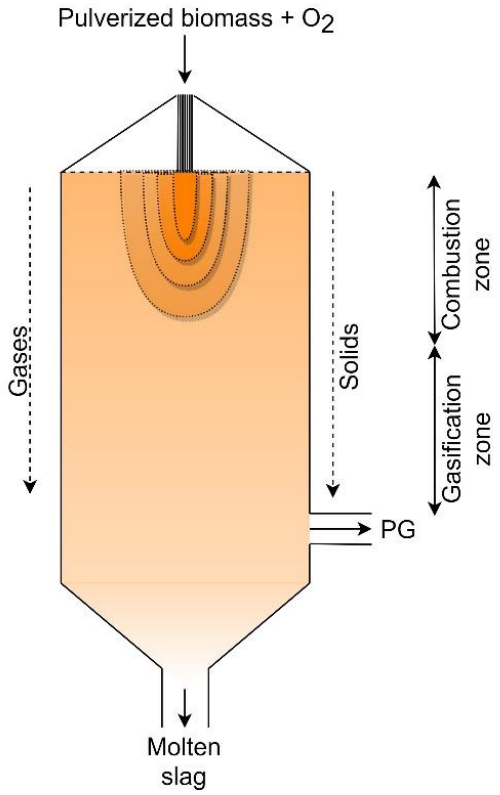

Figure 2.14 – Schematic representation of an entrained-flow gasifier.

2.2.4 STATUS IN EUROPE

In this Section, it is analyzed and evaluated the status of gasification technologies in Europe, focusing on Sweden, Finland, Germany, The Netherlands, Austria, Denmark and Italy. In Table 2.7, it is shown current industrial-scale (>3 MW_{th}) gasification plants in Europe, according to operation status, location, technology, inputs and outputs. In Table 2.8, the typical composition of the PG obtained in some of these plants is shown. In Figure 2.15, it can be observed the spatial distribution of these projects in Europe.

Table 2.7 – Industrial-scale (>3 MW_{th}) gasification plants in Europe.

Reference	Plant	Status	Location	Reactor type	Capacity	Input	Final output
[103,173,174]	Oberwart	On hold	Austria	DFB	9 MW_{th} input 3 MW_e power output 4 MW_{th} heat output	Wood chips	CHP
[103]	Güssing	On hold	Austria	DFB	8 MW_{th} input 3 MW_e power output	Wood chips	CHP
[66,103,174,198]	Harboøre	Operational	Denmark	Updraft	4 MW_{th} heat input 2 MW_{th} heat output 1 MW_e power output	Wood chips	CHP
[103,173,174]	Pyroneer	Canceled	Denmark	CFB	6 MW_{th} heat output	Wheat straw	Heat
[173]	Sindal District Heating Company	Operational	Denmark	Updraft	9 MW_{th} input 5 MW_{th} heat output 1 MW_e power output	Wood wastes	CHP
[236]	Skive	Operational	Denmark	BFB	20 MW_{th} input 6 MW_e power output 12 MW_{th} heat output	Wood pellets	CHP
[174]	Kiteen Lämpö Oy	Operational	Finland	Updraft	6 MW_{th} heat output	Wood chips	Heat
[173]	Jalasjaerven Lämpö Oy	Operational	Finland	Updraft	6 MW_{th} heat output	Wood chips, pellets and peat	Heat
[174]	Ilomantsin district heating	Operational	Finland	Updraft	6 MW_{th} heat output	Wood chips and peat	Heat
[174,208]	Varkaus Stora Enso	Operational	Finland	CFB	12 MW_{th} input	Bark and wood wastes	Fuel gas to lime kiln
[174]	Kauhajoen Lämpöhuolto Oy	Operational	Finland	Updraft	13 MW_{th} heat output	Wood chips and peat	Heat
[174]	Metsä Fibre Oy, Joutseno Mill	Operational	Finland	CFB	48 MW_{th} input	Bark and wood wastes	Fuel gas to lime kiln
[173,174,208,237]	Varkaus Corenso	Operational	Finland	BFB	50 MW_{th} h input	Plastic wastes	Syngas
[173,238]	Lahti Energia Kymijärvi I	Operational	Finland	CFB	70 MW_{th} input	Wood wastes	CHP

Table 2.7 – (cont.).

Reference	Project name/owner	Status	Location	Reactor type	Capacity	Input	Final output
[173]	Metsä Fibre Oy, Äänekoski Mill	Operational	Finland	CFB	87 MW_{th} output	Bark	Fuel gas to lime kiln
[173,174]	Lahti Valmet Kymijärvi II	Operational	Finland	CFB	160 MW_{th} input 50 MW_e power output 90 MW_{th} heat output	SRF	CHP
[174,239]	Bioliq	Operational	Germany	Pressurized entrained flow	5 MW_{th} input 608 t/y gasoline-type fuels output	Straw	DME and gasoline
[173]	RegaWatt Abensberg	Operational	Germany	Updraft	4 MW_{th} heat output 2 MW_e power output	Woody biomass	CHP
[173,201]	Blue Tower	On hold	Germany	Specific design	13 MW_{th} input	Wood wastes	H_2
[240]	Stadtwerke Ulm/Neu	Operational	Germany	DFB	15 MW_{th} input 5 MW_e power output	Wood chips	CHP
[173]	Muensterland Energy Gmbh	Operational	Germany	Downdraft	8.6 MW_{th} heat output 6 MW_e power output	Wood pellets and chips	CHP
[173,241]	Waermeversorgung Grossenhain	Operational	Germany	BFB	21 MW_{th} heat output 6 MW_e power output	Woody biomass	CHP
[240]	Choren Freiberg BtL production β-plant	On hold	Germany	Entrained flow	45 MW_{th} input 2 m^3/hour FT diesel	Wood chips	FT diesel
[173,174, 242]	Duchi Fratelli Societa Agricola/Agroenergia	Operational	Italy	Downdraft	7 MW_{th} input 1 MW_e power output 3 MW_{th} heat output	Wood chips	CHP
[173,174, 243]	Rossano Calabro	Operational	Italy	Specific design	20 MW_{th} input 4 MW_e power output	Wood and agricultural wastes	Electricity
[173,174]	LTU Green Fuels DP1+DME pilot	On hold	Sweden	Chemrec	3 MW_{th} input 2 MW syngas output 4 t/day DME 4 t/day methanol	Black liquor and pyrolysis oil	Syngas, DME and methanol

Table 2.7 – (cont.).

Reference	Plant	Status	Location	Reactor type	Capacity	Input	Final output
[173,174]	Chalmers gasifier	Operational	Sweden	DFB	4 MW_{th} heat output	Woody biomass	Heat
[174,244]	Växjö Värnamo Biomass Gasification Center AB	On hold	Sweden	CFB	18 MW_{th} input 6 MW_e power output 8 MW_{th} heat output	Woody biomass and agricultural wastes	CHP and syngas
[103,104,174,201,202]	GoBiGas	Cancelled	Sweden	DFB	32 MW_{th} input 3 MW_e power input 11 MW_{th} heat output 20 MW_{th} methane output	Wood wastes	Heat and SNG
[174,205,242]	Värmlandsmetanol AB	Awaiting investment (390 M €)	Sweden	CFB	125 MW_{th} input 130000 m^3/year methanol output	Woody biomass	Methanol
[174,205,245,246]	Bio2G	Awaiting investment (450 M €)	Sweden	Pressurized BFB	345 MW_{th} input 200 MW_{th} SNG output 55 MW_{th} heat output 15 to 23 MW_e power output	Wood wastes	CHP and biomethane
[173,247]	Kombi Power System Charmey	Operational	Switzerland	Updraft	5 MW_{th} heat output 1 MW_e power output	Wood chips	CHP
[173,242,247]	Puidoux Woodgasifier	Operational	Switzerland	Updraft	6 MW_{th} input 5 MW_{th} heat output 1 MW_e power output	Wood chips	CHP
[174]	CFB Tzum	On hold	The Netherlands	CFB	3 MW_{th} heat output	Chicken manure	CHP
[173,248]	Baas Energie BV	Operational	The Netherlands	Updraft	5 MW_{th} input 4 MW_{th} heat output 0.5 MW_e power output	Wood chips	CHP
[173,174]	ESKA Waste Paper Rejects Gasification	Operational	The Netherlands	CFB	15 MW_{th} input 12 MW_{th} heat output	Paper wastes	Heat

Table 2.7 – (cont.).

Reference	Plant	Status	Location	Reactor type	Capacity	Input	Final output
[249]	BioMCN Farmsum	Operational	The Netherlands	Specific design	200000 ton/year methanol output	Glycerin	Methanol
[173,250]	BioMCN Groningen	Operational	The Netherlands	Specific design	413000 ton/year methanol output	Wood chips	Methanol
[103,174]	Wood gasifier RWE Essent	On hold	The Netherlands	CFB	85 MW_{th} heat input 34 MW_e power output	Wood wastes and RDF	Power
[173]	GoGreenGas	Under construction	United Kingdom	Fluidized bed	4 MW_{th} input	RDF and waste wood	SNG

Table 2.8 – Average composition (H_2, CO, CO_2, CH_4, N_2, C_xH_y and tar) and LHV of the PG from different commercial gasifiers (>3 MW_{th}) in Europe.

			Gas composition [%v, dry gas]							
Reference	Plant/Company	Gasifier design	H_2	CO	CO_2	CH_4	N_2*	C_XH_Y	LHV [MJ/Nm^3]*	Tar [g/Nm^3]
[200]	Oberwart	DFB	39	25	22	10	2	3	11	nr
[201]	Güssing	DFB	37	31	17	9	3	2	11	3
[174]	Harboøre	Updraft	19	29	9	4	41	nr	7	nr
[251]	Pyroneer	CFB	8	15	18	10	34	nr	6	nr
[174]	Skive	BFB	16	20	12	4		nr	6	nr
[205]	Lahti Energia Kymijärvi I	CFB	11	15	18	5	51		4	10
[252]	Bioneer	Updraft	11	30	7	3	49	nr	6	75
-	Metsä Fibre Oy, Äänekoski Mill	CFB	6	9	12	3		2	5	24
[253]	Bioliq	Pressurized entrained-flow	31	33	23	0	15	nr	8	nr
[207]	Stadtwerke Ulm/Neu	DFB	38	23	22	11		4	13	14
[254,255]	Choren Freiberg BtL production β-plant	Entrained-flow	34	41	24	0	1	nr	9	nr
[256]	PRMES Model KC-18 Gasifier	Specific design	14	18	12	5	50	nr	5	nr
[206]	LTU Green Fuels DP1+DME pilot	Chemrec (Entrained-Flow)	38	26	33	1	1	nr	8	nr
[207]	Chalmers gasifier	DFB	40	14	30	6	4	2	9	12
[257]	Växjö Värnamo Biomass Gasification Center AB	CFB	11	18	16	7	50	nr	6	10
[202]	GoBiGas	DFB	40	24	20	9	5	2	10	1
[258]	Puidoux Woodgasifier	Updraft	18	27	nr	4	nr	nr	7	nr
[259]	ESKA Waste Paper Rejects Gasification	CFB	4	6	15	3	66	3	4	15
[238]	Wood gasifier RWE Essent	CFB	11	13	15	4	51	nr	6	nr

*- N_2 in DFB designs often result from inserting N_2 to pressurize feeding silos; LHV was sometimes determined by the author using the methodology detailed in [4]; nr – not referred.

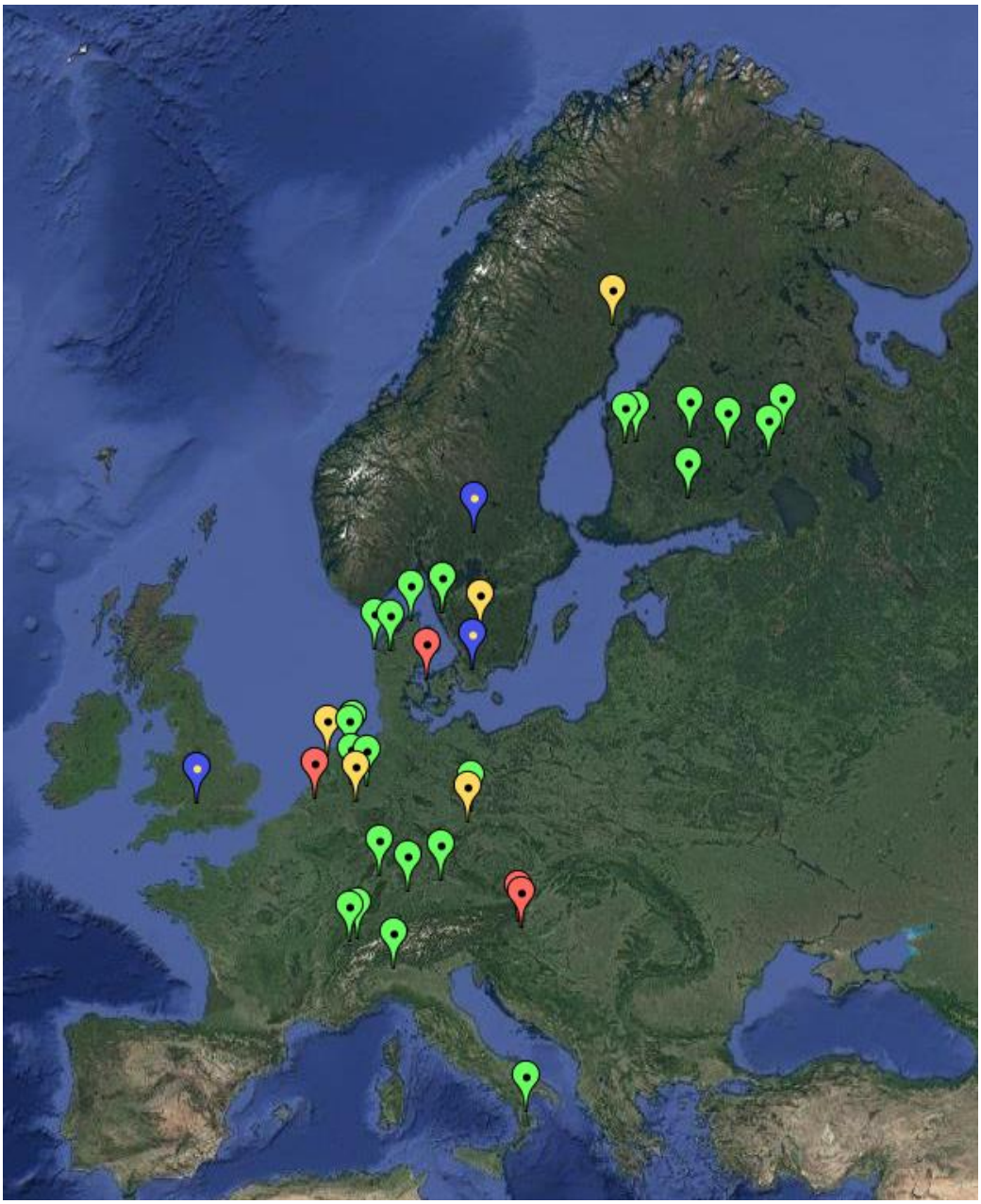

Figure 2.15 – Industrial-scale (>3 MW_{th}) gasification plants in Europe, countries participating on IEA Task 33. Green – Operational; Yellow – On hold; Red – Cancelled; Blue – Planned.

2.2.4.1 SWEDEN

In Sweden, there are several large-scale gasification plant projects for the production of biofuels at various stages, however, most of them are currently cancelled or awaiting investment [205]. Amongst these, the GoBiGas in Gothenburg can be considered as one of the most relevant, which was funded by the Swedish Energy Agency and recognized by the European Commission [26,103]. The plant performed the gasification of wood wastes and refined the obtained PG to biomethane in a methanation process [26]. The obtained biomethane was mixed and fed in the natural gas grid [26]. The plant was in operation from 2014 to 2018, with a 32 MW_{th} thermal load capacity and an output of 20 MW_{th} of biomethane [104,202]. It was built to reduce local emissions, such as soot particles from buses, as well as restricting GHG emissions [104]. The project included two main phases, the first phase was the construction of a demonstration plant to

produce 20 MW_{th} of biomethane, and the second was the construction of a commercial plant of 100 MW_{th} [104]. The first phase accumulated over 12000 hours of operation since 2014 [103]. However, due to unfavorable market conditions, particularly the actual price of biomethane not following projections and imported biomethane (biogas) from Denmark being cheaper [103], the second phase was not initiated [104]. The company decided to stop the project in 2018 due to direct production cost being higher that sales revenues [103]. The Chalmers demonstration gasifier (4 MW_{th} heat output), which is still in operation [173], served as a pilot plant for the GoBiGas project.

In Sweden, it was also built a pioneer large-scale plant for black liquor gasification, namely the LTU Green Fuels plant (Table 2.7). This technology is extremely relevant for the integration of gasification in the PP industry. The plant operated under 3 MW_{th} capacity and outputted 4 t/day of DME. The DME was used in trucks for transportation purposes, resulting in about 400 tons of DME produced and over 80000 km of truck operation [103]. However, when subsidies ended, the plant revenues could not support the process costs and commercial operation was stopped [103].

The largest gasification plant project in Europe is also associated to Sweden, namely the Bio2G project, which consists in a 345 MW_{th} pressurized BFB to be located somewhere in the Scania province. The plant has suffered significant delays in construction due to other "green" energy projects having priority, and is currently on hold and awaiting investment (450 million Euro) [205]. The decision regarding its construction is pending on oil prices variations in combination with uncertainties in Sweden policies [205]. Nonetheless, a grant of 203 million Euro was approved in 2014 [205]. The objective is the production of biomethane for distribution in the natural gas grid, thus providing natural gas supply security [245]. The gas cleaning procedure will include hot gas filters, catalytic reforming and acid gases removal. Furthermore, the gas will be cooled and pressurized to the required conditions of methane synthesis [245].

2.2.4.2 FINLAND

In Finland, there are several large-scale gasification plants in operation, such as Joutseno, Lahti Energia Kymijärvi I, Lahti Valmet Kymijärvi II, Varkaus Stora Enso, Varkaus Corenso and Äänekoski, whose technology has been supplied by Andritz, Valmet, Volter, VTT, among others [208]. There seems to be a trend in this country for the use of large-scale gasification processes to produce district heating and fuel gas for the PP kilns. Employed gasification technologies include BFBs and CFBs at higher scales (12 to 160 MW_{th}) and updrafts at lower scales (6 to 13 MW_{th}). Amongst these, is the largest gasification plant currently operating in Europe, namely the Kymijärvi II located in Lahti, with 7 years of commercial operation [208]. The infrastructure includes two 80 MW_{th} atmospheric CFB gasifiers (installed by Valmet) and produces 50 MW_e of electricity and 90 MW_{th} of district heat [174]. This covers the heating need of 30000 single-family homes for an entire year and the annual electricity consumption of 75000 apartments [174]. The total investment for this plant was 160 million euros [260].

In the Kymijärvi II plant, the gasifiers are started with natural gas before switching to solid recovered fuel (SRF) gasification, which takes place between 850 and 900 ºC. The fuel feeding has been reported as working properly, however, some blockages occur due to metals and oversize particles present in the SRF [238]. The gas cleaning process includes cooling down and hot filtration. The gas cooling is a relevant process because impurities present in the PG from SRF (e.g., alkali chlorides) must be removed prior to the gas combustion to avoid corrosion of the boiler [174]. Thus, the PG is cooled down from 900 ºC to 400 ºC, to condense these impurities while avoiding the condensation of tars. The cooling is performed by a heat exchanger with water as working fluid, which is then used to preheat the feedwater to the boiler [174]. The cooled PG is cleaned of particulate material by heated filters, which are replaced every 2 to 3 years [174]. The combustion boiler contains 4 burners, which are designed to use both PG (4.6 to 5.8 MJ/Nm^3) and natural gas, and are firstly ignited with natural gas before switching to PG [174,238]. The PG

combustion produces a temperature of 850 ºC and the obtained steam temperature and pressure is 540 ºC and 121 bar, respectively [174]. The plant operated over 6000 hours per year from 2013 to 2016 [238]. The first year of operation (2012) only had 4267 hours of operation due to carbon-containing ash clogging the gas filter [238]. This drawback led to the oxidation of these particles during start-up and shutdown procedures and consequent local overheating [238]. Thereafter, an alternative solution was implemented, involving periodic offline filter cleaning procedures, which presented satisfactory results and consequently increased the operation time of the plant [238]. Nonetheless, despite the promising results obtained with the operation of the Kymijärvi II plant, Valmet has not installed another similar gasification plant elsewhere [238].

2.2.4.3 GERMANY

In Germany, about 400 biomass gasification plants have been built until 2015, providing approximately 35 MW_e of electricity [90]. In the last decades, several companies have been developing and building small-scale gasification plants, namely Burkhardt GmbH, Spanner Re^2 GmbH, Holzenergie Wegscheid GmbH and REGAWATT GmbH [90,103]. A higher degree of decentralized small-scale gasification implementation can be found in the country, in comparison with large-scale gasification plants implementation, which is a common behavior in the central and southern Europe [103]. Nonetheless, some large-scale gasification plants are also in operation and development, for example the CHP Agnion Biomasse Heizkraftwerk Pfaffenhofen (45 MW_{th}), which seems to be the largest plant in operation, however, information about this infrastructure is scarce and uneven [174,240], thus it was not considered here for further analysis. Another large-scale facility in operation is the Waermeversorgung, which includes a 21 MW_{th} input BFB [173,241], and is located in Grossenhain. The largest DFB gasification plant currently in operation in Europe is also located in Germany, specifically in Neu-Ulm. This infrastructure presents a thermal load of 15.1 MW_{th} and an output of 4.6 MW_e [240], and has been in operation since 2011 [174]. The plant employs a gas engine and an ORC [174], and provides power for 21000 inhabitants of Senden, a town in the district of Neu-Ulm, Germany [240].

In Germany, the planning, construction and operation of large-scale gasification plants for the production of synthetic fuels, such as bioliq, Choren Freiberg BtL production β-plant and Blue Tower facility, is also occurring. The bioliq is composed by a 2 MW_{th} fast pyrolysis reactor coupled with a 5 MW_{th} pressurized entrained flow gasifier (up to 8 MPa) [240]. The facility is a demonstration plant for the bioliq process, which was developed at the Karlsruhe Institut für Technologie (KIT), and seeks the production of DME and gasoline from biomass [240]. The β-plant of Choren in Freiberg is planned to be a BtL 45 MW_{th} plant based on biomass gasification in an entrained flow gasifier (Carbo-V process) in combination with FT synthesis, for the production of 2 m^3/hour of FT liquids [240]. The plant is in a commission phase and the investment costs are reported to be approximately 190 million euros [240]. The Choren Industrietech-nik Carbo-V concept for air-blown gasification of biomass was initially tested in a 1 MW_{th} alpha pilot in Freiberg in 2003 [26]. The Blue Tower project remounts to 2009 [174], and is reported to be planned for construction in Herten [240]. The project concept includes a multi-stage reforming process to produce H_2 from wood wastes (roadside greenery) [174]. It seems the project is currently on hold and awaiting an investment of 25 million euros [173,240].

2.2.4.4 THE NETHERLANDS

In The Netherlands, due to the country specificities, the biomass resources are limited and there is an even higher focus in gasifying wastes (e.g., wood and plastics), with various projects currently under research and ongoing [103,174,249]. The Essent/RWE wood waste gasifier is the largest plant built in the country and includes an 85 MW_{th} CFB reactor based on Lurgi technology [103]. This infrastructure is connected to a 600 MW_e coal-fired power plant and was operated from 2001 to 2013 at approximately 5000 hours per year, with interruptions caused by feeding

issues and tar related fouling [249]. Subsidies on renewable power for this plant ended in 2013 and since then the gasifier has been offline [261]. In this respect, new options to attain an economically viable operation, such as gasifying cheaper waste materials, have been under research [249,261].

In this country, another relevant large-scale gasification plant is the BioMCN in Delfzijl, which produces methanol from biomass, with an output capacity of 200 kton/year, representing the second largest biofuel plant in the world [249]. The process is based on the gasification of crude glycerin, thus turning biodiesel synthesis into a more sustainable process by reducing the problem of surplus glycerin disposal [26]. BioMCN has another plant planned for the production of more 400 kton/year of methanol, which seems to have started operating recently [250]. For this installation, a grant of 199 million euro through European NER300 innovations program was obtained [249].

Another large-scale gasification plant was installed by ESKA at Hoogezand in 2016. The infrastructure is currently in operation and includes a 15 MW_{th} CFB plant for the gasification of paper rejects from the manufacturing process of high quality solid board [103,173]. The main objective is the production of fuel gas to replace natural gas in the manufacturing process of solid board [262]. The plant also comprises a boiler for the production of steam (5 to 16 ton/hour at 196 ºC and 13.6 bar) [259]. During the operation of this plant, the following challenges have been identified: difficulties to maintain continuous full capacity, large variation in the composition and LHV of the PG and blockages in the gasifier and boiler [259].

2.2.4.5 AUSTRIA

In Austria, implementation of gasification technologies is scarce and the focus has been more centered on small-scale gasification for CHP (e.g., Urbas Energietechnik, 100 to 150 kW_e), because large-scale gasification plants operation seldom is economically viable [90,103,263]. Regardless, the most successful and commercial indirect gasification system was developed by the Vienna University of Technology, namely the Güssing type DFB gasifier [15,101,263], which is highly suitable for large-scale operation. This concept of gasifier (described in Section 2.2.3) has been installed in Austria, Germany (Neu-Ulm plant) and Sweden (GoBiGas project), with different thermal load capacities [66,101,103].

The two largest gasification plants built in Austria, namely at Güssing and Oberwart, included this concept of DFB gasifier. However, both the Güssing and Oberwart plants were closed due to economic reasons [103]. Regarding the Güssing plant, the operation was economically viable from 2001 to 2016 due to supporting tariffs, which ended recently, leading the owners to stop the operation [103,263]. The PG from this plant was used in various research projects, including production of FT diesel and SNG and application in SOFCs [263]. From a technical viewpoint, it is argued that the plant could still be operated for several years [103,263]. The Oberwart plant and the Güssing plant shared similar designs, particularly the gasification process occurring in a Güssing type DFB gasifier and the PG cleaning performed in a bag filter followed by a tar scrubber; after cleaning, the PG was used in two gas engines for power generation [263]. In this process, the PG is cooled immediately after the gasification reactor to the necessary operation temperature of the bag filter (<200 ºC), which may lead to tar condensation in the gas coolers and consequent fouling during operation [264]. The main differences between these two plants were the installation in the Oberwart plant of a larger gasification reactor, with increased inner reaction volume in relation to the thermal biomass input, a biomass drying unit and an ORC for electric efficiency increase [263,264]. This infrastructure was also in operation for several years, namely from 2008 to 2015 [263].

2.2.4.6 DENMARK

In Denmark, there has been a green and sustainable energy policy since the oil embargo in 1973 [236]. Accordingly, there are various subsidies to support gasification projects, however, it is questionable if they are sufficient and as attractive as other green energy subsidies available in the country, for example subsidies for biogas [236]. In this country, 4 large-scale gasification plants were implemented, namely Harboøre, Pyroneer, Sindal, and Skive, with capacities of 4, 6, 9 and 20 MW_{th}, respectively (Table 2.7). Amongst these, the gasification plants in Harboøre and Skive have been operating for several years with success [103], while the Sindal plant has started operation more recently (2018) [173], and the Pyroneer plant was mothballed in 2015 after 4 years of operation [236]. The Harboøre plant is composed by a 3.7 MW_{th} updraft gasifier with an output of 1 MW_e power and 2 MW_{th} heat [236]. The plant operates 8000 hours per year and supplies heat to approximately 700 consumers [236]. The plant includes an updraft gasifier with an ash extraction system, air humidifier, gas cooling and cleaning system, two ICEs for CHP and a waste water cleaning system [236]. The Skive gasification plant is composed by an 20 MW_{th} BFB gasifier with an output of 6 MW_e power and 11.5 MW_{th} heat [236]. The PG is cleaned in a catalytic process and used in three ICEs for CHP application [236]. The produced heat is consumed in the local district heating network and the electricity is sold to the grid [236]. The plant seeks to be further upgraded to use the gas for the synthesis of gasoline and other biofuels [103].

2.2.4.7 ITALY

In Italy, there has been a long and significant focus on the energetic valorization of biomass wastes, with gasification attracting considerable interest [265]. In this country, gasification plants are mostly confined to small-scales, with over 150 biomass gasification plants installed with capacities between 100 and 150 kW_{th} [90]; only two plants were found over 3 MW_{th} (Table 2.7) [174,265]. The total nominal power installed seems to be around 50 MW_{th}, with a higher number of plants located in the north of Italy due to the presence of forestry industry [103]. However, there are various commercial gasifier technologies installed in almost all Italian regions [265]. The designs implemented are essentially downdraft gasifiers, developed and supplied by ESPE SRL and CMD SpA [103,265]. This design has been preferred due to the production of a PG with low tar concentration, thus not requiring filters and increasing the system reliability at long term [103]. These aspects show that the use of gasification for biofuels production has not been a priority in this country. Nevertheless, gasification processes are being researched in the Enea Trisaia Research Center, which is a R&D infrastructure focused on the development of gasification technologies [265]. In this infrastructure, various pilot-scale gasification reactors (10 kW_{th} to 1 MW_{th}) are under research, including DFB, downdraft, CFB, multi-stage and updraft designs [265]. Primary and secondary PG cleaning methods are being researched to reduce particle and tar concentration. In this respect, the integration of a high-temperature gas purification system in the freeboard of a 1 MW_{th} BFB showed promising results, namely a particle removal efficiency of 99 % from the PG [265].

2.2.5 FUTURE TRENDS AND PERSPECTIVES

Europe has been a pioneer in the development and implementation of biomass gasification technologies, with significant research and technological development performed [266]. Germany, The Netherlands, Finland, Denmark and Sweden are leaders in this area with several distinct types of gasification technologies planned and implemented at a commercial level. In the southern and central Europe, gasification technologies are more relevant at small-scales, while in the northern Europe large-scale installations have been more relevant [103], which can be associated to district heating necessities. In fact, Nordic countries have always been forerunners in the development of large-scale biomass thermal and co-generation plants [202]. The investment costs of industrial-scale (>3 MW_{th}) gasification plants in Europe can be grossly placed between

171 and 1000 €/kW_{th} (611 €/kW_{th} average) for CHP generation and between 1304 and 5000 €/kW_{th} (3114 €/kW_{th} average) for bioproducts synthesis (Table 2.9).

Table 2.9 – Investment costs of different industrial-scale (>3 MW_{th}) gasification plants in Europe.

Reference	Plant	Capacity [MW_{th} input]	Investment [M€]	Investment [€/kW_{th}]
[238]	Varkaus Corenso	50	20	400
[238]	Lahti Energia Kymijärvi I	70	12	171
[238]	Lahti Valmet Kymijärvi II	160	160	1000
[238]	ESKA Waste Paper Rejects Gasification	15	14.5	967
[238]	Wood gasifier RWE Essent	85	44	518
[103]	GoBiGas	32	160	5000
[103]	Värmlandsmetanol AB	125	390*	3120
[103]	Bio2G	345	450*	1304
[240]	Choren Freiberg BtL production β-plant	45	190*	4222
[240]	Blue tower	13	25*	1923

*- Predicted necessary investment for planned large-scale gasification plants

Currently, various shifts can be observed regarding gasification implementation in Europe in recent years and several trends can be predicted for the future. For example, in the last years several new large-scale gasification plants were planned or built, while others were closed [103]. Furthermore, using clean and expensive woody biomass is no longer considered economically viable for gasification processes [103]. Using expensive feedstocks to obtain PG turns the gasification process unprofitable in almost all scenarios. Thus, the scientific community is highly focused on developing and improving gasification and co-gasification technologies to use various abundant low-cost wastes (e.g., wood wastes, plastics and sludges) as feedstock [3,267,268]. The valorization of these wastes can help overcome their disposal problem, consequently increasing the sustainability of waste management and energy supply in the future [3,269]. For example, RFB resulting from forestry operations increases wildfire risks when left on site [176] and 45 % of the wastes generated (25 % being MSW) in the EU are still disposed in landfills, constituting several environmental risks [3]; both these low-cost wastes are potential feedstocks for gasification and co-gasification processes. Furthermore, mixing distinct feedstocks can lead to synergistic effects and be used as a technique to achieve desired PG quality and consequently reduce gas cleaning needs [3,270]. In fact, various large-scale gasification plants are already operating on waste feedstocks or seeking potential wastes feedstocks, for example paper rejects in the ESKA gasification plant in The Netherlands, glycerin in the BioMCN gasification plant in The Netherlands, SRF in the Energia Kymijärvi II gasification plant in Finland and RDF in the planned GoGreenGas plant in United Kingdom.

Another relevant trend is CHP applications becoming more relevant at small-scale gasification plants, and biofuels and biochemicals synthesis applications more relevant at large-scale gasification plants [103]. On one hand, this is related to the high market potential of decentralized small-scale gasification systems for CHP, which allows an effective valorization of local biomass resources collection and use [90]. On the other hand, this is related to scaling-down issues of advanced gasification processes, for example BFBs, CFBs and DFBs are not suited for small-scale implementation; it is also argued that large-scale gasification processes usually offer benefits in terms of efficiency to investment ratio [90].

In Europe, small-scale gasification implementation has been significantly prominent in the recent years, with over 1100 small-scale gasifiers installed [263], and this trend seems to be continued in the future. Germany and Italy have been particularly active at implementing small-scale gasifiers, with various companies and stakeholders involved. Regarding large-scale gasification plants, these are becoming increasingly considered to produce FT-diesel, methanol, SNG and

hydrogen, among other bioproducts, and there are already some plants in operation, for example the BioMCN in The Netherlands (methanol) and the Bioliq in Germany (DME and gasoline). The importance of generating these bioproducts from renewable sources is acknowledged due to environmental aspects and policies based on renewable energy sources [263].

Furthermore, the economy of generating renewable bioproducts from wastes is becoming significantly more attractive than power or CHP [238], mainly because it creates a new chain of value, contributing to fulfil the goals of circular economy and sustainable development, instead of competing with well-established renewable technologies [238], such as waste incineration and biomass power plants; this further highlights the interest of large-scale gasification plants. Nevertheless, these plants are still having trouble penetrating the market, due to high investment costs and economically unviable commercial operation, despite significant quantities of RFB and wastes being available [238]. On one hand, these large-scale processes may present issues related to biomass availability resulting from biomass seasonality, heterogeneity and local shortage. A high amount of local and sustainable biomass supply is required to support large-scale gasification plants, and local existing RFB by itself may not be enough to satisfy the needs at all times, which means that significant local areas to grow biomass are required. This may lead to the displacement of food crops to unused lands and consequent potential conversion of forest to arable lands, which may also cause biodiversity harm and increased GHG emissions [24,25]. In fact, it is considered that due to the logistical costs of transporting biomass feedstocks from far distances often turns bioenergy plants larger than 50 MW_{th} economically unviable [271]. These aspects must be addressed when implementing large-scale gasification plants, for example by integrating food and bioenergy cropping systems within farmlands [25] and by mixing local existing solid wastes in the feedstock, as previously discussed. This further supports the shift to using various types of wastes, such as wood and agricultural wastes, sludges, RDF and SRF, as feedstock in large-scale gasification plants. On another hand, high-end catalytic synthesis applications require a very high quality PG, with high H_2/CO molar ratio and low tar and particles concentration [272], among other requirements, leading to the mandatory implementation of expensive gas cleaning and upgrading processes and equipment (e.g., water-gas shift reactor, H_2S and CO_2 scrubbers, OLGA/RME scrubber, ceramic filters, bag filters), which have significant investment and operating costs.

Based on these aspects, it can be stated that without significant supporting economic subsidies and incentives, the implementation of large-scale gasification plants seldom can compete with fossil fuels technologies. For example, the GoBiGas plant in Sweden was in operation from 2014 to 2018, producing methanol from the gasification of wood wastes, however, when subsidies ended in 2018, the company decided to stop operation due to direct production cost being higher that sales revenues [103]. Other similar examples include the Güssing and Oberwart plants in Austria, as discussed in Section 2.2.4.5. Furthermore, in large-scale gasification plants, various distinct gasification technologies are employed with distinct PG cleaning procedures, including specific gasifiers designs (Table 2.7), which shows that the technology is neither mature or based on proven technologies that are more cost-efficient and reliable, in comparison with one another [238]. This leads to uncertainty and lack of confidence from the stakeholders.

The economic viability of large-scale waste gasification processes can be improved by the development and implementation of innovative gas upgrading processes, for example those that are integrated within the gasifier to use and preserve the thermal energy of the PG [15,123]. In this regard, catalysts for in-situ application have been developed with high activity for tar reforming [123,124]. However, these materials have been mostly tested at a laboratory-scale and the obtained results may diverge from real large-scale application, where various unpredictable factors have impact on the activity of the catalyst [125]. Using natural minerals or gasification byproducts (e.g., ashes and chars) as catalysts is also a promising pathway due to its proven activity, low-cost and abundance [123,125]. Development of low-cost catalysts with known composition, that can be easily regenerated in large-scale infrastructures, can also be an alternative approach [125]. Other potential strategies to improve the economic viability of the process can include retrofitting existing fluidized bed boilers to reduce investment costs

[15,104,273], residual char and ash valorization in suitable processes [274–276] and using polygeneration strategies for the production of more than one product in a combined process, such as combined SNG, heat and power [15]. Furthermore, projects on hold (e.g., GoBiGas) obtained significant sets of information, for example experimental and costs data, that must be used to plan future investments in advanced large-scale gasification plants for bioproducts [104]. These aspects are of major relevance because the current status of gasification and PG cleaning technologies is still in a demonstration phase and consequently entails technical and non-technical risks [238].

2.2.6 CONCLUSIONS

Biomass is the only non-transient renewable energy source that can be adjusted to current consumption needs. Gasification is a key technology for the use of biomass because it allows the production of fuel gas that can fit in the current carbon-based energy infrastructure through distinct thermal, power and synthesis applications. Despite still being at a demonstration level, biomass gasification technologies, and respective integration in biorefineries, have been profiled as a potential answer to global warming and fossil fuel depletion concerns.

The survey performed in this work shows that Europe has been active in the implementation and development of gasification technologies, with various large-scale gasification plants planned, idle and in operation. Recent trends and shifts, that reflect the need of new knowledge and cost-competitive technologies to attain the commercial breakthrough of biomass gasification, were identified and analyzed. CHP applications are becoming more relevant at small-scale gasification plants, due to an easier sustainable local biomass collection, while large-scale applications are becoming increasingly considered for the catalytic synthesis of bioproducts, due to scale-down issues of advanced gasification processes. Small-scale implementation of gasification for CHP has been prominent in recent years and this trend seems to be continued in the future. However, this will not be enough to answer climate neutrality or energy supply concerns, and significant implementation of large-scale processes for bioproducts synthesis is also required.

The economy of generating renewable bioproducts from biomass wastes is becoming significantly more attractive than power or CHP, because it creates a new value chain, instead of competing with well-established renewable technologies, and allows biomass to compete with current petrochemical refineries. However, large-scale gasification plants still entail significant issues and risks (e.g., biomass availability, PG upgrading costs) that decrease the project economic viability, and can cause the interruption of the operation of existing gasification plants upon the end of governmental subsidies. Furthermore, there are various distinct types of gasification technologies employed in gasification plants, and investments costs vary greatly, which hinders techno-economic analyses and reveals the lack of gasification technology maturity and proven cost-efficiency. These aspects cause significant investment risks and decrease confidence from stakeholders, consequently hampering the implementation of large-scale gasification projects, particularly for bioproducts synthesis.

To avoid drawbacks associated with biomass costs, availability and logistics, and competition with food supply and other land uses, the replacement of high quality wood by low-cost wastes feedstocks (e.g., RFB, RDF, SRF and respective mixtures) is under research by the scientific community and already occurring in some demonstration and large-scale gasification plants. The valorization of these wastes can also help overcome the problematic of their disposal, simultaneously promoting the sustainability of waste management and energy supply, and thus acting in accordance with circular economy principles. To reduce the costs associated to the required PG upgrading for synthesis applications, development and implementation of innovative and cost-efficient gas upgrading processes, particularly those that are integrated within the gasifier to use and preserve the thermal energy of the PG, are mandatory. To further increase stakeholders confidence, available information from pioneer demonstration and industrial-scale gasification plants should be used to optimize gasification technologies and support future plants construction

and operation. Governments should also present a stronger sense of concern and ensure necessary policies for gasification technologies to be cost-competitive with conventional fossil fuel technologies. Furthermore, to avoid biased markets, economic subsidies should always present levels equivalent to the ones provided to other “green” energies.

3 NUMERICAL TOOLS TO PREDICT PG COMPOSITION DURING BIOMASS GASIFICATION

This Chapter is composed by Article III, named "Empirical and chemical equilibrium modelling for prediction of biomass gasification in an autothermal pilot-scale bubbling fluidized bed reactor". This Article develops, compares and evaluates two distinct types of models to predict PG composition from direct (air) biomass gasification processes in BFBs, namely empirical and chemical equilibrium modelling. This Article was published in the Energy Journal in 2020 (https://doi.org/10.1016/j.energy.2020.117654).

3.1 ARTICLE III - EMPIRICAL AND CHEMICAL EQUILIBRIUM MODELLING FOR PREDICTION OF BIOMASS GASIFICATION IN AN AUTOTHERMAL PILOT-SCALE BUBBLING FLUIDIZED BED REACTOR

3.1.1 ABSTRACT

In this work, two approaches to predict the PG composition obtained by direct (air) biomass gasification in bubbling fluidized beds were developed and compared, namely empirical modelling based on reported experimental results in the literature and non-stoichiometric chemical equilibrium modelling. For this purpose, an extensive database containing a set of 19 published experimental results from the literature was compiled and a non-stoichiometric chemical equilibrium model developed.

The prediction capability of the empirical and chemical equilibrium model was evaluated by comparison with experimental data obtained in an 80kWth bubbling fluidized bed direct (air) biomass gasifier. The empirical model shows moderate accuracy in the determination of the PG composition (CO, H_2 and CH_4), whereas the chemical equilibrium clearly overestimates the concentration of H_2 and CO, and underestimates the concentration of CH_4, leading to subpar accuracy in the determination of typical gasification efficiency parameters. Thus, the empirical model is suited for preliminary estimates of gasification products, while black-box chemical equilibrium modelling, without experimental knowledge integration, is considered as unreliable for these gasification conditions.

Keywords: Biomass; Bubbling fluidized bed; Gasification; PG; Chemical equilibrium; Empirical modelling.

3.1.2 INTRODUCTION

Biomass gasification modelling is recognized as a promising approach for designing, up-scaling and operating gasification processes and technologies [52,277,278], serving as an useful complement to experimental research [56,278–280]. This technique allows the evaluation of the impact of operating parameters, such as ER, feedstock composition and temperature on the PG quality and overall process efficiency [26]. The desired composition of the PG is a major parameter that defines the configuration and design of the gasifier and the selection of the process operating parameters. Thus, numerical modelling is a relevant supporting tool for the configuration and design of gasification plants, including equipment size, startup and shutdown requirements, process control and the determination of the necessary infrastructures to handle the feedstock and the gasification agent [277]. During the gasification plant operation, modelling tools can also be important to predict the impact of unintended operating parameters modifications, such as the variation of feedstock characteristics, to interpret the causes behind gas

composition changes [277], to assist in reducing problems related to tar and char formation [52] and to be able to continuously optimize the process.

In this respect, several mathematical modelling approaches have been under research and were proposed in the literature to characterize and predict this complex process [52,279,281–283]. Generally, these can be classified into the following main groups [13,52]:

i) Kinetic models.
ii) CFD models.
iii) ANN models.
iv) CEM.

Kinetic models study the progress of reactions in the reactor, giving the products composition in distinct locations along the gasifier [52]. It is argued that these models provide accurate and reliable results, however, they are complex and computationally intensive and have limited application for distinct gasification plants with different design and characteristics [13,283]. CFD models can simulate physical phenomena, solving equations of balance of mass, momentum and energy over a discrete region of the gasifier, providing an accurate prediction of temperature and gas yield in the whole reactor [13,52]. However, these models require large amount of information (detailed reactor design, material properties, etc.,) and high computational resources [13]. ANN models are relatively novel for modelling gasification processes [52]. These models do not require a mathematical description of the phenomena associated with the system [279] but require large amount of consistent experimental data to train the network to be able to predict the behavior of the gasifier with accuracy [52]. A more detailed explanation and in-depth review of these models is out of the scope of this work. Readers can refer to other published works [56,281,283,284].

CEMs are the most common modelling approach for biomass gasification [56,285]. These models can predict the products of gasification by assuming that the reactants are allowed to react in fully mixed conditions for an infinite period of time [286], reproducing ideal gasification performance and predicting the maximum yields attainable by the reagent system [52]. The main advantages are the possibility of running the model without knowing the gasifier design [278,283] and the simplicity and reduced computational time [52]. CEMs are promising to determine first estimates of the composition of the PG, taking in account the influence of the process operating parameters (e.g., ER, temperature and pressure) and the feedstock characteristics (e.g., the chemical composition) [286] and to perform concept studies, preliminary analysis and optimization procedures [278]. These models are commonly used as a first approach to predict the PG composition from biomass gasification and to determine the optimal biomass feedstock for specific applications [52,69,287–289].

There are two main types of CEMs: stoichiometric models, which are based on equilibrium constants and require knowledge regarding the reactions paths and reactions equations, and non-stoichiometric models, which are based on minimizing the Gibbs free energy in the system and do not require knowledge of the process reactions mechanisms [282,283,286]. Puig-Arnavat et al., [283] argues that the two approaches are equally suitable to model biomass gasification processes. Sikarwar et al., refer that stoichiometric models can present significant deviations from real life scenarios if important reactions are neglected, and that the non-stoichiometric approach is more suitable for biomass gasification processes due to the uncertainty of gasification reaction mechanisms [26]. These modelling techniques can also have different approaches, for example by integrating experimental knowledge [290,291] and kinetics [283] or considering that only part of the process attains equilibrium [278]. In this respect, modified CEMs [292–294] and restricted CEMs [285,295] are under research.

In practical gasifier plants, the chemical interactions inside the gasifier take place in a finite time, and the CEM predictions have mixed success depending on the reaction temperature and residence time [26]. Therefore, assumptions of infinite reaction speed and that all reactions will be complete can be far from realistic for several practical gasifiers [286]. In fact, it is argued that chemical equilibrium may not be achieved when the gasification temperature is lower than 900 ºC and only a finite time is available for the reactants to react in the gasifier [52,66,278]. Besides, it

is also suggested that CEMs are not reliable when the ER of the gasification process is between 0.10 and 0.30 [296]. Unfortunately, the common operating conditions for biomass direct (air) gasification in BFBs fall between these ranges (Bed temperature: 600-900 ºC and ER: 0.20-0.30 [4]). Accordingly, it has been argued [13,26] that CEMs typically present better results for entrained flow gasifiers and downdraft gasifiers than for fluidized beds. In fact, reasonable agreement has been reported by some authors regarding CEMs predictions and experimental biomass gasification data obtained in these type of gasifiers [13,297–302]. Nonetheless, CEMs have also been intensively used for biomass gasification in fluidized beds [283,285,295,303–305].

Furthermore, several assumptions are also reported to lead to deviation between experimental observed values and predicted values [26]. For example, assuming ash as inert [26], neglecting tar production, even though tar is one of the major barriers of biomass gasification [4,286], and considering char as pure solid carbon [26]. Thus, CEMs determine ideal yields [52] that may not be attained in practical gasifiers (e.g., H_2 and CO overestimation [286] and hydrocarbon underestimation [66]), consequently leading to deviations in the prediction of the lower heating value (LHV) of the PG and the process efficiency parameters. These aspects need to be analyzed to determine the suitability of CEMs to support and model direct (air) gasification of biomass in BFBs.

In this work, two models to predict PG composition from direct (air) biomass gasification processes in BFBs were developed, compared and evaluated, namely a non-stoichiometric CEM and an empirical model. For this purpose, an extensive database regarding direct (air) gasification experiments of biomass in BFB reactors, including experimental data obtained in previous works performed by the authors [4,123], was compiled and organized. First, the CEM predictions were compared to the experimental database to identify deviations. Afterwards, correlations were derived from this experimental data and from the CEM predictions. The objective of both these correlations is to be used as tools for determining first estimates of gasification products from direct (air) gasification processes in BFBs. The empirical and CEM correlations prediction capability was addressed briefly by comparison with experimental data obtained in an 80 kW_{th} BFB gasifier with different operating conditions.

The comparison and evaluation of these two types of modeling approaches can help in determining weaknesses and strengths, and consequently in guiding researchers to adopt and develop more suitable and integrated modelling approaches. This may contribute for the successful development of these numerical prediction tools, which represents an important step for the up-scale, demonstration and commercial breakthrough of biomass gasification technologies, potentially diminishing the gap between existing theoretical and practical knowledge in the estimation of gasification products and process efficiency parameters.

3.1.3 METHODS AND LITERATURE DATA COLLECTION

The database was compiled by collecting and organizing published experimental results from the literature (Table 3.1), regarding direct (air) gasification processes in BFBs reactors with distinct biomass types (Table 3.2) and different operating conditions [4,183,307–314,184–188,229,287,306].

Table 3.1 – Experiment references and operating conditions of the studies reported in the literature.

Experiment reference		Biomass type	BFB scale	T [ºC]	ER	Ref
AE	AE0.17	Woodchips	Pilot	718	0.17	[183]
	AE0.18	Woodchips	Pilot	722	0.18	[183]
	AE0.23	Woodchips	Pilot	733	0.23	[183]
BC	BC0.22	Rice husk	Pilot	784	0.22	[229]
	BC0.24 - 790	Rice husk	Pilot	790	0.24	[229]
	BC0.24 - 828	Rice husk	Pilot	828	0.24	[229]
	BC0.28 - 821	Rice husk	Pilot	821	0.28	[229]
	BC0.28 - 823	Rice husk	Pilot	823	0.28	[229]
	BC0.28 - 846	Rice husk	Pilot	846	0.28	[229]
	BC0.28 - 874	Rice husk	Pilot	874	0.28	[229]
	BC0.28 - 781	Rice husk	Pilot	781	0.28	[229]
	BC0.32 - 812	Rice husk	Pilot	812	0.32	[229]
	BC0.32 - 866	Rice husk	Pilot	866	0.32	[229]
	BC0.34	Rice husk	Pilot	864	0.34	[229]
CP	CP0.35	Wood pellets	Pilot	812	0.35	[184]
GE-CE	GE-CE-1	RFB eucalyptus type A	Pilot	804	0.22	[4]
	GE-CE-2	RFB eucalyptus type A	Pilot	798	0.24	[4]
	GE-CE-3	RFB eucalyptus type A	Pilot	812	0.25	[4]
	GE-CE-4	RFB eucalyptus type A	Pilot	810	0.26	[4]
	GE-CE-5	RFB eucalyptus type A	Pilot	818	0.28	[4]
	GE-CE-6	RFB eucalyptus type B1	Pilot	706	0.28	[4]
	GE-CE-7	RFB eucalyptus type B1	Pilot	714	0.30	[4]
	GE-CE-8	RFB eucalyptus type B1	Pilot	700	0.36	[4]
	GE-CE-9	RFB eucalyptus type B2	Pilot	736	0.17	[4]
	GE-CE-10	RFB eucalyptus type B2	Pilot	709	0.18	[4]
	GE-CE-11	RFB eucalyptus type B2	Pilot	719	0.20	[4]
	GE-CE-12	RFB eucalyptus type B2	Pilot	800	0.25	[4]
	GE-CE-13	RFB eucalyptus type B2	Pilot	813	0.35	[4]
GE-CP	GE-CP-1	RFB pine	Pilot	786	0.23	[4]
	GE-CP-2	RFB pine	Pilot	811	0.26	[4]
	GE-CP-3	RFB pine	Pilot	830	0.30	[4]
	GE-CP-4	RFB pine	Pilot	824	0.29	[123]
	GE-CP-5	RFB pine	Pilot	786	0.24	[123]
	GE-CP-6	RFB pine	Pilot	798	0.19	[123]

Table 3.1 – (cont.).

Experiment reference		Biomass type	BFB Scale	T [ºC]	ER	Ref
GE-WP	GE-WP-1	Wood pellets	Pilot	816	0.22	[4]
	GE-WP-2	Wood pellets	Pilot	802	0.24	[4]
	GE-WP-3	Wood pellets	Pilot	854	0.25	[4]
	GE-WP-4	Wood pellets	Pilot	833	0.30	[4]
	GE-WP-5	Wood pellets	Pilot	793	0.24	[123]
	GE-WP-6	Wood pellets	Pilot	828	0.21	[123]
IPE	IPE0.29	Torrefied woodchips	Bench	760	0.29	[185]
IPP	IPP0.24	Straw pellets	Bench	780	0.24	[185]
IPPC	IPPC0.21	Softwood pellets	Bench	760	0.21	[185]
KC	KC0.25 - 650	Rice husk	Pilot	650	0.25	[287]
	KC0.25 - 675	Rice husk	Pilot	675	0.25	[287]
	KC0.25 - 700	Rice husk	Pilot	700	0.25	[287]
	KC0.25 - 725	Rice husk	Pilot	725	0.25	[287]
	KC0.35 - 600	Rice husk	Pilot	600	0.35	[287]
	KC0.35 - 650	Rice husk	Pilot	650	0.35	[287]
	KC0.35 - 700	Rice husk	Pilot	700	0.35	[287]
	KC0.35 - 725	Rice husk	Pilot	725	0.35	[287]
	KC0.35 - 750	Rice husk	Pilot	750	0.35	[287]
	KC0.45 - 600	Rice husk	Pilot	600	0.45	[287]
	KC0.45 - 650	Rice husk	Pilot	650	0.45	[287]
	KC0.45 - 700	Rice husk	Pilot	700	0.45	[287]
	KC0.45 - 725	Rice husk	Pilot	725	0.45	[287]
	KC0.45 - 800	Rice husk	Pilot	800	0.45	[287]
KCA	KCA0.36	Cotton stalk	Bench	770	0.36	[307]
	KCA0.71	Cotton stalk	Bench	770	0.71	[307]
KCS	KCS0.25	Hazelnut shell	Bench	775	0.25	[307]
	KCS0.68	Hazelnut shell	Bench	775	0.68	[307]
KE	KE0.32	Rubber woodchip	Pilot	750	0.32	[315]
	KE0.36	Rubber woodchip	Pilot	770	0.36	[315]
	KE0.38	Rubber woodchip	Pilot	790	0.38	[315]
	KE0.41	Rubber woodchip	Pilot	810	0.41	[315]
	KE0.43	Rubber woodchip	Pilot	840	0.43	[315]
KP	KP0.19	Wood pellets	Pilot	775	0.19	[186]

Table 3.1 – (cont.).

Experiment reference		Biomass type	BFB Scale	T [ºC]	ER	Ref
KP	KP0.24	Wood pellets	Pilot	775	0.24	[186]
	KP0.27	Wood pellets	Pilot	775	0.27	[186]
	KP0.32	Wood pellets	Pilot	775	0.32	[186]
KWP	KWP0.19	Pistachio shell	Bench	770	0.19	[308]
	KWP0.37	Pistachio shell	Bench	770	0.37	[308]
KWS	KWS0.19	Walnut shell	Bench	770	0.19	[308]
	KWS0.37	Walnut shell	Bench	770	0.37	[308]
MC	MC0.25 - 670	Rice husk	Pilot	670	0.25	[309]
	MC0.25 - 700	Rice husk	Pilot	700	0.25	[309]
	MC0.25 - 665	Rice husk	Pilot	665	0.25	[309]
	MC0.30 - 744	Rice husk	Pilot	744	0.30	[309]
	MC0.30 - 750	Rice husk	Pilot	750	0.30	[309]
	MC0.30 - 766	Rice husk	Pilot	766	0.30	[309]
	MC0.35 - 811	Rice husk	Pilot	811	0.35	[309]
	MC0.35 - 822	Rice husk	Pilot	822	0.35	[309]
	MC0.35 - 828	Rice husk	Pilot	828	0.35	[309]
MM	MM0.18	*Miscanthus*	Pilot	750	0.18	[310]
	MM0.26	*Miscanthus*	Pilot	800	0.26	[310]
	MM0.27	*Miscanthus*	Pilot	750	0.27	[310]
	MM0.30	*Miscanthus*	Pilot	800	0.30	[310]
	MM0.31	*Miscanthus*	Pilot	850	0.31	[310]
	MM0.37	*Miscanthus*	Pilot	850	0.37	[310]
NS	NS0.26	Pine sawdust	Bench	800	0.26	[187]
	NS0.32	Pine sawdust	Bench	800	0.32	[187]
	NS0.36	Pine sawdust	Bench	790	0.36	[187]
	NS0.37	Pine sawdust	Bench	800	0.37	[187]
	NS0.47	Pine sawdust	Bench	810	0.47	[187]
SB	SB0.27	Sugarcane bagasse	Bench	800	0.27	[311]
SC	SC0.30	Rice husk	Pilot	850	0.30	[188]
	SC0.40	Rice husk	Pilot	860	0.40	[188]
	SC0.50	Rice husk	Pilot	870	0.50	[188]

Table 3.1 – (cont.).

Experiment reference		Biomass type	BFB Scale	T [ºC]	ER	Ref
SCT	SCT0.26	Bana grass	Bench	800	0.26	[311]
	SCT0.27	Bana grass	Bench	800	0.27	[311]
	SCT0.30	Bana grass	Bench	800	0.30	[311]
	SCT0.33	Bana grass	Bench	800	0.33	[311]
SF	SF0.30	Coir pith	Pilot	750	0.30	[188]
	SF0.40	Coir pith	Pilot	760	0.40	[188]
	SF0.50	Coir pith	Pilot	770	0.50	[188]
SP	SP0.25	Alfalfa pellets	Pilot	-	0.25	[312]
	SP0.30	Alfalfa pellets	Pilot	-	0.30	[312]
SS	SS0.30	Sawdust	Pilot	840	0.30	[188]
	SS0.40	Sawdust	Pilot	860	0.40	[188]
	SS0.50	Sawdust	Pilot	880	0.50	[188]
VC	VC0.20 - 750	Olive kernel	Bench	750	0.20	[313]
	VC0.20 - 800	Olive kernel	Bench	800	0.20	[313]
	VC0.20 - 850	Olive kernel	Bench	850	0.20	[313]
	VC0.30 - 750	Olive kernel	Bench	750	0.30	[313]
	VC0.30 - 800	Olive kernel	Bench	800	0.30	[313]
	VC0.30 - 850	Olive kernel	Bench	850	0.30	[313]
	VC0.40 - 750	Olive kernel	Bench	750	0.40	[313]
	VC0.40 - 800	Olive kernel	Bench	800	0.40	[313]
	VC0.40 - 850	Olive kernel	Bench	850	0.40	[313]
XM	XM0.23	*Miscanthus*	Pilot	639	0.23	[314]
	XM0.26	*Miscanthus*	Pilot	645	0.26	[314]
	XM0.28	*Miscanthus*	Pilot	693	0.28	[314]
	XM0.37	*Miscanthus*	Pilot	723	0.37	[314]

Table 3.2 – Proximate and ultimate analysis of the biomass used for the models development.

	% wt, daf					% wt, db	
Biomass	C	H	N	S	O	Ash	Reference
CEM							
Cellulose ($C_6H_{10}O_5$)	44.45	6.22	0.00	0.00	49.34	-	-
Lignin	63.77	5.99	0.27	0.32	29.45	-	[289]
Miscanthus	49.20	6.00	0.40	0.15	44.20	3.00	[316]
Rice husk	49.30	6.10	0.80	0.08	43.70	18.00	[316]
RFB from eucalyptus	49.66	6.53	0.07	0.00	43.74	1.19	[4]
Empirical model							
Alfalfa pellets	50.10	5.90	2.88	0.30	40.88	16.98	[312]
Bana grass	49.33	5.54	0.46	0.17	43.89	4.50	[311]
Coir pith	47.18	3.60	1.01	0.01	48.20	6.00	[188]
Cotton stalk	52.80	5.62	1.00	0.18	40.71	6.91	[307]
Hazelnut shell	56.96	5.05	0.43	0.13	37.42	2.60	[307]
Miscanthus-1	44.50	5.20	5.30	0.00	45.00	-	[310]
Miscanthus-2	47.63	6.19	0.40	0.00	45.78	4.47	[314]
Olive kernel	48.59	5.73	1.57	0.05	44.06	2.17	[313]
Pine sawdust	50.42	5.75	0.20	0.03	44.47	0.85	[187]
Pistachio shell	50.03	5.93	0.40	0.10	43.55	0.27	[308]
RFB from eucalyptus-1	47.08	6.29	0.36	0.00	46.00	2.60	[4]
RFB from eucalyptus-2	49.66	6.53	0.07	0.00	43.74	1.19	[4]
RFB from pine	51.42	6.58	0.25	0.01	41.75	1.20	[4]
Rice husk-1	45.41	7.23	4.11	0.01	43.24	19.40	[229]
Rice husk-2	47.00	6.78	0.48	0.04	45.70	20.00	[309]
Rice husk-3	49.07	3.79	0.63	0.01	46.42	21.68	[287]
Rice husk-4	38.92	5.10	2.17	0.12	53.69	19.33	[188]
Rubber woodchip	46.40	5.70	0.20	0.00	47.70	1.10	[315]
Sawdust	51.33	6.13	0.12	0.02	41.97	1.80	[188]
Softwood pellets	54.61	5.83	0.00	0.03	39.53	0.57	[185]
Straw pellets	52.86	6.11	0.82	0.14	40.07	6.32	[185]
Sugarcane bagasse	49.15	5.59	0.13	0.05	45.01	5.80	[311]
Torrefied woodchips	58.77	5.53	0.15	0.01	35.50	0.18	[185]
Walnut shell	54.84	5.50	0.44	0.12	39.10	1.95	[308]
Wood pellets-1	47.65	6.22	0.09	0.00	46.04	0.32	[4]
Wood pellets-2	51.02	7.16	0.09	0.00	41.73	0.80	[186]

The database information was processed for equivalent units and basis, namely: i) biomass composition was expressed by mass fractions in dry ash-free fuel basis (C,H,O,N,S, kg i/kg daf fuel) and by mass fractions in dry basis (ash content, kg ash/kg dry fuel), ii) gas composition was

expressed in volumetric dry basis (%v, dry gas). Conversions between basis were performed as deemed necessary. The recorded data comprises the following parameters:

1. Biomass feedstock characteristics:
    a. Category (woody or non-woody) and type (miscanthus, rice husk, wood pellets, sawdust, bagasse, etc.,).
    b. Elemental composition (C,H,N,O,S).
    c. Ash content.
2. BFB characteristics and operating parameters:
    a. Scale (bench or pilot).
    b. Average bed temperature (600-880 ºC).
    c. ER (0.17-0.71).
3. Experimental results:
    a. PG composition (CO_2, CH_4, CO and H_2).
    b. PG LHV.
    c. Efficiency parameters (Y_{gas}, CGE and CCE).

Additional operating parameters, such as the fluidization velocity, residence time of gases and biomass, particle size of the biomass or heat supply, were not considered for the empirical model development because they are seldom detailed in the literature. Furthermore, the CEM approach, whose comparison with empirical modelling was the main focus of this work, only requires the knowledge of the feedstock and gasifying agent composition and the definition of the temperature, pressure and most common products. Accordingly, the strict CEM approach is a function of these parameters and is independent of the reactor design, and its hydrodynamics.

The methodologies used in the studies organized in this database were also briefly addressed for comparison purposes. In the analyzed literature, distinct measurement techniques are referred for determining the PG composition, for example infrared analysis for determination of CO, CO_2 and CH_4 concentration, thermal conductivity measurement for determination of H_2 concentration and paramagnetic analysis for determination of O_2 concentration [4,185,307,311]. N_2 concentration determination by mass balance is referred in some works [4,123,185,307]. Collection of gas samples in sampling bags, such as *Flexfoil* bags [4], with the objective of determining the PG composition (H_2, CO_2, CO, CH_4, etc.,) in GC-TCD equipment is also commonly referred [4,123,287,311,312,314]. Chemiluminescence analysis for detection of nitrogen oxides as NO was referred by one author [311]. The flow rate of the PG is determined by mass flow meters by some authors, such as Coriolis mass flow meters [314], and by calculation methodologies by other authors, namely nitrogen mass balances [4,123,312]. Regarding the necessary PG conditioning measures for sampling and equipment analysis, it is commonly referred tar condensation and particle removal by moisture traps, impinger bottles filled with isopropanol, ceramic filters, among other equipment [4,313,314].

Some parameters were not reported in all the analyzed studies; thus, their determination was performed as necessary when the required data was available. The LHV of the distinct types of biomass was determined according to the correlation developed by Parikh et al., [12]. The LHV of the PG and the process efficiency parameters (Y_{gas}, CGE and CCE) were determined based on the methodology explained in Section 1.4. Some deviations can occur due to some authors including other combustible gaseous species in the LHV calculation formula (e.g., propane). In this work, the gaseous species considered for the determination of the LHV were CO, H_2, CH_4 and C_2H_4. The reasoning behind this consideration results from the concentration of other minor components (e.g., propane) seldom being available in the published works and their abundance being relatively low, consequently presenting low contribution to the LHV value.

The CEM was developed considering the biomass and gasifying agent composition (CHNOS) and the chemical products of the process containing these elements; the products selected are the most commonly reported in biomass gasification processes. Other minor elements, such as Chlorine, were not considered. Thus, a total of 13 compounds in the products of gasification were considered: N_2, H_2O, CO_2, CO, O_2, H_2, CH_4, C_2H_4, C_2H_6, C_3H_8, H_2S, SO_2 and unconverted solid

carbon ($C_{(s)}$). All products were assumed to act as ideals gases, except for $C_{(s)}$. Steady state conditions of operation were assumed. Tar formation was neglected and ash in the feedstock was assumed to be inert. All the reactants were assumed to enter and leave the reactor at process temperature. The process temperature is assumed as homogeneous inside the gasifier, which is a common procedure in other non-stoichiometric thermodynamic models [13]. Hydrodynamics and kinetics were not considered. More information about the methodology employed for the development of the CEM can be found in Section 1.4.

The CEM was applied to calculate the composition of the PG for distinct direct (air) gasification parameters. Then, the respective efficiency parameters were calculated based on the obtained compositions. The software tool used for the model development was GASEQ (http://www.gaseq.co.uk/). The following parameters were used as input in the model:

- Feedstock: RFB from eucalyptus, rice husk, *miscanthus*, cellulose ($C_6H_{10}O_5$) and lignin (Table 3.2).
- Bed temperature: 600 ºC, 700 ºC, 800 ºC and 900 ºC.
- ER: 0 (pyrolysis), 0.10, 0.20, 0.25, 0.30 and 0.40.
- Pressure: 1 atm.

The compiled experimental database and the CEM predictions were analyzed using multiple regression tools in Microsoft Excel according to the methodologies described in Section 1.4. This type of regression describes the relationship between the analyzed data and outputs functions for the determination of process parameters. Linear empirical and CEM correlations were developed due to finding similar coefficients of determination (R-Squared and adjusted R-Squared) for distinct regressions (e.g., linear, polynomial) for the experimental and CEM data. Thus, linear correlations were adopted due to their simplicity and easier interpretation. The prediction capability of the correlations was briefly addressed by comparison with experimental biomass gasification data obtained in an 80kWth BFB direct (air) gasifier. Pearson's correlation test was used to measure the strength of the correlation between two variables. It must be noted that correlation does not imply causation [14]. PCC was determined between inputs and outputs for both experimental and CEM results and between actual and predicted outputs for both empirical and CEM correlations.

3.1.4 EXPERIMENTAL AND CEM RESULTS COMPARISON

In this Section, the experimental results reported in the literature and the CEM predictions are compared, and correlations based on these data were developed and evaluated. The objective of these correlations is to serve as simple and immediate tools for determining first estimates of gasification products. The main parameters of the gasification process were considered, namely the reactor bed temperature and ER. The comparison between reported experimental results and CEM predictions is performed for similar operating conditions: ER between 0.20 and 0.40 and bed temperature between 600 and 900 ºC. Accordingly, both empirical and CEM correlations were developed for those conditions. Reported experimental results with other conditions and CEM predictions for pyrolysis conditions (ER=0) and gasification under unsuitable low ER (ER=0.10) are shown for comparison purposes, but not used in the correlations development. The CEM results for lignin and cellulose were not included in the correlations development and are analyzed separately. Pearson's correlation test was performed to measure the strength of the correlation between operating parameters and results.

3.1.4.1 PROPERTIES OF THE PG

3.1.4.1.1 Combustible gases yield (H_2, CO and CH_4)

The influence of the reactor bed temperature and ER in the hydrogen concentration in the PG is shown in Figure 3.1. For similar operating conditions, the experimental H_2 results (2.0 to 24.0 %v) are lower than those predicted by the CEM (12.9 and 29.1 %v). Furthermore, the relation between H_2 concentration and reactor bed temperature or ER is distinct for both CEM and experimental results. The CEM shows that H_2 concentration is dependent on the employed ER, while the experimental results do not show any evident relation for both ER and temperature. Accordingly, PCC was found close to -1 for the relation of H_2 concentration and ER in the CEM results (Table 3.3). These differences may be justified by the impact of other parameters that were not analyzed in this work and are not related to chemical equilibrium, e.g., the physical properties of the biomass feedstock.

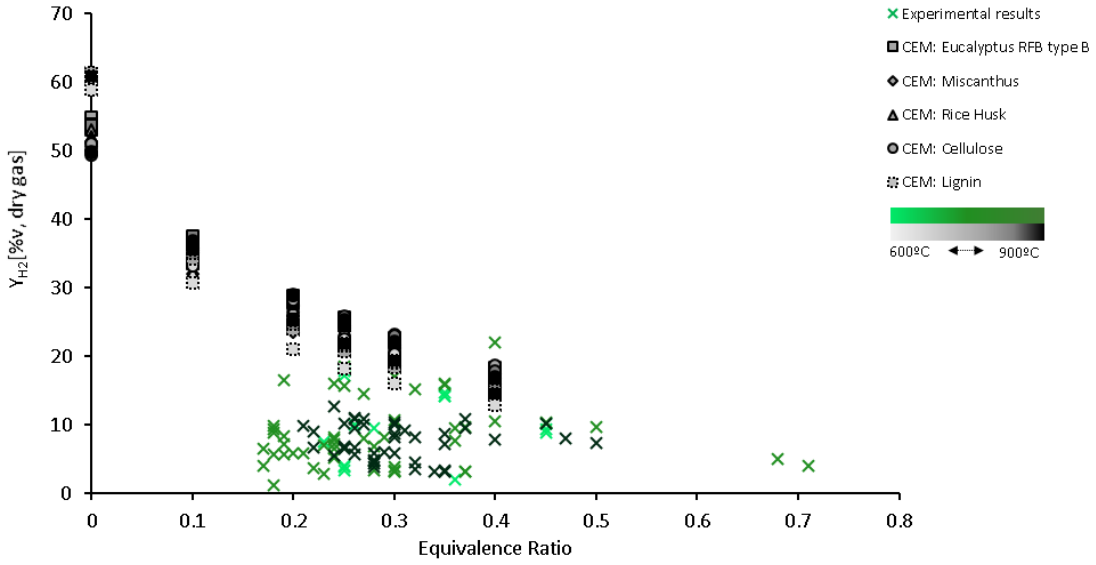

(a)

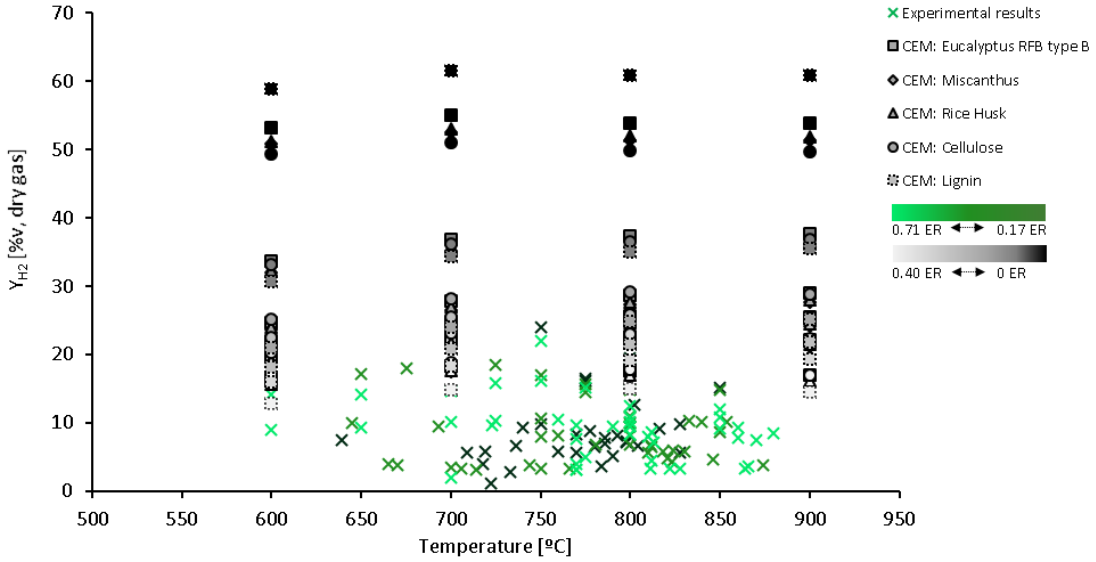

(b)

Figure 3.1 – Influence of the ER (a) and bed temperature (b) on the H_2 concentration in the PG for the experimental results reported in the literature and CEM results.

For pyrolysis conditions (ER=0) and gasification conditions with ER=0.10, the CEM results show H_2 concentration values between 32.0 and 54.9 %v for the range of temperatures considered (600 ºC to 900 ºC). Thus, higher production of H_2 is expected for pyrolysis conditions and gasification conditions with lower ER than that typically employed in practical gasifiers. The maximum value of H_2 concentration was found for pyrolysis of RFB from eucalyptus (T=700 ºC).

The CEM results for lignin conversion indicate higher H_2 concentration values in the PG than those predicted for the biomass feedstocks studied (miscanthus, rice husk and RFB from eucalyptus), predicting a maximum of 61.4 %v for pyrolysis condition (T=700 ºC, Figure 3.1).

Table 3.3 – PCC values for the correlation between operating conditions (temperature (T) and ER) and the PG composition (H_2, CO and CH_4), LHV, Y_{gas}, CGE and CCE, for the experimental results reported in the literature and CEM predictions.

	H_2		CO		CH_4		LHV		Y_{gas}		CGE		CCE	
PCC	Exp	CEM	Exp	CEM	Exp	CEM	Exp	CEM	Exp	CEM	Exp	CEM	Exp	CEM
T	-0.2	0.2	-0.4	0.8	0.2	-0.9	-0.2	0.6	0.3	0.4	-0.2	0.8	0.0	0.8
ER	0.0	-0.9	-0.3	-0.4	-0.4	-0.3	-0.5	-0.7	0.5	0.7	0.1	-0.3	0.3	0.3

*- Exp refers to the experimental results reported in the literature; CEM refers to the chemical equilibrium model predictions.

In Figure 3.2, it is observed that the CO concentration values predicted by the CEM are higher than the CO concentration values found in the experimental results. For similar operating conditions, experimental results show CO concentration values between 7.2 and 26.6 %v, while the CEM results show CO concentration values between 11.3 and 38.6%v. Furthermore, the CEM results show that CO concentration increases significantly with temperature increase, which is a phenomenon not observed in the experimental results (Figure 3.2 (b)). The PCC value for the relation between the predicted CO concentration value in the CEM and the process temperature is close to 0.8, showing positive correlation between these variables (Table 3.3). On the other hand, the PCC value for the relation between the CO concentration value found in the experimental results and the process temperature is close to -0.4, showing a slightly negative correlation. The reasoning behind this difference may be associated to the fact that in practical autothermal direct (air) gasifiers, the increase of bed temperature is associated to the increase of ER, which is known to lower CO concentration in the PG. In fact, in the developed database in the present work, the average ER for experimental studies with bed temperature above 800 ºC is 0.32 (Table 3.1). Nonetheless, it is observed a similar tendency for the decrease of CO with the increase of ER in both experimental and CEM results (Figure 3.2 (a)).

Analogous to the observations previously made regarding H_2 concentration, higher concentration values of CO were predicted by the CEM for pyrolysis conditions and gasification with ER=0.10. For these conditions, the CEM results show CO concentration values between 13.8 and 47.3 %v, with the maximum value found for the pyrolysis of miscanthus at 900 ºC. Nonetheless, a higher CO concentration value (49.21 %v) was predicted for the pyrolysis of cellulose at 900 ºC.

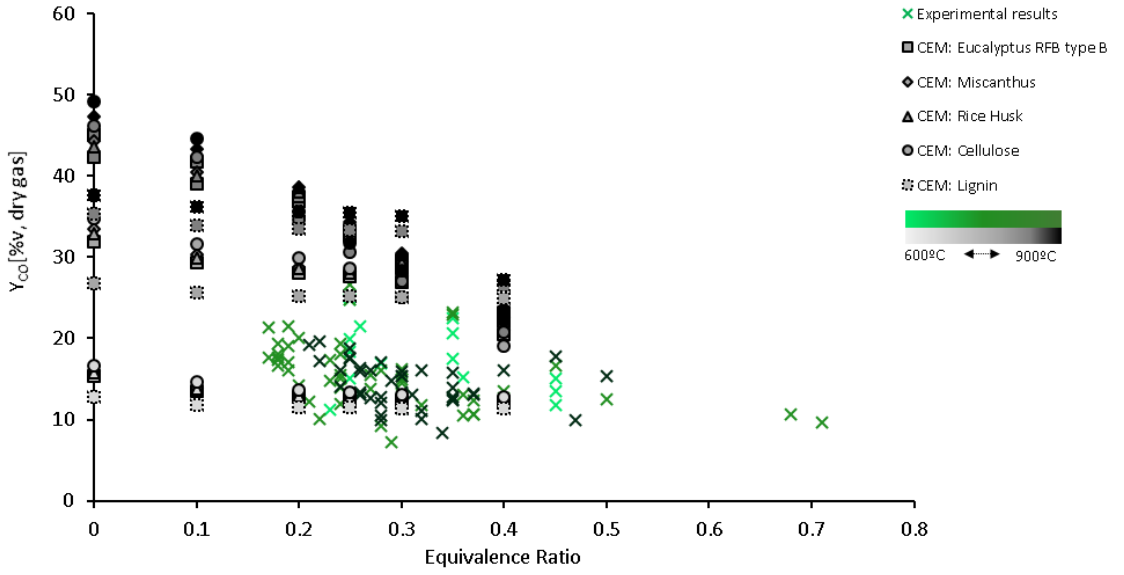

(a)

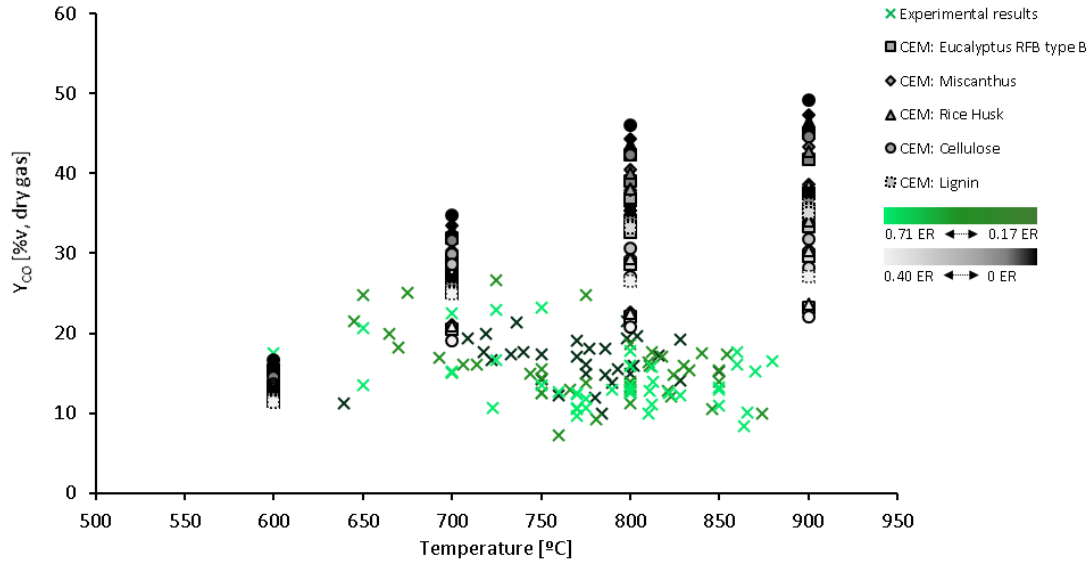

(b)

Figure 3.2 – Influence of the ER (a) and bed temperature (b) on the CO concentration in the PG for the experimental results reported in the literature and CEM results.

In contrast to the observations made regarding the concentration of CO and H_2, the concentration of CH_4 is typically higher in the reported experimental results than in the CEM results (Figure 3.3). For similar operating conditions, experimental results show CH_4 concentration between 0.7 and 8.4 %v, while the CEM results show CH_4 concentration between 0.0 and 2.6 %v. A similar negative correlation between CH_4 concentration and ER is observed in both experimental and CEM results (Figure 3.3 (a)). However, CEM results shows a significant decrease of CH_4 concentration with temperature increase, which is not observed in the experimental results (Figure 3.3 (b)). The determined PCC values are in accordance with this analysis (Table 3.3).

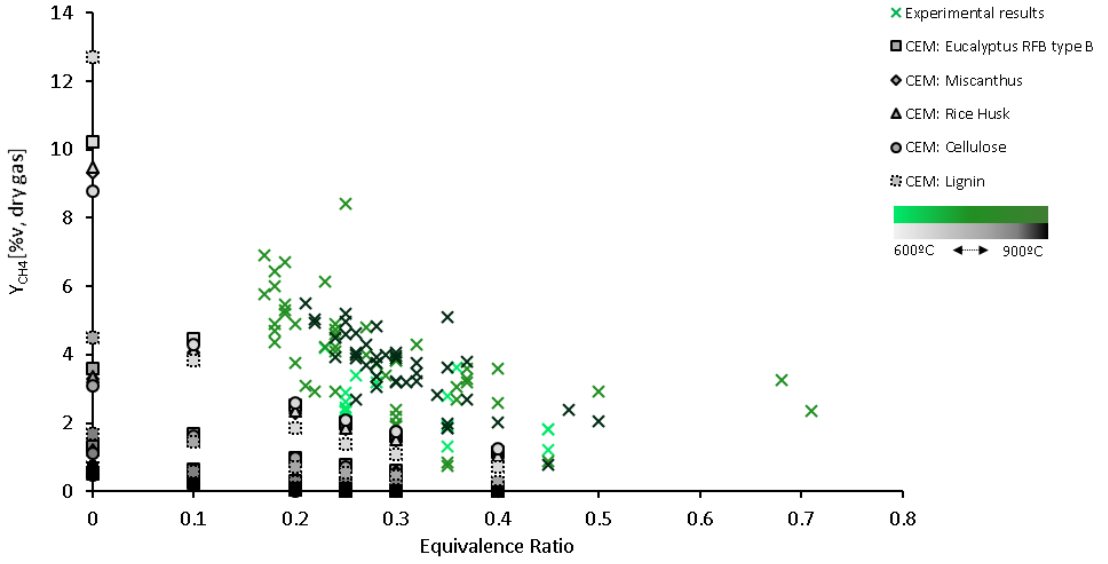

(a)

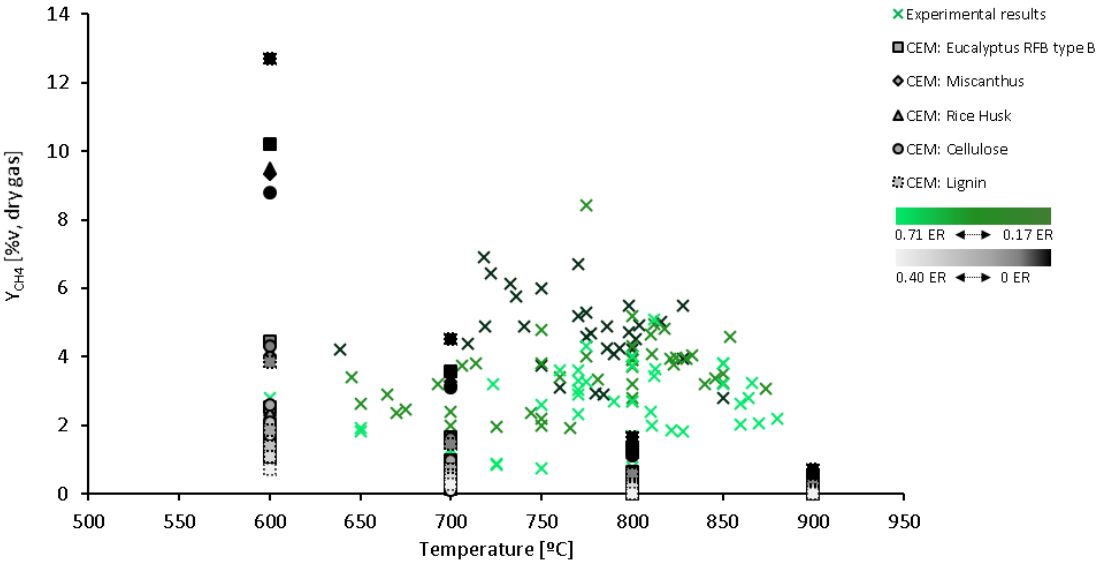

(b)

Figure 3.3 – Influence of the ER (a) and bed temperature (b) on the CH_4 concentration in the PG for the experimental results reported in the literature and CEM results.

CEM results for biomass pyrolysis conditions shows CH_4 concentration values between 0.3 and 10.2 %v, with the highest value predicted for the pyrolysis of RFB from eucalyptus at 600 ºC; this concentration value is higher than the values typically found in the experimental results analyzed. Furthermore, CEM results for lignin conversion show even higher values of CH_4 concentration, attaining a maximum value of 12.7 %v for pyrolysis conditions at 600 ºC (Figure 3.3).

The developed empirical correlations based on experimental results reported in the literature (Equations 3.1, 3.2 and 3.3) show a significantly lower R^2 and observable deviations from the correlations developed using the CEM results (Equations 3.4, 3.5 and 3.6). This shows the high variability of the values reported in the literature regarding the composition (e.g., H_2, CO and CH_4) of the PG obtained in biomass direct (air) gasification processes in BFB reactors, and their significant differences from chemical equilibrium predictions, for similar operating conditions.

$$Y_{H_2,exp} = -0.01564 \times T - 0.65738 \times \text{ER} + 21.45107 \quad \text{(Equation 3.1)}$$

$$R^2 = 0.04$$

$$Y_{CO,exp} = -0.02735 \times T - 15.3379 \times \text{ER} + 41.0061 \quad \text{(Equation 3.2)}$$

$$R^2 = 0.23$$

$$Y_{CH_4,exp} = 0.005132 \times T - 9.99971 \times \text{ER} + 2.401523 \quad \text{(Equation 3.3)}$$

$$R^2 = 0.26$$

$$Y_{H_2,eq} = 0.008173 \times T - 49.5472 \times \text{ER} + 30.2562 \quad \text{(Equation 3.4)}$$

$$R^2 = 0.93$$

$$Y_{CO,eq} = 0.060842 \times T - 47.7011 \times \text{ER} - 6.70893 \quad \text{(Equation 3.5)}$$

$$R^2 = 0.79$$

$$Y_{CH_4,eq} = -0.00563 \times T + -2.91807 \times \text{ER} + 5.6700002 \quad \text{(Equation 3.6)}$$

$$R^2 = 0.81$$

3.1.4.1.2 Gas phase products yield ratios

The relation between H_2:CO molar ratios and the temperature and ER is shown in Figure 3.4. This ratio is relevant for the configuration of gasification processes for production of fuel gas for advanced applications that require specific H_2:CO molar ratios, such as methanol production (2 mol.mol^{-1}), synthetic fuels production through FT synthesis (0.6 mol.mol-1) and DME production (1 mol.mol^{-1}) [72,180–182]. Figure 3.4 shows that the H_2:CO molar ratios for the CEM results are typically higher than the H_2:CO ratios found in the experimental results. This is a consequence of the H_2 experimental yield being further away from equilibrium than the CO experimental yield, as observed in the previous Section.

For similar operating conditions, the H_2:CO molar ratio was found between 0.1 and 1.7 for the experimental results, which is in accordance with typical values referred for gasification processes in BFBs [72], and between 0.7 and 1.9 for the CEM results. Thus, concerning H_2:CO molar ratio requirements, it can be observed that the PG from direct (air) gasification in BFB might be potentially used for FT synthesis but need further refinement to be used in other advanced applications, such as methanol synthesis. CEM results for pyrolysis conditions and gasification with ER=0.10 show higher H_2:CO molar ratios, namely between 0.8 and 3.5, with the maximum value observed for the pyrolysis of RFB from eucalyptus at 600 ºC. Furthermore, CEM results for lignin conversion show an even higher H_2:CO molar ratio, with a maximum value of 4.6 predicted for lignin pyrolysis at 600 ºC (Figure 3.3).

In Figure 3.3 (a), it can be observed a tendency for the decrease of the H_2:CO molar ratio with the increase of ER for the CEM results, which is not observed in the experimental results. Furthermore, in the CEM results, it is also observed a significant decrease of this molar ratio with temperature increase, which is not observed in the analyzed experimental results (Figure 3.3 (b)). A decrease of H_2:CO molar ratio with temperature increase has also been discussed in the literature [317] and can be justified by the occurrence of the exothermic WGS reaction (Reaction 2.8) thus, high temperatures do not favor the CO conversion rate, leading to lower H_2:CO molar ratio values [317].

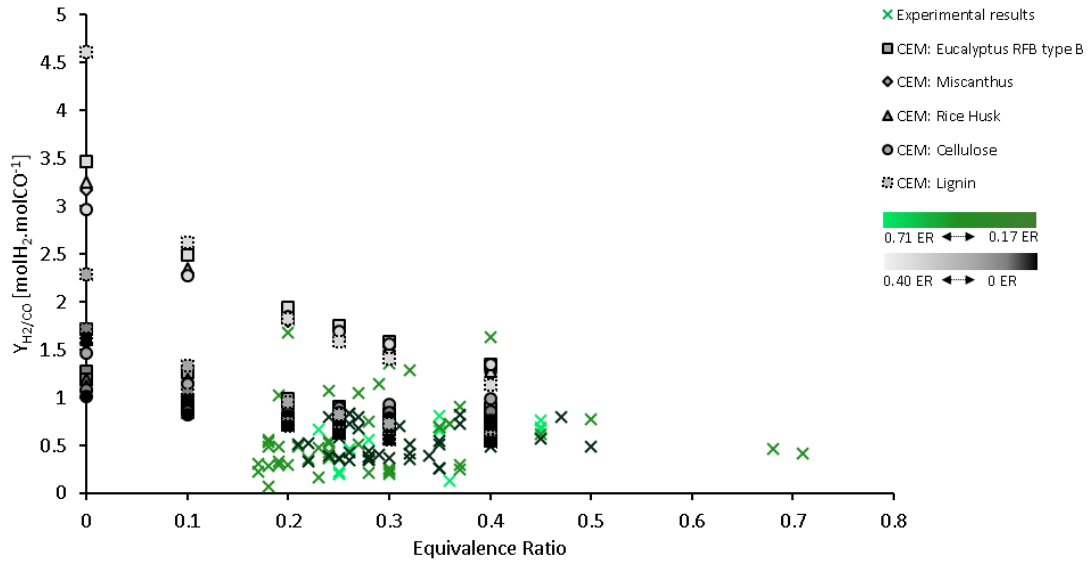

(a)

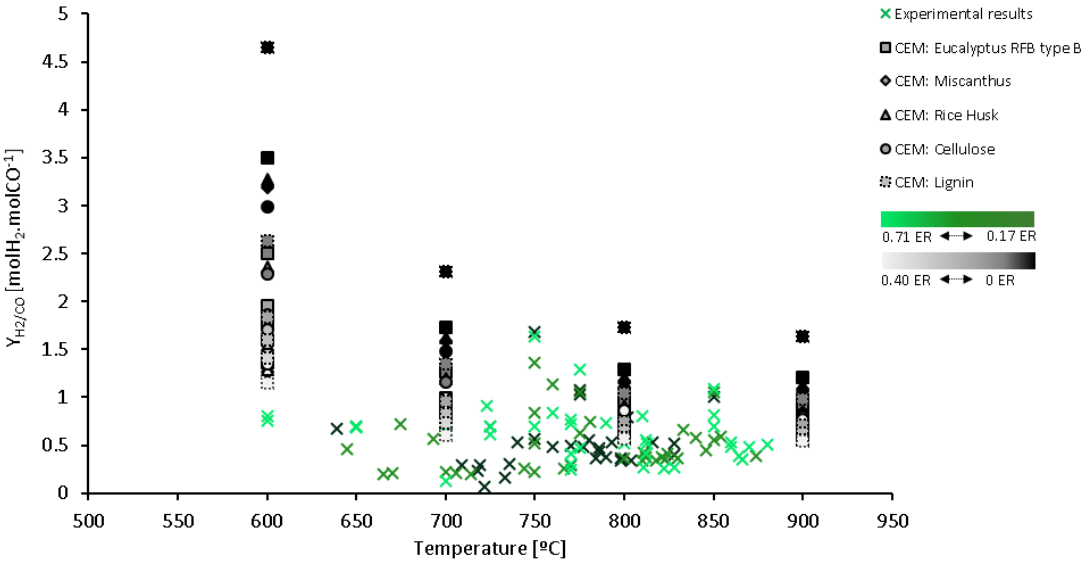

(b)

Figure 3.4 – Influence of the ER (a) and bed temperature (b) on the H_2:CO molar ratio in the PG for the experimental results reported in the literature and CEM results.

The CO:CO_2 molar ratio is shown in Figure 3.5, and although this ratio is not commonly referred in the literature, it can be used as an indicator of the efficiency of the process and the balance between the occurrence of gasification/combustion reactions [318]. It can be noticed that the experimental CO:CO_2 molar ratio values are significantly lower than the ones predicted by the CEM (Figure 3.5). For similar operating conditions, experimental results show CO:CO_2 molar ratios between 0.6 and 2.1, while CEM results show CO:CO_2 molar ratios between 0.7 and 22.1. Furthermore, CEM results show higher CO:CO_2 molar ratios, between 0.7 and 84.7, for pyrolysis and gasification with ER=0.10, with the maximum value obtained for gasification of RFB from eucalyptus at ER=0.10 and 900 ºC.

The influence of ER and bed temperature on the experimental CO:CO_2 molar ratios is not evident (Figure 3.5). On the other hand, the CEM results show that there is an increase of this molar ratio with temperature increase and ER decrease. For similar operating conditions, it is also observed

that biomass with higher total carbon content typically leads to higher $CO:CO_2$ molar ratio in the PG for both CEM and experimental results. The reasoning behind this phenomenon may be related to a higher occurrence of carbon gasification by CO_2 (Boudouard reaction, Reaction 2.5).

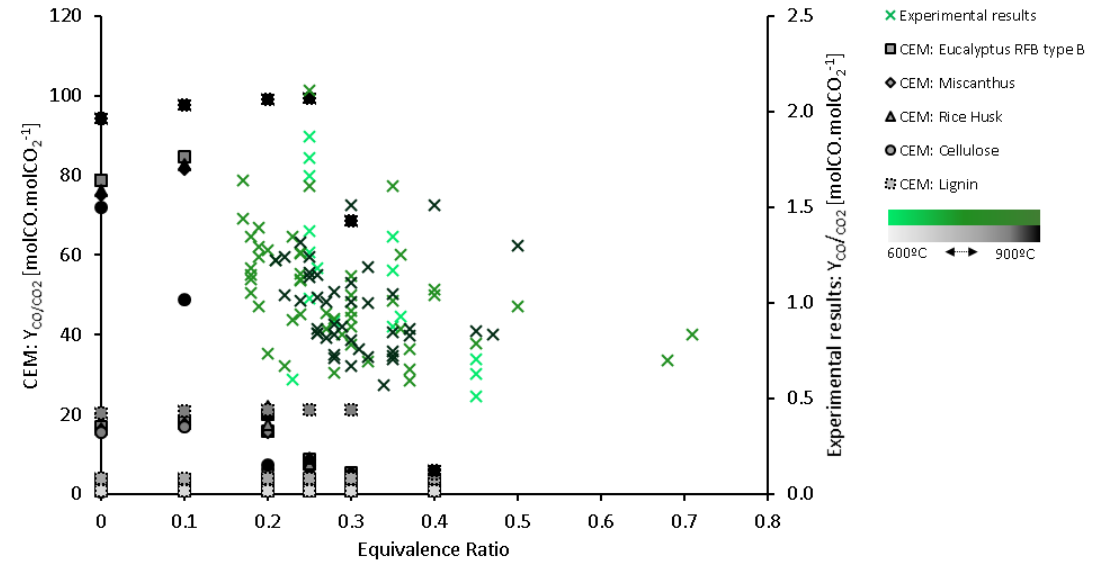

(a)

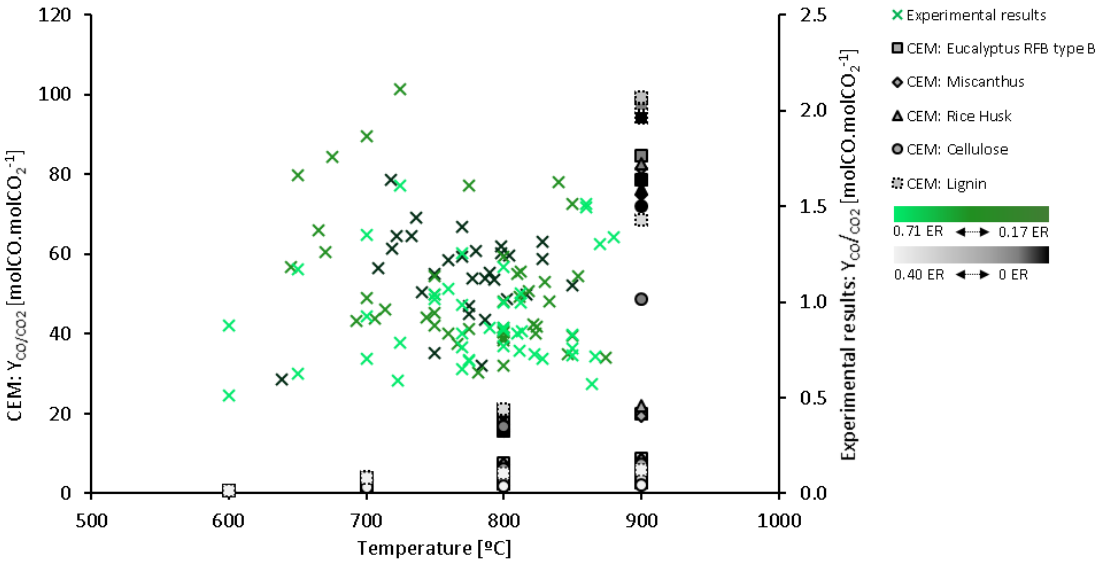

(b)

Figure 3.5 – Influence of the ER (a) and bed temperature (b) on the $CO:CO_2$ molar ratio in the PG for the experimental results reported in the literature and CEM results.

3.1.4.2 PROCESS EFFICIENCY PARAMETERS

3.1.4.2.1 LHV and Y_{gas}

The LHV of the PG for the experimental results reported in the literature and CEM results is shown in Figure 3.6. It is observed that the experimental LHV values are slightly lower than the LHV values predicted by the CEM. For similar operating conditions, the experimental and CEM results show LHV between 2.4 and 7.8 MJ/Nm^3 and between 3.6 and 7.9 MJ/Nm^3, respectively. Pyrolysis conditions and gasification with ER=0.10 show a higher LHV, namely between 6.7 and

11.7 MJ/Nm^3, with the maximum value obtained for the pyrolysis of RFB from eucalyptus at 900 ºC. For lignin conversion, an even higher LHV value (12.5 MJ/Nm^3), is observed in the CEM results for pyrolysis conditions and 600 ºC.

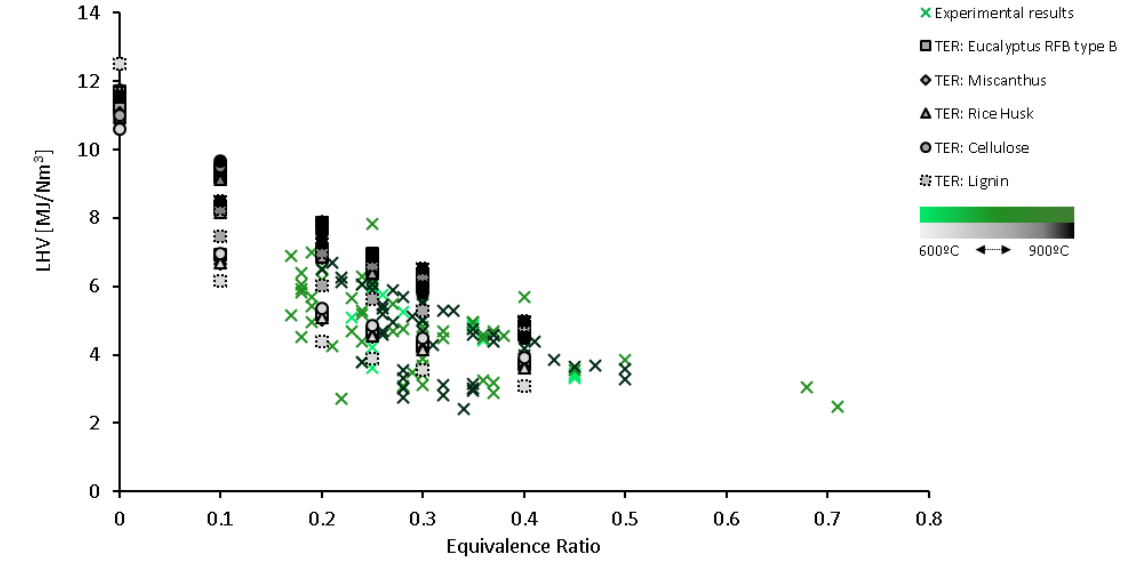

(a)

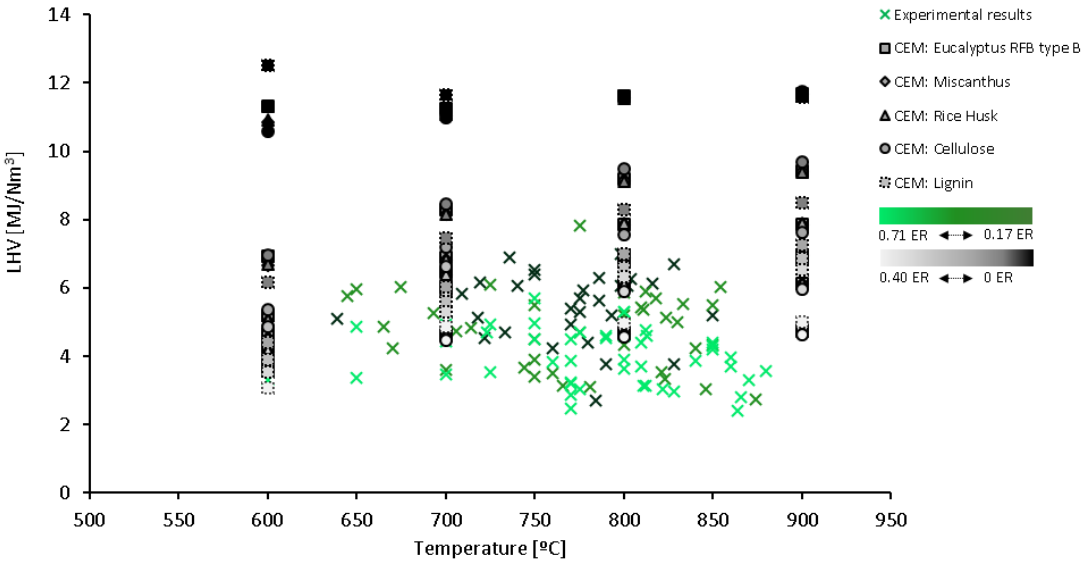

(b)

Figure 3.6 – Influence of the ER (a) and bed temperature (b) on the LHV of the PG for the experimental results reported in the literature and CEM results.

Regarding the variation of LHV with the operating parameters, there is an evident trend for the decrease of LHV with ER increase for both experimental and CEM results (Figure 3.6 (a)). The influence of temperature on LHV is not evident for the experimental results (Figure 3.6 (b)). For the CEM results, there is an observable tendency for the increase of LHV with temperature increase. PCC values are in concordance with this analysis and indicate that the CEM results present less dispersion (Table 3.3). Accordingly, the empirical correlation (developed based in experimental data) for LHV (Equation 3.7) presents a lower R^2 value than the correlation developed based in the CEM results (Equation 3.8).

$$LHV_{exp} = -0.00299 \times T + -8.87018 \times \mathrm{ER} + 9.637507 \qquad \text{(Equation 3.7)}$$

$$R^2 = 0.24$$

$$LHV_{eq} = 0.006549 \times T + -12.4161 \times \mathrm{ER} + 4.339622 \qquad \text{(Equation 3.8)}$$

$$R^2 = 0.85$$

The Y_{gas} for both experimental and CEM results is shown in Figure 3.7. For similar operating conditions, the experimental and CEM results show Y_{gas} values between 1.2 and 3.5 Nm^3/kg biomass db and 1.4 and 2.9 Nm^3/kg biomass db, respectively. CEM results for pyrolysis conditions and gasification with unusually low ER (ER=0.10), show significantly lower Y_{gas}, namely between 0.6 and 1.8 Nm^3/kg biomass db. Nonetheless, the maximum Y_{gas} value (3.7 Nm^3/kg biomass db) was found in the CEM results for lignin gasification with ER=0.40 and 800 ºC. In the experimental results, a higher Y_{gas} value is referred in the literature, namely 4.1 Nm^3/kg biomass db during gasification of sawdust with ER=0.50 and T=880 ºC [188]. However, these conditions are not suitable for typical direct (air) biomass gasification processes in BFB reactors due to the high ER employed, which leads to excessive combustion and low PG quality.

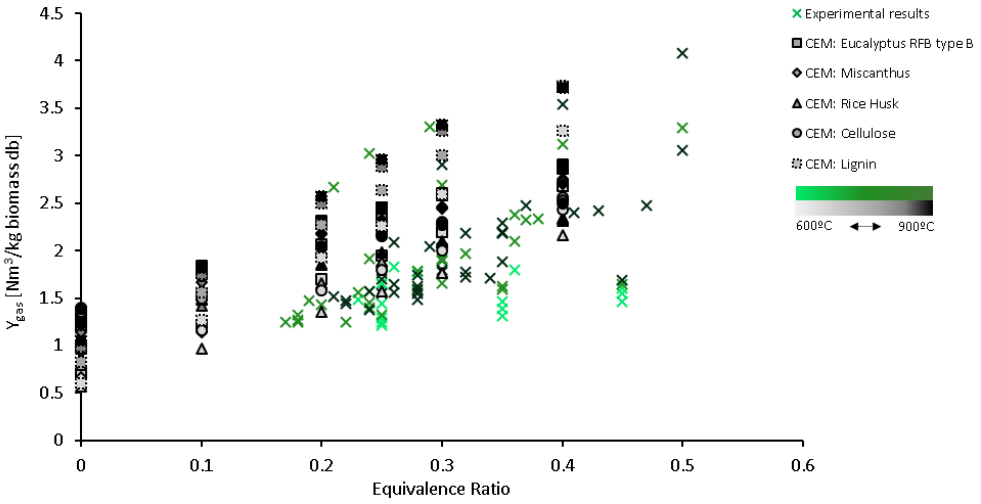

(a)

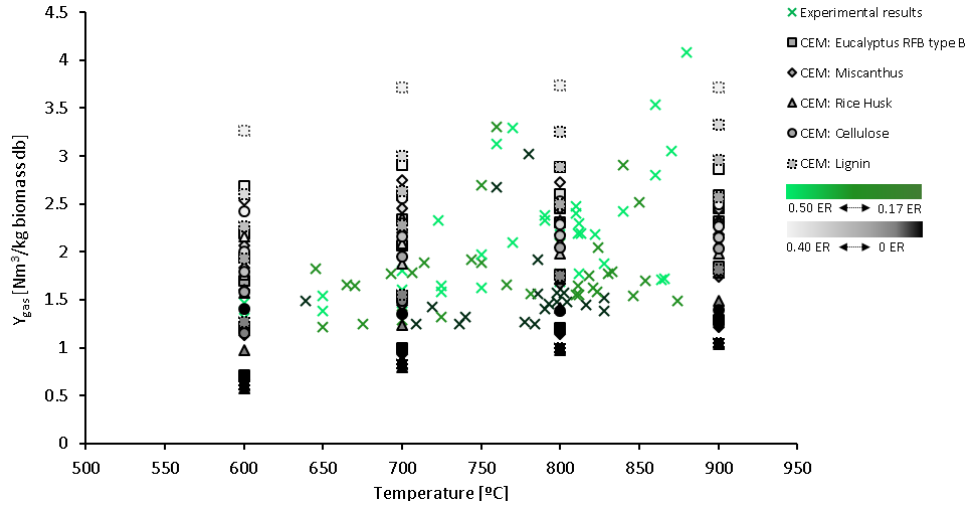

(b)

Figure 3.7 – Influence of the ER (a) and bed temperature (b) on the Y_{gas} for the experimental results reported in the literature and CEM results.

In Figure 3.7 (a), it can be observed an evident tendency for the increase of Y_{gas} with the ER for both experimental and CEM results. This can be explained by the higher ratio of gasifying agent per unit of biomass, which results directly from the increase of ER. A slight positive tendency is also observed between Y_{gas} and temperature increase, for both experimental and CEM results (Figure 3.7 (b)). Accordingly, the developed empirical and CEM correlations for Y_{gas} determination (Equations 3.9 and 3.10) present closer R^2 values than the correlations developed for other parameters.

$$Y_{gas,exp} = 0.001936 \times T + 4.630323 \times \text{ER} - 0.97472 \qquad \text{(Equation 3.9)}$$

$$R^2 = 0.30$$

$$Y_{gas,eq} = 0.001246 \times T + 3.400375 \times \text{ER} + 0.31634 \qquad \text{(Equation 3.10)}$$

$$R^2 = 0.62$$

3.1.4.2.2 CGE and CCE

The CGE and CCE are parameters typically used in the literature to evaluate the efficiency of biomass gasification processes [4,123].

Regarding CGE, the experimental results show significantly lower values than the CEM predictions (Figure 3.8). For biomass gasification processes under similar operating conditions, CGE values are between 23.5 and 78.8 % for experimental results and between 45.1 and 98.7 % for CEM results. The CEM results for pyrolysis conditions and gasification with unsuitable low ER (ER=0.10) show lower CGE values, namely between 24.8 and 93.6 %. Nonetheless, a maximum CGE value of 105.9 % was predicted by the CEM for cellulose gasification with ER=0.10 at 900 ºC; this value means that the PG has higher energy content than the initial biomass, which is not possible according to the laws of thermodynamics. This inconsistency may be related to the equation used to estimate the LHV of the distinct biomass types [12] (see Section 3.1.3).

The CEM results show a tendency for the increase of CGE with temperature increase, whereas no clear tendency is observed in the experimental results (Figure 3.8 (b)). No evident tendency is observed between CGE and ER for both experimental and CEM results (Figure 3.8 (a)). This may be related to the fact that low ER favor the concentration of combustible gases in the PG but also favor a decrease in gas production, thus creating a trade-off between these parameters, as it has been previously suggested by the authors [4]. Accordingly, PCC values for the relation between CGE and the operating parameters typically indicate high dispersion (Table 3.3), except for the PCC value found for the relation between the CGE predicted by the CEM and the process temperature (0.8). Thus, the developed empirical correlation (Equation 3.11) presents a significantly lower R^2 value than the correlation developed based on CEM results (Equation 3.12).

$$CGE_{exp} = -0.03761 \times T + 15.64463 \times \text{ER} + 73.98776 \qquad \text{(Equation 3.11)}$$

$$R^2 = 0.06$$

$$CGE_{eq} = 0.12096 \times T + -59.3921 \times \text{ER} + 0.916735 \qquad \text{(Equation 3.12)}$$

$$R^2 = 0.71$$

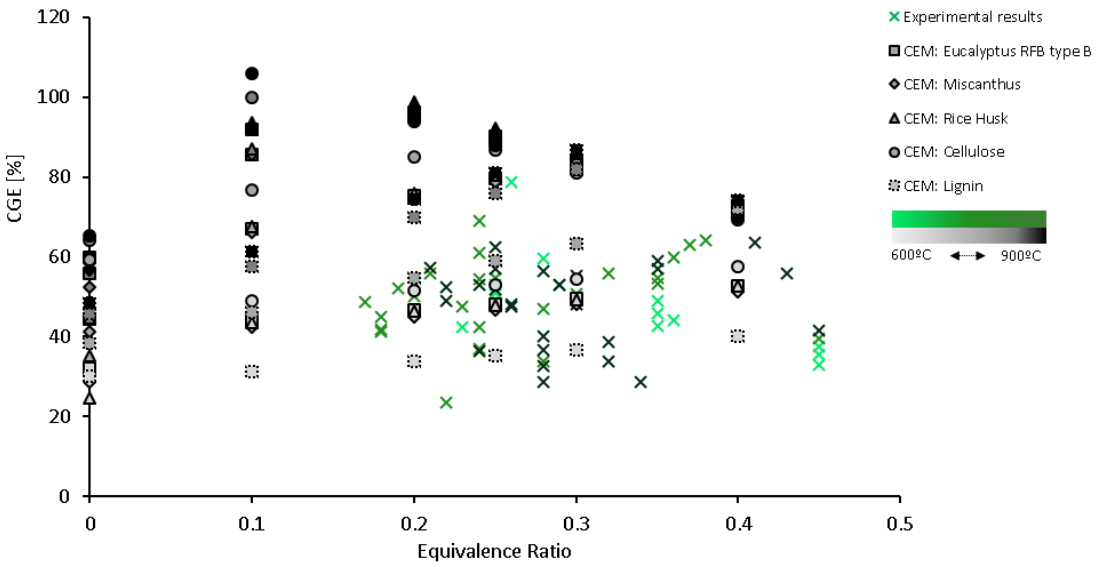

(a)

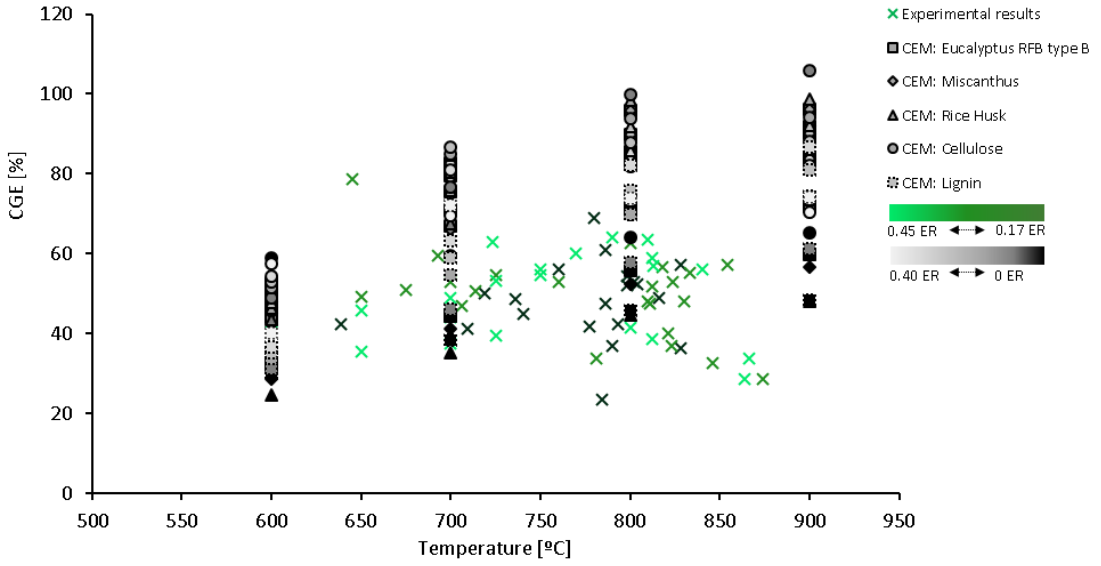

(b)

Figure 3.8 – Influence of the ER (a) and bed temperature (b) on the CGE for the experimental results reported in the literature and CEM results.

The influence of temperature and ER in the CCE, for both CEM and experimental results, is shown in Figure 3.9. For biomass gasification under similar operating conditions, the experimental and CEM results show similar values for CCE, namely between 55.0 and 94.8 % and 59.0 and 99.5 %, respectively. The CEM results for pyrolysis conditions and gasification with unsuitable low ER (ER=0.10) show lower CCE values, namely between 22.9 to 86.3 %, depending on biomass type and temperature. The CEM results for lignin and cellulose also show similar CCE values (20.5 to 99.5 %). The highest CCE value (99.5 %) was predicted by the CEM for various conditions, for example RFB from eucalyptus gasification with ER=0.20 and 800 ºC.

A tendency for the increase of CCE with ER is observed for both experimental and CEM results (Figure 3.9 (a)). A tendency for the increase of CCE with temperature can also be observed for the CEM results (Figure 3.9 (b)), which is in accordance with some other works [68]. For the experimental results, no evident tendency for the relation between CCE and temperature is

observed. Accordingly, PCC values for the experimental results are significantly low and indicate high dispersion (Table 3.3) and the developed empirical correlation (Equation 3.13) has a significantly lower R^2 value than the correlation developed based on CEM results (Equation 3.14).

$$CCE_{exp} = 0.005378 \times T + 45.36009 \times \text{ER} + 58.86143 \quad \text{(Equation 3.13)}$$

$$R^2 = 0.07$$

$$CCE_{eq} = 0.093148 \times T + 52.28168 \times \text{ER} + 5.825285 \quad \text{(Equation 3.14)}$$

$$R^2 = 0.7$$

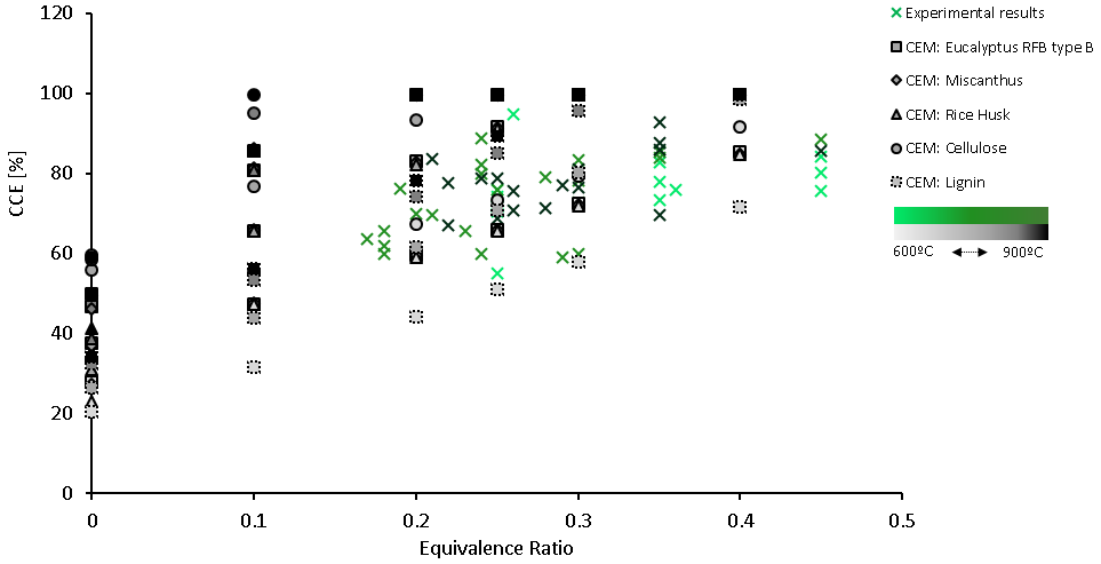

(a)

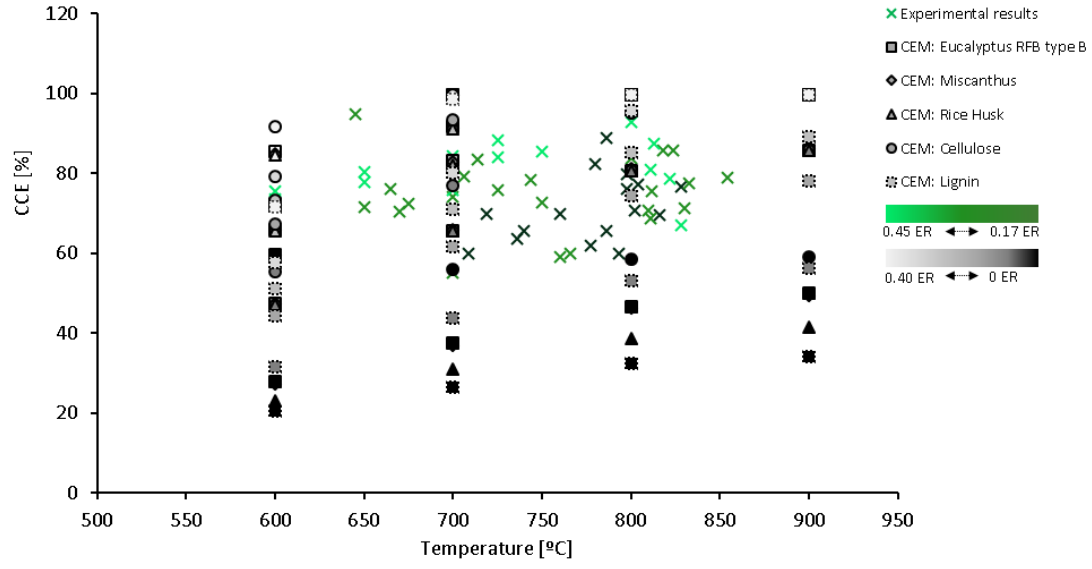

(b)

Figure 3.9 – Influence of the ER (a) and bed temperature (b) on the CCE for the experimental results reported in the literature and CEM results.

3.1.5 EMPIRICAL AND CEM CORRELATIONS EVALUATION

In this section, the empirical and CEM correlations prediction capability was briefly evaluated. For this purpose, direct (air) gasification experiments were performed in the DAO-UA 80 kW_{th} pilot-scale BFB gasifier (described in Section 1.3.1) with distinct biomass types and operating conditions. The operating conditions of the gasification experiments performed are detailed in Table 3.4. The correlations were evaluated by using these operating conditions (ER and bed temperature) as inputs and comparing the predicted results with the experimental results.

Table 3.4 – Operating conditions during the biomass gasification experiments performed in the pilot-scale BFB.

Biomass feedstock	Average bed temperature [ºC]	ER	Biomass feed rate [kg/h]	Air feed rate [L NPT/min]
Eucalyptus RFB	747	0.26	11.1	200
Eucalyptus RFB	754	0.26	11.1	200
Eucalyptus RFB	775	0.26	11.1	200
Wood pellets	814	0.33	8.7	200
Wood pellets	815	0.32	8.9	200
Eucalyptus RFB	816	0.28	10.5	200
Eucalyptus RFB	816	0.20	14.8	200
Wood pellets	817	0.33	8.8	200
Eucalyptus RFB	825	0.26	11.1	200

In Table 3.5, the experimental results and the empirical and CEM correlations predictions are summarized and compared. The composition of the PG (H_2, CO and CH_4), LHV, Y_{gas}, CGE and CCE are considered as parameters. Pearson's correlation test was performed to measure the strength of the correlation between the empirical and CEM correlations predictions and the experimental results, thus characterizing the accuracy of the predictions. In this analysis, a PCC value of 1 indicates that the values predicted by the correlations are perfectly linearly correlated with the observed experimental results [319].

The comparison between the empirical correlations predictions and the experimental results (Table 3.5) allowed the following general observations:

- Prediction of CH_4 concentration, H_2/CO molar ratio, LHV, Y_{gas} and CCE with low relative errors.
- Overestimation of H_2 and CO concentration and slight overestimation of CGE.

Maximum relative mean error associated to the prediction of H_2 and CO concentration (16.9 and 13.2 %, respectively), with the remaining relative mean errors being lower than 8.0 % (CGE). High positive PCC values were found for CH_4, H_2/CO molar ratio, Y_{gas} and CCE, showing positive correlations between the experimental results and the empirical correlations predictions. However, a significantly lower PCC value was found for LHV (close to 0), despite this parameter prediction average relative error being low. Furthermore, PCC values were found negative for H_2 (-0.9), CO (-0.5) and CGE (-0.4), showing negative correlations. These phenomena can be related to the high dispersion of values found in the literature for similar operating conditions, which were used in the development of the empirical correlations, as indicated by the low R^2 values found previously (see Section 3.1.4). Thus, for direct (air) gasification processes in BFB reactors, the developed empirical correlations show capacity to predict first estimates of gasification products and process efficiency parameters, specifically CH_4 concentration, H_2/CO molar ratio, Y_{gas} and CCE, however, require further improvement for higher reliability.

Table 3.5 – Comparison between obtained results in direct (air) gasification of biomass experiments in a BFB reactor and predicted by the empirical correlations and CEM correlations for the same operating conditions (Table 3.4).

		% vol, db			$Mol.mol^{-1}$	MJ/Nm^3	Nm^3/kg biomass db	%	
		H_2	CO	CH_4	H_2/CO	LHV	Y_{gas}	CGE	CCE
Experimental results	$\bar{x}$	7.3	12.9	3.8	0.6	4.6	1.8	44.5	73.2
	σ	1.0	1.7	0.4	0.1	0.5	0.2	7.8	10.2
Empirical correlations	$\bar{x}$	8.8	14.9	3.7	0.6	4.8	1.9	48.4	75.8
	Error $\bar{x}$ [%]	16.9	13.2	-2.0	4.1	3.0	5.3	8.0	3.5
	σ	0.5	1.1	0.4	0.0	0.4	0.2	1.1	1.9
	Error σ [%]	-114.8	-48.1	2.2	-142.5	-21.2	1.4	-602.5	-432.1
	PCC	-0.9	-0.5	0.6	0.7	0.0	1.0	-0.3	0.9
CEM correlations	$\bar{x}$	22.9	28.5	0.4	0.8	6.2	2.3	85.7	94.7
	Error $\bar{x}$ [%]	68.1	54.6	-926.0	29.7	25.4	22.0	48.1	22.8
	σ	2.0	2.3	0.2	0.1	0.5	0.2	3.5	3.8
	Error σ [%]	51.2	27.3	-76.2	-16.0	4.1	-36.3	-125.3	-166.9
	PCC	-0.4	0.8	-0.2	-0.4	0.5	1.0	0.8	0.9

The lack of accuracy of the CEM correlations to determine gasification products was expected due to the previously noticed difference between the PG composition predicted by the CEM and the gas composition reported in the literature regarding direct (air) biomass gasification in BFB reactors (see Section 3.1.4). These combined observations prove that chemical equilibrium is not attained in practical BFB direct (air) gasifiers. Nonetheless, H_2/CO molar ratio values obtained through the CEM are significantly closer to the values observed experimentally (relative mean error of 29.7 %). A positive PCC value (0.8) was found for the correlation between CO concentration found in the experimental results and predicted by the CEM, however, negative correlations were found for H_2, CH_4 and H_2/CO molar ratio (PCC = -0.2 to -0.4). Positive PCC values (0.5 to 1.0) were also found for LHV, Y_{gas}, CGE and CCE.

Thus, these results indicate that the developed CEM correlations are not suited to characterize and predict gasification products from direct (air) biomass gasification processes in BFBs reactors. Nevertheless, these correlations present higher accuracy for the prediction of H_2/CO molar ratios and efficiency parameters, than for the prediction of the volumetric concentration of major combustible gases (CO, H_2 and CH_4) present in the PG. The lack of accuracy of CEMs for the prediction of the PG composition under certain operating conditions has also been recognized in other works [13,26,66,283], nonetheless, chemical equilibrium modelling is still the most commonly used approach for determining PG composition in biomass gasification [56,285], and has been intensively used for fluidized beds in recent years [283,285,295,303–305,320]. Therefore, these results also indicate that the focus of modelling studies should be shifted from black-box chemical equilibrium modelling to other modelling approaches, such as approaches that integrate experimental knowledge. In this respect, integrating chemical equilibrium modelling with experimental knowledge, for example an integration between the CEM and empirical model developed in this work, may allow higher agreement between the model predictions and experimental data. These aspects are relevant to increase confidence in the predicted results from numerical tools and consequently facilitate the upscaling of biomass gasification technologies to the industrial level.

3.1.6 CONCLUSIONS

This works shows that the PG composition reported in the literature regarding direct (air) biomass gasification in BFB gasifiers has significant deviations from the one predicted by chemical

equilibrium. In fact, H_2 and CO concentrations are grossly overestimated by the CEM predictions, while CH_4 is largely underestimated. Furthermore, in some cases, the effect of temperature and ER on these concentration values is distinct for the reported experimental results and the CEM predictions. For example, the CEM predicted a significant decrease of H_2 concentration with ER increase and this phenomenon was not observed in the reported experimental results. Regarding typical gasification efficiency parameters (LHV, Y_{gas}, CGE and CEE), it was also observed deviations from the CEM predictions, however, these were not as significant as the ones observed for the PG composition. Thus, for the analyzed operating conditions, it is considered that non-stoichiometric chemical equilibrium modelling is not suited to predict gasification products and support the design and operation of BFB reactors in direct (air) biomass gasification. At most, black-box chemical equilibrium modelling should be used to obtain first estimates of LHV, Y_{gas} or CCE.

On the other hand, the empirical model development was hindered by the variability of the experimental results (for similar operating conditions) reported in the literature and by the lack of information regarding the specific design and operating conditions of the BFB gasifiers. Nonetheless, the empirical model showed moderate accuracy for the prediction of preliminary estimates of gasification products and process efficiency parameters, specifically CH_4 concentration, H_2/CO molar ratio, Y_{gas} and CCE. However, further development is necessary to improve the accuracy of the model predictions (with special emphasis on the prediction of H_2 and CO concentration), and consequently increase its reliability in the design, up-scale and operation of direct (air) BFB gasifiers. For this purpose, outlier exclusion, increase of database size and the inclusion of the biomass feedstock elemental composition in the correlations development, may be beneficial.

Currently, despite some studies revealing the flaws of the CEM approach, this is still the most commonly used technique to predict the products composition from biomass gasification and has been intensively used for simulating fluidized bed gasification in recent years. Accordingly, this work clearly shows that using CEMs to predict PG composition from direct (air) biomass gasification processes in BFBs can result in significant deviations from practical experimental results. Thus, alternative modeling techniques, for example approaches that integrate theoretical and experimental knowledge, such as integrating CEMs with empirical modelling, could be more reliable for the up-scale, design and operation of gasification technologies.

Biomass gasification technologies still require significant improvements to be cost-competitive and to be able to compete with conventional technologies based on fossil fuels. In this respect, modelling approaches are less expensive and time consuming than experimental research, and may improve the research progress of biomass gasification technologies and optimize the operation and design of gasification plants, leading to reduced costs. For this purpose, models based on suitable modelling approaches must be developed, for example by integrating practical knowledge from available experimental works. Accordingly, this Article results give a relevant insight on the variability of reported experimental results regarding direct (air) biomass gasification in BFBs and the applicability and accuracy of empirical and chemical equilibrium modelling approaches. In result, adopting and developing suitable modelling approaches is facilitated.

4 CHARACTERIZATION OF THE PG FROM DIRECT BIOMASS GASIFICATION

This Chapter characterizes the PG obtained from the direct gasification of distinct types of biomass in three distinct BFB reactors, namely the DAO-UA 80 kW_{th} pilot-scale BFB gasifier, the DAO-UA 3 kW_{th} bench-scale BFB gasifier and the KTH 5 kW_{th} bench-scale BFB gasifier (Section 1.3). The Chapter is composed by Articles IV, V, VI and VII.

Article IV, named "Characteristics of the gas produced during direct gasification of biomass in an autothermal pilot-scale bubbling fluidized bed reactor", demonstrated the direct (air) gasification process of distinct types of RFB in the DAO-UA pilot-scale BFB gasifier (Section 1.3) for the replacement of natural gas in some applications, such as gas furnaces for process heat production. This study also includes an extended survey of published data concerning direct gasification of biomass in fluidized beds, which is integrated with the new data obtained in this work, constituting a helpful tool to support decisions on biomass gasification related projects. This Article was published in the Energy Journal in 2017 (https://doi.org/10.1016/j.energy.2016.11.145).

Article V, named "Superheated steam injection as primary measure to improve PG quality from biomass air gasification in an autothermal pilot-scale gasifier", evaluated the influence of superheated water steam injection in the DAO-UA 80 kW_{th} pilot-scale BFB gasifier during the direct (air) gasification of distinct types of biomass, focusing on the effect of steam to biomass ratio in the PG composition and gasification efficiency parameters. The process was also evaluated in the DAO-UA 3 kW_{th} bench-scale BFB gasifier (Section 1.3) and simulated in a thermodynamic equilibrium model. The Article is currently submitted and under review in the Renewable Energy Journal.

Article VI, named "Co-gasification of refused derived fuel and biomass in a bubbling fluidized bed reactor", demonstrated the direct (air) co-gasification process of RDF with woody biomass in the DAO-UA 80 kW_{th} pilot-scale BFB gasifier as a valid WtE solution. The main objective was the evaluation of the RDF weight percentage in the feedstock mixture (0, 10, 20, 50 and 100 %wt). The Article was published in the Energy Conversion and Management Journal in 2020 (https://doi.org/10.1016/j.enconman.2020.112476).

Article VII, named "Tar formation during eucalyptus gasification in a bubbling fluidized bed reactor: Effect of feedstock and reactor bed composition", determined and evaluated tar concentration in the PG from the direct gasification of distinct types of RFB in the KTH 5 kW_{th} BFB gasifier (Section 1.3). The main objective was the evaluation of the feedstock chemical composition and gasifier operation time. The Article is currently submitted and under review in the Energy Conversion and Management Journal.

4.1 ARTICLE IV - CHARACTERISTICS OF THE GAS PRODUCED DURING DIRECT GASIFICATION OF BIOMASS IN AN AUTOTHERMAL PILOT-SCALE BUBBLING FLUIDIZED BED REACTOR

4.1.1 ABSTRACT

Direct (air) biomass gasification was demonstrated in a pilot-scale bubbling fluidized bed reactor and the influence of process parameters analyzed. For the operating conditions used, namely ER between 0.17 and 0.36 and bed temperature between 700 and 850ºC, the process was demonstrated as autothermal and operating under steady-state. The dry gas produced shows the following composition (volumetric basis): 14.0 to 21.4 % CO, 14.2 to 17.5 % CO_2, 3.6 to 5.8 % CH_4, 1.3 to 2.4 % C_2H_4, 2.0 to 12.7 % H_2 and 48.9 to 61.1 % N_2. The lower heating value of the dry gas was between 4.4 and 6.9 MJ/Nm^3, with the highest values observed during the experiments with lower ER. The specific dry gas production was between 1.2 and 2.2 Nm^3/kg biomass (dry basis), the cold gas efficiency between 41.1 and 62.6 % and the carbon conversion efficiency between 60 and 87.5 %.

The integrated analysis of new data from this study and a survey of published data shows that direct (air) biomass gasification produces gas mixtures with a wide range of variation in characteristics, that can be correlated with the biomass fuel properties and operating conditions used. Therefore, for each type of process application it is required specific experimental information to support an adequate scaling to the industrial scale.

Keywords: Biomass; Bubbling fluidized bed; Gasification.

4.1.2 INTRODUCTION

The use of biomass for useful energy production has been increasing in the recent years and makes part of the energy strategies of developed and developing countries. The driving force for this interest in biomass has been the search for alternatives to fossil fuels that allow the use of established energy conversion technologies and promote the decrease of greenhouse gases emissions. Biomass is considered a renewable fuel and its thermochemical conversion to energy has been considered neutral in terms of global carbon balance. Several thermochemical processes are available for heat and power production from biomass, even though combustion is the most widely used [69]. However, the need for renewable fuels that can replace gaseous fossil fuels in distinct applications has turned the worldwide research to biomass gasification. Two main routes have been applied for biomass gasification [15,69]: the direct process and the indirect process. In the direct process the gasification agent can consist in air or pure oxygen, or, in order to produce a gaseous fuel with higher hydrogen content, a mixture of these gases with steam; under these conditions the reactor should be autothermal and operated under very low ER [15,69], and, part of the fuel is oxidized (combustion) to supply the heat needed for the endothermic gasification reactions. In the indirect process, the fluidizing agent is usually steam, thus allowing the production of a raw gas with higher heating value when compared to the one produced by the direct process. However, the process is allothermal, which means that a supplementary external heat source is necessary.

A recognized setback of biomass gasification is related to the high tar content of the raw gas; which causes some problems in the equipment downstream of the gasification reactor and contributes to the decrease of the quality of the raw gas [69]; as a result, an upgrade of the raw gas is needed in order to obtain a gaseous fuel with suitable quality for its diverse possible applications. Therefore, several primary and secondary measures have been developed and are under research in order to improve the raw gas quality through the decrease of the tar content [15,69,78,124,287,321–323].

Unlike biomass combustion, where the composition of the main product gases (CO_2, H_2O) is relatively easy to be predicted, the composition of the produced gas from biomass gasification, namely the relative amounts of main gases such as H_2O, CO_2, CO, CH_4, C_2H_4 and H_2, seems to vary in a wide range and is strongly influenced by the biomass characteristics, reactor configuration and operating conditions [69,78,188], and, therefore, it is relatively difficult to be predicted with accuracy. In this context, thermodynamic equilibrium models [69,287–289], kinetic models [324], or combinations of both [325], have been used as an approach to predict the gas composition from biomass gasification. Nevertheless, experimental validation of theoretical approaches is recognized as of major importance to support decisions related to biomass gasification to energy conversion options.

In fact, from experimental practice reported in the literature [92,287,309] it is observed a wide range of variation on the quality of the produced gas and related process performance parameters values of direct (air) biomass gasification, such as the Y_{gas}, CGE and CCE. These process parameters seem to be deeply influenced by the fuel type, operating conditions and reactor type. Similar observations were made regarding the produced gas quality from indirect (steam) biomass gasification [326–328]. This imposes the need to obtain specific knowledge regarding the biomass gasification process for each particular application in order to get a suitable support for the development and optimization of new industrial projects, and avoid the afterward project drawbacks that have undeniably been a barrier to the implementation of this thermochemical process worldwide.

In this scope, the study presented here was designed with the goal of supporting the demonstration of direct (air) gasification process in a pilot-scale BFB reactor, using RFB as fuel, to produce a gas with heating value suitable to be used in partial replacement of natural gas in some applications, as for example, in gas furnaces for process heat producing in the PP industry. The fuel was chosen according to the available residual forest biomass from wood processing activities, such as the PP industry. This work results include new relevant information concerning the demonstration of direct (air) gasification of biomass in a pilot-scale BFB reactor, along with the experimental and methodological approach followed, and experimental data analysis regarding the operating conditions and the properties of the produced gas during a set of gasification experiments with the residual forest biomass types selected.

Additionally, seeking the capacity to interpret the influence of distinct biomass fuels and operating conditions on the raw gas (PG) properties, an extended survey of published data concerning direct gasification of biomass in fluidized beds is also integrated, analyzed and complemented with the new data obtained in this study, thus, constituting a helpful tool for the decision support on biomass gasification related projects.

4.1.3 MATERIALS AND METHODS

The experimental facility used was the DAO-UA 80 kW_{th} pilot-scale BFB gasifier (Section 1.3.1). The direct gasifier was operated under autothermal and steady-state conditions without any external auxiliary heating systems, thus, with the necessary heat for the gasification process delivered from the partial combustion of the biomass fuel in the reactor. The methodologies used to determine ER, LHV, Y_{gas}, CGE and CCE are detailed in Section 1.4.

4.1.3.1 FEEDSTOCK CHARACTERIZATION

The fuel used in the gasification experiments included commercial pine pellets (6 mm diameter and 15 mm to 20 mm in length) and different types of residual forest biomass (RFB) derived from pine (*Pinus Pinaster*) and from eucalyptus (*eucalyptus globulus*). The RFB derived from pine resulted from forestry operations, namely tree logging for the wood industry, and consisted of fine branches and tops of the trees. This fuel was pre-treated by chipping, air drying at atmospheric

conditions and sieving to a particle size below 10 mm. The RFB derived from eucalyptus resulted from two different operations, namely from forestry operations, as for example trees logging, and from industrial operations related to the woodchip production from eucalyptus logs in the context of the PP industry; for future reference throughout this work, the first was named eucalyptus RFB type A and the second eucalyptus RFB type B, respectively. The eucalyptus RFB type A and B were chipped, dried at atmospheric conditions and sieved to a particle size below 5 mm. Furthermore, the eucalyptus RFB type B was dried to two different levels of moisture content; thus, it is named type B1 the eucalyptus RFB type B with the higher moisture content and B2 with the lower moisture content. All the types of biomass were further characterized in terms of properties with interest for thermochemical conversion of biomass (proximate and ultimate analysis, and heating value), as shown in Table 4.1.

Table 4.1 – Characteristics of the different types of biomass used as fuel in the gasification experiments performed in Article IV.

	Pine RFB	Wood pellets	Eucalyptus RFB type A	Eucalyptus RFB type B	
				B1	B2
Proximate analysis (%wt, wb)					
Moisture	11.0	4.6	11.8	32.5	11.4
Volatile matter	71.1	78.5	71.0	52.2	68.5
Fixed carbon	16.8	16.6	14.6	14.5	19.0
Ash	1.1	0.3	2.6	0.8	1.1
Ultimate analysis (%wt, db)					
Ash	1.20	0.32	2.87	1.19	
C	50.80	47.50	45.85	49.07	
H	6.50	6.20	6.13	6.45	
N	0.25	0.09	0.35	0.07	
S	nd	nd	nd	nd	
O (by difference)	41.25	45.89	44.80	43.22	
LHV (MJ/kg) (db)	18.5	18.0	17.6	18.3	

nd- not determined, below the detection limit of the method, 100 ppm wt.

4.1.3.2 OPERATING CONDITIONS

The operating conditions of the reactor were characterized, namely the fuel feed rate, air feed rate, ER, temperature and pressure along the reactor and gas composition at the exit. The average bed temperature was maintained between 700 and 854 ºC and the ER between 0.17 and 0.36, corresponding to a biomass feed rate between 7.0 and 15.3 kg db/h. The bed temperature and ER values comprise a comprehensive range to allow the evaluation of these parameters influence on direct (air) gasification processes of biomass in BFB gasifiers. The methodologies for monitoring these parameters are detailed on Section 1.4. Table 4.2 shows the information about the operating conditions and the respective reference of the experiments performed in this work.

Table 4.2 – Operating conditions during the gasification experiments performed in Article IV.

Experiment reference		Fuel	ER	Average bed Temperature (ºC)	Biomass feed rate (kg db/h)	Air feed rate (L NPT/ min)
BPE	BPE1	Pine RFB	0.23	786 ±12	11	200
	BPE2	Pine RFB	0.26	811 ±3	10	200
	BPE3	Pine RFB	0.30	830 ±2	9	200
WPE	WPE1	Wood pellets	0.22	816 ±17	13	200
	WPE2	Wood pellets	0.24	802 ±4	12	200
	WPE3	Wood pellets	0.25	854 ±6	11	200
	WPE4	Wood pellets	0.30	833 ±2	10	200
BEE	BEE1	Eucalyptus RFB type A	0.22	804 ±7	13	200
	BEE2	Eucalyptus RFB type A	0.24	798 ±8	12	200
	BEE3	Eucalyptus RFB type A	0.25	812 ±5	11	200
	BEE4	Eucalyptus RFB type A	0.26	810 ±9	11	200
	BEE5	Eucalyptus RFB type A	0.28	818 ±3	10	200
	BEE6	Eucalyptus RFB type B1	0.28	706 ±8	9	200
	BEE7	Eucalyptus RFB type B1	0.30	714 ±6	9	200
	BEE8	Eucalyptus RFB type B1	0.36	700 ±7	7	200
	BEE9	Eucalyptus RFB type B2	0.17	736 ±19	15	200
	BEE10	Eucalyptus RFB type B2	0.18	709 ±14	14	200
	BEE11	Eucalyptus RFB type B2	0.20	719 ±21	13	200
	BEE12	Eucalyptus RFB type B2	0.25	800 ±5	10	200
	BEE13	Eucalyptus RFB type B2	0.35	813 ±14	7	200

db – biomass dry basis; NPT – Normal Pressure (1.013×10^5) and Temperature (0ºC)

4.1.4 RESULTS AND DISCUSSION

The results presented here include information about the gasifier operating conditions, such as the air and fuel feed rate and ER used, temperature profile along the reactor height, temperature along time at several locations in the reactor and composition of the dry gas produced in terms of CO_2, CO, CH_4, C_2H_4, N_2 and H_2 at the exit of the gasifier. Concerning the efficiency of the gasification process and the quality of the gas produced during the experiments, some variables were calculated such as LHV of the dry gas, Y_{gas}, CGE and CCE. A compilation and analysis of data reported in the literature regarding biomass direct gasification in BFBs, and, in a lesser extent, in other type of reactors and/or with another gasification agent (steam), is also included.

4.1.4.1 STEADY-STATE OPERATION OF THE GASIFIER

The BFB gasifier was operated under steady-state conditions. From the beginning of the biomass feeding (at a bed temperature of about 500 ºC) to the achievement of steady-state conditions of operation under gasification regime it typically took 150 minutes. During this transition period the bed temperature was continuously monitored and the gas composition was monitored at periodic times (typically 5 to 10 minutes interval). When the temperature and the gas composition started to stabilize and exhibit minor fluctuations along time the system was considered as operating under steady-state conditions; thereafter the gas composition and temperature started to be monitored online and continuously.

The typical temperature profile along time at several locations along the reactor height during the gasification of the different types of biomass was analogous, as shown in Figure 4.1. It is also

observed that the temperature at several locations along the reactor was very stable along time. Nonetheless some differences were observed between the temperature profiles regarding the experiments performed with wood pellets and with chipped RFB, probably due to the different physical characteristics of the fuel particles and its influence on the fuel feeding system, namely in terms of regular feeding conditions; in fact, during the experiments performed with pellets, the temperature along time showed a more steady behavior, particularly in the lower part of the freeboard, i.e. immediately above the fuel feeding location, and this can reflect a more regular feeding of the pellets when compared to the RFB chips.

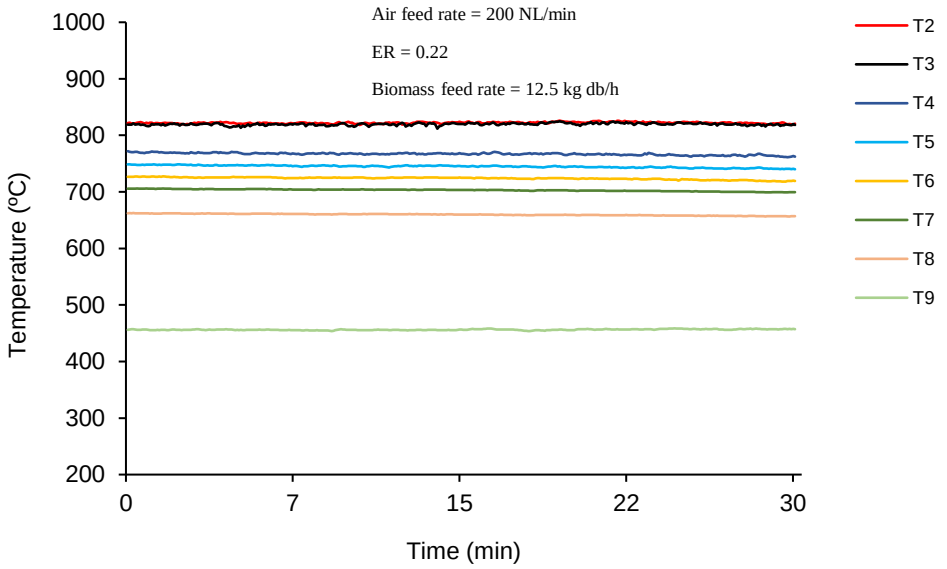

(a)

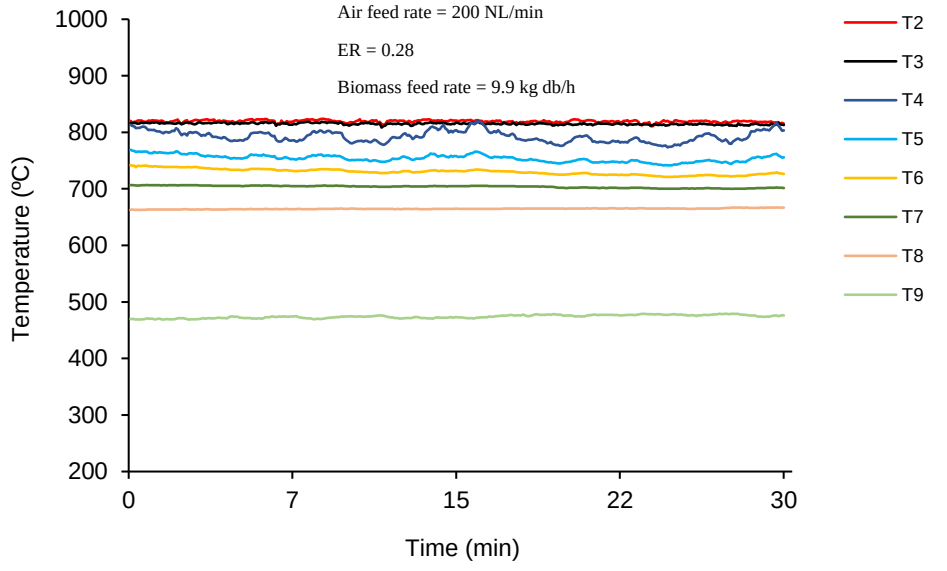

(b)

Figure 4.1 – Example of the typical evolution of the temperature along time at different locations along the reactor height during the gasification of: (a) wood pellets and (b) eucalyptus RFB type A.

It was observed that even at relatively low ER (as low as 0.17) it was possible to operate the BFB gasifier under stable autothermal conditions, with bed temperatures above 700 ºC (Figure 4.1,Table 4.2), without the need of any external heat source, as for example auxiliary electric

heating systems often used in other research works [184,314,329–331]. This result means that the exothermic reactions related to the partial oxidation of the biomass fuel released enough thermal energy to support the gasification process under autothermal conditions. The existence of steady-state operating conditions of the gasifier reflects the adequacy of the BFB reactor to study the process of direct biomass gasification.

Regarding the longitudinal temperature profile along the reactor, it was observed a continuous decrease of the temperature from the bed and its surface to the exit of the reactor (Figure 4.2). This can be explained by the specificities of the autothermal gasification process, in which the biomass fuel is oxidized mostly inside the bed and bed surface where it is discharged by the screw feeder and where O_2 is more available (from the primary air injection), thus releasing most of the thermal energy in this region in result of exothermal combustion reactions and generating higher temperatures at this location of the reactor. Afterwards, in the space above (freeboard region), the reactor becomes oxygen starved, as indicated by a zirconia cell probe installed in the freeboard (0.4 m above the biomass feeding location), and thus, the exothermic reactions typical of the combustion process are inhibited. Then, the thermal energy of the gas mixture decreases along the freeboard in result of being consumed by the endothermic reactions typical of the gasification process and lost by heat transfer throughout the reactor walls and by convection with the flue gas, therefore explaining the temperature decrease along the reactor height. The higher temperatures in the reactor were observed during conditions of higher ER (for example, 0.35), which can be explained in result of an increase of heat release from exothermic reactions, such as the combustion reactions, favored by the increase of oxygen availability.

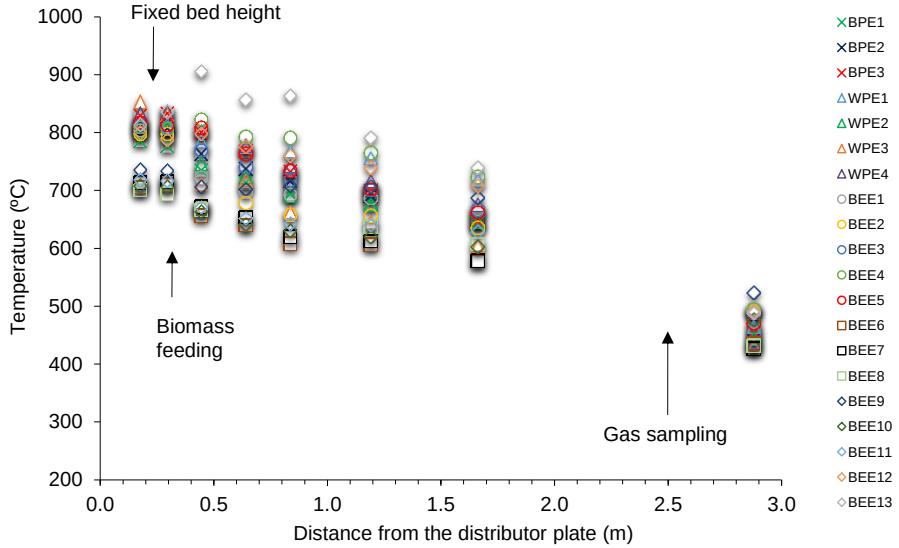

Figure 4.2 – Longitudinal temperature profile in the BFB reactor during the biomass gasification experiments performed. Legend according to experiments references in Table 4.2.

The continuous monitoring of the PG characteristics shows a relatively stable gas composition along time (Figure 4.3), which is coherent with the steady temperature profiles along time discussed previously (Figure 4.1), allowing to conclude that the BFB gasifier was operating at steady-state conditions. However, some fluctuations on the concentration of the gas species monitored along time can be observed and can be related to the fuel feeding conditions, namely the screw type feeding of biomass with heterogeneous physical characteristics, as for example the chipped RFB.

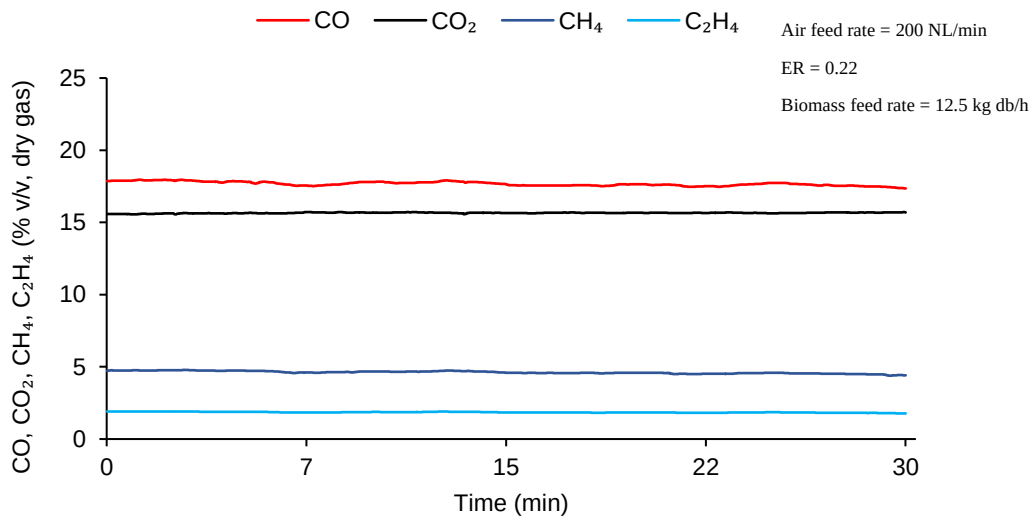

(a)

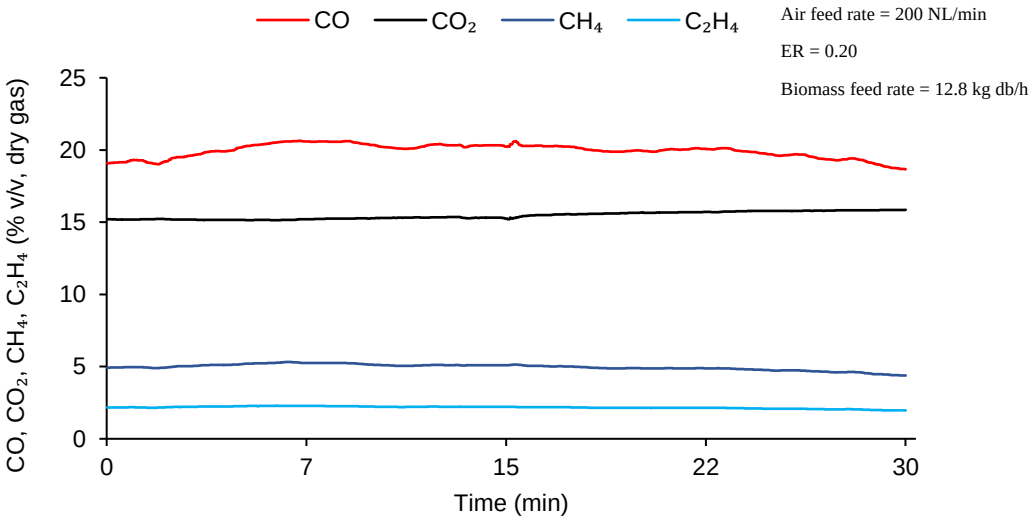

(b)

Figure 4.3 – Example of the typical dry gas composition (CO_2, CO, CH_4, C_2H_4) progress along time during the gasification of: (a) wood pellets and (b) eucalyptus RFB type B2.

4.1.4.2 INFLUENCE OF THE ER

The two gaseous components present in higher concentration (N_2 not considered) in the dry gas were CO_2 and CO, followed by H_2, CH_4 and C_2H_4 by decreasing order of abundance. The CO_2 concentration in the dry gas was between 14.2 and 17.5 %v, the CO concentration between 14.0 and 21.4 %v, the CH_4 concentration between 3.6 and 5.8 %v, the C_2H_4 concentration between 1.3 and 2.4 %v and the H_2 concentration between 2.0 and 12.7 %v, as shown in Figure 4.4 (a), (b) and (c). The highest concentration of CO, CH_4 and C_2H_4 was observed during the gasification of eucalyptus RFB type B2 with an ER of 0.17 (experiment reference BEE9 in Table 4.2 and Figure

4.4 (c)), however, the highest concentration of H_2 was observed during the gasification of wood pellets with an ER of 0.24 (experiment reference WPE2 in Table 4.2). The gas composition observed with distinct biomass fuels and operating conditions is in accordance with results reported in the literature regarding direct (air) gasification in BFBs (discussed in Section 4.1.4.4). In general, the concentration of combustible gases such as CO and H_2 increased with the decrease of ER in the range used (0.17 to 0.36) (Figure 4.4 (a), (b) and (c)), following a similar trend as reported in the literature (discussed in Section 4.1.4.4). This can be explained in result of the existence of a higher O/C ratio in the reaction environment with the increase of the ER, and thus more oxygen is available, which favors the oxidation reactions, and the consequent decrease in the concentration of combustible gases. Nevertheless, in some experiments it was observed that the concentration of H_2 decreased when the ER was decreased, and therefore, other reasons such as the reaction temperature should come into play.

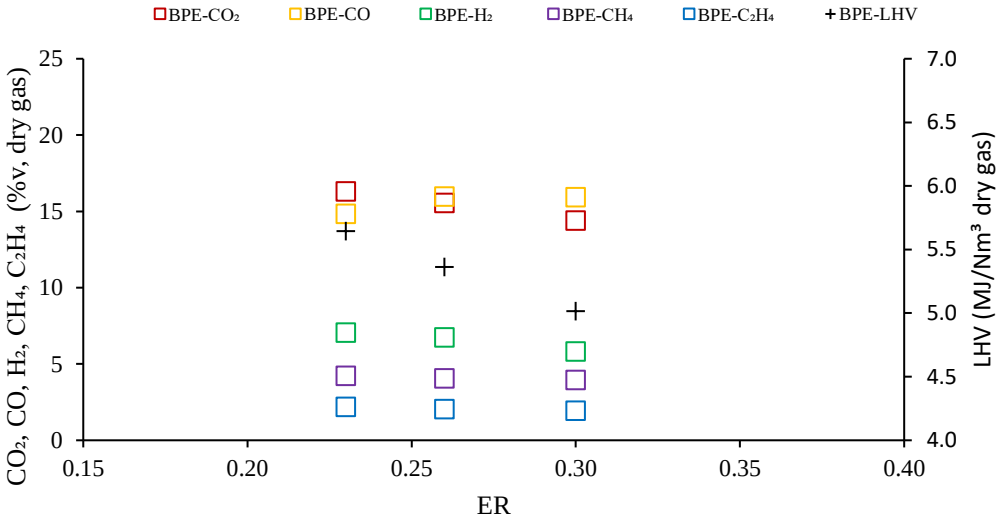

(a)

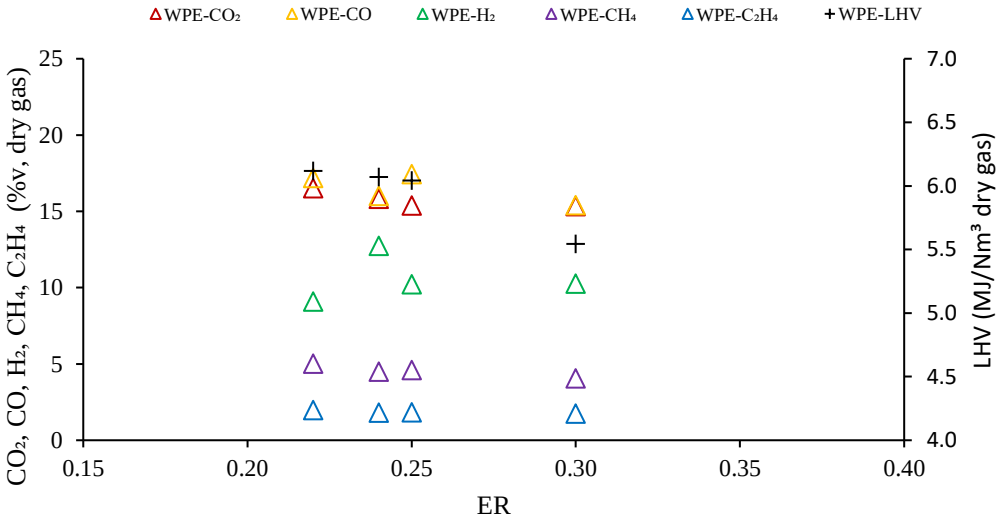

(b)

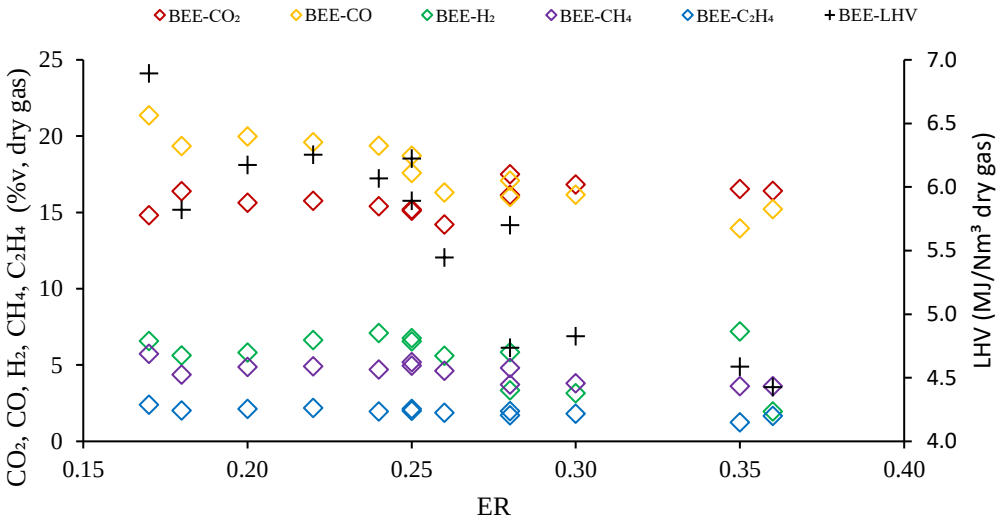

(c)

Figure 4.4 – Influence of ER on the average dry gas composition (CO_2, CO, H_2, CH_4 and C_2H_4) and LHV during the gasification experiments in the pilot-scale BFB with (a) pine RFB, (b) wood pellets and (c) eucalyptus RFB. Legend according to experiments reference in Table 4.2.

4.1.4.3 INFLUENCE OF THE TEMPERATURE

For the different fuels and operating conditions studied in this work, the most significant difference observed was related to the concentration of H_2 in the dry gas. During wood pellets gasification the H_2 concentration was between 6.6 and 12.7 %v, whereas during the gasification of the other types of biomass the concentration of H_2 was in the range 2.0 to 7.2 %v. Considering that the hydrogen content of these fuels is similar (around 6.1 to 6.5 %wt dry basis), with the highest value found in the chipped RFB derived from pine, and that the moisture content (an alternative source of H_2) of the pellets was lower, the reasoning for the observed differences in H_2 production could be related to other operating variables such as the ER and operating temperature. However, the ER during the wood pellets gasification was similar to that used for the other biomass fuels, and thus should not explain the observed differences on the H_2 production. On the other hand, the temperature in the reactor during the gasification of wood pellets is in the upper temperature range observed during the experiments done (Table 4.2), and it is recognized [289] that higher temperatures favor the formation of species such as H_2 and CO. Thus, for similar ER, the higher temperatures seem to be favoring the formation of H_2. In fact, the lower H_2 content in the dry gas was observed during the gasification experiments performed at lower temperatures, as those in range 700 ºC to 720 ºC. Besides the recognized influence of the temperature on H_2 production, it is also observed that for similar temperature and ER, the production of H_2 is always higher during the gasification of wood pellets. Thus, other phenomenon, such as the physical properties of the fuel, for example the pelletized form of particles instead of the chipped form, could have some influence on the mass ratio char/bottom bed, reactivity of particles, and gas-solid interaction and, consequently, on the results observed; considering the relevance of the subject, this must be further analyzed in future works in order to be clarified.

LHV in the range of 4.4 to 6.9 MJ/Nm^3 was observed (Figure 4.4), with the highest value observed during the gasification of eucalyptus RFB type B2 with ER 0.17 and bed temperature equal to 736 ºC (BEE9, Figure 4.4 (c)), and the lowest during the gasification of eucalyptus RFB type B1 with ER 0.36 and bed temperature equal to 700 ºC (BEE8, Figure 4.4 (c)). In general, for each

biomass fuel, and for similar operating temperature, the LHV of the dry gas decreased with the increase of the ER (Figure 4.4), and this is explained in result of the decrease of the concentration of the combustible gases produced with increasing ER, as already discussed in the previous Section. Nevertheless, it can also be observed that an increase in the ER in specific ranges, e.g. between 0.18 and 0.25, along with a temperature increase from around 700 ºC to 800 ºC, can result in an increase of the gas LHV (see for example BEE10 to BEE12, Figure 4.4 (c)). This means that an interplay exists between the ER and the temperature in determining the LHV of the gas. The values of LHV determined during the gasification experiments are in agreement with the range of LHV values often reported in literature for direct (air) biomass gasification in BFB (discussed in Section 4.1.4.4).

4.1.4.4 COMPARISON WITH LITERATURE DATA

In Figure 4.5, Figure 4.6, Figure 4.7, Figure 4.8 and Figure 4.9, it is made an integration of experimental data from this study with a survey of results concerning dry gas composition, LHV, Y_{gas}, CGE and CCE, respectively, from a set of studies available on the literature regarding direct (air) biomass gasification in BFB (Table 4.3). Regarding the composition of the dry gas (Figure 4.5), the CO concentration is between 7.2 and 26.6 %v and the H_2 concentration between 1.2 and 24 %v. When compared to literature data, the results obtained in the work developed here are within the upper range of reported values for CO concentration and in the lower range of reported values for H_2. Regarding the LHV of the PG (Figure 4.6), the values reported in literature are between 0.1 and 7.8 MJ/Nm^3. In this respect, the LHV values obtained in the present work are in the upper range of the values found in the literature. The analysis of published information and experimental results obtained in this work, point out for maximum LHV for ER in the range 0.17 to 0.27.

Table 4.3 – Survey of some published works in the literature regarding direct and indirect biomass gasification in distinct reactors.

Experiment reference		Biomass	Gasification agent	Reactor type	ER* or S/B**	Reference
KP	KP0.19	Wood pellets	Air	BFB	0.19*	[186]
	KP0.24	Wood pellets	Air	BFB	0.24*	[186]
	KP0.27	Wood pellets	Air	BFB	0.27*	[186]
	KP0.32	Wood pellets	Air	BFB	0.32*	[186]
KC	KCS0.25	Hazelnut shell	Air	BFB	0.25*	[307]
	KCS0.68	Hazelnut shell	Air	BFB	0.68*	[307]
	KCA0.36	Cotton stalk	Air	BFB	0.36*	[307]
	KCA0.71	Cotton stalk	Air	BFB	0.71*	[307]
BC	BC0.22	Rice husk	Air	BFB	0.22*	[229]
	BC0.24	Rice husk	Air	BFB	0.24*	[229]
	BC0.28	Rice husk	Air	BFB	0.28*	[229]
	BC0.32	Rice husk	Air	BFB	0.32*	[229]
	BC0.34	Rice husk	Air	BFB	0.34*	[229]
NS	NS0.26	Pine sawdust	Air	BFB	0.26*	[187]
	NS0.32	Pine sawdust	Air	BFB	0.32*	[187]
	NS0.36	Pine sawdust	Air	BFB	0.36*	[187]
	NS0.37	Pine sawdust	Air	BFB	0.37*	[187]
	NS0.47	Pine sawdust	Air	BFB	0.47*	[187]
KE	KE0.32	Rubber woodchip	Air	BFB	0.32*	[315]
	KE0.36	Rubber woodchip	Air	BFB	0.36*	[315]
	KE0.38	Rubber woodchip	Air	BFB	0.38*	[315]
	KE0.41	Rubber woodchip	Air	BFB	0.41*	[315]
	KE0.43	Rubber woodchip	Air	BFB	0.43*	[315]
CP	CP0.35	Wood pellets	Air	BFB	0.35*	[184]
KC	KC0.25	Rice husk	Air	BFB	0.25*	[287]
	KC0.35	Rice husk	Air	BFB	0.35*	[287]
	KC0.45	Rice husk	Air	BFB	0.45*	[287]
SF	SF0.30	Coir pith	Air	BFB	0.3*	[188]
	SF0.40	Coir pith	Air	BFB	0.4*	[188]
	SF0.50	Coir pith	Air	BFB	0.5*	[188]
SC	SC0.30	Rice husk	Air	BFB	0.3*	[188]
	SC0.40	Rice husk	Air	BFB	0.4*	[188]
	SC0.50	Rice husk	Air	BFB	0.5*	[188]
SS	SS0.30	Sawdust	Air	BFB	0.3*	[188]
	SS0.40	Sawdust	Air	BFB	0.4*	[188]
	SS0.50	Sawdust	Air	BFB	0.5*	[188]

Table 4.3 – (cont.).

Experiment reference		Biomass	Gasification agent	Reactor type	ER* or S/B**	Reference
XM	XM0.23	*Miscanthus*	Air	BFB	0.23*	[314]
	XM0.26	*Miscanthus*	Air	BFB	0.26*	[314]
	XM0.28	*Miscanthus*	Air	BFB	0.28*	[314]
	XM0.37	*Miscanthus*	Air	BFB	0.37*	[314]
SP	SP0.25	Alfalfa pellets	Air	BFB	0.25*	[312]
	SP0.30	Alfalfa pellets	Air	BFB	0.3*	[312]
IPP	IPP0.24	Straw pellets	Air	BFB	0.24*	[185]
IPPC	IPPC0.21	Softwood pellets	Air	BFB	0.21*	[185]
IPE	IPE0.29	Torrefied woodchips	Air	BFB	0.29*	[185]
MC	MC0.25	Rice husk	Air	BFB	0.25*	[309]
	MC0.30	Rice husk	Air	BFB	0.3*	[309]
	MC0.35	Rice husk	Air	BFB	0.35*	[309]
AE	AE0.17	Woodchips	Air	BFB	0.17*	[183]
	AE0.18	Woodchips	Air	BFB	0.18*	[183]
	AE0.23	Woodchips	Air	BFB	0.23*	[183]
VC	VC0.20	Olive kernel	Air	BFB	0.2*	[313]
	VC0.30	Olive kernel	Air	BFB	0.3*	[313]
	VC0.40	Olive kernel	Air	BFB	0.4*	[313]
SCT	SCT0.26	Bana grass	Air	BFB	0.26*	[311]
	SCT0.27	Bana grass	Air	BFB	0.27*	[311]
	SCT0.30	Bana grass	Air	BFB	0.3*	[311]
	SCT0.33	Bana grass	Air	BFB	0.33*	[311]
SB	SB0.27	Sugarcane bagasse	Air	BFB	0.27*	[311]
GCP	GCP0.15	Palm kernel shell	Air	BFB	0.15*	[306]
	GCP0.20	Palm kernel shell	Air	BFB	0.2*	[306]
	GCP0.25	Palm kernel shell	Air	BFB	0.25*	[306]
	GCP0.30	Palm kernel shell	Air	BFB	0.3*	[306]
	GCP0.45	Palm kernel shell	Air	BFB	0.45*	[306]
GCC	GCC0.15	Coconut shell	Air	BFB	0.15*	[306]
	GCC0.20	Coconut shell	Air	BFB	0.2*	[306]
	GCC0.25	Coconut shell	Air	BFB	0.25*	[306]
	GCC0.30	Coconut shell	Air	BFB	0.3*	[306]
	GCC0.45	Coconut shell	Air	BFB	0.45*	[306]

Table 4.3 – (cont.).

Experiment reference		Biomass	Gasification agent	Reactor type	ER* or S/B**	Reference
MM	MM0.18	Miscanthus	Air	BFB	0.18*	[310]
	MM0.26	Miscanthus	Air	BFB	0.26*	[310]
	MM0.27	Miscanthus	Air	BFB	0.27*	[310]
	MM0.30	Miscanthus	Air	BFB	0.3*	[310]
	MM0.31	Miscanthus	Air	BFB	0.31*	[310]
	MM0.37	Miscanthus	Air	BFB	0.37*	[310]
GNPP	GNPP0.20	Black pellets	Air	Updraft	0.2*	[332]
GNPC	GNPC0.20	Gray pellets	Air	Updraft	0.2*	[332]
PWP	PWP0.20	Wood pellets	Air	Updraft	0.2*	[189]
	PWP0.24	Wood pellets	Air	Updraft	0.24*	[189]
	PWP0.26	Wood pellets	Air	Updraft	0.26*	[189]
	PWP0.28	Wood pellets	Air	Updraft	0.28*	[189]
	PWP0.29	Wood pellets	Air	Updraft	0.29*	[189]
	PWP0.30	Wood pellets	Air	Updraft	0.3*	[189]
	PWP0.31	Wood pellets	Air	Updraft	0.31*	[189]
	PWP0.33	Wood pellets	Air	Updraft	0.33*	[189]
CEPM	CEPM0.29	Wood pellets	Air	Downdraft	0.29*	[190]
CEPB	CEPB0.29	Bagasse pellets	Air	Downdraft	0.29*	[190]
CEPC	CEPC0.30	EFB pellets	Air	Downdraft	0.3*	[190]
	CEPC0.39	EFB pellets	Air	Downdraft	0.39*	[190]
MDPP	MDPP0.26	Polish pellets	Air	Updraft	0.26*	[111]
	MDPT0.28	Torrified pellets	Air	Updraft	0.28*	[111]
MDPA	MDPA0.31	South African pellets	Air	Updraft	0.31*	[111]
MDSP	MDSP0.14	Polish sawdust	Air	Updraft	0.14*	[111]
CGP	CGP0.18	Corn straw	Air	Downdraft	0.18*	[333]
	CGP0.21	Corn straw	Air	Downdraft	0.21*	[333]
	CGP0.24	Corn straw	Air	Downdraft	0.24*	[333]
	CGP0.28	Corn straw	Air	Downdraft	0.28*	[333]
	CGP0.32	Corn straw	Air	Downdraft	0.32*	[333]
	CGP0.36	Corn straw	Air	Downdraft	0.36*	[333]
	CGP0.41	Corn straw	Air	Downdraft	0.41*	[333]

Table 4.3 – (cont.).

Experiment reference		Biomass	Gasification agent	Reactor type	ER* or S/B**	Reference
LISCPA	LISCPA0.22	Mixed PS sawdust	Air	CFB	0.22*	[92]
LISDB	LISDB0.26	Mixed sawdust	Air	CFB	0.26*	[92]
	LISDB0.30	Mixed sawdust	Air	CFB	0.3*	[92]
	LISDB0.46	Mixed sawdust	Air	CFB	0.46*	[92]
LISC	LISC0.34	Hemlock sawdust	Air	CFB	0.34*	[92]
	LISC0.52	Hemlock sawdust	Air	CFB	0.52*	[92]
	LISC0.45	Cypress sawdust	Air	CFB	0.45*	[92]
	LISC0.54	Cypress sawdust	Air	CFB	0.54*	[92]
LISAP	LISAP0.40	Mixed SPF sawdust	Air	CFB	0.4*	[92]
CLC	CLC1.00	Rice husk	Steam	BFB	1**	[326]
	CLC1.32	Rice husk	Steam	BFB	1.32**	[326]
	CLC1.70	Rice husk	Steam	BFB	1.7**	[326]
RCA	RCA1.00-1	Almond shell	Steam	BFB	1**	[327]
	RCA1.00-2	Almond shell	Steam	BFB	1**	[327]
	RCA1.00-3	Almond shell	Steam	BFB	1**	[327]
GCPV	GCPV1.00-1	Straw	Steam	-	0.15**	[328]
	GCPV1.00-2	Straw	Steam	-	0.15**	[328]
	GCPV1.00-3	Straw	Steam	-	0.15**	[328]
MPM	MPM0.83	Wood pellets	Steam	BFB	0.83**	[95]
	MPM0.84	Wood pellets	Steam	BFB	0.84**	[95]
	MPM1.00	Wood pellets	Steam	BFB	1**	[95]
	MPM1.20	Wood pellets	Steam	BFB	1.2**	[95]

Notes: EFB = Empty fruit bunch; PS = pine bark-spruce; SPF = Spruce-pine-fir.

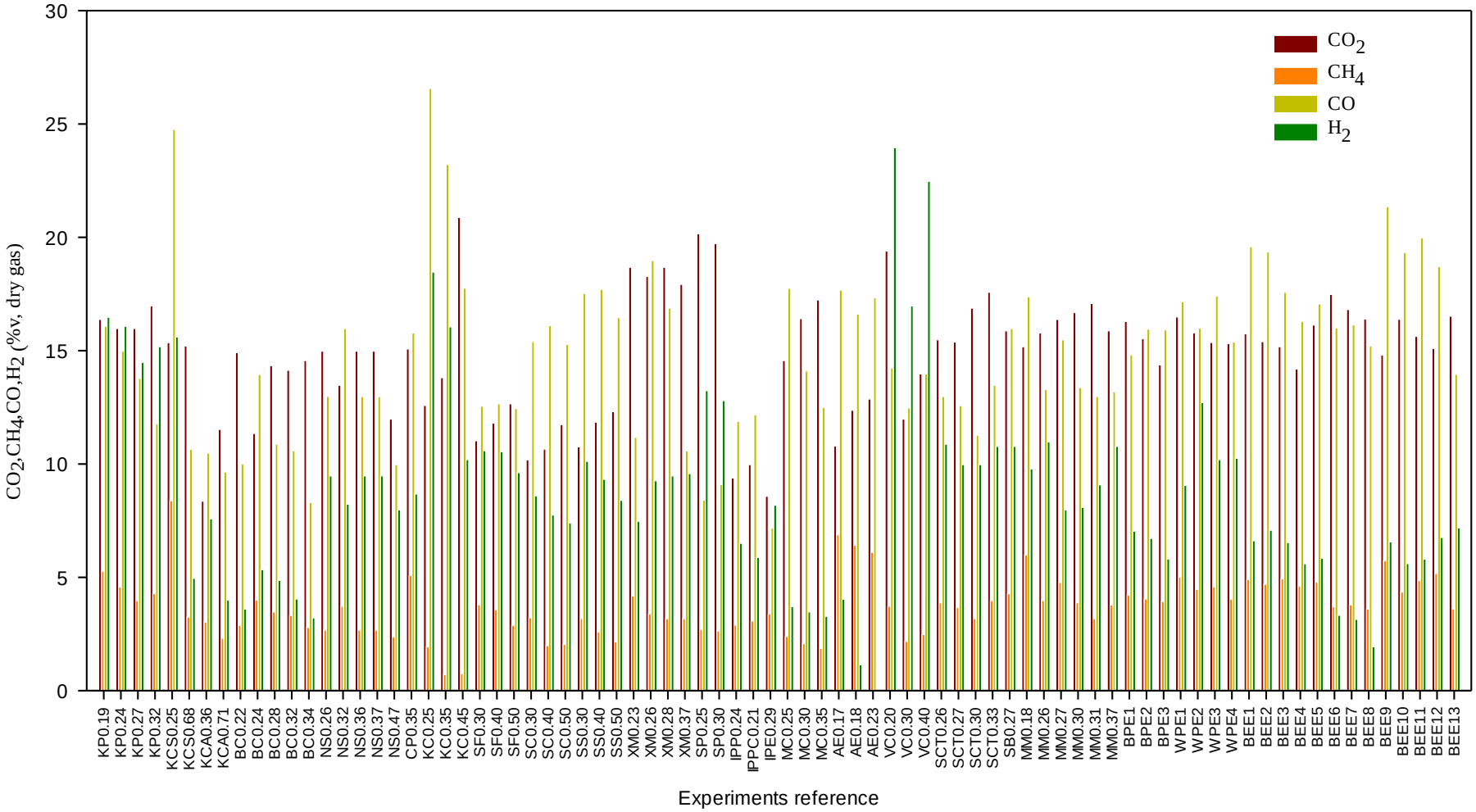

Figure 4.5 – Comparison between the composition of the PG from this work and the composition reported in the literature regarding direct (air) biomass gasification studies in BFB gasifiers. Experiments reference according to Table 4.2 (this work) and Table 4.3 (literature survey).

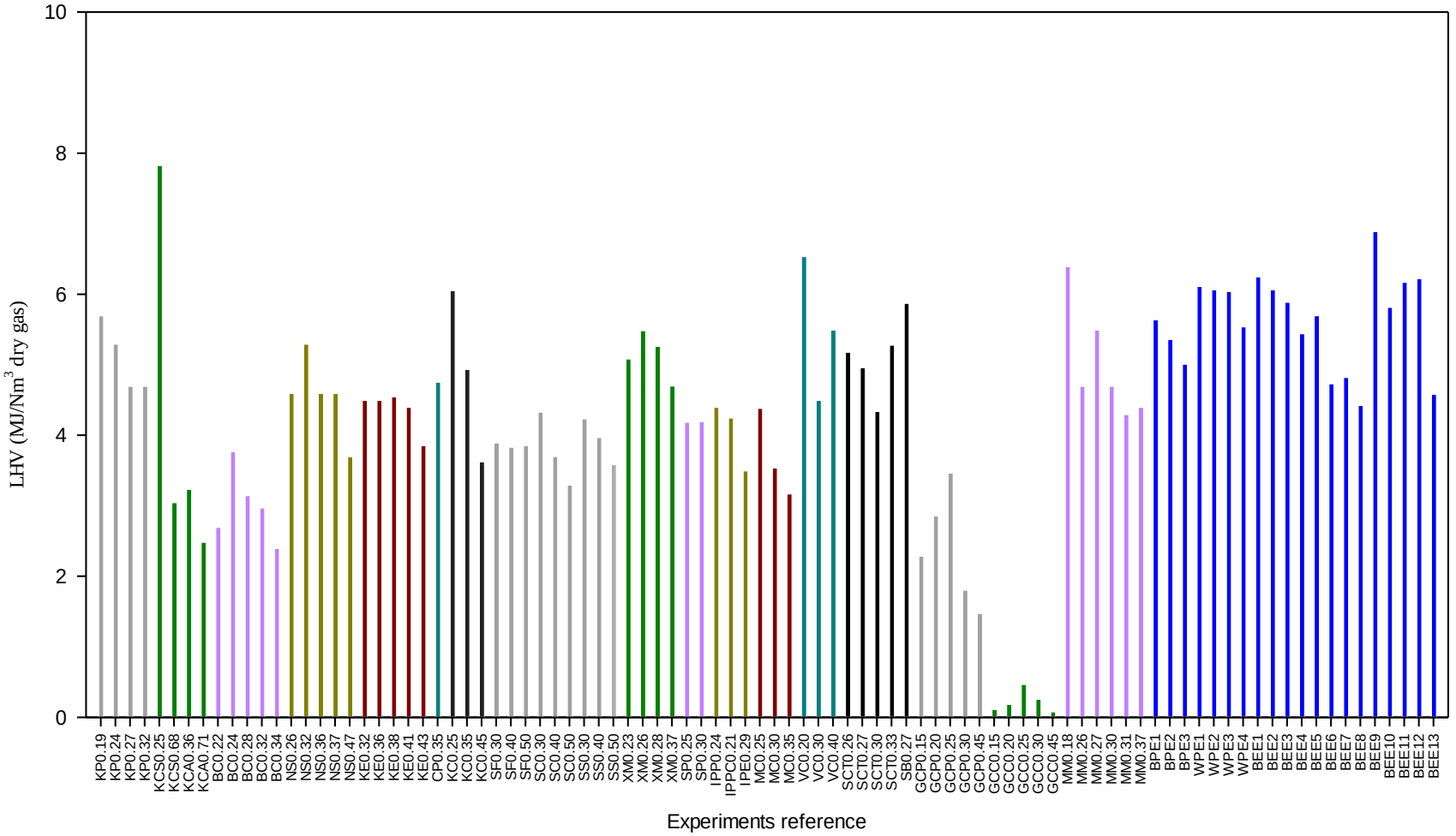

Figure 4.6 – Comparison between the LHV of the PG from the experiments performed in this work and the LHV reported in the literature regarding direct (air) biomass gasification studies in BFB gasifiers. Experiments reference according to Table 4.2 (this work) and Table 4.3 (literature survey).

The Y_{gas} values obtained for the gasification experiments were between 1.2 and 2.2 Nm^3 gas/kg biomass db (Figure 4.7). The highest value was obtained in the gasification of eucalyptus RFB type B2 with 0.35 ER (BEE13) and the lowest in the gasification of eucalyptus RFB type B2 with 0.18 ER (BEE10). Y_{gas} values between 1.2 and 4.1 Nm^3 gas/kg biomass db (dry basis) have been reported in the literature during direct gasification of biomass in BFB (Figure 4.7). The experimental results obtained during the gasification experiments from our study are in the lower/medium range of the values reported in the literature (Figure 4.7). In our work it was also found that the Y_{gas} is typically lower in experiments with lower ER, and a similar trend is observed in the literature.

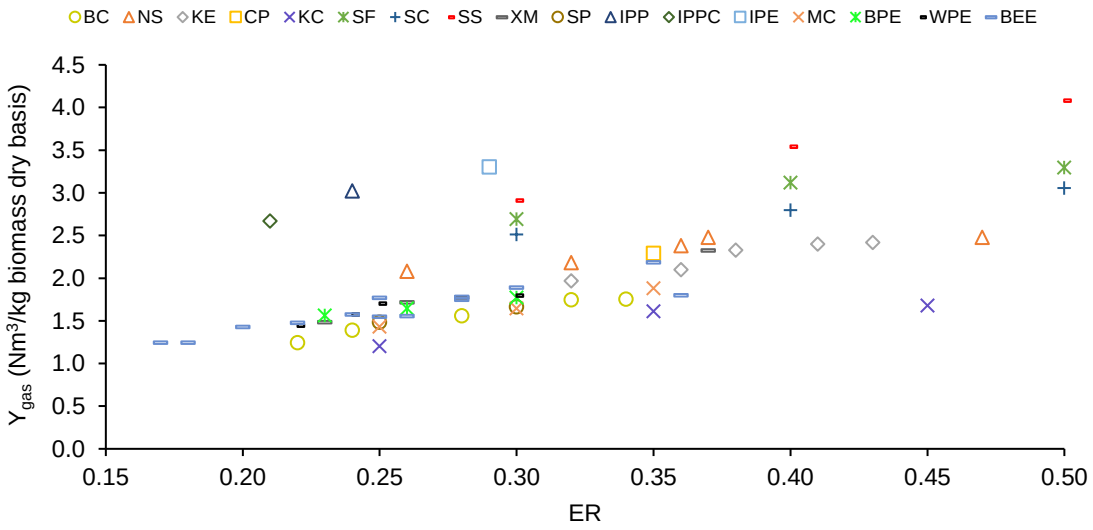

Figure 4.7 – Influence of ER on the Y_{gas} during the experiments performed in this work and reported in the literature regarding direct (air) biomass gasification in BFB reactors. Experiments reference according to Table 4.2 (this work) and Table 4.3 (literature survey).

Regarding the CGE, values between 37.4 and 62.6 % were calculated for the experimental conditions used (Figure 4.8). The highest value was obtained in the gasification of eucalyptus RFB type B2 with an ER of 0.25 (BEE12) and the lowest in the gasification of eucalyptus RFB type B2 with an ER of 0.18 (BEE10). These CGE values are coherent with those reported in the literature, which are between 23.5 and 69.0 %. These results are explained in accordance with the concentration of the combustible gases in the dry gas (CO, H_2, CH_4) and related to the effect of the ER on the process, i.e., too low ER should favor the existence of higher molecular weight hydrocarbons, as for example tars, which contribute to a decrease on the concentration of combustible permanent gases, whereas at too high ERs, for example above 0.27, the relevance of oxidation reactions should increase, and thus, a decrease in the concentration of combustible permanent gases should also occur [187]. Additionally, it should also be considered that higher ER are attained by increasing the air/fuel ratio and thus the Y_{gas} is typically higher for higher ERs, therefore contributing for higher CGE values. These trade-offs between operating parameters, e.g., lower or higher ER, and gasification performance parameters, e.g., CGE, are of major importance in defining the appropriate operation regime of the gasifier. From the results analyzed in this study, in order to achieve higher values of CGE (in average, over 50 %) the ER should not be lower than 0.20 or higher than 0.40 (Figure 4.8).

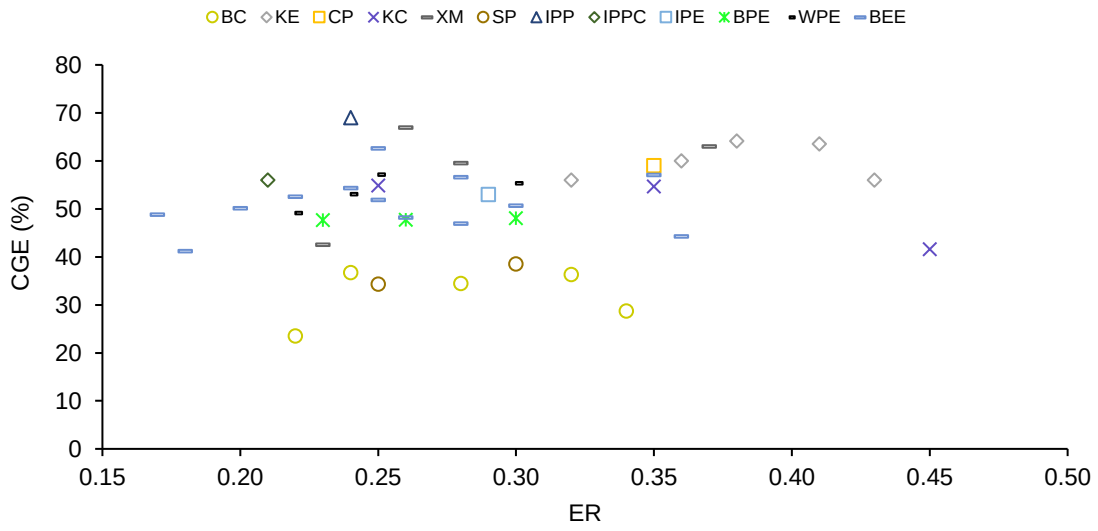

Figure 4.8 – Influence of ER on the CGE during the experiments performed in this work and reported in the literature regarding direct (air) biomass gasification in BFB reactors. Experiments reference according to Table 4.2 (this work) and Table 4.3 (literature survey).

Regarding CCE, values between 60.0 and 87.5 % were calculated for the gasification experiments performed (Figure 4.9). The maximum value was obtained in the gasification of eucalyptus RFB type B2 with an ER of 0.35 (BEE13) and the minimum in the gasification of eucalyptus RFB type B2 with an ER of 0.18 (BEE10). These values are in the medium/upper range of the results reported in the literature for direct (air) biomass gasification in BFBs, which are between 55.0 and 92.8 %. The trend for an increase of the CCE with the ER can be justified in result of an increase in the conversion of the carbon in the solid fuel into permanent gases containing carbon (e. g, CO and in particular CO_2) and Y_{gas}, due to an increase of the oxidant conditions in the reactor.

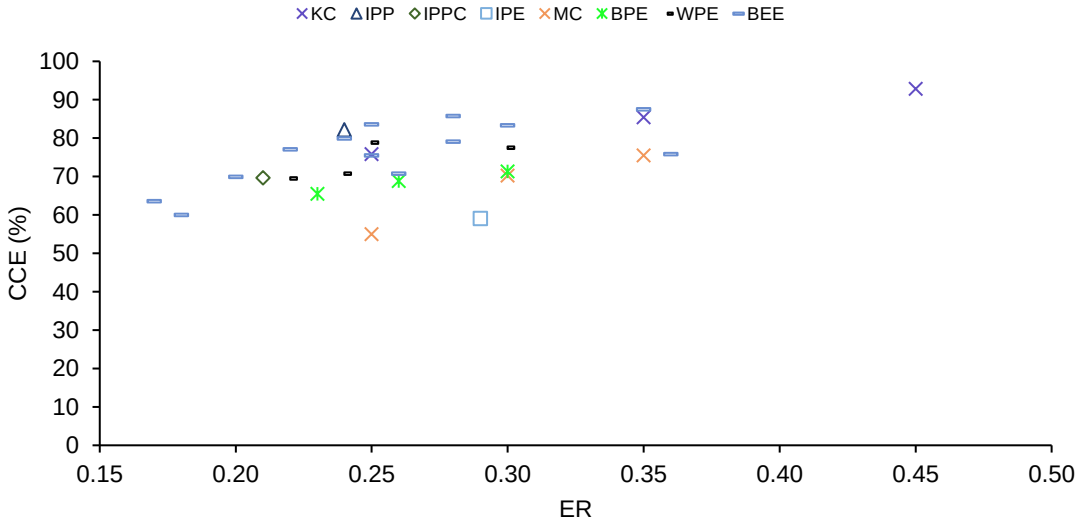

Figure 4.9 – Influence of ER on the CCE during the experiments performed in this work and reported in the literature regarding direct (air) biomass gasification in BFB reactors. Experiments reference according to Table 4.2 (this work) and Table 4.3 (literature survey).

Additionally, seeking a comparison between the PG characteristics and performance parameters obtained during biomass direct (air) gasification in BFB and in other types of reactors, a set of data from studies reported in the literature regarding fixed bed downdraft and updraft and CFB reactors was compiled and organized in Figure 4.10. The reported concentration values of CO and H_2 show a very wide range of variation and are between 6.9 to 32 %v and 3 to 17 %v, respectively. This wide range of CO and H_2 concentration is similar to that observed in the direct (air) gasification of biomass in BFB, reflecting the strong influence of fuel characteristics and operating conditions on the product gas quality. Regarding the LHV of the PG, the range of values reported in the literature is between 2.4 and 7.3 MJ/Nm^3 (Figure 4.10); these values of LHV are comparable to those obtained during direct (air) biomass gasification in BFB, previously reported and analyzed in this work. Regarding the Y_{gas}, values between 1.4 and 2.9 Nm^3 gas/kg biomass db were reported in literature; these values are within the range of values reported for the direct (air) gasification of biomass in BFB, reflecting the same trend of increasing dry gas yield with increasing ER. For the CGE, reported values between 44.2 and 77 % were found in literature; these values are in accordance with the CGE values from the experimental results in this work and also reported in the literature for BFB direct (air) gasification, with the maximum CGE value found within the same range of ER. Regarding the CCE, values between 81.6 and 102 % have been reported in the literature. The value of 102 % referred by Li et al., [92] is unexpected, and must be regarded carefully, because it probably is related to the occurrence of some miss data analysis during the mass balance performed in that study.

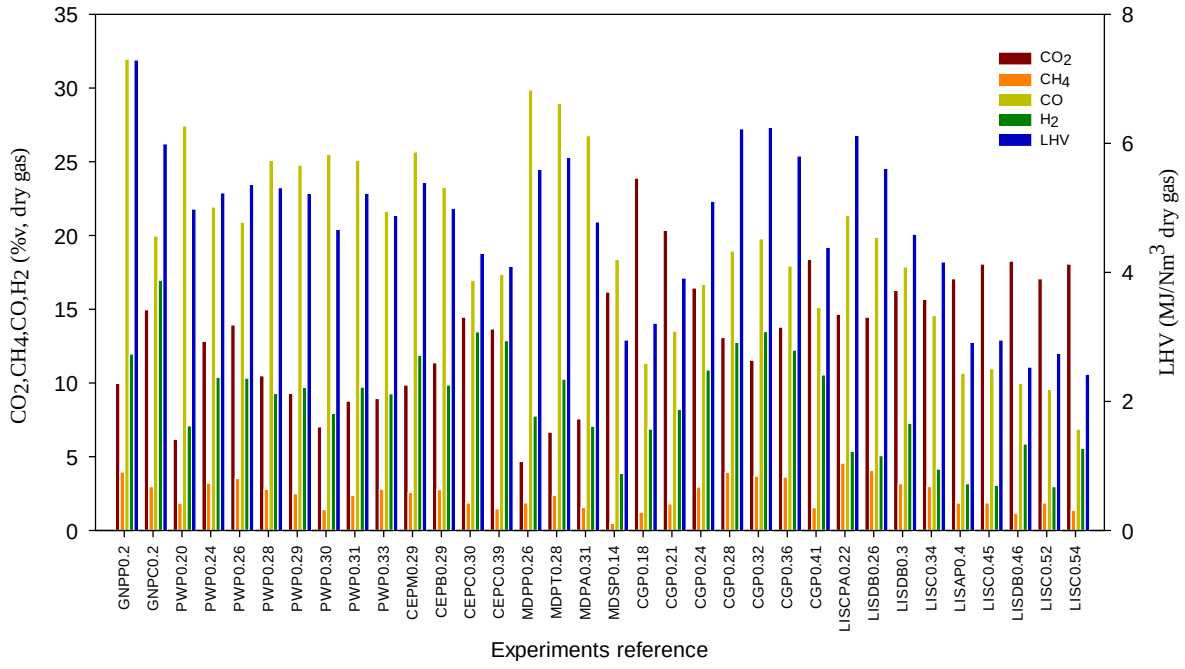

Figure 4.10 – Composition (CO_2, CH_4, CO and H_2) and LHV of the PG reported in the literature regarding biomass direct (air) gasification studies in downdraft/updraft fixed bed and CFB reactors. Experiments reference according to Table 4.3.

In general, the Y_{gas}, CGE and CCE obtained during the biomass direct (air) gasification experiments in BFB performed in this work are in the lower/medium range of the results reported in literature regarding biomass direct (air) gasification studies in fixed bed downdraft and updraft and CFB reactors. On the other hand, the LHV is in the upper range. It should be noted that fluidized beds and fixed beds have distinct hydrodynamic behavior and thus distinct operating patterns, for example, regarding the model of gas-solid contact, temperature and gas distribution profile in the reactor. Fixed beds have limitations regarding the use of distinct fuels with different characteristics and offer less

control over the temperature in comparison with fluidized beds; however, this type of reactors evade defluidization problems that could arise in fluidized beds when inappropriate high ash content fuels are used, which can consequently conduct to the unpredicted shutdown of the reactor. CFB reactors, in comparison with BFB, allow the achievement of improved gas-solid contact, and, consequently, a higher CCE, however, these have higher complexity of operation and frequent operational drawbacks [69]. Of major importance is also the influence of distinct gas-solid contact patterns on the amount of tars present in raw gas, being that the downdraft fixed bed typically leads to lower concentration values of these compounds when compared to the updraft fixed bed, BFB and CFB. A better description of these gasifier designs can be found in Chapter 2.

Regarding the influence of the scale-up of the biomass gasification process, in general, it is observed that the LHV of the produced gas from bench-scale direct (air) gasifiers is in average slightly higher (~ 0.5 MJ/Nm^3), mostly in result of a higher H_2 concentration in the dry gas, than that observed in pilot-scale reactors, including the results obtained in this work. Nonetheless, this difference may be related to other parameters than the scale-up of the reactor, for example, the biomass types used in distinct experiments (Table 4.3). It is observed that for both bench and pilot-scale reactors the PG with higher LHV is typically obtained at ER from 0.2 to 0.3, and that this parameter has a tendency to decrease with the increase of the ER. Concerning process efficiency parameters (Y_{gas}, CGE and CCE), similar values can be found for bench and pilot-scale reactors, however, the information for bench-scale reactors is scarce in this regard. From the analysis made, it can be inferred that the scale-up of the direct (air) gasification process from bench-scale to pilot-scale seems to have minor impact on the influence of operating variables on process performance parameters. This can be also extended to a higher scale, as observed in the work of Dudyński et al., [111] performed in an industrial fixed bed updraft gasifier.

Seeking another perspective, namely the comparison with indirect (steam) gasification of biomass in different types of reactors, in Figure 4.11 it is shown some results reported in the literature. The concentration of CO and H_2 was reported between 11.8 and 33.2 %v and 21.3 and 55.5 %v, respectively. Regarding the LHV, the values reported in the literature are comprehended between 9.6 and 15.8 MJ/Nm^3. These results reflect the improved quality of the produced gas during indirect gasification of biomass with steam, i.e., with higher concentration of CO, H_2 and CH_4, and consequently higher LHV, when compared to direct (air) gasification, as for example the PG in the experiments done in this work. Nevertheless, it is important to state that these two types of processes, direct and indirect biomass gasification, have distinct specificities, requirements and complexity of design and operation, and must be regarded in the context of distinct applications. Direct (air) gasification is less complex and easier to perform, however, the PG, while still presenting suitable properties for some applications such as burning in industrial furnaces for heat production, is diluted in N_2 and, consequently, has a lower heating value. Indirect (steam) gasification, despite allowing the production of a gas enriched in H_2 and with a higher heating value, and thus suitable for added value applications such as synthetic fuels production, has more complex design and operation requirements due to the necessity of an external heat source to support the gasifier and frequently requiring circulation of significant amounts of heat between two reactors, as for example in DFB gasifiers. More information about this can be found in Chapter 2.

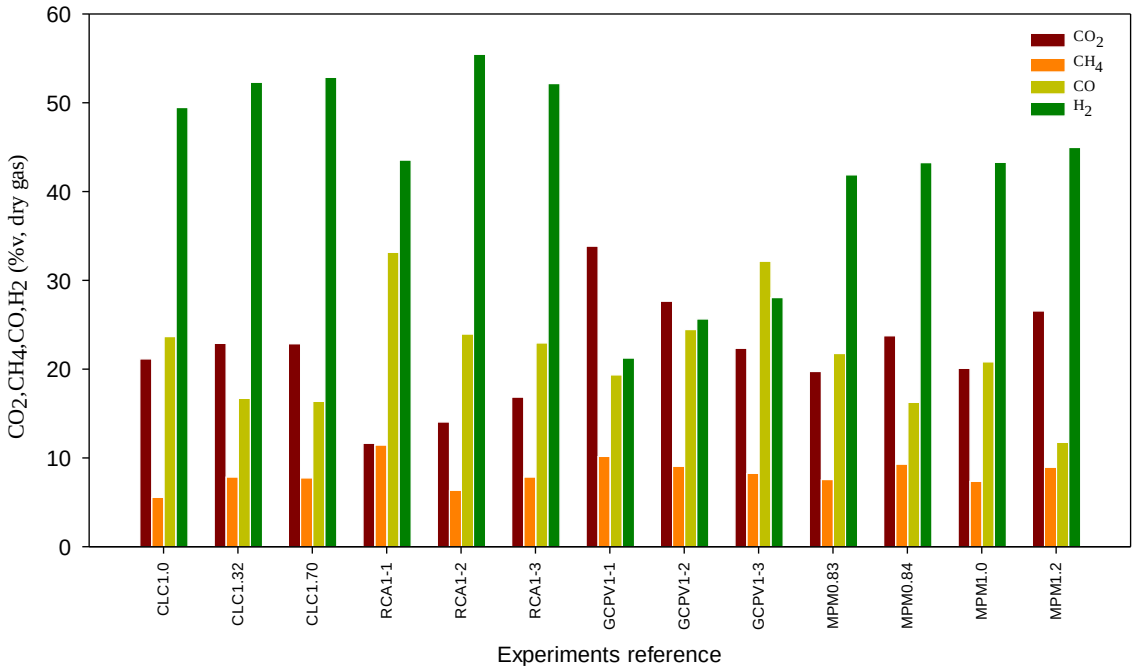

Figure 4.11 – Composition (CO_2, CH_4, CO and H_2) of the PG reported in the literature regarding biomass indirect (steam) gasification studies in different types of reactors. Experiments reference according to Table 4.3.

From the experimental results obtained in this work and literature review, it is observed that during direct (air) biomass gasification the characteristics of the gas produced and the process performance parameters can vary in a wide range (Table 4.2, Table 4.3 and Table 4.4), depending on the biomass fuel, operating conditions and gasifier type, and this must be accounted for and evaluated in order to properly support the development of each specific application.

Table 4.4 – Range of CO and H_2 concentration in the PG, LHV of the PG, Y_{gas}, CGE and CCE during the biomass gasification experiments. Comparison of data from this study with other studies of direct and indirect gasification, including BFB and other types of reactors (Table 4.3).

	CO [% vol, dry gas]	H_2 [% vol, dry gas]	LHV [MJ/Nm³ dry gas]	Y_{gas} [Nm³/kg biomass dry basis]	CGE [%]	CCE [%]
This work	13.2-21.4	2.0-12.7	4.4-6.9	1.2-2.2	41.1-62.6	60.0-87.5
BFB direct (air) gasification	7.2-26.6	1.2-24.0	0.1-7.8	1.2-4.1	23.5-69.0	55.0-92.8
Other reactors direct (air) gasification	6.9-32.0	3.0-17.0	2.4-7.3	1.4-2.9	44.2-77.0	81.6-102.0
Indirect (steam) gasification	11.8-33.2	21.3-55.5	9.6-15.8	nd	nd	nd

nd - no data provided in the analyzed studies.

4.1.5 CONCLUSIONS

In this work a set of new experimental results regarding the demonstration of direct (air) biomass gasification in a pilot-scale BFB reactor are presented and analyzed. The research was focused on the evaluation of distinct residual forest biomass quality as fuel and the influence of the operating variables on the quality of the dry gas produced. The pilot-scale BFB reactor was successfully operated under autothermal gasification conditions at bed temperatures between 700ºC and 850ºC, without the need of auxiliary external heat sources. The temperature at several locations along the reactor and the properties of the produced gas were very stable along time reflecting the existence of steady-state operating conditions and the adequacy of the BFB reactor, and its inherent characteristics as reactive system, to this thermochemical process. From the experimental results obtained and literature data integration it is concluded that it is possible to produce a combustible gas from direct (air) gasification of distinct biomass fuels under steady-state operation of BFB, providing reliable information to support the scale-up of the process.

For the experimental operating conditions used in the pilot-scale BFB, namely ERs in the range 0.17 to 0.36, the dry gas composition (volume basis) was 14.0 to 21.4 % CO, 14.2 to 17.5 % CO_2, 3.6 to 5.8 % CH_4, 1.3 to 2.4 % C_2H_4, 2.0 to 12.7 % H_2 and 48.9 to 61.1 % N_2. The highest concentration of CO, CH_4 and C_2H_4 was observed during the gasification of RFB derived from eucalyptus with an ER of 0.17 at a bed temperature of 736 ºC, however, the highest concentration of H_2 was obtained in the gasification of wood pellets with an ER of 0.24 and bed temperature of 802 ºC. The LHV of the PG was found between 4.4 and 6.9 MJ/Nm^3, with the higher values found for ER between 0.22 and 0.25 with average bed temperatures in the range 798 ºC to 816 ºC, and for ER between 0.17 to 0.20 with average bed temperatures between 719 ºC to 736 ºC. The Y_{gas} was between 1.2 and 2.2 Nm^3/kg biomass db, the CGE between 41.1 and 62.6 % and the CCE between 60.0 and 87.5 %.

In order to support a deeper understanding of the influence of distinct fuels and operating parameters on the quality of the dry gas produced during biomass gasification in BFB, the new experimental data obtained in this work was integrated with the analysis of a survey of published data about gas properties and process performance parameters of direct (air) biomass gasification. It was observed that there is a wide range of variation in the composition and LHV of the PG, and also on the Y_{gas}, CGE and CCE, and that these are deeply influenced by the fuel type, operating conditions and reactor type. Concerning the BFB gasifiers, the experimental results obtained in this work are in the medium to upper range of values found in the literature about direct biomass gasification, namely, the concentration of combustible gas components (e.g. CO between 7.2 and 26.6%v, H_2 between 1.2 and 24.0 %v, CH_4 between 0.7 and 8.4 %v), lower heating value (between 0.1 and 7.8 MJ/Nm^3), CGE (between 23.5 and 69.0 %) and CCE (between 55.0 and 92.8 %); the exception is the Y_{gas}, for which the experimental results obtained in this work are in the lower/medium range of the values reported on the literature (between 1.2 and 4.1 Nm^3 gas/kg biomass dry basis). The experimental results, complemented by the analysis of published information, point out for maximum LHV of the PG at ER in the range 0.17 to 0.27, and a strong dependence of this parameter with the operating temperature.

From the integrated analysis of published information, it is also shown how wide can be the variation of the quality of the produced gas and performance parameters values of the process of direct (air) biomass gasification. The analysis made shows how important it is to obtain specific knowledge regarding the experimental demonstration of the biomass gasification process for each particular application in order to provide a suitable support for the development and optimization of new industrial projects and to avoid the afterward project drawbacks that have undeniably been a barrier to the implementation of this process worldwide. Therefore, this work supports the adequacy of the direct (air) gasification of distinct types of RFB in BFB as an autothermal and steady state process to produce a low heating value combustible gas.

4.2 ARTICLE V - SUPERHEATED STEAM INJECTION AS PRIMARY MEASURE TO IMPROVE PG QUALITY FROM BIOMASS AIR GASIFICATION IN AN AUTOTHERMAL PILOT-SCALE GASIFIER

4.2.1 ABSTRACT

This work evaluated the influence of superheated water steam injection in an autothermal 80 kW_{th} pilot-scale bubbling fluidized bed during biomass direct (air) gasification, focusing on the effect of S/B in the PG composition and gasification efficiency parameters. The process was also evaluated in an allothermal 3 kW_{th} bench-scale BFB and simulated in a thermodynamic equilibrium model.

For low-density biomass, the steam injection resulted in a PG with higher H_2 concentration and H_2/CO molar ratio, although with lower heating value, and in a decrease of the process efficiency. Thus, steam injection promoted a trade-off between parameters, that can be associated with a higher occurrence of the WGS reaction. For high-density biomass, along with an increase of H_2 concentration and H_2/CO molar ratio, steam injection promoted an increase of the PG heating value and process efficiency, which can be justified by a higher char accumulation in the reactor bed and consequent higher occurrence of char-steam reforming reactions.

Therefore, steam injection shows high potential to improve the PG quality from high-density biomass air gasification, however, for low-density biomass, it shows limited potential and should only be used to adjust H_2/CO molar ratio.

Keywords: Steam injection; Gasification; Air-steam; Biomass; Bubbling fluidized bed; H_2/CO

4.2.2 INTRODUCTION

Gasification allows the production of a gaseous fuel (e.g., PG, syngas) from biomass that can fit in the current carbon-based energy infrastructure or be used to obtain other bioproducts, including chemicals and liquid fuels [219,220,334]. Thus, gasification is commonly acknowledged as a key technology for the use of biomass [15,90,215,223]. Furthermore, gasification technologies flexibility and potential have led to their integration in various biorefineries designs that are currently under research [26,150,153,158,159], and argued as relevant tools in the transition to a more sustainable bioeconomy and in the combat against climate change [138]. For example, gasification-based PP biorefineries that seek the production of various bioproducts from the byproducts resulting from pulp production (e.g., black liquor, eucalyptus chips). In fact, the integration of gasification processes in the PP industry can be seen as a pathway for the industry to generate new revenues, overcome a continuously declining paper market and become environmentally friendly [62,63]. Nonetheless, for gasification processes to perform as expected in these advanced biorefinery designs, development of more reliable and advanced gasification technologies is required.

In this respect, the PG can be refined and upgraded by two main approaches: treatment inside the gasifier (primary measures) and hot gas cleaning downstream of the gasifier (secondary measures) [123,124]. Gasification of biomass can also be performed using different gasifying agents, for example air, oxygen, water steam (thereafter referred as steam), CO_2 and their mixtures, which results in changes in the PG composition and yield, and respective process efficiency [1,29,335]. In fact, replacing the N_2 from air by active gasifying agents such as CO_2 and steam, can be used as a strategy to enhance the heating value of the PG from biomass gasification [336,337]. Thus, the injection of steam as a primary measure can be considered as a potential solution to improve the PG quality from biomass direct (air) gasification, particularly in industries where excess steam streams are highly available.

Steam addition to direct (air) biomass gasification processes is argued to result in an increase of the H_2/CO ratio and H_2 yield in the PG [1,74,337,338], due to a promotion of the WGS reaction (Reaction 2.8) [1,339,340], the reaction of unconverted char with steam (Reaction 2.6) [340] and the reforming of methane with steam (Reaction 2.9) [341]. This is relevant because H_2 is the most desired gaseous compound in the PG as its further use in energy applications does not generate greenhouse gases emissions at the point of use, thus being promoted as an ideal CO_2-neutral energy vector for heating and transport [77,221,222,267,342,343]. In fact, policies and economic forces are converging to create momentum in the H_2 sector and establish pathways for a rapid development and employment of green H_2 technologies [344]. Furthermore, PG requires high H_2/CO molar ratios to be suitable for further conversion into liquid fuels and chemicals, such as DME synthesis (2 $mol.mol^{-1}$), methanol synthesis (1 $mol.mol^{-1}$) and liquid fuel production by FT synthesis (0.6 $mol.mol^{-1}$) [6,72,182]. Unfortunately, H_2/CO molar ratio in the PG from direct (air) biomass gasification processes in BFBs falls between 0.2 and 0.6 $mol.mol^{-1}$ [4,272].

Air-steam gasification has been addressed in controlled reactive environments such as thermogravimetric analysis and single particle experiments, which focused on the kinetic of the reactions between char and steam [336,342,345], and various numerical tools have been developed to predict and characterize this process [290,342,343,346,347]. Air-steam gasification has also been studied in allothermal reactors [342,348–351], whose temperature is controlled by external heat supply from electric heaters, however, this method of supplying heat influences the temperature distribution in the reactor, and subsequent reaction progress along the reactor, and is not technically nor economically feasible for large-scale implementation, thus these results must be interpreted cautiously [184].

Considering demonstration of the process in fixed bed reactors, Sharma and Sheth [339] performed air-steam gasification of switchgrass in a pilot-scale downdraft gasifier and showed that steam addition led to an increase in the H_2 content in the PG, which was attributed to the promotion of the WGS reaction. The authors also found a decrease of the oxidation and reduction zones temperature with steam injection. Cerone et al., [6] performed air-steam and oxy-steam gasification of lignin-rich solid residues derived from lignocellulosic biomass enzymatic hydrolysis in an autothermal pilot-scale updraft reactor, and observed an increase of H_2/CO molar ratio from 0.4 to 1.2 by increasing S/B from 0 to 0.5 during air-steam gasification. The authors also observed that oxy-steam gasification resulted in the generation of a PG with a maximum H_2/CO molar ratio of 2.1 for a S/B of 0.3, which is an acceptable value for the catalytic synthesis of biofuels.

Concerning the demonstration of the process in fluidized bed reactors, which are more suitable for higher scales of operation than fixed beds due to their inherent characteristics [286,352], existing information at higher scales than laboratorial is very scarce, with only a limited set of results available in the literature. In this regard, Campoy et al., [353] performed air-steam gasification of wood pellets in a pilot-scale BFB and reported an increase of char and tar conversion with steam addition. The authors concluded that steam addition is an interesting option to improve the efficiency of direct (air) biomass gasification, without leading to significant capital costs increase. Nevertheless, wider sets of data concerning the demonstration of air-steam gasification processes in pilot-scale autothermal BFBs are still missing in the literature, particularly in-depths analyses regarding the influence of the physical-chemical characteristics of the biomass feedstock on the process and the determination of the effect of the S/B on the PG composition and efficiency parameters.

Thus, knowledge production is required, particularly at higher operating scales, to improve the understanding of the process and to be able to support further technology improvements and scale-up. To address this gap, in this work, superheated steam injection was performed and evaluated during direct (air) gasification of distinct types of biomass (*Eucalyptus Globulus* and *Pinus Pinaster*) in an autothermal pilot-scale BFB gasifier, focusing on the effect of S/B in the stability of the process (e.g., bed temperature, freeboard temperature), PG composition and gasification efficiency

parameters. The process was also conducted in an allothermal bench-scale BFB gasifier and simulated in a thermodynamic equilibrium model based on the minimization of Gibbs free energy. The interest in this analysis emerges from steam being potentially able to improve the H_2 concentration and H_2/CO molar ratio of the PG, which are two relevant parameters for the technical and economic viability of the application of this gaseous fuel in various scenarios. The interest is further highlighted by the fact that eucalyptus is a byproduct from the PP industry and steam is highly available at low-cost in this industry. Thus, the development of steam injection as primary measure for the improvement of PG quality from biomass direct (air) gasification can be a relevant driver to ease the integration of gasification processes in the PP industry.

4.2.3 MATERIALS AND METHODS

The experimental infrastructures used for Article V were the DAO-UA 80 kW_{th} pilot-scale BFB gasifier and the DAO-UA 3 kW_{th} bench-scale BFB gasifier (Section 1.3). The methodologies used in this work are described in Section 1.4.

4.2.3.1 FEEDSTOCK CHARACTERIZATION

The feedstocks used in the gasification experiments performed were pine (*Pinus Pinaster*) and eucalyptus (*Eucalyptus globulus*), namely residual fractions resulting from forestry and industrial operations involving these types of biomass. Eucalyptus was chosen as feedstock due to its relevance as a byproduct from the PP industry and pine was chosen for comparison purposes and because it is the most abundant tree species in the Portuguese forests [354]. In terms of feedstock pretreatment, sieving and drying was performed as deemed necessary, followed by chipping or pelletizing. Thus, the feedstocks include pellets made from pine (6 mm diameter), pellets made from eucalyptus RFB (2 to 4 mm diameter), chipped (2 to 4 mm) RFB derived from pine and chipped (<5 mm) RFB derived from eucalyptus. The RFB derived from pine resulted from forestry operations, namely tree logging for the wood industry, and consisted of fine branches from the tops of the trees, with a small content of olive kernel, hereafter referred by pine RFB. The RFB derived from eucalyptus resulted from fines generated during woodchip production from eucalyptus logs in the PP industry. Pelletizing was performed due to three main reasons, namely:

- To increase the uniformity of the physical characteristics of the feedstocks and consequently improve feeding regularity.
- To increase char accumulation in the bed due to the higher density of the pelletized form of biomass in comparison with the RFB chipped form, which leads to lower reactivity and entrainment with the flue gas, and consequently increase the contact between steam and char.
- To analyze the effect of the pelletized form of biomass in the H_2 concentration in the PG.

The feedstocks were characterized in terms of properties with interest for biomass thermochemical conversion, namely proximate and ultimate analysis, heating value and bulk density (Table 4.5).

Table 4.5 – Proximate and elemental analysis of the biomass types used as feedstock in the gasification experiments and as input for the thermodynamic equilibrium model (Article V).

	Pine Pellets	Pine RFB	Eucalyptus pellets	Eucalyptus RFB
Proximate analysis				
Moisture (%wt, wb)	4.6	10.6	7.9	27.5
Volatile matter (%wt, db)	82.3	69.0	77.1	77.3
Fixed carbon (%wt, db)	17.4	30.3	18.5	21.5
Ash (%wt, db)	0.3	0.7	4.4	1.2
Ultimate analysis (%wt, db)				
Ash	0.3	0.7	4.4	1.2
C	47.5	49.2	51.4	49.1
H	6.2	6.7	6.1	6.5
N	0.1	0.4	1.4	0.1
S	nd	nd	nd	nd
O (by difference)	45.9	43.0	36.7	43.1
LHV (MJ/kg db)	18.0	18.7	20.0	18.3
Bulk density (kg/m^3 wb)	614	403	437	154

nd- not determined, below the detection limit of the method, 100 ppm wt.

4.2.3.2 OPERATING CONDITIONS

The operating conditions of the gasification experiments performed Article V are detailed in Table 4.6. For the pilot-scale reactor, the ER was maintained between 0.24 and 0.26 and the bed temperature between 734 and 789 ºC. For the bench-scale reactor, the ER was kept at 0.25 and the bed temperature at 800 ºC (imposed by an electrical furnace and respective temperature controller). The S/B was varied between 0 and 0.6 in both experimental infrastructures.

Regarding the developed thermodynamic equilibrium model (methodology explained in Section 1.4.), the parameters used as input were analogous to the ones attained in the practical gasification experiments (Table 4.6), namely:

- Feedstock CHONS composition: Pine RFB, eucalyptus RFB, pine pellets and eucalyptus pellets.
- Bed temperature: 734 to 800 ºC.
- ER: 0.24 to 0.26.
- S/B: 0 to 0.6.
- Pressure: 1 atm.

Table 4.6 – Gasification experiments reference and respective operating conditions (Article V).

Experiment reference	Biomass type	BFB scale	ER	T_{bed} [ºC]	$T_{freeboard}$ [ºC]	$Q_{biomass}$ [kg/h]	Q_{Steam} [kg/h]	S/B [kg steam/kg biomass]	Q_{air} [NL/ min]
PE-0.0	Eucalyptus RFB	Pilot	0.24	751	711	15	0.0	0.0	200
PE-0.2	Eucalyptus RFB	Pilot	0.26	734	659	14	2.8	0.2	200
PE-0.4	Eucalyptus RFB	Pilot	0.25	748	687	14	5.7	0.4	200
PE-0.6	Eucalyptus RFB	Pilot	0.26	764	706	14	8.2	0.6	200
PP-0.0	Pine pellets	Pilot	0.25	789	715	12	0.0	0.0	200
PP-0.2	Pine pellets	Pilot	0.25	757	708	12	1.9	0.2	200
PP-0.4	Pine pellets	Pilot	0.25	769	722	12	4.9	0.4	200
PP-0.5	Pine pellets	Pilot	0.25	768	718	12	6.2	0.5	200
PP-0.6	Pine pellets	Pilot	0.25	764	703	12	6.9	0.6	200
BE-0.0	Eucalyptus pellets	Bench	0.25	800	800	0.21	0.00	0.0	4
BE-0.2	Eucalyptus pellets	Bench	0.25	800	800	0.21	0.04	0.2	4
BE-0.4	Eucalyptus pellets	Bench	0.25	800	800	0.21	0.08	0.4	4
BE-0.6	Eucalyptus pellets	Bench	0.25	800	800	0.21	0.13	0.6	4
BP-0.0	Pine RFB	Bench	0.25	800	800	0.23	0.00	0.0	4
BP-0.2	Pine RFB	Bench	0.25	800	800	0.23	0.05	0.2	4
BP-0.4	Pine RFB	Bench	0.25	800	800	0.23	0.09	0.4	4
BP-0.6	Pine RFB	Bench	0.25	800	800	0.23	0.14	0.6	4

4.2.4 RESULTS AND DISCUSSION

The results presented in this Section include temperature and PG composition (H_2, CO, CO_2, CH_4 and C_2H_4) profiles along time for the autothermal pilot-scale 80kW_{th} BFB reactor, and the average PG composition (H_2, CO, CO_2, CH_4, C_2H_4, C_2H_6, C_3H_8, N_2, H_2/CO) and efficiency parameters (LHV_G, Y_{gas}, CGE and CCE) for the autothermal 80 kW_{th} pilot-scale reactor and allothermal 3 kW_{th} bench-scale BFB reactor. The obtained results are compared to respective predictions from the developed non-stoichiometric thermodynamic model. The focus is the determination and analysis of the influence of steam injection (S/B parameter) during the direct (air) gasification process of biomass under different conditions of operation.

4.2.4.1 INFLUENCE OF S/B ON TEMPERATURE AND GAS COMPOSITION PROFILES ALONG TIME

For all gasification experiments performed (ER as low as 0.24 and steam flow as high as 8.2 kg/h), the gasifier was operated under autothermal regime (with average bed temperature above 734 ºC); it is important to state that electrical heating was needed to produce the steam in the external boiler. Furthermore, it was not observed any agglomeration or defluidization phenomena during the experiments, independently of the steam injection.

A typical temperature profile along time for the gasification experiments made in the autothermal pilot-scale reactor is shown in Figure 4.12. The temperature profiles for the distinct gasification experiments have similar behavior, however, it can be noticed some differences between feedstock type and a slight decrease of the temperature at different locations of the reactor with the insertion of steam. The latter can be justified by the fact that steam was produced at a temperature significantly lower (120 to 135 ºC) than the one observed at the reactor bottom bed and freeboard during the gasification experiments. Thus, the flow of steam absorbed thermal energy to rise the steam to the operating temperature of the gasifier. Thereafter, after a short period of time, the system reached a new steady-state condition of operation temperature (Figure 4.12). Slightly lower temperature and higher temperature fluctuations were also observed during experiments performed with RFB from

eucalyptus, which can be justified by the physical heterogenous characteristics and higher moisture content of this feedstock [4,355].

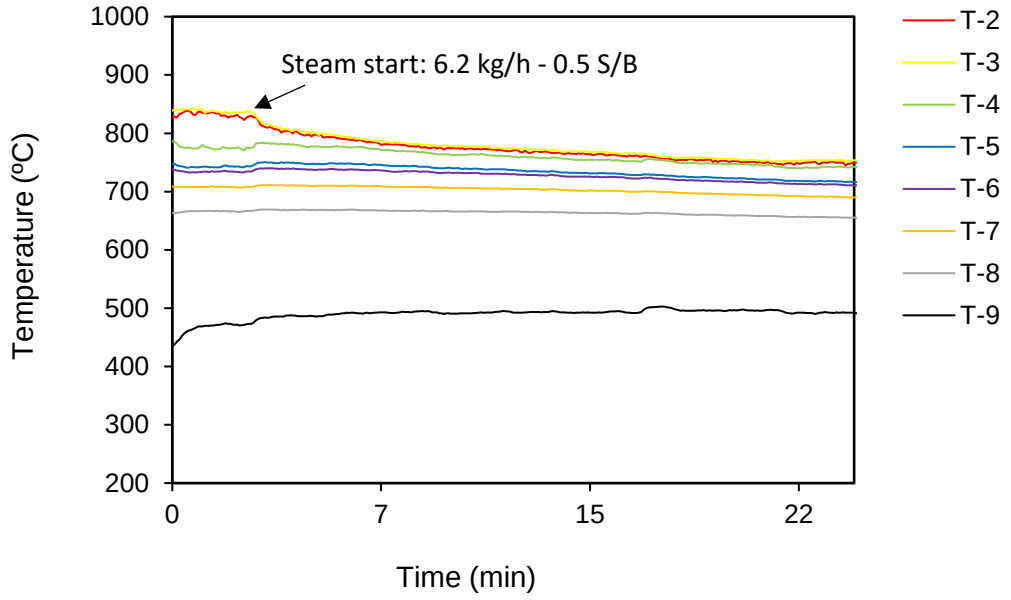

(a)

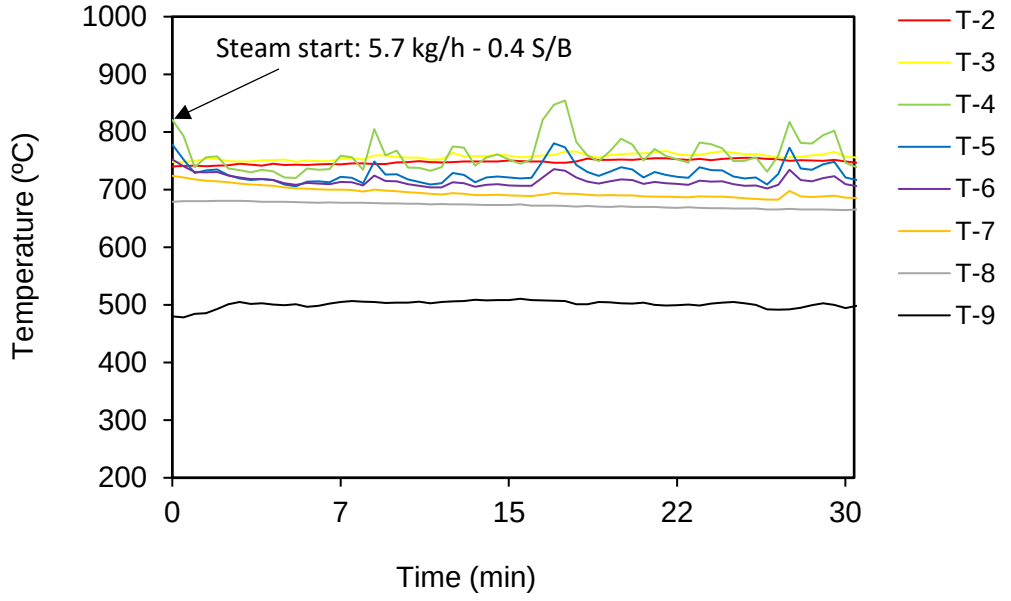

(b)

Figure 4.12 – Typical temperature profile along time at different locations of the pilot-scale BFB reactor for the experiment (a) PP-0.5 (Pine pellets, 6.2 kg/h steam) and (b) PE-0.4 (Eucalyptus RFB, 5.7 kg/h steam).

In Figure 4.13, it is shown the typical PG composition along time for distinct gasification experiments performed in the autothermal pilot-scale reactor. Analogous to the temperature profiles presented, it was observed a relatively stable PG composition along time, independently of the steam injection.

Thus, steady-state conditions of operation, similar to those observed during previous direct (air) biomass gasification studies performed in this pilot-scale infrastructure [4], were attained. However, slightly higher gas composition fluctuations were found for experiments performed with RFB from eucalyptus, which can be justified by the more irregular fuel feeding resulting from the heterogeneous physical characteristics and higher moisture content of this feedstock, as already stated regarding the temperature profiles.

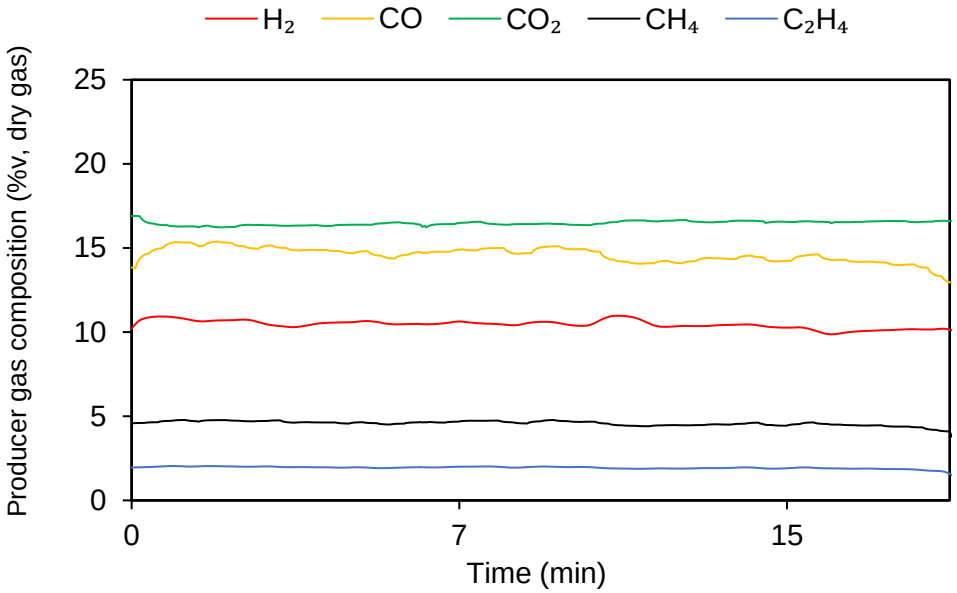

(a)

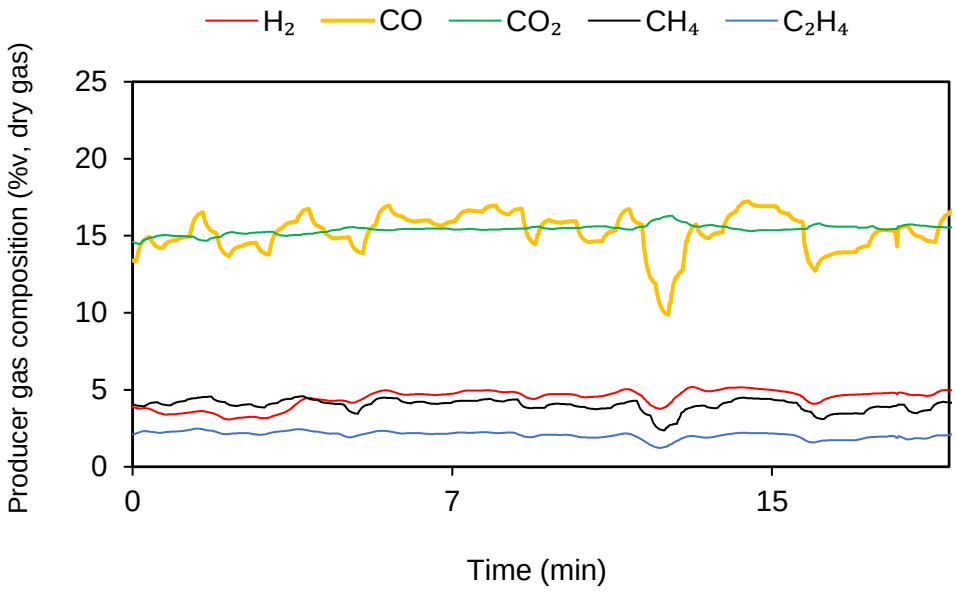

(b)

Figure 4.13 – Typical PG composition profile along time at different locations of the pilot-scale BFB reactor for the experiment (a) PP-0.5 (Pine pellets, 6.2 kg/h steam) and (b) PE-0.4 (Eucalyptus RFB, 5.7 kg/h steam).

4.2.4.2 INFLUENCE OF S/B ON PG COMPOSITION

The impact of the S/B on the composition of the PG (H_2, CO, CO_2, CH_4 C_2H_4, H_2/CO molar ratio) for the gasification experiments performed in the autothermal pilot-scale BFB gasifier and allothermal bench-scale BFB gasifier, and respective comparison with thermodynamic predictions for the same operating parameters (Table 4.6), is shown in Figure 4.14.

The H_2 concentration in the dry PG was found between 4.2 and 11.9 %v for the experiments in the autothermal pilot-scale BFB, with the maximum value found for the gasification of pine pellets with S/B equal to 0.6 (PP-0.6). It can be observed that the addition of steam led to an increase in H_2 concentration in the PG, which is in accordance with the thermodynamic predictions. This suggests a promotion of the WGS and char-steam reforming reactions with S/B increase. Nonetheless, H_2 increase with S/B increase is more evident for the thermodynamic predictions than for practical gasification experiments. It is also observed that the H_2 concentration is significantly higher in the thermodynamic predictions, independently of the operating parameters. This indicates that the PG composition is far from equilibrium during direct (air-steam) biomass gasification in BFBs. Furthermore, H_2 concentration was lower in experiments made with RFB feedstocks in comparison with experiments performed with pelletized biomass, suggesting the influence of the physical characteristics of the feedstock, namely the higher density of pellets promoting higher concentration of char inside the reactor bed and its subsequent reaction with steam to produce H_2. Accordingly, it was also observed a limited effect for the S/B in the H_2 concentration for the gasification experiments with RFB from eucalyptus in the autothermal pilot-scale gasifier, which can be justified by two main reasons:

1. A low occurrence of char-steam reforming reactions promoted by the low char concentration in the reactor bed. This was observed by subsequent combustion experiments of the bed material; the bottom bed temperature immediately decreased after stopping the eucalyptus RFB feeding, meaning that a very limited amount of residual char was burning in the bed. This is a consequence of the physical characteristics of the RFB from eucalyptus (e.g., low bulk density, small particle size, Table 4.5), which lead to high reactivity and char entrainment and elutriation with the upward flow gas. In fact, it was also observed lower CCE during eucalyptus RFB gasification experiments, in comparison with pine pellets gasification experiments (Section 4.2.4.3), which suggests higher losses of unreacted char, for example by elutriation and entrainment with the PG, despite the higher reactivity of the RFB and lower in-bed inventory of char.
2. Undesired variations of the reactor temperature and ER caused by the high variability of the moisture content of the eucalyptus RFB, in comparison with the more uniform moisture content of the pine pellets.

The CO concentration in the PG was found between 10.9 and 16.2 %v for the gasification experiments in the autothermal pilot-scale BFB, with the maximum value observed for the gasification of pine pellets with S/B equal to 0 (PP-0.0). It is observed a trend for a slight decrease of this gaseous specie concentration with S/B increase for both pilot-scale autothermal and bench-scale allothermal experiments. This trend was significantly more pronounced for the thermodynamic predictions. In fact, the predicted CO concentration for S/B equal to 0 was significantly higher than the value found in the experimental results, and, with increasing S/B, the predicted CO concentration values became significantly closer to the experimental values. However, for the gasification experiments using pine pellets in the autothermal BFB, the CO concentration remained almost unchangeable with S/B increase. This distinct behavior can result from the higher inventory of char found in the bottom bed during pine pellets gasification, as previously discussed for H_2 concentration. The increase in the bed char inventory promotes the occurrence of char-steam reforming reactions, and respective steam consumption in the bed, and consequently cause the decrease of the occurrence of the WGS reaction. Thus, under these conditions, an increase in the steam flow rate will promote

higher char-steam reforming reactions, leading to the increase in CO production, and may not have a significant effect on the WGS reaction, thus avoiding CO concentration decrease.

The H_2/CO molar ratio (Figure 4.14) in the PG is a fundamental parameter for the aplication of the PG for synthesis applications [6] and is a direct consequence of the concentration of H_2 and CO in the PG. For the gasification experiments in the autothermal pilot-scale BFB gasifier, this ratio was between 0.3 and 0.8 mol.mol^{-1}, with the maximum value found for the gasification of pine pellets with S/B equal to 0.6 (PP-0.6). This maximum value found is suitable for using the PG for FT liquid synthesis, which has a suggested lower limit of 0.6 mol.mol^{-1} for this ratio [72]. It can be observed an evident trend for the increase of the H_2/CO molar ratio with S/B increase for all the gasification experiments made and the thermodynamic predictions. Nonetheless, this trend is less pronounced for the gasification experiments in the autothermal pilot-scale gasifier, and more evident for the gasification experiments in the allothermal bench-scale gasifier. The latter is also closer to the predicted trends of the thermodynamic equilibrium, which generally show a stronger increase of the H_2/CO molar ratio with S/B increase. In fact, for eucalyptus pellets gasification experiments in the allothermal BFB gasifier, the experimental results and thermodynamic predictions show a very good match.

In this regard, it must be noted that apart from the aforementioned influence of the fuel morphology (e.g., lower bulk density of the feedstocks leading to lower char accumulation in the reactor bottom bed), the impact of S/B on the composition of the PG composition is also influenced by the characteristics of the BFB used, consequently hindering direct comparisons between the gasification experiments performed in the two gasifiers. For example, the smaller fluidization velocity (14 cm/s) used in the allothermal bench-scale gasifier, in comparison with the autothermal pilot-scale gasifier (30 cm/s), should push gas-gas reactions, such as water-gas shift, closer to equilibrium. Furthermore, this lower fluidization velocity also contributes to higher carbon conversion, consequently reducing char accumulation in the reactor bottom bed and increasing the occurrence of the water-gas shift reaction, due to lower steam consumption in the bed. However, the bed height and reaction chamber height of the bench-scale gasifier is also significantly lower than the pilot-scale gasifier (Section 2.2), compensating the lower fluidization velocity employed in terms of resulting residence time of the vapors/gasifying agent in the bottom bed and freeboard of the gasifier.

Thus, other factors should come into play, such as the temperature profiles of the gasifiers along the reactor chamber. In fact, the bench-scale gasifier typically showed a higher decay of temperature along the reactor height than the pilot-scale gasifier, and this is relevant because the forward water-gas shift reaction (consumption of CO and production of H_2) is exothermic and mainly active at temperatures lower than 700 ºC, consequently suggesting that steam addition will have a higher impact on the water-gas shift reaction occurrence in the bench-scale gasifier; this is in accordance with the higher increase of H_2/CO molar ratio with S/B increase found for the experiments performed in the bench-scale BFB. Nevertheless, the comprehensive analysis of these aspects is out of the scope of this work.

The CO_2 concentration was found between 15.3 and 16.8 %v for the gasification experiments in the autothermal pilot-scale BFB gasifier, with the maximum value found for the gasification of pine pellets with S/B equal to 0.4 (PP-0.4). The influence of S/B in the CO_2 concentration is not clear for the gasification experiments performed; this is in contrast with the thermodynamic predictions, which show a significant trend for the increase of CO_2 concentration with S/B increase. This difference can be justified by the fact that the thermodynamic model did not predict any char accumulation in the reactor bed for any operating condition (Section 4.2.4.3), including gasification with only air, consequently indicating that steam addition mainly has impact in gas-gas reactions. However, char accumulation in the reactor bed was observed during various gasification experiments with air and air with steam injection, which indicates that steam had significant contact with solid carbon and consequently was involved in gas-solid reactions. Accordingly, the experimental results suggest that

the CO_2 concentration variation with S/B is influenced by a trade-off between char-steam reforming reactions, and consequent steam consumption, and the WGS reaction. In fact, the CO_2 concentration variation with S/B indicates that the WGS reaction is not having as much relevance as expected, probably due to a low residence time of the PG in the freeboard of the reactors and the significant char accumulation observed in the reactor bed for some experiments.

The CH_4 concentration was found between 2.9 to 4.8 %v for experiments in the autothermal pilot-scale BFB gasifier, with the maximum value found for the experiment performed with pine pellets and S/B equal to 0.4. It can be observed a slight trend for the decrease of CH_4 concentration with S/B increase for the gasification experiments performed and thermodynamic predictions. This can be related to a promotion of the methane-steam reforming reaction (Reaction 2.9) with S/B increase and to the relative increase of other gaseous species (e.g., H_2). For example, the WGS reaction contributes to an increase of dry gas production (H_2O is consumed to generate CO and H_2, and this will be discussed ahead in terms of Y_{gas}). It can also be noticed that the CH_4 concentration values in the thermodynamic predictions are significantly lower than in the gasification experiments performed; this reflects that thermodynamic equilibrium conditions are far from being achieved during the gasification experiments performed, independently of the reactor size, feedstock or heating regime employed.

The concentration of light hydrocarbons, namely C_2H_4, C_2H_6 and C_3H_8, was found between 1.4 to 1.9, 0.2 to 0.3 and 0.1 to 0.2 %v, respectively, for the gasification experiments performed in the autothermal pilot-scale BFB gasifier. These gaseous species concentration values are not shown in Figure 4.14 because they were only found in very small amounts (0.0 to 1.9 %v for gasification experiments and thermodynamic predictions) and no evident impact from the steam injection was observed. In the thermodynamic equilibrium model, it is predicted that the PG does not contain any amount of these light hydrocarbons, thus these values corroborate the evidence that in direct (air-steam) gasification experiments in BFBs equilibrium is not attained.

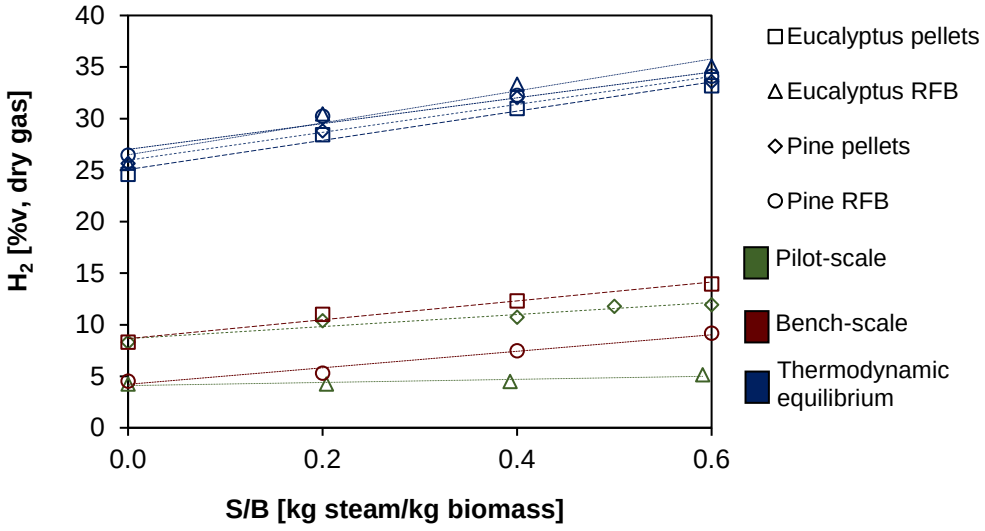

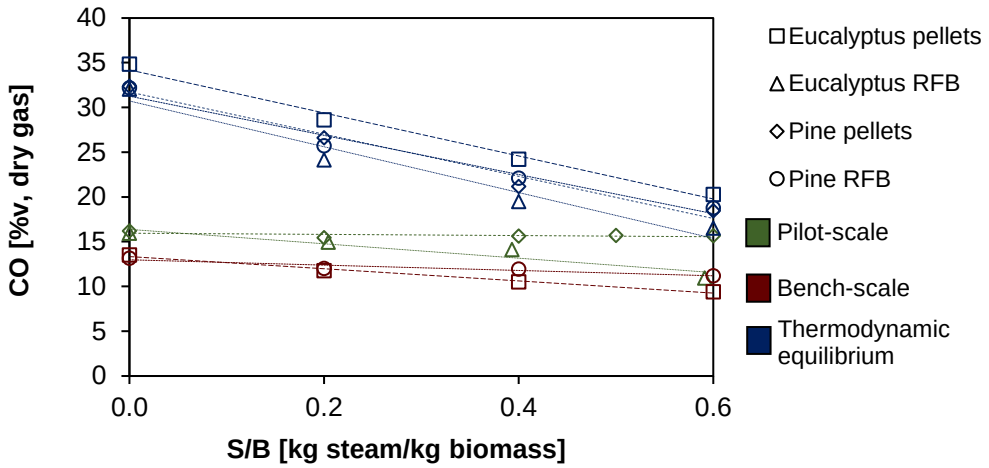
CO [%v, dry gas]
40
35
30
25
20
15
10
5
0
0.0
0.2
0.4
0.6
S/B [kg steam/kg biomass]
Eucalyptus pellets
Eucalyptus RFB
Pine pellets
Pine RFB
Pilot-scale
Bench-scale
Thermodynamic equilibrium

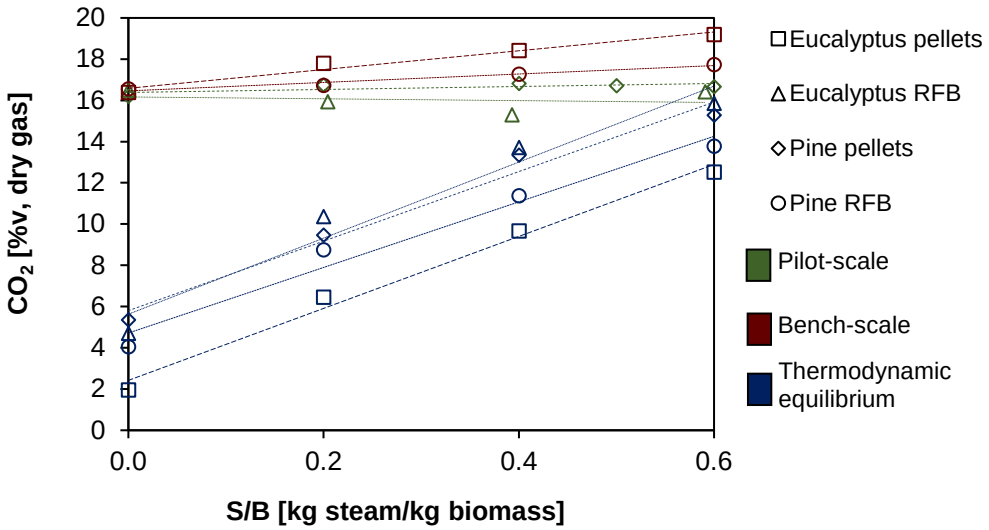
CO2 [%v, dry gas]
20
18
16
14
12
10
8
6
4
2
0
0.0
0.2
0.4
0.6
S/B [kg steam/kg biomass]
Eucalyptus pellets
Eucalyptus RFB
Pine pellets
Pine RFB
Pilot-scale
Bench-scale
Thermodynamic equilibrium

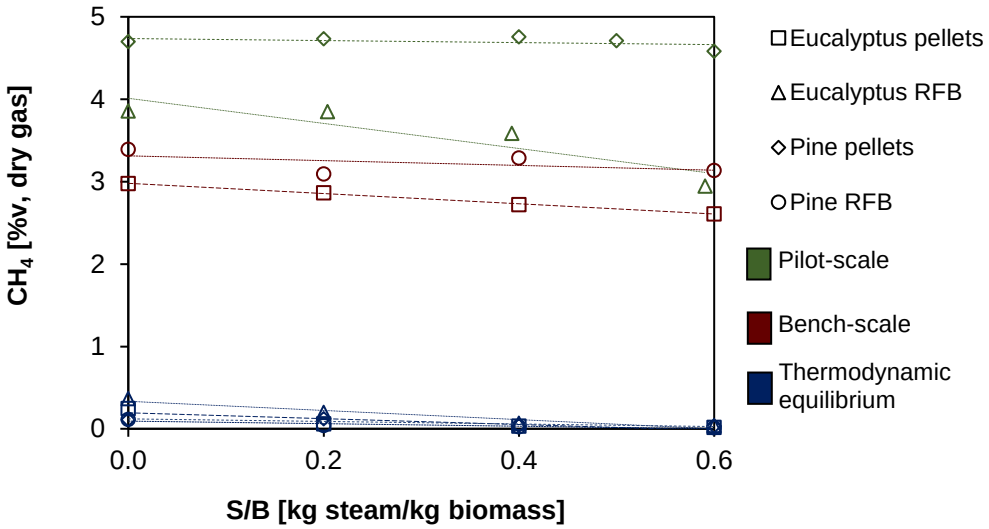
CH4 [%v, dry gas]
5
4
3
2
1
0
0.0
0.2
0.4
0.6
S/B [kg steam/kg biomass]
Eucalyptus pellets
Eucalyptus RFB
Pine pellets
Pine RFB
Pilot-scale
Bench-scale
Thermodynamic equilibrium

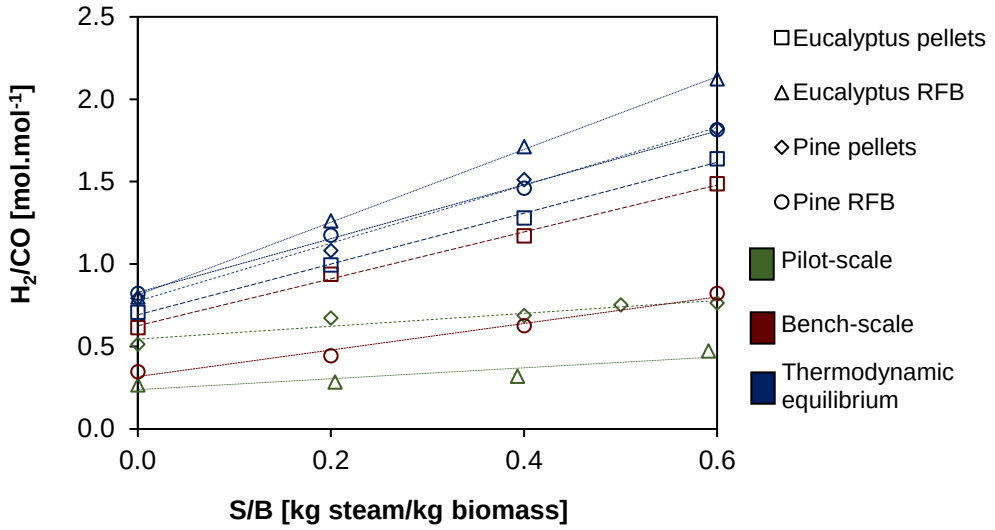

Figure 4.14 – Influence of the S/B on the composition of the dry PG (H_2, CO, CO_2, CH_4 and H_2/CO molar ratio) for the gasification experiments in the autothermal pilot-scale and allothermal bench-scale BFB reactors, and comparison with thermodynamic predictions for the same operating parameters. Operating parameters detailed in Table 4.6.

4.2.4.3 INFLUENCE OF STEAM ON PROCESS EFFICIENCY PARAMETERS

4.2.4.3.1 LHV and Y_{gas}

In Figure 4.15, it is shown the LHV of the PG and the Y_{gas} for the gasification experiments in the autothermal pilot-scale BFB gasifier and allothermal bench-scale BFB gasifier, and respective comparison with thermodynamic predictions for equal operating parameters (Table 4.6).

The LHV of the PG was found between 3.9 and 6.3 MJ/Nm^3 for the gasification experiments performed in the autothermal pilot-scale reactor, with the maximum value found for the gasification of pine pellets with S/B equal to 0.5. In general, it can be observed that the LHV of the PG decreases with S/B increase; the exception was the gasification of pine pellets in the pilot-scale BFB, where a slight increase was observed. This decrease of LHV of the PG with S/B increase was previously reported in other air-steam gasification experimental works [1]. This results from a trade-off between the concentration of combustible gases caused by the S/B increase, for example due to a promotion in the WGS reaction. The exception observed, namely for the pine pellets gasification in the autothermal pilot-scale BFB gasifier, can be justified by the fact that the CO concentration did not decrease with S/B increase, while H_2 concentration still increased in the same proportions as observed for the other experiments. This suggests a higher occurrence of char-steam reforming reactions and a lower occurrence of the WGS reaction, in comparison with other experiments, as previously discussed in the analysis regarding CO concentration (Section 4.2.4.2). Thus, it seems that with certain operating parameters, namely those that favor higher concentration of char within the reactor bed (e.g., low ER, high-density biomass feedstocks), steam addition may not lead to a decrease of the LHV of the PG. The thermodynamic equilibrium predictions also show a decrease on the LHV with increasing S/B; this effect is more pronounced that that observed in the experimental results.

The Y_{gas} was found between 1.5 and 1.8 Nm^3 dry gas/kg dry biomass for the gasification experiments performed in the autothermal pilot-scale BFB gasifier, with the maximum value found for the gasification of pine pellets with S/B equal to 0.5 (PP-0.5). In general, the experimental results show

a slight trend for the increase of Y_{gas} with S/B increase, which is in accordance with the trend observed in the thermodynamic equilibrium results, despite this latter being more pronounced. In the gasification experiments performed, this increase can be justified by the conversion of char with steam to gaseous species and to the WGS reaction, which contributes to an increase of the dry gas production (H_2O is consumed to generate CO and H_2). In the thermodynamic equilibrium model, this increase can only be associated with homogenous gaseous reactions (e.g., WGS reaction), because the model did not predict any char accumulation in the reactor bed for any operating condition, including conditions without steam addition, as previously discussed (Section 4.2.4.2).

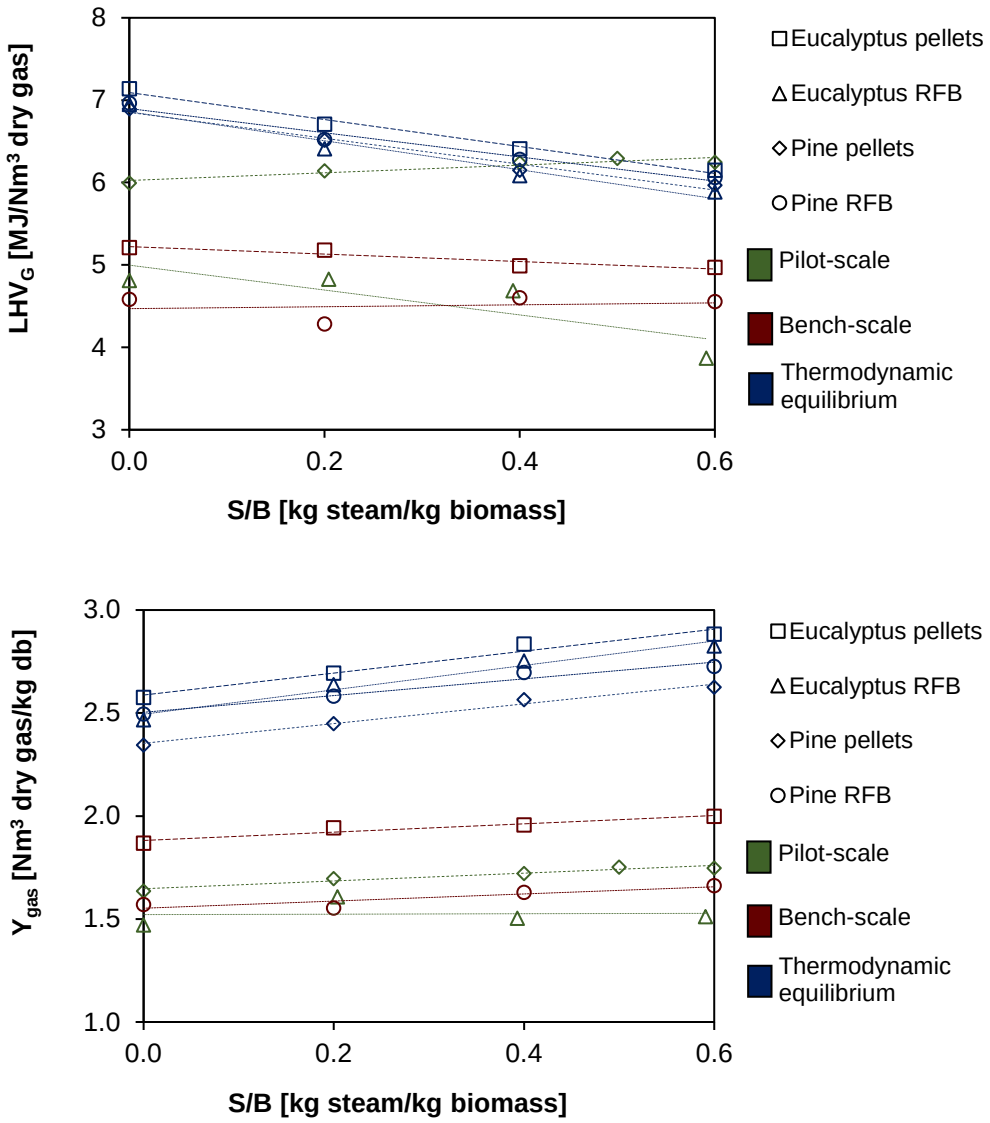

Figure 4.15 – Influence of the S/B on the LHV of the PG and Y_{gas} for the gasification experiments in the autothermal pilot-scale and allothermal bench-scale BFB reactors, and comparison with thermodynamic predictions for equal operating parameters. Operating parameters detailed in Table 4.6.

4.2.4.3.2 CGE and CCE

In Figure 4.16, it is shown the CGE and CCE for the gasification experiments performed, and respective comparison with thermodynamic predictions for equal operating parameters (Table 4.6).

For the gasification experiments performed in the autothermal pilot-scale BFB gasifier, the CGE was found between 33 and 62 % and the CCE between 56 and 82 %. It can be observed that both CGE and CCE follow similar trends with S/B increase, which are also analogous to the trend previously analyzed between LHV of the PG and S/B (Figure 4.15). This is further corroborated by the direct relation observed between these parameters for the experimental data (Figure 4.17). However, the influence of S/B on the CGE and CCE is not equal for each feedstock and reactor. In fact, for some gasification experiments, the S/B increase leads to an increase of these efficiency parameters, while for others it leads to a decrease. This phenomenon is related to the relevance of char accumulation in the reactor bed, which was particularly observed during the experiments performed with pine pellets in the autothermal pilot-scale BFB gasifier, and respective char-steam reforming reactions; in this case, S/B increase led to the highest observed relative increase of CGE and CCE. However, for the gasification experiments with RFB from eucalyptus (very low char accumulation in the reactor bed), the increase of S/B led to a significant decrease of CGE and CCE. These aspects also deviate from the thermodynamic model, which shows a decrease of CGE and a constant CCE with S/B increase for all operating conditions (Table 4.6). In fact, the thermodynamic model results show 100% CCE for all predicted cases and this reveals that the model did not predict any char accumulation in the bed, which is in contrast with experimental observations, and leads to significant deviations between the model and experimental results, as previously discussed.

These combined results indicate the importance of using high-density biomass for air-steam gasification processes in order to promote char accumulation and consequent char-steam reforming reactions. Furthermore, for similar operating parameters, all determined parameters (LHV, Y_{gas}, CGE and CCE) were higher for gasification experiments using high-density biomass (e.g., pellets), in comparison with gasification experiments using low-density biomass (e.g., chipped RFB); this further indicates the relevance of the physical characteristics of the biomass feedstock on the gasification process.

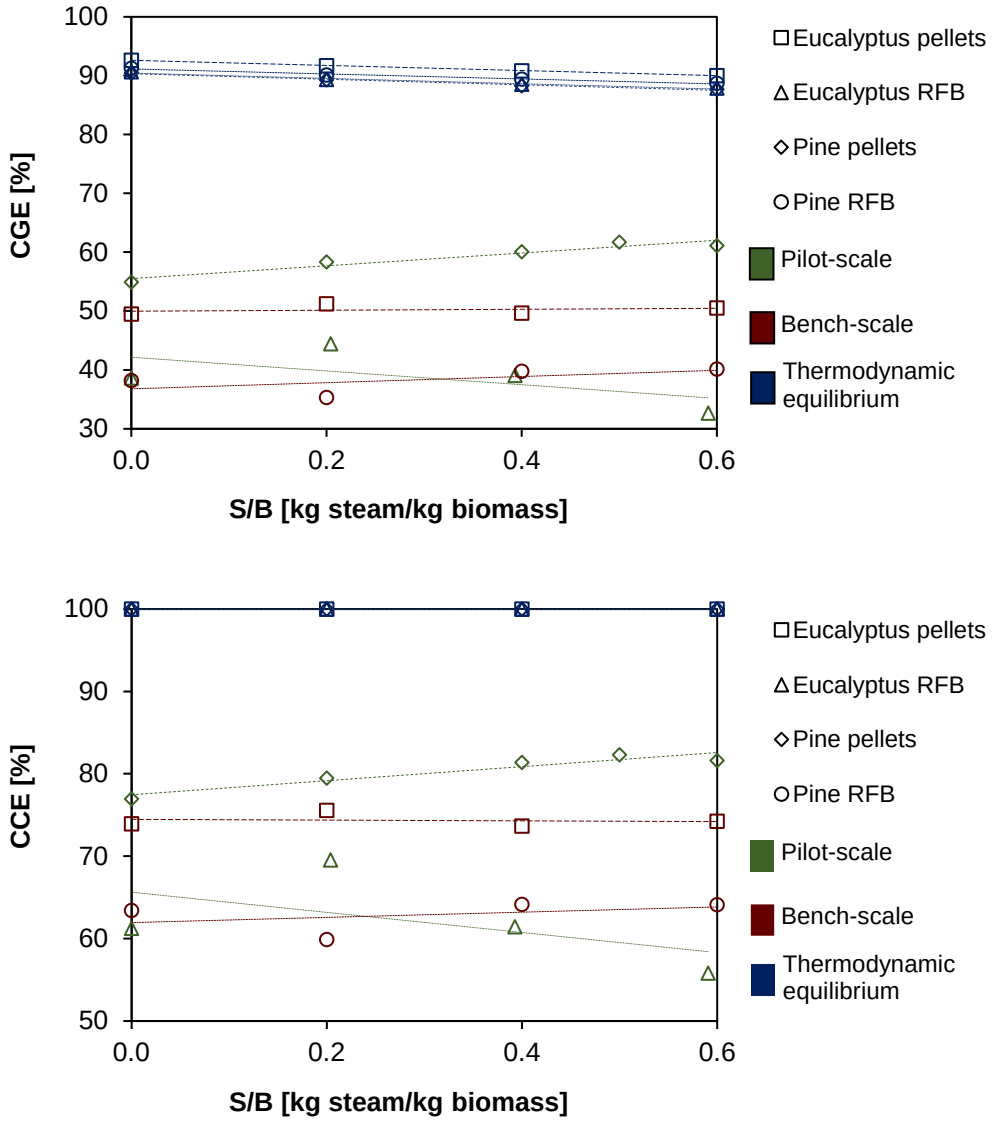

Figure 4.16 – Influence of the S/B on the CGE and CCE for the gasification experiments in the autothermal pilot-scale and allothermal bench-scale BFB reactors, and comparison with thermodynamic predictions for equal operating parameters. Operating parameters detailed in Table 4.6.

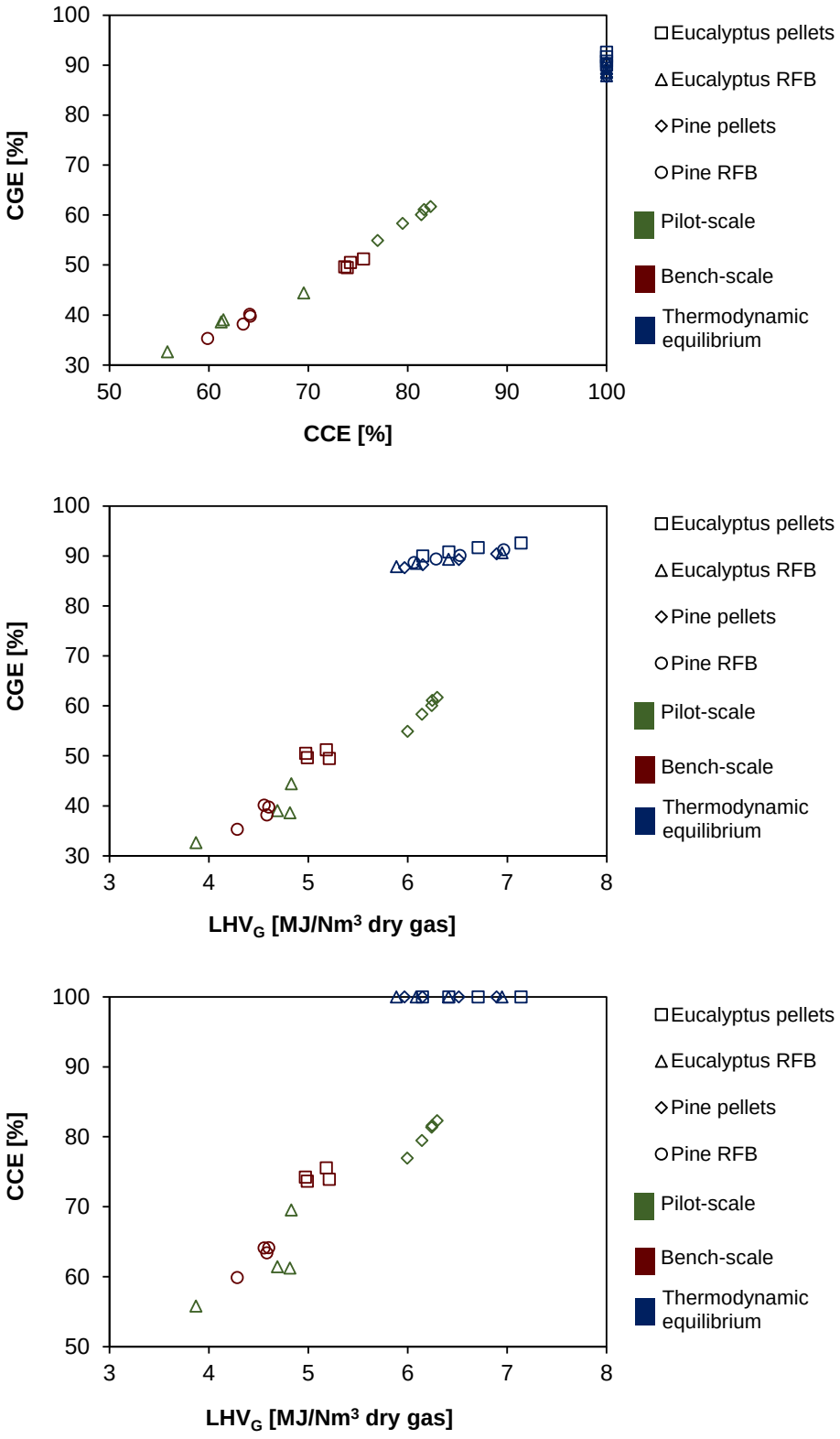

Figure 4.17 – Relation between CGE, CCE and the LHV of the PG for the gasification experiments performed in the autothermal pilot-scale and allothermal bench-scale BFB reactors and for the thermodynamic predictions (Article V). Operating parameters detailed in Table 4.6.

4.2.5 CONCLUSIONS

In this work, superheated steam injection was demonstrated as primary measure to improve PG quality during direct (air) gasification of biomass (*Eucalyptus globulus* and *Pinus Pinaster*) in an 80 kW_{th} pilot-scale autothermal BFB, focusing on the effect of S/B in the stability of the process, PG composition and gasification efficiency parameters. The process was also evaluated in a 3 kW_{th} allothermal bench-scale BFB and simulated in a thermodynamic equilibrium model.

Regarding the stability of the process, it was noticed a slight temperature decrease of the autothermal pilot-scale reactor with steam injection. Nevertheless, autothermal steady-state conditions of operation were achieved in all gasification experiments made, as reflected by stable temperature and gas composition profiles along time.

Regarding the PG composition, it was typically observed an increase of the H_2 concentration and a decrease of CO concentration with S/B increase, leading to an increase of the H_2/CO molar ratio in the PG. This is in accordance with thermodynamic equilibrium predictions and can be associated with the occurrence of the WGS reaction. However, some exceptions were observed, for example, during the gasification of pine pellets in the autothermal pilot-scale gasifier, the S/B did not show any effect on the CO concentration, despite H_2 concentration and H_2/CO molar ratio increasing with S/B increase. This could be related to the high char concentration observed in the reactor bed during these experiments, and consequent promotion of char-steam reforming reactions. This also deviates from thermodynamic equilibrium predictions because the developed model did not predict any char production for the conditions simulated.

In terms of process efficiency parameters, the effect of S/B in the LHV of the PG, CGE and CCE is not analogous for all the gasification experiments performed. For the gasification of low-density biomass, the increase in S/B caused a significant decrease of the LHV of the PG, CGE and CCE; this can be justified by steam injection mainly promoting the WGS reaction, which leads to the increase of H_2 concentration in detriment of CO concentration, and consequent decrease of the process efficiency parameters. For the gasification of high-density biomass, the increase in S/B caused an increase of the LHV of the PG, CGE and CCE; this can be justified by the significant char accumulation observed during these experiments and, consequently, steam addition promoting char-steam reforming reactions, in detriment of the WGS reaction, which corroborates the analysis performed in relation to PG composition. In terms of Y_{gas}, independently of the feedstock, an increase in the S/B caused a slight increase of this efficiency parameter, which can be associated with increased char conversion and WGS reaction occurrence with steam injection increase.

Therefore, this work demonstrates at a pilot-scale level that steam injection allows the improvement of the PG quality from the air gasification of high-density biomass in BFB gasifiers, revealing increased H_2 concentration and H_2/CO molar ratio in the PG and increased process parameters (LHV, Y_{gas}, CGE and CCE); a S/B of 0.5 is suggested to maximize the efficiency of the gasification. For air gasification of low-density biomass, steam injection can be used to adjust the H_2/CO molar ratio at the expense of the process efficiency parameters.

4.3 ARTICLE VI - CO-GASIFICATION OF REFUSED DERIVED FUEL AND BIOMASS IN A BUBBLING FLUIDIZED BED REACTOR

4.3.1 ABSTRACT

In this work, direct (air) co-gasification of RDF with biomass was demonstrated in an 80 kW_{th} pilot-scale BFB reactor. The influence of the process operating parameters, namely average bed temperature between 785 and 829 ºC, ER between 0.21 and 0.36 and RDF weight percentage in the fuel mixture (0, 10, 20, 50 and 100 %wt) was analyzed. For the operating conditions used, the process was demonstrated as autothermal and operating under steady-state conditions, with no defluidization phenomena observed. The increase of the RDF weight percentage in the fuel mixture led to an increase of the CH_4 and C_2H_4 concentration in the PG and, consequently, an increase of the PG LHV, reaching a maximum value of 6.4 MJ/Nm^3. In terms of efficiency parameters, CGE was found between 32.6 and 53.5 % and CCE between 56.0 and 84.1 %. A slight increase of the CGE was observed with the increase of the RDF weight percentage in the fuel mixture. Thus, RDF co-gasification with biomass was shown as a highly promising process for the valorization of wastes as an energetic resource.

Keywords: Refused derived fuel; Biomass; Co-gasification; Bubbling fluidized bed.

4.3.2 INTRODUCTION

Waste management and sustainable energy supply are two of the main challenges of society. On one hand, waste management should be improved and integrated with environment and human health protection while promoting the principles of circular economy [356]. On the other hand, current worldwide energy supply mainly relies on finite fossil fuel resources (coal, oil and natural gas), resulting in its excessive extraction and consumption. These aspects lead to negative economic and environmental consequences, such as the depletion of fossil fuel resources and emission of large quantities of GHGs. This means that the current worldwide energy supply is associated to pollution despite providing economic development and life quality increase [357]. Furthermore, continuous industrialization, population growth and general increase of living conditions, led to higher worldwide energy requirements and waste production in the last decades. Energy recovery from municipal and industrial wastes can contribute to solve these issues, and to reduce the EU dependence on fossil fuel-based feedstocks imports, by representing a new source of sustainable energy to satisfy the increasing society energy demands. Thus, a transition to a more sustainable waste management and circular economy model is facilitated [356].

In this context, WtE solutions can simultaneously contribute to overcome the problem of residues disposal and the reduction of GHGs emissions resulting from fossil fuels use [357]. WtE valorization options can be based on biochemical (e.g., hydrolysis, fermentation) or thermochemical conversion processes (e.g., combustion, pyrolysis, gasification). MSW, after separation of the fraction that can be reused or recycled, are an interesting feedstock for WtE conversion [358]. MSW are a mixture of distinct organic and inorganic components generated from households, offices, commerce and public institutions and, despite constituting only between 7 and 10 % of the total waste generated in EU, represent a significant challenge in terms of management [356]. In Portugal, MSW valorization as solid fuel is also considered as an opportunity to reduce GHGs emissions, minimize waste deposition in landfills, increase national energy independence and diversify the solid fuels supply [359].

Nonetheless, despite recent progresses in waste management, approximately 45 % of the wastes generated (25 % being MSW) in the EU are still disposed in landfill sites [360,361]. A higher value

(45 %) is seen in Portugal for MSW disposition in landfill [362]. These values are significantly higher than the value of 10 % that State Members should attain by 2035 [363]. Accordingly, in the EU, MSW production has increased from 150 million tons to 250 million tons between 1980 and 2017 [357,364]. Thus, the development and improvement of WtE valorization options for MSW management is relevant [5].

In this respect, to improve the effective use of MSW for WtE processes, two types of solid fuels can be produced from wastes, namely RDF and SRF [365]. These fuels can be composed by a mixture of distinct non-hazardous solid wastes, such as plastics, textiles, paper, biomass packages and rubber [5,365]. This composition can vary significantly depending on the waste origin, waste separation plant, season and the RDF/SRF production technique [5]. A more detailed description of the materials that typically compose these fuels can be found in the literature [366,367]. To be defined as SRF, the solid fuel must be produced in compliance with the European standard EN 15359 [368]. This means that the chlorine and mercury content and LHV of the solid fuel, must be determined [366,367]. Both RDF and SRF can be used for energy conversion processes, however, it has been argued that the SRF has commercial advantages in comparison with the RDF, because it eases the trade between producers and users [366], thus, contributing to higher confidence in the market [366]. In this work, the MSW used in the gasification and co-gasification (G-CG) experiments are referred as RDF, because their mercury and chlorine content were not determined.

Amongst the WtE valorization methods based on thermochemical conversion processes, combustion is the most conventional and commercial process, while pyrolysis and gasification are still in a demonstration phase. Combustion technologies are commercially available with several distinct configurations employed at industrial scale. Currently, thermal treatment plants, such as incineration plants, are commonly used for MSW disposal [5]. In fact, at least 450 MSW mass burning incineration plants are in operation in Europe [369]. Heat recovery and district heating based on waste mass burning incineration is currently performed in the EU and considered as an important technology to provide environmentally friendly heat for residential and industrial sectors [370].

MSW pyrolysis and co-pyrolysis with biomass is under research and its potential is recognized, however, it is argued that the upscaling and commercialization of this process still requires substantial efforts [371].

On the other hand, gasification is recognized as a highly promising and flexible process for waste energetic valorization [372], that allows the production of various bioproducts that neither combustion nor pyrolysis are suited to provide. In this respect, gasification can perform the valorization of waste energy into a fuel gas with flexible application in different scenarios, such as the replacement of natural gas in boilers or kiln ovens, liquid fuel production by FT process [373] or methanol synthesis [74]. Furthermore, there are several advantages in handling a gas in comparison with a solid waste, such as transport, storage and application [372].

In this context, co-gasification of wastes with biomass is a process that has been drawing significant attention in recent years [357]. In general, co-gasification of biomass with non-biomass fuels can be used as a strategy to reduce the ash content of a feedstock [374] and may lead to benefits in terms of PG quality, char reactivity and tar formation, in comparison with gasification processes using only biomass [375]. This practice can take advantage of synergistic effects that can occur between the two feedstocks used for the co-gasification process [357,375], for example, feedstocks with high ash content rich in alkali and alkali earth metals (e.g., sodium, potassium, magnesium and calcium) can have a catalytic effect during co-gasification with other fuels [374–376]. Furthermore, co-gasification of wastes with RFB can valorize both wastes and RFB [357,377]. On one hand, in comparison with gasification plants using 100 % biomass, adding wastes to the process avoids biomass excessive exploration and supply disruption. In fact, the high availability of wastes and its continuous generation, and the need of appropriate solutions for processing the non-recyclable

fraction of organic wastes, turns wastes into an almost inexhaustible resource for gasification processes [372]. On the other hand, in comparison with gasification plants using 100 % MSW, adding biomass may contribute to solve recognized process issues associated to the plastics gasification, such as feeding difficulties and contaminants formation [357].

In a recent literature review made by Ramos et al., [357], it is shown that only a small number of reports regarding co-gasification of biomass and wastes are currently available. The authors refer that the gasification products and yields are higher for co-gasification of MSW and biomass than for gasification processes of 100 % biomass or 100 % MSW, thus indicating synergy between these feedstocks. Accordingly, a recent co-gasification study of MSW and biomass [378] showed process benefits by adding wastes to the feedstock mixture, such as the increase of the LHV of the PG and the reduction of tar formation. Plastic addition to the fuel mixture in gasification processes has also been shown to lead to an increase in Y_{gas} and LHV [379–382]. It is argued that the thermal cracking of the plastic polymer chains leads to the production of diverse hydrocarbons with a wide range of molecular weight, including light hydrocarbons that contribute to the increase of both the Y_{gas} and LHV [380]. Some studies also evaluate the potential of more advanced applications for the produced gas from wastes gasification, such as methanol [383] and H_2 [221] production. In fact, a commercial biorefinery located in North America (Enerkem Alberta Biofuel) provides the industrial application of producing biofuels and renewable chemicals from non-recyclable waste and residues [383,384]. Despite these advances, studies regarding wastes gasification are still extremely scarce, particularly for higher scales (pilot and industrial) [357,385]. In this regard, further experimental research must be performed to characterize the effect of the addition of RDF on the PG quality and to evaluate potential synergistic effects.

Accordingly, in this work, distinct mixtures of RDF pellets (10, 20 and 50 %wt) were mixed with pine (chips and pellets) and used as feedstock in direct (air) co-gasification experiments in a BFB pilot-scale autothermal reactor. For comparison, gasification experiments with 100 % RDF pellets and 100 % pine (*pinus pinaster*, chips and pellets) were also performed. The influence of the RDF weight percentage on the operating conditions and process stability, in terms of temperature along time at several locations of the reactor and PG composition along time, was analyzed. Efficiency parameters were also determined to evaluate the influence of the RDF weight percentage on the process performance. This new information is relevant because it provides a systematic experimental analysis of the gasification of RDF and biomass, and their blends at different mixture ratios, in a BFB at a pilot-scale level, for which there exists a recognized lack of studies. Thus, the obtained results provide new knowledge that may serve as a complementary tool to support decisions related to co-gasification projects, including the upscale of the process to the industrial scale and the development of co-gasification plants. This can ease the commercial breakthrough of this technology and consequently promote both waste management and energy supply sustainability in the future.

4.3.3 MATERIALS AND METHODS

The experimental infrastructure used in this Article was the DAO-UA 80 kW_{th} pilot-scale BFB gasifier (Section 1.3). The methodologies used are described in Section 1.4.

4.3.3.1 FEEDSTOCK CHARACTERIZATION

Pine chips, pine pellets and RDF pellets produced from MSW were used as feedstock (Figure 4.18). The pine chips were dried at atmospheric conditions and sieved to a particle size below 15 mm. The feedstocks were characterized in terms of properties with interest for thermochemical conversion (proximate and elemental analysis and LHV), as shown in Table 4.7. The fusibility of the feedstock ashes was also determined (Table 4.8).

(a)

(b)

(c)

Figure 4.18 – Feedstocks used in the G-CG experiments, namely (a) RDF pellets, (b) pine pellets and (c) pine chips, over millimeter paper.

Table 4.7 – Proximate and elemental analysis of RDF and biomass types used as feedstock in the G-CG experiments in the pilot-scale BFB.

Material	RDF pellets	Pine Chips	Pine pellets
Proximate analysis (%wt, wb)			
Moisture	4.3	11.0	4.6
Volatile matter	75.2	77.9	78.5
Fixed carbon	7.1	10.8	16.6
Ash	13.4	0.3	0.3
Ultimate analysis (%wt, db)			
Ash	13.4	0.3	0.3
C	54.0	46.4	47.5
H	7.4	6.6	6.2
N	0.5	0.2	0.1
S	nd	nd	nd
O (by difference)	24.1	46.5	45.9
Ash composition (mg/kg db)			
Ca	29000	540	600
Al	20000	22	96
Si	18000	< 200	< 200
S	< 6000	< 6000	< 6000
Fe	3100	29	73
Na	1400	280	280
Mg	950	190	280
Cl^-	710	10	1500
K	680	410	590
Cu	380	< 3	3
P	370	33	48
Ti	200	< 3	4
Ba	190	< 3	< 3
Sr	180	3	5
Zn	180	5	7
Pb	42	< 3	< 3
Ni	34	6	< 3
Cr	21	< 3	< 3
V	19	< 3	< 3
Sn	9	< 1	< 1
Co	8	< 1	< 1
LHV (MJ/kg) (db)	24.8	18.8	18.0
Bulk Density (kg/m^3) (wb)	864	577	911

nd- not determined, below the detection limit of the method, 100 ppm wt.

Table 4.8 – Ash fusibility temperature for the different feedstocks used in the G-CG experiments.

	Ash		
	RDF pellets	Pine pellets	Pine chips
Shrinking starting temperature (ºC)	1200	1140	1020
Deformation temperature (ºC)	1250	1190	1100
Hemisphere temperature (ºC)	1420	1290	>1500
Flow temperature (ºC)	1450	1330	>1500

4.3.3.2 OPERATING CONDITIONS

The operating conditions of the G-CG experiments performed are detailed in Table 4.9. The ER was maintained between 0.21 and 0.36 and the bed temperature between 785 and 829 ºC. The RDF pellets were pre-mixed with two types of pine *(Pinus Pinaster)*, namely pine pellets and pine chips, in order to produce the fuel mixtures detailed in Table 4.9.

Table 4.9 – G-CG experiments reference and respective operating conditions (Article VI).

G-CG reference	Biomass type	Biomass [%wt]	RDF [%wt]	ER	Average bed Temperature [ºC]	Biomass feed rate [kg/h]	Air feed rate [L_{NPT}/ min]
PC100: ER023	Pine chips	100	0	0.23	803	14	200
PC100: ER031	Pine chips	100	0	0.31	806	10	200
PC90 - RDF10: ER022	Pine chips	90	10	0.22	803	14	200
PC90 - RDF10: ER025	Pine chips	90	10	0.25	804	12	200
PC90 - RDF10: ER030	Pine chips	90	10	0.30	807	10	200
PC80 - RDF20: ER022	Pine chips	80	20	0.22	785	13	200
PC80 - RDF20: ER025	Pine chips	80	20	0.25	794	12	200
PC80 - RDF20: ER031	Pine chips	80	20	0.31	811	9	200
PC50 - RDF50: ER032	Pine chips	50	50	0.32	819	8	200
PP100: ER022	Pine Pellets	100	0	0.22	791	13	200
PP100: ER030	Pine Pellets	100	0	0.30	829	10	200
PP90 - RDF10: ER022	Pine Pellets	90	10	0.22	797	13	200
PP90 - RDF10: ER031	Pine Pellets	90	10	0.31	816	9	200
PP80 - RDF20: ER022	Pine Pellets	80	20	0.22	801	12	200
PP80 - RDF20: ER031	Pine Pellets	80	20	0.31	806	9	200
PP50 - RDF50: ER021	Pine Pellets	50	50	0.21	812	12	200
PP50 - RDF50: ER030	Pine Pellets	50	50	0.30	818	8	200
RDF100: ER023	-	0	100	0.23	818	9	200
RDF100: ER027	-	0	100	0.27	793	8	200

4.3.4 RESULTS AND DISCUSSION

The results presented in this Section include the operating conditions of the gasifier, temperature profiles along time and along the reactor height, PG composition (CO, CO_2, CH_4 and C_2H_4) profile

along time and average PG composition (CO, CO_2, CH_4, C_2H_4, C_2H_6, C_3H_8, H_2 and N_2). The LHV of the PG and efficiency parameters, namely Y_{gas}, CGE and CCE are analyzed.

4.3.4.1 OPERATING CONDITIONS OF THE GASIFIER

For all G-CG experiments performed (ER as low as 0.21), the gasifier was operated under autothermal regime (with average bed temperature above 785 ºC). Thus, no external heating supply was necessary, independently of the inclusion of RDF in the fuel mixture. Slag, agglomeration or defluidization phenomena were not observed during the experiments made. This is also supported by the relatively high ash fusibility temperatures (>1000 ºC) of the feedstock ashes (Table 4.8), that are significantly higher than the maximum average bed temperature (829 ºC) measured during the G-CG experiments made.

The typical temperature profile along time for the G-CG experiments performed in the pilot-scale BFB reactor is shown in Figure 4.19. In general, the temperature profiles for the different gasification experiments performed present a similar behavior, however, the experiments performed with pine chips seem to have higher temperature fluctuations than the experiments performed with pine pellets. This is justified by the higher heterogeneity of the pine chips particles and consequent influence on the feeding regularity.

The inclusion of RDF in the fuel mixture seems to slightly increase temperature fluctuations in the reactor for experiments with pine pellets. In fact, gasification experiments with 100 % RDF presented the highest temperature fluctuations at the surface of the reactor bed (T-4), which can also be justified by the significant heterogeneity of this fuel. Regarding co-gasification experiments with pine chips, the addition of RDF does not seem to cause any significant changes in the temperature profiles. This may be related to the fact that this biomass already presents some heterogeneity, as previously discussed. Nevertheless, acceptable steady-state conditions of operation were attained in all G-CG experiments, as reflected by the temperature profiles along time at distinct locations along the reactor.

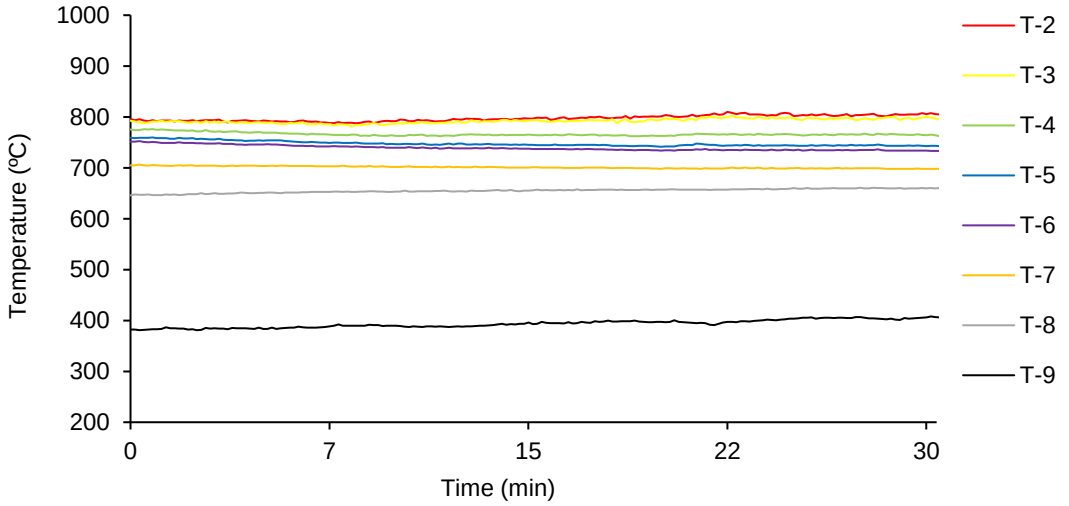

Figure 4.19 – Typical temperature profile along time at different locations of the pilot-scale BFB reactor.

Regarding the vertical temperature profiles along the reactor (Figure 4.20), the temperature shows a similar behavior for the distinct G-CG experiments performed. Typically, the temperature decreases from the surface of the bed to the exhaust of the reactor. This behavior is typical of biomass gasification processes and follows the general trend found in other works performed in this

infrastructure (see previous Sections). The addition of RDF does not seem to cause any major changes in the average temperature along the reactor or in the relationship between the temperature and the distance to the BFB reactor distributor plate.

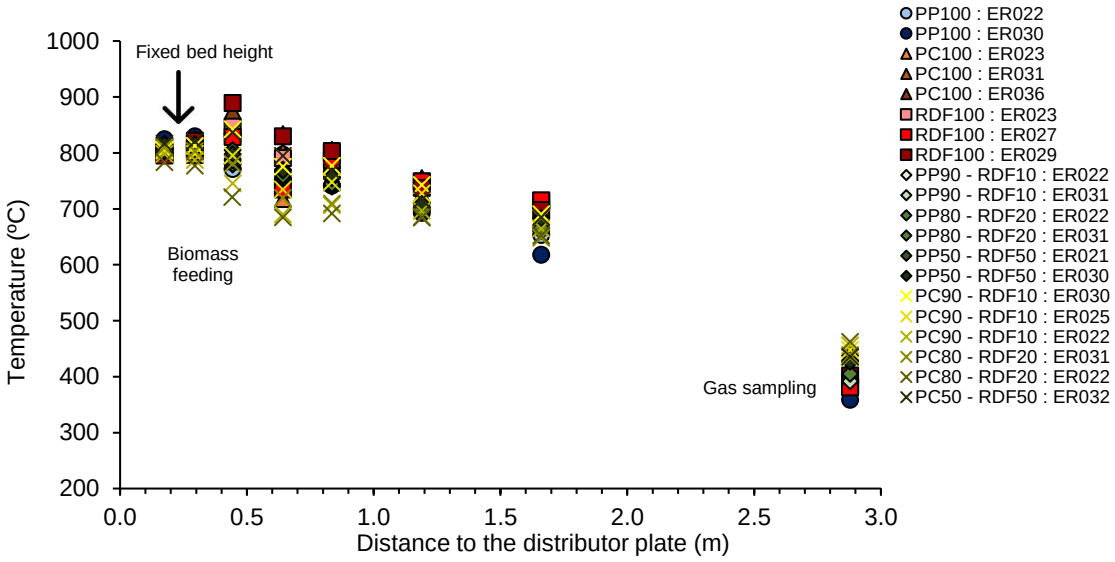

Figure 4.20 – Longitudinal temperature profile in the pilot-scale BFB reactor during the G-CG experiments performed. Legend according to experiments reference in Table 4.9.

Regarding the typical PG composition profiles along time (Figure 4.21), it can be observed that steady-state conditions of operation were achieved, as shown by the steady concentration of the selected compounds (CO, CO_2, CH_4 and C_2H_4) along time. Nonetheless, the gas composition profiles during the gasification of pine pellets shows less fluctuations than during the gasification of pine chips or RDF pellets. Accordingly, RDF weight percentage increase in the pine pellets fuel mixture increased the fluctuation of the concentration of the selected compounds, particularly the CO concentration. RDF weight percentage increase in the pine chips fuel mixture does not seem to have caused any significant stability changes in the gas composition profiles. Thus, the PG concentration profiles along time are in accordance with the stable temperature profiles presented, reflecting the suitability of the BFB pilot-scale reactor to conduct G-CG studies of biomass and RDF.

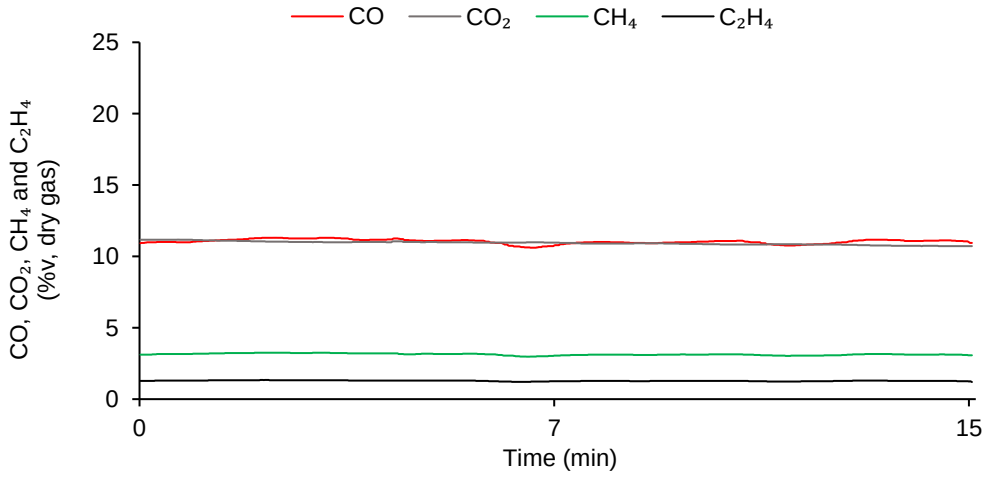

(a)

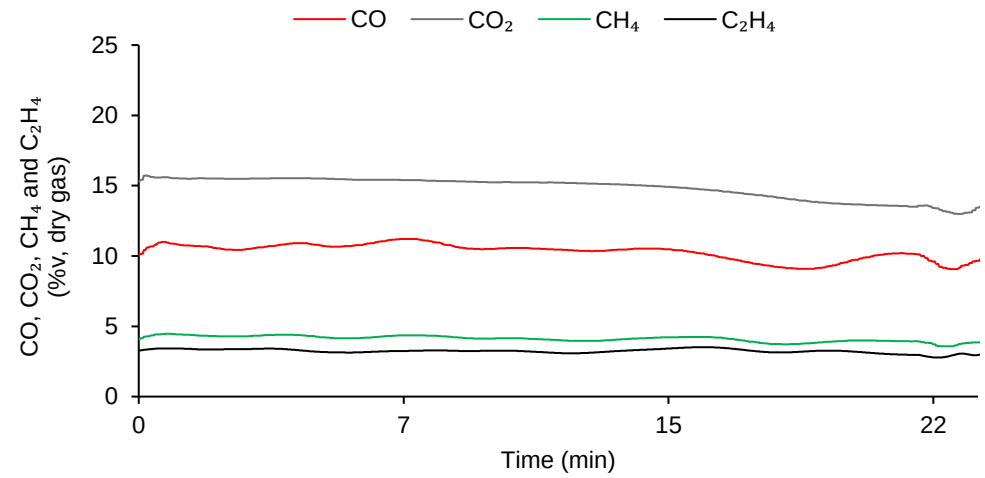

(b)

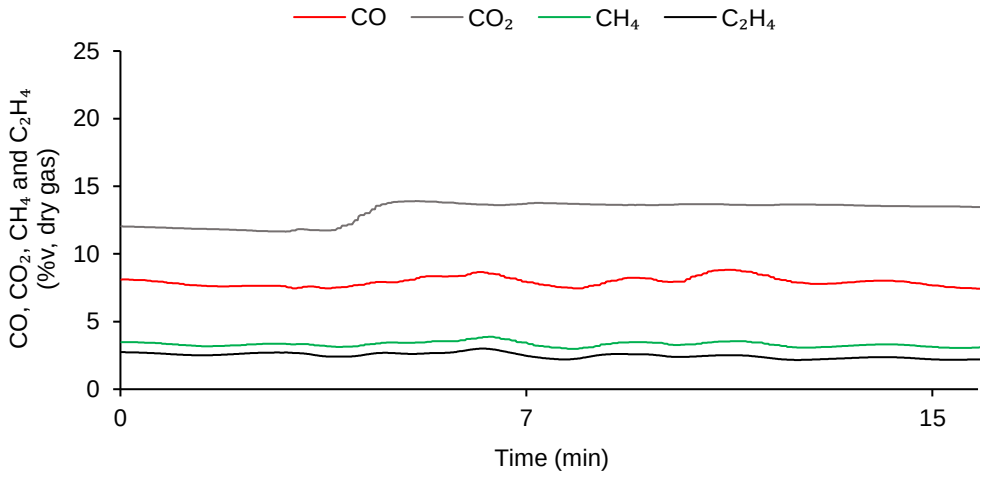

(c)

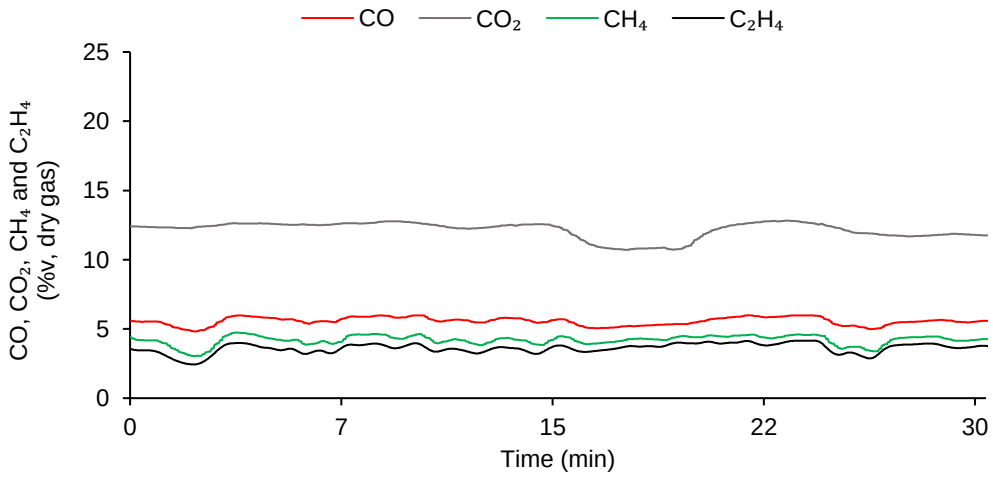

(d)

Figure 4.21 – Typical PG composition (CO_2, CO, CH_4 and C_2H_4) profiles along time for the G-CG experiments with: (a) 100 %wt pine pellets, (b) 50 %wt pine pellets - 50 %wt RDF, (c) 50 %wt pine chips - 50 %wt RDF and (d) 100 %wt RDF.

4.3.4.2 CHARACTERISTICS OF THE PG

4.3.4.2.1 Gas composition

The impact of the RDF weight percentage in the fuel mixture on the composition of the PG is shown in Figure 4.22 and Figure 4.23.

For similar ER, the RDF addition to the fuel mixtures caused a significant decrease of CO concentration in the PG. The effect seems to be related with the employed ER, i.e., the addition of RDF led to a steeper decrease of CO concentration values in experiments with lower ER. In fact, maximum CO concentration was found for the gasification of pine chips with 0.23 ER (18.6 %v, experiment reference PC100: ER0.23) and the minimum for the gasification of RDF with 0.23 ER (6.9 %v, experiment reference RDF100: ER0.23). In average, increasing RDF weight percentage in the feedstock mixture from 10 to 20 %, 20 to 50 % and 50 to 100 %, led to a CO decrease of 6.3, 1.5 and 42.0 %, respectively. In contrast, increasing RDF weight percentage in the fuel mixture, from 0 to 10 %, led to a CO increase (5.5 % in average). A CO concentration decrease in the PG with plastics weight percentage increase in the feedstock mixture has also been reported in other works [379,386]. In this case, a CO concentration decrease was unexpected due to the high carbon content present in the RDF (Table 4.7). This phenomenon may be related to an increase in the methanization reaction (Reaction 2.9) and to an increase of other combustible gases concentration, specifically those containing carbon, such as CH_4, C_2H_4, C_2H_6 and C_3H_8 (Figure 4.23). These aspects are discussed ahead.

The H_2 concentration values were found between 4.0 and 7.1 %v, however, the effect of the RDF weight percentage is not evident. It seems that the increase in RDF addition leads to slightly lower H_2 concentration values in the PG, which may also be related to an increase in the methanization reaction, however, this impact may be masked by more prominent effects such as the bed temperature or the ER.

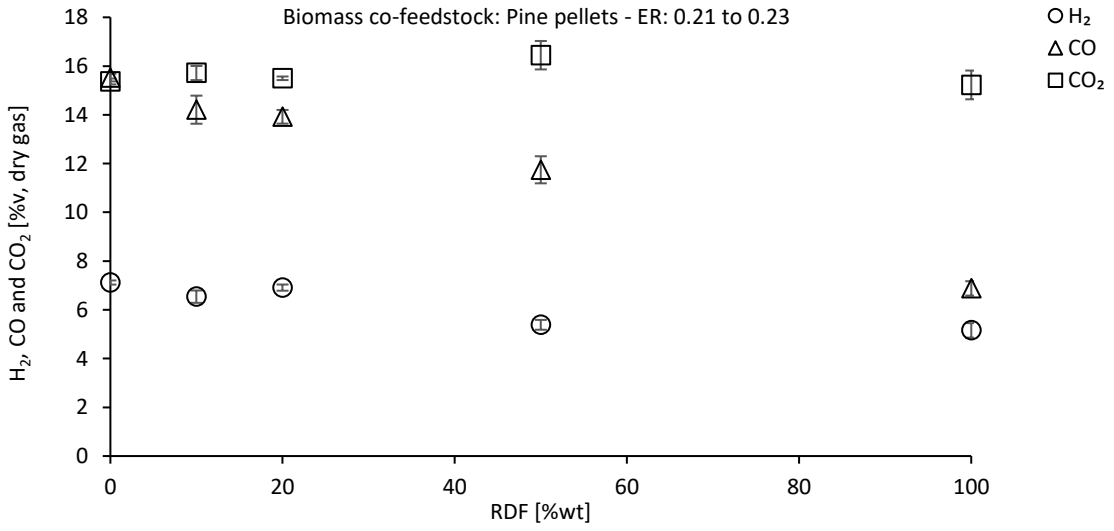

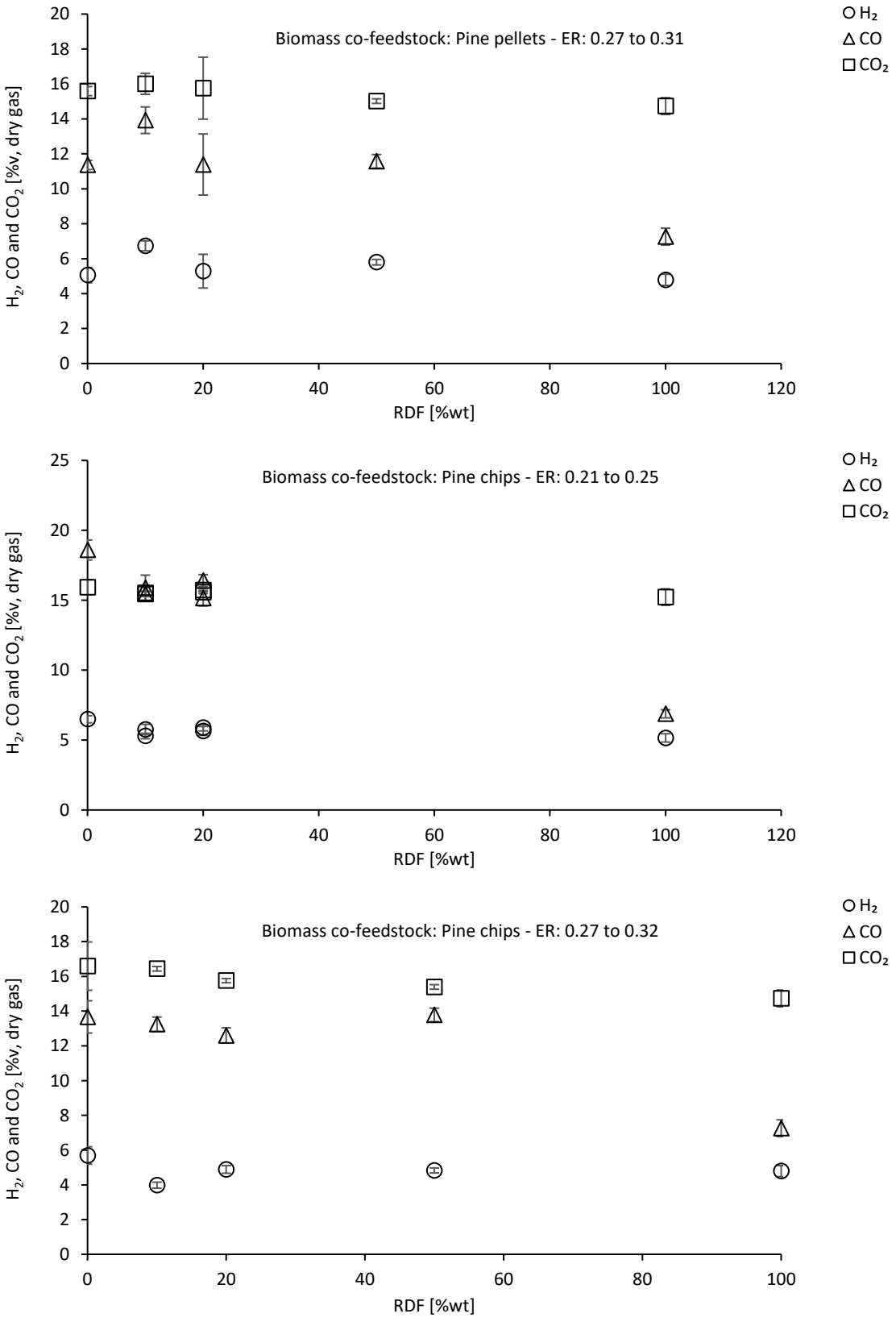

Figure 4.22 – Influence of the RDF weight percentage on the average PG composition (H_2, CO and CO_2) for the G-CG experiments.

Regarding CH_4 and C_2H_4, it can be observed that the addition of RDF increased the concentration of these compounds in the PG (Figure 4.23). Maximum CH_4 and C_2H_4 concentration values were found for the gasification of RDF with ER 0.27 (experiment reference RDF100: ER 0.27), namely 5.6 %v and 5.0 %v, respectively. On one hand, this may be justified by the thermal cracking of plastic polymers present in the RDF pellets, which lead to the production of light hydrocarbons [380]. On the other hand, the higher content of ashes rich in alkali and alkali earth metals (e.g., calcium, sodium, magnesium, potassium) present in the RDF pellets (Table 4.7), in comparison with biomass, may promote a catalytic effect [374–376] that also leads to the production of light hydrocarbons. Furthermore, the decrease in CO concentration and increase in CH_4 concentration also suggests an increase in methanization reactions. In fact, the CH_4 and C_2H_4 maximum concentration values observed are higher than the values typically reported in the literature regarding biomass direct (air) gasification [4]. Accordingly, the minimum CH_4 concentration value was found for the gasification of pine pellets with ER 0.30 (3.0 %v, experiment reference PP100: ER030), while the minimum C_2H_4 concentration value was found for the gasification of pine pellets with ER 0.30 (1.2 %v, experiment reference PP100: ER030).

It was also observed that the relative increase of the concentration of CH_4 and C_2H_4 with RDF addition to the fuel mixture was higher for experiments with higher ER. For example, for co-gasification experiments of pine pellets with RDF, the following was observed:

- For experiments with ER between 0.21 and 0.23 (Figure 4.23 (a)), the CH_4 increased from 4.5 to 5.1 %v and C_2H_4 from 1.8 to 4.3 %v with RDF weight percentage increase.
- For experiments with ER between 0.27 and 0.31 (Figure 4.23 (b)), the CH_4 increased from 3.0 to 5.6 %v and C_2H_4 from 1.2 to 5.0 %v with RDF weight percentage increase.

A similar observation can be made for the co-gasification experiments of pine chips with RDF (Figure 4.23 (c) and (d)). On one hand, this is justified by the fact that ER had a significant effect on the concentration of CH_4 and C_2H_4 in the PG from pine gasification (experiments reference PP100 and PC100), i.e., for these experiments, a decrease in ER led to significantly higher CH_4 and C_2H_4 concentration. This is related to a decrease of the oxygen availability with the decrease of ER, and thus a lower occurrence of oxidation reactions, leading to higher combustible gases concentration in the PG (e.g., H_2, CO, CH_4, C_2H_4). This is a typical behavior of biomass gasification processes and was also observed in the other papers composing this thesis (e.g., see previous Sections). On the other hand, it seems that the thermal cracking of the organic molecules present in the RDF compounds (e.g., plastics), which leads to the production of light hydrocarbons (e.g., CH_4 and C_2H_4) [380], is more effective at higher ER. In part, this may be related to the higher bed temperature and higher freeboard temperature generally attained during experiments with higher ER (Table 4.9), which promotes the thermal cracking of the plastic fraction. In fact, it is known that the reactor temperature is highly dependent of the ER in atmospheric gasifiers [387], due to the increase/decrease of oxidation reactions [4]. Furthermore, a higher bed and freeboard temperature is also known to favor tar cracking reactions and, consequently, increase the production of light hydrocarbons [387]. Therefore, for co-gasification experiments with lower ER, the addition of RDF led to a lower relative increase of CH_4 and C_2H_4 concentration.

In average, increasing the weight percentage of RDF in the fuel mixture from 0 to 10, 10 to 20, 20 to 50 and 50 to 100 %, led to a CH_4 concentration increase of 4.4, 1.3, 9.3 and 29.9 %, respectively, and a C_2H_4 concentration increase of 20.2, 16.1, 30.0 and 78.2 %, respectively. The concentration of C_2H_6 and C_3H_8 also shows a tendency to increase with RDF addition to the fuel mixture, however, this is not clear because these compounds were only found in very low concentrations (<0.5 %v, Figure 4.23).

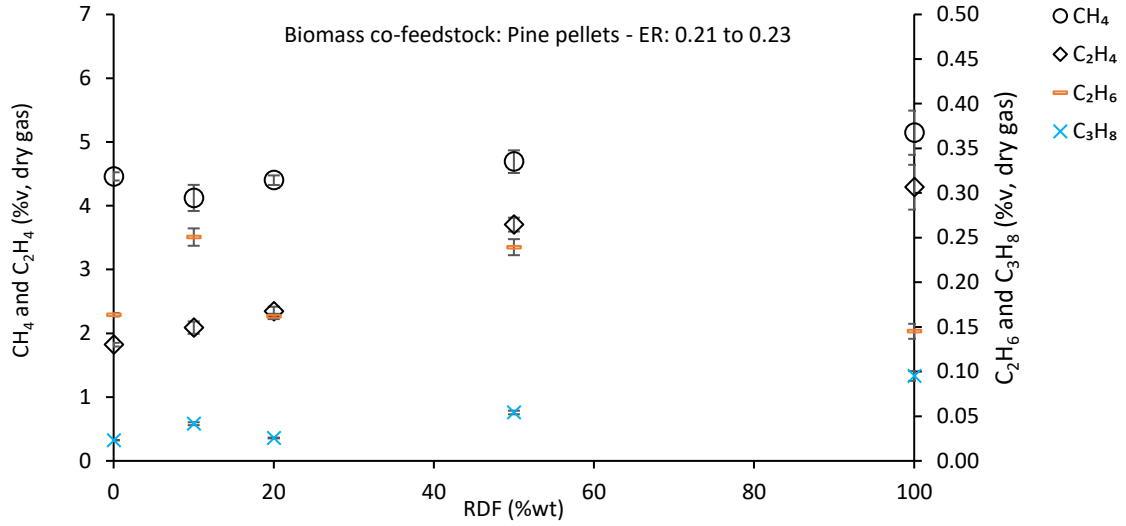
Biomass co-feedstock: Pine pellets - ER: 0.21 to 0.23
CH4 and C2H4 (%v, dry gas)
C2H6 and C3H8 (%v, dry gas)
RDF (%wt)
CH4
C2H4
C2H6
C3H8

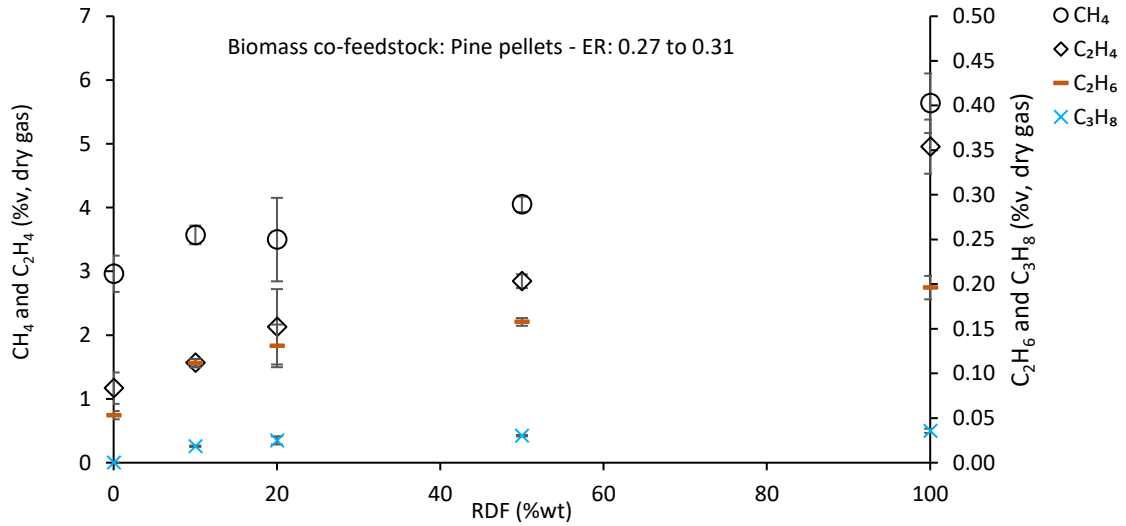
Biomass co-feedstock: Pine pellets - ER: 0.27 to 0.31
CH4 and C2H4 (%v, dry gas)
C2H6 and C3H8 (%v, dry gas)
RDF (%wt)
CH4
C2H4
C2H6
C3H8

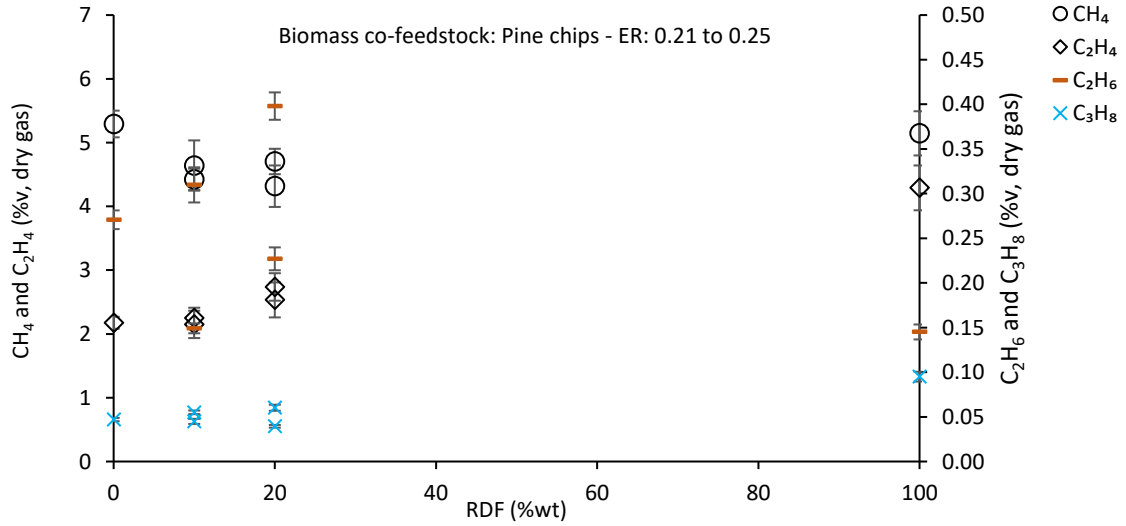
Biomass co-feedstock: Pine chips - ER: 0.21 to 0.25
CH4 and C2H4 (%v, dry gas)
C2H6 and C3H8 (%v, dry gas)
RDF (%wt)
CH4
C2H4
C2H6
C3H8

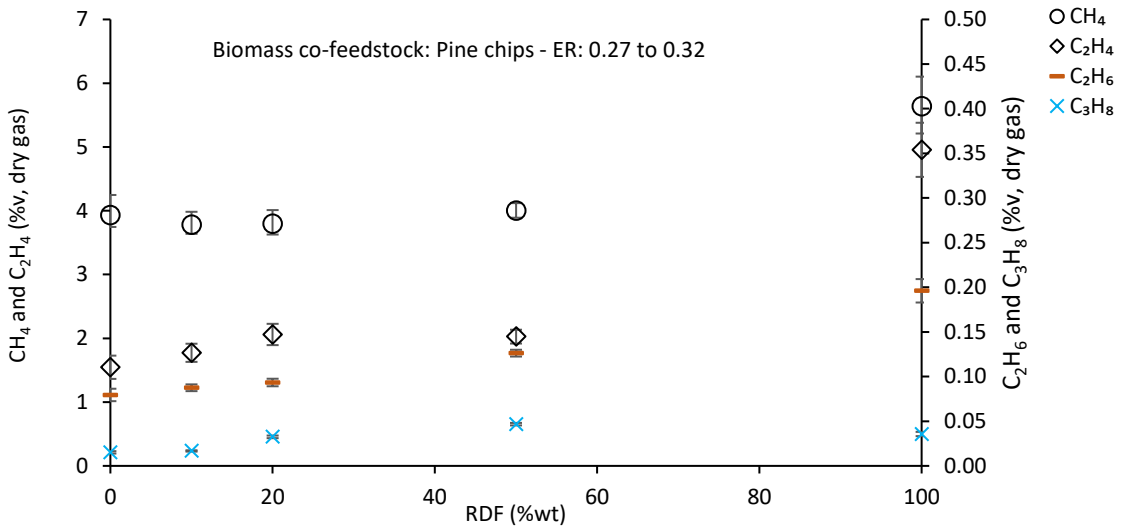

Figure 4.23 – Influence of the RDF weight percentage on the average PG composition (CH_4, C_2H_4, C_2H_6 and C_3H_8) for the G-CG experiments.

4.3.4.2.2 Gaseous products ratios

Two yield ratios are discussed in this Section, namely H_2:CO and CO:CO_2 molar ratios. H_2:CO molar ratio is relevant for the application of the PG in advanced applications that require high H_2:CO molar ratios, such as methanol production (2 mol·mol^{-1}), liquid fuel production through FT synthesis (0.6 mol·mol^{-1}) and DME production (1 mol·mol^{-1}) [180–182,388].

For the G-CG experiments performed, the H_2:CO molar ratio was found between 0.30 and 0.75 mol·mol^{-1} (Figure 4.24). The maximum value was found for the gasification of RDF with ER 0.23 (experiment reference RDF100: ER023) and the minimum for the co-gasification of pine chips and RDF with ER 0.30 (experiment reference PC90 – RDF 10: ER030). No significant trends were found for the variation of H_2:CO molar ratio with the RDF weight percentage increase from 0 to 50 %. However, in gasification experiments with 100 % RDF, this parameter value was significantly higher than in the other G-CG experiments performed, mainly due to the significantly lower CO concentration obtained (Figure 4.22).

The CO:CO_2 molar ratio is not commonly referred in the literature, however, it can be useful for the prediction of the process performance and the balance between gasification and combustion reactions [318]. For the G-CG experiments performed, CO/CO_2 molar ratio was found between 0.45 and 1.17 mol·mol^{-1} (Figure 4.24). The maximum value was found for the gasification of pine chips with ER 0.23 (experiment reference PC100: ER023) and the minimum value found for the gasification of RDF with ER 0.23 (experiment reference RDF100: ER023). In average, increasing RDF weight percentage in the feedstock mixture from 0 to 10 % led to CO:CO_2 molar ratio increase of 4.2 %, while increasing RDF weight percentage in the feedstock mixture from 10 to 20 %, 20 to 50 % and 50 to 100 %, led to a CO:CO_2 molar ratio decrease of 5.5, 0.6 and 39.3 %, respectively. This significant decrease of CO:CO_2 molar ratio in gasification experiments with 100 % RDF results from the low CO concentration values found in these experiments (Figure 4.22). This seems to indicate that the efficiency of the process decreases with RDF weight percentage increase. However, it must be noted that despite the CO concentration decrease, there is also an increase of the concentration of other combustible gases (e.g., CH_4 and C_2H_4), which compensates the effect of the decrease of the CO concentration on the energy content of the PG and the efficiency of the process (Section 4.3.4.3).

Thus, this ratio should be regarded with caution when used to characterize the effect of RDF weight percentage in co-gasification processes performance.

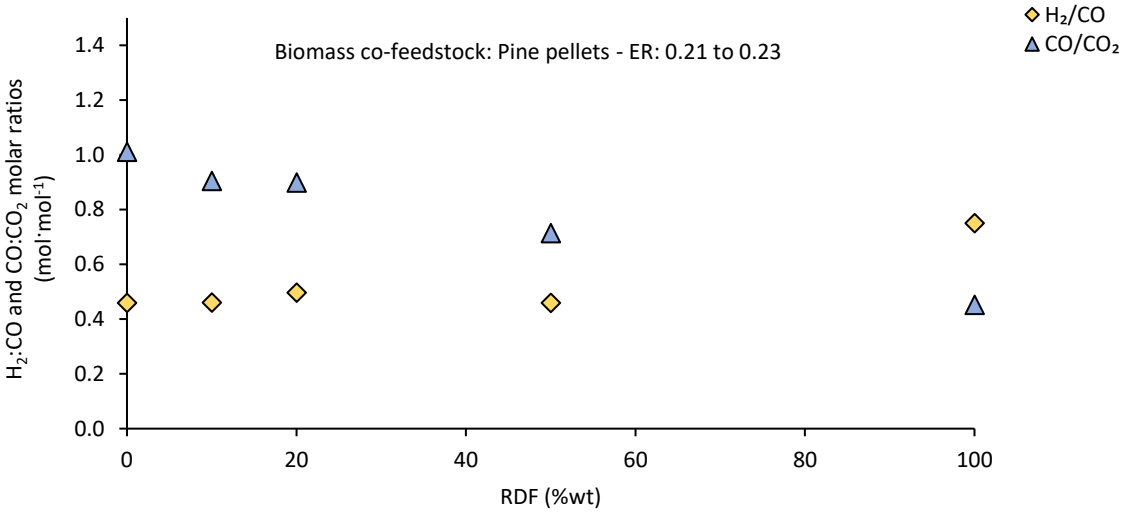

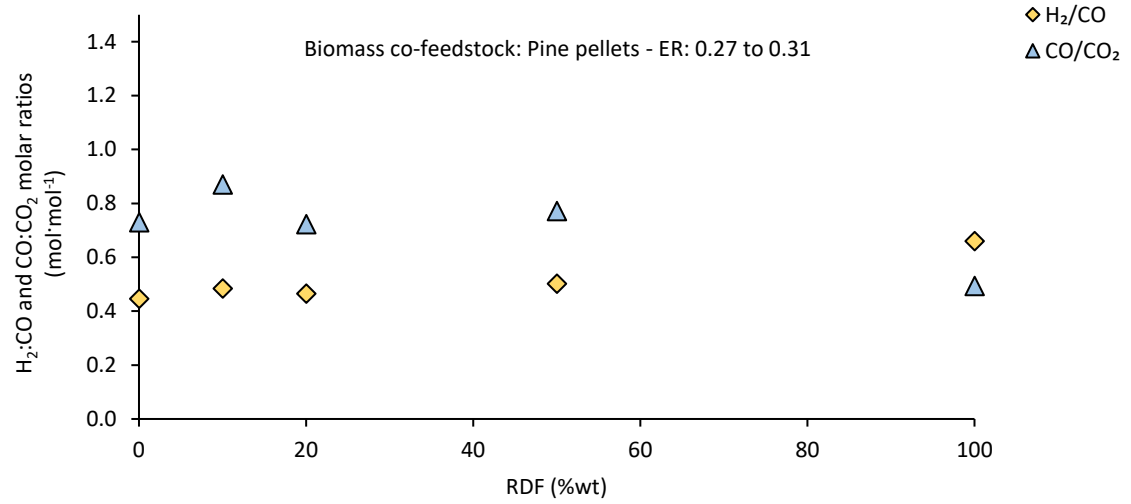

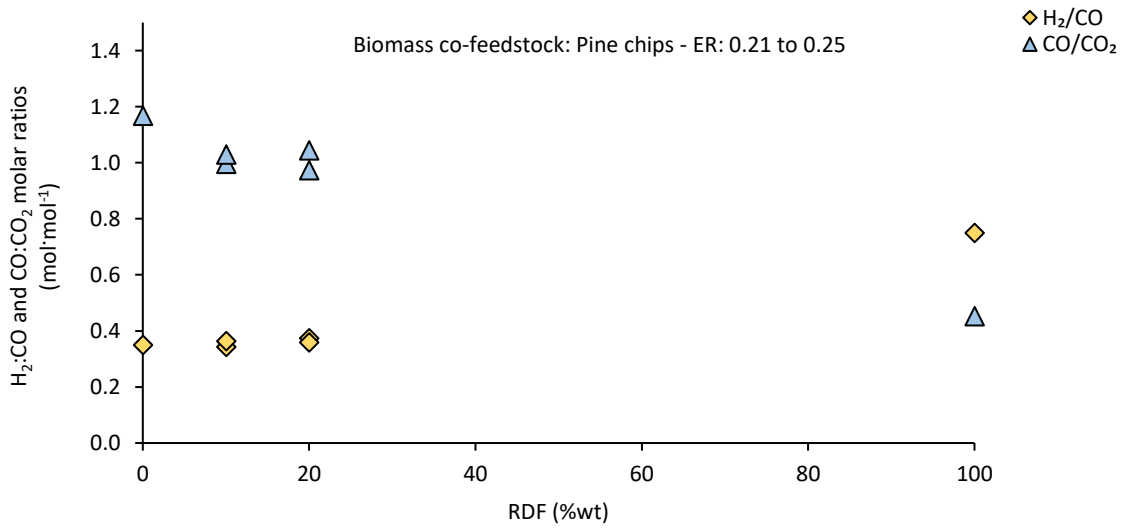

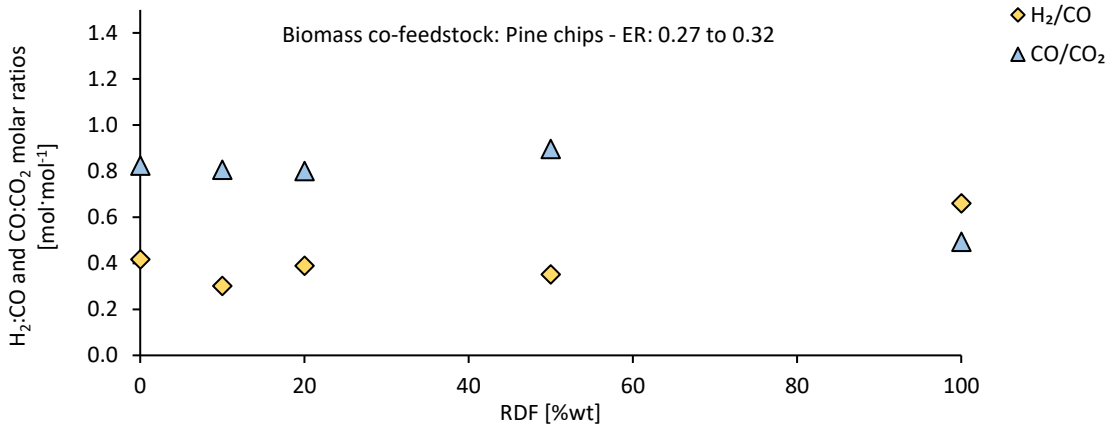

Figure 4.24 – Influence of the RDF weight percentage on the H_2:CO and CO:CO_2 molar ratios for the G-CG experiments.

4.3.4.3 PROCESS EFFICIENCY PARAMETERS

4.3.4.3.1 LHV and Y_{gas}

The influence of RDF weight percentage in the fuel mixture in the PG LHV and the Y_{gas} is shown in Figure 4.25.

Regarding the PG LHV, this parameter increased significantly with RDF weight percentage increase for experiments with higher ER (Figure 4.25 (b) and (d)). However, the effect of RDF addition on the LHV for experiments with lower ER was not clear (Figure 4.25 (a) and (c)). The effect of the RDF weight percentage on the LHV is mainly related to the influence of this parameter on the CH_4, C_2H_4 and CO concentration (4.3.4.2), which represent a significant part of the energy content of the PG. As previously discussed, the RDF weight percentage increase led to higher CH_4 and C_2H_4 concentration and lower CO concentration. For experiments with higher ER, the significant increase in CH_4 and C_2H_4 concentration caused a significant increase in the PG LHV. For experiments with lower ER, while the CH_4 and C_2H_4 concentration increase contributed to higher LHV, the observed significant decrease in CO concentration led to lower LHV, causing an unclear effect.

Furthermore, for the 100 % RDF gasification experiments performed (experiments reference RDF100: ER023 and RDF100: ER027), the LHV of the PG increased with ER (from 5.8 to 6.4 MJ/Nm^3), mainly due to an increase in the concentration of CH_4 and C_2H_4. This behavior is not common in biomass gasification processes [4] and may be explained by the increase in ER promoting the thermal cracking of the organic compounds present in the plastic fractions contained in the RDF, as previously discussed (Section 4.3.4.2). Accordingly, the maximum LHV value was found for the gasification of RDF with ER 0.27 (6.4 MJ/Nm^3) and the minimum value for the gasification of pine pellets with ER 0.30 (3.7 MJ/Nm^3). In average, increasing RDF weight percentage in the fuel mixture from 0 to 10, 10 to 20, 20 to 50 and 50 to 100 %, led to a LHV increase of 6.9, 1.4, 9.4 and 16.8 %, respectively. This general increase in the PG LHV is in accordance with the increase of the energy content in the feedstock mixture, resulting from the increase of RDF weight percentage, due to the RDF higher LHV in comparison with the pine pellets and chips (Table 4.7).

Regarding Y_{gas}, values between 1.3 and 2.1 Nm^3 dry gas/kg dry biomass were observed for the G-CG experiments performed. The maximum and minimum values were found for the co-gasification of pine chips with RDF, namely experiments with reference PC50 – RDF50: ER032 and PC90 –

RDF10: ER022, respectively. The effect of RDF weight percentage on Y_{gas} is not clear and may be masked by ER variations, which have significant influence on the Y_{gas} [4]. Nonetheless, a slight tendency for the increase of Y_{gas} with the increase of RDF weight percentage in the fuel mixture was noticed. In average, increasing RDF weight percentage from 0 to 10, 10 to 20, 20 to 50 and 50 to 100 % led to a Y_{gas} increase of 0.8, 3.3, 12.2 and 0.6 %, respectively. This increase may be related to an higher and faster degradation of plastic products [357], in comparison with biomass, and to the catalytic effect promoted by the high ash content rich in alkali and alkali earth metals (e.g., calcium, sodium, magnesium, potassium) present in the RDF pellets (Table 4.7), which are known promoters of combustible gaseous compounds formation during gasification processes [374–376], and consequent potential increase of light hydrocarbons production (see Section 4.3.4.2).

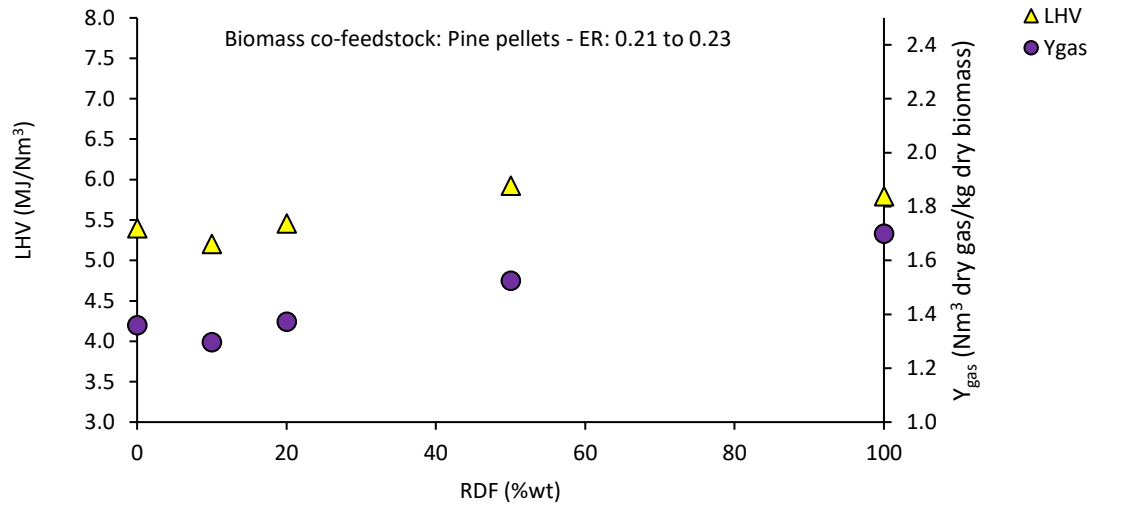

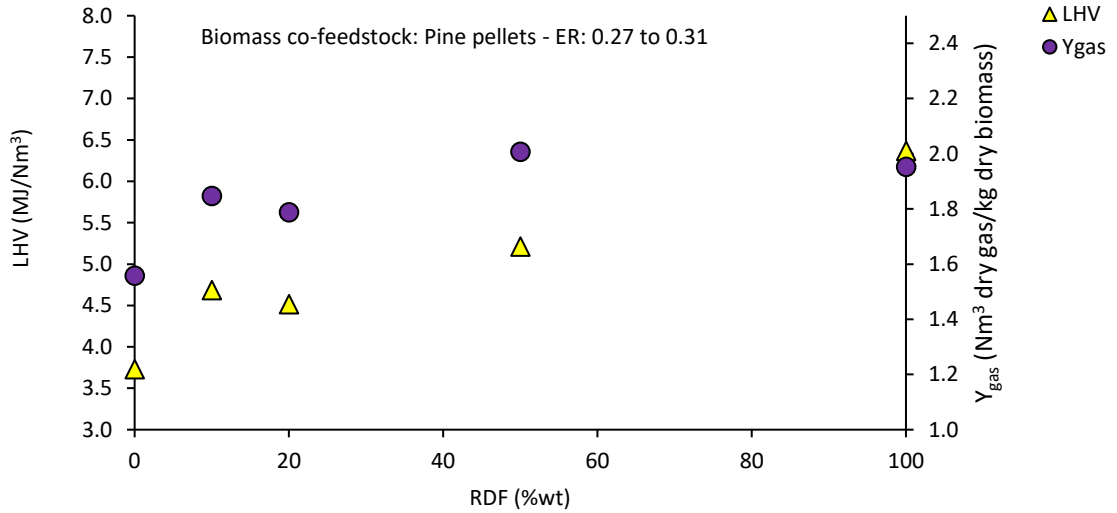

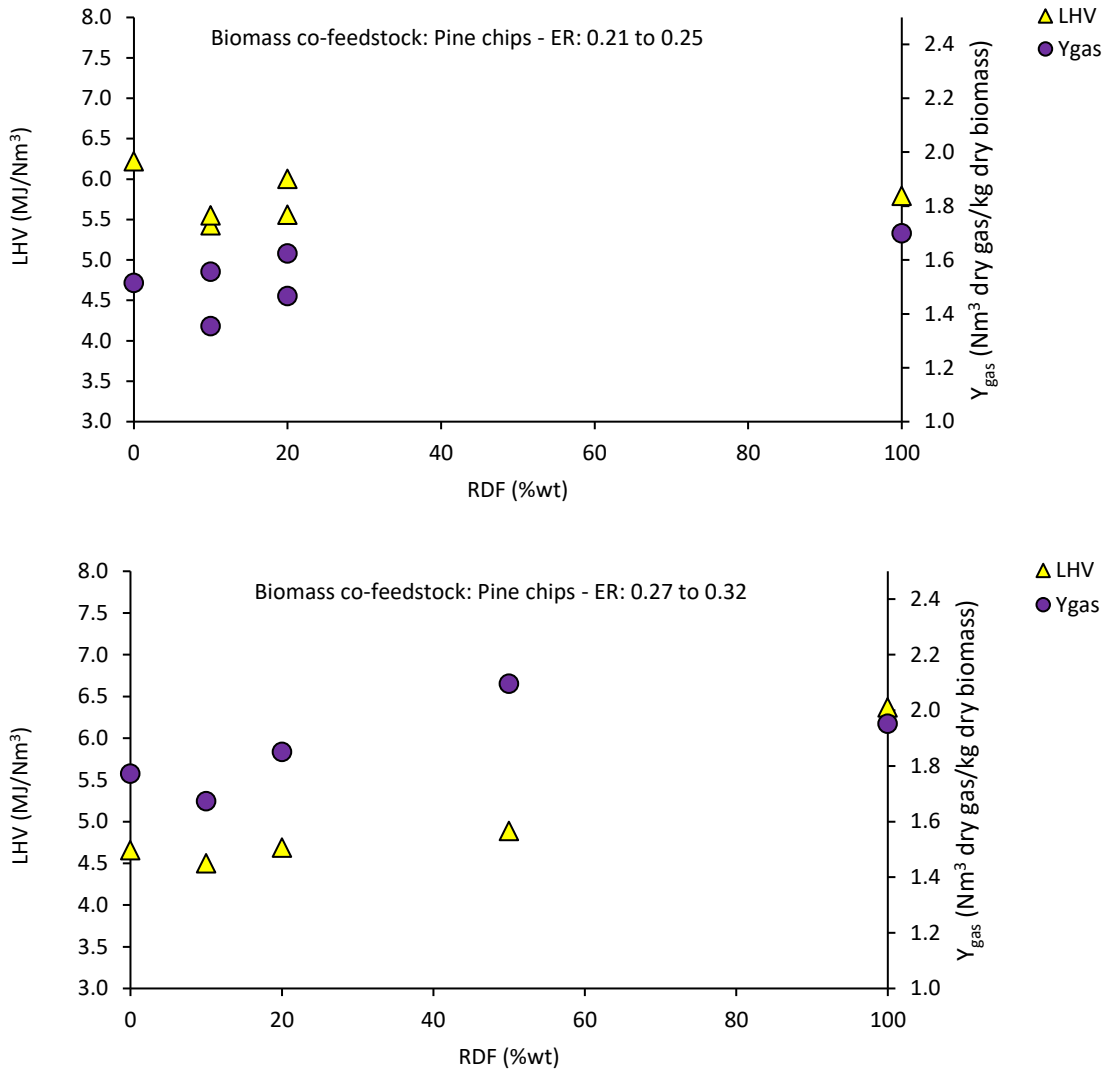

Figure 4.25 – Influence of the RDF weight percentage on the LHV and Y_{gas} for the G-CG experiments.

4.3.4.3.2 CGE and CCE

The effect of RDF weight percentage on the CGE and CCE is shown on Figure 4.26. It can be observed that RDF addition to the fuel mixture does not have significant effect on the CGE, however, a slight trend for the increase of CGE with the increase of RDF weight percentage can be noticed. In fact, maximum CGE value (53.5 %) was found for the gasification of RDF with ER 0.27 (experiment reference RDF100: ER0.27), while the minimum CGE value (32.6 %) was found for pine pellets gasification with ER 0.30 (experiment reference PP100: ER0.30). This is related to the RDF weight percentage increase leading to higher PG LHV and slightly higher Y_{gas} (Section 4.3.4.3.1), which contributes to higher CGE. However, the LHV of the RDF is higher than the LHV of the pine pellets and chips (Table 4.7), thus an increase in the RDF weight percentage means a feedstock mixture with higher energy content, and, consequently, higher values of PG LHV and Y_{gas} are required to maintain the efficiency of the process.

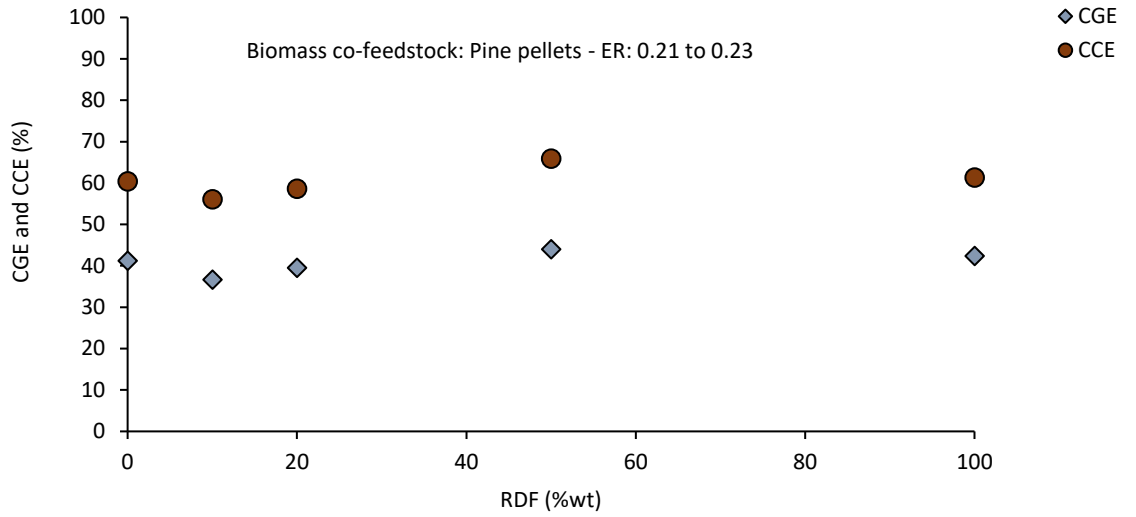
Biomass co-feedstock: Pine pellets - ER: 0.21 to 0.23
CGE
CCE
CGE and CCE (%)
RDF (%wt)
0
10
20
30
40
50
60
70
80
90
100
0
20
40
60
80
100

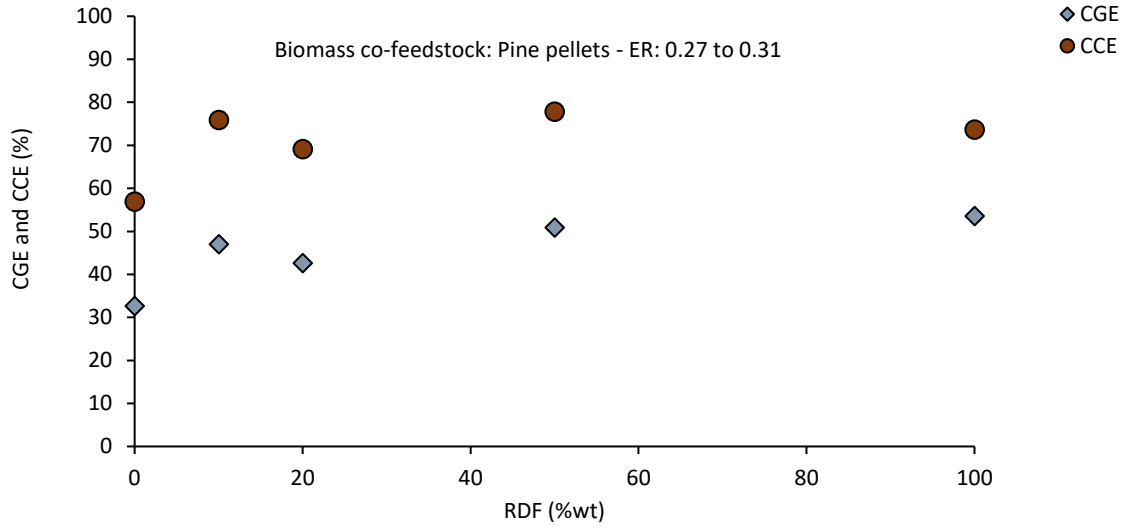
Biomass co-feedstock: Pine pellets - ER: 0.27 to 0.31
CGE
CCE
CGE and CCE (%)
RDF (%wt)
0
10
20
30
40
50
60
70
80
90
100
0
20
40
60
80
100

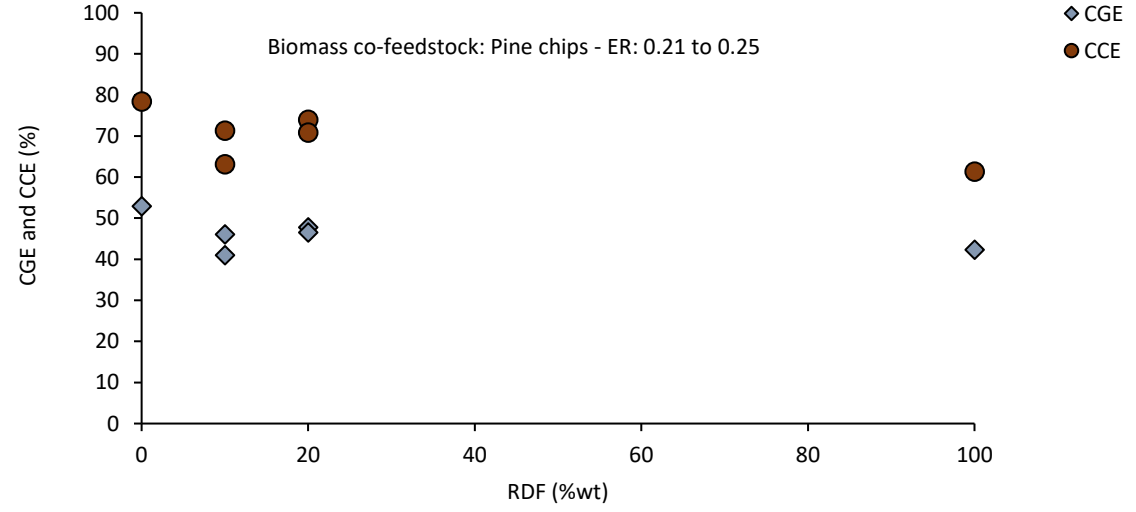
Biomass co-feedstock: Pine chips - ER: 0.21 to 0.25
CGE
CCE
CGE and CCE (%)
RDF (%wt)
0
10
20
30
40
50
60
70
80
90
100
0
20
40
60
80
100

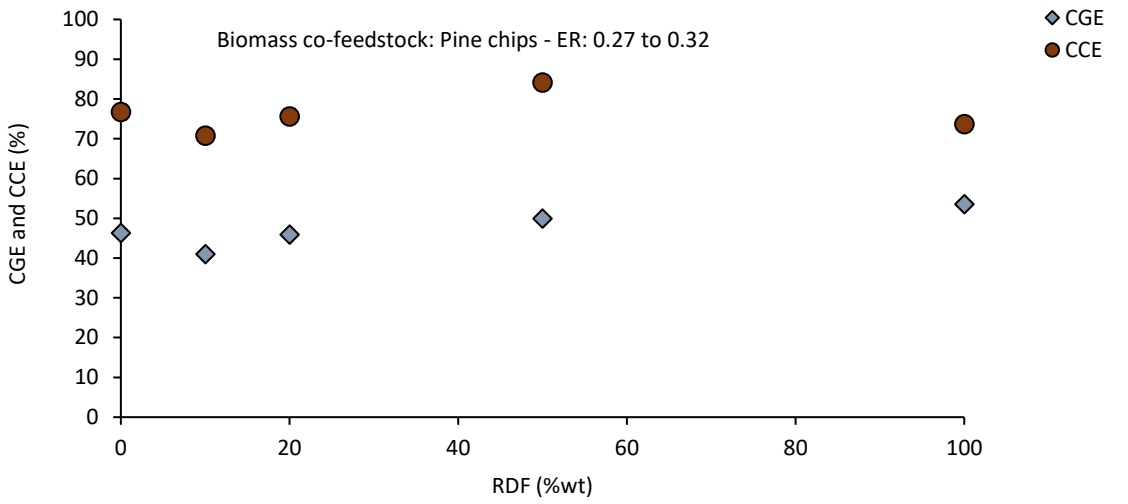

Figure 4.26 – Influence of the RDF weight percentage on the CGE and CCE for the G-CG experiments.

The CCE was found between 56.0 and 84.1 %; The maximum value was found for the co-gasification of pine chips and RDF with ER 0.32 (experiment reference PC50 – RDF50: ER032) and the minimum value for the co-gasification of pine pellets and RDF with ER 0.22 (experiment reference PP90 – RDF100: ER022). No evident trend was found for the effect of the RDF weight percentage increase on the CCE. This is justified by conflicting effects between these parameters. On one hand the RDF weight percentage increase led to higher CH_4 and C_2H_4 concentration in the PG (see Section 4.3.4.2.1), which contributes to higher CCE. On the other hand, the RDF weight percentage increase led to lower CO concentration values, which contributes to lower CCE.

4.3.5 CONCLUSIONS

This work performs a pilot-scale demonstration of the RDF potential as feedstock for gasification and co-gasification processes. Optimal operating conditions for the maximization of the PG quality and the efficiency of the process were determined, which are relevant to maximize rentability. The stability of the process and the synergy between RDF and biomass were shown, revealing enhanced gasification products during co-gasification, when compared to 100 % biomass gasification processes. Furthermore, no slag, agglomeration or defluidization phenomenona were observed during the experiments performed.

In terms of PG composition, increasing the RDF weight percentage led to a significant increase in CH_4 and C_2H_4 concentration and to a decrease in CO concentration. This may be related to a combined effect between the thermal cracking of the plastic polymers present in the RDF pellets and the catalytic effect promoted by the ashes (rich in alkali and alkali earth metal) from the RDF pellets. No significant trends were observed for the variation of H_2 concentration with RDF weight percentage, indicating that other parameters may have a more prominent effect on this gaseous compound production, such as the ER and bed temperature. Nonetheless, higher H_2:CO molar ratios were obtained with the increase of the RDF weight percentage, due to the CO concentration decrease.

In terms of efficiency parameters, the PG LHV increased with RDF weight percentage increase, mainly due to the CH_4 and C_2H_4 concentration increase. This phenomenon was more evident for experiments with higher ER. Increasing RDF weight percentage also led to slightly higher values of

Y_{gas}, however, this effect may be concealed by involuntary changes in the ER, which has a prominent effect on the Y_{gas}. Regarding CGE and CCE, the effect of the RDF weight percentage increase seems to be positive, although this is not clear due to conflicting effects. In terms of CGE, the RDF weight percentage increase generally led to higher PG LHV and slightly higher Y_{gas}, which contributes to higher CGE, however, due to the RDF higher heating value in comparison with the pine pellets and chips, an increase in the RDF weight percentage also means an increase of the feedstock mixture energy content, and, consequently, higher values of PG LHV and Y_{gas} are required to maintain the efficiency of the process. In terms of CCE, RDF weight percentage increase led to higher CH_4 and C_2H_4 concentration, which contributes to higher CCE values, however, the increase in the RDF weight percentage also led to lower CO concentration values, which contributes to lower CCE values.

Thus, this information supports the upscale and commercial breakthrough of RDF gasification technologies and promotes future research on this subject. In fact, adding RDF to the feedstock mixture of gasification plants may significantly improve the economic viability and environmental benefits of future gasification plants, due to the high availability and low cost of wastes; This needs to be properly analyzed in future works, for example by performing an integrated technoeconomic or life cycle analysis. Furthermore, gaseous pollutants (e.g., hydrochloric acid, sulfur oxides and nitrogen species), particulate matter and bottom bed and volatile ashes must also be characterized during RDF gasification and co-gasification with biomass, to fully evaluate the influence of this fuel in gasification processes. These aspects are relevant to support the valorization of both municipal and biomass wastes, and, consequently, may increase the sustainability of waste management and energy supply in the future.

4.4 ARTICLE VII - TAR FORMATION DURING EUCALYPTUS GASIFICATION IN A BUBBLING FLUIDIZED BED REACTOR: EFFECT OF FEEDSTOCK AND REACTOR BED COMPOSITION

4.4.1 ABSTRACT

Tar compounds are inevitably present in the raw PG from biomass gasification and currently represent the main barrier for the commercial breakthrough of gasification technologies. In the present work, tar concentration in the PG from direct gasification of distinct types of residual forest biomass from eucalyptus in a 5 kW_{th} bubbling fluidized bed reactor was investigated. The influence of the feedstock chemical composition and gasifier operation time was evaluated. Average tar concentration values in the raw PG were between 1.5 and 13.3 g/Nm^3, representing a tar production between 8.4 and 67.0 g tar/kg biomass db, which surpasses suggested tar concentration limits for various potential applications for the PG. Major average tar compounds present in the tar sampled from the raw PG were benzene (47.1 %wt), toluene (21.6 %wt), naphthalene (10 %wt) and indene (6.4 %wt). A significant decay of the tar concentration in the PG was observed with increasing gasifier operation time, namely up to 50 % within 45 minutes of operation, indicating its dependency on inorganics (e.g., $CaCO_3$, KCl, maximum 5.5 %wt) and solid carbon (maximum 22.7 %wt) accumulation in the reactor bed.

Keywords: Gasification; Biomass; Tars; Ash; Bubbling fluidized bed; Eucalyptus.

4.4.2 INTRODUCTION

The commercialization of large-scale biomass gasification plants still face technical and economic challenges associated to the presence of tars in the PG [26,58,115,123]. Tars are a mixture of highly aromatic organic condensable compounds formed during thermal or partial-oxidation (gasification) regimes of any organic material [114]. The composition of tars is highly dependent on the thermal conversion process temperature and can be divided in primary (e.g., phenol), secondary (e.g., benzene, toluene, xylene) and tertiary (e.g., pyrene, indene, naphthalene) products, roughly formed at 200 to 500 ºC, 500 to 1000 ºC and over 700 ºC, respectively [114,115]; primary and tertiary tars are mutually exclusive, being that primary products are destroyed before tertiary products appear [114]. In BFB gasifiers, as the operation takes place between 700 and 850 ºC [4], a mixture of second and tertiary tar products can be expected in the PG [114]. These undesired compounds represent a not negligible part of the chemical energy in the PG, which may be lost upon condensation [119]. Tars are also a major obstacle, causing several operating problems during the gasification process and downstream use of the PG, such as surface corrosion, blocking and fouling of engines, filter and pipe plugging and catalyst deactivation, leading to general malfunctions of equipment, breakdowns in operation and low efficiency [113,123,217].

The tar concentration in a PG from BFB gasifiers typically revolves around 1 to 30 g/Nm^3 [66,114], which is higher than the suggested tar concentration limit for most potential PG applications [26]. The employment of gas cleaning equipment for tar removal often turns the process economically unattractive. Accordingly, the effect of gasification operating parameters on tar compounds formation and concentration has been widely investigated in the literature, with particular emphasis on temperature [389–393], ER [335,389], pressure [394], residence time [395] and reactor bottom bed material [66,100,113]. In general, tar concentration in the PG decreases with temperature, ER and pressure increase [124]. Using active bed materials (e.g., dolomite, limestone and olivine) has also been demonstrated as a strategy to reduce tar concentration in the PG [66,100,124].

The effect of the chemical properties of the biomass feedstock has also been researched [396–401]. Yu et al., [398] compared the major biomass components (i.e. cellulose, hemicellulose and lignin) in relation to their differing tar formation characteristics during gasification and concluded that lignin leads to a higher tar yield with a higher thermal stability. Additionally, Hosoya et al., [399] observed that the primary tar fraction derived from lignin has a significantly lower reactivity than the one derived from cellulose, with the latter easily gasified into permanent gases. In accordance, Zhou et al., [400] showed that the main fraction of tar in the PG from biomass gasification was lignin-derived phenolics. In another study, Wang et al., [401] observed that adding potassium and calcium to the thermal decomposition of cellulose leads to a lower tar yield and an enhanced permanent gases production.

The gasification process is particularly interesting for converting eucalyptus byproducts from the PP industry due to the possibility of replacing natural gas by PG in kiln ovens and boilers, and the suitability of this industry to involve gasification-based biorefinery processes in the future [402]. Cross et al., [403] studied eucalyptus (*Eucalyptus Benthamii*) air gasification in a bench-scale BFB, focusing on the effect of harvesting age and bark content, and found tar yield between 1.3 and 1.7 g tar/kg biomass db, with higher amounts of naphthalene and indene and lower amounts of benzene (resulting in a lower total tar yield) in the PG from the gasification of older eucalyptus samples. Pinto et al., [404] performed steam gasification of eucalyptus (*Eucalyptus Globulus*) in a bench-scale BFB reactor, focusing on the influence of the feedstock torrefaction and pelletization, and found tar concentration in the PG between 4 and 16 g/m^3 (values retrieved from figures), with these pretreatment measures leading to a decrease of tar concentration in the raw PG of up to 72 %. Nonetheless, data regarding tar concentration in the PG from eucalyptus gasification is limited and investigation on tar formation during gasification of biomass usually neglects the depth of the influence of the feedstock chemical composition. For example, it is often neglected the catalytic effect promoted by alkali and alkaline earth metals (AAEMs) present in the biomass ashes, which are recognized promoters of tar cracking and reforming reactions [401,405,406]; this highlights the need for additional studies.

Thus, this work investigates tar formation during the direct gasification of distinct types of RFB from eucalyptus (*Eucalyptus Globulus)*, including eucalyptus byproducts from the PP industry, in a bench-scale BFB reactor. The main objective is to evaluate the influence of the eucalyptus chemical composition, and respective ashes, as well as chars', accumulation in the bed of the BFB gasifier with operation time, on the tar composition and concentration in the PG. An inert material (non-porous alumina, Al_2O_3) was used as bed material to minimize any potential activity from the fresh bed material towards char gasification and tar formation [355,407]. This provides valuable data for the evaluation of the gasification process of eucalyptus feedstocks, and consequent integration in the PP industry, as a valid valorization energetic option. It will also serve as a guideline for future research seeking tar reduction in the PG from biomass gasification in BFBs, which is the main barrier for the commercial breakthrough of these technologies [123].

4.4.3 MATERIALS AND METHODS

The experimental infrastructure used in this work was the KTH 5 kWth bench-scale BFB gasifier (Section 1.3.3). The methodologies used are described in Section 1.4.

4.4.3.1 FEEDSTOCK CHARACTERIZATION

The feedstocks used in the gasification experiments consisted of pellets (2 - 4 mm) produced from distinct fractions of RFB from eucalyptus (*Eucalyptus Globulus)*, namely:

- Pellets 1 - Eucalyptus wood fines (<1 mm) from industrial operations related to woodchip production from eucalyptus logs in the context of the PP industry, hereafter, called eucalyptus wood fines.
- Pellets 2 - Eucalyptus wood fines (<1 mm) and eucalyptus leaves.
- Pellets 3 - Eucalyptus branches (<30 mm in diameter).
- Pellets 4 - Eucalyptus wood fines (<1 mm), eucalyptus leaves and eucalyptus branches (<30 mm in diameter).

The biomass feedstocks preparation included chipping and sieving to a particle size below 5 mm, drying at atmospheric conditions to attain a moisture content between 15 and 20 %wt and pelletizing. The pelletization was performed to increase the uniformity of the physical characteristics of the feedstocks and to improve feeding regularity. The pellets were characterized in terms of relevant properties for the thermochemical conversion of biomass (proximate and ultimate analysis, ash composition, and LHV), as shown in Table 4.10.

Table 4.10 – Characteristics of the different types of eucalyptus pellets used as feedstock in the gasification experiments performed in the BFB (Article VII).

	Pellets			
	1	2	3	4
Proximate analysis				
Moisture (%wt, wb)	8.9	8.3	7.9	6.7
Volatile matter (%wt, db)	77.1	79	77.1	80.0
Fixed carbon (%wt, db)	15.6	17.7	18.5	16.6
Ash (%wt, db)	7.3	3.3	4.4	3.4
Ultimate analysis (%wt, db)				
Ash	7.3	3.3	4.4	3.4
C	48.2	50.9	51.4	51.2
H	6.2	6.1	6.1	6.1
N	<0.2	0.9	1.4	1.2
S	0.03	bd	bd	bd
O (by difference)	38.3	38.8	36.7	38.1
Ash composition (mg/kg biomass db)				
Ca	19856	7392	8052	6800
K	2088	2696	5148	2764
Cl	204	102	4893	75
S	518	281	176	177
P	515	307	471	286
Si	13	151	214	186
Al	322	112	74	117
Mg	718	591	1056	646
Na	558	360	792	462
Mn	112	159	96	109
Fe	147	101	122	115
Ti	5	3	2	2
Zn	9	6	7	5
Ba	24	11	36	19
AAEM	23244	11050	15084	10691
LHV (MJ/kg biomass db)	18.8	19.6	20.0	19.4

bd – below the detection limit of the method, 100 ppm wt.

4.4.3.2 OPERATING CONDITIONS

The operating conditions of the experiments performed in the present work are found in Table 4.11. The ER was maintained between 0.18 and 0.22 and the bed temperature at 800 ºC. The bottom bed of the reactor was composed by Al_2O_3 (approximately 3960 kg/m^3 bulk density) with a particle size between 63 and 125 µm; each gasification experiment started with a fresh Al_2O_3 bed. For the fluidization of the bed, 8.6 NL/min of a synthetic mixture of O_2 and N_2 (5.8 %v and 94.2 %v, respectively) was used. This synthetic mixture has a significantly lower O_2/N_2 molar ratio (0.06 mol·mol^{-1}) than atmospheric air (0.27 mol·mol^{-1}) to promote a higher dilution of the PG in N_2 and consequently reduce tar partial pressure and condensation. A flow of 2 NL/min of N_2 was added to the fuel hopper to prevent hot gases from escaping from the reactor through the water-cooled feeding screw, which could cause undesired biomass pyrolysis and consequent clogging and blockage in the feeding system.

Table 4.11 – Operating conditions during the gasification experiments in the BFB reactor.

Experiment reference	Feedstock	Bed material	Gasification agent	Bed temperature [ºC]	Biomass feeding rate [g/min]	ER	Tar sampling start** [mins]
LTS	Pellets 1	Al_2O_3	Synthetic mixture O_2/N_2*	800	2.8	0.20	129
	Pellets 2	Al_2O_3	Synthetic mixture O_2/N_2*	800	2.4	0.22	119
ETS	Pellets 3	Al_2O_3	Synthetic mixture O_2/N_2*	800	3.0	0.18	17
	Pellets 4	Al_2O_3	Synthetic mixture O_2/N_2*	800	2.7	0.20	32

*- Synthetic mixture with 5.8 %v O_2 and 94.2 %v N_2.

**- Tar sampling start time after initiating the gasification experiment

Tar sampling was conducted during two distinct times in each experiment, separated by 45 minutes. Three tar samples were taken at each time, representing approximately 10 minutes of operation time. For the experiments, performed with Pellets 1 and Pellets 2 (experiments reference LTS), at least 119 minutes of gasification were conducted before starting the tar sampling, while for the experiments with Pellets 3 and Pellets 4 (experiments reference ETS), the tar sampling start was performed before 32 minutes of operation. These operation times were chosen to analyze the effects of char and inorganics accumulation in the reactor bed over time on tar concentration in the raw PG.

The reactor bottom bed composition along time during the gasification experiments was estimated by a developed non-stoichiometric thermodynamic equilibrium model, based on the minimization of Gibbs free energy in the system (in-depth description in Section 1.4). The modelled compounds were assumed to reach equilibrium faster than the tar sampling start time. Quasi equilibrium conditions in the reactor bed were assumed during the tar sampling interval due to the low quantities of ash fed to the reactor along time, in comparison to the bed material. The model was implemented considering the molar input (biomass, gasifying agent and fresh reactor bed) and the predicted outputs (most abundant predicted gaseous and solid products). All the reactants were assumed to enter and leave the reactor at process temperature, namely 800 ºC. This temperature was assumed as homogenous inside the gasifier. The software tool used to implement the model was NASA Chemical Equilibrium with Applications (https://www.grc.nasa.gov/www/CEAWeb/). A similar methodology was used by the authors in Article III. The parameters used as input in the model were analogous to the ones attained in the gasification experiments (Table 4.11), namely:

- Feedstock composition: Pellets 1, 2, 3 and 4 (Table 4.10).
- Bed temperature: 800 ºC.

- Reactor bed: 350 g Al_2O_3.
- ER: 0.18 to 0.22.
- Pressure: 1 atm.
- Operation time: up to 8 hours.

4.4.4 RESULTS AND DISCUSSION

The results presented include information regarding the average concentration of CO_2, CO, CH_4, C_2H_4, H_2 in the dry and clean PG and the average tar compounds concentration (e.g., benzene, toluene, xylene, indene, naphthalene) in the raw PG, including tar composition profiles over time. The LHV of the dry and clean PG and the process efficiency parameters, namely Y_{gas}, CGE and CCE, are also presented and analyzed to characterize the process. The reactor bed composition over time in terms of Al_2O_3, char and inorganic solids, is also estimated from the developed thermodynamic model and correlated to the tar concentration in the PG.

4.4.4.1 GAS COMPOSITION AND GASIFICATION EFFICIENCY PARAMETERS

The composition of the dry and clean PG (after tar and particles removal) in terms of permanent gases and the gasification efficiency parameters for the different experiments performed with distinct biomass types is shown in Figure 4.27. In an inert free dry gas basis, the major compounds present in the PG are CO, CO_2, H_2, CH_4 and C_2H_4, by decreasing order of abundance. The gasification experiments of distinct eucalyptus pellets with similar operating conditions (temperature around 800 ºC and ER between 0.18 and 0.22), allowed for a production of PGes with similar permanent gases concentration and analogous efficiency parameters, although some differences were observed regarding the CGE and CCE. This is not surprising because the ER and bed temperature are commonly acknowledged as the main parameters governing the concentration of permanent gases in the PG from BFBs biomass gasification processes [4]; as these parameters were maintained almost constant between experiments, no significant differences in the dry and clean PG composition were expected.

The highest CO concentration (35.8 %v, dry N_2-free gas) is found for the gasification of Pellets 4 (ER:0.20), while the highest H_2 concentration (31.8 %v, dry N_2-free gas) is observed for the gasification of pellets 2 (ER:0.22). Nonetheless, the highest H_2:CO molar ratio (0.98 $mol \cdot mol^{-1}$) is found for the gasification of Pellets 3 (ER:0.18). The CH_4 concentration in the PG from the gasification of Pellets 4 (ER:0.20) is significantly lower (1 %v, dry N_2-free gas) than in the PG from the gasification of the other eucalyptus pellets (4.2 to 8.5 %v, dry N_2-free gas). The CO_2 concentration in the PG from the gasification of Pellets 2 (ER:0.22) is lower (23 %v, dry N_2-free gas) than in the PG from the gasification of the other eucalyptus pellets (27.6 to 31.5 %v, dry N_2-free gas). These differences may be relevant on a N_2-free gas basis, however, when considering N_2 in the PG composition, the differences are significantly smaller (CH_4 between 0.6 and 1.4 %v and CO_2 between 3.8 and 5.7 %v) and thus can be influenced by various external factors. For example, analytic errors associated with the GC-TCD analysis could have an impact due to the high quantity of N_2 present in the synthetic mixture used as gasification agent. Regarding C_2H_2, C_2H_6 and C_4H_8, the concentration of these compounds is always lower than 0.3 %v, dry gas N_2-free basis.

The LHV and Y_{gas} of the PGs are in the range of 10.5 to 11.2 MJ/Nm^3 N_2-free dry gas and 0.7 to 1.0 Nm^3 N_2-free dry gas/kg dry biomass, respectively. These values are in accordance with those typically referred to in the literature regarding direct biomass gasification in BFBs with similar bed temperature and ER [4]. In fact, the LHV is slightly lower and the Y_{gas} slightly higher than commonly reported [4]. However, when accounting for N_2 dilution, the LHV of the PG is significantly lower (2

to 2.1 MJ/Nm^3 dry gas) and the Y_{gas} significantly higher (4.5 to 5.5 Nm^3 dry gas/kg dry biomass) than the values reported in the literature for direct biomass gasification processes [4]. This is explained by the significantly lower O_2/N_2 ratio (0.06 mol·mol^{-1}) present in the synthetic mixture used as gasifying agent, in comparison with atmospheric air (0.27 mol·mol^{-1}), which causes a higher dilution of the PG in N_2.

Regarding CGE and CCE, these parameters are between 44.1 to 56.9 % and 58.2 to 74.8 %, respectively. Pellets 3 show the lowest CGE and CCE values, which can be related to the lower ER used in this experiment (Table 4.11). The highest CCE value is obtained for the gasification of Pellets 1, which can be justified by the higher alkali (e.g., K) content present in this feedstock, which are recognized promoters of tar cracking [3,123,376] and carbon gasification reactions [408], and consequent formation of combustible gaseous compounds (in this case containing carbon) during gasification processes. The discussion regarding this phenomenon in extended in Section 4.4.4.2. The CGE and CCE values observed are in the lower to average range of the values typically referred in the literature regarding direct biomass gasification processes in BFBs [4]. The lower values may be justified by the synthetic mixture of O_2 and N_2 used as gasification agent, which has a lower O_2/N_2 ratio (0.06 mol·mol^{-1}) than atmospheric air (0.27 mol·mol^{-1}); it is argued that the rate of gas char reactions lowers as the O_2/N_2 ratio decreases in the gasifying agent, which can be related to a higher convective cooling effect of the gas phase over the solid phase, caused by the higher N_2 content and consequent higher gas flow [1,409]. This contributes to lower radiation penetration and lower kinetic rates [409], thus causing lower char reactivity and conversion. In fact, Ismail et al., [334] suggested 0.67 mol·mol^{-1} as the optimal O_2/N_2 ratio for direct biomass gasification processes, which is significantly higher than the ratio present in the synthetic mixture used in the present work (0.06 mol·mol^{-1}).

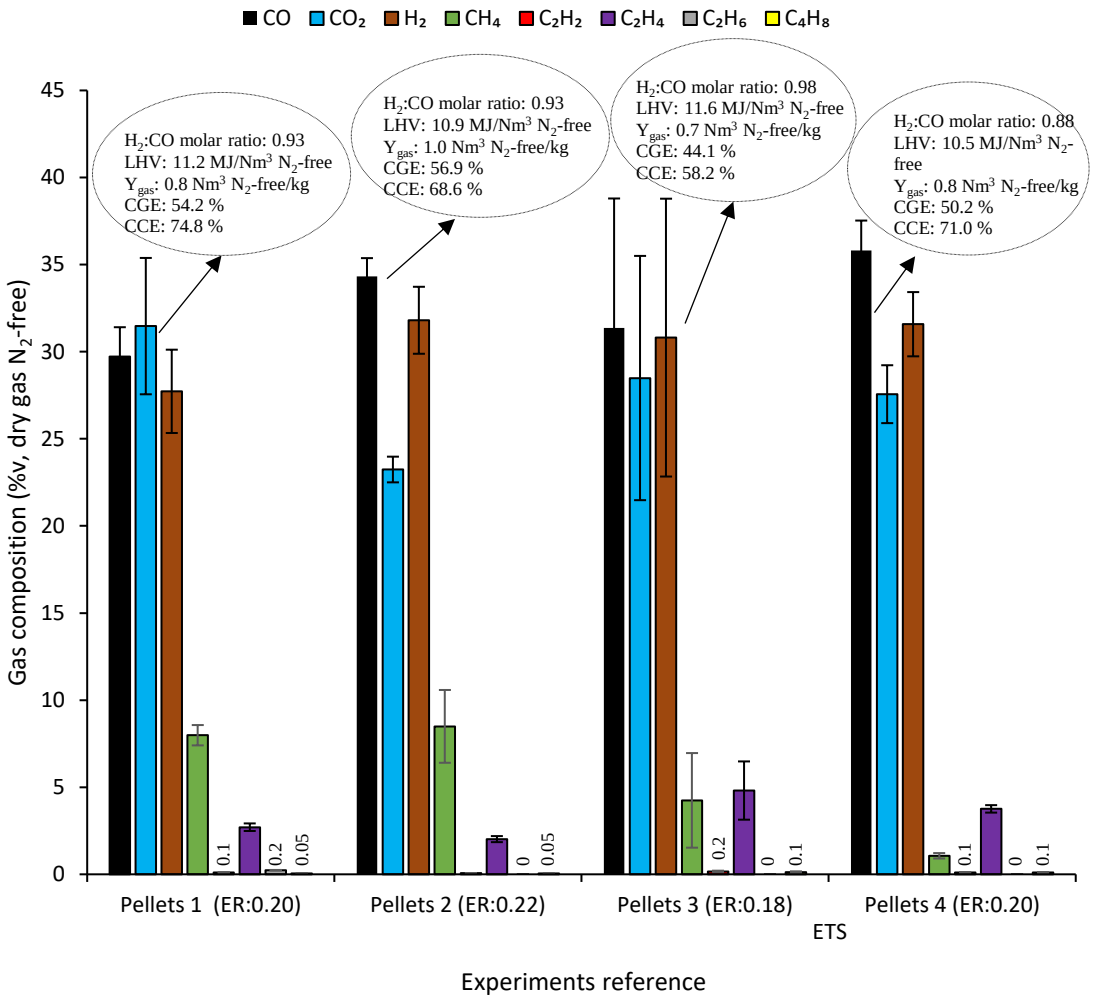

Figure 4.27 – Average dry gas composition for the gasification experiments performed with different eucalyptus pellets. Legend according to experiments reference in Table 4.11.

4.4.4.2 TAR COMPOSITION AND CONCENTRATION

In Figure 4.28, it is shown the tar production per unit of biomass (g tar/kg biomass db) for the distinct gasification experiments performed with different eucalyptus RFB pellets and similar operating parameters (e.g., bed temperature, ER, fluidization velocity). In average, the highest relative abundant compounds are benzene (47.1 %wt), toluene (21.6 %wt), naphthalene (10.0 %wt) and indene (6.4 %wt). Other compounds found include acenaphthylene, xylene, phenanthrene, pyrene, indane, among others. Similar tar composition during other biomass gasification processes has also been shown in the literature [410,411]. However, some authors also refer phenol, xylene or naphthalene as the main tar compounds found in the raw PG [114,412–414].

Significant distinct total tar production values, namely between 8.4 and 67.0 g tar/kg biomass db, which represent 1.5 and 13.3 g/Nm^3 concentration in the PG, are also observed; the gasification of Pellets 2 and 4 display the lowest and highest tar production, respectively. Considering that similar operating parameters (e.g., bed temperature, ER, fluidization velocity) were maintained between gasification experiments, these results suggest that the tar production, and consequent concentration in the PG, is highly dependent on the feedstock characteristics and gasification operation time. In

fact, for experiments with an early tar sampling start (17 to 32 minutes after starting the gasification experiments, reference ETS in Table 4.11), the tar production is significantly higher than in the experiments with a late tar sampling start (119 to 129 minutes after starting the gasification experiments, reference LTS in Table 4.11), namely 47.2 to 67.0 g tar/kg biomass db and 8.4 to 17.5 g tar/kg biomass db, respectively. This is further discussed in the next Section.

The tar concentration values obtained are in agreement with the literature for biomass direct gasification in fluidized beds (1 to 30 g/Nm^3) [66,114] and are significantly higher than the acceptable tar concentration limits for using the PG in fuel cells (1 mg/Nm^3), compressors (50 to 500 mg/Nm^3), internal combustion engines (50 mg/Nm^3) and gas turbines (5 mg/Nm^3) [26,50,113,120–122]. Even if benzene is excluded from the critical tar components, as suggested in the definition proposed by the International Energy Agency [113,415], the tar concentration of the remaining compounds is still higher (0.6 to 9.5 g/Nm^3) than the suggested tar concentration limits referred for the distinct potential applications for the PG. Important to note that a higher nitrogen content was used in the synthetic mixture used as gasifying agent, in comparison with air, and, consequently, this tar concentration is diluted in nitrogen, indicating that tar concentration in the raw PG most likely would be higher if air was used as gasifying agent. Thus, it is essential to remove the major quantity of tar from the PG from eucalyptus direct gasification to attain a gas quality, according to technical specifications, applicable to combustion engines, gas turbines or fuel cells.

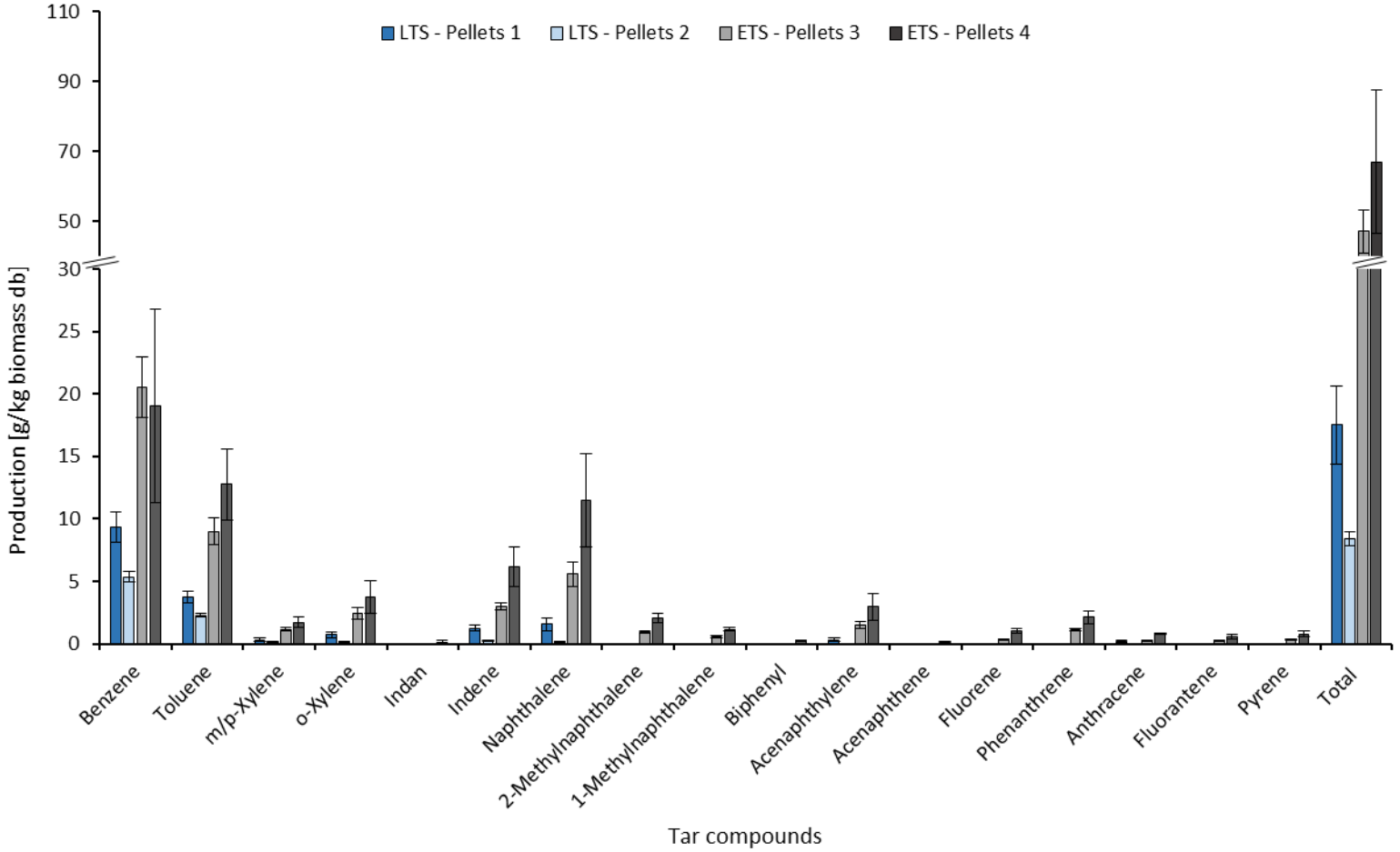

Figure 4.28 – Tar production values for the different gasification experiments. Legend according to experiments reference in Table 4.11.

4.4.4.2.1 Influence of gasification operation time

Figure 4.29 shows the decay of the total tar, BTX (benzene, toluene and xylene), naphthalene and indene concentration values with operation time for each gasification experiment. These tar compounds follow a similar behavior, i.e., a decay of concentration with time, which is especially relevant for experiments with a tar sampling start between 17 and 32 minutes (ETS, Table 4.11). An average decrease of up to 50 % in tar concentration is observed within 45 minutes of operation for these experiments. Note that the BTX concentration remains higher than the concentration of the original fractions of polyaromatic tars (indene and naphthalene), even after long operation times, which can be associated to the cracking of larger tar molecules to BTX compounds. For experiments with a tar sampling start between 119 and 129 minutes (LTS, Table 4.11), the decay of tar concentration with time was significantly smaller or inexistent. Furthermore, the variability of tar concentration values for three successive samplings is significantly lower for experiments LTS, as exemplified by the error bars in Figure 4.29, which indicates that the gasification process was attaining steady-state conditions in terms of tar concentration in the PG.

Considering all the gasification experiments made, a decrease of the total tar concentration of up to 5 times is observed with increasing operation time (Figure 4.29, (a)). In fact, for experiments LTS, the average total tar concentration was found between 1.5 and 3.6 g/Nm^3 (8.4 and 17.5 g tar/kg biomass db), which are lower values than commonly referred for fluidized beds [114]. Even when discounting the dilution caused by the low O_2/N_2 ratio present in the synthetic mixture used as gasifying the agent, the lowest average total tar concentration for experiments LTS was 8.8 g/Nm^3 N_2-free, which is still lower than commonly reported for direct (air) biomass gasification in atmospheric fluidized beds at 0.20 ER and 800 ºC [187].

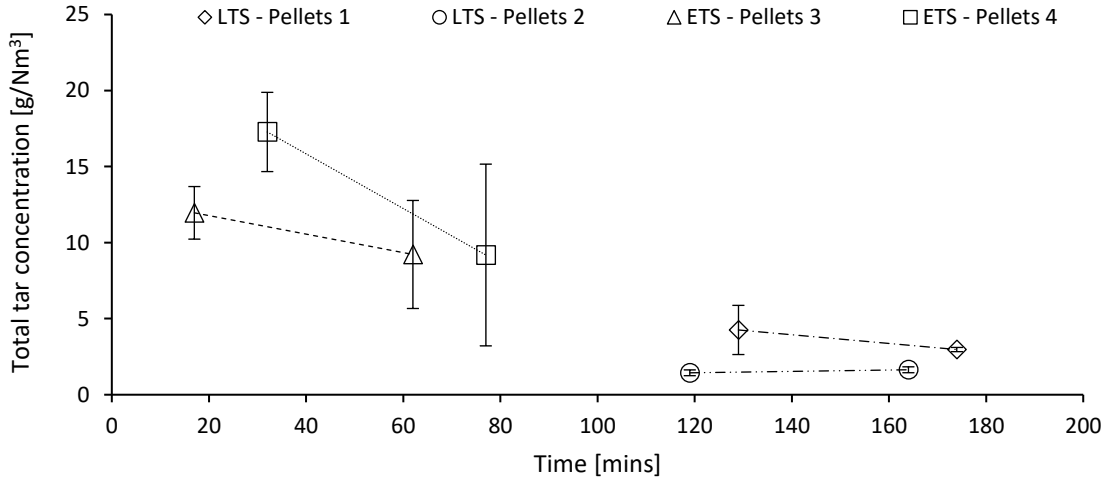

(a)

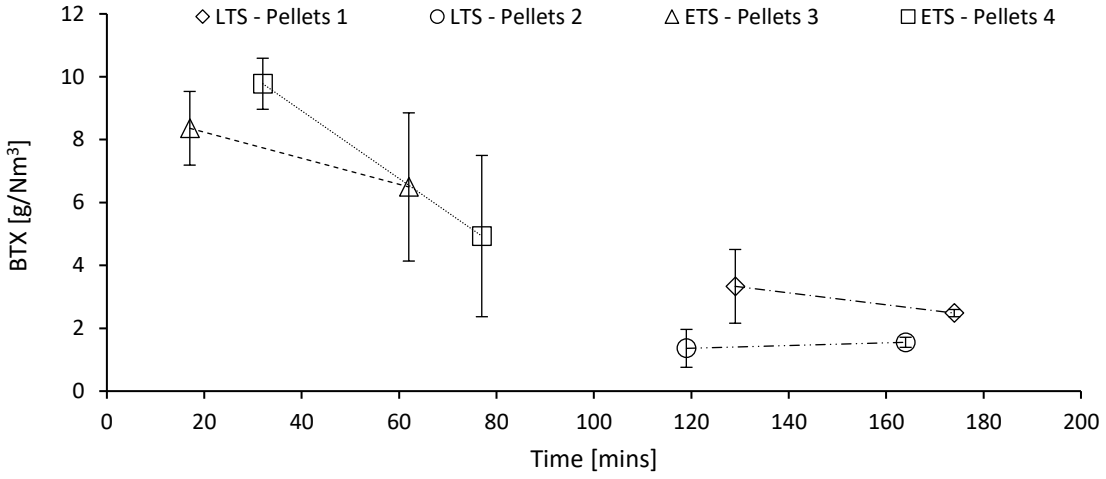

(b)

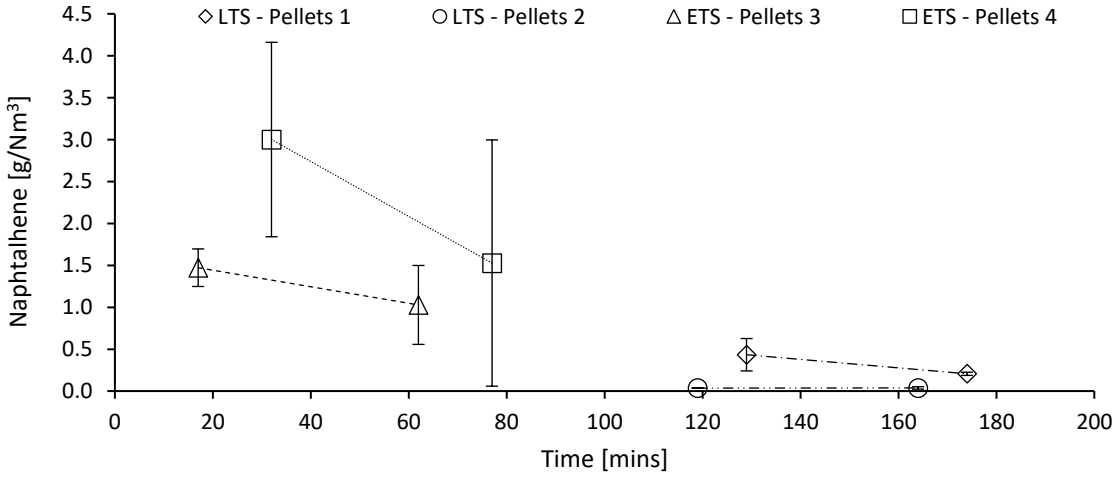

(c)

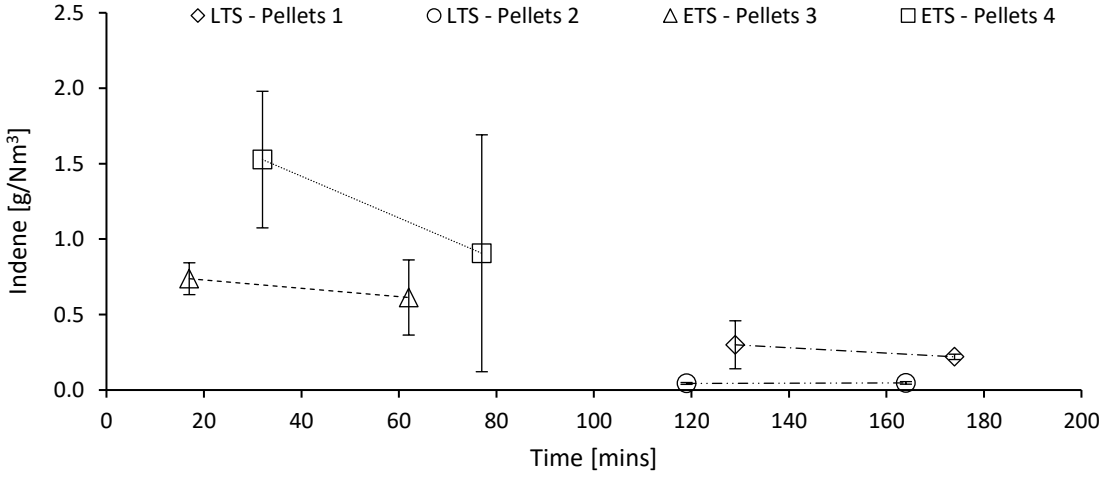

(d)

Figure 4.29 – Decay of the total tar (a), BTX (b), naphthalene (c) and indene (d) concentration in the raw PG with operation time. Experiments information in Table 4.11.

This decay of tar concentration in the raw PG along time indicates the dependence of tar formation on the accumulation of char and ash in the reactor bottom bed. Important to note that each experiment started with a fresh Al_2O_3 bed, and then there was an increase of inorganics and char concentration in the bed as the gasification process progressed, as shown by the results from the developed equilibrium thermodynamic model (Figure 4.30). The equilibrium thermodynamic predictions also show these compounds concentration in the reactor bed increased along time during the tar sampling procedure for all gasification experiments performed, and that equilibrium in terms of bed composition was still far from being attained, suggesting that long times of operation could be beneficial to further reduce tar concentration in the PG. Accordingly, the reactor bed showed higher contents of char and inorganics (e.g., $CaCO_3$, K_2CO_3, KCl, $Mg_2Al_2O_4$, Na_2AlO_2) in experiments LTS than in experiments ETS (Figure 4.30). However, some exceptions can also be observed, such as the highest content of KCl in the reactor bed predicted for experiment ETS – Pellets 3, which can be justified by the high content of K and Cl present in this biomass (Table 4.11, Figure 4.31), implying that these elements may be associated in the original biomass; this may also be important regarding deposit formation and corrosion issues in heat exchangers, due to the formation of low meting point eutectic layers from emitted KCl [416,417].

Thus, an evident trend between the tar concentration decrease in the PG and the increase of char and inorganics concentration in the reactor bottom bed (predicted by the equilibrium thermodynamic calculations) can be observed (Figure 4.32). This observed effect could be explained by the catalytic activity promoted by the chars and inorganics present in the reactor bed, which are recognized promoters of tar cracking and corresponding conversion to lighter gaseous species during gasification processes [3,131,374–376]. $CaCO_3$ was predicted to be the most abundant inorganic solid present in the reactor bed (0.4 and 4.6 %wt), which can be formed through the capture of CO_2 by CaO via a carbonation reaction [418]. CaO is a recognized catalyst for gasification processes [418–422], acknowledged to be able to catalytically reform tar compounds from higher ring species into polycyclic aromatic hydrocarbons with fewer ring species [418]. Accordingly, $CaCO_3$/CaO undoubtedly had a significant effect on tar reduction in the PG by promoting tar reforming/cracking reactions into gaseous products.

The results also show that at operation times longer than 2 to 3 hours, the tar concentration decay stops (Figure 4.29); this indicates that a limit for the catalytic effect promoted by the inorganics and char on the tar cracking was attained. Therefore, it can be inferred that further operation time and consequent additional ash and char accumulation in the bottom bed would not lead to lower tar concentration in the PG.

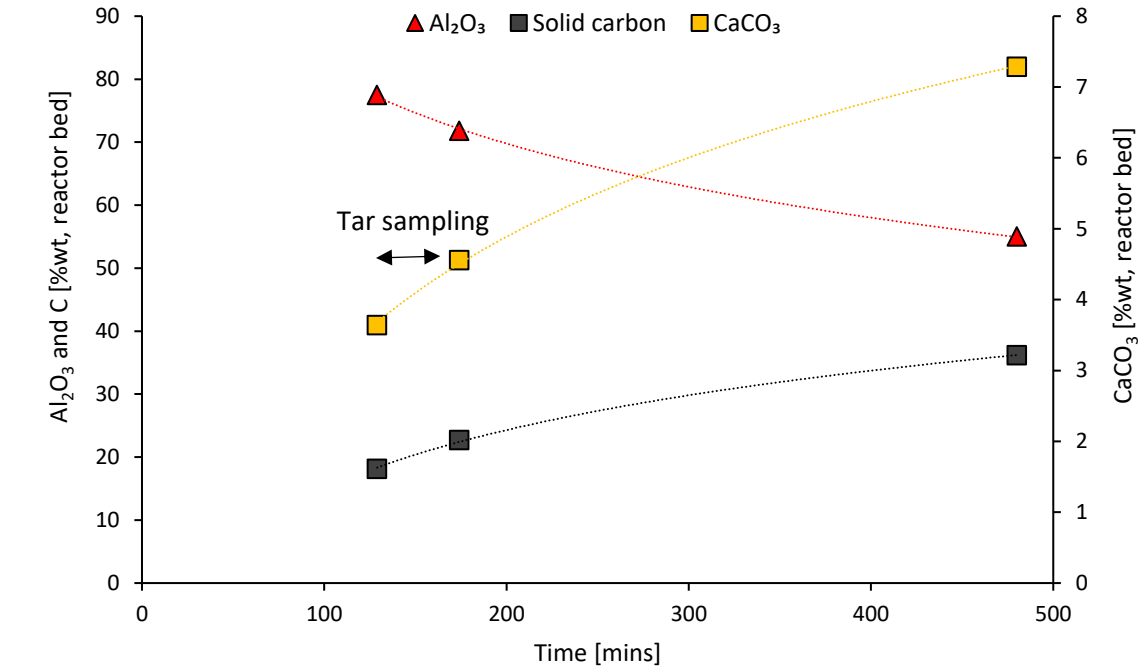
Al2O3
Solid carbon
CaCO3
Tar sampling
Al2O3 and C [%wt, reactor bed]
CaCO3 [%wt, reactor bed]
Time [mins]
0
10
20
30
40
50
60
70
80
90
0
1
2
3
4
5
6
7
8
0
100
200
300
400
500

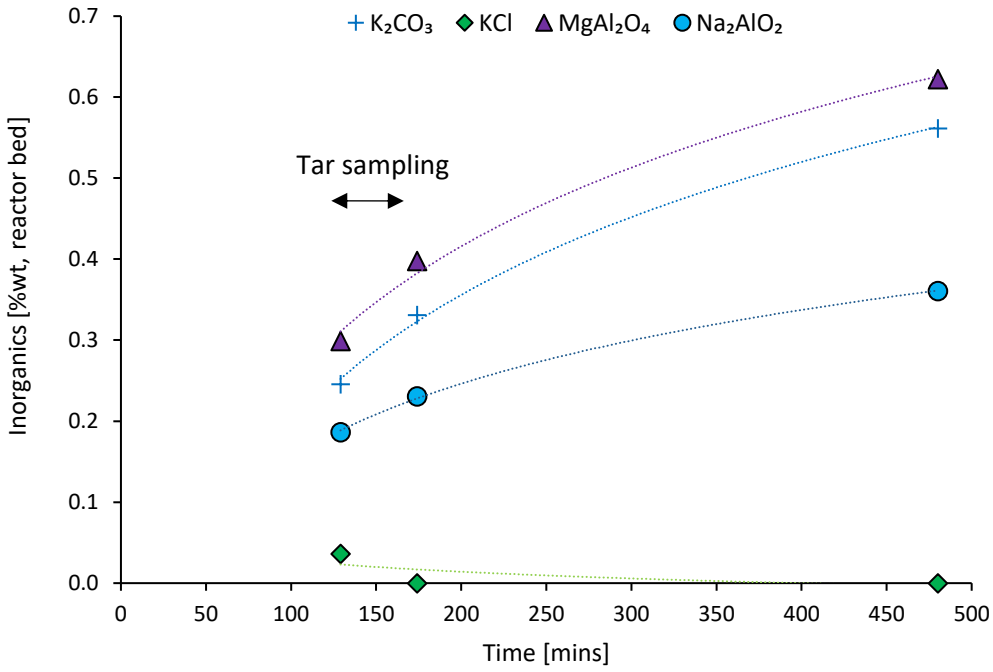
K2CO3
KCl
MgAl2O4
Na2AlO2
Tar sampling
Inorganics [%wt, reactor bed]
Time [mins]
0.0
0.1
0.2
0.3
0.4
0.5
0.6
0.7
0
50
100
150
200
250
300
350
400
450
500

(a)

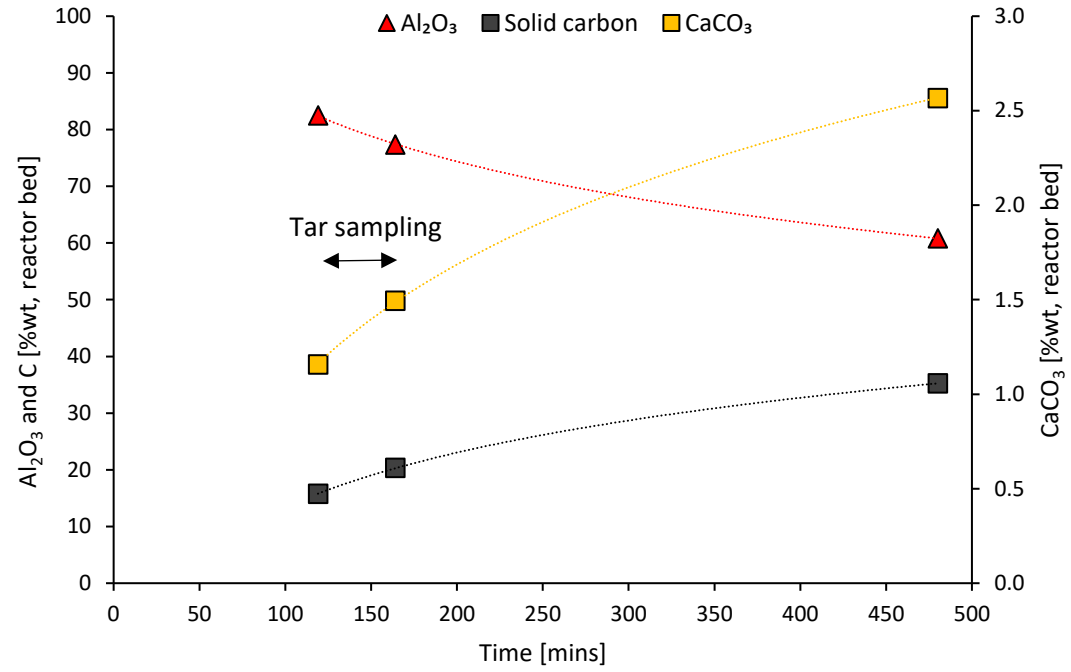
Al2O3
Solid carbon
CaCO3
Tar sampling
Al2O3 and C [%wt, reactor bed]
CaCO3 [%wt, reactor bed]
Time [mins]

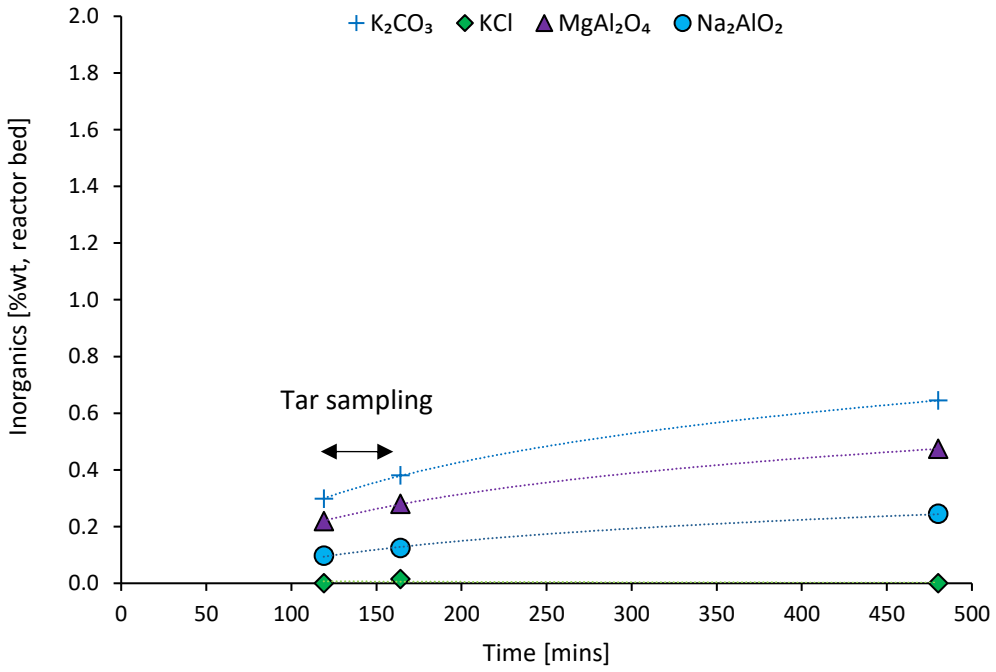
K2CO3
KCl
MgAl2O4
Na2AlO2
Tar sampling
Inorganics [%wt, reactor bed]
Time [mins]

(b)

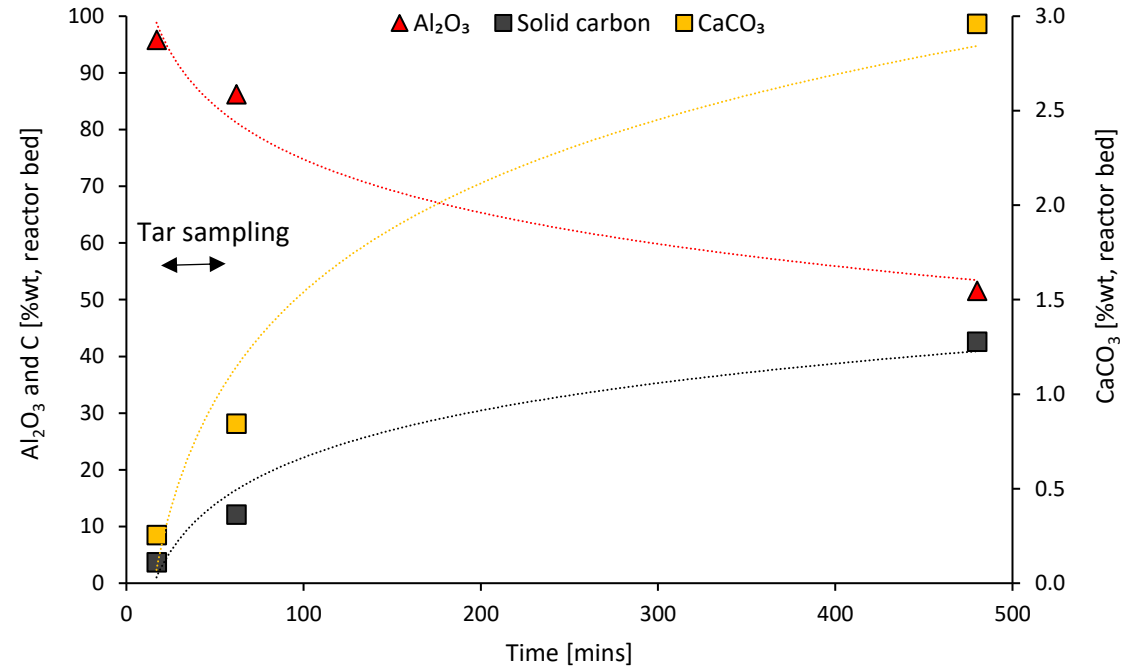
Al2O3
Solid carbon
CaCO3
Tar sampling
Al2O3 and C [%wt, reactor bed]
CaCO3 [%wt, reactor bed]
Time [mins]
0
10
20
30
40
50
60
70
80
90
100
0.0
0.5
1.0
1.5
2.0
2.5
3.0
0
100
200
300
400
500

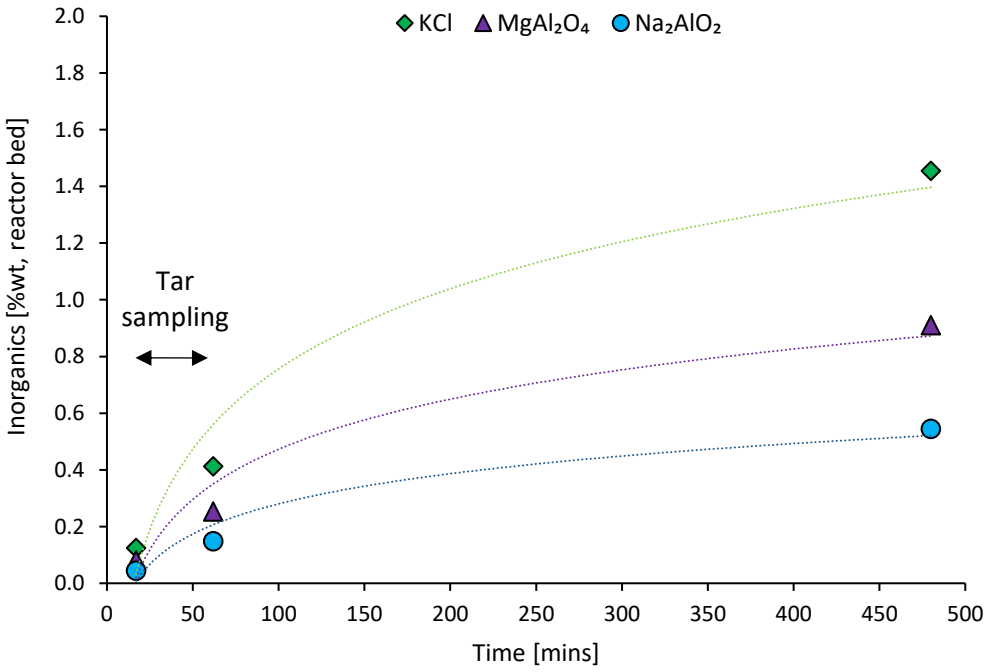
KCl
MgAl2O4
Na2AlO2
Tar sampling
Inorganics [%wt, reactor bed]
Time [mins]
0.0
0.2
0.4
0.6
0.8
1.0
1.2
1.4
1.6
1.8
2.0
0
50
100
150
200
250
300
350
400
450
500

(c)

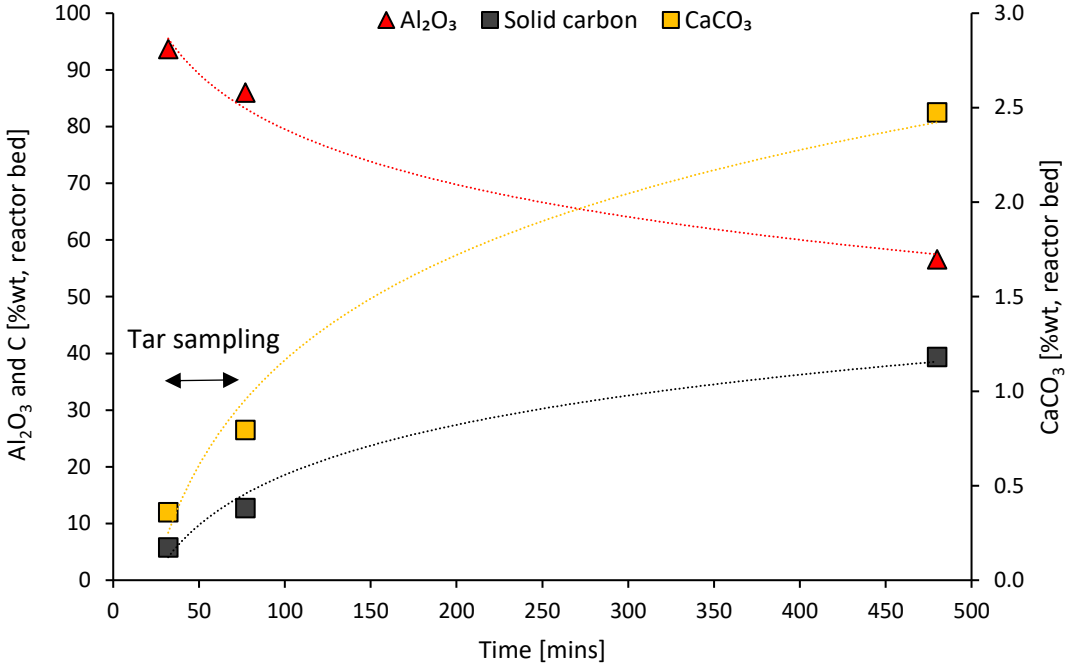

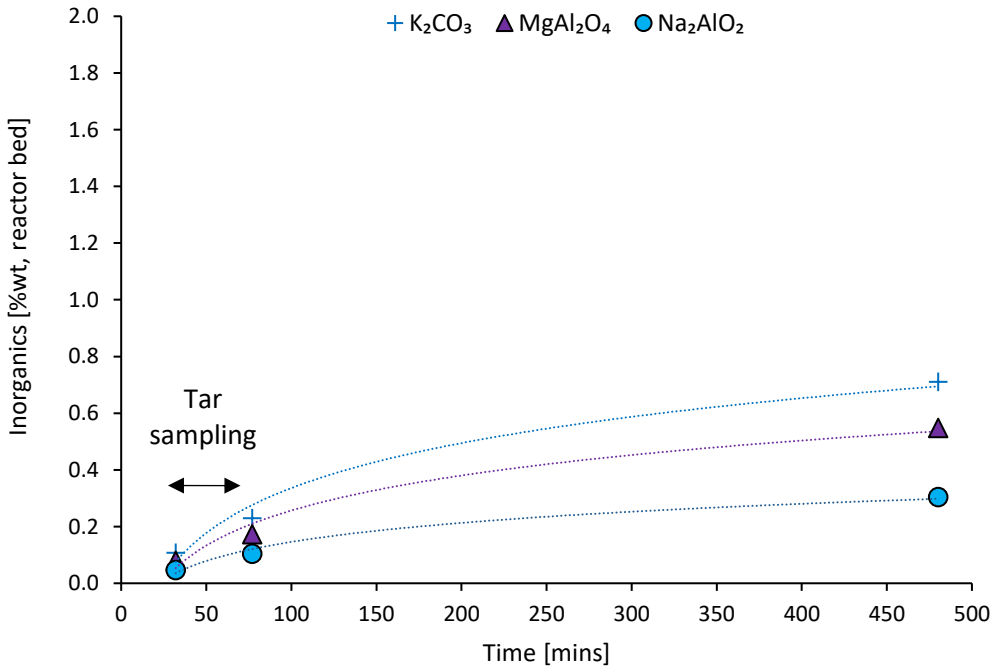

(d)

Figure 4.30 – Equilibrium thermodynamic prediction of the reactor bed composition along time for the experiments LTS – Pellets 1 (a), LTS – Pellets 2 (b), ETS – Pellets 3 (c) and ETS – Pellets 4 (d). Experiments information in Table 4.11.

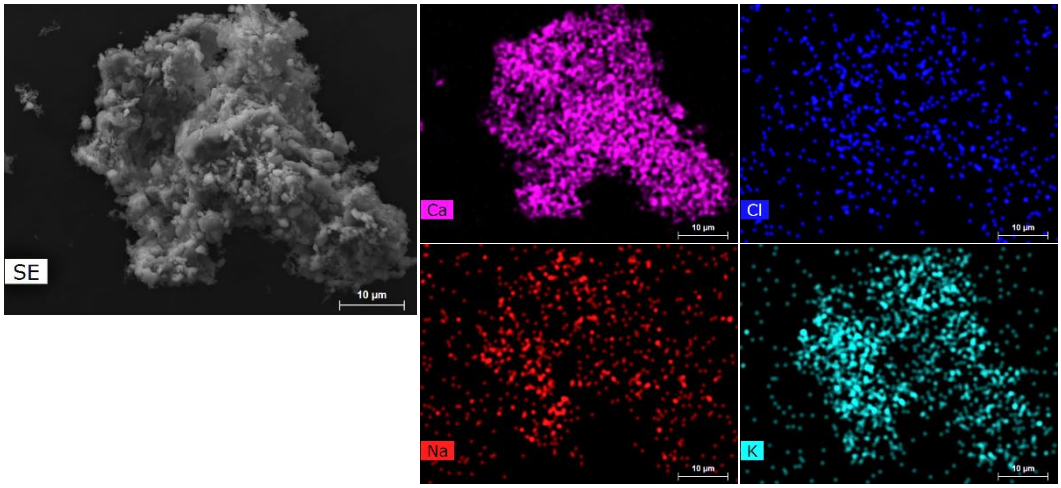

(a)

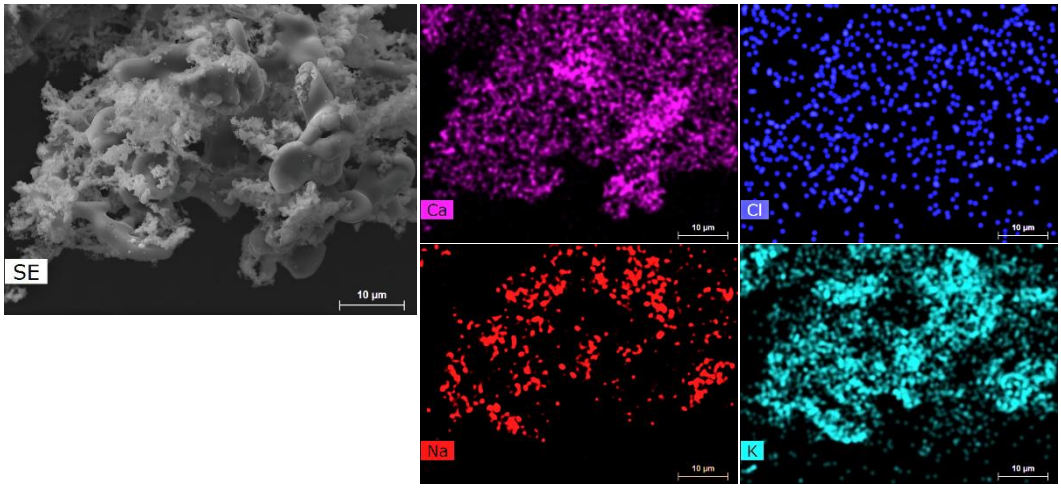

(b)

Figure 4.31 – SEM micrographs of a representative ash particle from Pellets 1 (a) and Pellets 3 (b), and respective Ca, Cl, Na and K elemental intensity maps.

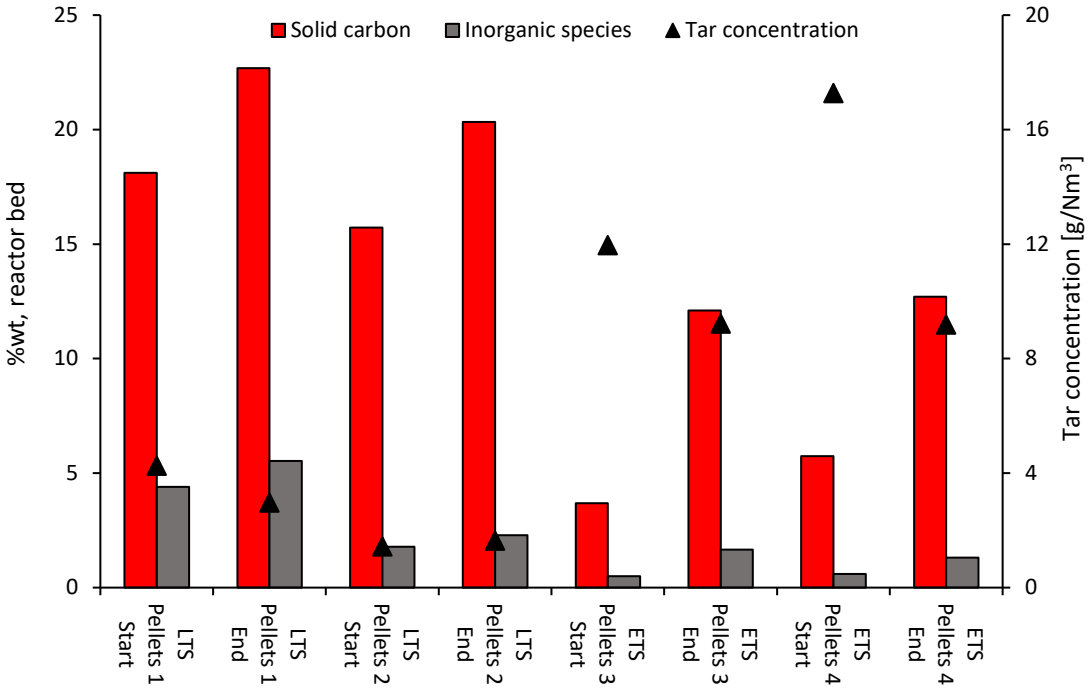

Figure 4.32 – Relation between the solid carbon and inorganic species content in the reactor bed (predicted by thermodynamic equilibrium) and the tar concentration in the PG for the different gasification experiments performed. Experiments information in Table 4.11.

The dependence of the LHV of the dry and clean PG with operation time and tar concentration in the raw PG (Figure 4.33), also confirms this gradual catalytic cracking of tars, and their conversion to lighter combustible gases. A trend for the increase of LHV with the increase in operation time, and consequent total tar concentration decrease, can also be observed, as discussed above. This may be relevant for the conceptualization of prediction models to support large-scale biomass gasification facilities that lack capacity to properly monitor tar concentration in the PG, as previously seen in other works [123]. In these cases, by developing a suitable prediction model, it may be possible to associate light combustible gases with tar compounds in the PG.

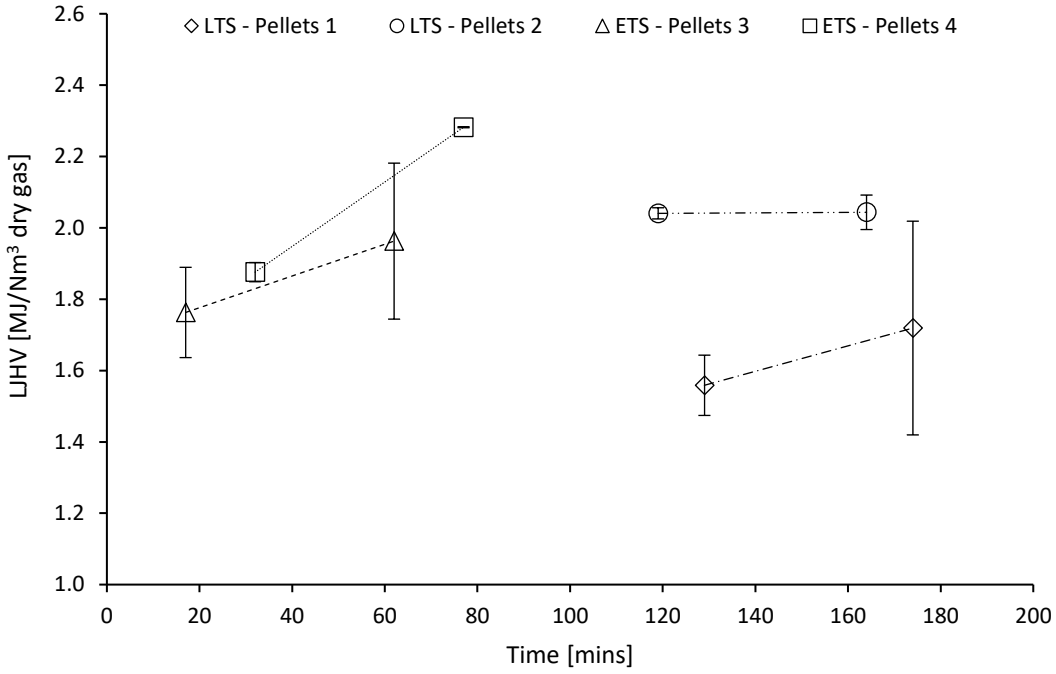

(a)

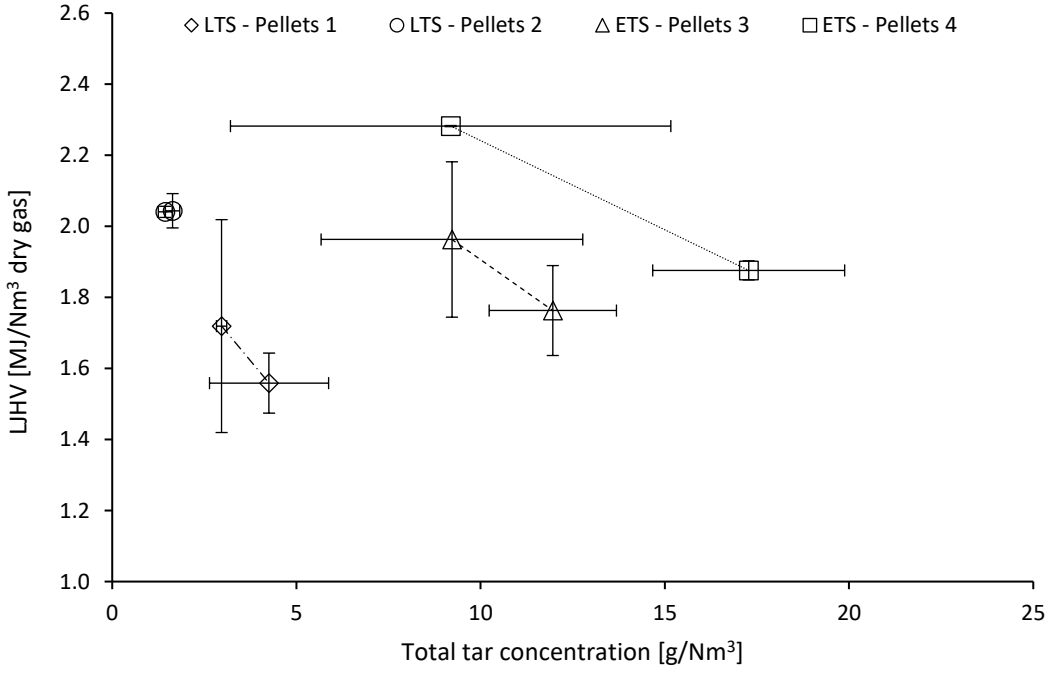

(b)

Figure 4.33 – Variation of the LHV of the dry and clean PG with (a) operation time and (b) total tar concentration in the raw PG. Experiments information in Table 4.11.

4.4.4.2.2 Influence of feedstock chemical composition

Despite the above discussed effect of operation time, and consequent char and ash accumulation in the reactor bed, on tar concentration in the raw PG, some differences for experiments with similar operation time and analogous operating parameters (e.g., bed temperature, ER, fluidization velocity) can also be observed. This suggests an influence of the characteristics of the distinct eucalyptus RFB feedstocks on tar formation mechanisms.

Figure 4.34 shows the variation of BTX, naphthalene and total tar concentration values in relation to several chemical properties of the eucalyptus RFB pellets, namely ash, volatile matter, fixed carbon and carbon and oxygen content. In experiments ETS, a significant decrease of total tar concentration with the increase of ash content in the biomass was observed, which can be explained by a faster ash inventory increase in the bottom bed reactor as the gasification progresses, with consequent catalytic effects promoted by inorganics [3], as previously discussed. It must be noted that the higher ash content present in Pellets 3 also has a significantly higher content of K and Cl (Table 4.10) in comparison to the ash content of the Pellets 4, consequently causing the accumulation of KCl in the reactor bottom bed (Figure 4.30 (c)). This indicates that the ash present in Pellets 3 has a higher catalytic activity for tar cracking and reforming than the ash present in Pellets 4, due to its high content of K, which is a recognized catalyst in gasification processes [423–425], and that this may be relevant in terms of tar production.

In experiments LTS, the increase of ash content did not lead to a lower tar concentration, suggesting that the reactive system converged to a nearly steady state regime in terms of potential ash catalytic effects, meaning that further ash accumulation in the bed would not result in a higher tar cracking and consequent lower concentration in the PG, as previously inferred.

Conclusively, these results indicate that the ash content and ash composition were the feedstock characteristics with highest influence on tar production. However, as the gasification process progresses, and the reactor bed gets richer in inorganic and char solids, these parameters influence on tar formation appear to decrease. Regarding other analyzed parameters (e.g., volatile matter, carbon and oxygen content), no obvious trends were observed, which may be explained by the similar composition of the eucalyptus RFB pellets (Table 4.10) and the operation time exerting a prevailing effect, as previously discussed. Important to note that the physical characteristics of the eucalyptus feedstocks were not evaluated in the present work. In fact, the distinct parts of the eucalyptus (e.g., branches, leaves) were processed to pellets to increase the uniformity of the physical characteristics of the feedstocks.

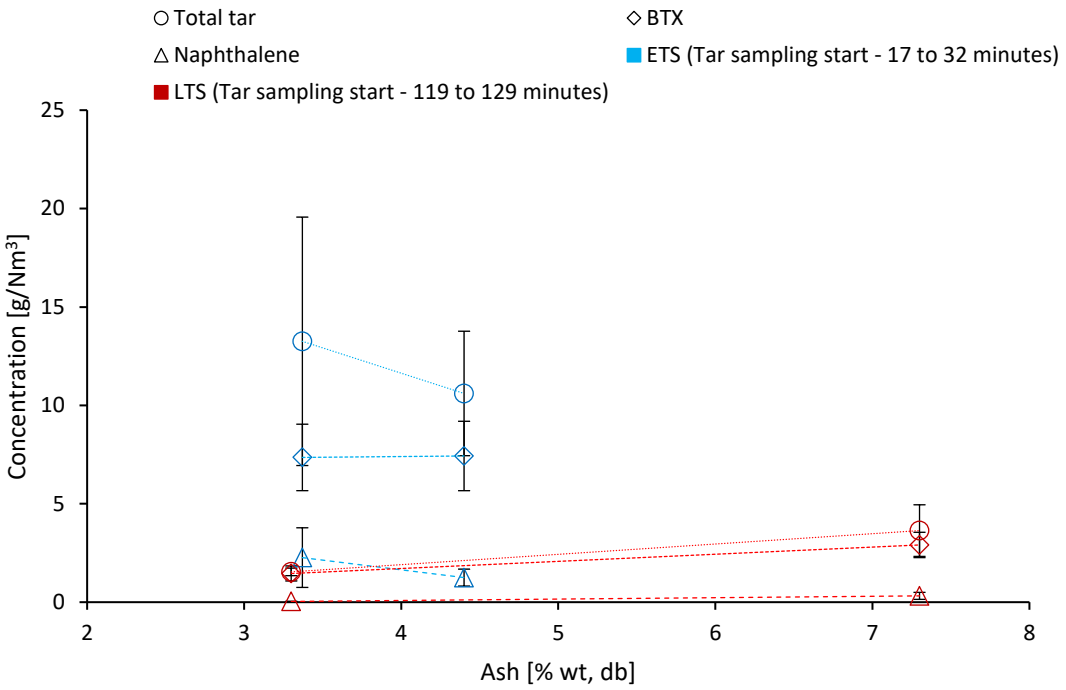
Total tar
BTX
Naphthalene
ETS (Tar sampling start - 17 to 32 minutes)
LTS (Tar sampling start - 119 to 129 minutes)
Concentration [g/Nm³]
25
20
15
10
5
0
2
3
4
5
6
7
8
Ash [% wt, db]

(a)

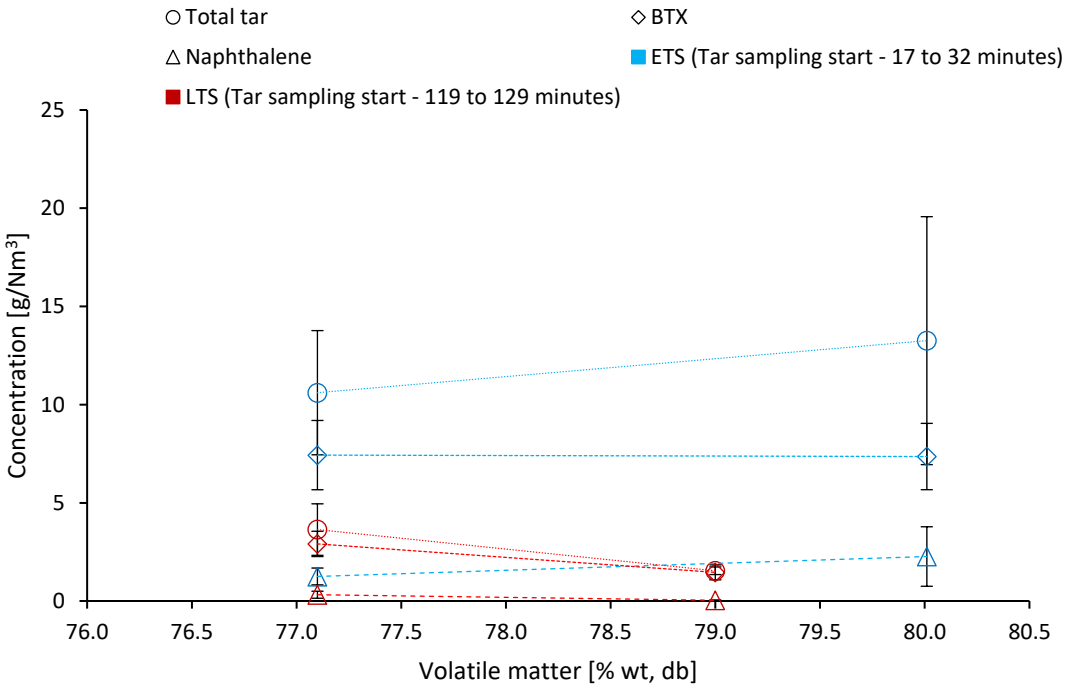
Total tar
BTX
Naphthalene
ETS (Tar sampling start - 17 to 32 minutes)
LTS (Tar sampling start - 119 to 129 minutes)
Concentration [g/Nm³]
25
20
15
10
5
0
76.0
76.5
77.0
77.5
78.0
78.5
79.0
79.5
80.0
80.5
Volatile matter [% wt, db]

(b)

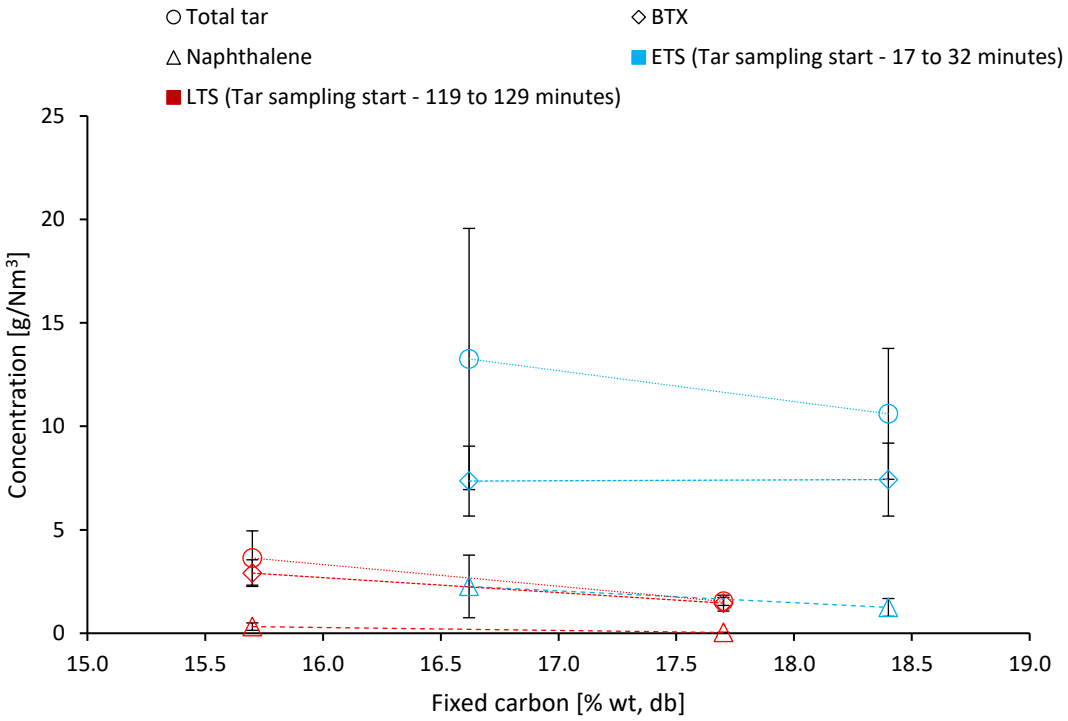
Total tar
BTX
Naphthalene
ETS (Tar sampling start - 17 to 32 minutes)
LTS (Tar sampling start - 119 to 129 minutes)
Concentration [g/Nm³]
25
20
15
10
5
0
15.0
15.5
16.0
16.5
17.0
17.5
18.0
18.5
19.0
Fixed carbon [% wt, db]

(c)

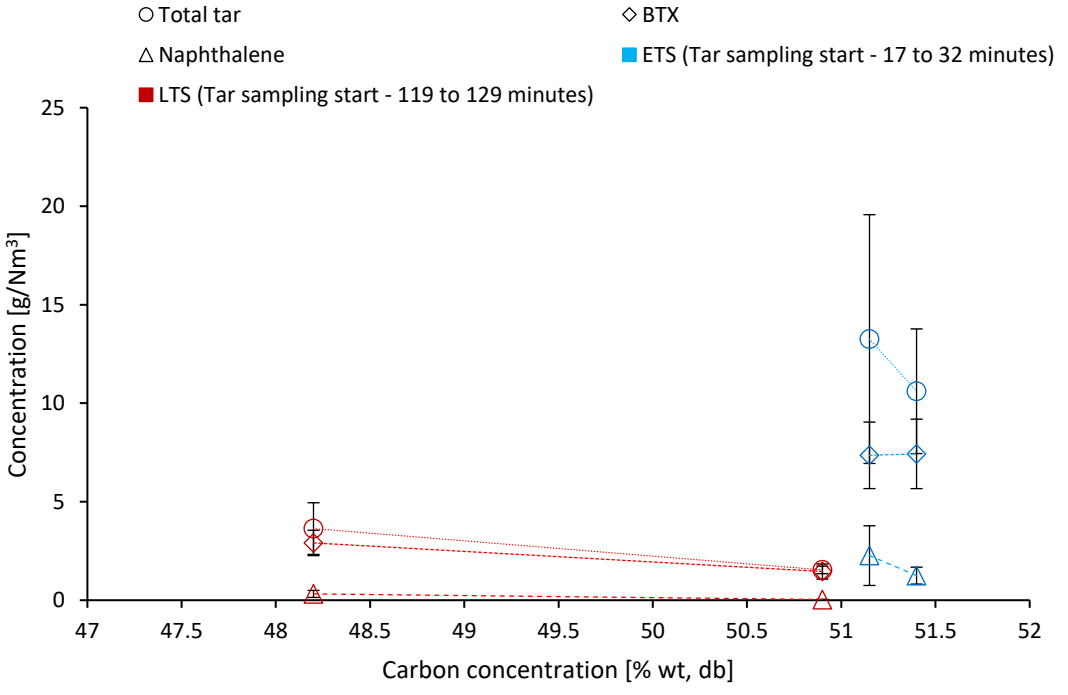
Total tar
BTX
Naphthalene
ETS (Tar sampling start - 17 to 32 minutes)
LTS (Tar sampling start - 119 to 129 minutes)
Concentration [g/Nm³]
25
20
15
10
5
0
47
47.5
48
48.5
49
49.5
50
50.5
51
51.5
52
Carbon concentration [% wt, db]

(d)

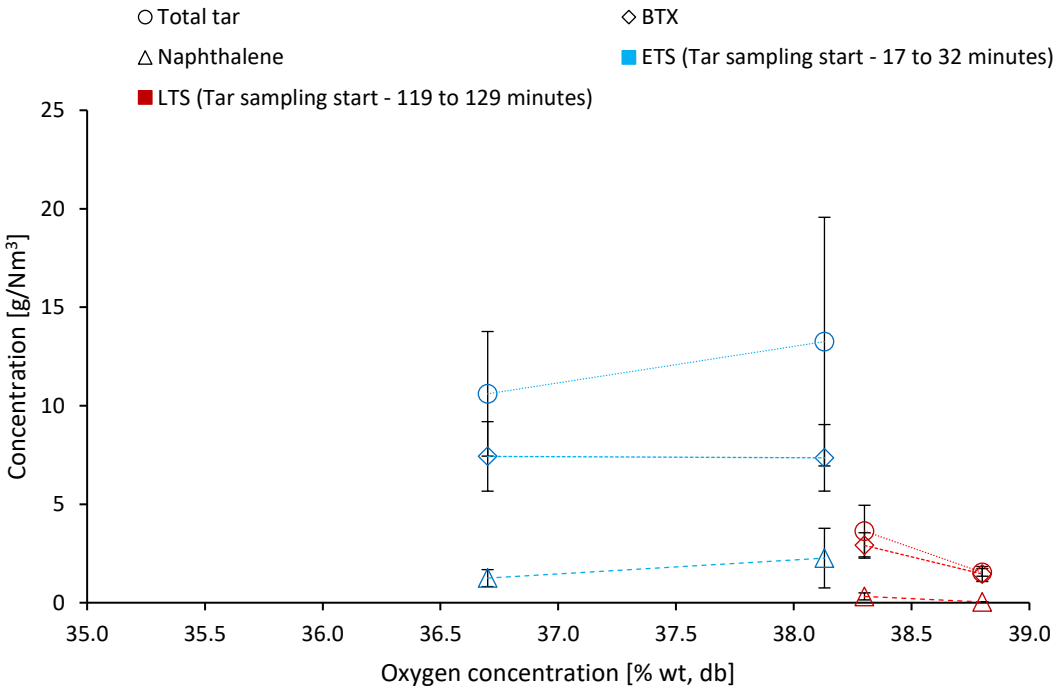

(e)

Figure 4.34 – Variation of total tar, BTX and naphthalene concentration in the raw PG with the chemical properties of the eucalyptus RFB pellets used in the gasification experiments: ash (a), volatile matter (b), fixed carbon (c), carbon concentration (d) and oxygen concentration (e). Feedstock characteristics in Table 4.10 and experiments reference in Table 4.11.

4.4.5 CONCLUSIONS

This work characterizes and evaluates the gasification of distinct types of RFB derived from eucalyptus with a synthetic mixture of O_2/N_2 (0.06 mol·mol^{-1}) in a 5 kW_{th} bench-scale BFB, focusing on tar composition and concentration in the PG.

The major components found in the clean and dry PG were CO, CO_2, H_2, CH_4 and C_2H_4 by decreasing order of abundance. The LHV of the clean and dry PG (2.0 to 2.1 MJ/Nm^3) was significantly lower than commonly reported in the literature for direct gasification processes, however, the Y_{gas} (4.5 to 5.5 Nm^3 dry gas/kg dry biomass) was significantly higher; the CGE (44.1 to 56.8 %) and CCE (58.2 to 74.8 %) were in the lower to average range. This is related to the synthetic mixture used as gasifying agent, which has a significantly lower O_2/N_2 ratio (0.06 mol·mol^{-1}) compared to atmospheric air (0.27 mol·mol^{-1}), and therefore promotes lower char conversion rates and causes a higher dilution of the PG in N_2.

The average tar concentration values in the raw PG were between 1.5 and 13.3 g/Nm^3, representing a tar production between 8.4 and 67.0 g tar/kg biomass db, which are significantly higher values than the tar concentration limits for various potential applications of the PG (can fall between 0.1 to 500 mg/Nm^3). The major tar compounds detected in the tar samples from the raw PG were benzene (47.1 %wt), toluene (21.6 %wt), naphthalene (10 %wt) and indene (6.4 %wt).

The tar concentration in the raw PG decayed significantly with the operation time of the gasification experiments. For experiments with a tar sampling start between 17 and 32 minutes after initiating the

gasification process (with a fresh Al_2O_3 bed), a tar concentration approximately 5 times higher, compared to experiments with tar sampling start between 119 to 129 minutes, was observed. For the prior case, the tar concentration decreased up to 50 % within 45 minutes of operation. For the latter case, the average total tar concentration was between 1.5 and 3.6 g/Nm^3 (8.4 to 17.5 g tar/kg biomass db), which are lower values than commonly reported for fluidized beds. These results indicate the influence of ash and char accumulation in the bed and the catalytic activity of these gasification byproducts for tar reforming/cracking.

The tar concentration showed a negative correlation with solid carbon and inorganics concentration in the reactor bed. It can be estimated that solid carbon (char) and $CaCO_3$/CaO had a significant effect on tar reduction by promoting tar reforming/cracking reactions into non-condensable gaseous products, due to their proven catalytic effect and predicted high accumulation and concentration in the reactor bed. However, 2 to 3 hours after the start of the gasification process, the tar concentration decay stopped, indicating a limit for the catalytic effect of ash and char on tar destruction.

The obtained results show the relevance of ash chemistry and ash/char bottom bed inventory during gasification processes in BFB reactors, and give a relevant contribution to support future works seeking tar reduction in the raw PG from biomass gasification.

4.5 INTEGRATED RESULTS DISCUSSION

This Chapter shows how wide can be the variability of the quality of the PG and the performance parameters values of the direct biomass gasification process. The values of ER, bed temperature, S/B (with steam injection as primary measure), char and ash accumulation in the reactor, as well as the addition of RDF and plastics to the feedstock mixture, all have significant impact on the PG quality and gasification efficiency, and the optimal combination of these parameters can significantly promote the viability of distinct gasification projects and plants. This reflects the importance of obtaining specific knowledge regarding the experimental demonstration of the biomass gasification process for each particular application; this is mandatory in order to provide a suitable support for the development and optimization of new industrial projects and avoid afterward drawbacks.

In this regard, from the extensive experimental practice performed in this work, it can be concluded that ER = 0.25 and bed temperature = 800 ºC allow an optimal balance between PG quality, efficiency parameters and stability of the process. Using a mixture of RDF and biomass wastes as feedstock also seems to lead to enhanced gasification products (due to synergies) and to be a promising strategy in terms of economic viability and environmental benefits of future gasification plants, due to the high availability and low costs of wastes. This may promote the valorization of both municipal and biomass wastes, consequently increasing the sustainability of waste management and energy supply in the future, thus acting in accordance with circular economy principles. The process may even be improved with the addition of steam as primary measure, which has shown very interesting results for the gasification of high-density solid fuels, particularly regarding H_2 concentration and H_2/CO molar ratio increase in the PG, and this needs to be analyzed and quantified in future works. The development of a techno-economic analysis that considers this integration is also of major relevance. Regarding the tar content of the PG, it has been found that ash chemistry and ash/char bottom bed inventory (directly related to operation time) have a prominent effect on tar reduction, and this must be accounted for in future studies concerning the analysis of tar concentration in the PG.

5 LOW-COST CATALYSTS AS PRIMARY METHODS TO IMPROVE THE PG QUALITY

This Chapter evaluates the in-situ application of distinct types of low-cost catalysts in the freeboard of two distinct BFB reactors, namely the DAO-UA 80 kW_{th} pilot-scale BFB gasifier and the DAO-UA 3 kW_{th} bench-scale BFB gasifier (Section 1.3). The Chapter is composed by Articles VIII, IX and X.

Article VIII, named "Low-cost catalysts for in-situ improvement of PG quality during direct gasification of biomass", analyzed and proposed an alternative configuration for studying primary tar destruction measures using catalysts in the DAO-UA 80 kW_{th} pilot-scale BFB gasifier. Three distinct low-cost catalysts were tested, namely bottom bed particles resulting from the combustion of eucalyptus RFB in an industrial BFB furnace, char particles resulting from wood pellets direct (air) gasification in a BFB reactor, and synthetic fayalite (Fe_2SiO_4). This Article was published in the Energy Journal in 2018 (https://doi.org/10.1016/j.energy.2018.09.119).

Article IX, named "Ilmenite as low-cost catalyst for PG quality improvement from a biomass pilot-scale gasifier", analyzed the application of natural-occurring ilmenite ($FeTiO_3$) in the same system proposed in Article VIII. This Article was published in the Energy Reports Journal (2020, https://doi.org/10.1016/j.egyr.2019.08.063) after being presented at the 6th International Conference on Energy and Environment Research (ICEER 2019), and serves as basis for Article X.

Article X, named "Concrete and Ilmenite as low-cost catalysts to improve gas quality during biomass gasification in a pilot-scale gasifier", evaluates the application of ilmenite and concrete as in-situ catalysts in the system proposed in Article VIII and in a new system developed in the DAO-UA 3 kW_{th} bench-scale BFB gasifier. The Article is currently submitted and under revision in a Special Issue of Energy & Fuels Journal for memory of Professor Mário Costa.

Because Article X is an extension of Article IX, only the contents of Article X were presented here.

5.1 ARTICLE VIII - LOW-COST CATALYSTS FOR IN-SITU IMPROVEMENT OF PG QUALITY DURING DIRECT GASIFICATION OF BIOMASS

5.1.1 ABSTRACT

In this work, the concept of biomass direct (air) gasification was demonstrated in a pilot-scale BFB and the influence of in-situ application of low-cost catalytic materials on the PG characteristics and gasifier performance was analyzed. Three different low-cost catalysts were tested: bottom bed ashes resulting from combustion of residual forest biomass derived from eucalyptus, char particles resulting from wood pellets direct (air) gasification, and synthetic fayalite (Fe_2SiO_4). Without using catalysts, the PG composition was 7.7-16.9 %v CO, 3.2-8.3 %v H_2, 0.5-3.4 %v CH_4 and 9.5-14.6 %v CO_2, with 2.4-4.3 MJ/Nm^3 LHV, Y_{gas} between 1.0 and 1.8 Nm^3 dry gas/kg biomass (dry basis), CGE between 13.7 and 30.5 % and CCE between 30.7 and 50.9 %. With the use of catalysts, the PG composition was 14.2-37.6 %v CO, 9.5-14.7 %v H_2, 2.6-3.5 %v CH_4 and 3.6-14.8 %v CO_2, with 3.9-6.3 MJ/Nm^3 LHV, Y_{gas} between 1.4 and 2.0 Nm^3 dry gas/kg biomass (dry basis), CGE between 38.1 and 66.3 % and CCE between 56.8 and 86.6 %. The highest increase in H_2 concentration (352 % increase) was observed on experiments using wood pellets char as catalyst while the highest increase in CO (305 % increase), LHV (123 % increase), Y_{gas} (62 % increase), CGE (262 % increase) and CCE (174 % increase), was observed on experiments using synthetic Fe_2SiO_4 as catalyst.

Keywords: Biomass; Bubbling fluidized bed; Gasification; Catalyst.

5.1.2 INTRODUCTION

Several thermochemical processes are available for heat and power production from biomass, amongst which combustion is the most widely used [69]. However, biomass gasification is gaining interest worldwide due to the process flexibility and the need of renewable fuels that can replace gaseous fossil fuels in distinct applications. Gasification is a promising alternative to direct biomass combustion due to the recognition that combustible gases have practical advantages over solid fuels, such as handling and application [112,426]. Different types of biomass can be converted by gasification into a fuel gas containing mainly hydrogen, carbon monoxide, carbon dioxide and methane and, from this gas, it is possible to produce heat, power, biofuels and chemicals [15,218]. Gasification of biomass is recognized as a partial solution to diverse environmental problems and societal needs, with emphasis on greenhouse gases accumulation in the atmosphere, fossil fuel depletion and waste disposal [174]. This process has the potential to partly replace the use of fossil fuels through liquid fuels/chemicals production, integrated gasification combined cycles for electricity/steam production, PG combustion in gas-fired kilns and furnaces and production of hydrogen-rich syngas and synthetic natural gas. Thus, biomass gasification technologies are expected to have an important role in future energy systems [15,58,430,100,112,116,231,426–429] and to be the basis of potential future biorefineries that will provide a variety of chemicals and energy products [231], including electricity and transportation fuels.

In addition to these advanced applications, which are particularly suitable for developed countries, biomass gasification can also meet the rural electrification and thermal needs of developing countries, mainly those with a high share of solid biofuels in their energy mix [218,431,432]. In fact, in developing countries with intense agricultural activities, and, consequently, strong potential for power generation from agricultural byproducts and wastes, such as rice husk [433], sugar cane bagasse [190] or almond shell [327], biomass gasification technologies have been considered of particular interest [431]. This interest is increased when considering integrated gasification combined cycles technologies which allow high efficiencies in electricity generation (about 40 %)

[157,434,435]. In developed countries, thermochemical conversion of biomass by gasification has been emerging as a suitable CO_2-neutral energy conversion process capable of providing distinct energy carriers [15,218]. This is important due to the imposed need to reduce CO_2 emissions from fossil fuels consumption [218], coupled to an increased necessity of biomass wastes valorization [436] and energy supply security. However, critical drawbacks associated to the use of biomass, such as its availability as energy resource and the impacts of energy crops [24,437], must also be taken in account. It has been argued that pressure on land will increase strongly under a growing biomass to energy demand, which can lead to adverse effects on biodiversity [437], and there exists resistance against the use of existing arable land to produce biomass instead of food, due to indications on endangerment of food security, especially in third world countries [438], as well as concerns regarding water scarcity [24]. Nonetheless, several studies propose that it is possible to sustainably increase biomass production if additional measures are provided, such as integrated policies for energy, land use and water management [17,24,439–441]. In fact, the European Union forest grew approximately 2% over the past decade [17]. Process efficiency and wastes valorization is also important in this context. For example, wood residues from industrial processes (e.g., small sawmills) can be efficiently used for power generation if integrated energy systems can be conceived [442], thus being an alternative to energy crops and respective land use needs. Another relevant drawback is related to the uncertainties regarding biomass stocks availability and prices and long-term national and European energy and climate policies. Unpredictable changes in energy policies or biomass availability can turn a current attractive biomass to energy conversion solution to a considerably expensive one in the future.

Furthermore, even though biomass gasification advantages are widely recognized and research on biomass gasification is not recent, being that industrial biomass gasifiers and commercial/demonstration plants have been developed in the past decades [69,72,91,174,427,443], it is acknowledged that some barriers must still be overcome in order to allow a commercial breakthrough of biomass gasification technologies. Gasification technologies for heat production are commercially available and deployed but their current application is scarce [444]. CHP gasification exists in the market, but its deployment is limited due to high costs and critical operational demands [444]. Gasification using integrated combined cycles, namely biomass integrated gasification/combined cycle for electricity production, has potential but is currently at a demonstration phase [444,445]. Several specific applications are also under demonstration/research phase, for example, integration in the PP industry [64,150,155], production of biofuels to offer small communities means to cover their energy demand for public transport by using local biomass feedstocks [432], production of electricity in agricultural intensive countries [431], production of oxymethylene ethers for blending with conventional diesel fuels [446–448], production of biomethane [449], solar-biomass power generation integrated with a gasifier [450], bio-oil gasification to act as bridge between bio-oil and transportation fuels [451], among several others [15,16,31,323,428,432,452]. Biomass gasification is a complex process in nature, with many reactants and many possible reaction paths, leading to difficult operation and variable gas composition. Thus, biomass gasification technologies are limited by diverse technological and operational aspects and are dependent on public and policy support [15,218,453]. Recognized drawbacks that need to be solved are related to difficulties regarding the control of the composition of the produced gas, heterogeneous composition and availability of biomass [70,429,454], environmental and safety questions [427,455], inorganics effect on the process performance, including agglomeration, fouling and corrosion problems [157], and, most importantly, the tars present in the produced gas [15,59,457,70,111,116,127,218,427,429,456] and the uncertainties regarding its cleaning and upgrading for downstream applications [58,70,218,427,429,458]. These issues, regardless of the current availability of vast literature on biomass gasification and the technological advances made [91], have not been overcome and are the reason behind the lack of commercial biomass gasification designs with economic competitiveness [58,59,218]. Thus, the application of this process at industrial scale is difficult [59,111], and, therefore, it is currently confined to specific applications and niche markets [218].

Tars present in the produced gas are recognized as the main technological barrier to the development and implementation of biomass gasification at industrial scale [15,16,59,111,112,116,127,429,456,457]. For sufficiently long reaction times, chemical equilibrium is reached and the products are mostly limited to light gases, however, gasifier temperatures and residence time are usually not enough to attain chemical equilibrium, and, therefore, the produced gas contains large amounts of tars [231]. In fluidized beds, which are a technology recognized as capable to offer a good performance in biomass gasification, average tar concentration is usually around 1-30g/Nm^3 [459]. Unfortunately, this concentration is too high for most raw gas applications [114,124,321] because tar condenses at relatively high temperatures [129]. Tar removal technologies can be broadly divided in primary measures (inside the gasification reactor) and secondary measures (downstream the gasification reactor) [124]. Several types of these measures have been developed and are under research in order to improve the raw gas quality through the decrease of the tar content [15,67,69,78,116,124,287,321,322]. Primary measures are interesting because they eliminate the need of downstream clean-up, however, they are not fully understood and still lack commercial implementation [124]. Primary measures consist mostly in changes in the operating parameters, such as the ER, changes in the reactor design and in the usage of bed additives/catalysts [124].

Catalysts can be used as primary measure, when for example mixed with the biomass feed prior to gasification [187] or used as bottom bed material [393], and as secondary measure when placed in a post gasification reactor [67,116]. When the PG passes over catalyst particles, tar can be reformed on the catalyst surface with either steam or carbon dioxide, thus producing additional hydrogen and monoxide carbon [286]. Even though primary measures for tar removal are considered more promising, research has been more focused on applying catalysts as secondary measure [15,69,78,116,124,287,321,322], due to the catalysts tendency to deactivate by carbon deposition, contamination (sulphur, chlorine, alkalis, etc.), microstructural changes, erosion related problems, etc., when inserted inside the gasification reactor [67]. In this regard, design and choice of catalysts for in-situ application in gasification processes must consider and seek these aspects: easy regeneration or absence of carbon deposition and sintering, cheap, capacity to decompose tar effectively and enhance the non-condensable gaseous products yields (particularly H_2, and respective H_2/CO molar ratio), and low pressure drop in the gasifier.

In this work, an alternative configuration for studying primary tars destruction measures using catalysts is proposed and analyzed. A small fixed bed reactor filled with catalyst materials was integrated on the high temperature region of the BFB freeboard, just above the bottom bed. The raw gas was characterized with/without passing the fixed bed of catalysts, thus allowing the evaluation of the performance of the catalyst on upgrading the gas quality. Three different low-cost catalysts were alternately tested, namely, bottom bed particles resulting from combustion of RFB derived from eucalyptus in an industrial BFB furnace (bottom bed ashes), char particles resulting from wood pellets direct (air) gasification in a pilot-scale BFB reactor, and synthetic fayalite (Fe_2SiO_4). Fe_2SiO_4 is the endmember of olivine minerals $(Fe,Mg)_2SiO_4$, and was selected as model catalyst for low cost catalysts based on natural minerals, with demonstrated catalytic activity in biomass gasification [460]. The low-cost catalysts performance was evaluated during direct (air) biomass gasification in a pilot-scale BFB gasifier, considering their influence in the produced gas composition (CO, CO_2, CH_4, C_2H_4, C_2H_6, C_3H_8, H_2 and N_2), LHV, Y_{gas}, CGE and CCE. The effect of the catalysts in the PG quality was evaluated throughout a relation between the concentration of combustible gases in the produced gas, such as H_2 and CO, and the catalysts applied as primary measures. In fact, it is assumed that the increase of the concentration of combustible light gases may result from tar destruction reactions promoted by the catalyst, as suggested in other works [124,393].

5.1.3 MATERIALS AND METHODS

The experimental infrastructure used in this work was the DAO-UA 80 kW_{th} pilot-scale BFB gasifier (Section 1.3.1). The methodologies used are described in Section 1.4.

5.1.3.1 FEEDSTOCK CHARACTERIZATION

The feedstocks used were commercial pine wood pellets (6 mm diameter and 15 mm to 20 mm in length) and RFB derived from pine (*pinus pinaster*). The RFB derived from pine required previous pretreatment, namely sieving and drying, to ensure more suitable feeding conditions and adequate thermochemical conversion. The pretreatment procedure of the RFB derived from pine was similar as described in Article IV (Section 4.1.3.1). Table 5.1 shows the proximate and ultimate analysis and heating value of both feedstocks.

Table 5.1 – Characteristics of the different types of biomass used as feedstock in the gasification experiments in the pilot-scale BFB (Article VIII).

	RFB Pine	Wood pellets
Proximate analysis (%wt, wb)		
Moisture	11.0	4.6
Volatile matter	71.1	78.5
Fixed carbon	16.8	16.6
Ash	1.1	0.3
Ultimate analysis (%wt, db)		
Ash	1.20	0.32
C	50.80	47.50
H	6.50	6.20
N	0.25	0.09
S	nd	nd
O (by difference)	41.25	45.89
LHV (MJ/kg) (db)	18.5	18.0

nd- not determined, below the detection limit of the method, 100 ppm wt.

5.1.3.2 LOW-COST CATALYSTS CHARACTERIZATION

The ash and char particles used in the fixed bed reactor were characterized and detailed in Table 5.2. The ash particles contain mainly silica, and minor amounts of oxides of other chemical elements such as K, Fe, Na, Ca, Mg, Mn. Thus, being representative of typical bottom bed ash particles from industrial BFB combustors, which are mainly composed of silica sand with a coating layer of several micrometers composed by chemical elements typical of the inorganic content of biomass, such as alkali and alkaline earth elements [461]. The char particles are mainly composed by carbon and minor amounts of hydrogen, nitrogen, sulfur and oxides of other chemical elements such as K, Ca and Mg. The ash particles physico-chemical characteristics were thoroughly analyzed previously [462]. Some additional information regarding the characterization of wood pellets char particles can be found in [289].

Table 5.2 – Characteristics of the different types of low-cost catalysts tested in gasification experiments in the pilot-scale BFB (Article VIII).

%wt, db	Bottom bed ashes	Wood pellets chars
C	-	88.000
H	-	0.350
N	-	0.370
S	-	0.024
Na_2O	0.387	0.045
K_2O	1.910	1.000
CaO	7.558	0.541
MgO	1.529	0.247
P_2O_5	0.474	0.065
Al_2O_3	2.249	0.054
Fe_2O_3	0.744	0.046
MnO	0.131	0.025
SiO_2	82.893	nd

nd - not determined.

The Fe_2SiO_4 catalyst was synthesized by reactive firing of silicon carbide (SiC) and hematite (Fe_2O_3) powder mixtures under CO_2 gas flow; this provided the required additional supply of oxygen and yielded suitable redox conditions imposed by $CO:CO_2$ equilibrium in the resulting atmosphere as follows:

$$SiC + Fe_2O_3 + 2\,CO_2 \rightarrow Fe_2SiO_4 + 3\,CO \qquad \text{Reaction 5.1}$$

Guidelines for firing conditions were obtained by thermodynamic predictions of redox stability (Figure 5.1). These redox stability diagrams were calculated using methods proposed earlier [463,464], and were superimposed with the redox conditions of $CO:CO_2$ equilibrium in the gas phase. In addition, thermogravimetric studies under controlled thermal cycles, and with CO_2-based atmospheres allowed to establish suitable conditions to obtain single phase Fe_2SiO_4 by heating at 2ºC/min up to 980 ºC, and then at 10 ºC/min up to 1100 ºC, with CO_2 flow. X-ray diffraction was used to monitor reactivity and to optimize the conditions to obtain single phase Fe_2SiO_4 catalysts. SEM was used to inspect relevant microstructural features (Figure 5.2). This shows that Fe_2SiO_4 catalysts can be processed as highly porous samples, with typical particle sizes in the micrometer range, provided that the precursor powders are also within or below this range. On combining the observed size range ($d \approx 1$ μm) and theoretical density ($\rho_{th} \approx 4.39\ g/cm^3$), it is expected typical values of specific surface area in the order of $3/(\rho_{th} d) \approx 0.7 cm^2/g$. In addition, the SEM microstructures also show that individual grains are connected by strong necks, which confers sufficient mechanical strength for catalytic testing in relatively high flow conditions such as fluidized beds. A more detailed description of the Fe_2SiO_4 characteristics and the relevant methods used for its synthesis was reported in [465].

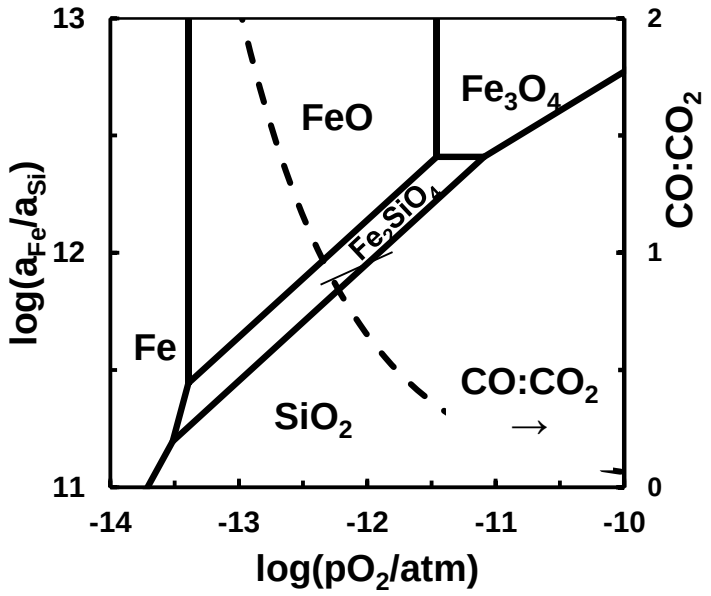

Figure 5.1 – Thermodynamic predictions of redox phase stability conditions for the Fe-Si-O system at 1373 K superimposed on $CO:CO_2$ equilibrium in the gas phase.

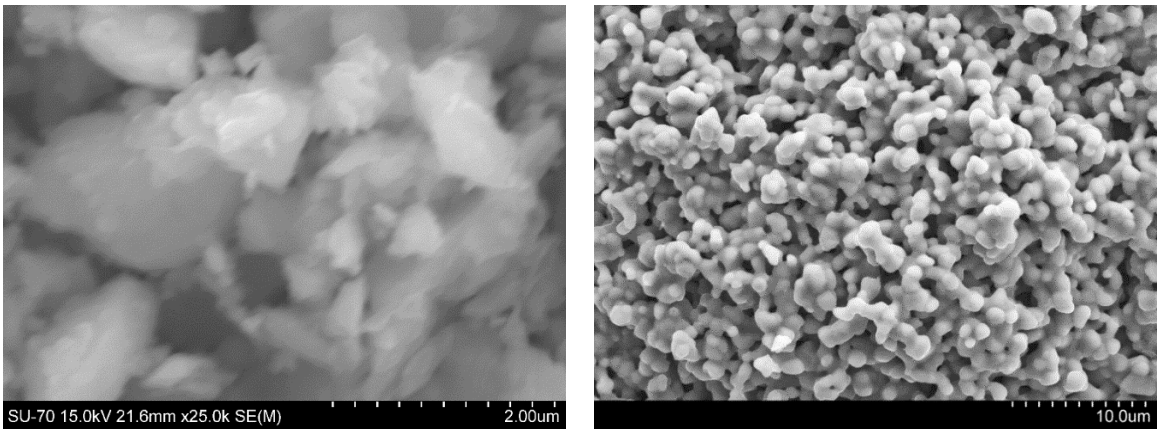

a) SiC b) Fe_2SiO_4

Figure 5.2 – SEM of SiC precursor powders (a) and one representative single phase Fe_2SiO_4 (b) sample prepared by solid state reaction of stoichiometric $SiC+Fe_2O_3$ powder mixtures, in CO_2 atmosphere, with optimized firing cycle.

5.1.3.1 OPERATING CONDITIONS

The conditions of the performed experiments in this work are visible in Table 5.3 and Table 5.4. The fluidized bed was operated at atmospheric pressure and in bubbling regime, with superficial gas velocity of around 0.28 to 0.30 m/s (depending on the operating conditions, namely the bed temperature). Pressure drop across the bed was 0.20m of water column. The ER was between 0.19 and 0.30 and the bed temperature between 780 and 880 ºC.

Table 5.3 – Pilot-scale BFB gasification experiments reference and respective operating conditions (Article VIII).

Experiment reference	Fuel	ER	Average bed temperature (ºC)	Biomass feed rate (kg/h)	Air feed rate (NL/ min)
GE-WP-1	Wood pellets	0.24	793	11.9	200
GE-WP-2	Wood pellets	0.21	828	13.4	200
GE-CP-1	RFB Pine	0.29	824	9.5	200
GE-CP-2	RFB Pine	0.24	786	11.5	200
GE-CP-3	RFB Pine	0.19	798	14.7	200
GB-WP-Ash-1	Wood pellets	0.22	814	13.1	200
GB-WP-Ash-2	Wood pellets	0.25	854	11.4	200
GB-WP-Fe:Olivine-1	Wood pellets	0.24	824	11.9	200
GB-WP-Fe:Olivine-2	Wood pellets	0.21	882	13.7	200
GB-CP-Char-1	RFB Pine	0.30	812	9.0	200
GBC-WP-Ash-1	Wood pellets	0.22	814	13.1	200
GBC-WP-Ash-2	Wood pellets	0.25	854	11.4	200
GBC-WP-Fe:Olivine-1	Wood pellets	0.24	849	11.9	200
GBC-WP-Fe:Olivine-2	Wood pellets	0.24	830	11.9	200
GBC-CP-Char-1	RFB Pine	0.27	836	10.2	200
GBC-CP-Char-2	RFB Pine	0.29	799	9.5	200

WP – Wood pellets; CP – Chipped pine; GE – Gas sampled at the reactor exhaust; GB – Gas sampled above the surface of the reactor bed; GBC – Gas sampled above the surface of the bed that passed through a fixed bed of catalysts.

Table 5.4 – Parameters of the experiments performed for testing the catalysts in direct (air) gasification regime in the pilot-scale BFB (Article VIII).

	Experiment reference	Catalyst	Mass of catalyst [g]	Granulometry [mm]
GBC	GBC-WP-Ash-1	Bottom bed ashes	200	1-1.4
	GBC-WP-Ash-2	Bottom bed ashes	200	1-1.4
	GBC-WP-Fe:Olivine-1	Synthetized Fe_2SiO_4	26	<1
	GBC-WP-Fe:Olivine-2	Synthetized Fe_2SiO_4	26	<1
	GBC-CP-Char-1	Wood pellets chars	40	>1
	GBC-CP-Char-2	Wood pellets chars	40	>1

5.1.4 RESULTS AND DISCUSSION

The results presented in this Section include the process operating conditions, such as the biomass feed rate, ER and reactor temperature, and the composition of the produced gas in terms of CO_2, CO, CH_4, C_2H_4, C_2H_6, C_3H_8, N_2 and H_2. The LHV of the dry gas and the efficiency parameters Y_{gas}, CGE and CCE were determined and discussed to evaluate the quality of the PG and the efficiency of the gasification experiments.

The composition of the PG and respective performance parameters of the gasification process were determined considering two perspectives: (i) the overall performance of the gasifier and (ii) the effects of the low-cost catalysts. For the evaluation of the overall performance of the gasifier, the produced gas was sampled at the exhaust of the BFB reactor; these experiments were named GE throughout this work. For the evaluation of the performance of the low-cost catalysts in improving the produced gas quality, the produced gas was sampled before and after passing the fixed bed of

catalysts located above the bottom bed of the BFB; the experiments in which the produced gas was sampled above the surface of the bottom bed and before passing the fixed bed of catalyst were named GB, while the experiments in which the produced gas was sampled after passing the fixed bed of catalysts were named GBC. Therefore, in the experiments reference (Table 5.3) it is included the acronyms GE, GB and GBC according to the position where the gas was sampled.

5.1.4.1 STEADY-STATE OPERATION OF THE GASIFIER

The infrastructure was considered as operating under steady-state conditions when the temperature of the fluidized bed pilot reactor and the composition of the produced gas were stable and only exhibited minor fluctuations along time; thereafter the gas was sampled for conditioning and composition analysis (CO, CO_2, CH_4, C_2H_4, C_2H_6, C_3H_8, H_2 and N_2) on the exhaust (GE experiments) or above the surface bed without (GB experiments) and with (GBC experiments) passing the fixed bed of catalyst particles.

The temperature profiles along time for different locations of the reactor, during the different gasification experiments performed, were similar and stable, as shown in the examples presented in Figure 5.3. However, the temperature showed a slightly steadier behavior during gasification experiments with wood pellets, particularly in the lower section of the freeboard, i.e. immediately above the fuel feeding location. This can reflect a more consistent feeding of the pellets when compared to the RFB chips. Stable autothermal conditions (with bed temperatures above 780 ºC) were achieved even at low ERs (as low as 0.19) (Table 5.3, Figure 5.3). Thus, the use of external heat sources was not found necessary, as often seen in other works regarding direct (air) gasification processes [184,314,329–331].

Regarding the vertical temperature profiles along the reactor, similar values were found for different gasification experiments (Figure 5.4). Furthermore, a typical trend for the continuous decrease of the temperature from the bottom bed and its surface towards the exit of the reactor was observed. This behavior was observed and described in other works performed here (see previous Sections). Nonetheless, some localized deviating behaviors were observed, namely a slight local temperature increase (by 15 ºC to 36 ºC) in some experiments (GE-WP-1, GE-WP-2, GE-CP-3, GB-WP-Fe:Olivine-1, GB-WP-Fe:Olivine-2), observed from 0.8 meters to 1.2 meters height. The reasoning for that behavior cannot at present be advanced based on the experimental data available; this issue must be object of further characterization in future experimental work.

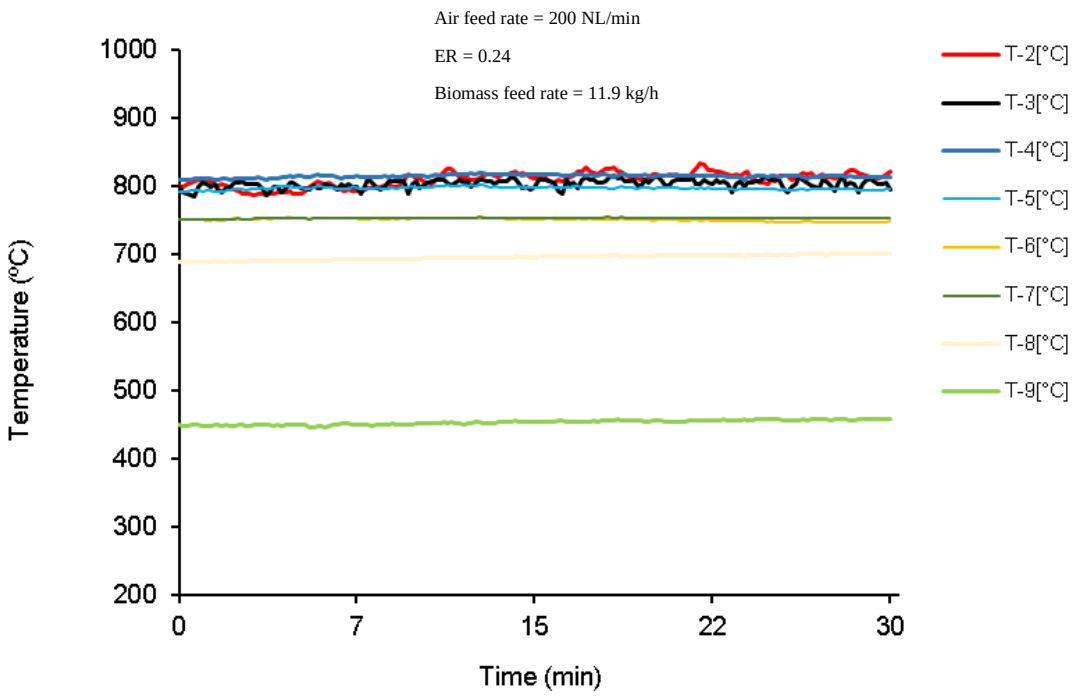

(a)

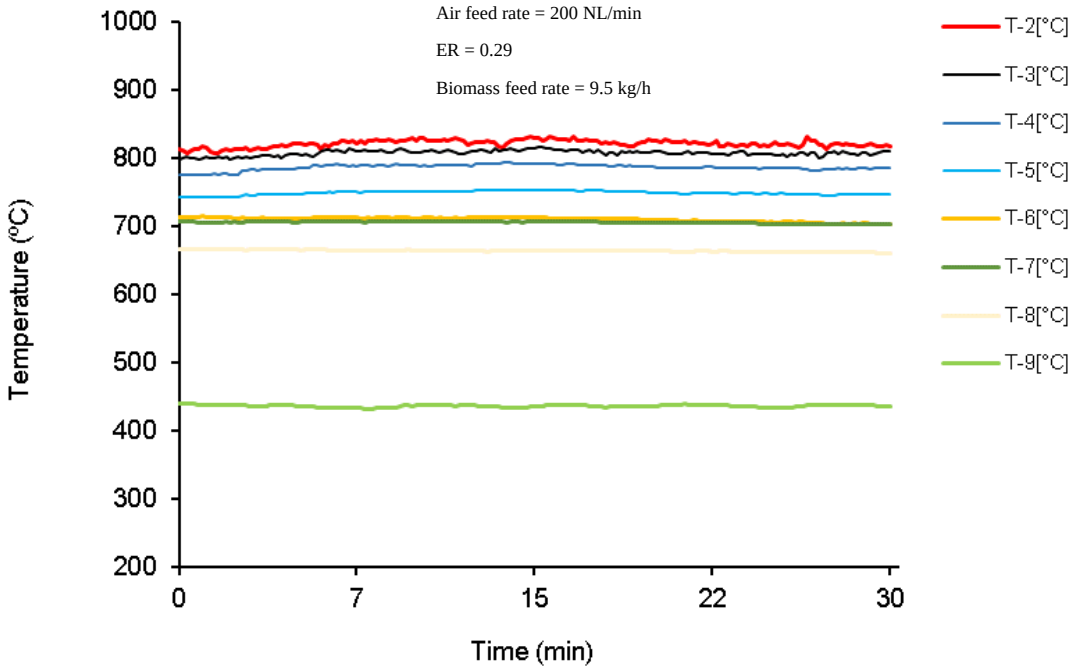

(b)

Figure 5.3 – Typical evolution of the temperature along time at different locations along the reactor height during the gasification of: (a) wood pellets and (b) RFB from pine.

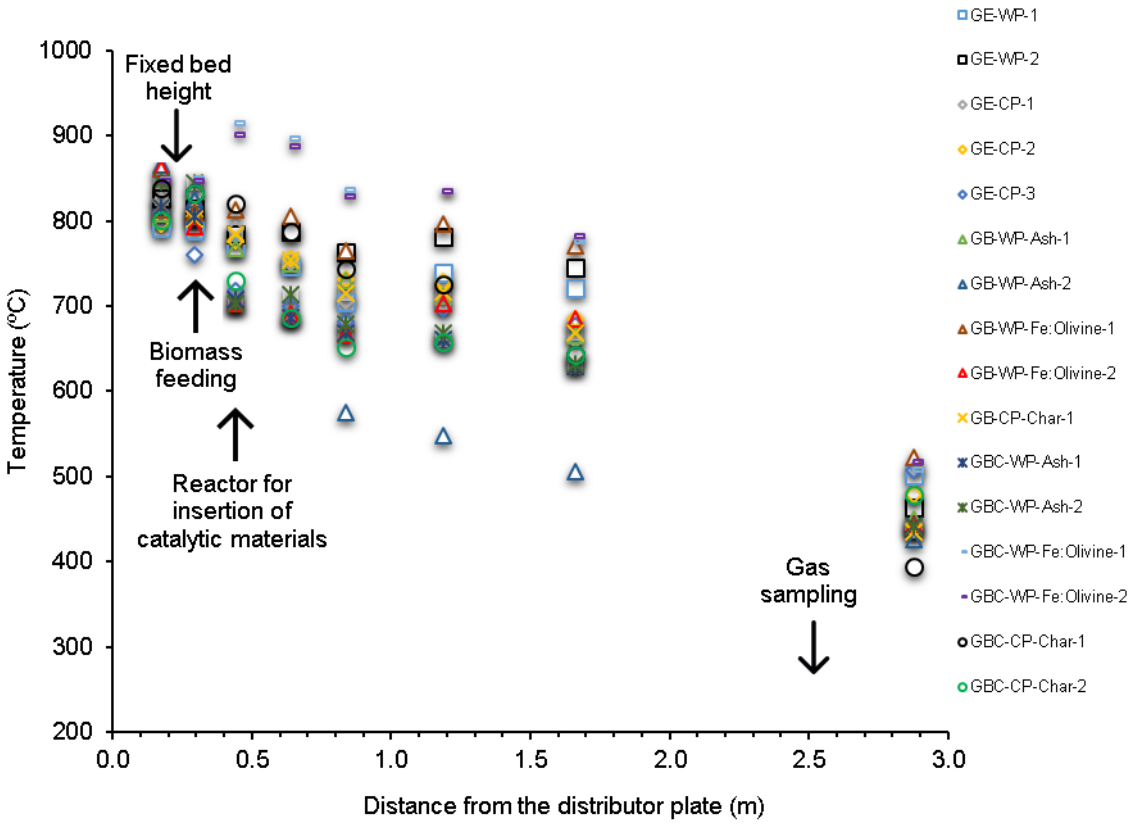

Figure 5.4 – Average vertical temperature profile in the BFB reactor for the biomass gasification experiments performed. Legend according to experiments references in Table 5.3.

Coherent with the steady temperature profiles discussed previously (Figure 5.3), the exhaust gas composition (CO, CO_2, CH_4 and C_2H_4) along time showed steady state conditions and exhibited only minor fluctuations (see examples in Figure 5.5), allowing to conclude that the BFB reactor operated at steady-state conditions. These steady-state operating conditions allow the conclusion that the developed pilot-scale BFB reactor is suitable to perform the thermochemical conversion of biomass by direct (air) gasification and validate the study of the application of the aforementioned low-cost catalysts as primary tar destruction measures in this pilot-scale gasifier. Nonetheless, some minor fluctuations along time were observed, which can be justified by feed rate irregularities caused by the biomass feedstock heterogenous physical characteristics. These are particularly relevant during the gasification experiments performed with RFB from pine.

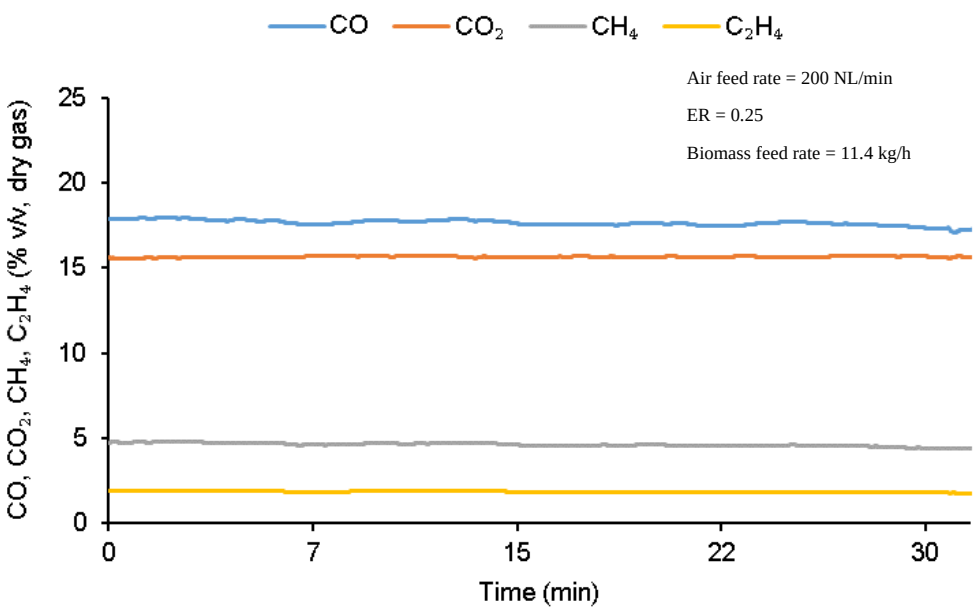

(a)

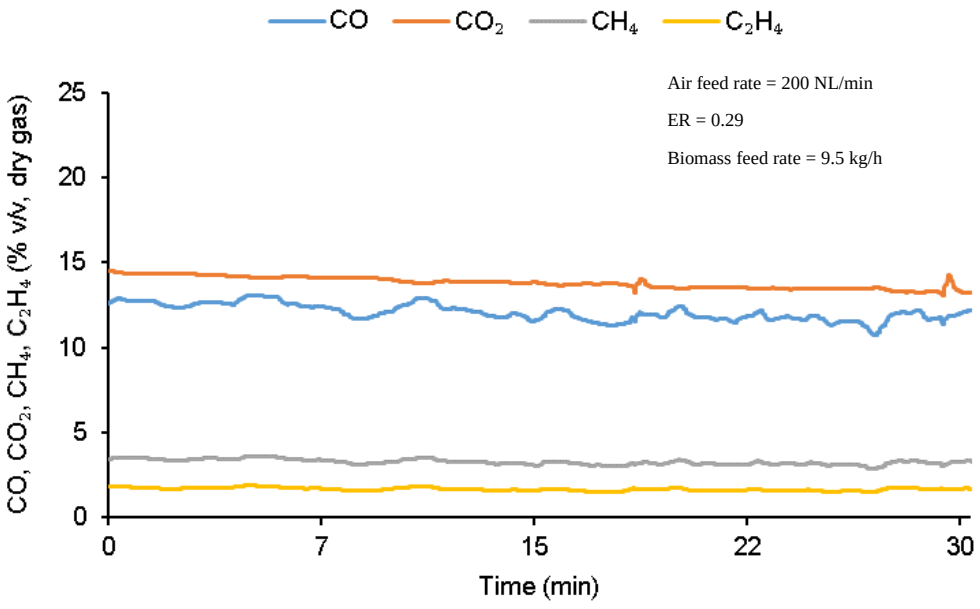

(b)

Figure 5.5 – Typical composition (CO_2, CO, CH_4, C_2H_4) along time of the dry gas produced at the exhaust (GE) during the gasification of: (a) wood pellets and (b) RFB from pine.

5.1.4.2 CHARACTERISTICS OF THE PG AT THE EXHAUST OF THE BFB GASIFIER

The composition of the produced gas sampled at the exhaust of the BFB gasifier, hereafter referred as gas composition GE, showed that the most abundant gaseous components present in the produced gas were CO and CO_2, followed by H_2, CH_4, C_2H_4, C_2H_6 and C_3H_8 by decreasing order of abundance (Excluding N_2, Figure 5.6). The CO_2 concentration in gas composition GE varied between 13.9 and 17.0 %v and the CO concentration between 14.8 and 21.5 %v, depending mostly on the ER and biomass type, which yields changes in the ratio of reduced to oxidized species ($CO:CO_2$). These variables also yield changes in the light hydrocarbon and hydrogen contents, thus the fuel gas produced presented CH_4 concentration between 4.0 and 5.5 %v, C_2H_4 concentration between 1.4 and 2.6 %v, C_2H_6 concentration ≤ 0.27 %v, C_3H_8 concentration ≤ 0.11 %v and H_2 concentration between 6.1 and 9.9%v. Highest H_2 concentration was observed during the gasification of wood pellets with an ER of 0.21 (experiment reference GE-WP-2 in Table 5.3 and Figure 5.6), while the highest concentration of CO was observed during the gasification of RFB from pine with an ER of 0.19 (experiment reference GE-CP-3 in Table 5.3 and Figure 5.6). These results are in the range of the values typically reported in the literature regarding direct (air) gasification in BFBs (see Section 4.1.1). In general, the concentration of combustible gases, such as CO and H_2, increased with the decrease of ER in the range used (0.19 to 0.30). This can be explained due to an increase in the O/C ratio in the reaction environment with the increase of the ER, thus favoring oxidation reactions that consume combustible gases.

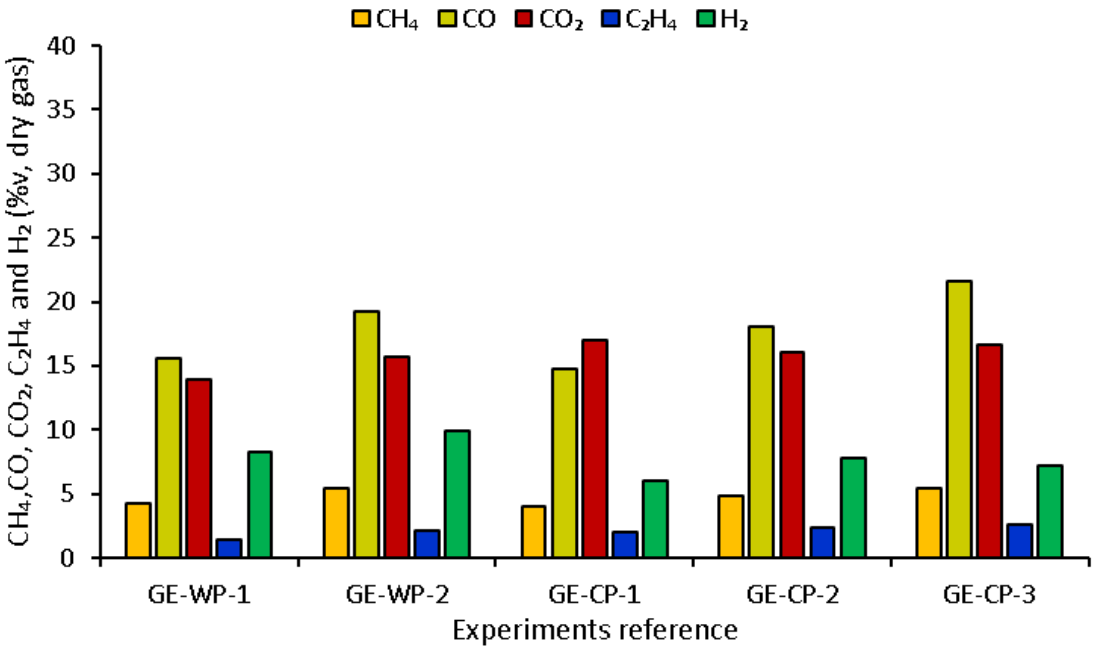

Figure 5.6 – Composition (CH_4, CO, CO_2, C_2H_4 and H_2) of the dry gas sampled at the exhaust (GE). Experiments reference according to Table 5.3.

Regarding the two fuels studied in this work, the most significant difference observed was related to the concentration of H_2 in the produced gas. During wood pellets gasification, the H_2 concentration varied between 8.2 and 9.9 %v, while during the gasification of RFB from pine the concentration of H_2 was found in the range 6.1 to 7.2 %v. This phenomenon was previously observed and described in a work performed in this infrastructure (see Section 4.1.1).

The LHV corresponding to gas composition GE was in range 5.1 to 6.9 MJ/Nm^3 (Figure 5.7). The highest LHV value was found during the gasification of RFB from pine with ER 0.19 and bed

temperature equal to 798 ºC (GE-CP-3, Table 5.3 and Figure 5.7), and the lowest during the gasification of RFB from pine with ER 0.29 and bed temperature equal to 824 ºC (GE-CP-1, Table 5.3 and Figure 5.7). It was observed that the LHV of the dry gas decreased with the increase of ER, and this is justified by the decrease of the concentration of the combustible gases with the increase of ER, previously discussed. The values of LHV determined during these gasification experiments are in the upper range of LHV values typically reported in literature for direct (air) biomass gasification in BFB reactors (see Section 4.1.1).

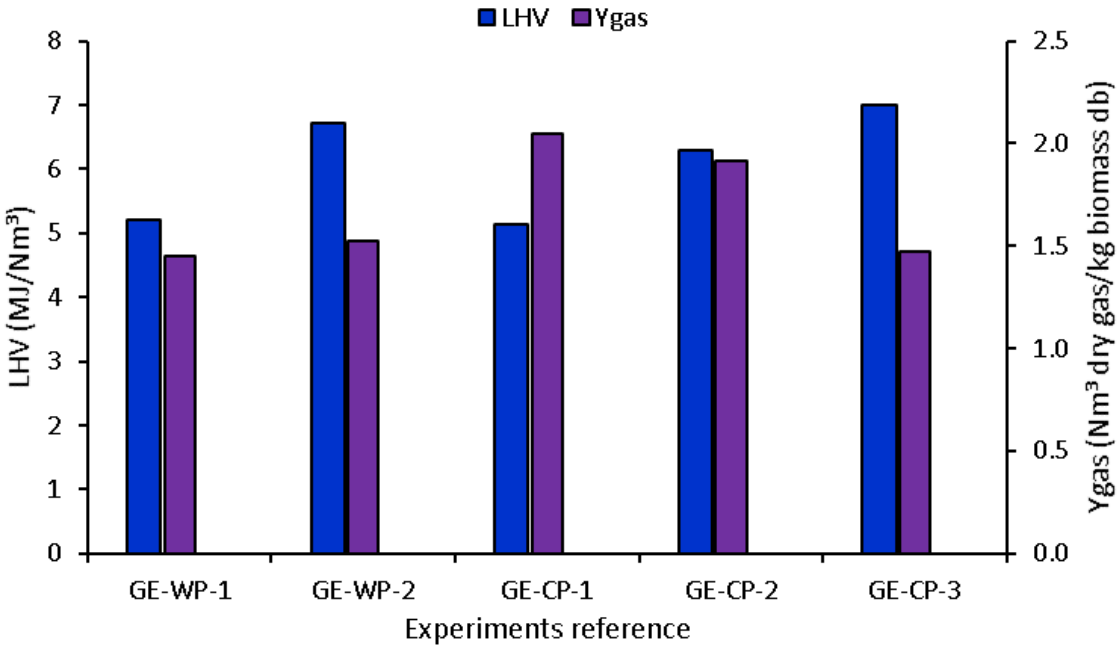

Figure 5.7 – LHV and Y_{gas} of the dry gas sampled at the exhaust (GE). Experiments reference according to Table 5.3.

The Y_{gas} values for GE experiments were between 1.5 and 2.0 Nm^3 gas/kg biomass dry basis (db) (Figure 5.7); the highest value was obtained in the gasification of RFB from pine with 0.29 ER (GE-CP-1) and the lowest in the gasification of wood pellets with 0.24 ER (GE-WP-1). The results obtained for Y_{gas} during the gasification experiments performed in this work are slightly lower than the range of values typically reported in the literature (see Section 4.1.1); it was also found that the Y_{gas} values determined here are typically lower in experiments with lower ER. Similar trends have been reported in the literature (see Section 4.1.1).

Regarding CGE, values between 42.4 and 61.0% were determined for GE experiments as shown in Figure 5.8. The highest CGE value was determined for the gasification of RFB from pine with an ER of 0.24 (GE-CP-2) and the lowest for the gasification of wood pellets with an ER of 0.24 (GE-WP-1). These CGE values are in accordance with the range of values generally reported in the literature for direct (air) biomass gasification in BFB reactors (see Section 4.1.1).

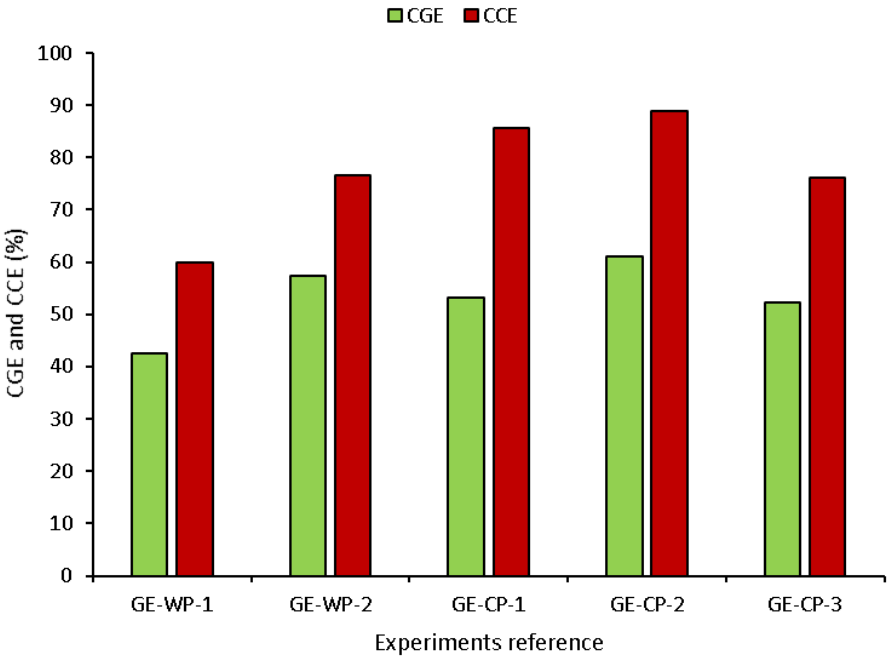

Figure 5.8 – CGE and CCE for experiments regarding the dry gas sampled at the exhaust (GE). Experiments reference according to Table 5.3.

The effect of the ER on the CGE is not obvious, because while low ERs seem to favor a higher concentration of combustible gases, such as H_2 and CO, and, consequently, higher CGE, decreasing the ER originates lower Y_{gas} values, thus contributing to lower CGE. This trade-off must be accounted for and properly defined in order to establish the appropriate operation regime of the gasifier. Nonetheless, based on this work results and previous results obtained in this experimental infrastructure (see previous Sections), for direct (air) gasification of biomass in fluidized bubbling bed, it is expected a maximum value of CGE for an ER close to 0.25.

Regarding CCE, values between 59.8 and 88.8 % were determined for GE experiments as shown in Figure 5.8. The maximum value was obtained for the gasification of RFB from pine with an ER of 0.24 (GE-CP-2) and the minimum for the gasification of wood pellets with an ER of 0.24 (GE-WP-1). These CCE values are in accordance with the typical range of values reported in the literature for direct (air) biomass gasification in BFB reactors (see Section 4.1.1).

5.1.4.3 INFLUENCE OF THE TESTED CATALYSTS ON THE PG COMPOSITION

The influence of the catalyst materials on the gas characteristics and consequently on the process efficiency parameters was evaluated based upon a comparison between the composition of the gas sampled above the surface of the bottom bed (GB experiments) and the gas sampled at the same location but passing through the fixed bed of catalytic materials (GBC experiments).

The composition of the sampled gas at the bed surface (Figure 5.9), hereafter referred as gas composition GB, for experiments with wood pellets (GB-WP-Ash-1, GB-WP-Ash-2, GB-WP-Fe:Olivine-1 and GB-WP-Fe:Olivine-2) and with RFB from pine (GB-CP-Char-1), was the following: CO between 7.7 and 16.9 %v, H_2 between 3.2 and 8.3 %v, CH_4 between 0.5 and 3.4 %v, CO_2 between 9.5 and 14.6 %v, C_2H_4 between 0.2 and 1.2 %v, $C_2H_6 \leq 0.1$ %v and $C_3H_8 \leq 0.03$ %v (Figure 5.9).

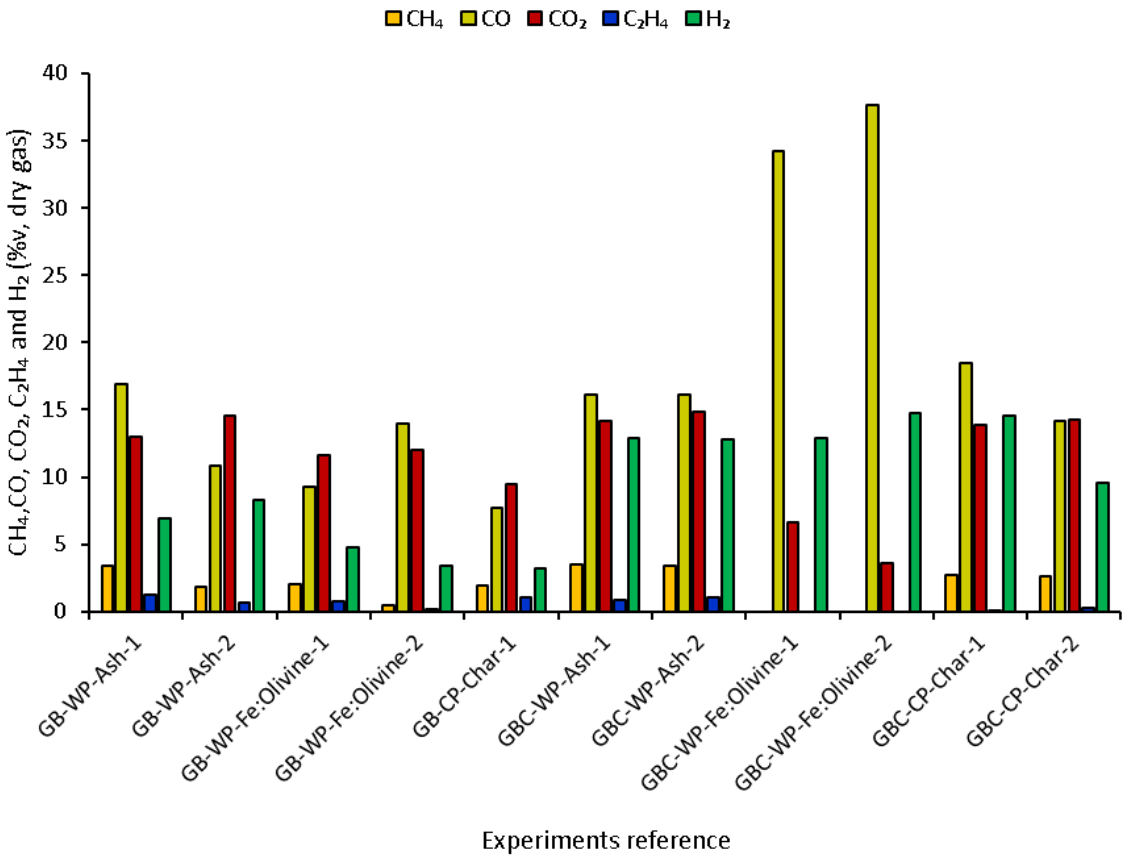

Figure 5.9 – Composition (CH_4, CO, CO_2, C_2H_4 and H_2) of the dry gas sampled above the surface of the bed (GB) and above the surface of the bed passing through a fixed bed of catalytic materials (GBC). Experiments reference according to Table 5.3.

For similar ER, namely 0.21 to 0.29, it was observed that gas composition GB presented distinct values, namely lower in terms of H_2 and CO concentration, in comparison with gas composition GE (experiments GE-WP-1, GE-WP-2, GE-CP-1, GE-CP-2 and GE-CP-3 (see Section 5.1.4.2).This can be related to the fact that gas composition GB is mainly composed by a mixture of gases coming from inside the bed and from biomass pyrolysis occurring at that location (feeding location), and thus resulted from a lower conversion of the solid feedstock and pyrolysis products into chemical species such as H_2 and CO. The higher concentration of H_2 and CO in the gas composition GE reflects the importance of the gas residence time and subsequent gas conversion along the freeboard of the BFB gasifier, and thus the impact of the system being even further away from attaining chemical equilibrium.

The gas composition after passing the catalyst, hereafter referred as gas composition GBC (in experiments GBC-WP-Ash-1, GBC-WP-Ash-2, GBC-WP-Fe:Olivine-1, GBC-WP-Fe:Olivine-2, GBC-CP-Char-1 and GBC-CP-Char-2), shows an increase in concentration of H_2 and CO concentration (Figure 5.9), therefore indicating that the different low-cost catalysts tested possibly provide an alternative pathway with lower activation energy for conversion of heavier hydrocarbons and, possibly, tar destruction reactions. Accordingly, heavier hydrocarbons such as C_2H_6 and C_3H_8 were only detected in the gas composition GB, i.e., before passing the bed of catalysts.

The volumetric gas composition GBC was the following:

- For experiments performed with bottom bed ashes (GBC-WP-Ash-1 and GBC-WP-Ash-2): 16.1 to 16.2 % CO, 12.8 to 12.9 % H_2, 3.4 to 3.5 % CH_4, 14.1 to 14.8 % CO_2 and 0.8 to 1.1 % C_2H_4.
- For experiments performed with synthetic Fe_2SiO_4 (GBC-WP-Fe:Olivine-1 and GBC-WP-Fe:Olivine-2): 34.2 to 37.6 % CO, 12.9 to 14.7 % H_2, 3.6 to 6.6% CO_2. CH_4, C_2H_4, C_2H_6 or C_3H_8 were not detected when synthetic Fe-Olivine was used as catalyst.
- For experiments performed using wood pellets chars: 14.2 to 18.5 % CO, 9.5 to 14.5 % H_2, 2.6 to 2.7 % CH_4, 13.9 to 14.3 % CO_2 and $C_2H_4 \leq 0.3$ %.

The comparison of these gases concentration values with those regarding gas composition GB, show that Fe-Olivine caused the highest increase of CO (305 %, GBC-WP-Fe:Olivine-2 compared to GB-WP-Fe:Olivine-1), wood pellets chars the highest increase of H_2 (352 %, GBC-CP-Char-1 compared to GB-CP-Char-1) and bottom bed ashes the highest increase of CH_4 (85 %, GBC-WP-Ash-2 compared to GB-WP-Ash-2), as shown in Figure 5.10. Despite the highest concentration of H_2 being found with the application of Fe_2SiO_4 (14.7 %v), the application of this material caused a lower H_2 concentration increase (209 % maximum increase) than the increase observed with the application of wood pellets chars (352 % maximum increase). Thus, it is noticed that the wood pellets chars had a more relevant positive effect on the H_2 concentration than the synthetic Fe_2SiO_4. This may be related to the alkaline and alkaline earth metals content present in the chars, such as Ca and K (Table 5.2), which seem to act as catalysts during gasification processes (see Section 4.4). However, the bottom bed ashes also contain a high alkaline metal content (Table 5.2) and only allowed a maximum increase of 85 % of the H_2 concentration value. These aspects and the fundamentals behind them need to be further clarified and studied in future work.

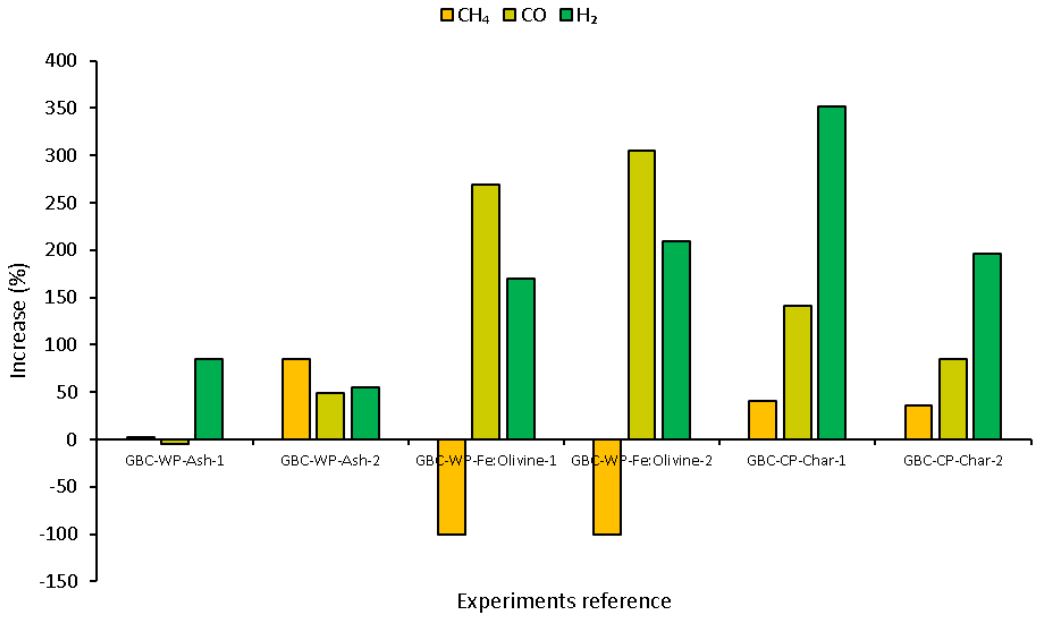

Figure 5.10 – Influence of the different catalytic materials tested in this work on the composition (CH_4, CO and H_2) of the PG sampled above the surface of the fluidized bed. Experiments reference according to Table 5.3.

It is thought that some loss of catalytic activity (deactivation) occurred during experiments performed with wood pellets chars, specifically on GBC-CP-Char-2, which was carried approximately 8 hours after the start-up of the gasification experiment. In fact, both CO and H_2 concentration were lower in

the PG from GBC-CP-Char-2 than in the PG from GBC-CP-Char-1 (approximately 5%v lower). Note that GBC-CP-Char-1 was conducted approximately 6 hours before GBC-CP-Char-2, i.e. immediately after steady-state operating conditions in the gasifier were achieved. This phenomenon must be further investigated in future works.

Based on the gas composition GB and GBC during these experiments, the following values of LHV, Y_{gas}, CGE and CCE (see Figure 5.11 and Figure 5.12) were determined:

- Experiments GB:
  - LHV = 2.4 to 4.3 MJ/Nm^3.
  - Y_{gas} = 1.0 to 1.8 Nm^3 dry gas/kg biomass db.
  - CGE = 13.7 to 30.5 %.
  - CCE = 30.7 to 50.9 %.
- Experiments GBC-Ash:
  - LHV = 5.1 to 5.3 MJ/Nm^3.
  - Y_{gas} = 1.4 to 1.7 Nm^3 dry gas/kg biomass db.
  - CGE = 40.2 to 48.6 %.
  - CCE = 56.8 to 68.3 %.
- Experiments GBC-Fe:Olivine:
  - LHV = 5.7 to 6.3 MJ/Nm^3.
  - Y_{gas} = 1.8 to 1.9 Nm^3 dry gas/kg biomass db.
  - CGE = 56.9 to 66.3 %.
  - CCE = 81.8 to 86.6 %.
- Experiments GBC-Char:
  - LHV = 3.9 to 4.9 MJ/Nm^3.
  - Y_{gas} = 1.9 to 2.0 Nm^3 dry gas/kg biomass db.
  - CGE = 38.1 to 50.3 %.
  - CCE = 64.4 to 75.4 %.

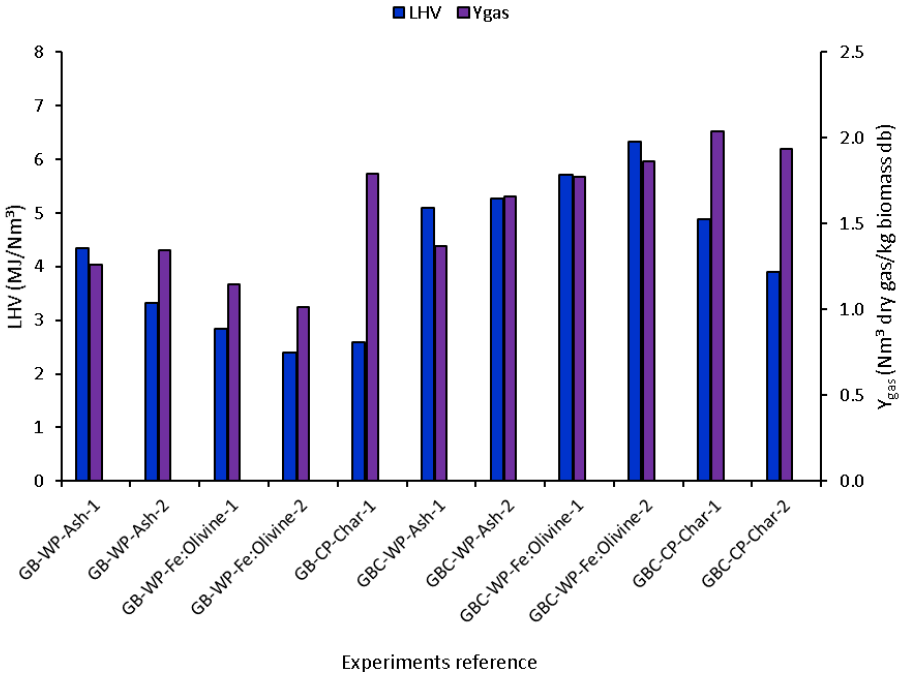

Figure 5.11 – LHV and Y_{gas} for the experiments regarding the PG sampled above the surface of the bed (GB) and above the surface of the bed after passing through a fixed bed of catalytic materials (GBC). Experiments reference according to Table 5.3.

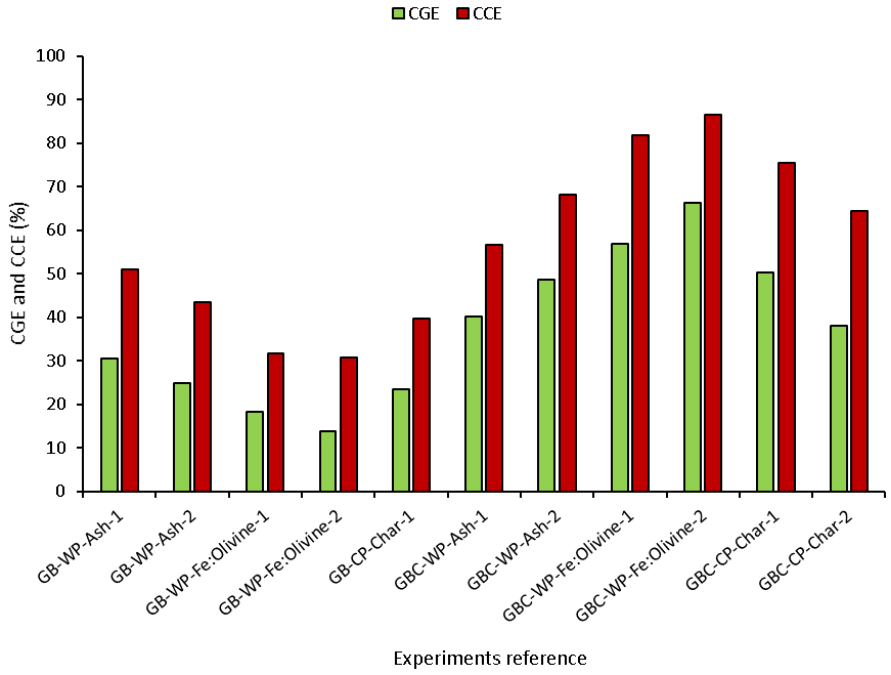

Figure 5.12 – CGE and CCE for the experiments regarding the PG sampled above the surface of the bed (GB) and above the surface of the bed after passing through a fixed bed of catalytic materials (GBC). Experiments reference according to Table 5.3.

The highest percentage increase in terms of comparison between the efficiency parameters determined based on the gas composition GB and gas composition GBC was obtained with the use of synthetic Fe-Olivine, specifically 123 % increase in LHV, 62 % increase in Y_{gas}, 262 % increase in CGE and 174 % increase in CCE (GBC-WP-Fe:Olivine-2 compared to GB-WP-Fe:Olivine-1, Figure 5.13). Therefore, based on these results, it can be concluded that the synthetized Fe-Olivine performed better than the bottom bed ashes or wood pellets chars tested in this work, in the improvement of the produced gas quality obtained from direct (air) biomass gasification in BFBs. Nonetheless, further studies must be performed to fully ascertain the influence of these low-cost catalysts on the produced gas quality and gasification efficiency parameters.

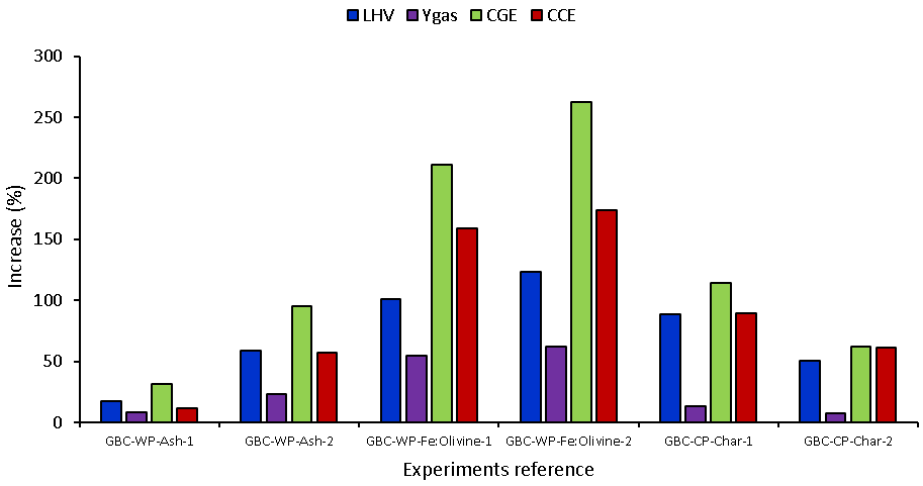

Figure 5.13 – Influence of the different catalytic materials tested on this work on LHV, Ygas, CGE and CCE. Experiments reference according to Table 5.3.

5.1.5 CONCLUSIONS

In this research, new results regarding the demonstration of direct (air) biomass gasification in a BFB pilot-scale reactor and the application of a new reactor configuration for in-situ low-cost catalytic materials for improvement of the PG quality were presented and analyzed. The research focused on the evaluation of the overall performance of the gasifier and of the low-cost catalytic materials adequacy for improving the PG quality in direct (air) gasification in BFB reactors. The pilot-scale gasification reactor was successfully operated under autothermal regime and for the operating conditions used, namely ER between 0.19 and 0.30 and average bed temperature between 780 and 880ºC, steady-state operating conditions suitable for studying the proposed research were attained.

For the evaluation of the overall performance of the gasifier, experiments were performed in which the PG was sampled at the exhaust of the BFB reactor. The dry gas sampled at this location presented the following volumetric composition: 14.8 to 21.5 %v CO, 6.1 to 9.9 %v H_2, 4.0 to 5.5 %v CH_4, 13.9 to 17.0 %v CO_2, 1.4 to 2.6 %v C_2H_4, ≤ 0.27 %v C_2H_6 and ≤ 0.11 %v C_3H_8 and LHV between 5.1 and 6.9 MJ/Nm^3. The highest concentration of CO was observed during the gasification of RFB from pine with an ER of 0.19 while the highest concentration of H_2 was observed during the gasification of wood pellets with an ER of 0.21. For these experiments, the Y_{gas} was found between 1.5 and 2.0 Nm^3 gas/kg biomass (dry basis), the CGE between 42.4 and 61.0 % and the CCE between 59.8 and 88.8 %. Most of these values are in the medium/upper range of the values typically referred in the literature for direct (air) biomass gasification in BFBs. Thus, this work attests the suitability of the direct (air) biomass gasification process in BFBs to produce low heating value combustible gas.

The evaluation of the low-cost catalysts performance for improving the produced gas quality was performed by sampling the gas before and after passing a fixed bed of catalysts located above the bottom bed of the pilot-scale BFB. The dry gas sampled at the bottom bed surface and before passing the fixed of catalysts presented the following volumetric composition: 7.7 to 16.9%v CO, 3.2 to 8.3 %v H_2, 0.5 to 3.4 %v CH_4, 9.5 to 14.6 %v CO_2, 0.2 to 1.2 %v C_2H_4, C_2H_6 ≤ 0.1 %v and C_3H_8 ≤ 0.03 %v and LHV between 2.4 and 4.3 MJ/Nm^3. For these experiments, the Y_{gas} was found between 1.0 to 1.8 Nm^3 dry gas/kg biomass (dry basis), the CGE between 13.7 and 30.5 % and the CCE between 30.7 and 50.9 %. This gas showed a distinct composition than the dry gas sampled at the exhaust of the reactor, namely lower in terms of H_2 and CO concentration. The higher concentration of H_2 and CO in the gas sampled at the exit of the gasifier is justified by the gas higher residence time and thus the system being closer to attaining chemical equilibrium, thus reflecting the importance of the gas residence time and gas conversion along the freeboard of the BFB gasifier. The dry gas sampled after passing the fixed bed of catalysts presented the following volumetric composition: 14.2 to 37.6 %v CO, 9.5 to 14.7 %v H_2, ≤ 3.5 %v CH_4, 3.6 to 14.8 %v CO_2, ≤ 1.1 %v C_2H_4 and 3.9 to 6.3 MJ/Nm^3 LHV. No C_2H_6 or C_3H_8 were detected in this gas. For these experiments, the Y_{gas} was found between 1.4 and 2.0 Nm^3 dry gas/kg biomass (dry basis), the CGE between 38.1 and 66.3 % and the CCE between 58.6 and 86.6 %.

The highest percentage increase in the concentration of CO, H_2 and CH_4 in the produced gas after passing the fixed bed of catalysts was observed with Fe_2SiO_4 for CO (305 % increase), with wood pellets chars for H_2 (352 % increase) and with bottom bed ashes for CH_4 (85 % increase). The highest increases observed in the process performance parameters were observed with the use of the synthetized Fe_2SiO_4 as catalyst, namely 123 % increase in LHV, 62 % increase in Y_{gas}, 262 % increase in CGE and 174 % increase in CCE.

Based on these results, it can be concluded that the introduction of low-catalysts for in-situ appliance improvement of the PG quality was successful; all catalysts tested in this work allowed the improvement of the PG quality during direct (air) biomass gasification in BFBs. Nonetheless, it was observed that the synthetized Fe-Olivine performed better than the bottom bed ashes or wood pellets chars tested in this work. Further studies must be conducted to fully ascertain the influence of these

low-cost catalysts on the produced gas quality and gasification efficiency parameters, and to identify the influence of long operation times on the performance of the catalysts.

5.2 ARTICLES IX AND X - CONCRETE AND ILMENITE AS LOW-COST CATALYSTS TO IMPROVE GAS QUALITY DURING BIOMASS GASIFICATION IN A PILOT-SCALE GASIFIER

5.2.1 ABSTRACT

Naturally occurring ilmenite ($FeTiO_3$) and synthetic concrete were compared as low-cost catalysts for in-situ application in the freeboard of an autothermal 80 kW_{th} pilot-scale BFB direct (air) biomass gasifier. For comparison purposes, the process was also evaluated in an allothermal 3 kW_{th} bench-scale BFB gasifier.
The in-situ application of the solid materials was successfully implemented in both infrastructures, showing promising results due to the increase of H_2 concentration and H_2/CO molar ratio in the PG, namely up to 99.2 and 77.4 % (relative), respectively. This indicates that these materials can promote the WGS reaction. However, this effect was highly dependent on the gas-solid contact time and catalyst temperature, being that it was only significant when these parameters were at least 4.7 s and 746 ºC, respectively. Regarding the efficiency parameters, significant impacts were only found for the application of concrete, namely an increase of up to 25.1, 55.3 and 47.0 % for the Y_{gas}, CGE and CCE. This suggests that, in addition to the promotion of the WGS reaction, this material also has the potential to promote tar reforming/cracking and carbon gasification reactions.

Keywords: Gasification; Ilmenite; Concrete.

5.2.2 INTRODUCTION

The growing environmental and economic concerns related to the use of fossil fuels resulted in the study of new energy solutions. Amongst them, biomass appears as a sustainable option for energy conversion, having some advantages over other types of renewable sources and fossil fuels, including high availability and worldwide distribution, possible application in the current energy carbon infrastructure and potential carbon neutrality [139,402]. However, several problems can be identified when using solid biomass feedstocks, such as handling, mass and heat transfer, material heterogeneity and application. In this regard, gasification can be an interesting solution, since it can process different types of biomass feedstocks to a fuel gas, denominated by PG, which present easier storage and handling, and can be used for the generation of heat and power, and for the synthesis of biofuels and chemicals [15,26,217].

Apart from the desirable compounds of the PG (e.g., H_2), other byproducts are generated during the process, including a complex mixture of condensable organic compounds, denominated by tar. Tar compounds can lead to clogging and blockage of the equipment downstream the gasifier and are one of the major constraints for PG applications [26]. Therefore, PG upgrading and refining is mandatory for various potential PG applications. In this regard, tar removal can be performed by two main types of measures: primary, which are applied inside the reactor, and secondary, which are applied downstream of the gasifier. The interest in primary measures surge from their potential to promote more efficient industrial applications by preserving and using the thermal energy of the PG [15]. In this regard, the PG can be refined by optimizing the reactor design and process parameters, such as the ER, using active bottom bed materials (e.g., olivine, limestone and dolomite) and applying catalytic materials in an integrated section of the gasifier [15,123,124]. A more extensive description of this subject can be found in Chapter 2.

Amongst the potential catalyst materials, $Ca(OH)_2$/CaO has been gaining interest due to its cheapness and promising activity towards tar and hydrocarbons reforming and carbon gasification reactions [421]. In this regard, concrete is one of the most important construction materials and produces more

than 900 million tons of waste each year worldwide [466]. Concrete is composed by aggregate material (e.g. sand) and calcium silicates that undergo hydration in the presence of water, being a source of $Ca(OH)_2$ and CaO [467,468]. Thus, concrete can be an interesting solution for the application of $Ca(OH)_2$ as a catalyst for biomass gasification processes. In a gasification system, $Ca(OH)_2$ will start dehydrating to CaO at about 500 ºC (Reaction 5.2), releasing H_2O in the process. The CaO will then act as a CO_2 sorbent (Reaction 5.3) and tar/hydrocarbon reforming catalyst [422], while the H_2O will act as reactant in other reactions (e.g., Reaction 2.6), including carbon gasification reactions [418,421]. Following the decrease in CO_2 partial pressure in the PG, the WGS reaction (Reaction 2.8) is driven forward, further increasing the H_2 concentration [420,421]. The drawback of this process is the deactivation of CaO after capturing CO_2, which constitutes a challenge for continuous application in gasification systems [418].

$$Ca(OH)_2 \leftrightarrow CaO + H_2O \qquad \text{Reaction 5.2}$$

$$CaO + CO_2 \leftrightarrow CaCO_3 \qquad \text{Reaction 5.3}$$

Hamad et al., [421] studied the production of H_2 rich PG from gasification of biomass in a bench-scale fixed bed reactor, using oxygen as gasifying agent and distinct catalytic materials as additives in the biomass feedstocks. The authors found that $Ca(OH)_2$ increased the gas yield and reduced both char and tar production during gasification processes. The authors also found higher H_2 yields with $Ca(OH)_2$ in comparison to CaO, which can be justified by the H_2O released during the $Ca(OH)_2$ dehydration process. Udomsirichakorn et al., [469] analyzed the combined role of CaO on CO_2 sorbent and tar reforming in a BFB biomass steam gasifier, and found that replacing the reactor sand bed by a CaO bed allowed 20 % higher concentration and almost double yield of H_2, and a decrease of 67 % in tar content. The authors also found that the tar species shifted from higher to lower ring structures with CaO addition, consequently reducing its carcinogenic potential and dew point. Nam et al., [422] analyzed the application of CaO as bed material during air and air-steam gasification of biomass in a BFB reactor. The authors found that the presence of CaO significantly reduced the tar content through thermal cracking and oxidation reactions, and also increased the WGS reaction leading to an increase of the H_2 concentration; the combination of steam and CaO allowed a H_2 concentration of approximately 50 %v. Jordan and Akay [470] analyzed the effect of CaO as bed material on tar production and dew point during gasification of cane bagasse in a pilot-scale downdraft gasifier, and found that the use of 2, 3 and 6 %wt in-bed CaO decreased tar yield ranging from 16 to 35 %, which corresponded to a tar concentration decrease between 44 to 80 % in the PG. The authors also found an increase in syngas yield of 17 to 37 % and a decrease of tar dew point of 37 to 60 ºC.

Natural-occurring ilmenite ($FeTiO_3$) is also an interesting potential low-cost catalytic material for gasification processes due to its mechanical and thermochemical properties at high temperature, catalytic activity for tar reforming and high WGS reaction activity [471,472]. In this regard, it is argued that the Fe content of the ilmenite, together with the H_2O and CO_2 content present in the PG, should significantly induce both steam and dry tar reforming (Reactions 5.4 and 5.5, respectively) [113,472]. The cost of the preparation of ilmenite catalysts is also argued to be low compared to other synthetized catalysts [473]. The drawback of the application of this mineral are the high level of coke deposits generated with its application, which consequently reduce its activity as catalyst [472]. This can be solved by removing the carbon deposits by oxidation, for example in a chemical-looping system [472].

$$C_N H_m + nH_2O \rightarrow \left(\frac{m}{2} + n\right) H_2 + nCO \qquad \text{Reaction 5.4}$$

$$C_N H_m + nCO_2 \rightarrow \left(\frac{m}{2}\right) H_2 + 2nCO \qquad \text{Reaction 5.5}$$

In this regard, Lind et al., [472] investigated tar reforming in a secondary catalytic reactor using ilmenite as the bed material, and found a reduction of the tar content in the PG by 35% and an increase of the H_2/CO ratio from 0.7 to almost 3, with a gas residence time in the bed ranging from 0.4 to 0.5 s. Min et al., [474] investigated ilmenite as a low-cost catalyst for the steam reforming of tars from the pyrolysis of mallee woody biomass. The authors found that ilmenite has good activity for steam reforming of tars due to its highly dispersed iron-containing species. Furthermore, the authors also found that the H_2O and CO_2 produced during the pyrolysis, play an important role for the minimization of coke deposition on the catalyst surface, and, consequently, the catalyst activity can be maintained for longer operation times.

Despite these works, information regarding the application of ilmenite and $Ca(OH)_2$/CaO is still limited, particularly regarding its application as in-situ catalysts in direct (air) pilot-scale biomass BFB gasifiers, and there are still various uncertainties regarding the capacity of these materials towards reducing tar formation and increasing non-condensable gases yields (e.g., H_2).

Thus, in this work, concrete and ilmenite were tested as in-situ catalysts in the freeboard of an autothermal 80 kW_{th} bubbling fluidized bed (BFB) direct (air) biomass gasifier. The process was also evaluated in an allothermal 3 kW_{th} BFB gasifier. The main objective is the determination of the performance of these low-cost catalysts as primary measures for the increase of the PG quality, during direct (air) biomass gasification in BFBs with distinct operating parameters (e.g., operating scale and gas-solid contact time). In this context, it was characterized the influence of both concrete and ilmenite on the PG composition (CO, CO_2, CH_4, C_2H_4, C_2H_6, C_3H_8, H_2 and N_2) and LHV and gasification process efficiency parameters, namely Y_{gas}, CGE and CCE. The influence of these solid materials on the tar concentration in the raw PG was qualitatively inferred by assuming that the increase of the concentration of combustion light gases results, in part, from tar destruction reactions promoted by the catalysts, as suggested in other works [124,393].

5.2.3 MATERIALS AND METHODS

The experimental infrastructures used for this work were the DAO-UA 80 kW_{th} pilot-scale BFB gasifier and the DAO-UA 3 kW_{th} bench-scale BFB gasifier (Section 1.3.2). The methodologies used are described in Section 1.4.

5.2.3.1 FEEDSTOCK CHARACTERIZATION

The feedstock chosen for the gasification experiments was commercial pine (*Pinus Pinaster)* pellets due to three main reasons:

1. Pine (*Pinus Pinaster*) is one of the most abundant tree species in the Portuguese Forests [354].
2. Pelletization allows an increase of the uniformity of the physical characteristics of biomass feedstocks, which leads to improved feeding regularity.
3. This biomass feedstock has an adequate chemical composition (e.g., low ash content) and has previously shown good performance in other works performed here (See previous Sections).

For the experiments carried out in the autothermal pilot-scale infrastructure, the pellets had 4 to 6 mm diameter depending on the experiments performed, i.e., for the experiments regarding concrete application the pellets used had 6 mm diameter, while for the experiments performed with ilmenite the pellets had 4 to 6 mm diameter. This latter lower size was used to try to increase the reactivity of

the pellets and consequently decrease char accumulation in the reactor bed, which caused some operational problems during the experiments performed with concrete. For the allothermal bench-scale infrastructure, the pellets were previously grounded and sieved to a size between 2 to 4 mm diameter, due to the lower dimensions of the reactor and respective feeding system. The characteristics of the biomass used as feedstock are detailed in Table 5.5.

Table 5.5 – Proximate and elemental analysis of the pine pellets used as feedstock in the gasification experiments.

	Pine pellets
Proximate analysis	
Moisture (%wt, wb)	4.6
Volatile matter (%wt, db)	82.3
Fixed carbon (%wt, db)	17.4
Ash (%wt, db)	0.3
Ultimate analysis (%wt, db)	
Ash	0.3
C	47.5
H	6.2
N	0.1
S	nd
O (by difference)	45.9
LHV (MJ/kg db)	18.0
Bulk density (kg/m^3 wb)	614

nd- not determined, below the detection limit of the method, 100 ppm wt.

5.2.3.2 CONCRETE AND ILMENITE CHARACTERIZATION

The concrete was prepared by combining Portland cement CIMPOR and quartzite sand (1:5). For this purpose, cement was mixed with sand and stirred evenly for a given water- ratio of 0.5 at controlled rotation speed (100 rpm). The samples were dried at 25ºC for 24 hours on a drying oven with controlled humidity. Hydration process was performed in an autoclave with curing time and controlled temperature to improve the $Ca(OH)_2$ phase.

The crystalline phases of the fresh solid materials were assessed by powder X-ray diffraction (XRD) (BrukerD8 Advance DaVinci). Diffraction patterns were analyzed using ICDD (International Centre of Diffraction Data, PDF 4). Brunauer–Emmett–Teller (BET) and Barrett–Joyner–Halenda (BJH) measurements were performed to determine the specific surface area and average pore diameter of the particles.

The XRD pattern shown in Figure 5.14 indicates ilmenite as the main phase ($FeTiO_3$) and alumina (α-Al_2O_3), rutile (TiO_2) and mayenite ($Ca_{12}Al_{14}O_{33}$) as residual phases. For the fresh concrete sample, it was observed quartz as the main phases and some residual silicates phases. Note that the low intensities peaks observed for silicate phases may suggest amorphization of Ca-species in the fresh concrete sample. Other relevant characteristics of the used solid materials are shown in Table 5.6.

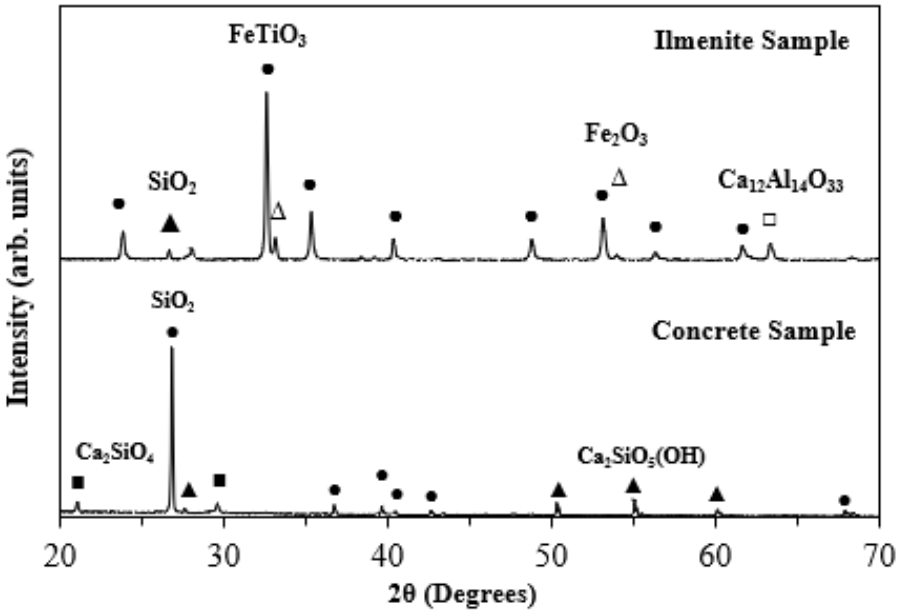

Figure 5.14 – Normalized XRD patterns of the fresh ilmenite and concrete samples.

Table 5.6 – Physical-chemical characteristics of the low-cost solid materials used as catalysts in the gasification experiments performed.

		Ilmenite	Concrete
Physical characteristics	Particle size [µm]	<355	<3000
	Apparent density [kg·m^{-3}]	2570	1750
	Surface specific area [m^2·g^{-1}]	0.52	1.2
	Pore diameter [nm]	3 to 4	9 to 10
Chemical composition [%wt]	Ti	26.680	0.058
	Fe	36.640	0.731
	Mg	1.980	0.372
	Si	0.990	32.676
	Al	0.380	0.779
	Ca	0.260	17.492
	Mn	0.230	0.016
	V	0.120	-
	S	0.160	0.708
	Na	-	0.057
	Cr	0.080	-
	Ni	0.043	-
	K	0.025	0.400
	P	0.011	0.013
	Zn	0.018	-
	Co	0.017	-
	Zr	0.015	-
	Cu	0.011	-
	Nb	0.005	-
	Cl	-	0.012
	Sr	0.004	-
	Pb	0.001	-
	O	32.330	46.686

5.2.3.3 OPERATING CONDITIONS

The operating conditions of the gasification experiments performed in the autothermal pilot-scale and allothermal bench-scale BFB reactors are detailed in Table 5.7. For the pilot-scale reactor, the ER was maintained between 0.22 and 0.26 and bed temperature between 781 and 809 ºC. For the bench-scale reactor, the ER was kept at 0.25 and the bed temperature at 800 ºC (imposed by an electrical furnace and respective temperature controller). The contact time between the sampled PG and the fixed bed of catalysts was maintained between 0.2 and 3.5 seconds for the bench-scale reactor, and between 4.7 and 5.2 s for the pilot-scale reactor. The gas-solid contact time is calculated by assuming that the sampling flow of the PG is constant throughout the whole sampling line, including the fixed bed of catalysts.

Table 5.7 – Gasification experiments reference and respective operating conditions.

Experiment reference	Pine pellets granulometry [mm]	BFB scale	ER	T_{bed} [ºC]	$Q_{biomass}$ [kg/h]	Q_{air} [NL/min]	Catalyst	$T_{catalyst}$ [ºC]	Gas-solid contact time [s]
BP Blank	2 to 4	Bench	0.25	800	0.154	2.7	-	-	-
BP Ilmenite 0.2	2 to 4	Bench	0.25	800	0.154	2.7	Ilmenite	620	0.2
BP Ilmenite 3.5	2 to 4	Bench	0.25	800	0.154	2.7	Ilmenite	585	3.5
BP Concrete 0.3	2 to 4	Bench	0.25	800	0.154	2.7	Concrete	620	0.3
BP Concrete 3.5	2 to 4	Bench	0.25	800	0.154	2.7	Concrete	585	3.5
PP Blank I	4 to 6	Pilot	0.26	809	10.9	200	-	-	-
PP Blank C	6	Pilot	0.22	781	13.2	200	-	-	-
PP Ilmenite 4.7	4 to 6	Pilot	0.26	801	11.2	200	Ilmenite	774	4.7
PP Concrete 5.2	6	Pilot	0.22	798	13.2	200	Concrete	746	5.2

5.2.4 RESULTS AND DISCUSSION

The results presented in this Section include the average PG composition (H_2, CO, CO_2, CH_4, C_2H_4, C_2H_6, C_3H_8, N_2, H_2/CO) and LHV, and gasification efficiency parameters (Y_{gas}, CGE and CCE), for the autothermal 80 kW_{th} pilot-scale BFB reactor and allothermal 3 kW_{th} bench-scale BFB reactor, with and without the in-situ application of concrete and ilmenite.

5.2.4.1 INFLUENCE OF THE TESTED CATALYSTS ON THE PG COMPOSITION

For the autothermal pilot-scale BFB, the highest concentration of H_2, CO and CH_4 was found for the experiment performed with concrete as catalyst (PP - Concrete 5.2, Figure 5.15), namely 16.9, 19.1 and 6.0 %v, respectively, corresponding to an average LHV of 7.5 MJ/Nm^3, which are values higher than commonly referred in the literature for direct (air) gasification of biomass in BFB reactors [4]. Important to note that the experiments performed with ilmenite in the pilot-scale BFB had a higher ER (Table 5.7), thus a direct comparison between the catalysts effect is not possible. Therefore,

concrete allowed a relative increase of 99.2, 12.1, 19.0 and 23.8 % for the concentration of H_2, CO and CH_4 and LHV (Figure 5.16), respectively, in comparison with the gasification experiment performed under the same conditions but without concrete (PP – Blank C). This increase in H_2 concentration suggests that CaO significantly promoted the WGS reaction by performing CO_2 absorption, consequently pushing the reaction forward. Accordingly, the CO_2 did not decrease and was maintained almost constant (relative increase of 1.2 %). However, its yield improved from 12.5 to 19.8 g/kg biomass db. Thus, despite the absorption of CO_2 performed by the CaO, the CO_2 concentration and yield did not decrease because of the consequent WGS reaction promotion and a potential increase in the specific dry gas production that can be associated to both tar reforming and carbon gasification reactions.

In this regard, as the concrete was not located at the bottom bed of BFB reactor, but instead was placed above it (Figure 1.3, M3, Section 1.3.1), it should not be expected any promotion of carbon gasification. However, the general increase of the yield of the non-condensable gases seems to be too high (Figure 5.17) to be justified only by tar reforming/cracking, i.e., the combined yield of CO, CO_2, H_2 and CH_4 increased from 544 to 585 g/Nm^3 dry gas; as the tar concentration in a PG from BFB gasifiers typically revolves around 1 to 30 g/Nm^3 [66,114], this would mean that even if all tar was converted to non-condensable gases, it would not be sufficient to justify this increase. Therefore, some carbon conversion must also have occurred, such as carbon particles elutriated with the upward gas flow of the reactor or soot/coke deposited on the concrete (further discussed in next Section in terms of Y_{gas}).

The highest H_2/CO molar ratio was also found for experiment PP – Concrete 5.2, namely 0.88 mol·mol^{-1}, and is a direct consequence from the higher occurrence of the WGS reaction. This value is suitable for Fischer-Tropsch synthesis processes (0.6 mol·mol^{-1}), but still needs to be higher for other applications, such as methanol synthesis or dimethyl ether production, which require molar ratios of 1 and 2, respectively [72,475].

Regarding the in-situ application of ilmenite in the autothermal pilot-scale BFB, a relative increase of 55.5, 15.7 and 5.8 % was found for the concentration of H_2, CO_2 and CH_4, respectively. On the other hand, a relative decrease of 12.1 % was found for the concentration of CO. Accordingly, a relative increase of 68.5 and 0.4 % was found for the H_2/CO molar ratio and LHV, respectively. These results indicate an increase in WGS activity induced by the ilmenite particles. The phenomenon was previously observed in other gasification processes involving ilmenite [272,472] and is typically associated to iron-based catalysts [123,471]. Analogous to the gasification experiments performed with concrete, it was also observed a general increase of the gases yields (Figure 5.17) that can be partly justified by the ilmenite promoting tar reforming/cracking and carbon gasification reactions. In fact, the combined yield of CO, CO_2, H_2 and CH_4 increased from 514 to 554 g/Nm^3 dry gas with ilmenite application (further discussed in the next Section in terms of Y_{gas}).

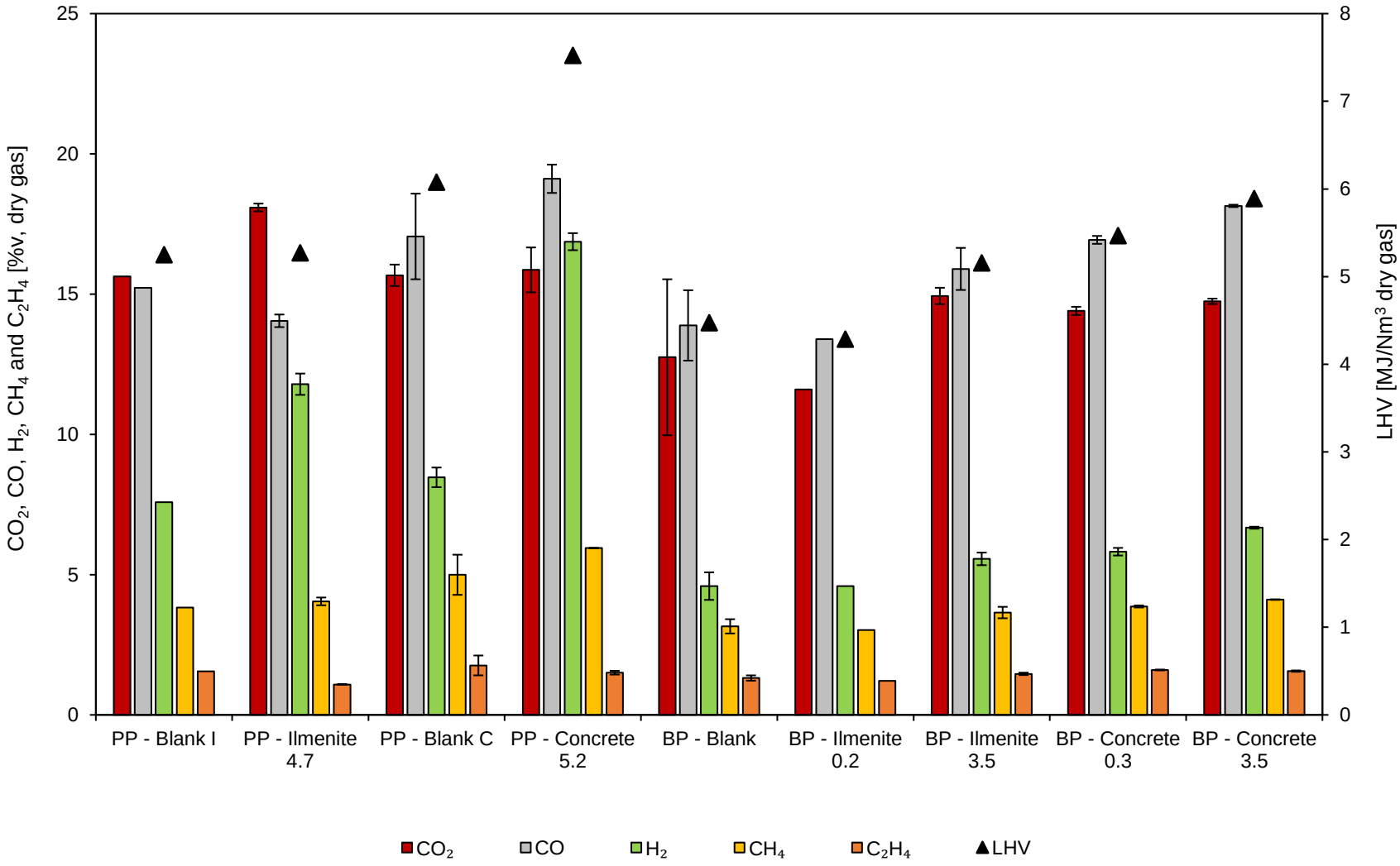

Figure 5.15 – PG composition and LHV for the distinct gasification experiments performed in the pilot and bench-scale fluidized bed reactors. Experiments reference according to Table 5.7.

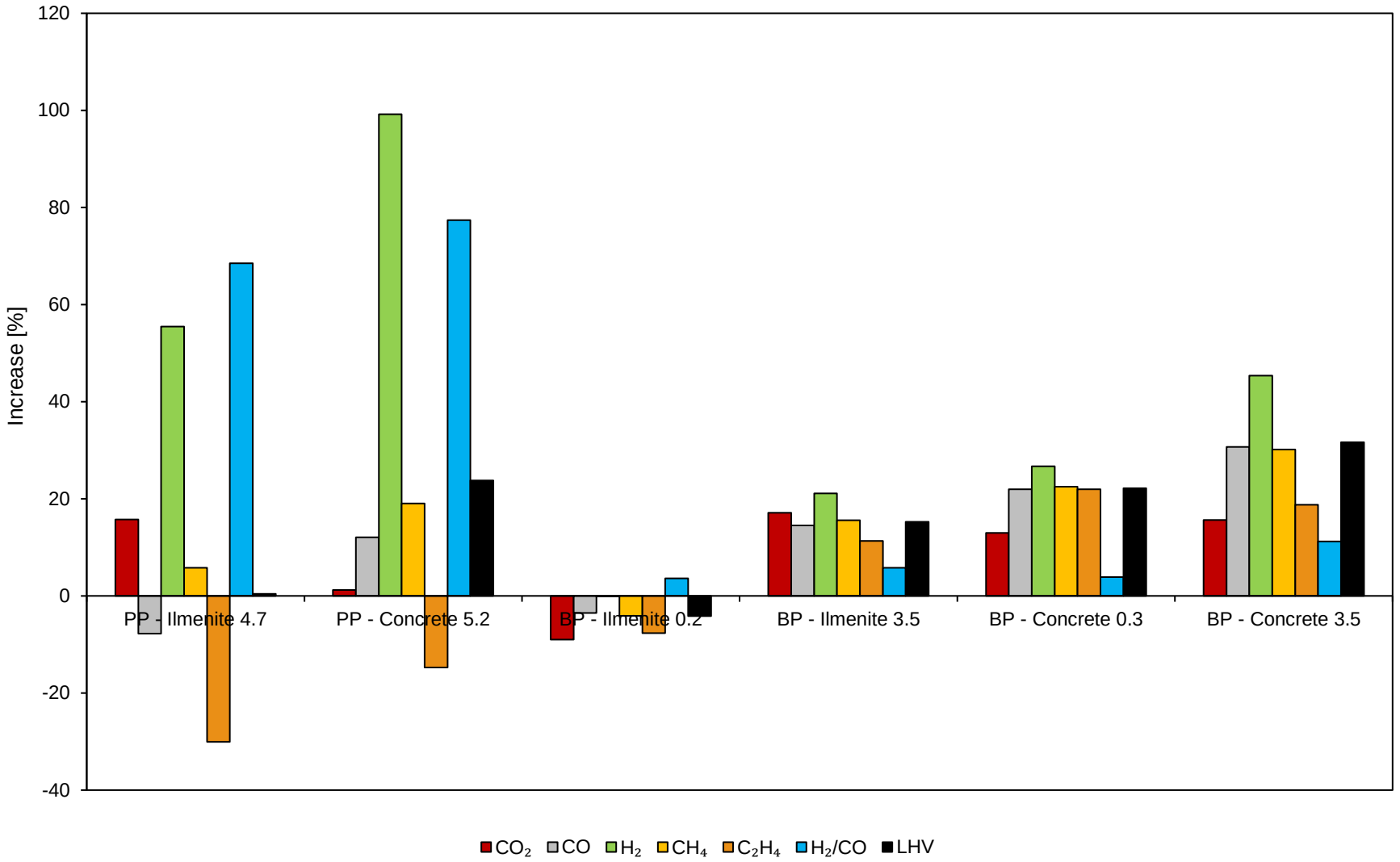

Figure 5.16 – Influence of the distinct low-cost catalytic materials on the composition and LHV of the PG for the different gasification experiments performed. Experiments reference according to in Table 5.7.

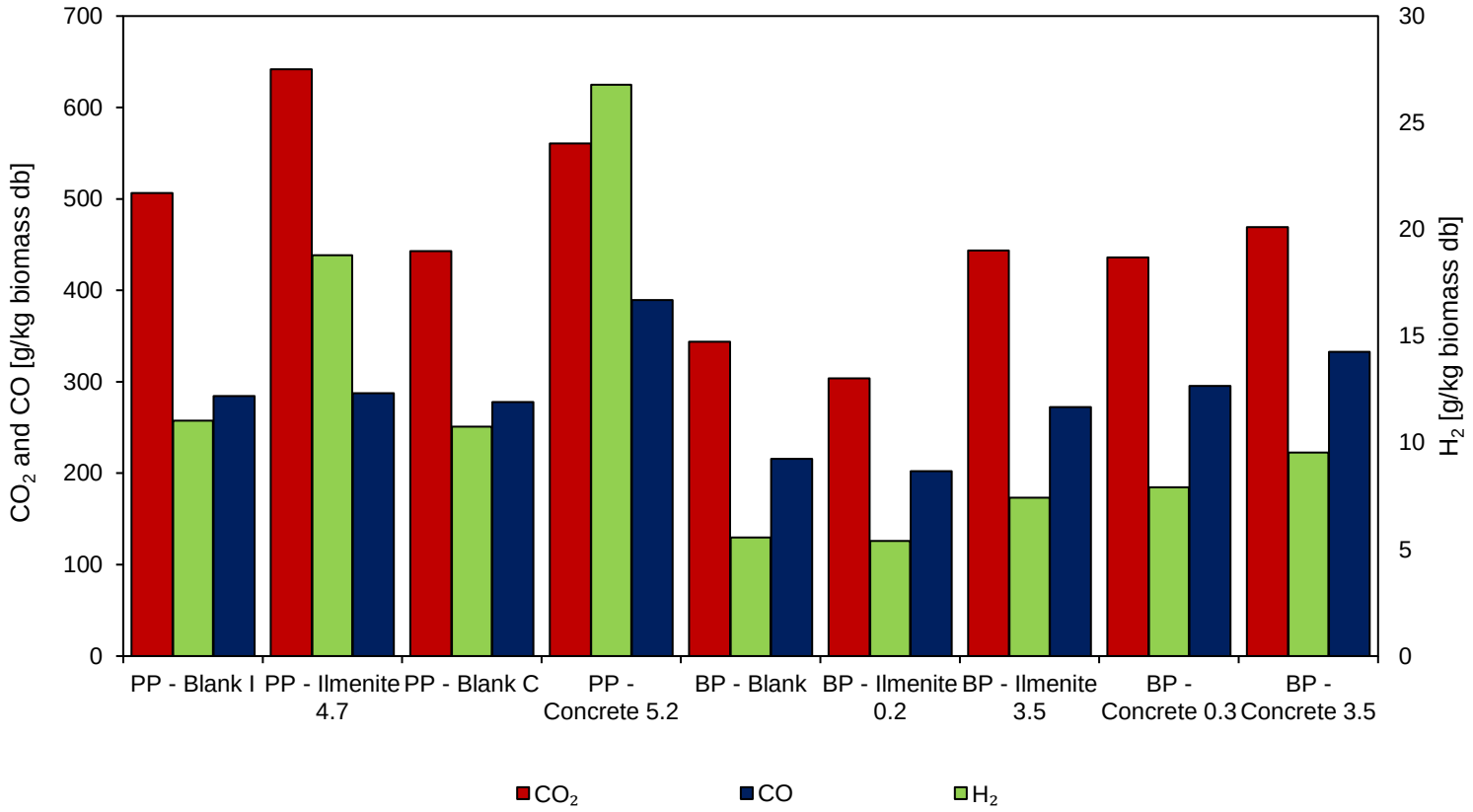

Figure 5.17 – CO_2, CO and H_2 yield for the distinct gasification experiments performed in the pilot and bench-scale fluidized bed reactors. Experiments reference according to Table 5.7

For the allothermal bench-scale BFB, the highest concentration of CO, H_2 and CH_4 was found for the in-situ application of concrete with 3.5 s gas-solid contact time (BP – Concrete 3.5), namely 18.2, 6.7 and 4.1 %v, respectively; this represented a relative increase of 30.7, 45.4 and 30.2 %, respectively. However, the CO_2 also increased in a similar relative amount to these gaseous species, namely 15.6 %. Accordingly, in experiment BP – Concrete 0.3, a relative increase of CO, H_2, CH_4 and CO_2 of 22.0, 13.0, 26.7 and 22.5 %, respectively, was also found. These similar relative increases, as well as the unexpected increase of CO and CO_2, indicate that the catalyst did not have a prominent influence on CO_2 absorption or the WGS reaction during the experiments BP – Concrete 3.5 and BP – Concrete 0.3, which is in contrast with the results observed for PP – Concrete 5.2. Accordingly, the H_2/CO molar ratio was also maintained almost constant, with the maximum relative increase being found for experiment BP – Concrete 3.5, namely 11.2 %.

The justification behind this phenomenon can be associated to the lower residence time and catalyst temperature employed in these experiments, in comparison with the experiments performed in the pilot-scale infrastructure (Table 5.7). Nonetheless, as the non-condensable gas yields increased (Figure 5.17), it can be inferred that there was some increase in tar reforming promoted by the concrete during these experiments, despite the lack of increased activity of the WGS reaction. Accordingly, the concrete also improved the LHV of the PG, allowing a maximum relative increase of 31.6 % (BP – Concrete 3.5).

Regarding the gasification experiments performed with ilmenite in the bench-scale BFB reactor, the effect was inexistent for lower residence times (BP – Ilmenite 0.2), however, the concentration of combustible gases was increased in the PG during experiments with higher gas-solid contact times (BP – Ilmenite 3.5). In this latter, a relative increase of the concentration of CO_2, CO, H_2 and CH_4 by 14.5, 17.1, 21.1 and 15.6 %, respectively, was found; this represented a relative increase of 15.3 % in terms of LHV. Analogous to the discussion performed for the application of concrete in this bench-scale infrastructure, as the non-condensable gases yield increased in similar amounts (Figure 5.17), it can be inferred that the activity of the WGS reaction did not increase, instead, the ilmenite particles seem to have induced an increase of tar reforming/cracking reactions, due to the specific gas production increase (further discussed in the next Section in terms of Y_{gas}). Accordingly, the H_2/CO molar ratio only showed a slight increase, namely between 3.6 and 5.8 %, further corroborating that the ilmenite only promoted the WGS activity at higher gas-solid contact times and catalyst temperature, namely in the experiments performed at the pilot-scale BFB (PP – Ilmenite 4.7).

Conclusively, it seems that the influence of the catalytic materials on the PG composition was not as evident in the experiments performed in the bench-scale infrastructure as in the pilot-scale infrastructure, particularly regarding the increase of the WGS reaction occurrence. This is justified by the lower gas-solid contact time and catalyst temperature employed in this smaller-scale reactor. Furthermore, due to the lower dimension of the bench-scale BFB, an increase in the contact time between the PG and the catalyst leads to a decrease of the catalyst average temperature (Table 5.7), as evidenced by the temperature profile of the reactor (Figure 5.18), thus constituting a trade-off between these parameters. This is in contrast to the autothermal pilot-scale BFB, where it is possible to employ high gas-solid contact times at temperatures closer to the reactor bed (Figure 5.19). Therefore, it seems that a high gas-solid contact time (over 3.5 s) and a high catalyst temperature (over 740 ºC) is beneficial for the application of both ilmenite and concrete as in-situ catalysts, particularly regarding the WGS activity and consequent increase of the H_2/CO molar ratio in the PG.

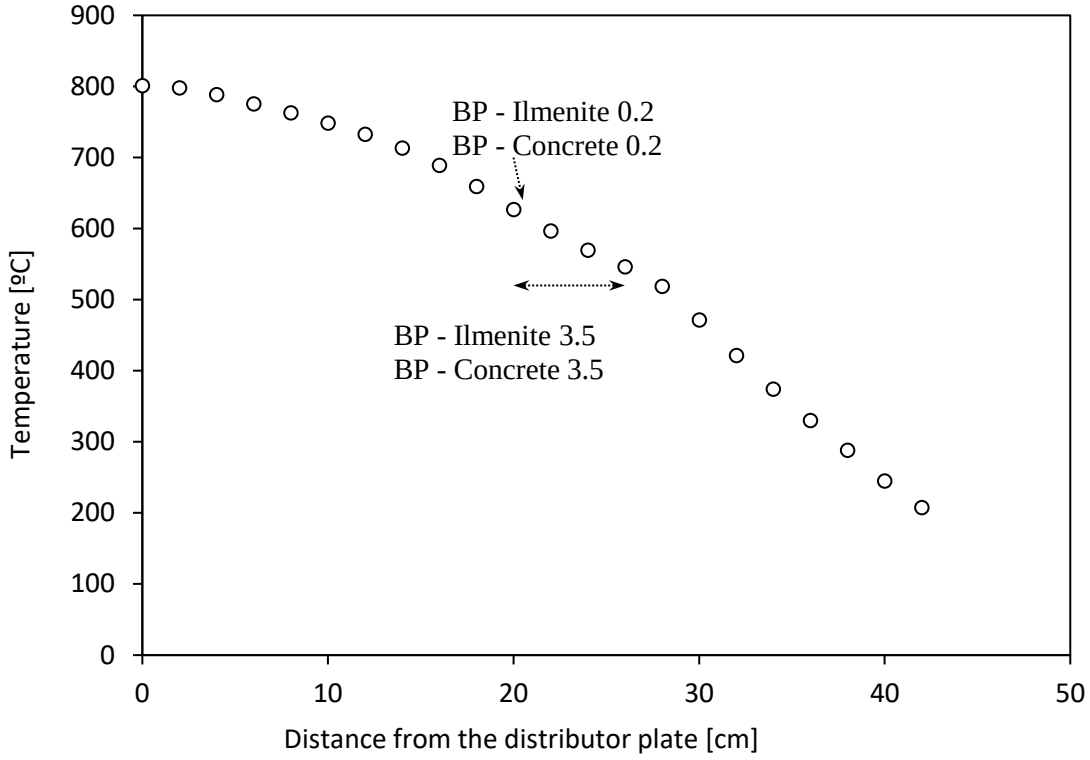

Figure 5.18 – Average vertical temperature profile in the allothermal bench-scale BFB reactor. Experiments reference according to Table 5.7.

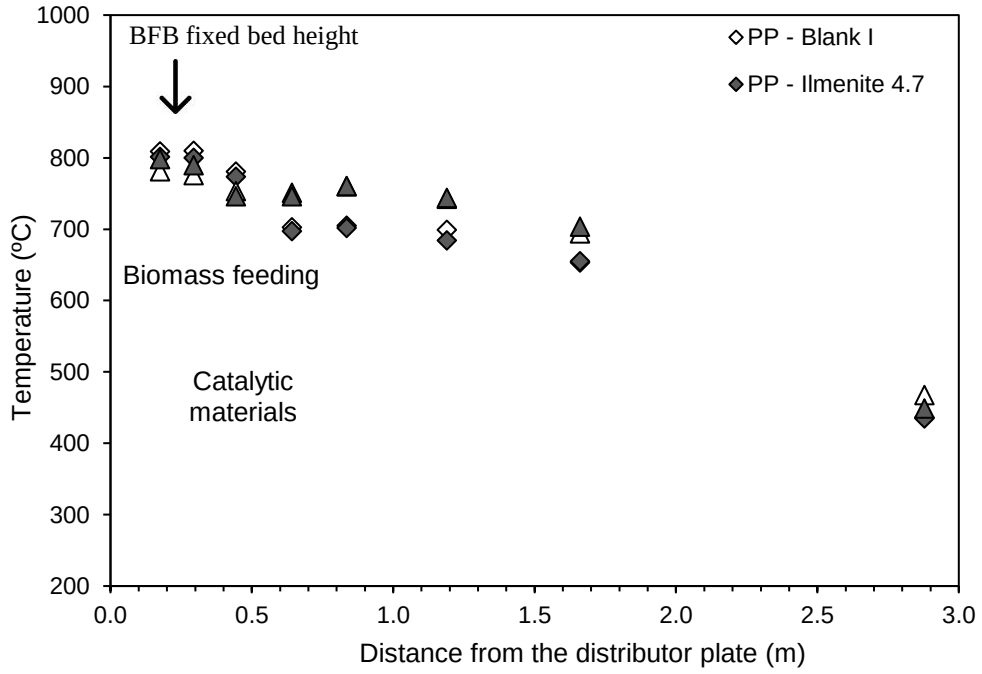

Figure 5.19 – Average vertical temperature profiles for the distinct gasification experiments performed in the autothermal pilot-scale BFB reactor. Experiments reference according to Table 5.7.

5.2.4.2 INFLUENCE OF THE TESTED CATALYSTS ON THE GASIFICATION EFFICIENCY PARAMETERS

Figure 5.20 shows the efficiency parameters (Y_{gas}, CGE and CCE) obtained for the distinct gasification experiments performed in the pilot-scale and bench-scale BFB reactors. For the prior, a maximum of 1.8 Nm^3 dry gas/kg biomass db was found for PP – Ilmenite 4.7, while the highest CGE and CCE, namely 74.8 and 90.3 %, were found for PP – Concrete 5.2. It must be noted that the experiment PP - Ilmenite 4.7 had a higher ER than the experiment PP – Concrete 5.2, and that higher ER contributes to higher Y_{gas} [4]. In terms of comparison with the blank experiments (PP – Blank I and PP – Blank C), performed under the same operating conditions, the highest relative increases were found for the experiments performed with concrete (PP – Concrete 5.2), namely 25.1, 54.4 and 33.9 % for the Y_{gas}, CGE and CCE (Figure 5.21), respectively. This indicates the positive influence of concrete on tar reforming/cracking reactions. However, as the increase of Y_{gas} and CCE, namely from 1.4 to 1.8 Nm^3 dry gas/kg biomass db and 67.4 to 90.3 %, respectively, seems to be too high to be caused only by tar destruction, some carbon conversion must also have been promoted by this catalytic material, as previously discussed regarding the increase of the non-condensable gases yields (Figure 5.17); this needs to be further assessed in future works. On the other hand, the efficiency parameters relative increases found for PP – Ilmenite 4.7, namely 9.6, 10.0 and 10.4 % for the Y_{gas}, CGE and CCE, respectively, were lower than the ones found for PP – Concrete 5.2. This indicates that this natural-occurring mineral has higher impact on permanent gas-gas reactions (e.g., WGS reaction) due to the significant gas composition changes previously discussed (Figure 5.15 and Figure 5.16), than tar reforming or carbon gasification reactions.

For the allothermal bench-scale BFB reactor, the highest relative increases of Y_{gas}, CGE and CCE, were found for the experiments made with concrete (BP – Concrete 3.5), namely 18.0, 55.3 and 47.0 %, respectively. For BP – Concrete 0.3, the relative increases were lower due to the lower gas-solid contact time. Regarding the experiments performed with ilmenite in this infrastructure, positive increases were only obtained for experiment BP – Ilmenite 3.5, while the efficiency parameters actually decreased for experiment BP – Ilmenite 0.2. This is justified by the low gas-solid contact time used during this latter, which was not enough for the catalyst to have sufficient activity to surpass the influence caused by the natural variability of the operating conditions of the gasifier. For example, fluctuations in the biomass feeding rate or feedstock chemical composition lead to changes in the ER, which consequently influences the efficiency parameters; this is particularly relevant for the bench-scale BFB reactor because the biomass feeding rate used was relatively low (Table 5.7).

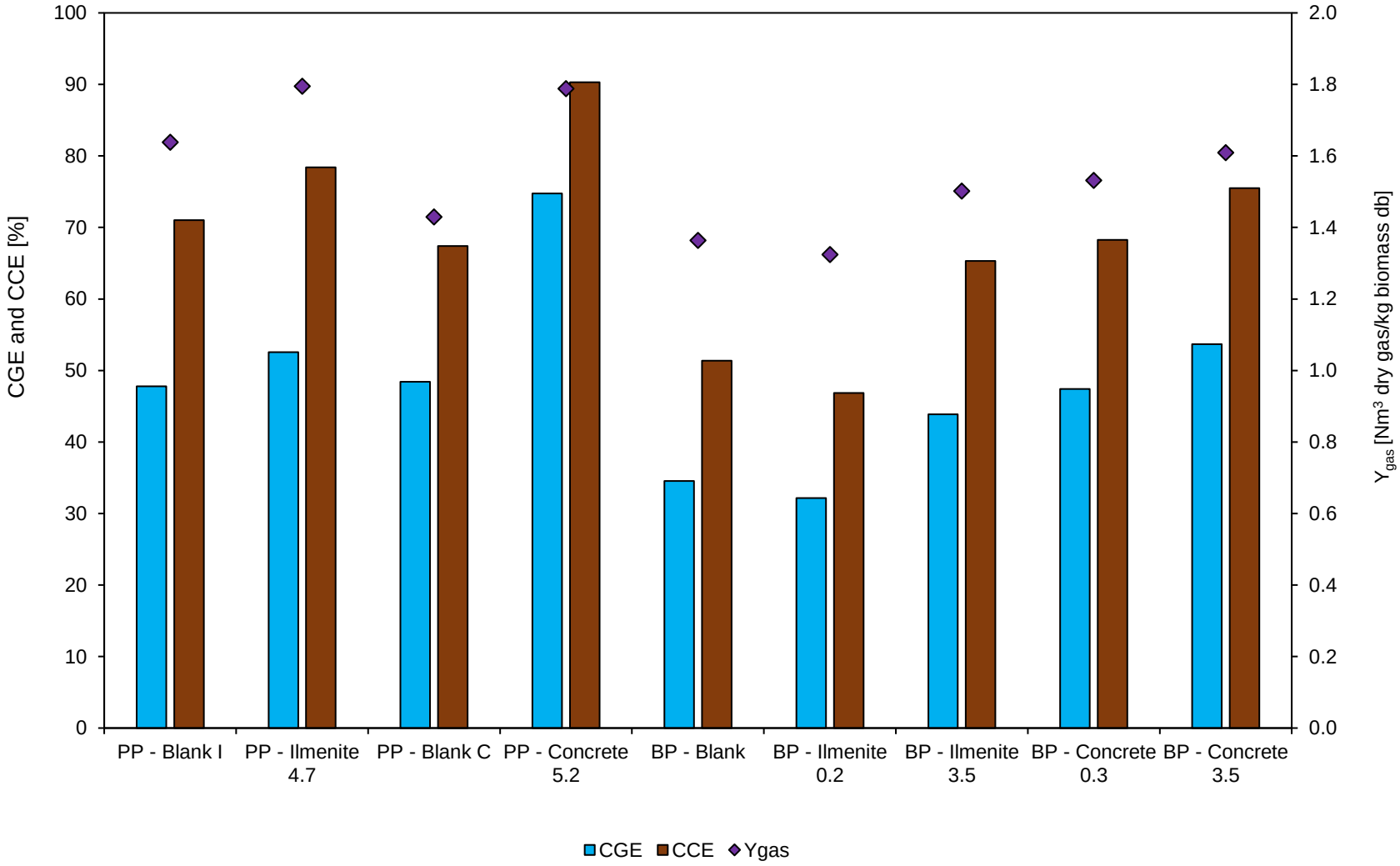

Figure 5.20 – Y_{gas}, CGE and CCE for the distinct gasification experiments performed in the pilot and bench-scale BFB reactors. Experiments reference according to Table 5.7.

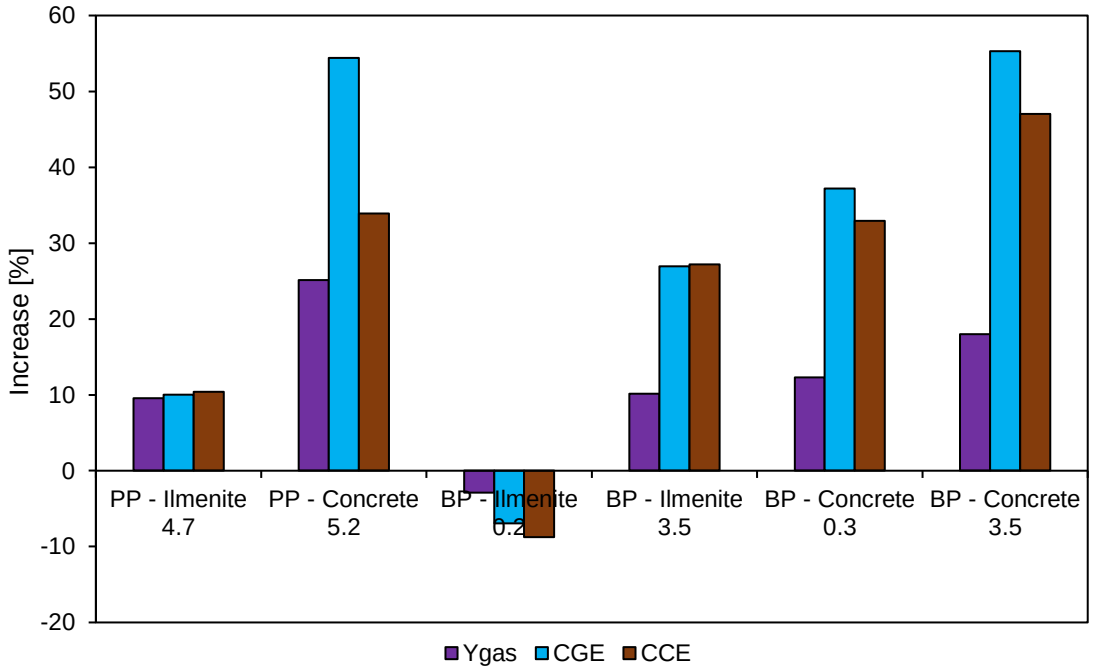

Figure 5.21 – Influence of the distinct low-cost catalytic materials on Y_{gas}, CGE and CCE for the different gasification experiments made. Experiments reference according to Table 5.7.

5.2.5 CONCLUSIONS

In this work, the in-situ application of concrete and ilmenite was evaluated as primary measure to improve PG quality during direct (air) gasification of biomass (*Pinus Pinaster*) in an 80 kW_{th} pilot-scale autothermal BFB reactor, focusing on the PG composition and process efficiency parameters. For comparison purposes, the process was also evaluated in a 3 kW_{th} allothermal bench-scale BFB reactor.

Regarding the PG composition and respective LHV, for the highest gas-solid contact times (4.7 to 5.2 s) and catalyst temperatures (746 to 774 ºC) employed in the gasification experiments, both ilmenite and concrete caused a significant relative increase of H_2 concentration and H_2/CO molar ratio in the PG, namely up to 99.2 and 77.4 %, respectively, reflecting the capacity of these materials to promote the WGS reaction. Regarding the concrete, this can be justified by the CaO performing CO_2 absorption, consequently pushing the WGS reaction forward. Regarding the ilmenite, this behavior can be justified by this solid material Fe content, which is known to promote the WGS activity. Despite the significant increase of H_2 concentration observed with concrete, this solid material also caused a small relative increase of the CO concentration (up to 12.1 %) and significant increase of the LHV of the PG (up to 23.8 %), indicating that the concrete promoted tar reforming/cracking and carbon gasification reactions, in addition to the WGS reaction. In contrast, the ilmenite did not have a significant effect on the LHV of the PG because it also promoted a relative decrease of the CO concentration (up to -7.8 %), which can be associated to the increase of the occurrence of the WGS reaction. For lower gas-solid contact times (0.2 to 3.5 s) and catalyst temperatures (585 to 620 ºC), the H_2/CO molar ratio did not show significant increases with both ilmenite and concrete, indicating that these materials did not promote the WGS reaction under these operating conditions. Nonetheless, the LHV of the PG still increased in similar amounts, consequently indicating that higher gas-solid contact times and catalyst temperature can be mainly

related to the promotion of the WGS reaction and not as relevant for tar reforming/cracking or carbon gasification reactions.

Regarding the process efficiency parameters, the maximum relative increases were found for the experiments performed with concrete, namely up to 25.1, 55.3 and 47.0 % for Y_{gas}, CGE and CCE, respectively. This further suggests the concrete capacity to promote tar reforming/cracking and carbon gasification reactions. On the other hand, the relative increases of process efficiency parameters for the experiments performed with ilmenite are significantly lower than for the experiments performed with concrete, thus, suggesting that this material can have higher impact on permanent gas chemistry (e.g., WGS reaction) than tar reforming or carbon gasification reactions.

Conclusively, the in-situ application of low-cost catalysts (ilmenite and concrete) for the improvement of the PG quality was successfully performed in the 80 kW_{th} pilot-scale BFB reactor and the 3 kW_{th} bench-scale BFB reactor. In fact, both low-cost catalysts showed very promising results regarding the increase of H_2 concentration and H_2/CO molar ratio in the PG. Nonetheless, it was observed that the concrete performed better than the ilmenite, due to the significant increase of the gasification efficiency parameters observed during the application of this material, which can be associated to a promotion of the occurrence of tar reforming/cracking and carbon gasification reactions. Further work must be performed to fully quantify the effect of these solid materials on tar conversion and composition, and to determine the influence of long operation times on the decay of their catalytic activity.

5.3 INTEGRATED RESULTS DISCUSSION

Based on the results of the developed Articles in this Section, it can be concluded that the introduction of low-cost catalysts for in-situ improvement of the PG quality was successfully performed in the two distinct reactive systems, namely the 80 kW_{th} pilot-scale BFB gasifier and the 3 kW_{th} bench-scale BFB gasifier. All tested materials (wood pellets chars, eucalyptus ashes, Fe_2SiO_4, ilmenite and concrete) allowed the improvement of the PG quality and efficiency parameters. Nevertheless, the configurations must still be improved, particularly regarding the possibility of using higher gas-solid contact times and catalyst temperatures in the bench-scale reactive system; this is easier to perform on the pilot-scale reactor due to its higher inner diameter.

Regarding the low-cost catalysts tested, it was found very promising results concerning the H_2 concentration and H_2/CO molar ratio relative increases for the experiments performed with concrete and wood pellet chars. On the other hand, synthetic Fe_2SiO_4 promoted the highest relative increases of the PG LHV, Y_{gas}, CGE and CCE, consequently showing suitability to be used when immediate direct combustion of the PG is desired. Nevertheless, the highest absolute values of H_2 concentration, LHV, CGE and CCE were found for the experiments performed with concrete as catalyst. This indicates that these low-cost materials can have significant distinct impacts on the gasification process, and must be chosen in accordance with the desired PG characteristics. The promotion of the tar reforming/cracking, carbon gasification, WGS and CO_2 absorption reactions, are inferred to be the reasons behind the increases found, depending on the material tested; this also seems to be highly dependent on the operating conditions (gas-solid contact time and temperature). These results further corroborate the conclusion from Chapter 4, i.e., the necessity of obtaining specific knowledge regarding the experimental demonstration of each type of biomass gasification process for each particular application, including the application of each potential catalyst and respective operating conditions.

Further work must be performed to fully quantify the effect of these low-cost solid materials on tar conversion and composition, and to understand the respective tar cracking mechanisms. For this purpose, in a first stage, it may be helpful to test the catalysts on selected tar model compounds (e.g, naphthalene), and then upscale the experiments to use real tar mixtures from distinct PGs. It must also be determined the influence of long gasification operation times on the performance of the catalysts, including their potential loss of activity (e.g., by carbon deposition and poisoning). In this case, the possibility of regeneration must also be considered and evaluated, depending on the material.

6 COMBUSTION OF PP BYPRODUCTS AS A CO-INTEGRABLE BIOREFINERY PROCESS

This Chapter is composed by Article XI, named "Co-combustion of residual forest biomass and sludge in a pilot-scale bubbling fluidized bed". This Article evaluates the co-combustion process of distinct types of byproducts from the PP industry in a BFB reactor. For this purpose, the DAO-UA 80 kW_{th} pilot-scale BFB infrastructure (Section 1.3.1) was modified (description in Section 6.1.3). The objective is to show this process as a valid energetic valorization solution to be used as co-integrable biorefinery process with other biomass gasification processes. This Article was published in the Journal of Cleaner Production in 2020 (https://doi.org/10.1016/j.egyr.2019.08.063).

6.1 ARTICLE XI - CO-COMBUSTION OF RESIDUAL FOREST BIOMASS AND SLUDGE IN A PILOT-SCALE BUBBLING FLUIDIZED BED

6.1.1 ABSTRACT

In this work, the co-combustion of RFB from eucalyptus and its blend with different amounts of primary and secondary sludge from the PP industry was studied in a pilot-scale bubbling fluidized bed reactor. The main objective was the determination of sludge addition influence on the overall process and on the composition of the exhaust gases, with emphasis on chlorine emissions, namely present in the solid phase (fly ashes) and in the gaseous phase (hydrogen chloride), and nitrogen oxides emissions. The co-combustion process of RFB with primary sludge (up to 5 % in mass) and secondary sludge (up to 10 % in mass) was successfully demonstrated as a valid energy valorization option. Except specific cases, no significant emissions increase of nitrogen oxides, carbon monoxide or hydrogen chloride were found with the addition of sludge. In fact, hydrogen chloride emissions decreased, potentially due to an increase in the chlorine retention in ashes caused by the high inorganic content present in the sludge. This high inorganic content can also lead to a significant increase in ash production during the combustion process. Thus, consequently, without proper maintenance, significant ash accumulation along the combustion system may occur, which can decrease the process efficiency and cause equipment damage.

Keywords: Biomass; Sludge; Bubbling fluidized bed; Combustion; Chlorine.

6.1.2 INTRODUCTION

Sewage sludge is an unavoidable byproduct of wastewater treatment processes [476]. This byproduct has been accumulating in the recent years due to lack of proper valorization and disposal methods [477]. In countries that produce PP, primary and secondary sludges from the PP industry may account for more sludge production than municipal wastewater treatment plants [478]. Co-combustion of these wastes with other fuels (e.g., residual forest biomass) is recognized as possible, due to the relatively moderate calorific value of sludges [479,480]. This process is also promising because it simultaneously allows the reduction of the sludges volume and the production of heat and power [481]. Furthermore, both waste sludge and RFB from eucalyptus are byproducts from the PP industry and considered as potential alternative fuels and renewable energy resources [477]. Regarding solid and exhaust gases emissions, it is commonly suggested that adding sludges to the combustion process of Cl-rich fuels may reduce Cl deposition and bed agglomeration, while increasing NOx emissions, due to the sludges high nitrogen content, and Cl gaseous emissions (HCl) [482–485].

Cl emissions are associated with diverse problems of deposition and corrosion in combustion systems. During biomass combustion processes, the Cl present in the fuel is released and can be present in both gas phase and solid phase. Furthermore, Cl can ease the mobilization of diverse inorganic compounds [486], such as alkali metals present in the burning biomass particles, easing the reaction between these and other substances [487]. Thus, Cl contributes to the increase of problems related to the alkali metals, such as corrosion and agglomeration in the combustion system. Depending on the temperature, it is recognized that a high Cl content in the fuel can cause a significant increase of the emissions of alkali metals [488]. Nonetheless, Cl release from the combustion particles can be controlled to a certain point by limiting the maximum temperature of the process [489]. Thus, the higher Cl content present in biomass (in comparison with coal [490]), limit the steam production process conditions in biomass combustion systems, due to temperature limitations [491–493].

Cl release during the devolatilization phase is related to the organic and inorganic fractions of Cl present in the fuel. Cl released at low temperature is associated to organic compounds or HCl and can be recaptured in the chars by secondary reactions with available alkali metals [494]. Then, re-release of the captured Cl can occur due to KCl sublimation during pyrolysis and combustion at high temperatures [494]. Thus, all relevant Cl species involved in combustion processes are highly volatile, and a high volatilization of Cl is expected [51,494].

Accordingly, Lith et al., [495] observed high Cl percentage release, including complete dechlorination, during combustion of spruce and fiberboard with process temperature between 500 and 850 ºC. Diaz-Ramírez et al., [496] observed Cl release near 50 % at temperatures below 700 ºC and complete dechlorination at around 800 ºC, during brassica and poplar combustion. Strömberg and Björkman [486] studied the pyrolysis and gasification of different types of biomass (sugarcane trash, switch grass, lucerne and straw rape) and observed that under biomass pyrolysis and gasification conditions, Cl release under 200 ºC is not significant, 20-50 % of Cl was released at low temperatures such as 300 to 400 ºC, and 30-60 % of the total Cl was still left in the chars at 900 ºC. Jensen et al., [489] studied the release and transformation of K and Cl as a function of temperature during the pyrolysis of straw in a laboratory batch operated reactor. The authors observed the release of Cl in two main phases: 60 % was released when the temperature was raised from 200 ºC to 400 ºC and the remaining fraction was released at temperatures between 700 and 900 ºC. Knudsen et al. [497], observed that 25 to 75 % of the Cl present in the fuel was released to the gaseous phase at temperatures lower than 500 ºC, during combustion experiments with different types of biomass. Afterwards, the Cl was released by volatilization under KCl form, mostly between 700 and 800 ºC. For temperatures above 800 ºC, the authors observed complete dechlorination for all experiments performed.

During devolatilization (200-400 ºC), Cl is released to the gaseous phase mainly under HCl form [498]; at these relatively low temperatures, the free Cl ion tends to react with hydrogen ions to form HCl, but not with alkaline metals to form alkali chlorines. With temperature increase, HCl formation tends to decrease [487]. For higher temperatures, a significant part of Cl is released under KCl form and associated to char combustion [487,489,496,497]. After formation and release to the gaseous phase in the combustion system, the alkali chlorines tend to condensate over fly ash particles or heat exchangers [51]. Thus, part of the released Cl during biomass combustion seems to become associated to the solid phase of the exhaust gases, namely fly ashes, or deposited in heat exchangers, while the other part is emitted in the gaseous phase as HCl in the exhaust gas [51].

Due to the close relation between K and Cl, the release behavior and reaction mechanism of these species is dependent on their initial molar ratio present in the biomass [494]. The major Cl compound in biomass is KCl, which is stable in solid phase until temperatures of 700 ºC to 800 ºC are attained [494]; for temperatures lower than 700 ºC to 800 ºC, the vapor pressure of KCl is negligible [494]. Nonetheless, the Cl initially present as KCl can react with functional groups present in the organic matrix of the biomass, leading to release of HCl according to Reaction 6.1 [498]:

$$R - COOH(s) + KCl(s) \rightarrow R - COOK(s) + HCl\ (g) \qquad \text{Reaction 6.1}$$

Jensen et al., [489] suggested that at temperatures between 200 and 400 ºC, the original organic matrix of the biomass is destroyed, and Cl can be released from the solid phase and transferred to a liquid tar phase. Afterwards, Cl is further released to the gaseous phase in the form of HCl (g) or suffers secondary reactions with K on the char surface. Some further release of Cl under the form of HCl might be due to the reaction of KCl with functional oxygenated groups present in the chars, where HCl is released and K is bound to the char matrix. Jensen et al., [489] concluded that by using adequate operating conditions, for example, low heating rates and large reactors, HCl emissions in gaseous phase can be significantly minimized during biomass pyrolysis.

As previously referred, the biomass type has a considerable influence on the Cl emissions [496,497]. Some studies suggest that the percentages of Cl emitted, in relation to the Cl content present in the fuel, are significantly higher for fuels with less Cl content, due to the fact that Cl emissions are conditioned by the number of proton donors, such as carboxyl and phenolic groups [496,497]. Cl-rich fuels, such as wheat, rice, brassica, etc., present limited interaction between the inorganic Cl and the proton donating sites, thus, leading to lower Cl percentage release [496]. The addition of sludges (typically rich in sulfur) modifies the chemistry involved due to the reaction between KCl and sulfur. Thus, a total removal of Cl from the fly ashes is theoretically possible if sulfur exists in sufficient amounts to react with all KCl present (Reaction 6.2 [499]).

$$2\ \mathrm{KCl(g)} + SO_2\mathrm{(g)} + 0.5\ O_2\mathrm{(g)} + H_2\mathrm{O(g)} \rightarrow K_2SO_4\mathrm{(s)} + 2\ \mathrm{HCl(g)} \qquad \text{Reaction 6.2}$$

In the literature, it is also suggested that adding sludges may be beneficial for inhibiting Cl deposits formation due to the following mechanisms [483]:

- S in the sludges may react with K, producing SO_4 and gaseous HCl.
- KCl may be removed by condensation on fly ash particles added with the sludge.
- K in gaseous phase may react with aluminosilicates present in the sludges.
- The deposits may be mechanically removed by the increased ash flows caused by the sludges.

Thus, with sludge addition it can be expected a decrease of Cl emissions in the solid phase and an increase of Cl emissions in the gaseous phase [485] (HCl, e.g. Reaction 6.2). Nonetheless, if the sludges are rich in Ca, Cl retention on ashes might increase while HCl concentration in the exhaust gases decreases. These aspects need to be characterized and studied experimentally.

In this work, the co-combustion process of RFB from eucalyptus with primary sludge (up to 5%wt) and secondary sludge (up to 10 %wt) from wastewater treatment was characterized. The sludge resulted from the wastewater treatment in the PP industry. The influence of the addition of sludge on the overall process and on the exhaust gases composition, with emphasis on Cl emissions, namely present in the solid phase (fly ashes) and in the gaseous phase (HCl), and NO_x emissions, was evaluated. The objective was to properly characterize the impact of the integration of this energy valorization solution for the sludges, on the solids and exhaust gases emissions during the co-combustion operation.

6.1.3 MATERIALS AND METHODS

The experimental infrastructure used in this work is based on the DAO-UA 80 kWth pilot-scale BFB (Section 1.3.1) but was properly updated for the co-combustion of RFB and sludges. The general layout of the updated experimental infrastructure is shown in Figure 6.1. The bottom bed of the

reactor consists of 20 kg of sand (98.3 %wt. SiO_2 content)) with particle size in range 0.250 mm to 1.00 mm; the bottom bed of the reactor has a static height of around 0.24 m above the primary air (fluidizing air) injectors. At typical operating conditions, the expanded (fluidized) bed height level is approximately 0.30 m above the distributor plate; the fluidizing bed height level can be controlled by the discharge bed level at port C in Figure 6.1. The fluidized bed was operated at atmospheric pressure and in bubbling regime, with superficial gas velocity of around 0.28 to 0.30 m/s (depending on the operating conditions), and with average bed temperatures in the range of 800 to 850 ºC. The total combustion air was maintained at 250 NL/min, distributed in 80 % primary air (fluidization) and 20 % secondary air, in order to maintain the bottom bed and freeboard hydrodynamic conditions. The stoichiometry conditions of the combustion process were controlled by continuously monitoring the O_2 concentration in the exhaust gases, and through proper adjustment of the biomass feed, which was maintained between 3 and 4 kg/h.

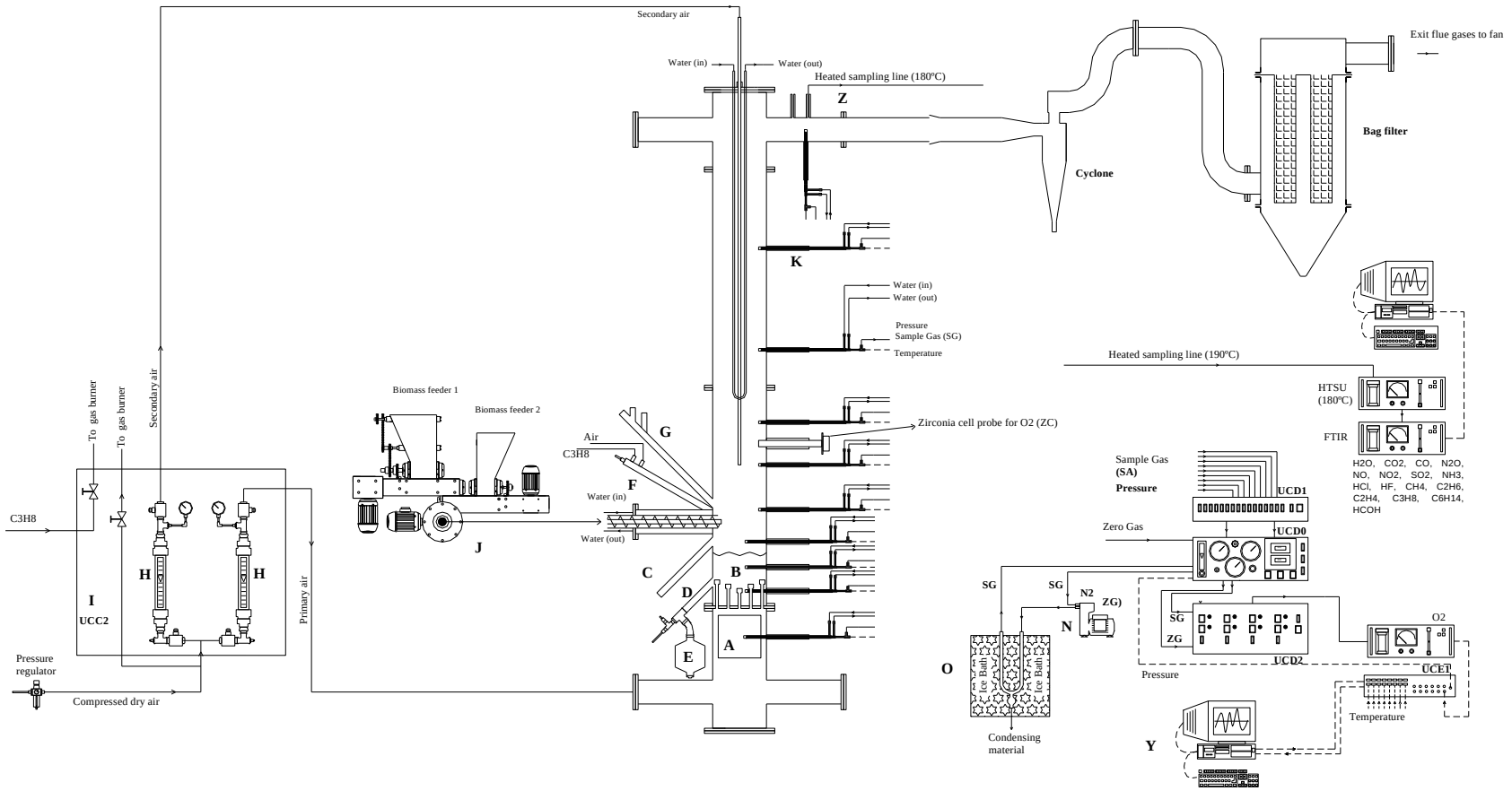

Figure 6.1 – Layout of the experimental infrastructure with the pilot-scale BFB reactor (combustion mode). Dashed line — Electric circuit, Solid line — Pneumatic circuit, A - Primary air heating system, B - Sand bed, C - Bed solids level control, D - Bed solids discharge, E - Bed solids discharge silo, F - Propane burner system, G - Port for visualization of bed surface, H - Air flow meter (primary and secondary air), I - Control and command unit (UCC2), J - Biomass feeder, K - Water-cooled gas sampling probe, , N - Gas sampling pump, O - Gas condensation unit for moisture removal, Y – Computer based control and data acquisition system, Z - Exhaust duct; O2 – Online paramagnetic analyzer for the determination of O_2 (ADC-700), FTIR – Online infrared analyzer for determination of H_2O, CO_2, CO, N_2O, NO, NO_2, SO_2, HCl, NH_3, CH_4, etc., UCD0, UCD1, UCD2 - Electro-pneumatic command and gas distribution units, UCE1 - Electronic command unit.

The monitoring of the operating conditions was performed according to the following methodologies:

1) Characterization of the exhaust gases.
   a) O_2 concentration determination in a paramagnetic analyzer (ADC-700).
   b) H_2O, O_2, CO, CO_2, CH_4, NO, SO_2 and HCl determination through heated sampling and analysis (180 ºC) with measuring principle by FTIR (Gasmet CEM-II).
   c) Total particles concentration determination through isokinetic sampling in quartz filters and their chemical characterization (Cl, Na, K and Ca). The isokinetic sampling for particle concentration determination was performed downstream of a cyclone and, in some cases, downstream of a bag filter located after the cyclone. The content of Cl, K, Na and Ca in the particles present in the exhaust gases (thinner fly ashes) was determined in terms of the content of soluble inorganic ions (Cl^-, K^+, Ca^{2+} and Na^+) by ion chromatography in liquid phase according to the procedure described by Calvo et al., in [500].
2) Characterization of bottom bed ash and fly ash deposited in different locations of the combustion system.
   a) Determination of chemical elements content (Cl, Na, K, Ca, Mg, Al, Mn and P) was performed in an external laboratory following acid digestion and ICP-MS analysis.

6.1.3.1 FEEDSTOCK CHARACTERIZATION

The biomass fuel used included distinct types of chipped RFB derived from eucalyptus (*Eucalyptus Globulus*), different types of pellets produced from distinct fractions of RFB from eucalyptus (branches with leaves, bark, etc.), and mixtures of these types of RFB with primary (up to 5 % wt.) and secondary (up to 10 % wt.) sludges resulting from wastewater treatment processes in the PP industry. The pelletizing process of the RFB from eucalyptus was performed to increase the uniformity of the physical characteristics of the fuel and improve the fuel feeding regularity. The RFB from eucalyptus resulted from two different operations, namely from forestry operations, as for example trees logging, and was named eucalyptus RFB type A, and from industrial operations in the context of the PP industry, namely woodchip production from eucalyptus logs, and was named eucalyptus RFB type B. Both types of RFB were chipped, dried at atmospheric conditions, and sieved to a particle size below 5 mm. All the types of biomass were characterized in terms of properties with interest for thermochemical conversion of biomass (proximate and ultimate analysis, and heating value), as shown in Table 6.1. Some types of biomass were characterized in terms of inorganics composition, as shown in Table 6.2.

Table 6.1 – Characteristics of the different types of biomass used as feedstock in the combustion experiments in the pilot-scale BFB.

	Eucalyptus RFB		Pellets						Sludge	
	Type A	Type B	A	A*	B	C	D	E	Primary	Secondary
Proximate analysis (%wt, db)										
Moisture	11.4	11.8	7.7	10.2	8.3	8.9	8.3	7.9	11.3	20.0
Volatile matter	77.3	80.5	78.3	78.1	78.2	77.1	79.0	77.1	na	na
Fixed carbon	21.5	16.6	16.7	17.5	19.0	15.7	17.7	18.4	na	na
Ash	1.2	2.9	5.0	4.5	2.8	7.3	3.3	4.4	61.5	26.5
Ultimate analysis (%wt, db)										
Ash	1.2	2.9	5.0	4.5	2.8	7.3	3.3	4.4	61.5	26.5
C	49.1	48.2	44.4	46.4	50.6	48.2	50.9	51.4	32.4	36.7
H	6.5	6.2	5.4	5.7	6.2	6.2	6.1	6.1	4.2	5.0
N	0.1	<0.2	0.2	0.7	0.8	<0.2	0.9	1.4	0.5	2.2
S	nd	0.03	0.03	nd	nd	0.03	nd	nd	nd	0.4
O (by difference)	43.2	42.7	44.7	42.3	39.5	38.3	38.6	36.3	1.4	29.0
Cl	0.05	0.05	0.20	0.40	0.14	0.05	0.18	0.38	0.02	0.19

na – not available; nd – not determined, below the detection limit of the method, 100 ppm wt.

Table 6.2 – Concentration of Ca, Na, K, Mg, Al, Mn and P in the ashes from the different types of biomass used as feedstock in the combustion experiments in the pilot-scale BFB.

	Pellets				Sludge	
	A*	B	D	E	Primary	Secondary
Ash elemental analysis				Ppm wt., db		
Ca	8060	6960	7910	9480	245000	106166
Na	635	3920	396	952	4290	nd
K	3240	2750	2610	6310	291	1134
Mg	1730	668	546	1421	1800	1608
Al	367	41.9	63.3	61.2	313	869
Mn	219	139	157	99	168	nd
P	302	289	263	511	3450	2500

nd – not determined.

6.1.3.2 OPERATING CONDITIONS

The operating conditions during the combustion experiments in the pilot-scale reactor were characterized, namely the biomass fuel feed rate, air feed rate, temperature and pressure along the reactor and gas composition at the exit. Table 6.3 shows information regarding the operating conditions and the respective reference of the experiments performed in this work.

Table 6.3 – Combustion experiments reference and respective operating parameters.

Experiment reference	Biomass (%wt.)	Type of RFB	Average bed temperature [ºC]	O_2 (%v, dry gas) in the exhaust combustion gases
EL-0	100% eucalyptus	Eucalyptus RFB type A	804	7.0
EL-0 #2	100% eucalyptus	Diverse pellets	821	8.1
EL-5	5% SS + 95% eucalyptus	Eucalyptus RFB type A	815	7.0
EL-10	10% SS + 90% eucalyptus	Eucalyptus RFB type A	810	6.2
EL-10 #2	10% SS + 90% eucalyptus	Eucalyptus RFB type B	825	7.4
EL-10 #3	10% SS + 90% eucalyptus	Pellets A	837	7.1
EL-10 #4	10% SS + 90% eucalyptus	Pellets B	848	7.2
EL-10 #5	10% SS + 90% eucalyptus	Pellets C	839	6.9
EL-10 #6	10% SS + 90% eucalyptus	Pellets A*	830	5.9
EL-10 #7	10% SS + 90% eucalyptus	Pellets E	828	6.0
EL-10 #8	10% SS + 90% eucalyptus	Pellets A*	836	4.5
ELP-5	5% PS + 95% eucalyptus	Pellets D	837	8.0
ELP-5 #2	5% PS + 95% eucalyptus	Pellets E	819	6.0
ELP-5 #3	5% PS+ 95% eucalyptus	Pellets A*	838	5.5
ELP-5 #4	5% PS + 95% eucalyptus	Pellets E	820	7.9

Legend: PS – Primary sludge; SS – Secondary sludge; Diverse pellets – Different pellets used during the combustion experiment, namely, commercial pine pellets (2h), pellets A (5h) and pellets B (2h); Pellets A – Pellets from eucalyptus bark resulting from operations in the PP industry (sample 1); Pellets A*- Pellets from eucalyptus bark resulting from operations in the PP industry (sample 2); Pellets B – Pellets from eucalyptus branches, resulting from forest maintenance operations, with residual amounts of eucalyptus foliage; Pellets C – Pellets from powdered eucalyptus chips (<1mm) Pellets D – Pellets resulting from eucalyptus RFB type A and type B and eucalyptus foliage; Pellets E – Pellets from powdered eucalyptus branches.

6.1.4 RESULTS AND DISCUSSION

This Section includes results regarding the combustion experiments performed, namely, reactor temperature profiles (with time and longitudinal), combustion exhaust gas composition profiles along time (CO_2, H_2O, HCl, NO, CO and SO_2), chemical composition (Cl, Na, K and Ca) of fly ash present in the exhaust gases, chemical composition (Cl, Na, K, Ca, Mg, Al, Mn and P) of bottom bed ashes and of fly ashes deposited in surfaces along the combustion system.

6.1.4.1 TEMPERATURE PROFILES

The evolution of temperature with time in different locations along the reactor during the combustion of the different mixtures of biomass follows a similar pattern and shows steady-state conditions of operation. These conditions were observed when using only RFB from eucalyptus or mixtures of this biomass with primary (up to 5 %wt) and secondary sludge (up to 10 %wt) (Figure 6.2). The temperature stability, despite the fuel mixtures variability and feeding irregularities caused by the heterogeneous physical characteristics of the RFB, is justified based on the recognized suitable mass and energy transfer characteristics provided by the BFB operation regime [51,69,501]. The bed material allows the absorption, storage and release of thermal energy and its mixing contributes to the existence of uniform temperature in the bottom bed section. Consequently, the biomass is rapidly converted after being fed to the reactor, due to the high heat transfer. In this work, the bed temperature was maintained between 800 and 850 ºC.

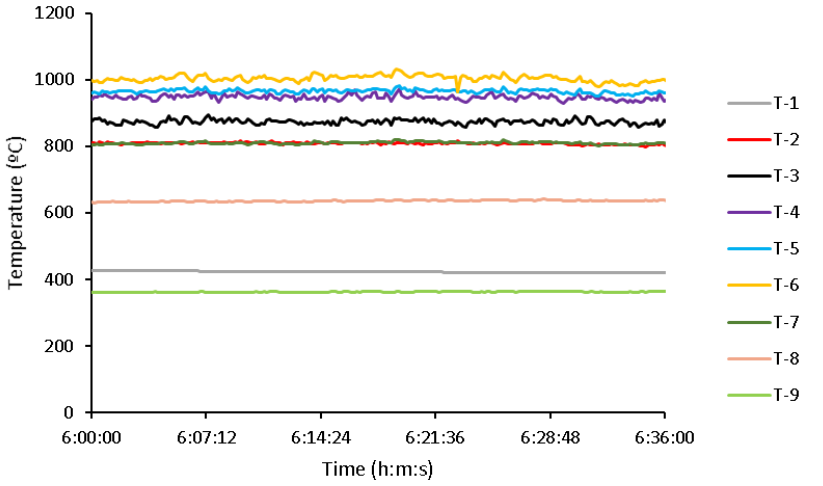

(a)

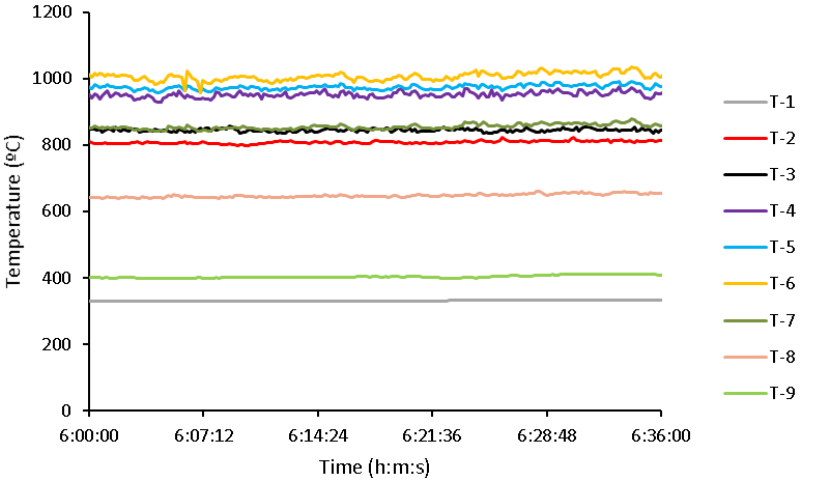

(b)

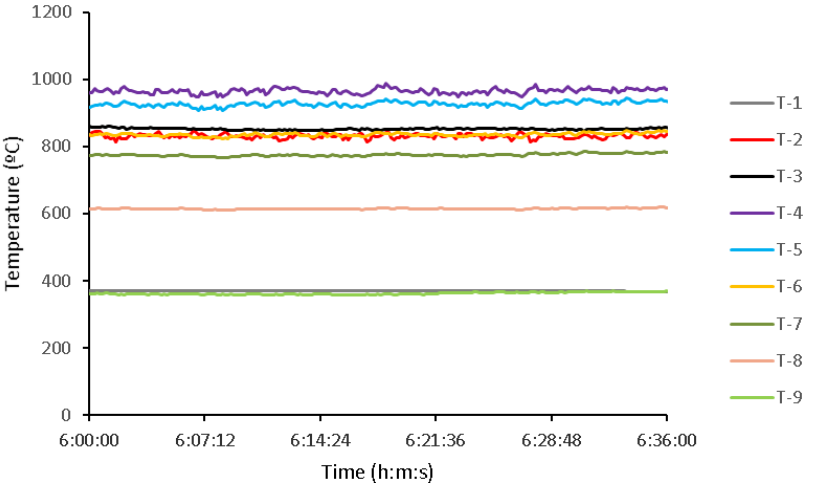

(c)

Figure 6.2 – Typical evolution of the temperature with time at different locations along the reactor height during the combustion experiments: (a) EL-O, (b) EL-10 and (c) ELP-5. Experiments reference according to Table 6.3.

The longitudinal temperature profile for the different combustion experiments performed is shown in Figure 6.3. It is observed that the temperature increases from the inside of the bed to the freeboard zone located immediately above the bed, where the biomass is fed. The maximum temperature is observed close to the secondary air injection. Above this region the temperature decreases with height due to heat losses through the reactor walls, convection with the flue gas and the existence of a heat exchanger (liquid water with a flow rate of 0.6 L/min) located 1 m above the distributor plate (Figure 6.1). Similar to the observation performed regarding the temperature profiles along time, it was observed that the introduction of sludge mixed with RFB did not cause major changes in the longitudinal temperature profile.

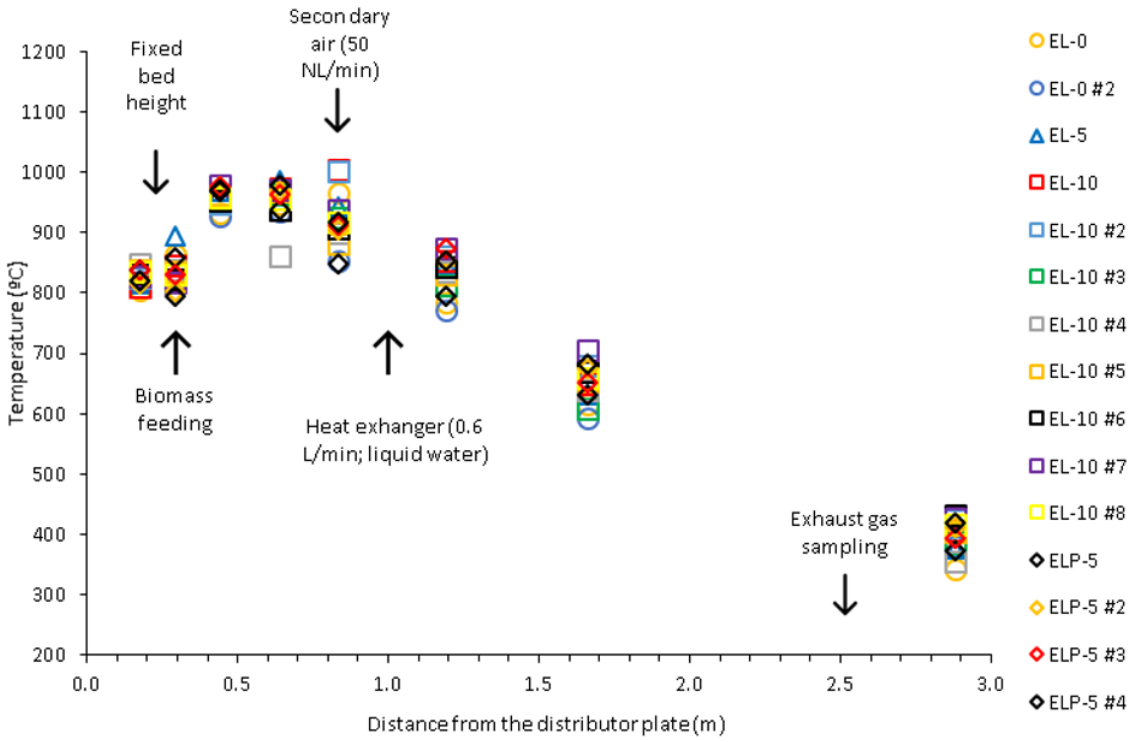

Figure 6.3 – Longitudinal temperature profile in the BFB reactor during the biomass combustion experiments performed. Legend according to experiments references in Table 6.3.

6.1.4.2 GAS COMPOSITION PROFILES

In this Section, it is analyzed the typical concentration profile along time of different gaseous species (CO_2, H_2O, HCl, NO, CO and SO_2) present in the exhaust gases, during the combustion experiments with different biomass mixtures (Table 6.3).

6.1.4.2.1 CO_2 and H_2O

Figure 6.4 shows the typical CO_2 and H_2O concentration profiles for the exhaust gases in the distinct experiments performed. It can be observed that both CO_2 and H_2O show small fluctuations with time which can be justified by irregularities in the biomass feeding rate and the heterogeneous physical and chemical characteristics of the biomass mixtures used. Nonetheless, for long periods of operation, it can be assumed that the system was operating in steady-state conditions in terms of CO_2 and H_2O concentration. CO_2 concentration was typically between 12 and 17 %v (dry gas), which are

typical values of industrial combustion systems [51]. The addition of primary and secondary sludge did not cause any noticeable change in the CO_2 and H_2O concentration profiles.

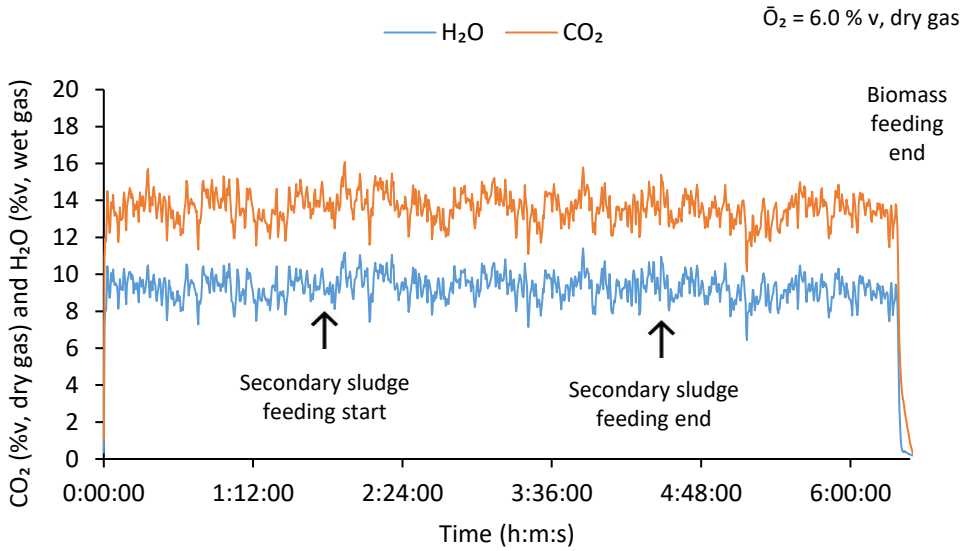

(a)

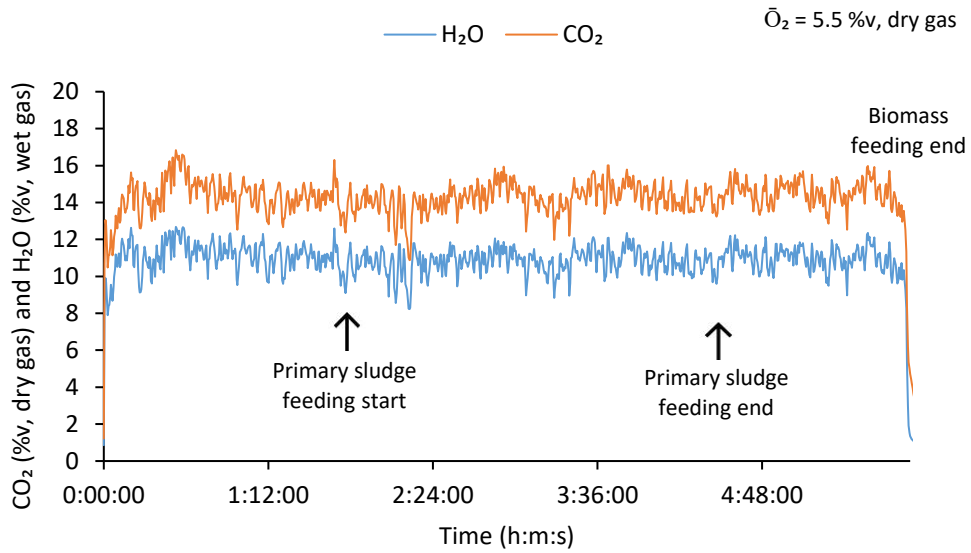

(b)

Figure 6.4 – Typical CO_2 and H_2O concentration with time in the exhaust gases for (a) EL-10 #7 and (b) ELP-5 #3.

6.1.4.2.2 HCl

The HCl concentration profiles along time (Figure 6.5 and Figure 6.6) show a distinct behavior from the other chemical species (e.g., CO_2, H_2O) analyzed. While these species show a concentration that fluctuate around an average value, the HCl concentration increases immediately after the introduction of biomass until attaining a maximum value. Afterwards, HCl concentration decreases with time

until reaching a value that changes only in minor amounts with time. This behavior is more evident in experiments with sludge addition. For these experiments, the addition of sludge to the feedstock mixture caused an immediate decrease of HCl concentration in the combustion flue gases (see Figure 6.5). This can be justified by the sludges high content in ashes rich in CaO (Table 6.2), which acts as adsorbent for acid species such as HCl. In fact, the addition of Ca is recognized as an effective measure for HCl removal in combustion systems [487]. Therefore, sludge addition seems to promote a decrease of the HCl concentration.

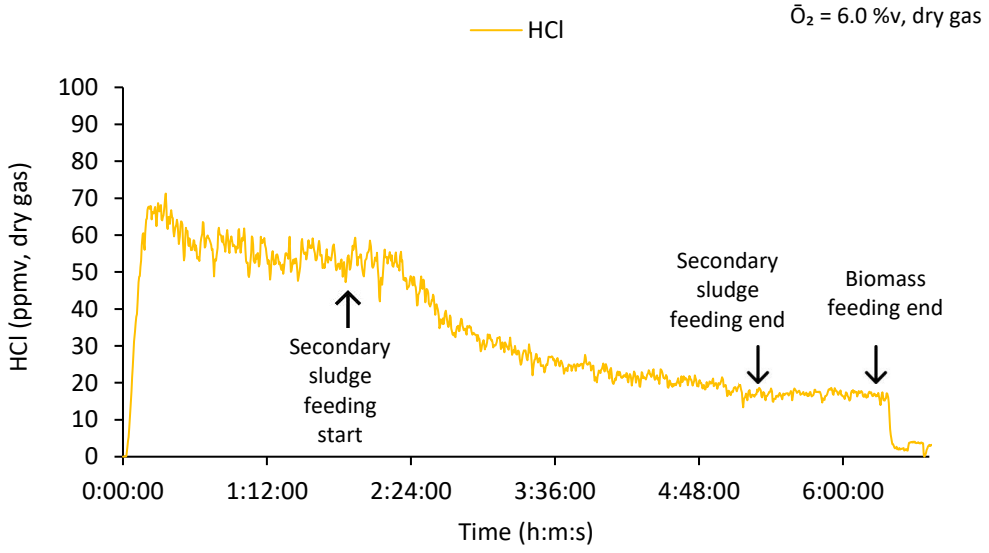

(a)

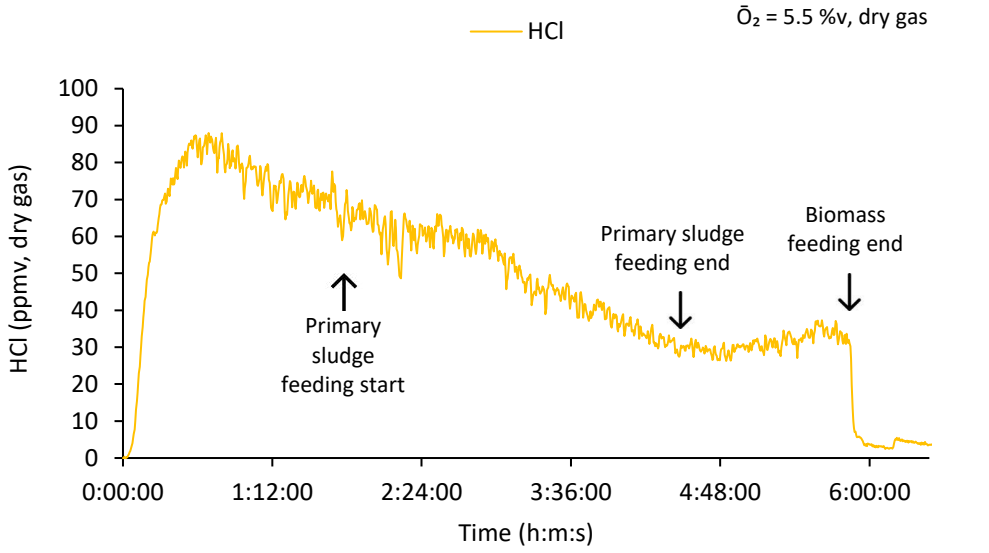

(b)

Figure 6.5 – Typical HCl concentration with time in the exhaust gases for (a) EL-10 #7 and (b) ELP-5 #3. Experiments reference according to Table 6.3.

Despite the analogous conditions of operation obtained for the different combustion experiments performed (e.g., Figure 6.3), it is observed that the HCl concentration presents significant differences

between experiments (Figure 6.6). On one hand, this can be justified by the distinct Cl content present in each type of biomass used as feedstock (Table 6.1). On the other hand, it seems that lower stoichiometric ratios (assumed by lower O_2 concentration in the combustion exhaust gases) tends to contribute to higher HCl concentration in the exhaust gases, being that for the same fuel mixture and bed temperature, lower HCl concentration values were found for lower O_2 concentration in the exhaust gases (e.g., ELP-5 #2 and ELP-5 #4). This needs to be investigated in future works.

It was also observed an effect of the operation time on the concentration of HCl in the exhaust gases (Figure 6.5), i.e., with the increase of operation time, the concentration of HCl in the exhaust gases tended to decrease. This effect might be related to the fact that at the end of each combustion experiment the reactor bed was replaced by a new sand bed. Thus, each experiment started with a clean bed without biomass/sludge ashes. Therefore, it is reasoned that the concentration of HCl might be influenced by the equilibrium between ash accumulation in the bottom bed and their capacity to adsorb HCl. This effect was particularly relevant during combustion experiments where sludge was included in the biomass mixture used as feedstock; the sludge promoted a higher introduction of Ca compounds in the reactor, and thus increased the capacity of the ashes to adsorb HCl.

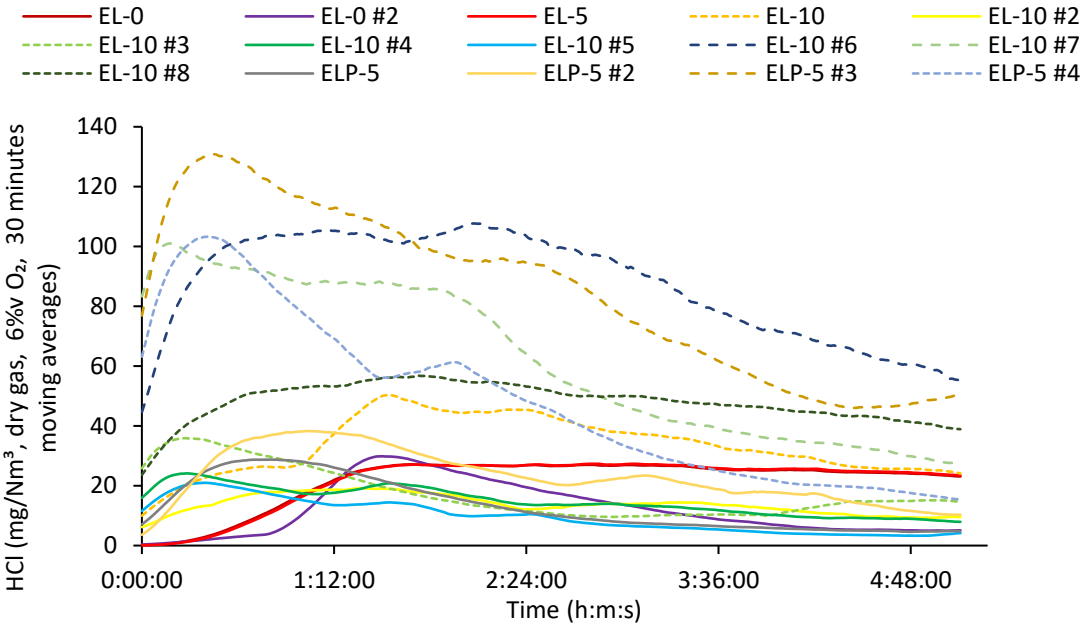

Figure 6.6 – HCl concentration with time (30 minutes moving average) for the distinct combustion experiments performed. Experiments reference according to Table 6.3.

6.1.4.2.3 NO

In Figure 6.7 and Figure 6.8, it can be observed the NO concentration for the different combustion experiments performed and its relation with the primary and secondary sludges addition. The addition of secondary sludge caused a major increase in NO concentration during the combustion of eucalyptus RFB type A (Figure 6.7 (a)). This can be justified by the difference between the nitrogen content present in the secondary sludges in comparison to the RFB from eucalyptus (Table 6.1). Analogous results were obtained for eucalyptus RFB type B (EL-5, EL-10 and EL-10#2). The addition of secondary sludge caused only a slight increase in the average NO concentration during the combustion of pellets from eucalyptus bark (Pellets A and A*), however, it led to the increase of the fluctuation of the NO concentration value (Figure 6.7 (b)). The addition of secondary sludge did not cause noticeable changes in NO concentration during combustion experiments with pellets from

eucalyptus branches (Pellets E, Figure 6.7 (c)). This can be justified by the already relatively high nitrogen content present in this type of biomass (Table 6.1). The addition of primary sludge (up to 5 %wt) does not seem to promote any major change in the concentration of NO for all the experiments performed (Figure 6.7 (d)).

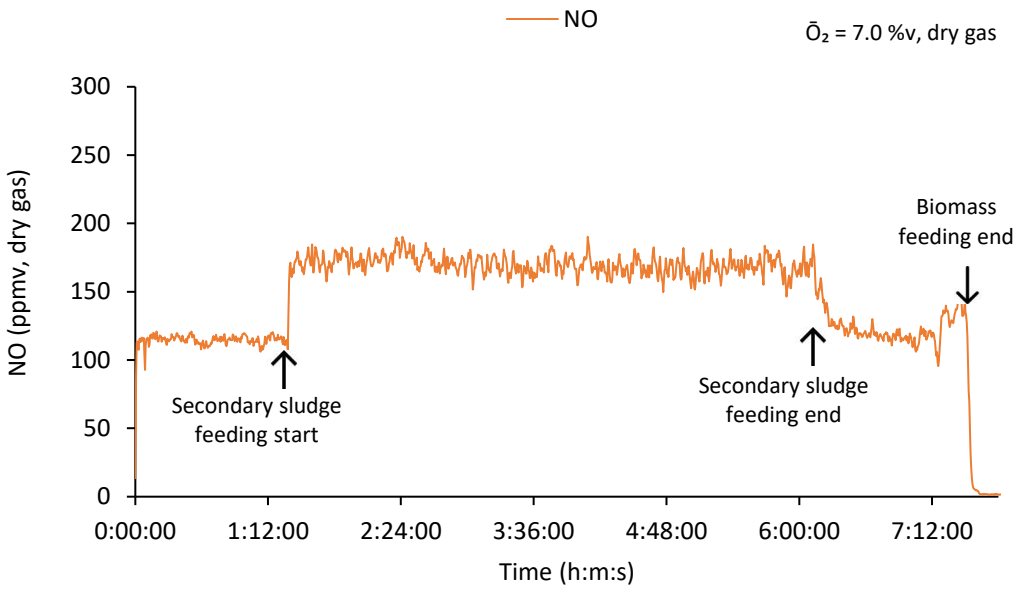

(a)

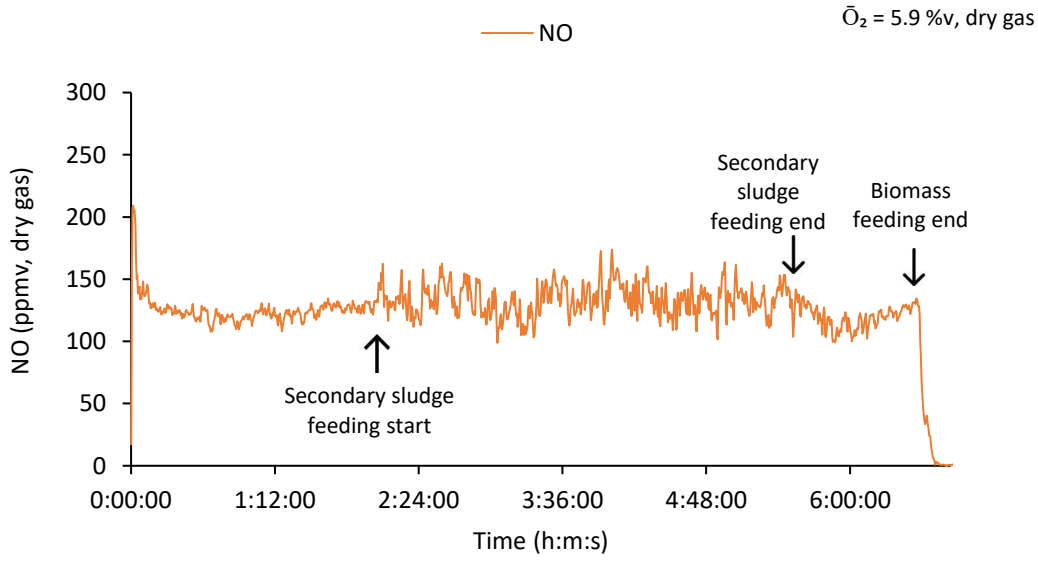

(b)

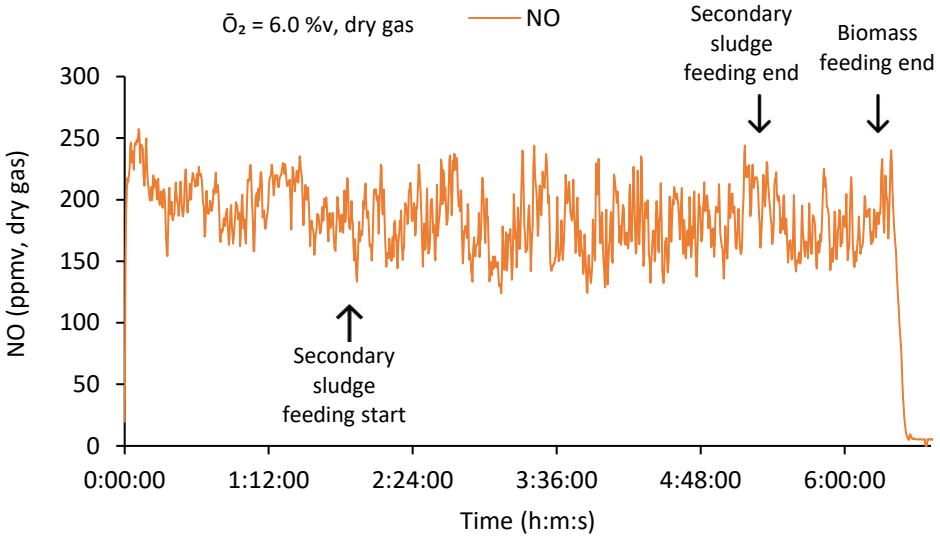

(c)

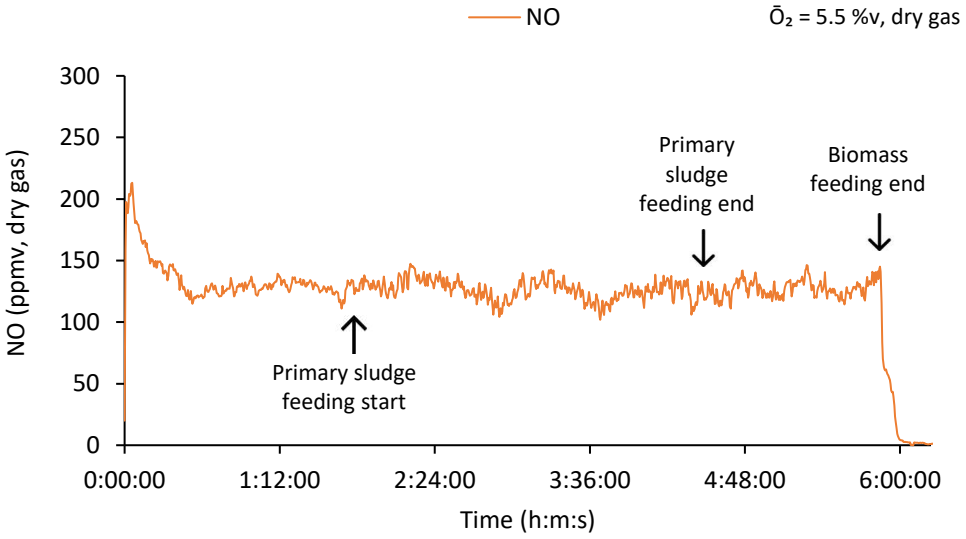

(d)

Figure 6.7 – Typical NO concentration with time in the exhaust gases for (a) EL-10, (b) EL-10 #6, (c) EL-10 #7 and (d) ELP-5 #3. Experiments reference according to Table 6.3.

Thus, in some cases, it was observed that the addition of secondary sludge promoted an increase in NO concentration in the exhaust gases; however, in general, it was not observed a significant difference between the NO concentration values in experiments performed without sludges addition or with sludges addition in the referred mass percentages. Typically, it was observed that the nitrogen content of the biomass has direct influence on the NO concentration in the exhaust gases. NO concentration values expressed as NO_2 (at 6 %v O_2, dry gas) were typically between 215 mg/Nm^3 and 433 mg/Nm^3. The highest values were found during combustion experiments with pellets from eucalyptus branches, which is justified by the higher nitrogen content present in this biomass (Table 6.1). For comparison, the values obtained for the NO concentration in these experiments were plotted

against the ELV referred in the Best Available Technologies (BAT) reference document for Large Combustion Plants [502] (180 mg/Nm^3, 6 % O_2) in Figure 6.8. It is observed that the experimental values obtained are always above the referred limit.

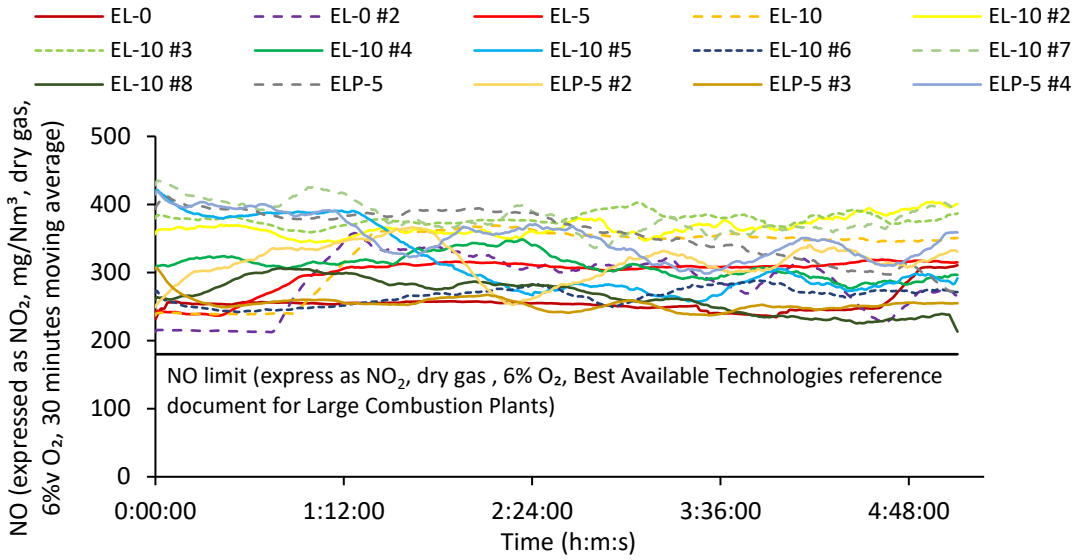

Figure 6.8 – NO concentration with time (30 minutes moving average) for the distinct combustion experiments performed and comparison with the limit value referred on the BAT reference document for Large Combustion Plants [502]. Experiments reference according to Table 6.3.

6.1.4.2.4 CO

In general, it is observed that the concentration of CO in the exhaust gases is below the emission limit value (ELV) (500 mg/Nm^3, 11 % O_2, Figure 6.9 (a)) imposed for biomass boilers in the Portuguese legislation (in Portaria n.º 677/2009 [503], Portaria n.º 190-B/2018 [504] does not include CO ELVs). Nonetheless, during some experiments the CO concentration value exceeded the ELV (e.g., EL-10# 2, Figure 6.9 (b)). This is related to significant biomass feeding fluctuations caused by the heterogenous physical characteristics of the biomass used as feedstock in these experiments. Sludge addition did not promote any visible change in CO concentration.

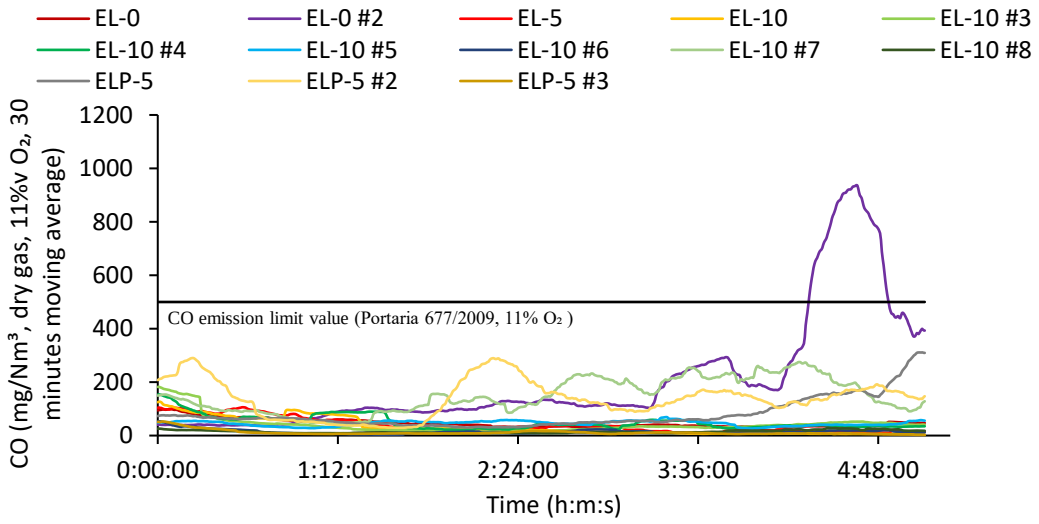

(a)

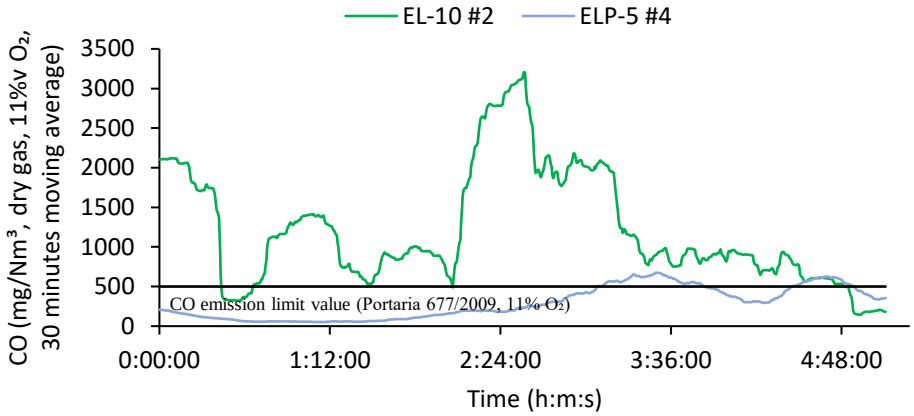

(b)

Figure 6.9 – CO concentration with time (30 minutes moving average) for the distinct combustion experiments performed and comparison with the limit value referred to biomass boilers in the Portuguese legislation, in Portaria 677/2009 [503]: (a) experiments with lower CO concentration values and (b) experiments with higher CO concentration values. Experiments reference according to Table 6.3.

6.1.4.2.5 SO_2

It is observed that SO_2 concentration values are relatively low (Figure 6.10), which results from the relatively low concentration of sulfur present in the biomass used as feedstock (Table 6.3). It is also observed that the addition of sludge did not cause any significant change on the SO_2 concentration profiles, even though the secondary sludges have higher sulfur content than all the types of RFB from eucalyptus tested. This behavior may result from the fact that the sludge incorporation (up to 10 %wt) is not high enough to influence SO_2 concentration in the exhaust gases. Furthermore, these sludges have a high Ca content, which can cause retention of SO_2 on ashes [499]. The highest concentration value of SO_2 found was 17.2 mg/Nm^3 (dry gas, 11 % O_2) during experiment EL-10, which is significantly lower than the ELV (500 mg/Nm^3, 11 %O_2, Figure 6.10) referred for biomass boilers in the Portuguese legislation (in Portaria n.º 677/2009 [503], Portaria n.º 190-B/2018 [504] does not stipulate O_2 reference value for SO_2 concentration ELV).

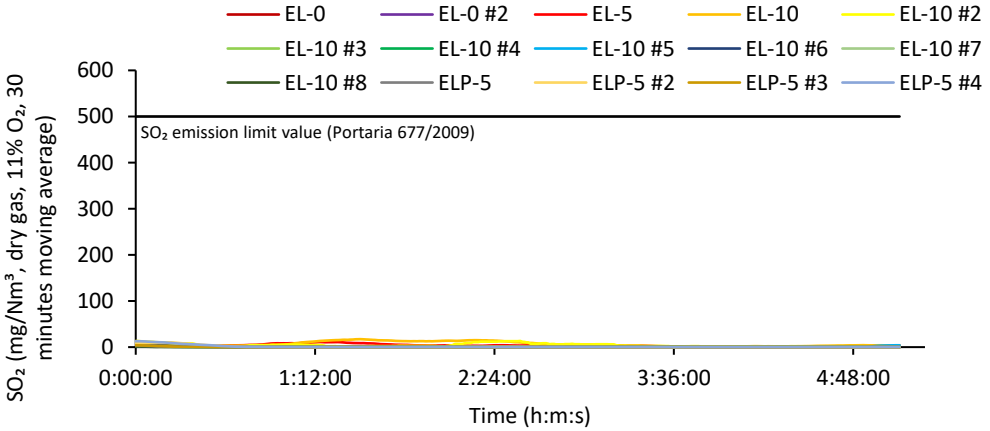

Figure 6.10 – SO_2 concentration along time (30 minutes moving average) for the distinct combustion experiments performed and comparison with the limit value referred to biomass boilers in the Portuguese legislation, in Portaria 677/2009 [503]. Experiments reference according to Table 6.3.

6.1.4.3 PARTICULATE MATTER ANALYSIS

6.1.4.3.1 Fly ashes in the exhaust gases

In this Section, the average particle concentration and composition (Cl, K, Ca, and Na) in the exhaust gases during the co-combustion experiments performed is presented and analyzed.

The average particle concentration in the exhaust gases during each combustion experiment performed is shown in Figure 6.11. It is typically observed lower particle concentration in experiments with chipped RFB from eucalyptus (EL-0, EL-5, EL-10 and EL-10 #2) than in experiments performed with pellets produced from fractions of RFB from eucalyptus (EL-0 #2, EL-10 #3, EL-10 #4, EL-10 #5, EL-10 #6, EL-10 #7, EL-10 #8, ELP-5, ELP-5 #2, ELP-5 #3 and ELP-5 #4). In part, this is justified by the lower ash content of the chipped RFB (Table 6.1); bark and leaves typically have higher ash content than fractions of wood. In fact, combustion experiments of pellets from eucalyptus bark (EL-10 #6, EL-10 #8 and ELP-5 #3) and pellets from eucalyptus branches (Pellets E, EL-10 #7, ELP-5 #2 and ELP-5 #4) presented particle concentration significantly higher than other combustion experiments with other types of pellets. Nonetheless, the co-combustion experiment performed with the biomass feedstock with highest ash content (Pellets C, EL-10 #5) did not present higher fly ash concentration in the exhaust gases. Thus, other factors apart from the ash content of the biomass may have influenced the formation of fly ash, such as the physical characteristics of the pellets (e.g., density and hardness) and the chemical composition of the ashes [505]. Future works should address this behavior.

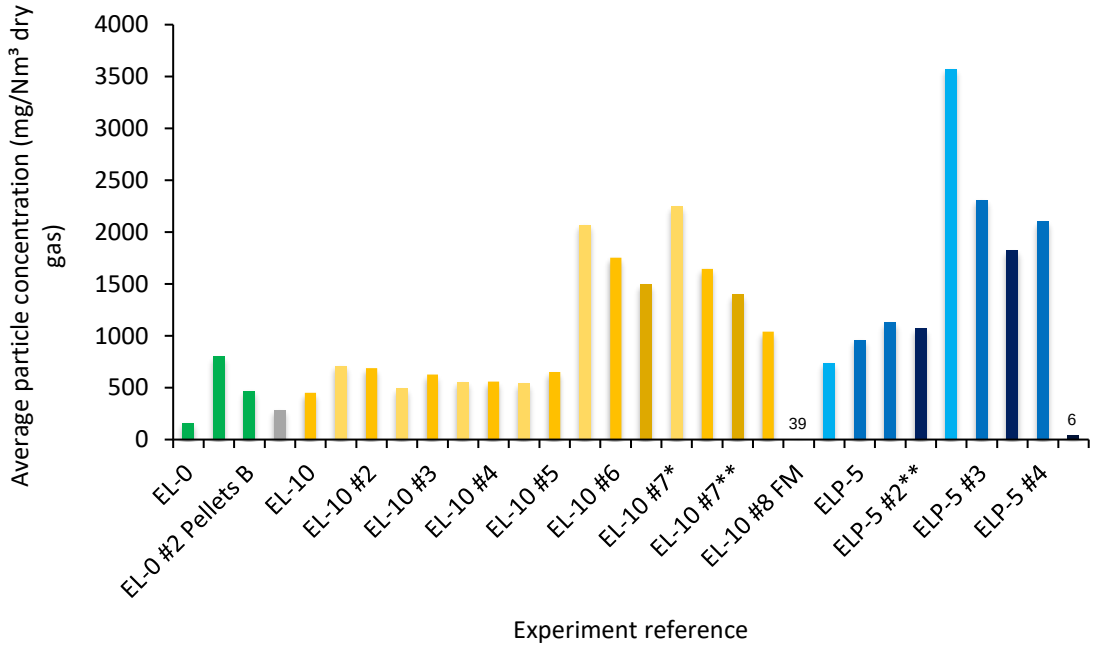

*- Only RFB, before introducing sludge.

**- Only RFB, after the co-combustion process of sludge with RFB.

FM- gas sampling after the bag filter.

Figure 6.11 – Average particle (fly ash) concentration in the exhaust gases during the combustion experiments. The gas sampling was performed after the cyclone, except for references with FM, where the gas sampling was downstream of the bag filter. Experiments reference according to Table 6.3.

Two main observations can be made regarding the effect of the addition of primary and secondary sludge on the particle concentration in the exhaust gases. In some cases, the sludge addition seems to promote a small increase of the particle concentration (e.g., EL-10 #3 and ELP-5), which is justified by the higher ash content present in the sludge in comparison to the RFB from eucalyptus (Table 6.1). In other cases, it was observed the opposite, i.e., the decrease of particles concentration after the addition of sludge (e.g., EL-10 #6, EL-10 #7 and ELP-5 #3). Nonetheless, in these experiments, when the sludge feeding ended, the particles concentration continued to decrease. The justification for this phenomenon may be related to the high content of Ca present in the ashes retained in the bed and on the exhaust duct, which may have prevented the formation of thinner fly ashes. In fact, the major components present in the fly ashes from the exhaust gases are Cl and K (Figure 6.12), whereas Ca was found as the major element in the composition of bottom bed ashes and ashes deposited in inner surfaces of the combustion system (Figure 6.15). This will be discussed in the following Section. Similar results were observed in other works regarding co-combustion of RFB with sludge from the PP industry [499].

K concentration (Figure 6.12) in the fly ashes was typically higher for experiments with pellets from eucalyptus bark (e.g., Pellets A*, EL-10 #6, EL-10 #8 and ELP-5 #3) and pellets from eucalyptus branches (Pellets E, EL-10 #7, ELP-5 #2 and ELP-5 #4). Furthermore, a linear correlation between K and Cl concentration was found for the particle matter in the exhaust gas (Figure 6.13 (a)). This relation is close to the mass ratio 1:0.91 for K:Cl in the compound KCl, which indicates that a significant part of Cl in the fly ashes present in the exhaust gases might be in the form of KCl, as suggested by some other works [51].

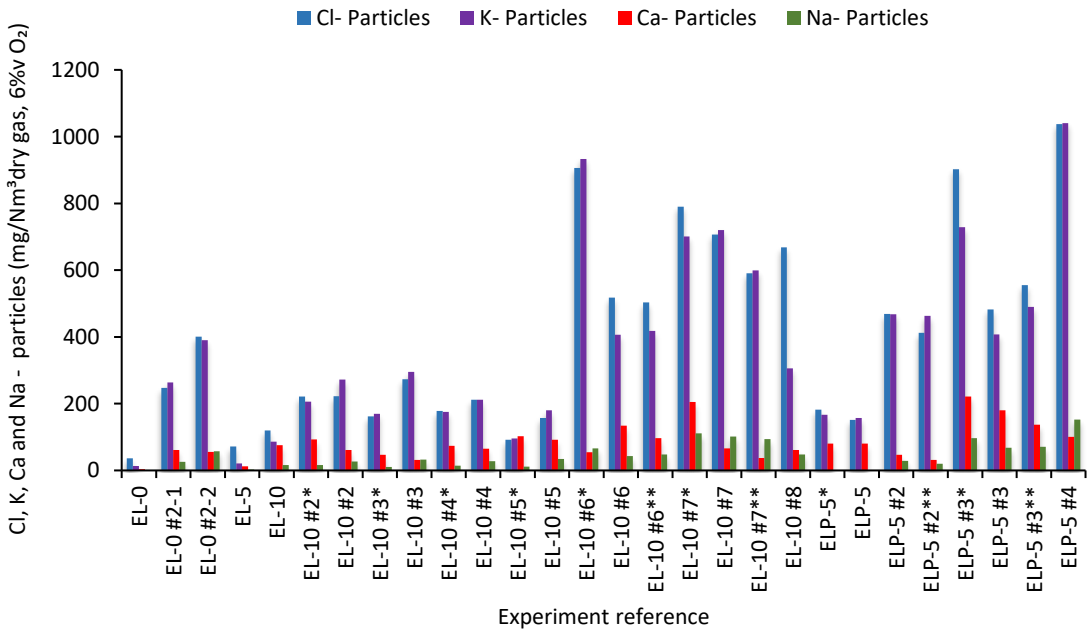

*- Only RFB, before introducing sludges.

**- Only RFB, after the co-combustion process of sludges with RFB.

Figure 6.12 – Average Cl, K, Ca and Na concentration emitted associated with the fly ashes present in the exhaust gases during the combustion experiments. These elements were measured as ion Cl^-, K^+, Ca^{2+} and Na^+, and expressed as mg chemical element/Nm^3 dry gas, corrected to 6 %v O_2. Sampling was performed downstream of the cyclone (Figure 6.1). Experiments reference according to Table 6.3.

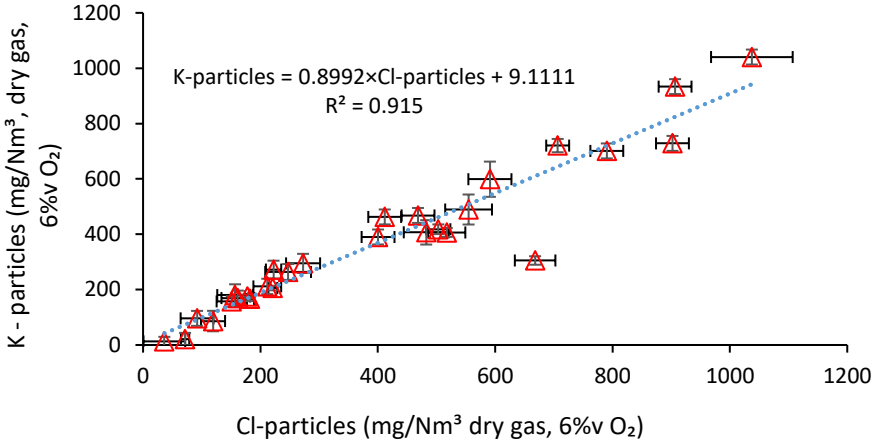

(a)

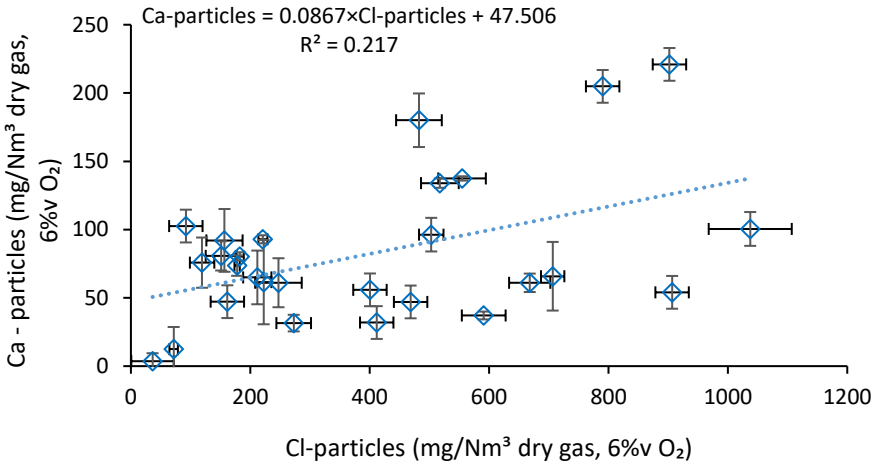

(b)

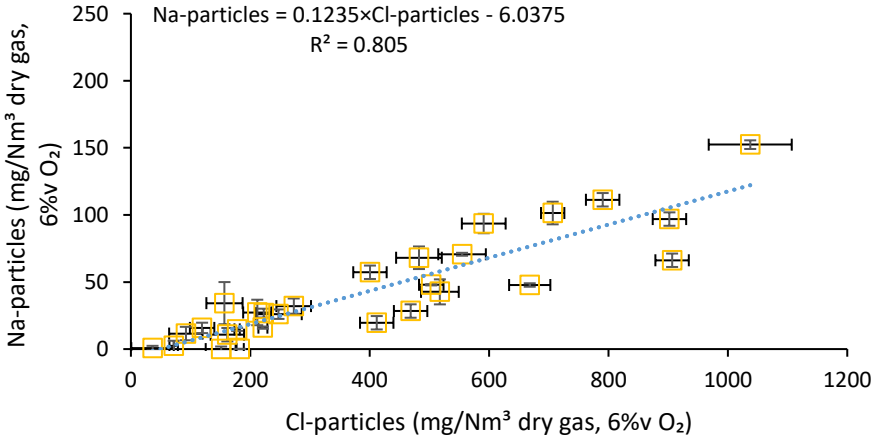

(c)

Figure 6.13 – Relation between the content of K, Ca and Na with Cl in the fly ashes present in the exhaust gas during the combustion experiments: (a) K and Cl, (b) Ca and Cl and (c) Na and Cl.

Ca and Na concentration values in the fly ashes present in the exhaust gases (Figure 6.12) are significantly lower than the K and Cl concentration values. Furthermore, even though Ca has the capacity to remove Cl in gaseous effluents [506], only a weak relationship between Ca and Cl in the fly ashes was observed (Figure 6.13 (b)). The relatively low concentration value found for Ca in the fly ashes is in contrast with that found for the bottom bed ashes and ashes deposited in inner surfaces of the BFB reactor (Figure 6.15, next Section). In fact, Ca is the main alkali element present in the ashes from the RFB and sludges used (Table 6.2). The Na concentration in the fly ashes present in the exhaust gases is lower than Ca, however, it is observed a stronger linear relation between the mass concentration of Na and Cl (Figure 6.13 (c)). Nonetheless, this relation is significantly lower than the mass ratio of 1:1.5 for Na:Cl present in the compound NaCl. In summary, it is observed that the mass concentration of chemical elements in the fly ashes sampled in the exhaust gases during the combustion experiments shows the following decreasing order of abundance: Cl > K > Ca > Na.

In Figure 6.14, it is shown the contribution from the gaseous phase (measured as HCl) and the particulate phase (fly ashes present in the exhaust gases) to the emission of Cl during the combustion experiments. It is observed that the concentration of Cl (quantified as the chlorine ion Cl^-, by ion chromatography) in the solid phase (associated to fly ashes in the exhaust gases and denoted as Cl-particles in Figure 6.14) is higher than in the gaseous phase (associated to HCl and denoted as Cl-HCl in Figure 6.14) for the combustion experiments performed. It is also observed that the Cl emissions for both solid and gas phases are related to the Cl content in the biomass mixture used as feedstock. For example, experiments with pellets from eucalyptus bark (e.g. Pellets A*, EL-10 #6, EL-10 #8 and ELP-5 #3) or eucalyptus branches (Pellets E, EL-10 #7, ELP-5 #2 and ELP-5 #4), which have a high Cl content (Table 6.1), caused higher average emissions of Cl in both solid and gaseous phase (Figure 6.14). Similar to the observations made regarding Cl concentration in the gaseous phase (HCl), discussed in the previous Section, the addition of sludge seems to have caused a decrease of Cl concentration in the fly ashes present in the exhaust gases (e.g. EL-10 #2, EL-10 #6, EL-10 #7, ELP-5 and ELP-5 #3), which can be related to the Ca present in the sludge ashes and the respective adsorption of Cl by heavier particles retained in the BFB, e.g., in the bottom bed; however, some exceptions were observed that must be accounted (EL-10 #3, EL-10 #4 and EL-10 #5). This phenomenon should be addressed in future works.

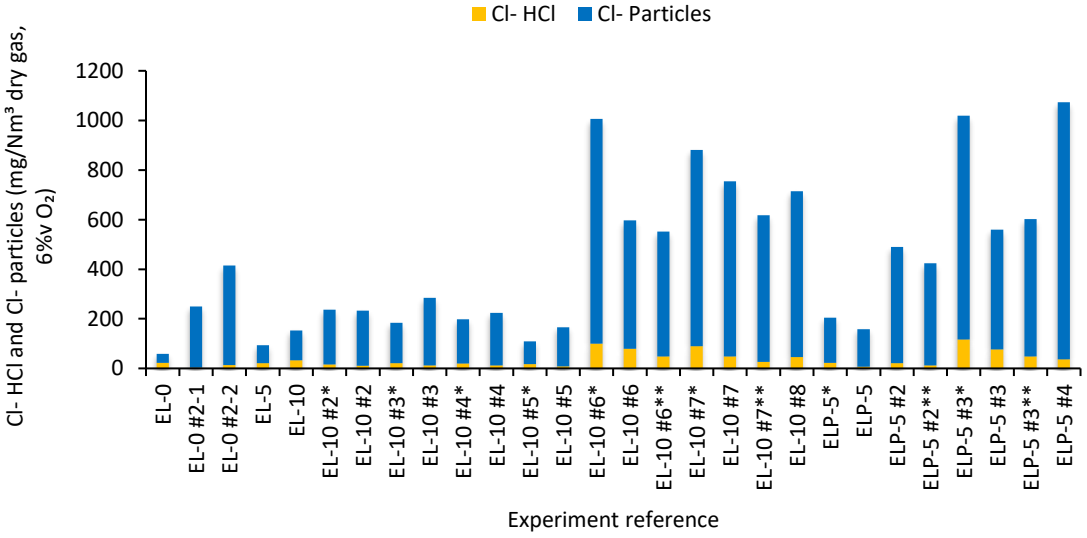

Figure 6.14 – Average Cl concentration in the solid phase, measured as ion Cl^- in fly ashes (denoted as Cl-particles), and expressed as mg Cl/Nm^3 dry gas corrected to 6 %v O_2, and in gaseous phase (denoted as Cl-HCl), measured as HCl in the flue gas and expressed as mg Cl/Nm^3 dry gas corrected to 6 %v O_2, in the exhaust gases during the combustion experiments. Sampling was performed downstream of the cyclone (Figure 6.1). Experiments reference according to Table 6.3.

6.1.4.3.2 Bottom bed ashes and fly ashes deposited along the combustion system

In this Section, results regarding the chemical characterization (Ca, K, Mg, P, Na, Al, Mn and Cl) of samples of bottom bed ashes and fly ashes deposited along the combustion system are presented and analyzed. The chosen locations of the combustion system for sampling the ashes were the bottom bed surface layer, the reactor walls above the distributor plate, a cold (liquid water cooling) deposition probe located 2.2 m above the distributor plate, the bottom of the horizontal exhaust duct of the reactor and the ash retained in the cyclone located downstream of the BFB reactor. The ashes were sampled after the experiments with reference EL-10 #4, EL-10 #6, EL-10 #7, ELP-5 #3 and ELP-5 #4 (Table 6.3). The average concentration values (Ca, K, Mg, P, Na, Al, Mn and Cl) found are shown in Figure 6.15.

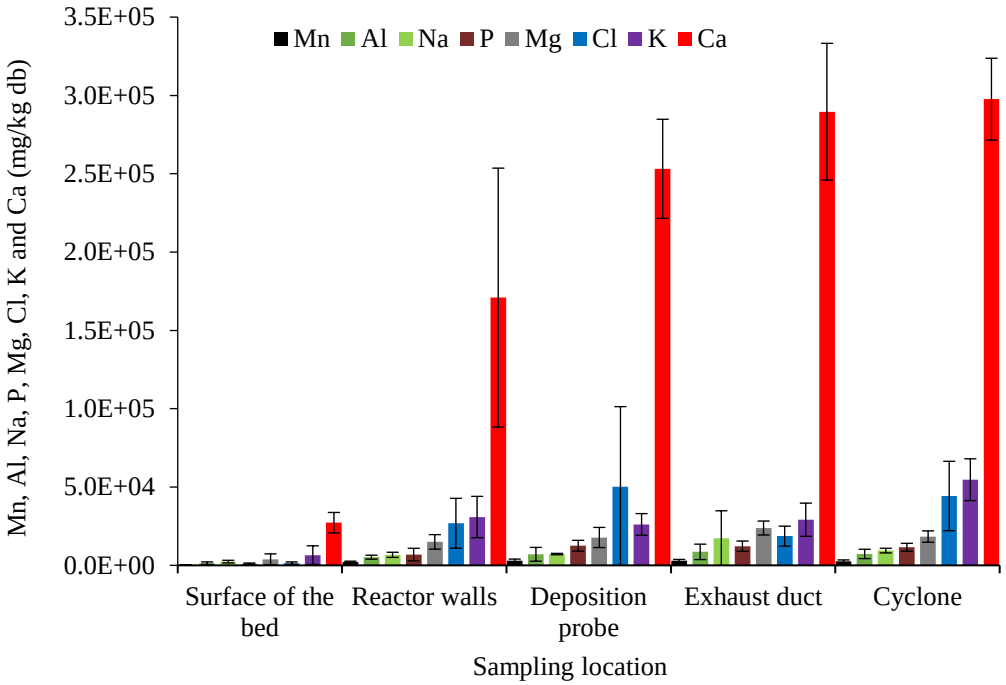

Figure 6.15 – Average composition (Ca, K, Mg, P, Na, Al, Mn and Cl) (and respective standard deviation) of the ashes deposited or settled in different locations of the combustion system.

It is observed that Ca is present in significantly higher concentration in the different ash samples than the other analyzed elements (Figure 6.15). This results from Ca being the main chemical element present in the ashes for both RFB from eucalyptus and sludges (Table 6.2). Regardless of the sampling location, the average concentration of chemical elements on the ashes is by descending order of abundance: Ca>K>Cl>Mg>P>Na>Al>Mn. This composition is distinct from that observed for the fly ashes in the exhaust gases, where K and Cl were the main chemical elements (Figure 6.12). Nevertheless, K and Cl are still present in relatively high concentration in the bottom bed ashes and deposited ashes along the reactor surfaces. These elements are associated with corrosion processes [51,492,493,499,507], thus, their retention in the bottom bed ashes is desired. In fact, co-combustion of RFB with sludge from the PP industry has been referred as beneficial to prevent corrosion from compounds derived from Cl and K [482–484,499], which could be related to the high Ca content of the ashes.

The concentration of the analyzed chemical elements in the bottom bed ashes is significantly lower than in the fly ashes deposited in other locations of the combustion system. This is justified by the fact that even after the combustion process, the bottom bed particle samples are composed mainly of the original sand (98.3 %wt of SiO_2) and silicon was not analyzed. Nonetheless, the sum of the

average concentration of the analyzed chemical elements on the particle samples collected at the surface layer of the bottom bed is around 4.4%wt., which means that the sand from the bed is enriched with typical elements from the ashes of the biomass.

Accordingly, it is observed a trend for the increase of the concentration of the analyzed chemical elements with the increase of the distance to the distributor plate. Furthermore, the maximum concentration value for these analyzed chemical elements was typically found in the ashes collected on the exhaust duct or the cyclone. Some exceptions observed are: experiment EL-10 #4 where Cl concentration decreased from the surface of the bed to the exhaust duct and experiment EL-10 #7 where the highest Cl concentration value was found in the ashes collected in the deposition probe located at the top of the combustion chamber. In fact, the maximum average Cl concentration value was found in the ashes collected on the deposition probe. It was also found that the average sum of chemical elements analyzed (Na, K, Mg, Al, Mn, P, Ca and Cl) in the ashes collected in the deposition probe and exhaust duct was 40.2 % and 44.6 %wt db, respectively. This shows that the fly ashes deposited along the reactor are significantly enriched in typical elements of biomass inorganics, which in industrial scenarios may lead to relevant corrosion issues.

Thus, the excess Ca introduced through the sludge addition seems to have caused a higher retention of Cl in the bottom bed ashes and fly ashes deposited on solid surfaces exposed to the exhaust gases. This might justify the reduction in HCl concentration in the exhaust gases observed with the addition of sludge, which was previously discussed.

6.1.5 CONCLUSIONS

The objective of this work was the evaluation of the co-combustion process of RFB from eucalyptus with primary (up to 5 %wt) and secondary (up to 10%wt) sludge from the PP industry in a pilot-scale BFB reactor, with emphasis on NO and Cl related emissions.

The continuous monitoring of the operating parameters, such as temperature and exhaust gas composition along time in the BFB, during the co-combustion process of the different mixtures of RFB and sludge, showed that the reactor was operating under steady-state conditions.

Regarding the composition of the exhaust gases, a continuous HCl concentration decrease with time until reaching an almost constant value was observed during the combustion process. This behavior can be related to the Cl retention promoted by the alkaline elements present in the biomass, such as Ca and K. In fact, sludge addition typically caused a decrease in the concentration of HCl in the exhaust gases, which can be related to the high content of alkaline elements present in the sludge (e.g., Ca).

Regarding NO concentration in the exhaust gases, it was observed that it is mainly influenced by the characteristics of the feedstock used. It was also observed that the addition of sludge to RFB with low N content (e.g., eucalyptus wood chips) caused a significant increase in NO concentration during the combustion process. On the other hand, addition of sludge to RFB with high N content (e.g., eucalyptus bark) did not seem to promote any noticeable increase in the NO concentration. For all the combustion experiments performed, the NO concentration (expressed as NO_2) values found in the exhaust gases met the stipulated ELV for biomass furnaces in the Portuguese legislation (Portaria 677/2009 [503]), but are above the ELV indicated in the BAT reference document for Large Combustion Plants [502].

Regarding CO concentration in the exhaust gases, it was observed that it is immensely influenced by the regularity of the biomass feeding and that sludge introduction in the fuel mixture did not seem to promote any noticeable changes. Furthermore, by using an adequate control of the feeding conditions and an appropriate stoichiometric ratio, it was possible to meet the stipulated ELV for CO

concentration in the exhaust gases from biomass furnaces according to the Portuguese legislation (Portaria 677/2009 [503]).

Regarding SO_2 concentration in the exhaust gases, it was observed that this value was significantly lower than the ELV stipulated for biomass furnaces in the Portuguese legislation (Portaria 677/2009 [503]). Furthermore, sludge addition to the fuel mixture did not cause a noticeable increase in the concentration of SO_2.

Regarding the fly ashes particles emitted with the exhaust gases, it was observed that Cl and K were the major inorganic chemical elements present in the fly ashes. It is reasoned that these two elements might be in the form of KCl, due to the observation of a linear relation between Cl and K with a mass ratio K:Cl close to 1:0.91. It was also observed that the mass of Cl emitted in the particulate phase was significantly higher than that emitted in the gas phase as HCl.

The characterization of the bottom bed ashes and ashes deposited in inner surfaces along the combustion system, considering the chemical elements Ca, K, Mg, P, Na, Al, Mn and Cl, showed that the average concentration of chemical elements in the sampled ashes is (by decreasing order of abundance) Ca>K>Cl>Mg>P>Na>Al>Mn, regardless of the location of the sampling point. This knowledge is relevant to understand the potential negative effects that ashes can cause on combustion equipment, such as slagging and fouling, and upon the environment after emission to the atmosphere.

Thus, this work demonstrates the potential of the co-combustion of RFB from eucalyptus with primary or secondary sludge in BFB. Except specific cases, it was not found a significant increase of NO, CO or HCl emissions with the addition of sludge to the fuel mixture. In fact, the addition of sludge typically promoted a decrease of HCl concentration in the exhaust gases, which can be related to Cl retention in Ca rich ashes. Nonetheless, for RFB from eucalyptus with low N content, the addition of sludge to the fuel mixture led to higher NO emissions. Furthermore, the high inorganic content present in the sludge can originate a significant increase in the amount of ash production. The accumulation of these ashes along time and along the combustion system (e.g. heat exchangers), can promote operational problems, such as the decrease of the process efficiency, increase of maintenance operation needs and equipment damage. This must be investigated in future works.

7 TECHNO-ECONOMIC ANALYSIS OF DIRECT BIOMASS GASIFICATION

This Chapter is composed by Article XII, named "Biomass direct gasification for electricity generation and natural gas replacement in the lime kilns of the pulp and paper industry: A techno-economic analysis". This Article performs a comparative techno-economic analysis for the integration of biomass gasification in the PP industry for electricity generation and for the replacement of the natural gas used in the lime kilns and is currently submitted in the Energy Journal. In this Article, D.T. Pio had the role of co-author (see List of publications), which is in contrast with all the other Articles (Articles I to XI) present in this PhD thesis document, where D.T. Pio had the role of first author and was the main contributor (e.g., Methodology, Investigation, Validation, Formal analysis, Writing – Original Draft, Writing – Review & Editing, Visualization, Supervision). Accordingly, this Chapter presents a slightly distinct structure and organization in comparison with the other Chapters of this document. For example, specific methodology and nomenclature Sections are included in this Chapter.

7.1 ARTICLE XII - BIOMASS DIRECT GASIFICATION FOR ELECTRICITY GENERATION AND NATURAL GAS REPLACEMENT IN THE LIME KILNS OF THE PULP AND PAPER INDUSTRY: A TECHNO-ECONOMIC ANALYSIS

7.1.1 ABSTRACT

This study aims to present a comparative techno-economic analysis of the integration of biomass gasification for the generation of PG for electricity generation and to replace natural gas in the lime kilns of the PP industry. Three possible configurations of the process were analyzed, including generation of electricity, generation of heat and co-generation of electricity and heat. The process chosen was the direct (air) gasification of RFB from eucalyptus, resulting from logging activities in the context of the PP industry, in BFBs. The analysis is based on review reports, evaluation of the existing literature on investment projects in biomass power plants and experimental investigation. An economic model was developed that combines the NPV, IRR and PBP. The main results of the energy analysis show that the net electricity generation (cases I and III) is greater than 70.00 GWh/year, while the production of CaO by direct combustion of PG in the lime kiln (cases II and III) is 82.12 kt/year; a global efficiency between 21.70 and 34.17 % was achieved. The results predict the viability of the project due to a positive NPV of between 0.50 to 6.61 M€, an IRR between 8.99 to 9.78 % and PBP of between 19.16 to 21.22 years. The sensitivity analysis yielded quite favorable investment projections given the low probability that the NPV will reach negative values. The NPV of the project is considerably more sensitive to the sale price of electricity and the efficiency of the gasification system for the scenarios with electricity generation, while for the scenario of thermal energy generation, the NPV is more sensitive to the price of natural gas and the purchase price of the RFB.

Keywords: Techno-economic analysis; Gasification; Biomass; Bubbling fluidized bed; PP industry.

7.1.2 NOMENCLATURE

A	Last year with a negative cumulative NPV, years
B	Absolute value of cumulative NPV at the end of that year, €
C	Costs, €
CFAT	Cash flows after taxes, €
CFBT	Cash flow before taxes, €
Cp	Specific heat capacity, kJ/kg.K
D	Total annual cash flow during the year after, €
DEP	Depreciation, €
$\dot{E}$	Energy flows, kW
$\dot{Ep}$	Electricity power, kW
h	Enthalpy, kJ/kg
I	Initial investment, €
IR	Inflation rate, %
LHV	Lower heating value, kJ/kg
$\dot{m}$	Mass flow, m/s
N	Plant lifetime
$\dot{Q}_G$	Losses, kW
r	Discount rate, %
t	Time, years
t	Tons, t
TXI	Taxable Income, €
TXR	Tax Rate, %
ΔT	Temperature variation, K
η	Efficiency, %

Subscripts	
CC	Combined cycle
EG	Exhaust gases
el	Electric
EP	Electricity produced
LK	Lime kiln
Self-con	Electrical self-consumption
th	Thermal

Acronyms	
BFB	Bubbling fluidized bed
BIGCC	Biomass-based integrated gasification combined cycle system
GT	Gas Turbine
IRR	Internal rate of return
NG	Natural gas
NPV	Net present value
OLGA	Dutch Acronym for oil-based gas washer
PBP	Payback period
PG	Producer gas
PP	Pulp and paper
RFB	Residual forest biomass
ST	Steam Turbine
WI	Wobbe index

7.1.3 INTRODUCTION

To achieve the EU goals of a climate-neutral economy by 2050 [508], an adjustment of the current economy to one based on renewable raw materials (bioeconomy) must occur [57,509,510]. For this purpose, current and new renewable and sustainable energy technologies must be developed and improved. These renewable solutions must be introduced into our existing production chain and must be conceived not as immediate solutions, but as long-term solutions, which must be employed as soon as possible and improved along time. Nonetheless, a complete transition of the current production system to a more sustainable one is a difficult challenge [511]; this will require technological development and significant scientific advancements, as well as innovative thinking and research approaches and proper support from governments and stakeholders.

Lignocellulosic biomass is recognized as a key material for this transition to a bioeconomy [224,509], by being the main source of renewable carbon. The use of biomass for energy sectors offers benefits that other renewable sources of energy are unable to provide, such as adjustable energy production or the direct replacement of fossil fuels in the current carbon infrastructure. Gasification is a key technology for biomass to energy conversion because it provides flexibility, i.e., the generation of PG that can be used in distinct applications to obtain multiple bioproducts, including heat, electricity, biofuels and biochemicals [26]. Thus, biomass gasification technologies can reduce the reliance on fossil fuels in different scenarios and, consequently, represent a main role in the transition to a sustainable bioeconomy and in future biorefineries that will compete with conventional petrochemical refineries for the production of various value-added products [26,56,123,512].

The PP industry is one of the world largest consumers of biomass and producer of bioenergy and biomaterials and is highly suitable to transform into complete biorefineries due to decades long experience with biomass handling, process integration opportunities and existence of partly processed byproducts [61,64,151]. Replacing the natural gas and oil used in the manufacturing process of this industry (e.g., in the lime kilns and boilers) by PG from biomass gasification, is perhaps the most immediate step for the integration of gasification processes in the PP industry. This immediately leads to reduced fossil fuel dependence in the industry manufacturing process and has the potential to promote additional profits, reduced emissions, energy security and rural economic development [44]. Unfortunately, biomass gasification technologies often are not cost-competitive or reliable due to various technical and commercial barriers (e.g., tars present in the PG and associated necessary cleaning equipment costs [123]), leading to the lack of gasification plants construction and even the stoppage of operation of fully functioning plants [103]; this decreases confidence from the stakeholders.

In this regard, techno-economic analysis is a tool of most relevance in supporting the deployment of the technology, by providing estimation of the performance, emissions and costs of the gasification plant before it is integrated in the PP industry [513]. Pettersson et al., [160] analyzed the integration of black liquor gasification in the PP industry for the production of electricity and DME and showed that this latter was the most profitable option. Naqvi et al., [164] showed significant potential production of SNG production by integrating black liquor gasification in small pulp mills without chemical recovery. Isaksson et al., [154,155,158] showed that the integration of wood wastes gasification in the PP industry was feasible and presented good potential for obtaining four distinct bioproducts, namely methanol, FT diesel, SNG and electricity by IGCC, with net annual profits for all biofuels production scenarios. Wetterlund et al., [159] showed that the integration of the gasification of wood wastes and purchased wood in the PP industry for the production of electricity by IGCC and DME was economically feasible, however, the authors stated that the economic results have a high degree of uncertainty due to the dependence on energy market parameters. Akbari et al., [153] showed that ammonia can be synthetized with competitive market prices from the PG of the gasification of distinct byproducts from the PP industry, namely black liquor, and mixtures of black liquor with different types of sludge from wastewater treatment.

Despite these promising studies, it was not found in the literature any comprehensive techno-economic analysis of the replacement of natural gas by PG in industrial gas burners of the PP industry manufacturing process, which is the most immediate step towards the transformation of this industry into complete gasification-based biorefineries. To address this gap, this work performs a techno-economic pre-feasibility analysis of the integration of biomass gasification for PG production to replace natural gas in the lime kiln of a PP industry, using the case study of a Portuguese medium scale Portuguese PP facility. Generation and co-generation of electricity were also considered as possible integrations. For this purpose, RFB from eucalyptus (*Eucalyptus Globulus*) in the context of the PP industry manufacturing process were considered as feedstock for direct (air) gasification in BFBs. The composition of the obtained PG was determined by experimental research in an 80 kW_{th} pilot-scale BFB. Investment analysis was performed by calculating the NPV, IRR and PBP. A sensitivity analysis was conducted to measure the risks associated to the variations of the biomass and natural gas costs and PG composition. The main technical and economic challenges and barriers associated to this integration were analyzed and highlighted.

7.1.4 MATERIALS AND METHODS

This study followed three steps:

1. Energy analysis, based on process engineering principles and the first law of thermodynamics, to identify the mass and energy flows of each process involved in the processing and generation of energy from RFB.

2. Economic analysis, using economic engineering principles, a spreadsheet-based model was formulated to identify cash flows, calculate costs and revenues throughout the life of the project and obtain the NPV, IRR and PBP.

3. Sensitivity analysis based on the Monte Carlos method to allow the measure of the risks associated with the project, namely by analyzing the behaviour of the main economic indicators.

For this purpose, three possible cases for the direct (air) gasification of RFB from eucalyptus in BFBs were analyzed. In Case I, it is analysed the generation of electricity from RFB in an IGCC. In Case II, it is analised the generation of PG by gasification for replacement of natural gas in the burners of the lime kiln to produce calcium oxide (CaO). In Case III, it is analised the integration of Case I with Case II (co-generation of electricity and heat). The detailed configuration of each Case and respective formulation for energetic analysis is made in Section 7.1.4.3.

7.1.4.1 FEEDSTOCK CHARACTERIZATION

The case study location in Aveiro region coincides with one of the areas with the highest availability of forest biomass in Portugal. In this region, the maximum availability of forest biomass is estimated to be over 83 kt/year [514,515], which ensures the biomass supply to the plant. Table 7.1 shows the characteristics of the eucalyptus RFB considered for this study.

Table 7.1 – Characteristics of the eucalyptus RFB considered as feedstock in this work.

	Eucalyptus RFB
Proximate analysis (%wt, wb)	
Moisture	11.8
Volatile matter	71.0
Fixed carbon	14.6
Ash	2.6
Ultimate analysis (%wt, db)	
Ash	2.87
C	45.85
H	6.13
N	0.35
S	nd
O (by difference)	44.8
LHV (MJ/kg) (db)	17.6

nd-not determined, below the detection limit of the method, 100 ppm wt.

7.1.4.2 TECHNOLOGIES AND PG CHARACTERISTICS

The technology chosen to be used in this analysis is the direct (air) gasification in BFBs. The data (Table 7.2) related to the gasification of eucalyptus RFB was obtained from experiments carried out in the DAO-UA 80 kW_{th} BFB gasifier (Article IV, Section 4.1).

Table 7.2 – Operating conditions of the gasifier and characteristics of the PG.

Operating conditions	
Average bed temperature (°C)	785
Y_{gas} ($Nm^3_{gas}/kg_{biomass\ db}$)	1.58
ER [-]	0.25
CGE (%)	52.7
CCE (%)	80.0
Characteristics of the PG	
CO_2 [%,db]	15.4
CH_4 [%,db]	4.8
CO [%,db]	18.0
H_2 [%,db]	6.4
C_2H_4 [%,db]	2.0
N_2 [%,db]	53.4
LHV (MJ/Nm^3)	5.9

Despite this experimental data, practical PG from biomass gasification processes also contain small amounts of distinct organics compounds (e.g., tars). [1–7]. Tars are a mixture of highly aromatic (e.g., benzene, toluene, naphthalene, phenol) organic condensable compounds formed during thermal or partial-oxidation regimes (gasification) of any organic material [114,124,516]. These compounds are responsible for causing several operating problems during the gasification process and downstream use of the PG, such as surface corrosion, blocking and fouling of engines, filter and pipe plugging and catalyst deactivation, leading to the general malfunction of equipment, breakdowns in operation and low efficiency. A more in-depth description and analysis of this subject can be found in Section 4.4 (Article VII). According to Ríos et al., [113], the tar content should be less than <100 mg/Nm^3, particulate matter must not exceed 30 mg/Nm^3, while the sulfur compounds must be <30 ppmv and nitrogen compounds (N_2 not included) must be <50 ppmv, in order to use the PG in gas turbines. Accordingly, the PG must be subjected to a cleaning process in Cases I and III.

In this context, a wet cleaning system based on multi-stage scrubbers denominated by OLGA technology is proposed for the analysis made in this work. The technology uses vegetable oil as scrubbing agent and is capable of efficiently removing tar and particles from the gas at levels suitable for multiple end applications. To date, this process is considered as one of the most efficient PG cleaning processes [517,518]. OLGA technology is divided into two stages, as shown in Figure 7.1. In the first stage (collector), the gas is cooled by the wash oil, allowing the heavy tars to condense and separate from the gas stream. In the second stage (absorbent/stripper), the wash oil absorbs the lighter gaseous tars (phenol and aromatic with one to two rings). Subsequently in the stripper, the light tars are separated from the oil by the action of a hot air stream and are fed together with the air to the gasifier [519,520].

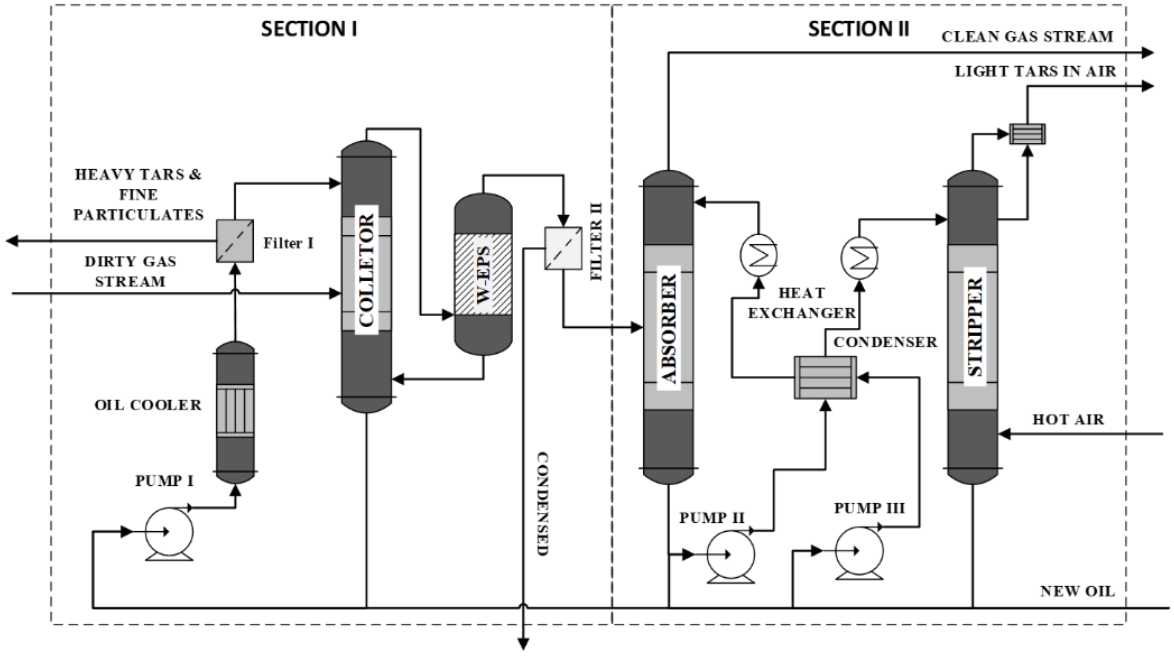

Figure 7.1 – OLGA syngas cleaning system [521].

7.1.4.3 CASES DEFINITION

For the energetic analysis, some key technical parameters must be considered, such as the efficiency of biomass dryers, compressors, gas turbines and recovery boilers, and the self-consumption of electrical energy from the plant. Table 7.3 shows the values considered for the Case studies. The Cases I, II and III respective formulation for energetic analysis are defined in the following Sections.

Table 7.3 – Predetermined data of the PP industry.

Parameter	Value
η_{Dryer} (%) [522]	60
η_{HRSG} (%)[522]	80
$\eta_{comp.}$ (%) [523]	85
η_{GT} (%) [524]	35
η_{ST} (%)[523]	90
Cp_g (kJ/kg.K) [525]	1.25
Hours of operation (h/year)	7884
Self-consumption energy (%)	12

7.1.4.3.1 Case I: Direct (air) gasification of eucalyptus RFB for electricity generation in CC

In Case I, it is analyzed the direct (air) gasification of RFB for generation of electricity in a BIGCC system. The schematic representation of the set of integrated processes is shown in Figure 7.2. The eucalyptus RFB, after being dried, is gasified in an atmospheric BFB reactor, which uses air as the oxidizing agent. Impurities from the raw PG stream are removed by an OLGA-type cleaning system (Figure 7.1). The clean PG is used as fuel for the generation of electricity in the gas turbine (GT). The exhaust gases from the GT are recovered in heat recovery steam generators (HRSG) for the generation of steam that is later converted into electricity in the steam turbine (ST). Exhaust gases must leave the HRSG at temperatures above 150 °C to avoid acid condensation [526]. These gases, which are still at a high temperature, are used at the dryer to decrease RFB moisture content from 40 %wt (as received at the plant) to an average moisture content of 10 %wt [527]. Decreasing the moisture content of RFBs to 10%wt is important to achieve efficiency levels above 50 % in the gasification system [4]. In this configuration, the system was designed with a processing capacity of approximately 17.1 t/h of eucalyptus RFB (40 %wt moisture), corresponding to a thermal power of approximately 50 MW_{th} and electric power of 10.8 MWe.

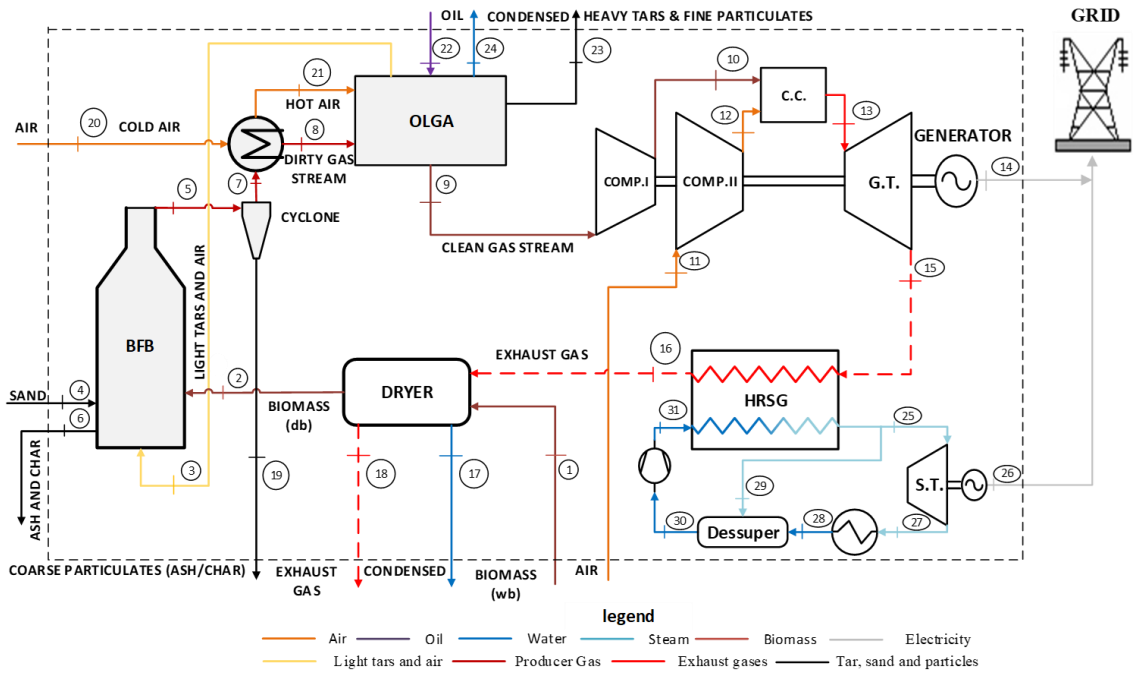

Figure 7.2 – Integrated schematics of Case I.

A theoretical model based on the principle of conservation of mass and energy (first law of thermodynamics) was developed to describe the BIGCC system (Figure 7.2), including the production of electricity and the energy efficiency of the process. The general equation for energy balance can be written as follows:

$$\dot{E} + \sum \dot{m}_{in} \times \left(h_{in} + \frac{V_{in}^2}{2} + g \times Z_{in}\right) = \dot{W} + \sum \dot{m}_{out} \times \left(h_{out} + \frac{V_{out}^2}{2} + g \times Z_{out}\right) \quad \text{Equation 7.1}$$

To simplify the analysis, the system is considered in steady-state operation and the contribution of kinetic and potential energy is considered negligible in comparison to the other terms. So, the energy balance becomes:

$$\dot{E} + \sum \dot{m}_{in} \times h_{in} = \dot{W} + \sum \dot{m}_{out} \times h_{out} \quad \text{Equation 7.2}$$

The above energy balance is applied to the gasification system and to the CC system; for the biomass drying and OLGA processes it is used the global efficiency parameters described in Table 7.3. For the gasification system, the energy balance is described in Equations 7.3 to 7.8. The LHV of tar is calculated using Equation 7.9 and the data present in Table 7.4 [528–530]. The CGE was determined according to the methodology described in Section 1.4.

$$\dot{E}_{RFB} + \dot{E}_{Air} \times Cp \times \Delta T = \dot{E}_{PG} + \dot{E}_{Tar} + \dot{E}_{ash} + Q_G \quad \text{Equation 7.3}$$

$$\dot{E}_{RFB} = \dot{m}_{RFB} \times LHV_{RFB} \quad \text{Equation 7.4}$$

$$\dot{E}_{Air} = \dot{m}_{Air} \times Cp \times \Delta T \quad \text{Equation 7.5}$$

$$\dot{E}_{PG} = \dot{m}_{PG}(Cp \times \Delta T + LHV_{PG}) \quad \text{Equation 7.6}$$

$$\dot{E}_{Tar} = \dot{m}_{Tar} \times LHV_{Tar} \quad \text{Equation 7.7}$$

$$\dot{E}_{Ash} = \dot{m}_{ash} \times Cp \times \Delta T \quad \text{Equation 7.8}$$

$$LHV_{tar} = 0.4879 \times [C_5H_{12}] + 0.4202 \times [C_6H_6] + 0.3245 \times [C_6H_6O] \quad \text{Equation 7.9}$$

Table 7.4 – Assumed concentration for the main compounds present in the tar in the raw PG, and its LHV [528–530].

Model tar compound	Remarks	LHV (MJ/kg)	% wt of each compound in tar
Naphthalene (C_5H_{12})	Represents the LPAHs tars or tertiary tars, at 900 °C, Naphthalene is the major single compound in the tars. These tars condense at low temperature even in very low concentration.	48.79	45
Phenol (C_6H_6O)	Represents heterocyclic tars, highly water-soluble compounds.	32.45	9
Benzene (C_6H_6)	It represents a stable aromatic structure, formed in high-temperature processes; It is a light hydrocarbon with a single ring; it does not pose a problem about condensability and solubility	42.02	46

The energy balance of the CC will conveniently be divided into two parts: first it is shown the GT (Brayton cycle) and then the ST (Rankine cycle). Although there is still no clear definition of how the efficiency of the GT is affected by the LHV of the PG, it is possible to make some general assumptions. GT are designed primarily for the combustion of NG, a fuel composed primarily of CH_4, with a high LHV (near 40 MJ/Nm^3) and a high Wobbe index (WI) between 48 and 53 MJ/Nm^3 [531]. On the other hand, the PG is a mixture of several combustible gases H_2, CO_2, CH_4, with inert components such as CO_2 and N_2, the latter in high concentration, and show a low WI (5 to 13 MJ/Nm^3) [532]. Since the WI of the PG is smaller, a larger volume of fuel must enter the combustion chamber of the GT, to provide the same power as with NG. This results in a higher mass

flow of gas through the turbine section, increasing shaft power. This is the main impact of the use of PG in the gas turbines. According to Brooks [533], in most cases of operation with fuels of low LHV, it can be assumed that the output power and efficiency of the gas turbine will be equal to or greater than that obtained with NG.
The combustion chamber of the GT is designed to burn fuel efficiently, reduce emissions and decrease the wall temperature. In recent years, GT manufacturers have developed flexible combustion chambers that can handle solid, liquid and gaseous fuels [534]. Amongst gaseous fuels, those derived from biomass gasification and with medium (12 to 20 MJ/Nm^3) to low (3 to 7 MJ/Nm^3) LHV, can also be burned [535], although an increase in the PG flow must be considered to maintain the same power as when NG is burned. The results obtained by Ghenai [534] and Park et al., [536] in studies about combustion of PG in the combustion chamber of GTs show that low LHV fuels can be burned efficiently, leading to reduced emissions of polluting gases and without significantly affecting the performance of the turbine.

The general reaction for the complete combustion of PG with the theoretical amount of air required is given by Equation 7.10, with unknown coefficients a, b, c, d, and e, determined by applying the principle of conservation of mass to each element that constitutes the PG..

$$C_X H_Y N_Z + a(O_2 + 3.76N_2) = bCO_2 + cH_2O + dO_2 + eN_2 \qquad \text{Equation 7.10}$$

The electrical efficiency of the GT is determined as the ratio between the electric power output and incoming fuel power, as given by Equation 7.11:

$$\eta_{GT} = \frac{\dot{E}p_{GT}}{(\dot{E}_{PG} - \dot{E}_{GS})} \qquad \text{Equation 7.11}$$

The HRSG is used to recover thermal power from the GTs exhaust gases to generate steam and to run the ST to generate electricity. The performance of HRSG and ST is determined according to Equations 7.12 to 7.15:

$$\eta_{ST} = \frac{\dot{E}p_{ST}}{\dot{E}_{EG} \cdot \eta_{HRSG}} \qquad \text{Equation 7.12}$$

$$\eta_{HRSG} = \frac{\dot{E}_{Steam}}{\dot{E}_{EG}} \qquad \text{Equation 7.13}$$

$$\dot{E}_{Steam} = \dot{m}_{Steam} \times (h_{int} - h_{Out}) \qquad \text{Equation 7.14}$$

$$\dot{E}_{EG} = \dot{m}_{EG} \times cp_{EG} \times (T_{int} - T_{Out}) \qquad \text{Equation 7.15}$$

The operating parameters of the plant designed in Case I (Figure 7.2) are shown in Table 7.5. The global efficiency is determined by Equation 7.16:

$$\eta_{Global} = \frac{\dot{E}p_{GT} + \dot{E}p_{ST} - \dot{E}p_{Self-con}}{\dot{E}_{RFB}} \qquad \text{Equation 7.16}$$

Table 7.5 – Operating parameters for the plant designed in Case I.

Description	m (kg/s)	T (K)	P (kPa)	W (MW)
1	4.7	298.2	101.3	50.0
2	3.2	333.0	101.3	50.0
3	3.7	298.2	101.3	0.3
4	0.02	298.2	101.3	-
5	6.6	1073.0	101.3	38.3
6	0.3	298.2	101.3	4.5
7	6.6	1073.0	101.3	38.3
8	6.6	973.0	101.3	36.0
9	6.0	298.0	101.3	28.0
10	6.0	323.1	1519.5	28.2
11	22.4	298.2	101.3	-
12	22.4	323.1	1519.5	0.6
13	28.4	927.0	1443.5	27.3
14	-	-	-	9.8
15	28.4	763.0	106.4	15.2
16	28.4	373.2	101.3	2.7
17	1.5	373.2	101.3	2.8
18	28.4	373.2	101.3	2.3
19	0.01	298.2	101.3	0.1
20	2.8	298.0	101.3	-
21	2.8	398.0	101.3	0.4
22	0.01	298.0	101.3	0.5
23	0.2	298.0	1001.3	0.7
24	0.4	373.2	101.3	0.6
25	3.0	530.0	6400.0	9.1
26	-	-	-	2.5
27	3.0	803.0	6400.0	9.1
28	3.0	378.0	121.0	0.1
29	0.01	530.0	6400.0	0.03
30	3.0	378.0	121.0	0.1
31	3.0	378.2	6400.0	0.1

7.1.4.3.2 Case II: Direct (air) gasification of eucalyptus RFB for natural gas replacement in the lime kiln

In Case II, it is analysed the use of PG as fuel for the lime kiln (calcination process) of a PP industry. The PG is generated by the eucalyptus RFB gasification, as shown in Figure 7.3. This system is made up of the following processes: dryer, BFB gasifier, and lime kiln. Considering that the PG can be burned directly in a lime kiln, the raw gas stream from the gasifier will be subjected to a minimal clean process to remove particulates through a cyclone-filter placed at the outlet of the gasifier. This system was designed with a processing capacity of approximately 2.7 t/h of eucalyptus RFB (40 %wt moisture) with thermal power of approximately 8 MW_{th} and the capacity to produce 10.4 t/h of CaO.

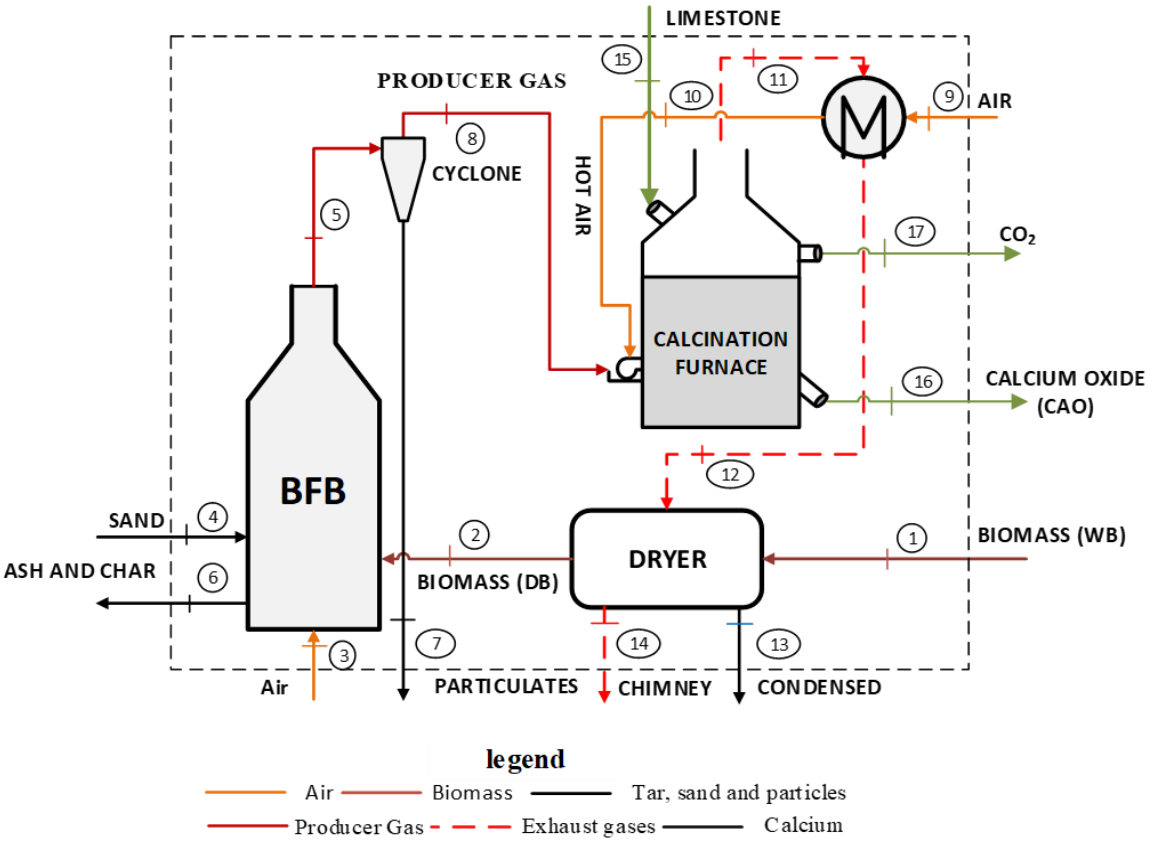

Figure 7.3 – Integrated schematics of Case II.

Lime production is an energy-intensive process, mainly due to the highly endothermic calcination reaction that requires a high energy consumption (~1.78 MJ/kg $CaCO_3$, at 1173 K [537,538]) to decompose the limestone into calcium oxide and carbon dioxide (Reaction 7.1). This high energy demand implies the emissions of large volumes of CO_2 caused by high fuel consumption.

$$CaCO_{3\,(s)} + \Delta H_R \rightarrow CaO_{(s)} + CO_{2\,(g)} \qquad \text{Reaction 7.1}$$

According to Granados et al., [537], for rotary kilns fed with dry limestone, the energy consumption for the calcination process is between 6 to 8 MJ/kg of CaO produced, more than double when compared to the heat required for the reaction (3.04 MJ/kg of CaO). This shows that there is considerable scope to improve the efficiency of the process. In Equation 7.17 it is shown the energy balance of the lime kiln.

$$\dot{m}_{CaCO_3} \times h_{CaCO_3} + \dot{E}_{PG} = \dot{m}_{CaO} \times h_{CaO} + \dot{m}_{CO_2} \times h_{CO_2} + \dot{E}_{EG} \qquad \text{Equation 7.17}$$

The operating parameters of the plant designed in Case II (Figure 7.3) are shown in Table 7.6. The global efficiency is determined by Equation 7.18, with the efficiency of the lime kiln (η_{LK}) estimated at 61.2 %, according to [539].

$$\eta_{Global} = \frac{(\dot{E}_{PG} \times \eta_{LK})}{\dot{E}_{RFB}} \qquad \text{Equation 7.18}$$

Table 7.6 – Operating parameters for the plant designed in Case II.

Description	m (kg/s)	T (K)	P (kPa)	W (MW)
1	0.74	298.2	101.3	7.8
2	0.50	333.0	101.3	7.8
3	0.23	298.2	101.3	-
4	0.01	298.2	101.3	-
5	0.73	973.0	101.3	4.4
6	0.01	298.2	101.3	-
7	0.001	298.2	101.3	-
8	0.73	973.0	101.3	4.4
9	2.51	398.2	101.3	0.4
10	2.51	398.2	101.3	0.4
11	3.24	573.0	101.3	1.1
12	3.24	448.2	101.3	0.8
13	0.24	373.2	101.3	0.5
14	3.24	373.2	101.3	0.3
15	5.12	298.2	101.3	-
16	2.89	298.2	101.3	-
17	2.23	298.2	101.3	-

7.1.4.3.3 Case III: Direct (air) gasification of eucalyptus RFB for electricity generation in CC and natural gas replacement in the lime kiln

In Case III, it is analyzed the direct (air) gasification of eucalyptus RFB for the generation of PG to be used in a CC for electricity generation and as fuel to replace the natural gas in the burner of a lime kiln for production of CaO (Figure 7.4). This configuration integrates in a single plant the system described in Cases I and II. For this purpose, the system is made up of the following elements: dryer, BFB gasifier, OLGA, GT, HRSG, ST and lime kiln. The eucalyptus RFB, after undergoing a drying process, is gasified in a direct (air) atmospheric BFB reactor. The raw PG stream from the gasification reactor passes through a high temperature cyclone filter to remove the particulate material, and then, a fraction of the PG is burned directly in the lime kiln and the other fraction is subjected to deeper cleaning in the OLGA system, in order to be used as fuel in the GT. The organic stream resulting from the OLGA process is fed to the burner of the lime kiln, together with the PG. The thermal power from the GTs exhaust gases is recovered in an HRSG for steam generation which is then fed to the ST for electricity production. For the drying of the biomass, it is used the residual thermal energy of the exhaust gases of the HRSG, together with the exhaust gases from the lime kiln. In this configuration, the system was designed with a processing capacity of approximately 17.1 t/h of eucalyptus RFB (40 %wt moisture), with thermal power of approximatelly 50 MW_{th} and electric power of 8.9 MW_e, allowing the generation of 10.4 t/h CaO.

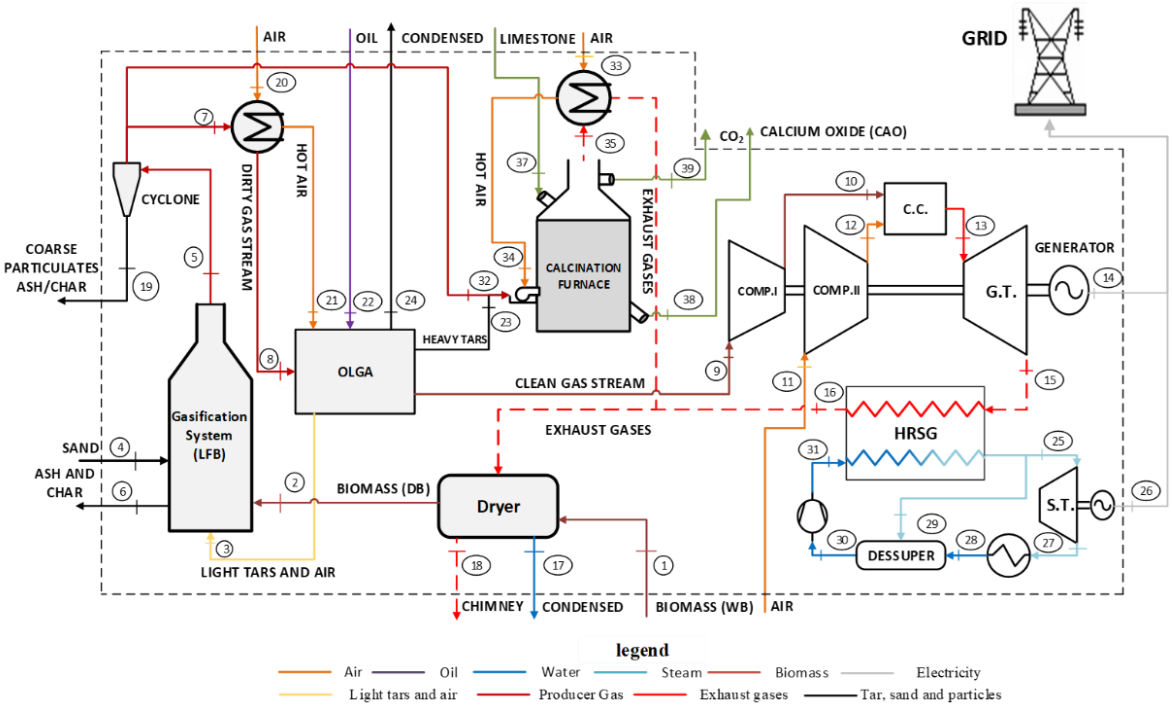

Figure 7.4 – Integrated schematics of Case III (combination of Cases I and II).

The operating parameters of the plant designed in Case III (Figure 7.4) are shown in Table 7.7 and the global efficiency is determined by Equation 7.19.

$$\eta_{Global} = \frac{\dot{E}p_{GT} + \dot{E}p_{ST} + (E_{PG} \times \eta_{LK}) - \dot{E}p_{Self-con}}{\dot{E}_{RFB}} \qquad \text{Equation 7.19}$$

Table 7.7 – Operating parameters for the plant designed in Case III.

Description	m (kg/s)	T (K)	P (kPa)	W (MW)
1	4.7	298.2	101.3	50.0
2	3.2	333.0	101.3	50.0
3	3.2	298.2	101.3	0.3
4	0.0	298.2	101.3	-
5	5.1	1073.0	101.3	29.6
6	0.3	298.2	101.3	4.5
7	5.1	1073.0	101.3	29.6
8	5.1	973.0	101.3	27.8
9	5.1	298.0	101.3	23.6
10	5.1	323.1	1519.5	23.8
11	23.1	298.2	101.3	-
12	23.1	323.1	1519.5	0.6
13	28.1	927.0	1443.5	24.3
14	-	-	-	8.5
15	28.1	763.0	106.4	15.0
16	32.3	373.2	101.3	3.0
17	1.5	373.2	101.3	2.8
18	32.3	373.2	101.3	2.7
19	0.01	298.2	101.3	0.1
20	2.9	298.0	101.3	-
21	2.9	398.0	101.3	0.4
22	0.01	298.0	101.3	0.5
23	0.3	298.0	1001.3	0.8
24	0.4	373.2	101.3	0.6
25	1.9	530.0	6400.0	6.0
26	-	-	-	1.6
27	1.9	803.0	6400.0	6.0
28	2.9	378.0	121.0	0.1
29	1.0	530.0	6400.0	3.1
30	2.9	378.0	121.0	0.1
31	1.9	378.2	6400.0	0.0
32	0.9	298.0	101.3	4.4
33	3.2	298.2	101.3	-
34	3.2	398.2	101.3	0.5
35	4.2	573.0	101.3	1.0
36	4.2	448.2	101.3	1.3
37	5.1	298.2	101.3	-
38	2.9	298.2	101.3	-
39	2.2	298.2	101.3	-

7.1.4.4 METHODOLOGY FOR THE ECONOMIC AND SENSITIVITY ANALYSIS

The general approach to an economic analysis is to compare the costs of the project with the expected income during its useful life. Basically, this analysis includes the evaluation of the performance of the system designed in terms of its efficiency, capital cost, operation and maintenance cost, energy generation cost, periods of recovery of the investment, acceptance of the technology and the profitability of the whole system. Such research depends on many parameters, such as the availability and cost of biomass at the gasification site, the capacity for energy production, the quality of the energy produced, the efficiency of the process, the optimization of the system and the applications of the energy produced [91,540]. Table 7.8 presents the financial data and details the annually considered cost factors to model the economic feasibility of the plant considered for each of the developed Cases (I, II and III).

Table 7.8 – Initial input financial data and cost factors considered to model the plant configurations preconized in the developed Cases (I, II and III).

Item	Value	Comments	Reference
$I_{Gasifier}$ (€/kW_{th})	800	Costs related to the acquisition of the dryer and the BFB gasifier system.	[541,542]
I_{OLGA} (€/Nm^3)	100	Costs related to the acquisition of the OLGA system.	[520]
I_{CC} (€/kW_e)	700	Costs related to the acquisition of the GT, the HRSG and the ST.	[104]
$C_{Electricity}$ (€/kWh)	0.13	Electricity sales price practiced in Portugal.	[543]
$C_{O\&M}$ (%)	3.2	Operation and maintenance (O&M) costs refer to 3.2% of the total investment, applied accordingly to both systems. Includes salaries, electricity, water, ash removal and equipment maintenance costs.	[271]
r (%)	1.4	Interest rates on credit operations	[544]
C_{RFB} (€/t)	35	RFB acquisition costs for Portugal include transportation and splintering.	[377]
$C_{NG_{Cons.}}$ (€/Nm^3)	0.25	Value paid per cubic meter (standard pressure and temperature) of natural gas consumed	[545]
CO_2 (€/t_{CO2})	24.8	Economic value for CO_2 emission rights.	[546]
$(i)_{2020}$ (%)	8.5	Average discount rate considered per year. Applied to both systems.	[547]
IR (%)	1.6	Inflation rate; Harmonised inflation Portugal 2020.	[548]
Project lifetime (years)	25	Plant lifetime	[549]

Economic analysis methods are based on the costs and benefits of investments. In the literature, it is possible to find several methods of economic analysis that allow identifying with great precision the potential costs and benefits of a specific investment. Total present value is one of the most used economic methods to assess the economic viability of a project. This method is the combination of three economic indicators, namely the NPV, the IRR and the PBP, each of these indicators have their strengths and limitations. To calculate the economic indicators, an analysis of the cash flows is performed. First, the costs and income of cash flow before taxes (CFBT) incurred in:

I. An initial investment period related to the design and construction phase of the plant.
II. Amortizations of the debt contracted with the acquisition of the project.
III. Investments in fixed assets and working capital, which will be deducted from amortizations to recover the investments.
IV. Costs related to operation and maintenance (O&M), employees and structure.
V. Financial income from capital investments.
VI. Income is obtained from the sale of electricity to the network, from the values saved in the purchase of natural gas and the payment of CO_2 emission rights.

Then, the CFBT is calculated by balancing revenues and expenses while further applying the discount rate, as shown in Equation 7.20 [550]:

$$CFBT = (\sum Revenues - \sum Expenses)/(1+i)^t \quad \text{Equation 7.20}$$

The cash flow after taxes (CFAT) is one of the most useful liquidity measures to assess the financial health of a project or company since it considers the effect of the tax burdens on the obtained profits. It also allows the determination of the economic viability of the future investments while measuring the profitability growth of an investment. In this work, the CFAT was determined by Equation 7.21, which relates CFBT minus taxation [551].

$$CFAT = CFBT - Tax \quad \text{Equation 7.21}$$
$$Tax = TXI \times TXR \quad \text{Equation 7.22}$$
$$TXI = CFBT - (DEP \times Inv) \quad \text{Equation 7.23}$$

In Equations 7.22 and 7.23, TXI represent the Taxable Income, TXR the Tax Rate, Inv the initial investment, and DEP is the Depreciation, which is the amount that tax authorities allow to deduct from taxes. The depreciation of assets in Portugal follows the regulatory decree 25/2009 from the Ministry of Finance and Public Administration, which considers a depreciation rate of 8.3% for power generation companies [552]. Before and after-tax cash-flows for cost and revenue calculations over the life of the project are applied to an economic model based on a spreadsheet developed to calculate these economic indicators.

The NPV is an economic indicator that allows the evaluation of the profitability of a project by considering all the inflows and outflows of cash throughout its useful life. A positive NPV indicates that the project is profitable, while a negative NPV indicates losses. Thus, the NPV refers to the current values of all costs and revenues associated with the system and in this work it is calculated by Equation 7.24 [549], with the plant lifetime estimated for 25 years (N).

$$NPV(i,N) = \sum_{t=0}^{N} \frac{\text{CFBT}}{(1+i)^t} \qquad \text{Equation 7.24}$$

The period t=0 is the initial investment stage of the project, and corresponds to the investment costs associated to the purchase and installation of the equipment.

The IRR is the interest or return rate offered by an investment. The higher the IRR, the greater the profitability of the project will be. Also, the IRR is the discount rate that makes the NPV of all cash flows equal to zero, determining the minimum rate of return for the project to be viable. If the IRR is higher than the discount rate (i), then the project is feasible [377]. In this work, the IRR is calculated by Equation 7.25.

$$NPV(IRR,N) = \sum_{t=0}^{N} \frac{\text{CFBT}}{(1+IRR)^t} = 0 \qquad \text{Equation 7.25}$$

The PBP is the payback period i.e., the time needed to earn back the initial capital investments. The shorter the PBP, the stronger the financial viability of the project. In this analysis, PBP is calculated by finding the year in which the cumulative NPV cash flow becomes positive[549]. For this purpose, it was used the Equation 7.26, where A is the last year with a negative cumulative NPV, B is the absolute value of cumulative NPV at the end of that year, and C is the total annual cash flow during the year after.

$$PBP = A + \frac{B}{C} \qquad \text{Equation 7.26}$$

The methodology used for the economic analysis of Cases I, II and III considers various assumptions related to the sector of biomass conversion into useful energy, so it is important to perform a sensitivity analysis. The analysis was performed to measure the influence of different techno-economic variables and assumptions on the results of the economic analysis of the distinct designed plants. This approach allows changes in the results of the economic analysis, indicating the importance of specific risk parameters when evaluating their influence on system performance. It is worth noting that some of these input variables comprise a greater range of uncertainty than others. In this sensitivity analysis, it was chosen a set of techno-economic variables assumed to be those with higher influence on the performance of the plant, namely:

I. Efficiency of the gasification system, because it influences the amount of biomass consumed, the characteristics of the PG and the global efficiency of the plant.
II. Initial investment, given the large initial amount of capital outflow from which the project needs to recover.
III. Cost of the RFB, considering that it constitutes the main raw feedstock of the plant, on which the production is sustained.
IV. Discount rate, because it influences the present value of future costs and benefits.
V. Sale price of electricity (for Cases I and III) and purchase price of natural gas (for Cases II and III), due to its importance for expected energy revenues and long-term uncertainty from market fluctuations and policies.

The sensitivity analysis was evaluated by the Monte Carlo method implemented in the MATLAB program version 2019b. The model was programmed for a total of 10000 iterations following a triangular distribution considering a lower limit (unfavorable value), a most likely value (baseline value) and the upper limit (favorable value). This type of distribution is often applied to sensitivity analysis due to its relative mathematical simplicity while generating enough random samples to identify the most sensitive parameters [553]. For each iteration, the input variables move based on the defined range of sensitivity limits (± 10 % over the reference value of the selected input variables), while the other variables within the model were maintained constant during this analysis. This uncertainty in the variables of selected inputs has an impact on the results of the financial indicators (NPV, IRR and PBP) selected as the corresponding products in the risk model.

7.1.5 RESULTS AND DISCUSSION

7.1.5.1 ENERGY ANALYSIS RESULTS

The results of the mass and energy analysis of the integration of biomass gasification in the PP industry following the system configuration of Cases I, II and III (Table 7.5, Table 7.6 and Table 7.7) allows the analysis of the energy performance of each component of the plant for each configuration. Eucalyptus RFB consumption, total electricity generated, CaO production and the global efficiency of electricity generation and CaO production for the three configurations studied with the implementation of biomass direct gasification in BFB, are presented in Table 7.9. In Case I, an electrical power of 10.9 MW_e is achieved, with a eucalyptus RFB consumption of 17.1 t/h, and global system efficiency of 21.7 %. In Case II, a production of 10.4 t/h of CaO is achieved, with an eucalyptus RFB consumption of 3.6 t/h and global system efficiency of 34.2 %. In Case III, an electric power of 8.9 MW_e is achieved, producing 10.3 t/h of CaO, with an eucalyptus RFB consumption of 17.1 t/h and global system efficiency of 25.0 %.

Table 7.9 – Eucalyptus RFB consumption, total electricity generated, CaO production and the global efficiency of electricity generation for the three configurations studied.

Configuration	E_E [MWh]	CaO [t/h]	$\dot{m}_{RBF}$ [t/h]	η_{Global} [%]
Case I	10.85	-	17.05	21.70
Case II	-	10.42	3.60	34.17
Case III	8.92	10.42	17.05	24.94

Figure 7.5 shows the Sankey diagram of the energy flows of each configuration analyzed. To simplify the analysis of the Sankey diagram, only the main energy flows are considered: i) in Case I, it is shown the energy flows for the biomass gasification system and for the CC power generation system, ii) for Case II, it is shown the energy flows for the biomass gasification system and for the production of CaO by combustion of the PG in the lime kiln, and iii) for the Case III, it is shown the energy flows for the biomass gasification system, for the CC power generation system and for the CaO production by combustion of the PG in the lime-kiln.

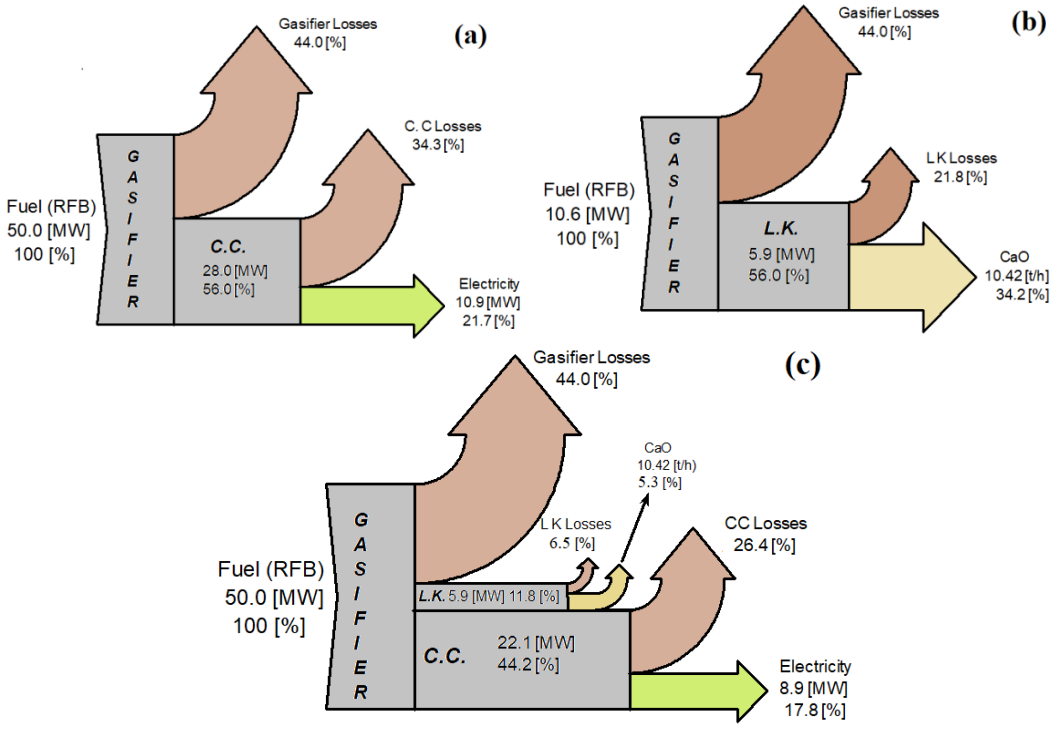

Figure 7.5 – Sankey diagram for the main energy flows in the system configurations studied: a) Case I, b) Case II and c) Case III.

The energy contained in the eucalyptus RFB is converted into thermal and chemical energy in the PG during the gasification process. Thermal energy and solids discharged (ash, unconverted char) become the main sources of energy loss during the gasification process, representing 44.0 % of total losses for all configurations. In Case I, the PG is used as fuel in the CC for electricity generation, and the energy losses in this process reach 34.30 %, and are mainly due to the loss of thermal energy in the exhaust gases and to inefficiencies in the CC; the global efficiency of the system configuration in Case I is 21.70 %. In Case II, the PG is used as fuel in the burner of the lime kiln for the production of CaO, and the energy losses in this stage reach 21.80 %. According to Watkinson & Brimacombe [538], these losses are mainly associated with the thermal energy in the exhaust gases and the inefficiency in the limestone calcination process; the system achieves a global efficiency of 34.20 %. In Case III, 78.90 % of the PG is used as fuel for the generation of electricity in the CC, and the energy losses in this process are 26.40 %, and 21.10 % of PG is burned in the lime kiln to produce CaO, with energy losses of 4.60 %; the global efficiency for this system is 23.13 %.

7.1.5.2 ECONOMIC ANALYSIS RESULTS

Figure 7.6 shows the cash-flow calculated after taxes and the total annual inflows and outflows for the system configurations of Case I, II and III. During the investment period (year 0), the initial disbursement for Case I is around 49.4 M€, for Case II is 6.3 M€ and for Case III is 47.62 M€. It is considered that 30 % of the initial investment comes from own capital and 70 % from borrowed capital [554]. The capital is lent with an interest rate of 1.6 % [544] and the debt must be amortized in 12 years.

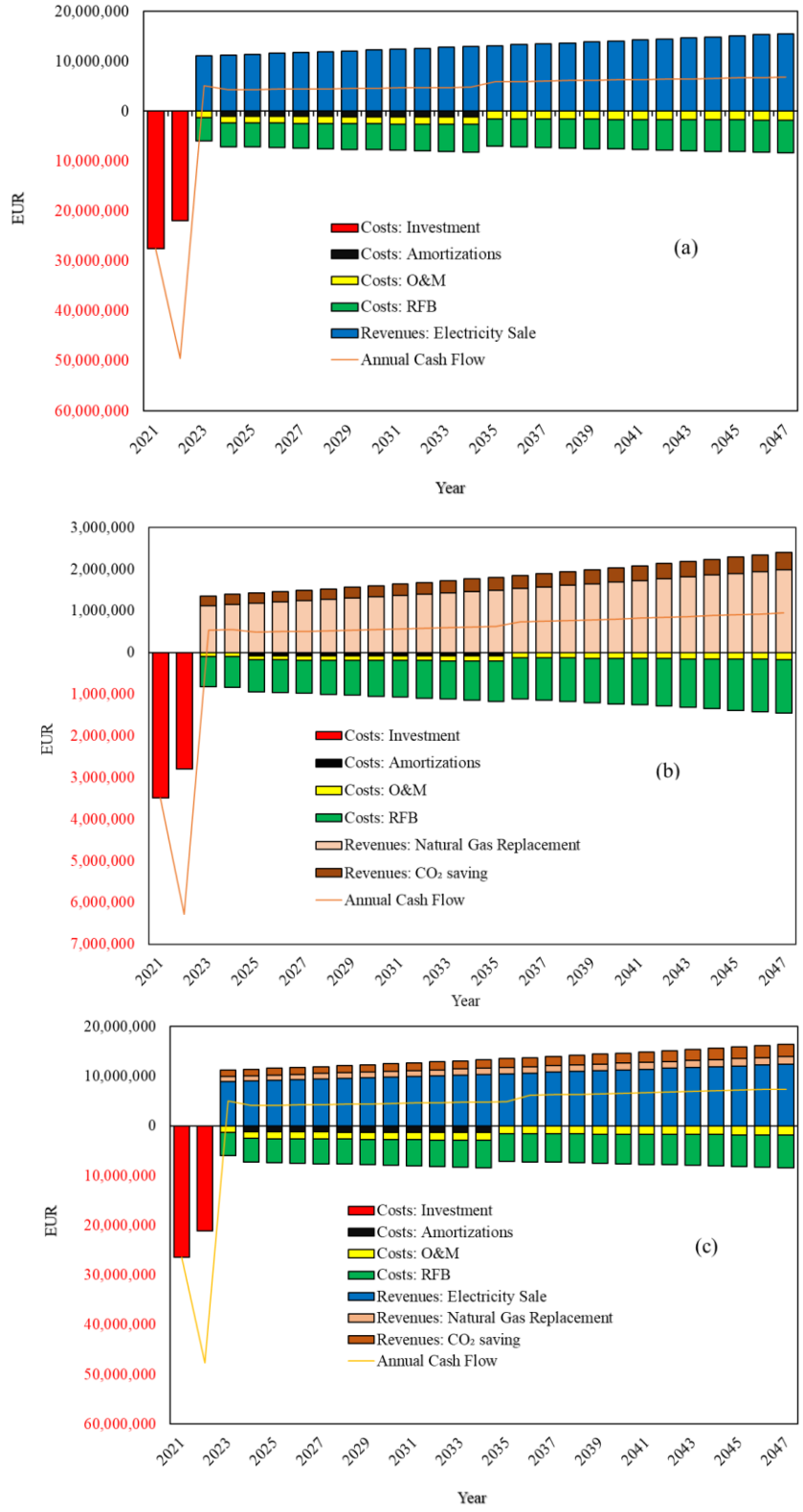

Figure 7.6 – Cash-flows through the useful lifetime of the plant for (a) Case I, (b) Case II and (c) Case III.

In all the cases analyzed, the useful life of the plant was considered 25 years [549]. For year 1, the projects after-tax cash-flow will increase to positive as it reaches the operating phase. For the Case I, the inputs come from electricity sales revenues and the outputs come from the first period of debt amortization and expenses with O&M, employees, structure and purchase of the eucalyptus RFB. It is assumed that, from the first year, the plant will generate approximately 85.52 GWh/year for the rest of the useful lifetime of the project, achieving an average income of more than 12.0 M€/year. For the Case II, the inputs come from the costs avoided in the purchase of NG, which is replaced with PG for the production of CaO, and from the costs avoided by saving CO_2 certificates. The outputs are derived from the amortization of the debt and the expenses with O&M, employees, structure and purchase of the eucalyptus RFB. It is assumed that, from the first year, the plant will save approximately 4.3×10^6 Nm^3/year of NG during the rest of the useful lifetime of the project, which translates into an average income of over 1.8 M€/year. For Case III, the inputs come from electricity sales, from the costs avoided in the purchase of NG, which is replaced with PG for the production of CaO, and from costs avoided by saving CO_2 certificates. The outputs derive from the amortization of the debt and expenses with O&M, employees, structure and the purchase of the eucalyptus RFB. It is assumed that, from the first year, the plant will generate approximately 63.37 GWh/year and save approximately 4.3×10^6 Nm^3/year of NG during the rest of the useful lifetime of the project, achieving an average income of over 12 M€/year.

For the three cases analyzed, the projects cash-flows tend to increase steadily as the income exceeds the expenses, which is derived from these inflows and outflows growing at the inflation rates imposed throughout the useful lifetime of the plant. Revenue shows a fairly positive incremental cash flow for all the cases analyzed over the years, emphasizing the relevance of the benefits of the electricity sale price for the Cases I and III, in terms of the viability of the project. In the year 12 of the project, a sudden increase in cash flow is observed, which is caused by the completion of the payment of the debt contracted with the acquisition of the main equipment and the construction of the plant.

According to the results of the financial analysis for the Case I, the plant will be debt-free at the end of year 16.0 of operation, in Case II it is estimated that the investment will recover from year 19.0, and for Case III, after year 18.2. For all the cases analyzed, in addition to the initial investment that is only reflected during the investment period, the annual costs with the acquisition of the eucalyptus RFB, constitute the largest cash outflow during the useful lifetime of the project; these expenses represent approximately 65 to 85% of the total annual expenses. The annual expenses in O&M, responsible for keeping the plant operational, are also high and rank as the second most important expenses, representing approximately between 7 to 20 % of total annual expenses; this results from the high initial investment because the O&M is calculated as a percentage of the initial investment (Table 7.8). Finally, the debt amortization expenses, account between 10 to 16 % of total annual expenses, and its weight is reflected in the first 12 years of the project.

After obtaining the cash-flows, it was analyzed the behavior of the economic indicators NPV, IRR and PBP, to determine if the project is economically acceptable. Figure 7.7 shows the results of the economic analysis considering these three indicators for each case in study. For all the cases analyzed, the NPV profile is evaluated for various discount rates (0 to 25 %), which allows the determination of whether the project is accepted or rejected. Based on this approach, the project is accepted if the NPV is greater than zero and rejected if it is less than zero. In this study, for all the analyzed cases, as the discount rate increases, the value of the NPV decreases, which shows that the comportment of the NPV is inversely proportional to the discount rate. Applying an after-tax discount rate of 8.5 % [547], the NPV of the project for Case I, is 6.61 M€ (Figure 7.7 (a)), 0.50 M€ for Case II (Figure 7.7 (b)) and 5.81 M€ for Case III (Figure 7.7 (c)). The IRR is given by the time the NPV equals zero, and the IRR is 8.99 % for Case I, 9.36 % for Case II and 9.78 % for Case III. Note that the IRR is calculated concerning the results of the cash-flows after-tax, as given by Equation 7.25. Finally, the payback period (PBP), which is the year in which the accumulated cash-flow turns positive, is equal to 19.52 years for Case I, 21.22 years for Case II and 19.16 years for Case III.

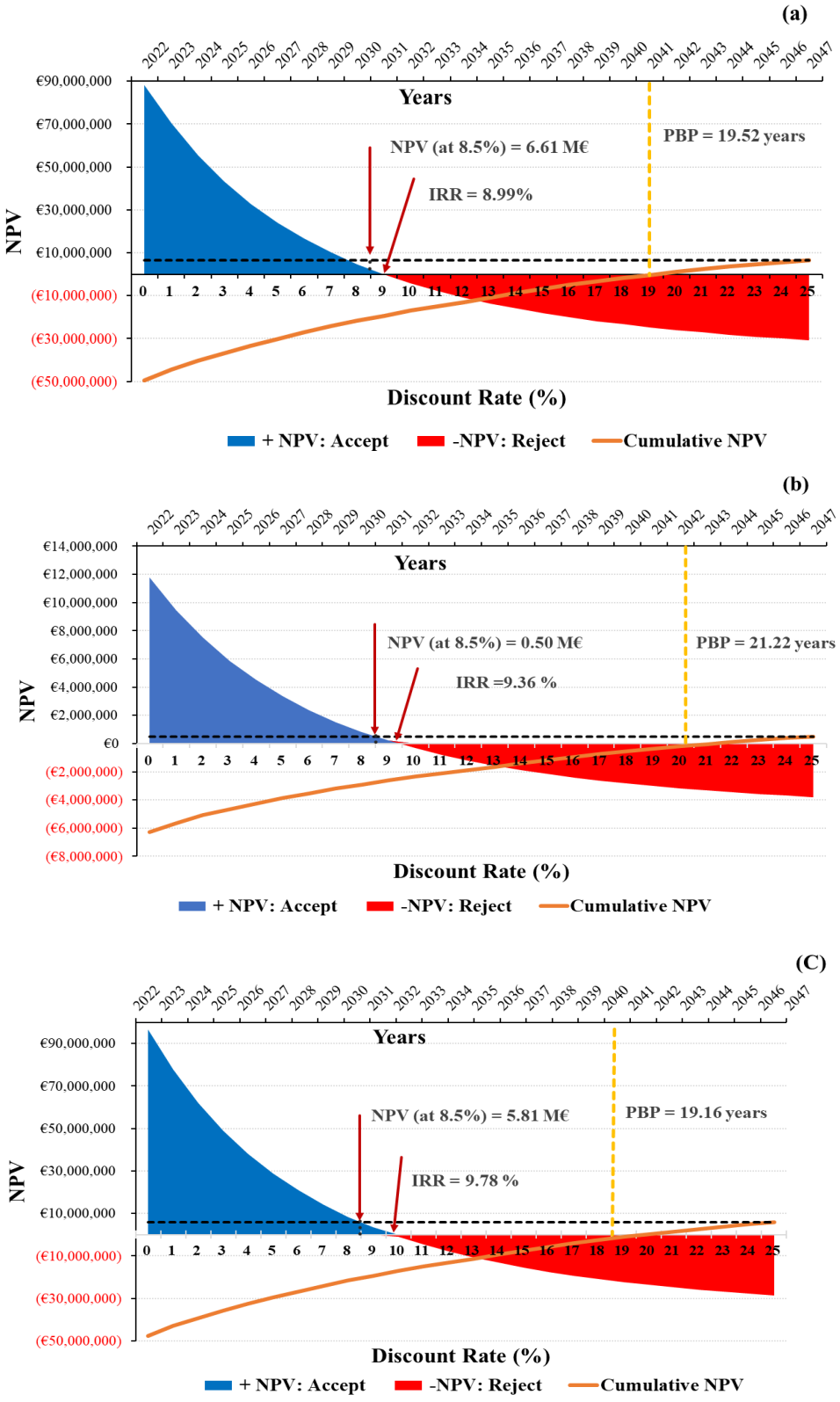

Figure 7.7 – Financial indicators (NPV, IRR and PBP) throughout the useful lifetime of the plant, for (a) Case I, (b) Case II and (c) Case III.

According to the results of the economic indicators, the projects (Case I, II and III) show a positive NPV, an IRR greater than the discount rate and a PBP less than the useful lifetime of the plants, turning them to a viable investment from the economic point of view. However, according to the World Bank Group's considerations for international financial cooperation [549], typical benchmarks for key financial parameters in biomass projects point out that the NPV must be positive, the IRR must be greater than 10 % and the PBP less than 10 years. Based on these criteria, neither of the three configurations considered (Cases I, II and III) are attractive to investors because the IRR is less than 10 % and the PBP exceeds 10 years. In particular, the PBP is between 19.16 to 21.22 years, which is approximately 80 % higher than recommended by the World Bank [549]. It is evident that the longer the PBP, the less desirable the project is to investors. It is also clear that these criteria vary according to the specific conditions of each country and according to the economic evaluation methodology used. Table 7.10 shows a summary of the main results for the three cases analyzed.

Table 7.10 – Summary of the results of the economic evaluation.

Items	Case I	Case II	Case III
Gasifier system cost (M€)	40.00	6.28	40.00
Cleaning system cost (M€)	1.84	-	1.55
Combined Cycle cost (M€)	7.59	-	6.22
Total capital cost (M€)	49.43	6.28	47.62
Electricity cost (k€/kW)	4.51	-	4.68
Limestone cost (k€/t_{CaO})	-	0.01	0.01
NPV (k€)	6.61	0.50	5.81
IRR (%)	8.99	9.36	9.78
PBP (Years)	19.52	21.22	19.16

7.1.5.3 SENSITIVITY ANALYSIS RESULTS

Figure 7.8 shows the NPV risk forecast histograms as a function of the probability density and the cumulative probability for the three cases analyzed, following the methodology presented in Section 7.1.4.4. The average distribution values, given by the vertical line "Mean" in the NPV probability distribution figures, are very close to the average values previously calculated in the economic analysis, demonstrating the validity of the simulation. The standard deviation (referred as “St. dev.” in Figure 7.8) indicates how dispersed the data is from the mean; the widest standard deviation value is observed for Case II, namely St. dev.=0.70 M€ and mean of 0.45 M€ (Figure 7.8 (b)), followed by Case I with St. dev.=7.29 M€ and a mean of 6.35 M€, (Figure 7.8 (b)), and the lowest value in Case III with St. dev.=5.00 M€ and a mean of 5.08 M€ (Figure 7.8 (c)). These results show that a higher probability of loss of investment is more likely to occur in Case II, followed by Case I, and then Case III. In describing the NPV projection, the probability of reaching a negative NPV is given by the probability density area to the left of NPV=0 in the X-axis of Figure 7.8. This area for Case I is around 19.52 %, while for Case II it is 26.55 %, and in Case III it is 15.75 %. On the other hand, the probability of this investment exceeding an NPV of 12 M€, for Cases I and III, it is approximately 21.93 % and 8.69 %, respectively. For Case II, the probability of this investment exceeding the NPV of 1 M€ is approximately 21.98 %. In general, the probability distribution for the NPV presents a positive prognosis, with a probability of total gain of approximately 80.48 % for the Case I, 73.45 % for Case II and 84.25 % for Case III.

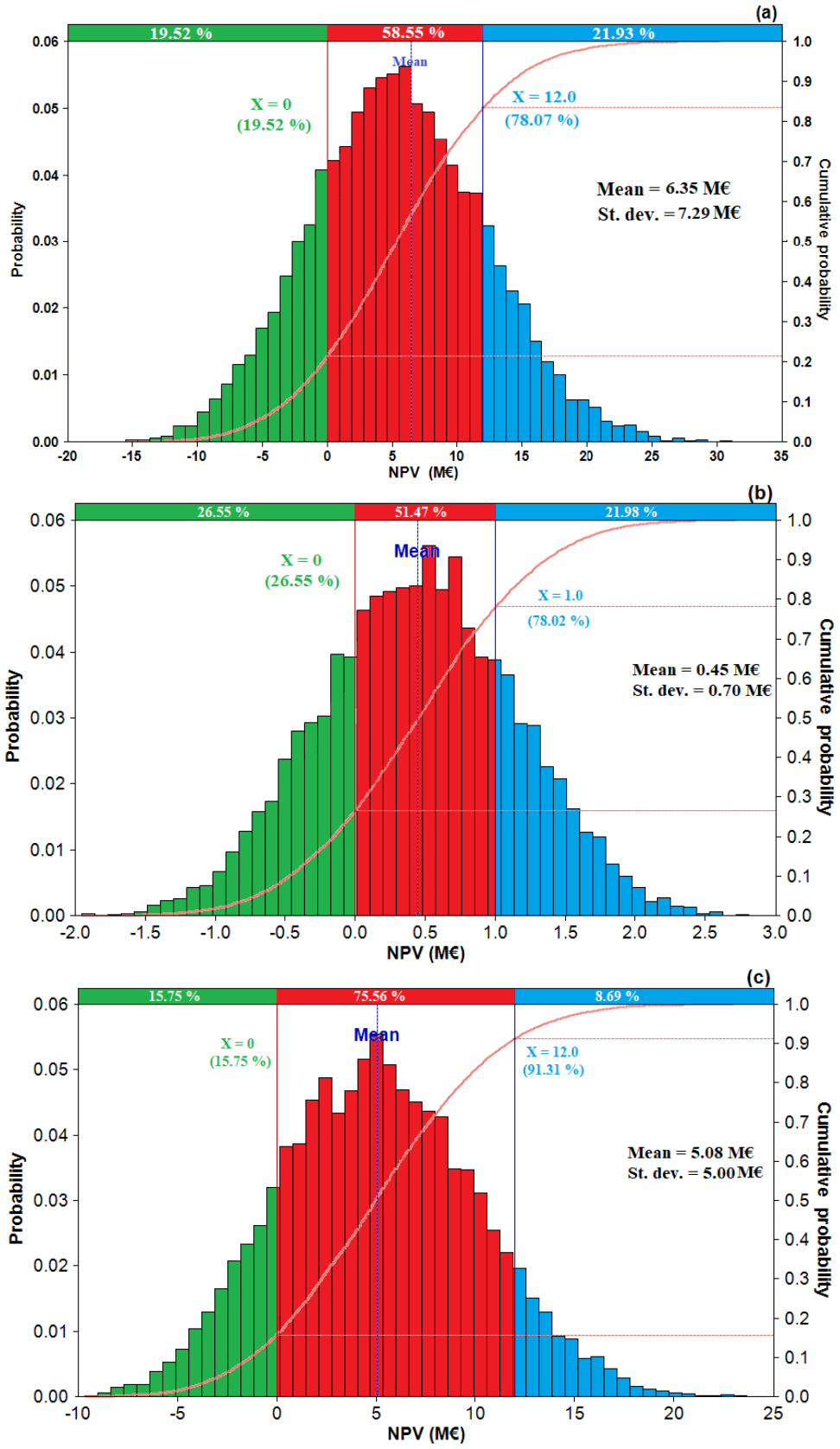

Figure 7.8 – Probability distribution for NPV for (a) Case I, (b) Case II and (c) Case III.

It was also made an analysis to the IRR and PBP risk forecast histograms as a function of the probability density and the cumulative probability for the three cases analyzed, following the methodology presented in Section 7.1.4.4. The results for the mean and standard deviation values relative to the parameters IRR and PBP are summarized in Table 7.11. The standard deviation of the IRR is between 0.01 % to 0.02 %, while the standard deviation of the PBP varies from 4.14% to 5.39 %. These results indicate that all the expected values tend to be close to the mean, which means that the investment presents a low flaw risk.

Table 7.11 – Parameters of the probability distributions for IRR and PBP, considering Cases I, II and III.

	IRR		PBP	
	Mean (%)	St. dev (%)	Mean (Years)	St. dev. (Years)
Case I	8.98	0.02	19.58	5.39
Case II	9.49	0.02	20.55	4.75
Case III	9.78	0.01	19.93	4.14

These results show that the NPV has higher standard deviation values than the IRR and PBP, meaning that the NPV is the financial indicator for which the uncertainty can represent the highest risk for the investment. Therefore, the following discussion is focused on how the uncertainty of each of the input variables considered will influence the NPV for each analyzed case.

Figure 7.9 shows the impact of each input variable on the NPV and its sensitivity range. For Cases I and III, the profitability of the project (as reflected by the uncertainty in NPV) is more sensitive to the electricity sale price, followed by the gasification system efficiency and the eucalyptus RFB costs. For Case I, the less striking variables are the initial investment followed by the discount rate, while for Case III, it is the discount rate followed by the initial investment. For Case II, the NPV is more sensitive to the price of natural gas, followed by the eucalyptus RFB cost, initial investment, discount rate, and the gasification system efficiency.

For Case I, the electricity sale price and the efficiency of the gasification system show a considerable impact on the NPV, compared to the other input variables. In fact, these two variables can greatly compromise the economic viability of the project, including the attainment of a negative NPV in an unfavorable and stressful scenario, namely up to −1.30 M€ and −1.02 M€, respectively. On the other hand, the NPV of the project can also increase considerably in result of more favorable scenarios for the electricity sale price and gasification system efficiency, namely up to a maximum of 14.24 M€ and 14.38 M€, respectively (mean value = 6.35 M€).

For Case II, the purchase price of natural gas (which translates into avoided costs) and the purchase price of the eucalyptus RFB can compromise the NPV in an unfavorable and stressful scenario, namely up to −0.47 M€ and −0.17 M€, respectively. On the other hand, in more favorable scenarios of natural gas and RFB prices, the NPV of the project can also be benefited up to a maximum of 1.36 M€ and 1.12 M€, respectively (mean value = 0.45 M€).

For Case III, the electricity sale price is the variable with higher influence on the economic viability of the project, allowing a negative NPV in an unfavorable and stressful scenario of up to −1.23 M€. On the other hand, in more favorable scenarios for electricity sales prices the NPV can also increase up to 11.43 M€ (mean value = 5.08 M€).

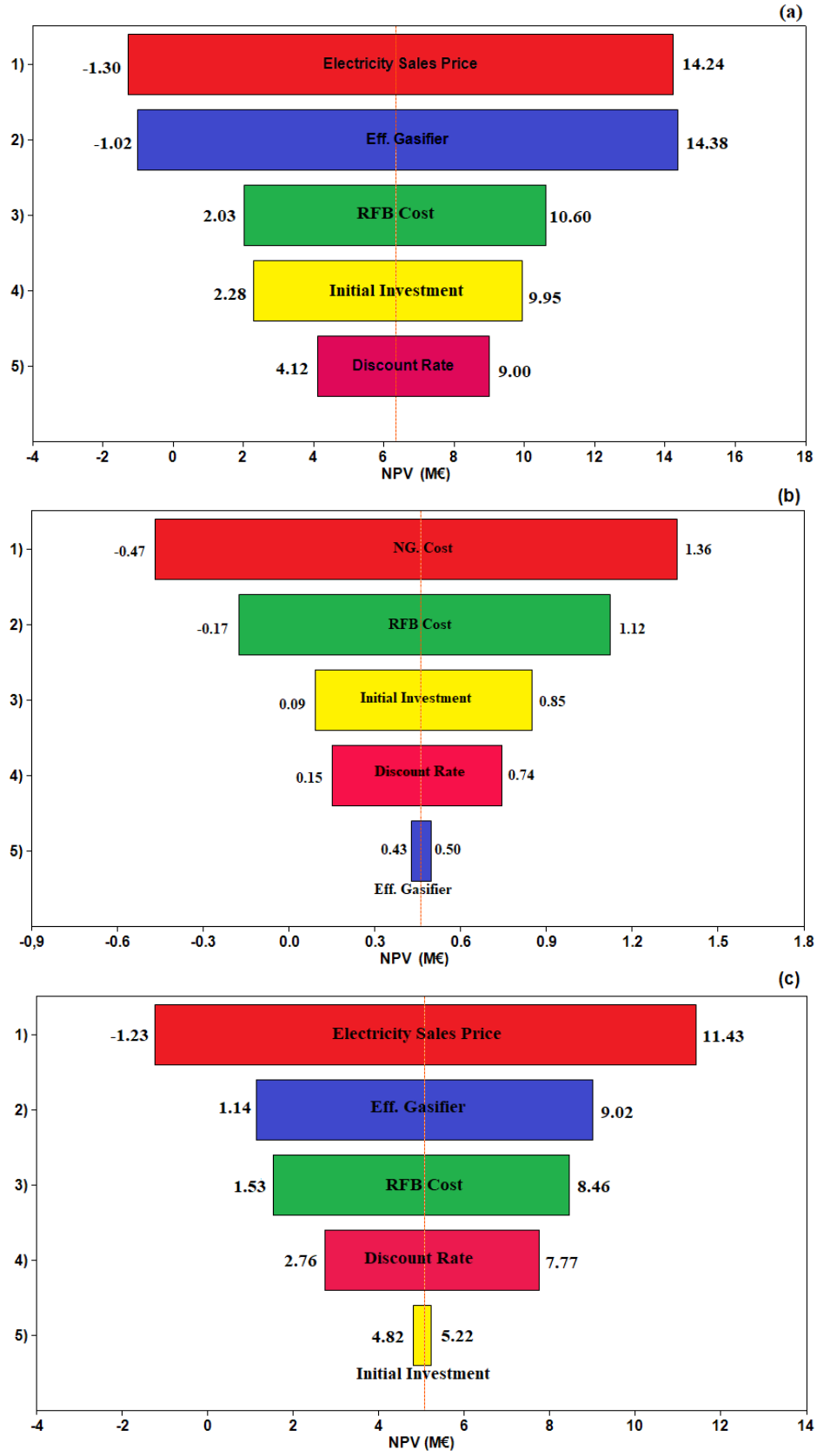

Figure 7.9 – Impact of changes in selected input variables on the NPV for (a) Case I, (b) Case II and (c) Case III.

7.1.6 CONCLUSIONS

This work presented a techno-economic analysis of three possible configurations for the energetic integration of eucalyptus RFB gasification in the PP industry. In Case I, it was analyzed the generation of electricity from RFB in a BIGCC. In Case II, it was analyzed the production of CaO from the combustion of PG in the lime kiln, consequently replacing natural gas. In Case III, it was analyzed the integration of Case I with Case II, namely a BIGCC system for electricity generation integrated with combustion of PG (replacing the NG) in the lime kiln for CaO production. All the data related to the gasification of the eucalyptus RFB was obtained from experiments carried out in the DAO-UA 80 kW_{th} pilot-scale BFB gasifier (see Section 4.1).

For Case I, a net electricity generation of 85.46 GWh/year is achieved, with an RFB consumption of 134.39 kt/year and a global system efficiency of 21.70 %. In Case II, it is produced 82.12 kt/year of CaO in the lime kiln using PG as fuel, corresponding to an eucalyptus RFB consumption of 21.10 kt/year and a global system efficiency of 34.17 %. In Case III, a combined electricity generation of 70.34 GWh/year and a production of 82.12 kt/year of CaO in the lime kiln is achieved, with an RFB consumption of 134.38 kt/h and global system efficiency of 25.0 %.

For all the analyzed configurations (Case I, II and III), the financial indicators (NPV, IRR and PBP) of the economic model presented positive perspectives. For Case I, the financial results showed a NPV equal to 6.61 M€, an IRR of 8.99 % and a PBP of 19.52 years. For Case II, the NPV is 0.50 M€, the IRR is 9.36 % and the PBP is 21.22 years. For Case III, the NPV is 5.81 M€, the IRR is 9.76 % and the PBP is 19.16 years. In general, the results of the economic analysis show a positive NPV, an IRR greater than the discount rate (8.5 %) and a PBP less than the useful life of the plant, which makes this project a viable investment the for the three cases analyzed, from an economic point of view.

The sensitivity analysis shows that the risk assessment yielded quite favorable investment projections with a probability that the NPV will reach positive values of 80.48 % for Case I, 73.45 % for Case II and 84.25 % for Case III. Compared to the NPV, the IRR and the PBP had lower standard deviation values, between 0.01 % to 0.02 % and 4.14 % to 5.39 %, respectively; this means that a lower investment risk is associated to these two financial indicators. The NPV is considerably more sensitive to the electricity sale price and the gasification system efficiency for Cases I and III, whereas for Case II, the NPV is more sensitive to the price of the NG and the purchase price of the eucalyptus RFB.

Finally, despite the economic viability of the three considered Cases, it must be analyzed how attractive the projects are to potential investors. If it is taken into account the recommendations of the World Bank [549], the calculated IRR is less than the minimum of 10 % recommended and the PBP exceeds the maximum 10 years recommended. In particular, the PBP for all analyzed Cases is close to 20 years, which represents a long period to recover the total investment. Another aspect to consider is that gasification technologies are not fully mature, nor highly available on a commercial scale. Nonetheless, as previously stated in this PhD document, biomass gasification technologies can have a main role in terms of the future transition to a bioeconomy and be the basis of future biorefineries that will compete with current conventional petrochemical refineries for the production of various commodities (see Chapter 2); this must be accounted for during the decision-making process. The role of governmental policies and appropriate economic instruments will also be of major relevance in this context.

8 DISCUSSION

This work sought the production of new scientific knowledge for the development of direct (air) biomass gasification process in BFBs to produce a gaseous fuel with suitable properties to replace natural gas in industrial gas burners. Accordingly, various solutions were analyzed to improve the raw PG quality (e.g., H_2 concentration, LHV) and the process performance indicators (e.g., Y_{gas}, CGE and CCE).

In this regard, it was demonstrated the feasibility of direct gasification of biomass in BFBs to produce a combustible gas that can replace fossil fuels in various applications. The addition of superheated steam as primary measure showed promising results by allowing the increase of H_2 concentration and H_2/CO molar ratio in the PG, without compromising the stability of the process. However, this measure mainly showed potential for the gasification of high-density biomass due to the necessity of char accumulation in the reactor bottom bed for the occurrence of char-steam reforming reactions. Addition of RDF to the biomass feedstock also led to enhanced gasification products, without changing the stability of the process. This latter seems as a highly promising strategy in terms of economic viability and environmental benefits of future gasification plants, due to the high availability and low costs of wastes. The energetic valorization of RDF also acts in accordance with circular economy principles, contributing to the sustainability of both energy supply and waste management. In the same vein, the application of low-cost catalysts as primary measure allowed the improvement of the PG quality and process efficiency parameters with distinct solid materials. This measure was successfully implemented in different experimental infrastructures, allowing the use and preservation of the PG thermal energy for the catalysis process; this may be relevant to avoid excessive plant investment and operation costs. On one hand, wood pellets chars and concrete showed high potential for the relative increase of the H_2 concentration and H_2/CO molar ratio in the PG, which is relevant for advanced PG applications (e.g., FT synthesis). On the other hand, synthetic Fe_2SiO_4 promoted the highest relative increases of PG LHV, Y_{gas}, CGE and CCE, consequently showing suitability to be used when immediate direct combustion of the PG is desired (e.g., replacement of natural gas in industrial burners). Nevertheless, the highest absolute values of H_2 concentration, LHV, CGE and CCE were found for the experiments performed with concrete as catalyst.

The results obtained indicate that an optimal direct (air) gasification process in BFBs could potentially involve the use of a mixture of RFB and RDF as feedstock with the addition of superheated steam in the reactor bottom bed. In this case, the high density of the RDFs may be beneficial for char accumulation in the reactor bottom bed and consequent occurrence of char-steam reforming reactions with steam injection. The results also suggest that an optimal balance between PG quality, efficiency parameters and stability of the process, could potentially be attained with ER = 0.25, bed temperature = 800 ºC, S/B = 0.5 and a feedstock mixture containing a 50/50 %wt ratio of RDF and RFB. In addition, the integration of a second section in the gasifier freeboard for low-cost catalysts (e.g., concrete) insertion could improve the PG quality and process efficiency even further. This section could also act as a catalytic filter to allow particle removal in the gasifier. In this configuration, thermal losses would be reduced. These aspects need to be quantified in future works and properly analyzed in techno-economic and life cycle analyses.

Regarding tar formation, it was found that inorganics and char accumulation in the reactor bed (directly related to operation time), and respective chemistry and composition, have significant impact on the tar concentration in the PG. In fact, a decrease of tar concentration of up to 50 % within 45 minutes of operation was found. Thus, operation times over 2 hours are suggested to attain steady-state conditions in terms of tar concentration in the PG; this needs to be accounted for in future works seeking tar reduction in gasification processes.

Regarding the prediction of the gasification products by numerical modelling tools, two main aspects are of major relevance: On one hand, the significant variability of experimental results found in the

literature regarding direct biomass gasification in BFB reactors significantly hinders the development and applicability of empirical models, consequently reflecting the necessity of obtaining specific knowledge for the experimental demonstration of distinct gasification processes for each particular application. On the other hand, chemical equilibrium modelling showed various limitations and significant deviations from practical experimental results obtained in direct (air) BFB gasifiers. Thus, the development of alternative modelling techniques, for example approaches that integrate theoretical and experimental knowledge, such as the integration of chemical equilibrium with empirical modelling, can be of major relevance for the development of suitable supporting tools for the up-scale, design and operation of gasification plants.

Regarding the techno-economic pre-feasibility analysis of the biomass gasification process, the economic viability of the integration of direct (air) biomass gasification technologies in the PP industry was shown for three distinct cases, including electricity generation and natural gas replacement in the lime kiln. However, the financial indicators are not attractive for potential investors. In this regard, supporting policies, technology roadmaps, market-driven research, policy goals and frameworks, are fundamental to reduce the risks and uncertainties associated with this investment. Regarding the transformation of the PP industry into a complete biorefinery design, the development of biomass conversion technologies for co-integration with gasification processes is also of major relevance. In this regard, the co-combustion of RFB from eucalyptus with primary or secondary sludges from the PP industry was shown as a valid co-integrable energy valorization option.

9 CONCLUSIONS

The society currently faces the greatest environmental threat of the 21st century: Climate Change. The answer to this man-made disaster must be made by changing our economy to one more based in renewable materials, and whose energy is provided by the eternal nature energies (e.g., wind, solar). In this context, biomass has a very important role by being an adjustable and renewable feedstock that allows the replacement of fossil fuels in various applications. In fact, biorefineries have the potential to compete with petrochemical refineries for the production of various commodities. In these industries, gasification can represent a key technology due to its flexibility and the obtainable PG is a very promising intermediate feedstock for the generation of heat and power and synthesis of biochemicals and biofuels.

This work performs an extensive pilot-scale demonstration of the production of PG from various types of biomass (including eucalyptus RFB), and under distinct operating conditions, as a valid solution for the replacement of natural gas in industrial gas burners. In this regard, H_2 and CO concentration in the PG was found between 2.0 and 16.9 %v and 5.7 and 37.6 %v, respectively. PG LHV was found between 3.7 to 7.5 MJ/Nm^3, Y_{gas} between 1.2 to 2.2 Nm^3/kg biomass db, CGE between 31.9 to 74.8 % and CCE between 55.7 to 90.3 %. Thus, various measures that reflect potential opportunities to improve the PG quality and process efficiency were identified and analyzed. Amongst these, using mixtures of RDF and RFB as feedstock, injecting superheated steam in the reactor bottom bed and applying low-cost catalysts (e.g., concrete and wood pellets chars) above the surface of the bed, seem to be very promising and potentially combinable strategies.

The economic viability of the integration of gasification processes in the PP industry was also shown, despite the determined economic parameters lacking interest to potential investors. In this regard, various uncertainties and barriers still hinder the commercial breakthrough of biomass gasification technologies and respective integration in the PP industry, and these were discussed throughout this document. At this stage, demonstration and industrial-scale experimental research is required to tackle these issues and further advance the technology integration in the markets. For this purpose, the first step is the production of PG from RFB for natural gas replacement at the lime kilns of the local PP industry. Afterwards, a gradual and phased transformation into complete biorefinery designs can be considered, which will require the improvement of various co-integrable biorefinery concepts and key technologies to competitive market levels. Suitable economic tools must also be developed and employed to support the first years of biorefinery operation and respective development towards market maturity and production stability. To this end, and to avoid the interruption of operation of fully functioning gasification-based biorefineries, a strong support from governments is mandatory. Finally, solving these enormous challenges can give stakeholders the confidence necessary to invest in this industry, consequently leading to the establishment of relevant competition with the current petrochemical refineries. This will allow biomass, and gasification, to have a key role in the combat against Climate Change.

10 FUTURE WORK

The results from this thesis can be combined to provide an adequate support to decisions related to biomass gasification to energy conversion options and projects. Nevertheless, distinct aspects must still be evaluated, and various issues solved, to improve the understanding of the biomass gasification process and properly support these investments. In this regard, the following proposal of future studies and technologic development are considered of major relevance:

- Development of a PG gas burner and in-depth analysis of the combustion characteristics of the PG (and mixtures of PG with natural gas). Relevant combustion properties to characterize the PG combustion include laminar flame speed, adiabatic flame temperature, Wobbe Index, flame stability and extinction limits. Evaluation of tar clogging issues and exhaust gases emissions must also be performed. For this purpose, a suitable gas burner must be developed, allowing the insertion and control of air flow, as well as sampling and conditioning of the exhaust gases. Experimental research regarding PG combustion is extremely relevant to serve as a tool to support biomass gasification related projects decisions, specifically those that seek to use PG in combustion systems or as a middle platform compound in a gasification-based biorefinery design.

- Development and implementation of a demonstration gasification plant (~1 MW_{th}) in the PP industry site for gradual replacement of the natural gas used in the current industrial gas burners (e.g., boilers, lime kiln). In a first stage, very small percentages of natural gas should be replaced, for example using PG to provide 5% of the necessary energy for the calcination process. Excessive heat from the gasification unit can be evaluated as an opportunity to dry the RFB to lower values than 25 %. As the PG is burned immediately downstream of the gasifier, only minimal cleaning procedures will be required (e.g., cyclone-filter placed at the outlet of the gasifier). However, in this configuration, the temperature of the PG must be maintained above 400 ºC to avoid tar condensation in the ducts. The operation of this prototype unit will allow the production of valuable practical knowledge, such as the identification of in-site operating issues and respective best problem-solving approaches, to support the implementation of future gasification plants with higher thermal power and future gasification-based biorefineries.

- Determination of the effect of the tested solid materials (wood pellets chars, eucalyptus ashes, Fe_2SiO_4, ilmenite and concrete) on tar conversion and composition. In a first stage, this should be performed by testing the materials on selected tar model compounds (e.g., naphthalene), and then the experiments should be upscaled to real tar mixtures from distinct PGs. It should also be quantified the influence of long gasification operation times on the decay of the activity of the tested solid materials. In this context, it is important to determine the effect of coke deposition and the release of potassium, chlorine and sulfur, amongst other species, on the poisoning of the catalysts.

- Evaluation of the direct (air + steam) co-gasification of distinct mixtures of RFB, RDF and sludges in BFBs. Improvement of the process can also be evaluated by applying in-situ low-cost catalysts (e.g., natural minerals, ashes rich in alkali metals, chars) integrated within the gasifier to use and preserve the thermal energy of the PG. The influence of the hydrodynamic behavior of the BFBs should be considered, for example fluidization velocity, vapors

residence time in the bed/freeboard, among other aspects. Then, the following aspects should be analyzed: mass percentage of RDF, sludges and RFB in the feedstock blend, S/B ratio, and impact of the chosen low-cost catalysts, and respective operating parameters (gas-solid contact time and temperature). Seeking the valorization of residual O_2 from adjacent processes (e.g., water electrolysis for H_2 production), the enrichment of air with O_2 (e.g., up to 40 %v) can also be evaluated. At this stage, determination of the tar concentration in the PG is of the utmost importance to properly evaluate these gasification processes. The understanding of these processes can be improved by determining the devolatilization kinetics of the distinct feedstock mixtures under controlled conditions in bench-scale reactors, before the upscale to gasification at pilot-scale, due to their relevant subsequent impact on the process. In this respect, thermogravimetric analyses of the fuel blends may also be beneficial.

- Development and evaluation of secondary measures to improve the PG quality, such as tar scrubbing and high temperature filtration. The implementation of this latter in the DAO-UA experimental infrastructures will also improve the reliability of tar characterization because it will allow the reduction of particles retained in the syringes during the sampling procedure. It is acknowledged that the pathway to affordable clean PG will require gasifier designs that reduce secondary gas cleaning requirements as much as possible by implementing primary gas cleaning measures, particularly those with low complexity and costs. Nonetheless, post-processing treatment measures must be analyzed and considered in comprehensive techno-economic analyses for comparison purposes with primary measures effectiveness. Furthermore, the use of primary measures may not be enough to attain the desired PG quality for some applications; in these cases, a combination of primary and secondary measures may be beneficial.

- Improvement of the accuracy of the developed empirical model by increasing the quality of the input data, excluding outliers, increasing database size and including the biomass feedstock chemical composition in the correlations development. This will be relevant to provide a more adequate supporting tool for the design and operation of gasification plants.

- Development of holistic techno-economic and life cycle analyses to integrate and evaluate the aforementioned aspects.

11 ACKNOWLEDGMENTS

The author acknowledges the following projects and institutions:

- FCT/MCTES and The Navigator Company for providing financial support to the PhD scholarship granted to Daniel Pio (ref. PD/BDE/128620/2017), endorsed by the Doctoral Program FCT PD00158/2012.

- Project inpactus – innovative products and technologies from eucalyptus, Project N.º 21874 funded by Portugal 2020 through European Regional Development Fund (ERDF) in the frame of COMPETE 2020 nº246/AXIS II/2017.

- SusPhotoSolutions - Soluções Fotovoltaicas Sustentáveis, PO Centro 2020 (ref. CENTRO-01-0145-FEDER-000005).

- Cellular oxide catalysts for emission lean combustion in porous media, project PO Centro 2020 (ref. CENTRO-01-0145-FEDER-000005).

- PoliTechWaste – Policy and technology analysis of waste/biomass residue gasification for energy production in Portugal, Project CMU/TMP/0032/2017, Exploratory Research Proposals under the Carnegie Mellon Portugal Program – 2017.

- PTDC/AAC-AMB/ 116568/2010 (Project n.º FCOMP-01-0124-FEDER-019346) - BiomAshTech - Ash impacts during thermo-chemical conversion of biomass.

- Portuguese Foundation for Science and Technology (FCT)/Ministry of Science, Technology and Higher Education (MCTES) for the financial support to CESAM (UIDP/50017/2020+UIDB/50017/2020), through national funds.

- NOTARGAS – Novel catalyst concepts for tar-free oxy-steam gasification of biomass. POCI-01-0145-FEDER-030661. Financed by FCT/MCTES.

12 BIBLIOGRAPHY

[1] C.A.V.B. de Sales, D.M.Y. Maya, E.E.S. Lora, R.L. Jaén, A.M.M. Reyes, A.M. González, R.V. Andrade, J.D. Martínez, Experimental study on biomass (eucalyptus spp.) gasification in a two-stage downdraft reactor by using mixtures of air, saturated steam and oxygen as gasifying agents, Energy Convers. Manag. 145 (2017) 314–323. https://doi.org/10.1016/j.enconman.2017.04.101.

[2] P.H. Moud, K.J. Andersson, R. Lanza, J.B.C. Pettersson, K. Engvall, Effect of gas phase alkali species on tar reforming catalyst performance: Initial characterization and method development, Fuel. 154 (2015) 95–106. https://doi.org/10.1016/j.fuel.2015.03.027.

[3] D.T. Pio, L.A.C. Tarelho, A.M.A. Tavares, M.A.A. Matos, V. Silva, Co-gasification of refused derived fuel and biomass in a pilot-scale bubbling fluidized bed reactor, Energy Convers. Manag. 206 (2020). https://doi.org/10.1016/j.enconman.2020.112476.

[4] D.T. Pio, L.A.C. Tarelho, M.A.A. Matos, Characteristics of the gas produced during biomass direct gasification in an autothermal pilot-scale bubbling fluidized bed reactor, Energy. 120 (2017) 915–928. https://doi.org/10.1016/j.energy.2016.11.145.

[5] M. Hervy, D. Remy, A. Dufour, G. Mauviel, Air-blown gasification of Solid Recovered Fuels (SRFs) in lab-scale bubbling fluidized-bed: Influence of the operating conditions and of the SRF composition, Energy Convers. Manag. 181 (2019) 584–592. https://doi.org/10.1016/j.enconman.2018.12.052.

[6] N. Cerone, F. Zimbardi, L. Contuzzi, M. Prestipino, M.O. Carnevale, V. Valerio, Air-steam and oxy-steam gasification of hydrolytic residues from biorefinery, Fuel Process. Technol. 167 (2017) 451–461. https://doi.org/10.1016/j.fuproc.2017.07.027.

[7] T. Waldheim, L. Nilsson, Heating value of gases from biomass gasification, 2001. http://www.ieatask33.org/app/webroot/files/file/publications/HeatingValue.pdf.

[8] C. Brage, Q. Yu, G. Chen, K. Sjöström, Use of amino phase adsorbent for biomass tar sampling and separation, Fuel. 76 (1997) 137–142. https://doi.org/10.1016/S0016-2361(96)00199-8.

[9] CEN/TS 15148 Solid biofuels - Method for the determination of the content of volatile matter, 2005. https://www.nen.nl/pdfpreview/preview_82570.pdf (accessed July 24, 2019).

[10] CEN/TS 14775 Solid biofuels - Method for the determination of ash content, 2004. https://www.nen.nl/pdfpreview/preview_82572.pdf (accessed July 24, 2019).

[11] CEN/TS 14774-1 Solid biofuels - Methods for determination of moisture content - Oven dry method - Part 1: Total moisture - Reference method, 2004.

[12] J. Parikh, S.A. Channiwala, G.K. Ghosal, A correlation for calculating HHV from proximate analysis of solid fuels, Fuel. 84 (2005) 487–494. https://doi.org/10.1016/j.fuel.2004.10.010.

[13] A. Gambarotta, M. Morini, A. Zubani, A non-stoichiometric equilibrium model for the simulation of the biomass gasification process, Appl. Energy. 227 (2018) 119–127. https://doi.org/10.1016/j.apenergy.2017.07.135.

[14] V. Grech, WASP (Write a Scientific Paper) using Excel – 13: Correlation and Regression, Early Hum. Dev. 122 (2018) 60–63. https://doi.org/10.1016/j.earlhumdev.2018.04.009.

[15] S. Heidenreich, P.U. Foscolo, New concepts in biomass gasification, Prog. Energy Combust. Sci. 46 (2015) 72–95. https://doi.org/10.1016/j.pecs.2014.06.002.

[16] A. Molino, S. Chianese, D. Musmarra, Biomass gasification technology: The state of the art overview, J. Energy Chem. 25 (2016) 10–25. https://doi.org/10.1016/j.jechem.2015.11.005.

[17] D. Bourguignon, Biomass for electricity and heating. Opportunities and challenges., 2015. http://www.europarl.europa.eu/RegData/etudes/BRIE/2015/568329/EPRS_BRI(2015)568329_EN.pdf.

[18] R.J. Henry, Evaluation of plant biomass resources available for replacement of fossil oil, Plant Biotechnol. J. 8 (2010) 288–293. https://doi.org/10.1111/j.1467-7652.2009.00482.x.

[19] J. Kjarstad, F. Johnsson, The role of biomass to replace fossil fuels in a regional energy system: The case of west Sweden, Therm. Sci. 20 (2016) 1023–1036. https://doi.org/10.2298/TSCI151216113K.

[20] D. Sengupta, Chemicals from Biomass, CRC Press, 2012. https://doi.org/10.1201/b12341.

[21] W. van Swaaij, S. Kersten, W. Palz, Biomass power for the world: Transformations to effective use, 2015.

[22] H. Long, X. Li, H. Wang, J. Jia, Biomass resources and their bioenergy potential estimation: A review, Renew. Sustain. Energy Rev. 26 (2013) 344–352. https://doi.org/10.1016/j.rser.2013.05.035.

[23] D.A. Landis, C. Gratton, R.D. Jackson, K.L. Gross, D.S. Duncan, C. Liang, T.D. Meehan, B.A. Robertson, T.M. Schmidt, K.A. Stahlheber, J.M. Tiedje, B.P. Werling, Biomass and biofuel crop effects on biodiversity and ecosystem services in the North Central US, Biomass and Bioenergy. 114 (2018) 18–29. https://doi.org/10.1016/j.biombioe.2017.02.003.

[24] J. Popp, Z. Lakner, M. Harangi-Rákos, M. Fári, The effect of bioenergy expansion: Food, energy, and environment, Renew. Sustain. Energy Rev. 32 (2014) 559–578. https://doi.org/10.1016/j.rser.2014.01.056.

[25] O.C.D. Anejionu, J. Woods, Preliminary farm-level estimation of 20-year impact of introduction of energy crops in conventional farms in the UK, Renew. Sustain. Energy Rev. 116 (2019) 109407. https://doi.org/10.1016/j.rser.2019.109407.

[26] V.S. Sikarwar, M. Zhao, P.S. Fennell, N. Shah, E.J. Anthony, Progress in biofuel production from gasification, Prog. Energy Combust. Sci. 61 (2017) 189–248. https://doi.org/10.1016/j.pecs.2017.04.001.

[27] K. Waldron, Advances in Biorefineries: Biomass and Waste Supply Chain Exploitation, 2014. https://books.google.pt/books/about/Advances_in_Biorefineries.html?id=2KaoZwEACAAJ&redir_esc=y (accessed November 22, 2017).

[28] A. Pandey, R. Höfer, M. Taherzadeh, K.M. Nampoothiri, C. Larroche, Industrial Biorefineries and White Biotechnology, 2015. https://doi.org/10.1016/c2013-0-19082-4.

[29] E. Shayan, V. Zare, I. Mirzaee, Hydrogen production from biomass gasification; a theoretical comparison of using different gasification agents, Energy Convers. Manag. 159 (2018) 30–41. https://doi.org/10.1016/j.enconman.2017.12.096.

[30] A. Arregi, M. Amutio, G. Lopez, J. Bilbao, M. Olazar, Evaluation of thermochemical routes for hydrogen production from biomass: A review, Energy Convers. Manag. 165 (2018) 696–719. https://doi.org/10.1016/j.enconman.2018.03.089.

[31] C.M. van der Meijden, H.J. Veringa, L.P.L.M. Rabou, The production of synthetic natural gas (SNG): A comparison of three wood gasification systems for energy balance and overall efficiency, Biomass and Bioenergy. 34 (2010) 302–311. https://doi.org/10.1016/j.biombioe.2009.11.001.

[32] T.M.H. Dabros, M.Z. Stummann, M. Høj, P.A. Jensen, J.D. Grunwaldt, J. Gabrielsen, P.M. Mortensen, A.D. Jensen, Transportation fuels from biomass fast pyrolysis, catalytic

hydrodeoxygenation, and catalytic fast hydropyrolysis, Prog. Energy Combust. Sci. 68 (2018) 268–309. https://doi.org/10.1016/j.pecs.2018.05.002.

[33] G. Perkins, N. Batalha, A. Kumar, T. Bhaskar, M. Konarova, Recent advances in liquefaction technologies for production of liquid hydrocarbon fuels from biomass and carbonaceous wastes, Renew. Sustain. Energy Rev. 115 (2019) 109400. https://doi.org/10.1016/j.rser.2019.109400.

[34] F. Shen, X. Xiong, J. Fu, J. Yang, M. Qiu, X. Qi, D.C.W. Tsang, Recent advances in mechanochemical production of chemicals and carbon materials from sustainable biomass resources, Renew. Sustain. Energy Rev. 130 (2020) 109944. https://doi.org/10.1016/j.rser.2020.109944.

[35] G. Fiorentino, M. Ripa, S. Ulgiati, Chemicals from biomass: technological *versus* environmental feasibility. A review, Biofuels, Bioprod. Biorefining. 11 (2017) 195–214. https://doi.org/10.1002/bbb.1729.

[36] C.A. García-Velásquez, C.A. Cardona, Comparison of the biochemical and thermochemical routes for bioenergy production: A techno-economic (TEA), energetic and environmental assessment, Energy. 172 (2019) 232–242. https://doi.org/10.1016/j.energy.2019.01.073.

[37] H.C. Ong, W.H. Chen, Y. Singh, Y.Y. Gan, C.Y. Chen, P.L. Show, A state-of-the-art review on thermochemical conversion of biomass for biofuel production: A TG-FTIR approach, Energy Convers. Manag. 209 (2020) 112634. https://doi.org/10.1016/j.enconman.2020.112634.

[38] P. Ibarra-Gonzalez, B.G. Rong, A review of the current state of biofuels production from lignocellulosic biomass using thermochemical conversion routes, Chinese J. Chem. Eng. 27 (2019) 1523–1535. https://doi.org/10.1016/j.cjche.2018.09.018.

[39] R.C. Neves, B.C. Klein, R.J. da Silva, M.C.A.F. Rezende, A. Funke, E. Olivarez-Gómez, A. Bonomi, R. Maciel-Filho, A vision on biomass-to-liquids (BTL) thermochemical routes in integrated sugarcane biorefineries for biojet fuel production, Renew. Sustain. Energy Rev. 119 (2020). https://doi.org/10.1016/j.rser.2019.109607.

[40] E. Hosseini Koupaie, S. Dahadha, A.A. Bazyar Lakeh, A. Azizi, E. Elbeshbishy, Enzymatic pretreatment of lignocellulosic biomass for enhanced biomethane production-A review, J. Environ. Manage. 233 (2019) 774–784. https://doi.org/10.1016/j.jenvman.2018.09.106.

[41] W. Luo, J. Wang, X. Liu, H. Li, H. Pan, Q. Gu, X. Yu, A facile and efficient pretreatment of corncob for bioproduction of butanol, Bioresour. Technol. 140 (2013) 86–89. https://doi.org/10.1016/j.biortech.2013.04.063.

[42] K. Thangavelu, R. Desikan, O.P. Taran, S. Uthandi, Delignification of corncob via combined hydrodynamic cavitation and enzymatic pretreatment: Process optimization by response surface methodology, Biotechnol. Biofuels. 11 (2018) 1–13. https://doi.org/10.1186/s13068-018-1204-y.

[43] A.P. Moshi, S.G. Temu, I.A. Nges, G. Malmo, K.M.M. Hosea, E. Elisante, B. Mattiasson, Combined production of bioethanol and biogas from peels of wild cassava Manihot glaziovii, Chem. Eng. J. 279 (2015) 297–306. https://doi.org/10.1016/j.cej.2015.05.006.

[44] S. Consonni, R.E. Katofsky, E.D. Larson, A gasification-based biorefinery for the pulp and paper industry, Chem. Eng. Res. Des. 87 (2009) 1293–1317. https://doi.org/10.1016/j.cherd.2009.07.017.

[45] K.C. Pagnoncelli, A.R. Pereira, G.C. Sedenho, T. Bertaglia, F.N. Crespilho, Ethanol generation, oxidation and energy production in a cooperative bioelectrochemical system, Bioelectrochemistry. 122 (2018) 11–25. https://doi.org/10.1016/j.bioelechem.2018.02.007.

[46] G.M. Figueroa-Torres, W.M.A. Wan Mahmood, J.K. Pittman, C. Theodoropoulos, Microalgal biomass as a biorefinery platform for biobutanol and biodiesel production, Biochem. Eng. J. 153 (2020) 107396. https://doi.org/10.1016/j.bej.2019.107396.

[47] X. Liu, X. Yu, Enhancement of Butanol Production: From Biocatalysis to Bioelectrocatalysis, ACS Energy Lett. 5 (2020) 867–878. https://doi.org/10.1021/acsenergylett.9b02596.

[48] A. Sanchez, I. Valdez-Vazquez, A. Soto, S. Sánchez, D. Tavarez, Lignocellulosic n-butanol co-production in an advanced biorefinery using mixed cultures, Biomass and Bioenergy. 102 (2017) 1–12. https://doi.org/10.1016/j.biombioe.2017.03.023.

[49] A. Anca-Couce, Reaction mechanisms and multi-scale modelling of lignocellulosic biomass pyrolysis, Prog. Energy Combust. Sci. 53 (2016) 41–79. https://doi.org/10.1016/j.pecs.2015.10.002.

[50] P. Basu, Biomass Gasification, Pyrolysis and Torrefaction, Elsevier, 2013. https://doi.org/10.1016/C2011-0-07564-6.

[51] J. Koppejan, The Handbook of Biomass Combustion and Co-firing, Earthscan, 2012. https://doi.org/10.4324/9781849773041.

[52] M. La Villetta, M. Costa, N. Massarotti, Modelling approaches to biomass gasification: A review with emphasis on the stoichiometric method, Renew. Sustain. Energy Rev. 74 (2017) 71–88. https://doi.org/10.1016/j.rser.2017.02.027.

[53] J. Kluska, M. Ochnio, D. Kardaś, Carbonization of corncobs for the preparation of barbecue charcoal and combustion characteristics of corncob char, Waste Manag. 105 (2020) 560–565. https://doi.org/10.1016/j.wasman.2020.02.036.

[54] H. Suopajärvi, E. Pongrácz, T. Fabritius, The potential of using biomass-based reducing agents in the blast furnace: A review of thermochemical conversion technologies and assessments related to sustainability, Renew. Sustain. Energy Rev. 25 (2013) 511–528. https://doi.org/10.1016/j.rser.2013.05.005.

[55] W. Ma, B. Liu, R. Zhang, T. Gu, X. Ji, L. Zhong, G. Chen, L. Ma, Z. Cheng, X. Li, Co-upgrading of raw bio-oil with kitchen waste oil through fluid catalytic cracking (FCC), Appl. Energy. 217 (2018) 233–240. https://doi.org/10.1016/j.apenergy.2018.02.036.

[56] S. Safarian, R. Unnþórsson, C. Richter, A review of biomass gasification modelling, Renew. Sustain. Energy Rev. 110 (2019) 378–391. https://doi.org/10.1016/j.rser.2019.05.003.

[57] V. Dhyani, T. Bhaskar, A comprehensive review on the pyrolysis of lignocellulosic biomass, Renew. Energy. 129 (2018) 695–716. https://doi.org/10.1016/j.renene.2017.04.035.

[58] M. Asadullah, Barriers of commercial power generation using biomass gasification gas: A review, Renew. Sustain. Energy Rev. 29 (2014) 201–215. https://doi.org/10.1016/j.rser.2013.08.074.

[59] J.A. Ruiz, M.C. Juárez, M.P. Morales, P. Muñoz, M.A. Mendívil, Biomass gasification for electricity generation: Review of current technology barriers, Renew. Sustain. Energy Rev. 18 (2013) 174–183. https://doi.org/10.1016/j.rser.2012.10.021.

[60] D.T. Pio, L.A.C. Tarelho, Empirical and chemical equilibrium modelling for prediction of biomass gasification products in bubbling fluidized beds, Energy. 202 (2020) 117654. https://doi.org/10.1016/j.energy.2020.117654.

[61] G. Mongkhonsiri, R. Gani, P. Malakul, S. Assabumrungrat, Integration of the biorefinery concept for the development of sustainable processes for pulp and paper industry, Comput. Chem. Eng. 119 (2018) 70–84. https://doi.org/10.1016/j.compchemeng.2018.07.019.

[62] A. Toppinen, S. Pätäri, A. Tuppura, A. Jantunen, The European pulp and paper industry in

transition to a bio-economy: A Delphi study, Futures. 88 (2017) 1–14. https://doi.org/10.1016/j.futures.2017.02.002.

[63] B. Ben Daya, M. Nourelfath, Sustainability assessment of integrated forest biorefinery implemented in Canadian pulp and paper mills, Int. J. Prod. Econ. 214 (2019) 248–265. https://doi.org/10.1016/j.ijpe.2018.06.014.

[64] J. Isaksson, Biomass Gasification-Based Biorefineries in Pulp and Paper Mills – Greenhouse Gas Emission Implications and Economic Performance, Chalmers University of Technology, 2015. http://publications.lib.chalmers.se/publication/213227.

[65] C. Higman, M. van der Burgt, Gasification, Elsevier, 2003. https://doi.org/10.1016/B978-0-7506-7707-3.X5000-1.

[66] S. Heidenreich, M. Müller, P.U. Foscolo, Advanced Biomass Gasification, Elsevier, 2016. https://doi.org/10.1016/C2015-0-01777-4.

[67] E. Dahlquist, Technologies for converting biomass to useful energy combustion, gasification, pyrolysis, torrefaction and fermentation, CRC Press, 2013. https://doi.org/10.1201/b14561.

[68] K.J. Timmer, Carbon conversion during bubbling fluidized bed gasification of biomass, Iowa State University, 2008. http://digitalcollections.dordt.edu/cgi/viewcontent.cgi?article=1075&context=faculty_work.

[69] H. Knoef, Handbook of Biomass Gasification, BTG Gr. 2012 (2005) 378.

[70] M. Siedlecki, W. de Jong, A.H.M. Verkooijen, Fluidized bed gasification as a mature and reliable technology for the production of bio-syngas and applied in the production of liquid transportation fuels-a review, Energies. 4 (2011) 389–434. https://doi.org/10.3390/en4030389.

[71] J.J. Cheng, Biomass to renewable energy processes, second edition, CRC Press/Taylor & Francis, 2017. https://doi.org/10.1201/9781315152868.

[72] J.P. Ciferno, J.J. Marano, Benchmarking biomass gasification technologies for fuels, chemicals and hydrogen production, 2002. http://seca.doe.gov/technologies/coalpower/gasification/pubs/pdf/BMassGasFinal.pdf.

[73] M. Barrio, Experimental Investigation of Small-Scale Gasification of Woody Biomass, 2002. http://www.diva-portal.org/smash/get/diva2:126378/FULLTEXT01.pdf.

[74] M. Puig-Gamero, J. Argudo-Santamaria, J.L. Valverde, P. Sánchez, L. Sanchez-Silva, Three integrated process simulation using aspen plus®: Pine gasification, syngas cleaning and methanol synthesis, Energy Convers. Manag. 177 (2018) 416–427. https://doi.org/10.1016/j.enconman.2018.09.088.

[75] A.M. Parvez, T. Wu, S. Li, N. Miles, I.M. Mujtaba, Bio-DME production based on conventional and CO2-enhanced gasification of biomass: A comparative study on exergy and environmental impacts, Biomass and Bioenergy. 110 (2018) 105–113. https://doi.org/10.1016/j.biombioe.2018.01.016.

[76] V. Belgiorno, G. De Feo, C. Della Rocca, R.M.A. Napoli, Energy from gasification of solid wastes, Waste Manag. 23 (2003) 1–15. https://doi.org/10.1016/S0956-053X(02)00149-6.

[77] P. Parthasarathy, K.S. Narayanan, Hydrogen production from steam gasification of biomass: Influence of process parameters on hydrogen yield - A review, Renew. Energy. 66 (2014) 570–579. https://doi.org/10.1016/j.renene.2013.12.025.

[78] N. Couto, A. Rouboa, V. Silva, E. Monteiro, K. Bouziane, Influence of the biomass gasification processes on the final composition of syngas, Energy Procedia. 36 (2013) 596–606. https://doi.org/10.1016/j.egypro.2013.07.068.

[79] T. Robinson, B. Bronson, P. Gogolek, P. Mehrani, Comparison of the air-blown bubbling fluidized bed gasification of wood and wood-PET pellets, Fuel. 178 (2016) 263–271. https://doi.org/10.1016/j.fuel.2016.03.038.

[80] X. Tan, Z. Wang, B. Meng, X. Meng, K. Li, Pilot-scale production of oxygen from air using perovskite hollow fibre membranes, J. Memb. Sci. 352 (2010) 189–196. https://doi.org/10.1016/j.memsci.2010.02.015.

[81] Q. Fu, Y. Kansha, C. Song, Y. Liu, M. Ishizuka, A. Tsutsumi, An elevated-pressure cryogenic air separation unit based on self-heat recuperation technology for integrated gasification combined cycle systems, Energy. 103 (2016) 440–446. https://doi.org/10.1016/j.energy.2015.09.095.

[82] L. V. van der Ham, S. Kjelstrup, Exergy analysis of two cryogenic air separation processes, Energy. 35 (2010) 4731–4739. https://doi.org/10.1016/j.energy.2010.09.019.

[83] S.Y. Yoon, B.S. Choi, J.H. Ahn, T.S. Kim, Improvement of integrated gasification combined cycle performance using nitrogen from the air separation unit as turbine coolant, Appl. Therm. Eng. 151 (2019) 163–175. https://doi.org/10.1016/j.applthermaleng.2019.01.110.

[84] M. Puig-Arnavat, S. Soprani, M. Søgaard, K. Engelbrecht, J. Ahrenfeldt, U.B. Henriksen, P.V. Hendriksen, Integration of mixed conducting membranes in an oxygen-steam biomass gasification process, RSC Adv. 3 (2013) 20843–20854. https://doi.org/10.1039/c3ra44509g.

[85] T. Antonini, K. Gallucci, P.U. Foscolo, A biomass gasifier including an ionic transport membrane system for oxygen transfer, Chem. Eng. Trans. 37 (2014) 91–96. https://doi.org/10.3303/CET1437016.

[86] T. Antonini, K. Gallucci, V. Anzoletti, S. Stendardo, P.U. Foscolo, Oxygen transport by ionic membranes: Correlation of permeation data and prediction of char burning in a membrane-assisted biomass gasification process, Chem. Eng. Process. Process Intensif. 94 (2015) 39–52. https://doi.org/10.1016/j.cep.2014.11.009.

[87] L. Liu, Y. Huang, J. Cao, C. Liu, L. Dong, L. Xu, J. Zha, Experimental study of biomass gasification with oxygen-enriched air in fluidized bed gasifier, Sci. Total Environ. 626 (2018) 423–433. https://doi.org/10.1016/j.scitotenv.2018.01.016.

[88] S. Ayyadurai, L. Schoenmakers, J.J. Hernández, Mass and energy analysis of a 60 kWth updraft gasifier using large size biomass, Fuel. 187 (2017) 356–366. https://doi.org/10.1016/j.fuel.2016.09.080.

[89] K.J. Ptasinski, M.J. Prins, A. Pierik, Exergetic evaluation of biomass gasification, Energy. 32 (2007) 568–574. https://doi.org/10.1016/j.energy.2006.06.024.

[90] Y.A. Situmorang, Z. Zhao, A. Yoshida, A. Abudula, G. Guan, Small-scale biomass gasification systems for power generation (<200 kW class): A review, Renew. Sustain. Energy Rev. 117 (2020) 109486. https://doi.org/10.1016/j.rser.2019.109486.

[91] S.K. Sansaniwal, K. Pal, M.A. Rosen, S.K. Tyagi, Recent advances in the development of biomass gasification technology: A comprehensive review, Renew. Sustain. Energy Rev. 72 (2017) 363–384. https://doi.org/10.1016/j.rser.2017.01.038.

[92] X.T. Li, J.R. Grace, C.J. Lim, A.P. Watkinson, H.P. Chen, J.R. Kim, Biomass gasification in a circulating fluidized bed, Biomass and Bioenergy. 26 (2004) 171–193. https://doi.org/10.1016/S0961-9534(03)00084-9.

[93] J.J. Hernández, G. Aranda-Almansa, A. Bula, Gasification of biomass wastes in an entrained flow gasifier: Effect of the particle size and the residence time, Fuel Process. Technol. 91 (2010) 681–692. https://doi.org/10.1016/j.fuproc.2010.01.018.

[94] A. Tremel, D. Becherer, S. Fendt, M. Gaderer, H. Spliethoff, Performance of entrained flow and fluidised bed biomass gasifiers on different scales, Energy Convers. Manag. 69 (2013) 95–106. https://doi.org/10.1016/j.enconman.2013.02.001.

[95] M. Mayerhofer, P. Mitsakis, X. Meng, W. De Jong, H. Spliethoff, M. Gaderer, Influence of pressure, temperature and steam on tar and gas in allothermal fluidized bed gasification, Fuel. 99 (2012) 204–209. https://doi.org/10.1016/j.fuel.2012.04.022.

[96] S. Turn, C. Kinoshita, Z. Zhang, D. Ishimura, J. Zhou, An experimental investigation of hydrogen production from biomass gasification, Int. J. Hydrogen Energy. 23 (1998) 641–648. https://doi.org/10.1016/s0360-3199(97)00118-3.

[97] C.O. Colpan, F. Hamdullahpur, I. Dincer, Y. Yoo, Effect of gasification agent on the performance of solid oxide fuel cell and biomass gasification systems, Int. J. Hydrogen Energy. 35 (2010) 5001–5009. https://doi.org/10.1016/j.ijhydene.2009.08.083.

[98] S. Koppatz, C. Pfeifer, R. Rauch, H. Hofbauer, T. Marquard-Moellenstedt, M. Specht, H2 rich product gas by steam gasification of biomass with in situ CO2 absorption in a dual fluidized bed system of 8 MW fuel input, Fuel Process. Technol. 90 (2009) 914–921. https://doi.org/10.1016/j.fuproc.2009.03.016.

[99] P. Kaushal, R. Tyagi, Steam assisted biomass gasification-an overview, Can. J. Chem. Eng. 90 (2012) 1043–1058. https://doi.org/10.1002/cjce.20594.

[100] C. Pfeifer, S. Koppatz, H. Hofbauer, Steam gasification of various feedstocks at a dual fluidised bed gasifier: Impacts of operation conditions and bed materials, Biomass Convers. Biorefinery. 1 (2011) 39–53. https://doi.org/10.1007/s13399-011-0007-1.

[101] J. Karl, T. Pröll, Steam gasification of biomass in dual fluidized bed gasifiers: A review, Renew. Sustain. Energy Rev. 98 (2018) 64–78. https://doi.org/10.1016/j.rser.2018.09.010.

[102] K. Göransson, U. Söderlind, W. Zhang, Experimental test on a novel dual fluidised bed biomass gasifier for synthetic fuel production, Fuel. 90 (2011) 1340–1349. https://doi.org/10.1016/j.fuel.2010.12.035.

[103] IEA Bioenergy Task 33 special report, Status report on thermal gasification of biomass and waste, 2019. http://www.task33.ieabioenergy.com/app/webroot/files/file/publications/T33 Projects/Status report final.pdf.

[104] H. Thunman, C. Gustavsson, A. Larsson, I. Gunnarsson, F. Tengberg, Economic assessment of advanced biofuel production via gasification using cost data from the GoBiGas plant, Energy Sci. Eng. 7 (2019) 217–229. https://doi.org/10.1002/ese3.271.

[105] C.M. van der Meijden, A. van der Drift, B.J. Vreugdenhil, Experimental results from the allothermal biomass gasifier Milena, 15th Eur. Biomass Conf. (2007) 7–11.

[106] J.P. Simanjuntak, Z.A. Zainal, Experimental study and characterization of a two-compartment cylindrical internally circulating fluidized bed gasifier, Biomass and Bioenergy. 77 (2015) 147–154. https://doi.org/10.1016/j.biombioe.2015.03.023.

[107] F. Miccio, G. Ruoppolo, S. Kalisz, L. Andersen, T.J. Morgan, D. Baxter, Combined gasification of coal and biomass in internal circulating fluidized bed, Fuel Process. Technol. 95 (2012) 45–54. https://doi.org/10.1016/j.fuproc.2011.11.008.

[108] X. Xiao, D.D. Le, K. Morishita, S. Zhang, L. Li, T. Takarada, Multi-stage biomass gasification in Internally Circulating Fluidized-bed Gasifier (ICFG): Test operation of animal-waste-derived biomass and parametric investigation at low temperature, Fuel Process. Technol. 91 (2010) 895–902. https://doi.org/10.1016/j.fuproc.2009.08.009.

[109] M.J. De Kam, R. Vance Morey, D.G. Tiffany, Biomass Integrated Gasification Combined

Cycle for heat and power at ethanol plants, Energy Convers. Manag. 50 (2009) 1682–1690. https://doi.org/10.1016/j.enconman.2009.03.031.

[110] E.T. Liakakou, B.J. Vreugdenhil, N. Cerone, F. Zimbardi, F. Pinto, R. André, P. Marques, R. Mata, F. Girio, Gasification of lignin-rich residues for the production of biofuels via syngas fermentation: Comparison of gasification technologies, Fuel. 251 (2019) 580–592. https://doi.org/10.1016/j.fuel.2019.04.081.

[111] M. Dudyński, J.C. Van Dyk, K. Kwiatkowski, M. Sosnowska, Biomass gasification: Influence of torrefaction on syngas production and tar formation, Fuel Process. Technol. 131 (2015) 203–212. https://doi.org/10.1016/j.fuproc.2014.11.018.

[112] P. Kaushal, R. Tyagi, Advanced simulation of biomass gasification in a fluidized bed reactor using ASPEN PLUS, Renew. Energy. 101 (2017) 629–636. https://doi.org/10.1016/j.renene.2016.09.011.

[113] M.L. Valderrama Rios, A.M. González, E.E.S. Lora, O.A. Almazán del Olmo, Reduction of tar generated during biomass gasification: A review, Biomass and Bioenergy. 108 (2018) 345–370. https://doi.org/10.1016/j.biombioe.2017.12.002.

[114] T. a Milne, R.J. Evans, N. Abatzoglou, Biomass Gasifier "Tars": Their Nature, Formation, and Conversion, 1998. https://doi.org/10.2172/3726.

[115] J. Ren, Y.L. Liu, X.Y. Zhao, J.P. Cao, Biomass thermochemical conversion: A review on tar elimination from biomass catalytic gasification, J. Energy Inst. (2019). https://doi.org/10.1016/j.joei.2019.10.003.

[116] Y. Shen, K. Yoshikawa, Recent progresses in catalytic tar elimination during biomass gasification or pyrolysis - A review, Renew. Sustain. Energy Rev. 21 (2013) 371–392. https://doi.org/10.1016/j.rser.2012.12.062.

[117] N.E. Carpenter, Chemistry of sustainable energy, CRC Press/Taylor and Francis, 2014. https://doi.org/10.1201/b16687.

[118] S. Kyritsis, 1st World Conference on Biomass for Energy and Industry, in: 1st World Conf. Biomass Energy Ind., James & James, 2001: p. 1494. https://doi.org/10.13140/2.1.2777.7601.

[119] B. De Caprariis, C. Bassano, P. Deiana, V. Palma, A. Petrullo, M. Scarsella, P. De Filippis, Carbon dioxide reforming of tar during biomass gasification, Chem. Eng. Trans. 37 (2014) 97–102. https://doi.org/10.3303/CET1437017.

[120] Z. Wang, T. He, J. Li, J. Wu, J. Qin, G. Liu, D. Han, Z. Zi, Z. Li, J. Wu, Design and operation of a pilot plant for biomass to liquid fuels by integrating gasification, DME synthesis and DME to gasoline, Fuel. 186 (2016) 587–596. https://doi.org/10.1016/j.fuel.2016.08.108.

[121] H. Boerrigter, H.P. Calis, D.J. Slor, H. Bodenstaff, Gas Cleaning for Integrated Biomass Gasification (Bg) and Fischer-Tropsch (Ft) Systems ; Experimental Demonstration of Two Bg-Ft Systems, 2nd World Conf. Technol. Exhib. Biomass Energy, Ind. Clim. Prot. (2004) 10–14. https://doi.org/ECN-RX--04-041.

[122] R.N. Singh, S.P. Singh, J.B. Balwanshi, D.A. Vishwavidhlya, Tar removal from Producer Gas: A Review, Res. J. Eng. Sci. 3 (2014) 16–22. www.isca.me.

[123] D.T. Pio, L.A.C. Tarelho, R.G. Pinto, M.A.A. Matos, J.R. Frade, A. Yaremchenko, G.S. Mishra, P.C.R.R. Pinto, Low-cost catalysts for in-situ improvement of producer gas quality during direct gasification of biomass, Energy. 165 (2018) 442–454. https://doi.org/10.1016/j.energy.2018.09.119.

[124] L. Devi, K.J. Ptasinski, F.J.J.G.J.G. Janssen, A review of the primary measures for tar elimination in biomass gasification processes, Biomass and Bioenergy. 24 (2003) 125–140.

https://doi.org/10.1016/S0961-9534(02)00102-2.

[125] J. Ren, J.P. Cao, X.Y. Zhao, F.L. Yang, X.Y. Wei, Recent advances in syngas production from biomass catalytic gasification: A critical review on reactors, catalysts, catalytic mechanisms and mathematical models, Renew. Sustain. Energy Rev. 116 (2019) 109426. https://doi.org/10.1016/j.rser.2019.109426.

[126] A. Paethanom, S. Nakahara, M. Kobayashi, P. Prawisudha, K. Yoshikawa, Performance of tar removal by absorption and adsorption for biomass gasification, Fuel Process. Technol. 104 (2012) 144–154. https://doi.org/10.1016/j.fuproc.2012.05.006.

[127] S. Anis, Z.A. Zainal, Tar reduction in biomass producer gas via mechanical, catalytic and thermal methods: A review, Renew. Sustain. Energy Rev. 15 (2011) 2355–2377. https://doi.org/10.1016/j.rser.2011.02.018.

[128] H. Boerrigter, S.V.B. van Paasen, P.C. a Bergman, J.W. Könemann, R. Emmen, A. Wijnands, "Olga" Tar Removal Technology, 2005.

[129] R. Zwart, S. Van Der Heijden, R. Emmen, J.D. Bentzen, J. Ahrenfeldt, P. Stoholm, J. Krogh, Tar removal from low-temperature gasifiers, 2010.

[130] I.U. Hai, F. Sher, G. Zarren, H. Liu, Experimental investigation of tar arresting techniques and their evaluation for product syngas cleaning from bubbling fluidized bed gasifier, J. Clean. Prod. 240 (2019) 118239. https://doi.org/10.1016/j.jclepro.2019.118239.

[131] D.A. Buentello-Montoya, X. Zhang, J. Li, The use of gasification solid products as catalysts for tar reforming, Renew. Sustain. Energy Rev. 107 (2019) 399–412. https://doi.org/10.1016/j.rser.2019.03.021.

[132] L. Lang, W. Yang, J. Xie, X. Yin, C. Wu, J.Y.S. Lin, Oxidative filtration for flyash & tar removal from 1.0 MWth fixed-bed biomass air gasification, Biomass and Bioenergy. 122 (2019) 145–155. https://doi.org/10.1016/j.biombioe.2019.01.018.

[133] T. Tarnpradab, S. Unyaphan, F. Takahashi, K. Yoshikawa, Tar removal capacity of waste cooking oil absorption and waste char adsorption for rice husk gasification, Biofuels. 7 (2016) 401–412. https://doi.org/10.1080/17597269.2016.1147919.

[134] H. Boerrigter, S.V.B. van Paasen, P.C. a Bergman, J.W. Könemann, R. Emmen, a Wijnands, "Olga" Tar Removal Technology, 2005.

[135] H. Chen, Lignocellulose Biorefinery Engineering: Principles and Applications, 2015. https://doi.org/10.1016/C2014-0-02702-5.

[136] O. Ajao, M. Marinova, O. Savadogo, J. Paris, Hemicellulose based integrated forest biorefineries: Implementation strategies, Ind. Crops Prod. 126 (2018) 250–260. https://doi.org/10.1016/j.indcrop.2018.10.025.

[137] G. Jungmeier, R. Van Ree, E. De Jong, H. Stichnothe, I. De Bari, H. Jørgensen, M. Wellisch, G. Bell, J. Spaeth, K. Torr, Assessing Biorefineries Using Wood for the BioEconomy – Current Status and Future Perspective of IEA Bioenergy Task 42 " Biorefining ," 2015. http://www.iea-bioenergy.task42-biorefineries.com (accessed September 5, 2019).

[138] IEA Bioenergy Task 42, Biorefineries: adding value to the sustainable utilisation of biomass, 2009. http://www.ieabioenergy.com/wp-content/uploads/2013/10/Task-42-Booklet.pdf (accessed September 5, 2019).

[139] A. Demirbas, Biorefineries: For biomass upgrading facilities, Green Energy Technol. 26 (2010) 240. https://doi.org/10.1007/978-1-84882-721-9.

[140] J. Moncada B, V. Aristizábal M, C.A. Cardona A, Design strategies for sustainable biorefineries, Biochem. Eng. J. 116 (2016) 122–134.

https://doi.org/10.1016/j.bej.2016.06.009.

[141] P. Bajpai, Biorefinery Opportunities in the Pulp and Paper Industry, 2013. https://doi.org/10.1016/b978-0-12-409508-3.00002-x.

[142] P.A. Schieb, H. Lescieux-Katir, M. Thénot, B. Clément-Larosière, Biorefinery 2030: Future prospects for the bioeconomy, Springer, 2015. https://doi.org/10.1007/978-3-662-47374-0.

[143] UN, UN Sustainable Development Knowledge Platform, (n.d.). https://sustainabledevelopment.un.org/ (accessed June 16, 2020).

[144] A.T. Ubando, C.B. Felix, W.H. Chen, Biorefineries in circular bioeconomy: A comprehensive review, Bioresour. Technol. 299 (2020). https://doi.org/10.1016/j.biortech.2019.122585.

[145] F. Cherubini, The biorefinery concept: Using biomass instead of oil for producing energy and chemicals, Energy Convers. Manag. 51 (2010) 1412–1421. https://doi.org/10.1016/j.enconman.2010.01.015.

[146] R. van Ree, Biorefinery Approach in the EU and Beyond (Task 42), 2017.

[147] W. Stafford, W. De Lange, A. Nahman, V. Chunilall, P. Lekha, J. Andrew, J. Johakimu, B. Sithole, D. Trotter, Forestry biorefineries, Renew. Energy. 154 (2020) 461–475. https://doi.org/10.1016/j.renene.2020.02.002.

[148] C. Bergeron, D.J. Carrier, S. Ramaswamy, Biorefinery Co-Products: Phytochemicals, Primary Metabolites and Value-Added Biomass Processing, John Wiley & Sons, 2012. https://doi.org/10.1002/9780470976692.

[149] J.A. Ferreira, M.J. Taherzadeh, Improving the economy of lignocellulose-based biorefineries with organosolv pretreatment, Bioresour. Technol. 299 (2020) 122695. https://doi.org/10.1016/j.biortech.2019.122695.

[150] K. Pettersson, M. Mahmoudkhani, A. von Schenck, Opportunities for biorefineries in the pulping industry, 2012. http://www.chalmers.se/en/areas-of-advance/energy/Pages/Energy/E-book/Biorefineries-Chapter-5.aspx.

[151] T. Rafione, M. Marinova, L. Montastruc, J. Paris, The Green Integrated Forest Biorefinery: An innovative concept for the pulp and paper mills, Appl. Therm. Eng. 73 (2014) 74–81. https://doi.org/10.1016/j.applthermaleng.2014.07.039.

[152] S.S. Hassan, G.A. Williams, A.K. Jaiswal, Lignocellulosic Biorefineries in Europe: Current State and Prospects, Trends Biotechnol. 37 (2019) 231–234. https://doi.org/10.1016/j.tibtech.2018.07.002.

[153] M. Akbari, A.O. Oyedun, A. Kumar, Ammonia production from black liquor gasification and co-gasification with pulp and waste sludges: A techno-economic assessment, Energy. 151 (2018) 133–143. https://doi.org/10.1016/j.energy.2018.03.056.

[154] J. Isaksson, M. Jansson, A. Åsblad, T. Berntsson, Transportation fuel production from gasified biomass integrated with a pulp and paper mill – Part A: Heat integration and system performance, Energy. 103 (2016) 557–571. https://doi.org/10.1016/j.energy.2016.02.091.

[155] J. Isaksson, K. Pettersson, M. Mahmoudkhani, A. Åsblad, T. Berntsson, Integration of biomass gasification with a Scandinavian mechanical pulp and paper mill - Consequences for mass and energy balances and global CO2 emissions, Energy. 44 (2012) 420–428. https://doi.org/10.1016/j.energy.2012.06.013.

[156] EPA, Biomass Combined Heat and Power Catalog of Technologies, 2007. https://www.epa.gov/sites/production/files/2015-07/documents/biomass_combined_heat_and_power_catalog_of_technologies_v.1.1.pdf.

[157] A. Demirbas, Biofuels securing the planet's future energy needs, Energy Convers. Manag. 50

(2009) 2239–2249. https://doi.org/10.1016/j.enconman.2009.05.010.

[158] J. Isaksson, M. Jansson, A. Åsblad, T. Berntsson, Transportation fuel production from gasified biomass integrated with a pulp and paper mill - Part B: Analysis of economic performance and greenhouse gas emissions, Energy. 103 (2016) 522–532. https://doi.org/10.1016/j.energy.2016.02.092.

[159] E. Wetterlund, K. Pettersson, S. Harvey, Systems analysis of integrating biomass gasification with pulp and paper production - Effects on economic performance, CO2 emissions and energy use, Energy. 36 (2011) 932–941. https://doi.org/10.1016/j.energy.2010.12.017.

[160] K. Pettersson, S. Harvey, Comparison of black liquor gasification with other pulping biorefinery concepts - Systems analysis of economic performance and CO2 emissions, Energy. 37 (2012) 136–153. https://doi.org/10.1016/j.energy.2011.10.020.

[161] E.T.D.F. Ferreira, J.A.P. Balestieri, Black liquor gasification combined cycle with CO2 capture - Technical and economic analysis, Appl. Therm. Eng. 75 (2015) 371–383. https://doi.org/10.1016/j.applthermaleng.2014.09.026.

[162] M. Naqvi, J. Yan, E. Dahlquist, Energy conversion performance of black liquor gasification to hydrogen production using direct causticization with CO2 capture, Bioresour. Technol. 110 (2012) 637–644. https://doi.org/10.1016/j.biortech.2012.01.070.

[163] E. Andersson, S. Harvey, System analysis of hydrogen production from gasified black liquor, Energy. 31 (2006) 3426–3434. https://doi.org/10.1016/j.energy.2006.03.015.

[164] M. Naqvi, E. Dahlquist, A.S. Nizami, M. Danish, S. Naqvi, U. Farooq, A.S. Qureshi, M. Rehan, Gasification Integrated with Small Chemical Pulp Mills for Fuel and Energy Production, Energy Procedia. 142 (2017) 977–983. https://doi.org/10.1016/j.egypro.2017.12.156.

[165] L. Carvalho, J. Lundgren, E. Wetterlund, J. Wolf, E. Furusjö, Methanol production via black liquor co-gasification with expanded raw material base – Techno-economic assessment, Appl. Energy. 225 (2018) 570–584. https://doi.org/10.1016/j.apenergy.2018.04.052.

[166] J. Andersson, E. Furusjö, E. Wetterlund, J. Lundgren, I. Landälv, Co-gasification of black liquor and pyrolysis oil: Evaluation of blend ratios and methanol production capacities, Energy Convers. Manag. 110 (2016) 240–248. https://doi.org/10.1016/j.enconman.2015.12.027.

[167] P. Bajpai, Black Liquor Gasification, Elsevier Ltd, 2014. https://doi.org/10.1016/C2013-0-12854-1.

[168] M. Naqvi, J. Yan, E. Dahlquist, Black liquor gasification integrated in pulp and paper mills: A critical review, Bioresour. Technol. 101 (2010) 8001–8015. https://doi.org/10.1016/j.biortech.2010.05.013.

[169] D.M. Neiva, S. Araújo, J. Gominho, A. de C. Carneiro, H. Pereira, Potential of Eucalyptus globulus industrial bark as a biorefinery feedstock: Chemical and fuel characterization, Ind. Crops Prod. 123 (2018) 262–270. https://doi.org/10.1016/j.indcrop.2018.06.070.

[170] E. Dahlquist, M. Naqvi, E. Thorin, J. Yan, K. Kyprianidis, P. Hartwell, Experimental and numerical investigation of pellet and black liquor gasification for polygeneration plant, Appl. Energy. 204 (2017) 1055–1064. https://doi.org/10.1016/j.apenergy.2017.05.008.

[171] H. Wiinikka, P. Carlsson, M. Marklund, C. Grönberg, E. Pettersson, M. Lidman, R. Gebart, Experimental investigation of an industrial scale black liquor gasifier. Part 2: Influence of quench operation on product gas composition, Fuel. 93 (2012) 117–129. https://doi.org/10.1016/j.fuel.2011.06.066.

[172] P. Carlsson, H. Wiinikka, M. Marklund, C. Grönberg, E. Pettersson, M. Lidman, R. Gebart, Experimental investigation of an industrial scale black liquor gasifier. 1. the effect of reactor operation parameters on product gas composition, Fuel. 89 (2010) 4025–4034. https://doi.org/10.1016/j.fuel.2010.05.003.

[173] IEA Bioenergy, Task 33 Database: Gasification of Biomass and Waste, (2020). http://www.ieatask33.org/content/Task 33 Projects (accessed March 27, 2020).

[174] J. Hrbek, Status report on thermal biomass gasification in countries participating in IEA Bioenergy Task 33, 2016. http://www.ieatask33.org/content/publications/Status_report%5Cnhttp://www.ieatask33.org/app/webroot/files/file/2016/Status_report.pdf.

[175] G. Mongkhonsiri, P. Charoensuppanimit, A. Anantpinijwatna, R. Gani, S. Assabumrungrat, Process development of sustainable biorefinery system integrated into the existing pulping process, J. Clean. Prod. 255 (2020). https://doi.org/10.1016/j.jclepro.2020.120278.

[176] K. Mitchell, S. Berkeley, Draft Report: Potential for Biofuel Production from Forest Woody Biomass, 2015. http://biomass.ucdavis.edu/wp-content/uploads/2016/07/Forestry-Biomass-Fuel-Potential-6_24_2015-web-version.pdf.

[177] L.D. Gottumukkala, K. Haigh, F.X. Collard, E. van Rensburg, J. Görgens, Opportunities and prospects of biorefinery-based valorisation of pulp and paper sludge, Bioresour. Technol. 215 (2016) 37–49. https://doi.org/10.1016/j.biortech.2016.04.015.

[178] X. Ku, J. Wang, H. Jin, J. Lin, Effects of operating conditions and reactor structure on biomass entrained-flow gasification, Renew. Energy. 139 (2019) 781–795. https://doi.org/10.1016/j.renene.2019.02.113.

[179] J. Schneider, C. Grube, A. Herrmann, S. Rönsch, Atmospheric entrained-flow gasification of biomass and lignite for decentralized applications, Fuel Process. Technol. 152 (2016) 72–82. https://doi.org/10.1016/j.fuproc.2016.05.047.

[180] J.M. Saad, P.T. Williams, Manipulating the H2/CO ratio from dry reforming of simulated mixed waste plastics by the addition of steam, Fuel Process. Technol. 156 (2017) 331–338. https://doi.org/10.1016/j.fuproc.2016.09.016.

[181] D. Tristantini, S. Lögdberg, B. Gevert, Ø. Borg, A. Holmen, The effect of synthesis gas composition on the Fischer-Tropsch synthesis over Co/γ-Al2O3 and Co-Re/γ-Al2O3 catalysts, Fuel Process. Technol. 88 (2007) 643–649. https://doi.org/10.1016/j.fuproc.2007.01.012.

[182] N. Clausen, L. R., Elmegaard, B., & Houbak, Design of novel DME/methanol synthesis plants based on gasification of biomass, 2011.

[183] M.T. Lim, Z. Alimuddin, Bubbling fluidized bed biomass gasification-Performance, process findings and energy analysis, Renew. Energy. 33 (2008) 2339–2343. https://doi.org/10.1016/j.renene.2008.01.014.

[184] M. Campoy, A. Gómez-Barea, F.B. Vidal, P. Ollero, Air-steam gasification of biomass in a fluidised bed: Process optimisation by enriched air, Fuel Process. Technol. 90 (2009) 677–685. https://doi.org/10.1016/j.fuproc.2008.12.007.

[185] I. Isik-Gulsac, P. Gafarova-Aksoy, H. Karatas, Y. Durak-Cetin, A. Sarioglan, Biomass gasification in bubbling fluidized bed: Effect of biomass type on syngas properties, (2015) 1–4.

[186] Y.D. Kim, C.W. Yang, B.J. Kim, K.S. Kim, J.W. Lee, J.H. Moon, W. Yang, T.U. Yu, U. Do Lee, Air-blown gasification of woody biomass in a bubbling fluidized bed gasifier, Appl. Energy. 112 (2013) 414–420. https://doi.org/10.1016/j.apenergy.2013.03.072.

[187] I. Narváez, A. Orío, M.P. Aznar, J. Corella, Biomass gasification with air in an atmospheric bubbling fluidized bed. Effect of six operational variables on the quality of the produced raw gas, Ind. Eng. Chem. Res. 35 (1996) 2110–2120. https://doi.org/10.1021/ie9507540.

[188] P. Subramanian, A. Sampathrajan, P. Venkatachalam, Fluidized bed gasification of select granular biomaterials, Bioresour. Technol. 102 (2011) 1914–1920. https://doi.org/10.1016/j.biortech.2010.08.022.

[189] P. Plis, R.K. Wilk, Theoretical and experimental investigation of biomass gasification process in a fixed bed gasifier, Energy. 36 (2011) 3838–3845. https://doi.org/10.1016/j.energy.2010.08.039.

[190] C. Erlich, T.H. Fransson, Downdraft gasification of pellets made of wood, palm-oil residues respective bagasse: Experimental study, Appl. Energy. 88 (2011) 899–908. https://doi.org/10.1016/j.apenergy.2010.08.028.

[191] H. Wiinikka, P. Carlsson, F. Granberg, J. Löfström, M. Marklund, R. Tegman, M. Lindblom, R. Gebart, Design and methodology of a high temperature gas sampling system for pressurized black liquor gasification, Fuel. 89 (2010) 2583–2591. https://doi.org/10.1016/j.fuel.2010.02.021.

[192] G. Nong, L. Huang, H. Mo, S. Wang, Investigate the variability of gas compositions and thermal efficiency of bagasse black liquor gasification, Energy. 49 (2013) 178–181. https://doi.org/10.1016/j.energy.2012.11.012.

[193] J.J. Hernández, M. Lapuerta, J. Barba, Flame stability and OH and CH radical emissions from mixtures of natural gas with biomass gasification gas, Appl. Therm. Eng. 55 (2013) 133–139. https://doi.org/10.1016/j.applthermaleng.2013.03.015.

[194] L. Chanphavong, Z.A. Zainal, Characterization and challenge of development of producer gas fuel combustor: A review, J. Energy Inst. 92 (2019) 1577–1590. https://doi.org/10.1016/j.joei.2018.07.016.

[195] C. Serrano, J.J. Hernández, C. Mandilas, C.G.W. Sheppard, R. Woolley, Laminar burning behaviour of biomass gasification-derived producer gas, Int. J. Hydrogen Energy. 33 (2008) 851–862. https://doi.org/10.1016/j.ijhydene.2007.10.050.

[196] E. Monteiro, M. Bellenoue, J. Sotton, N.A. Moreira, S. Malheiro, Laminar burning velocities and Markstein numbers of syngas-air mixtures, Fuel. 89 (2010) 1985–1991. https://doi.org/10.1016/j.fuel.2009.11.008.

[197] B. Yan, Y. Wu, C. Liu, J.F. Yu, B. Li, Z.S. Li, G. Chen, X.S. Bai, M. Aldén, A.A. Konnov, Experimental and modeling study of laminar burning velocity of biomass derived gases/air mixtures, Int. J. Hydrogen Energy. 36 (2011) 3769–3777. https://doi.org/10.1016/j.ijhydene.2010.12.015.

[198] J. Ahrenfeldt, Characterization of biomass producer gas as fuel for stationary gas engines in combined heat and power production, Technical University of Denmark, 2007.

[199] A. Saliamonas, R. Navakas, N. Striūgas, A. Džiugys, K. Zakarauskas, Generatorinių dujų priemaišų įtaka gamtinių dujų liepsnos spektrinėms charakteristikoms, Energetika. 60 (2014) 210–219. https://doi.org/10.6001/energetika.v60i4.3017.

[200] M. Kraussler, M. Binder, H. Hofbauer, Behavior of GCMS tar components in a water gas shift unit operated with tar-rich product gas from an industrial scale dual fluidized bed biomass steam gasification plant, Biomass Convers. Biorefinery. 7 (2017) 69–79. https://doi.org/10.1007/s13399-016-0205-y.

[201] K. Göransson, U. Söderlind, J. He, W. Zhang, Review of syngas production via biomass DFBGs, Renew. Sustain. Energy Rev. 15 (2011) 482–492.

https://doi.org/10.1016/j.rser.2010.09.032.

[202] H. Thunman, M. Seemann, T. Berdugo Vilches, J. Maric, D. Pallares, H. Ström, G. Berndes, P. Knutsson, A. Larsson, C. Breitholtz, O. Santos, Advanced biofuel production via gasification – lessons learned from 200 man-years of research activity with Chalmers' research gasifier and the GoBiGas demonstration plant, Energy Sci. Eng. 6 (2018) 6–34. https://doi.org/10.1002/ese3.188.

[203] I. Kirm, J. Brandin, M. Sanati, Shift catalysts in biomass generated synthesis gas, Top. Catal. 45 (2007) 31–37. https://doi.org/10.1007/s11244-007-0236-5.

[204] K. Ståhl, M. Neergaard, J. Nieminen, Progress Report : Varnamo Biomass Gasification Plant, in: 1999 Gasif. Technol. Conf., San Francisco, California, 1999: pp. 1–16.

[205] L. Waldheim, IEA Bioenergy Task 33 Country Report Sweden, 2018. http://ieatask33.org/app/webroot/files/file/country_reports/2019/CR_Sweden1.pdf.

[206] I. Landälv, R. Gebart, B. Marke, F. Granberg, E. Furusjö, P. Löwnertz, O.G.W. Öhrman, E.L. Sørensen, P. Salomonsson, Two years experience of the BioDME project-A complete wood to wheel concept, Environ. Prog. Sustain. Energy. 33 (2014) 744–750. https://doi.org/10.1002/ep.11993.

[207] T. Berdugo Vilches, Operational strategies to control the gas composition in dual fluidized bed biomass gasifiers, Chalmers University Of Technology, 2018.

[208] K. Suomesta, IEA Task 33 Gasification activities in Finland, 2019. http://www.ieatask33.org/app/webroot/files/file/2018/Alkmaar-Petten/CR/Finland.pdf.

[209] P.R. Bhoi, S.A. Channiwala, Optimization of producer gas fired premixed burner, Renew. Energy. 33 (2008) 1209–1219. https://doi.org/10.1016/j.renene.2007.07.014.

[210] N.L. Panwar, B.L. Salvi, V.S. Reddy, Performance evaluation of producer gas burner for industrial application, Biomass and Bioenergy. 35 (2011) 1373–1377. https://doi.org/10.1016/j.biombioe.2010.12.046.

[211] K.B. Sutar, M.R. Ravi, S. Kohli, Design of a partially aerated naturally aspirated burner for producer gas, Energy. 116 (2016) 773–785. https://doi.org/10.1016/j.energy.2016.10.019.

[212] S. Dattarajan, R. Kaluri, G. Sridhar, Development of a Combustor to burn raw producer gas, Fuel Process. Technol. 126 (2014) 76–87. https://doi.org/10.1016/j.fuproc.2014.04.017.

[213] W. De Jong, J.R. Van Ommen, Biomass as a Sustainable Energy Source for the Future, John Wiley & Sons, Inc, Hoboken, NJ, 2014. https://doi.org/10.1002/9781118916643.

[214] M. Schlaf, Z.C. Zhang, Reaction pathways and mechanisms in thermocatalytic biomass conversion I: Cellulose structure, depolymerization and conversion by heterogeneous catalysts, Springer, 2015. https://doi.org/10.1007/978-981-287-688-1.

[215] S. Singh Siwal, Q. Zhang, C. Sun, S. Thakur, V. Kumar Gupta, V. Kumar Thakur, Energy production from steam gasification processes and parameters that contemplate in biomass gasifier – A review, Bioresour. Technol. 297 (2020) 122481. https://doi.org/10.1016/j.biortech.2019.122481.

[216] C. Higman, M. van der. Burgt, Gasification, Gulf Professional Pub./Elsevier Science, 2008.

[217] V.S. Sikarwar, M. Zhao, P. Clough, J. Yao, X. Zhong, M.Z. Memon, N. Shah, E.J. Anthony, P.S. Fennell, An overview of advances in biomass gasification, Energy Environ. Sci. 9 (2016) 2939–2977. https://doi.org/10.1039/c6ee00935b.

[218] A.F. Kirkels, G.P.J. Verbong, Biomass gasification: Still promising? A 30-year global overview, Renew. Sustain. Energy Rev. 15 (2011) 471–481. https://doi.org/10.1016/j.rser.2010.09.046.

[219] J. Yan, R. Sun, L. Shen, H. Bai, S. Jiang, Y. Xiao, T. Song, Hydrogen-rich syngas production with tar elimination via biomass chemical looping gasification (BCLG) using BaFe2O4/Al2O3 as oxygen carrier, Chem. Eng. J. 387 (2020) 124107. https://doi.org/10.1016/j.cej.2020.124107.

[220] M. Cortazar, G. Lopez, J. Alvarez, A. Arregi, M. Amutio, J. Bilbao, M. Olazar, Experimental study and modeling of biomass char gasification kinetics in a novel thermogravimetric flow reactor, Chem. Eng. J. 396 (2020) 125200. https://doi.org/10.1016/j.cej.2020.125200.

[221] M. Materazzi, R. Taylor, M. Cairns-Terry, Production of biohydrogen from gasification of waste fuels: Pilot plant results and deployment prospects, Waste Manag. 94 (2019) 95–106. https://doi.org/10.1016/j.wasman.2019.05.038.

[222] M.A. Salam, K. Ahmed, N. Akter, T. Hossain, B. Abdullah, A review of hydrogen production via biomass gasification and its prospect in Bangladesh, Int. J. Hydrogen Energy. 43 (2018) 14944–14973. https://doi.org/10.1016/j.ijhydene.2018.06.043.

[223] A. Ebrahimi, M. Ziabasharhagh, Energy and exergy analyses of a novel integrated process configuration for tri-generation heat, power and liquefied natural gas based on biomass gasification, Energy Convers. Manag. 209 (2020) 112624. https://doi.org/10.1016/j.enconman.2020.112624.

[224] Y. Xiang, L. Cai, Y. Guan, W. Liu, T. He, J. Li, Study on the biomass-based integrated gasification combined cycle with negative CO2 emissions under different temperatures and pressures, Energy. 179 (2019) 571–580. https://doi.org/10.1016/j.energy.2019.05.011.

[225] N. Radenahmad, A.T. Azad, M. Saghir, J. Taweekun, M.S.A. Bakar, M.S. Reza, A.K. Azad, A review on biomass derived syngas for SOFC based combined heat and power application, Renew. Sustain. Energy Rev. 119 (2020) 109560. https://doi.org/10.1016/j.rser.2019.109560.

[226] H. Shi, Q. Li, W. Tan, H. Qiu, C. Su, Solid oxide fuel cells in combination with biomass gasification for electric power generation, Chinese J. Chem. Eng. (2020) 1–6. https://doi.org/10.1016/j.cjche.2020.01.018.

[227] R. Moradi, V. Marcantonio, L. Cioccolanti, E. Bocci, Integrating biomass gasification with a steam-injected micro gas turbine and an Organic Rankine Cycle unit for combined heat and power production, Energy Convers. Manag. 205 (2020) 112464. https://doi.org/10.1016/j.enconman.2019.112464.

[228] G. Chidikofan, A. Benoist, M. Sawadogo, G. Volle, J. Valette, Y. Coulibaly, J. Pailhes, F. Pinta, Assessment of Environmental Impacts of Tar Releases from a Biomass Gasifier Power Plant for Decentralized Electricity Generation, Energy Procedia. 118 (2017) 158–163. https://doi.org/10.1016/j.egypro.2017.07.034.

[229] J.J.R. Behainne, J.D. Martinez, Performance analysis of an air-blown pilot fluidized bed gasifier for rice husk, Energy Sustain. Dev. 18 (2014) 75–82. https://doi.org/10.1016/j.esd.2013.11.008.

[230] N. Mazaheri, A.H. Akbarzadeh, E. Madadian, M. Lefsrud, Systematic review of research guidelines for numerical simulation of biomass gasification for bioenergy production, Energy Convers. Manag. 183 (2019) 671–688. https://doi.org/10.1016/j.enconman.2018.12.097.

[231] R.C. Brown, T.R. Brown, Biorenewable Resources: Engineering New Products from Agriculture: Second Edition, Iowa State Press, 2014. https://doi.org/10.1002/9781118524985.

[232] A.A.P. Susastriawan, H. Saptoadi, Purnomo, Small-scale downdraft gasifiers for biomass gasification: A review, Renew. Sustain. Energy Rev. 76 (2017) 989–1003. https://doi.org/10.1016/j.rser.2017.03.112.

[233] Z. Wan, S. Yang, Y. Wei, J. Hu, H. Wang, CFD modeling of the flow dynamics and gasification in the combustor and gasifier of a dual fluidized bed pilot plant, Energy. 198 (2020). https://doi.org/10.1016/j.energy.2020.117366.

[234] S. Koppatz, C. Pfeifer, H. Hofbauer, Comparison of the performance behaviour of silica sand and olivine in a dual fluidised bed reactor system for steam gasification of biomass at pilot plant scale, Chem. Eng. J. 175 (2011) 468–483. https://doi.org/10.1016/j.cej.2011.09.071.

[235] K.H. A. van der Drift, H. Boerrigter, B. Coda, M.K. Cieplik, Entrained flow gasification of biomass: Ash behaviour, feeding issues, and system analyses, 2004.

[236] M. Hansen, Thermal Biomass Gasification in Denmark: IEA Bioenergy Task 33 Country Report, 2019. http://ieabioenergytask33.org/download.php?file=files/file/country_reports/2019/Danish Coutry Report 2019 final.pdf.

[237] H. Jörgen, International Seminar on Gasification, 2008.

[238] L. Waldheim, Gasification of waste for energy carriers: A review, 2018. https://www.ieabioenergy.com/wp-content/uploads/2019/01/IEA-Bioenergy-Task-33-Gasification-of-waste-for-energy-carriers-20181205-1.pdf.

[239] K.I. of Technology, The Bioliq process - High Pressure Entrained Flow Gasification, (n.d.). https://www.bioliq.de/english/67.php (accessed March 28, 2020).

[240] IEA Bioenergy, Country Report Germany for IEA Task 33 Thermal Gasification of Biomass, n.d.

[241] V.D.N. Topf, D.M. Berger, D. Gert, The "CombiPower Process" – a Possibility for Decentralized Generation of Power , Heat and Industrial Gas from Coal and Biomass*), n.d.

[242] Global Syngas Technologies Council: Woldwide Syngas Database, (n.d.). https://www.globalsyngas.org/resources/world-gasification-database/vaermlands-methanol-plant (accessed March 29, 2020).

[243] J. R. Bailey, M. Colombo, W.N.Scott, A 4 MWe biogas engine plant fueled by the gasification of olive oil production wastes (sansa), 2001. https://p2infohouse.org/ref/35/34010.pdf.

[244] J. Hansson, A. Leveau, Biomass Gasifier Database for Computer Simulation Purposes, 2011.

[245] B. Fredriksson Möller, K. Ståhl, A. Molin, A.M. B. Fredriksson Möller, K. Ståhl, Bio2G - A full-scale reference plant for production of Bio-SNG (biomethane) based on thermal gasification of biomass in Sweden, in: 21st Eur. Biomass Conf. Exhib., ETA-Florence Renewable Energies, Copenhagen, 2013: pp. 147–150. https://doi.org/10.5071/21steubce2013-4ao.5.3.

[246] B. Fredriksson, Bio2G - A commercial-scale gasification to SNG plant, n.d.

[247] ReGaWatt GmbH – Ihr schlüsselfertiges Kombi Power System, (n.d.). https://www.regawatt.de/startsite/ (accessed March 30, 2020).

[248] D. Baas, Baas Energie BV, NL-Ens, Kombi Power System, 2017.

[249] B. van der Drift, Biomass gasification in the Netherlands, 2013. http://www.ieatask33.org/app/webroot/files/file/country_reports/NL_July2013.pdf.

[250] BioMCN successfully starts M2, (n.d.). https://www.chemieparkdelfzijl.nl/actueel/2019/09/810480-biomcn-start-m2-met-succes-op (accessed April 10, 2020).

[251] M. Martin, Status of DONG Energy's Pyroneer gasification technology for high alkaline fuels like straw: an efficient and sustainable method to replace fossil fuels in our energy system,

2013.

[252] E. Kurkela, Review of Finnish biomass gasification technologies, 2002. https://www.researchgate.net/publication/30482338_Review_of_Finnish_biomass_gasification_technologies.

[253] B. Zimmerlin, M. Eberhard, N. Dahmen, T. Kolb, H. Lam, R. Mai, B. Michelfelder, A. Niebel, C. Pfitzer, Residual biomass to gasoline – operations of the bioliq® pilot plant, in: Adv. Bioeconomy Leadersh. Conf., San Francisco, 2018.

[254] J. Vogels, Industrial scale hydrogen production from biomass via CHOREN's unique Carbo-V-process, in: 18th World Hydrog. Energy Conf., 2010: pp. 1–6.

[255] M. Rudloff, Entrained-flow gasification to convert biomass into synthesis gas, 2009.

[256] T. Mustafa, Biomass potential in Turkey & Gasification technology, in: 3th Forebiom Work., 2014.

[257] L. Ståhl, Krister & Waldheim, Lars & Morris, Michael & Johnsson, Ulf & Gårdmark, Biomass IGCC at Värnamo, Sweden: past and future, in: GCEP Energy Work., 2004. http://gcep.stanford.edu/pdfs/energy_workshops_04_04/biomass_stahl.pdf.

[258] C. Giulio, CHP plant based on wet wood gasification - Puidoux (CH), in: 5th Biomass Swiss Energy Futur. Conf., 2018.

[259] J. Hrbek, K. Whitty, IEA Bioenergy, Task 33 – Gasification of Biomass and Waste, in: Work. Waste Gasif., 2018: pp. 1–25. http://www.eti.co.uk/project/waste-gasification/.

[260] J. Isaksson, Metso Waste Gasification, in: Valtakunnalliset Jätteen Hyötykäyttöpäivät, 2013.

[261] B. Vreugdenhil, Country report The Netherlands: Gasification of biomass and waste, n.d.

[262] L.& L. Technologies, Eska Graphic Board: 12 MWth Waste Paper Rejects Gasification System, 2015.

[263] J. Hrbek, IEA Bioenergy Task 33: Gasification of biomass and waste Country Report Austria, 2018.

[264] J. Kotik, R. Rauch, H. Hofbauer, K. Bosch, F. Schwenninger, 8.5 MWth CHP Plant in Oberwart, Austria - based on DFB Steam Gasification of Solid Biomass - Achieves Continuous Full Load Operation Through Stringent Optimization, Eur. Biomass Conf. Exhib. Proc. (2012) 1033–1037. https://doi.org/10.5071/20theubce2012-2bv.2.10.

[265] Biomass and Waste Gasification: Country Report ITALY, 2019. http://www.ieatask33.org/app/webroot/files/file/country_reports/2019/ITALY2018.pdf.

[266] Y.A. Situmorang, Z. Zhao, A. Yoshida, Y. Kasai, A. Abudula, G. Guan, Potential power generation on a small-scale separated-type biomass gasification system, Energy. 179 (2019) 19–29. https://doi.org/10.1016/j.energy.2019.04.163.

[267] R. Alipour Moghadam Esfahani, L. Osmieri, S. Specchia, S. Yusup, A. Tavasoli, A. Zamaniyan, H2-rich syngas production through mixed residual biomass and HDPE waste via integrated catalytic gasification and tar cracking plus bio-char upgrading, Chem. Eng. J. 308 (2017) 578–587. https://doi.org/10.1016/j.cej.2016.09.049.

[268] C. Cao, C. Bian, G. Wang, B. Bai, Y. Xie, H. Jin, Co-gasification of plastic wastes and soda lignin in supercritical water, Chem. Eng. J. 388 (2020) 124277. https://doi.org/10.1016/j.cej.2020.124277.

[269] Y. Chai, N. Gao, M. Wang, C. Wu, H2 production from co-pyrolysis/gasification of waste plastics and biomass under novel catalyst Ni-CaO-C, Chem. Eng. J. 382 (2020) 122947. https://doi.org/10.1016/j.cej.2019.122947.

[270] A. AlNouss, G. McKay, T. Al-Ansari, Production of syngas via gasification using optimum blends of biomass, J. Clean. Prod. 242 (2020) 118499. https://doi.org/10.1016/j.jclepro.2019.118499.

[271] IRENA International Renewable Energy Agency, Renewable Power Generation Costs in 2018, 2018. https://doi.org/10.1007/SpringerReference_7300.

[272] D.T. Pio, H.G.M.F. Gomes, L.A.C. Tarelho, L.C.M. Ruivo, M.A.A. Matos, R.G. Pinto, J.R. Frade, F.M.S. Lemos, Ilmenite as low-cost catalyst for producer gas quality improvement from a biomass pilot-scale gasifier, Energy Reports. 6 (2020) 325–330. https://doi.org/10.1016/j.egyr.2019.08.063.

[273] A. Bridgwater, The future for biomass pyrolysis and gasification: status, opportunities and policies for Europe, 2002.

[274] A. Ramos, J. Berzosa, F. Clarens, M. Marin, A. Rouboa, Environmental and socio-economic assessment of cork waste gasification: Life cycle and cost analysis, J. Clean. Prod. 249 (2020) 119316. https://doi.org/10.1016/j.jclepro.2019.119316.

[275] V. Benedetti, S.S. Ail, F. Patuzzi, D. Cristofori, R. Rauch, M. Baratieri, Investigating the feasibility of valorizing residual char from biomass gasification as catalyst support in Fischer-Tropsch synthesis, Renew. Energy. 147 (2020) 884–894. https://doi.org/10.1016/j.renene.2019.09.050.

[276] M.M. Parascanu, M. Puig-Gamero, G. Soreanu, J.L. Valverde, L. Sanchez-Silva, Comparison of three Mexican biomasses valorization through combustion and gasification: Environmental and economic analysis, Energy. 189 (2019) 116095. https://doi.org/10.1016/j.energy.2019.116095.

[277] C. Higman, M. van der Burgt, R.L. Bain, K. Broer, Gasification, Gulf Professional Publishing, 2011. https://books.google.com/books?id=IjlMBi_Q6kIC&pgis=1 (accessed February 7, 2015).

[278] G. Mirmoshtaghi, H. Li, E. Thorin, E. Dahlquist, Evaluation of different biomass gasification modeling approaches for fluidized bed gasifiers, Biomass and Bioenergy. 91 (2016) 69–82. https://doi.org/10.1016/j.biombioe.2016.05.002.

[279] D. Baruah, D.C. Baruah, M.K. Hazarika, Artificial neural network based modeling of biomass gasification in fixed bed downdraft gasifiers, Biomass and Bioenergy. 98 (2017) 264–271. https://doi.org/10.1016/j.biombioe.2017.01.029.

[280] P. Meenaroch, S. Kerdsuwan, K. Laohalidanond, Development of Kinetics Models in Each Zone of a 10 kg/hr Downdraft Gasifier using Computational Fluid Dynamics, Elsevier B.V., 2015. https://doi.org/10.1016/j.egypro.2015.11.485.

[281] A. Gómez-Barea, B. Leckner, Modeling of biomass gasification in fluidized bed, Prog. Energy Combust. Sci. 36 (2010) 444–509. https://doi.org/10.1016/j.pecs.2009.12.002.

[282] B. Fortunato, G. Brunetti, S.M. Camporeale, M. Torresi, F. Fornarelli, Thermodynamic model of a downdraft gasifier, Energy Convers. Manag. 140 (2017) 281–294. https://doi.org/10.1016/j.enconman.2017.02.061.

[283] M. Puig-Arnavat, J.C. Bruno, A. Coronas, Review and analysis of biomass gasification models, Renew. Sustain. Energy Rev. 14 (2010) 2841–2851. https://doi.org/10.1016/j.rser.2010.07.030.

[284] D. Baruah, D.C. Baruah, Modeling of biomass gasification: A review, Renew. Sustain. Energy Rev. 39 (2014) 806–815. https://doi.org/10.1016/j.rser.2014.07.129.

[285] M.C. Acar, Y.E. Böke, Simulation of biomass gasification in a BFBG using chemical

equilibrium model and restricted chemical equilibrium method, Biomass and Bioenergy. 125 (2019) 131–138. https://doi.org/10.1016/j.biombioe.2019.04.012.

[286] P. Basu, Biomass Gasification, Pyrolysis and Torrefaction: Practical Design and Theory, 2013. https://doi.org/10.1016/C2011-0-07564-6.

[287] M.K. Karmakar, J. Mandal, S. Haldar, P.K. Chatterjee, Investigation of fuel gas generation in a pilot scale fluidized bed autothermal gasifier using rice husk, Fuel. 111 (2013) 584–591. https://doi.org/10.1016/j.fuel.2013.03.045.

[288] S. Jarungthammachote, A. Dutta, Equilibrium modeling of gasification: Gibbs free energy minimization approach and its application to spouted bed and spout-fluid bed gasifiers, Energy Convers. Manag. 49 (2008) 1345–1356. https://doi.org/10.1016/j.enconman.2008.01.006.

[289] D. Neves, Evaluation of thermochemical conversion in fluidized bed, 2013.

[290] Y. Il Lim, U. Do Lee, Quasi-equilibrium thermodynamic model with empirical equations for air-steam biomass gasification in fluidized-beds, Fuel Process. Technol. 128 (2014) 199–210. https://doi.org/10.1016/j.fuproc.2014.07.017.

[291] I. Hannula, E. Kurkela, A semi-empirical model for pressurised air-blown fluidised-bed gasification of biomass, Bioresour. Technol. 101 (2010) 4608–4615. https://doi.org/10.1016/j.biortech.2010.01.072.

[292] D.A. Rodriguez-Alejandro, H. Nam, A.L. Maglinao, S.C. Capareda, A.F. Aguilera-Alvarado, Development of a modified equilibrium model for biomass pilot-scale fluidized bed gasifier performance predictions, Energy. 115 (2016) 1092–1108. https://doi.org/10.1016/j.energy.2016.09.079.

[293] M. Puig-Arnavat, J.C. Bruno, A. Coronas, Modified thermodynamic equilibrium model for biomass gasification: A study of the influence of operating conditions, Energy and Fuels. 26 (2012) 1385–1394. https://doi.org/10.1021/ef2019462.

[294] P. Sittisun, N. Tippayawong, S. Pang, Biomass gasification in a fixed bed downdraft ractor with oxygen enriched air: A modified equilibrium modeling study, Energy Procedia. 160 (2019) 317–323. https://doi.org/10.1016/j.egypro.2019.02.163.

[295] L.P.R. Pala, Q. Wang, G. Kolb, V. Hessel, Steam gasification of biomass with subsequent syngas adjustment using shift reaction for syngas production: An Aspen Plus model, Renew. Energy. 101 (2017) 484–492. https://doi.org/10.1016/j.renene.2016.08.069.

[296] J. Yu, J.D. Smith, Validation and application of a kinetic model for biomass gasification simulation and optimization in updraft gasifiers, Chem. Eng. Process. - Process Intensif. 125 (2018) 214–226. https://doi.org/10.1016/j.cep.2018.02.003.

[297] A. Gagliano, F. Nocera, M. Bruno, G. Cardillo, Development of an Equilibrium-based Model of Gasification of Biomass by Aspen Plus, Energy Procedia. 111 (2017) 1010–1019. https://doi.org/10.1016/j.egypro.2017.03.264.

[298] C. Torres, L. Urvina, H. de Lasa, A chemical equilibrium model for biomass gasification. Application to Costa Rican coffee pulp transformation unit, Biomass and Bioenergy. 123 (2019) 89–103. https://doi.org/10.1016/j.biombioe.2019.01.025.

[299] D. Antolini, A.S. Shivananda, F. Patuzzi, M. Grigiante, M. Baratieri, Experimental and modeling analysis of Air and CO2 biomass gasification in a reverse lab scale downdraft gasifier, Energy Procedia. 158 (2019) 1182–1187. https://doi.org/10.1016/j.egypro.2019.01.304.

[300] Z.A. Zainal, R. Ali, C.H. Lean, K.N. Seetharamu, Prediction of performance of a downdraft

gasifier using equilibrium modeling for different biomass materials, Energy Convers. Manag. 42 (2001) 1499–1515. https://doi.org/10.1016/S0196-8904(00)00078-9.

[301] A. Melgar, J.F. Pérez, H. Laget, A. Horillo, Thermochemical equilibrium modelling of a gasifying process, Energy Convers. Manag. 48 (2007) 59–67. https://doi.org/10.1016/j.enconman.2006.05.004.

[302] P. Brachi, R. Chirone, F. Miccio, M. Miccio, G. Ruoppolo, Entrained-flow gasification of torrefied tomato peels: Combining torrefaction experiments with chemical equilibrium modeling for gasification, Fuel. 220 (2018) 744–753. https://doi.org/10.1016/j.fuel.2018.02.027.

[303] W. Doherty, A. Reynolds, D. Kennedy, The effect of air preheating in a biomass CFB gasifier using ASPEN Plus simulation, Biomass and Bioenergy. 33 (2009) 1158–1167. https://doi.org/10.1016/j.biombioe.2009.05.004.

[304] G. Zang, J. Jia, Y. Shi, T. Sharma, A. Ratner, Modeling and economic analysis of waste tire gasification in fluidized and fixed bed gasifiers, Waste Manag. 89 (2019) 201–211. https://doi.org/10.1016/j.wasman.2019.03.070.

[305] M. Ruggiero, G. Manfrida, An equilibrium model for biomass gasification processes, Renew. Energy. 16 (1999) 1106–1109. https://doi.org/10.1016/s0960-1481(98)00429-7.

[306] W.A.W.A.K. Ghani, R.A. Moghadam, M.A.M. Salleh, A.B. Alias, Air gasification of agricultural waste in a fluidized bed gasifier: Hydrogen production performance, Energies. 2 (2009) 258–268. https://doi.org/10.3390/en20200258.

[307] H. Karatas, H. Olgun, F. Akgun, Experimental results of gasification of cotton stalk and hazelnut shell in a bubbling fluidized bed gasifier under air and steam atmospheres, Fuel. 112 (2013) 494–501. https://doi.org/10.1016/j.fuel.2013.04.025.

[308] H. Karatas, F. Akgun, Experimental results of gasification of walnut shell and pistachio shell in a bubbling fluidized bed gasifier under air and steam atmospheres, Fuel. 214 (2018) 285–292. https://doi.org/10.1016/j.fuel.2017.10.061.

[309] K.G. Mansaray, A.E. Ghaly, A.M. Al-Taweel, F. Hamdullahpur, V.I. Ugursal, Air gasification of rice husk in a dual distributor type fluidized bed gasifier, Biomass and Bioenergy. 17 (1999) 315–332. https://doi.org/10.1016/S0961-9534(99)00046-X.

[310] E. Monteiro, P. Brito, L. Calado, Gaseificação Térmica de Miscanthus, (2015) 1–7.

[311] S.Q. Turn, C.M. Kinoshita, D.M. Ishimura, J. Zhou, The fate of inorganic constituents of biomass in fluidized bed gasification, Fuel. 77 (1998) 135–146. https://doi.org/10.1016/S0016-2361(97)00190-7.

[312] S. Sarker, F. Bimbela, J.L. Sánchez, H.K. Nielsen, Characterization and pilot scale fluidized bed gasification of herbaceous biomass: A case study on alfalfa pellets, Energy Convers. Manag. 91 (2015) 451–458. https://doi.org/10.1016/j.enconman.2014.12.034.

[313] V. Skoulou, G. Koufodimos, Z. Samaras, A. Zabaniotou, Low temperature gasification of olive kernels in a 5-kW fluidized bed reactor for H2-rich producer gas, Int. J. Hydrogen Energy. 33 (2008) 6515–6524. https://doi.org/10.1016/j.ijhydene.2008.07.074.

[314] G. Xue, M. Kwapinska, A. Horvat, Z. Li, S. Dooley, W. Kwapinski, J.J. Leahy, Gasification of miscanthus x giganteus in an air-blown bubbling fluidized bed: A preliminary study of performance and agglomeration, Energy and Fuels. 28 (2014) 1121–1131. https://doi.org/10.1021/ef4022152.

[315] S. Kaewluan, S. Pipatmanomai, Potential of synthesis gas production from rubber wood chip gasification in a bubbling fluidised bed gasifier, Energy Convers. Manag. 52 (2011) 75–84.

https://doi.org/10.1016/j.enconman.2010.06.044.

[316] S. V. Vassilev, D. Baxter, L.K. Andersen, C.G. Vassileva, An overview of the chemical composition of biomass, Fuel. 89 (2010) 913–933. https://doi.org/10.1016/j.fuel.2009.10.022.

[317] P. Lv, Z. Yuan, C. Wu, L. Ma, Y. Chen, N. Tsubaki, Bio-syngas production from biomass catalytic gasification, Energy Convers. Manag. 48 (2007) 1132–1139. https://doi.org/10.1016/j.enconman.2006.10.014.

[318] Z. Ravaghi-Ardebili, F. Manenti, C. Pirola, F. Soares, M. Corbetta, S. Pierucci, E. Ranzi, Influence of the effective parameters on H2:CO Ratio Of Syngas At Low-Temperature Gasification, Chem. Eng. Trans. 37 (2014) 253–258. https://doi.org/10.3303/CET1437043.

[319] M.B. de Souza, L. Couceiro, A.G. Barreto, C.P. B. Quitete, Neural Network Based Modeling and Operational Optimization of Biomass Gasification Processes, Gasif. Pract. Appl. (2012). https://doi.org/10.5772/48516.

[320] J. Amaro, A.Z. Mendiburu, I. Ávila, Modeling of syngas composition obtained from fluidized bed gasifiers using Kuhn–Tucker multipliers, Energy. 152 (2018) 371–382. https://doi.org/10.1016/j.energy.2018.03.141.

[321] J. Han, H. Kim, The reduction and control technology of tar during biomass gasification/pyrolysis: An overview, Renew. Sustain. Energy Rev. 12 (2008) 397–416. https://doi.org/10.1016/j.rser.2006.07.015.

[322] L.P.L.M. Rabou, R.W.R. Zwart, B.J. Vreugdenhil, L. Bos, Tar in biomass producer gas, the Energy research Centre of The Netherlands (ECN) experience: An enduring challenge, Energy and Fuels. 23 (2009) 6189–6198. https://doi.org/10.1021/ef9007032.

[323] R. Zhang, K. Cummer, A. Suby, R.C. Brown, Biomass-derived hydrogen from an air-blown gasifier, Fuel Process. Technol. 86 (2005) 861–874. https://doi.org/10.1016/j.fuproc.2004.09.001.

[324] P. Kaushal, J. Abedi, N. Mahinpey, A comprehensive mathematical model for biomass gasification in a bubbling fluidized bed reactor, Fuel. 89 (2010) 3650–3661. https://doi.org/10.1016/j.fuel.2010.07.036.

[325] A. Gómez-Barea, B. Leckner, Estimation of gas composition and char conversion in a fluidized bed biomass gasifier, Fuel. 107 (2013) 419–431. https://doi.org/10.1016/j.fuel.2012.09.084.

[326] C. Loha, P.K. Chatterjee, H. Chattopadhyay, Performance of fluidized bed steam gasification of biomass - Modeling and experiment, Energy Convers. Manag. 52 (2011) 1583–1588. https://doi.org/10.1016/j.enconman.2010.11.003.

[327] S. Rapagnà, N. Jand, A. Kiennemann, P.U. Foscolo, Steam-gasification of biomass in a fluidised-bed of olivine particles, Biomass and Bioenergy. 19 (2000) 187–197. https://doi.org/10.1016/S0961-9534(00)00031-3.

[328] G. Cheng, Q. Li, F. Qi, B. Xiao, S. Liu, Z. Hu, P. He, Allothermal gasification of biomass using micron size biomass as external heat source, Bioresour. Technol. 107 (2012) 471–475. https://doi.org/10.1016/j.biortech.2011.12.074.

[329] F. Pinto, R.N. André, C. Carolino, M. Miranda, P. Abelha, D. Direito, N. Perdikaris, I. Boukis, Gasification improvement of a poor quality solid recovered fuel (SRF). Effect of using natural minerals and biomass wastes blends, Fuel. 117 (2014) 1034–1044. https://doi.org/10.1016/j.fuel.2013.10.015.

[330] G. Xue, M. Kwapinska, A. Horvat, W. Kwapinski, L.P.L.M. Rabou, S. Dooley, K.M. Czajka,

J.J. Leahy, Gasification of torrefied Miscanthus×giganteus in an air-blown bubbling fluidized bed gasifier, Bioresour. Technol. 159 (2014) 397–403. https://doi.org/10.1016/j.biortech.2014.02.094.

[331] M. Campoy, A. Gómez-Barea, P. Ollero, S. Nilsson, Gasification of wastes in a pilot fluidized bed gasifier, Fuel Process. Technol. 121 (2014) 63–69. https://doi.org/10.1016/j.fuproc.2013.12.019.

[332] D.S. Gunarathne, A. Mueller, S. Fleck, T. Kolb, J.K. Chmielewski, W. Yang, W. Blasiak, Gasification characteristics of steam exploded biomass in an updraft pilot scale gasifier, Energy. 71 (2014) 496–506. https://doi.org/10.1016/j.energy.2014.04.100.

[333] C. Gai, Y. Dong, Experimental study on non-woody biomass gasification in a downdraft gasifier, Int. J. Hydrogen Energy. 37 (2012) 4935–4944. https://doi.org/10.1016/j.ijhydene.2011.12.031.

[334] T.M. Ismail, A. Ramos, E. Monteiro, M.A. El-Salam, A. Rouboa, A. Ramos, M.A. El-Salam, A. Rouboa, Parametric studies in the gasification agent and fluidization velocity during oxygen-enriched gasification of biomass in a pilot-scale fluidized bed: Experimental and numerical assessment, Renew. Energy. 147 (2020) 2429–2439. https://doi.org/10.1016/j.renene.2019.10.029.

[335] J. Gil, J. Corella, M.P. Aznar, M.A. Caballero, Biomass gasification in atmospheric and bubbling fluidized bed: Effect of the type of gasifying agent on the product distribution, Biomass and Bioenergy. 17 (1999) 389–403. https://doi.org/10.1016/S0961-9534(99)00055-0.

[336] V.M. Jaganathan, O. Mohan, S. Varunkumar, Intrinsic hydrogen yield from gasification of biomass with oxy-steam mixtures, Int. J. Hydrogen Energy. 44 (2019) 17781–17791. https://doi.org/10.1016/j.ijhydene.2019.05.095.

[337] A. Galvagno, M. Prestipino, S. Maisano, F. Urbani, V. Chiodo, Integration into a citrus juice factory of air-steam gasification and CHP system: Energy sustainability assessment, Energy Convers. Manag. 193 (2019) 74–85. https://doi.org/10.1016/j.enconman.2019.04.067.

[338] N. Gil-Lalaguna, J.L. Sánchez, M.B. Murillo, E. Rodríguez, G. Gea, Air-steam gasification of sewage sludge in a fluidized bed. Influence of some operating conditions, Chem. Eng. J. 248 (2014) 373–382. https://doi.org/10.1016/j.cej.2014.03.055.

[339] S. Sharma, P.N. Sheth, Air-steam biomass gasification: Experiments, modeling and simulation, Energy Convers. Manag. 110 (2016) 307–318. https://doi.org/10.1016/j.enconman.2015.12.030.

[340] J.J. Hernández, G. Aranda, J. Barba, J.M. Mendoza, Effect of steam content in the air-steam flow on biomass entrained flow gasification, Fuel Process. Technol. 99 (2012) 43–55. https://doi.org/10.1016/j.fuproc.2012.01.030.

[341] A.M. Sharma, A. Kumar, R.L. Huhnke, Effect of steam injection location on syngas obtained from an air-steam gasifier, Fuel. 116 (2014) 388–394. https://doi.org/10.1016/j.fuel.2013.08.026.

[342] M. Prestipino, V. Chiodo, S. Maisano, G. Zafarana, F. Urbani, A. Galvagno, Hydrogen rich syngas production by air-steam gasification of citrus peel residues from citrus juice manufacturing: Experimental and simulation activities, Int. J. Hydrogen Energy. 42 (2017) 26816–26827. https://doi.org/10.1016/j.ijhydene.2017.05.173.

[343] T. Nakyai, S. Authayanun, Y. Patcharavorachot, A. Arpornwichanop, S. Assabumrungrat, D. Saebea, Exergoeconomics of hydrogen production from biomass air-steam gasification with methane co-feeding, Energy Convers. Manag. 140 (2017) 228–239.

https://doi.org/10.1016/j.enconman.2017.03.002.

[344] Hydrogen Council, Path to hydrogen competitiveness: a cost perspective, 2020. www.hydrogencouncil.com.

[345] A. Fernandez, L.R. Ortiz, D. Asensio, R. Rodriguez, G. Mazza, Kinetic Analysis and Thermodynamics Properties of Air/Steam Gasification of Agricultural Waste, 2020. https://doi.org/10.1016/j.jece.2020.103829.

[346] S. Yang, H. Wang, Y. Wei, J. Hu, J.W. Chew, Eulerian-Lagrangian simulation of air-steam biomass gasification in a three-dimensional bubbling fluidized gasifier, Energy. 181 (2019) 1075–1093. https://doi.org/10.1016/j.energy.2019.06.003.

[347] M. Echegaray, D.Z. García, G. Mazza, R. Rodriguez, Air-steam gasification of five regional lignocellulosic wastes: Exergetic evaluation, Sustain. Energy Technol. Assessments. 31 (2019) 115–123. https://doi.org/10.1016/j.seta.2018.12.015.

[348] P.M. Lv, Z.H. Xiong, J. Chang, C.Z. Wu, Y. Chen, J.X. Zhu, An experimental study on biomass air-steam gasification in a fluidized bed, Bioresour. Technol. 95 (2004) 95–101. https://doi.org/10.1016/j.biortech.2004.02.003.

[349] P. Lv, J. Chang, Z. Xiong, H. Huang, C. Wu, Y. Chen, J. Zhu, Biomass air-steam gasification in a fluidized bed to produce hydrogen-rich gas, Energy and Fuels. 17 (2003) 677–682. https://doi.org/10.1021/ef020181l.

[350] H. Karatas, H. Olgun, F. Akgun, Experimental results of gasification of waste tire with air&CO 2, air&steam and steam in a bubbling fluidized bed gasifier, Fuel Process. Technol. 102 (2012) 166–174. https://doi.org/10.1016/j.fuproc.2012.04.013.

[351] Y. Tian, X. Zhou, Y. Yang, L. Nie, Experimental analysis of air-steam gasification of biomass with coal-bottom ash, J. Energy Inst. 93 (2020) 25–30. https://doi.org/10.1016/j.joei.2019.04.012.

[352] T. Zhou, S. Yang, Y. Wei, J. Hu, H. Wang, Impact of wide particle size distribution on the gasification performance of biomass in a bubbling fluidized bed gasifier, Renew. Energy. 148 (2020) 534–547. https://doi.org/10.1016/j.renene.2019.10.059.

[353] M. Campoy, A. Gómez-Barea, A.L. Villanueva, P. Ollero, Air-steam gasification of biomass in a fluidized bed under simulated autothermal and adiabatic conditions, Ind. Eng. Chem. Res. 47 (2008) 5957–5965. https://doi.org/10.1021/ie800220t.

[354] Instituto da Conservação da Natureza e das Florestas (ICNF), Perfil Florestal - Portugal, (2018) 1–4.

[355] I.L. Motta, N.T. Miranda, R. Maciel Filho, M.R. Wolf Maciel, Biomass gasification in fluidized beds: A review of biomass moisture content and operating pressure effects, Renew. Sustain. Energy Rev. 94 (2018) 998–1023. https://doi.org/10.1016/j.rser.2018.06.042.

[356] European Comission, Directive (EU) 2018/851 of the European Parliament and of the Council of 30 May 2018 amending Directive 2008/98/EC on waste, Off. J. Eur. Union. (2018) 109–140. https://doi.org/10.1023/A:1009932427938.

[357] A. Ramos, E. Monteiro, V. Silva, A. Rouboa, Co-gasification and recent developments on waste-to-energy conversion: A review, Renew. Sustain. Energy Rev. 81 (2018) 380–398. https://doi.org/10.1016/j.rser.2017.07.025.

[358] F.J. Gutiérrez Ortiz, A. Kruse, F. Ramos, P. Ollero, Integral energy valorization of municipal solid waste reject fraction to biofuels, Energy Convers. Manag. 180 (2019) 1167–1184. https://doi.org/10.1016/j.enconman.2018.10.085.

[359] S. Dias, Como garantir a sustentabilidade do CDR no Mercado Nacional. Que futuro?, 10º

Fórum Nac. Resíduos, O Impacto Da Econ. Circ. No Set. Nac. Dos Resíduos. (2016).

[360] Statistics Abu Dhabi, Waste statistics, (2011) 1.

[361] Eurostat, Municipal waste statistics Statistics Explained, (2019) 1–6. https://ec.europa.eu/eurostat/statisticsexplained/ (accessed July 5, 2019).

[362] Pordata, Resíduos urbanos: total e por tipo de operação de destino, (2019). https://www.pordata.pt/Municipios/Resíduos+urbanos+total+e+por+tipo+de+operação+de+destino-67 (accessed June 19, 2019).

[363] European Union, Directive of the European Parliament and of the Council of 30 May 2018 amending Directive 1999/31/EC on the landfill of waste, Off. J. Eur. Union. 2018 (2018) 100–108. https://eur-lex.europa.eu/legal-content/EN/TXT/PDF/?uri=CELEX:32018L0850&from=EN.

[364] Eurostat, Municipal waste by waste management operations, Eurostat Press Off. (2019). http://appsso.eurostat.ec.europa.eu/nui/show.do?dataset=env_wasmun&lang=en%0Ahttps://ec.europa.eu/eurostat/web/products-datasets/-/env_wasmun.

[365] A. Białowiec, J. Pulka, P. Stępień, P. Manczarski, J. Gołaszewski, The RDF/SRF torrefaction: An effect of temperature on characterization of the product – Carbonized Refuse Derived Fuel, Waste Manag. 70 (2017) 91–100. https://doi.org/10.1016/j.wasman.2017.09.020.

[366] M. Paolo, M. Paola, RDF: From waste to resource - The Italian case, Energy Procedia. 81 (2015) 569–584. https://doi.org/10.1016/j.egypro.2015.12.136.

[367] E.C. Rada, M. Ragazzi, Selective collection as a pretreatment for indirect solid recovered fuel generation, Waste Manag. 34 (2014) 291–297. https://doi.org/10.1016/j.wasman.2013.11.013.

[368] I. Standard, Solid recovered fuels-Specifications and classes, 2011. https://infostore.saiglobal.com/preview/is/en/2011/i.s.en15359-2011.pdf?sku=1500480 (accessed July 25, 2019).

[369] H. Wilts, N. Von Gries, Europe's waste incineration capacities in a circular economy, Proc. Inst. Civ. Eng. Waste Resour. Manag. 168 (2015) 166–176. https://doi.org/10.1680/warm.14.00009.

[370] U. Persson, M. Münster, Current and future prospects for heat recovery from waste in European district heating systems: A literature and data review, Energy. 110 (2016) 116–128. https://doi.org/10.1016/j.energy.2015.12.074.

[371] A.T. Sipra, N. Gao, H. Sarwar, Municipal solid waste (MSW) pyrolysis for bio-fuel production: A review of effects of MSW components and catalysts, Fuel Process. Technol. 175 (2018) 131–147. https://doi.org/10.1016/j.fuproc.2018.02.012.

[372] J. Recari, C. Berrueco, N. Puy, S. Alier, J. Bartrolí, X. Farriol, Torrefaction of a solid recovered fuel (SRF) to improve the fuel properties for gasification processes, Appl. Energy. 203 (2017) 177–188. https://doi.org/10.1016/j.apenergy.2017.06.014.

[373] A. Shirazi, A. Rahbari, C.A. Asselineau, J. Pye, A solar fuel plant via supercritical water gasification integrated with Fischer–Tropsch synthesis: System-level dynamic simulation and optimisation, Energy Convers. Manag. 192 (2019) 71–87. https://doi.org/10.1016/j.enconman.2019.04.008.

[374] M.M. Yu, M.S. Masnadi, J.R. Grace, X.T. Bi, C.J. Lim, Y. Li, Co-gasification of biosolids with biomass: Thermogravimetric analysis and pilot scale study in a bubbling fluidized bed reactor, Bioresour. Technol. 175 (2015) 51–58. https://doi.org/10.1016/j.biortech.2014.10.045.

[375] R. Habibi, J. Kopyscinski, M.S. Masnadi, J. Lam, J.R. Grace, C.A. Mims, J.M. Hill, Co-gasification of biomass and non-biomass feedstocks: Synergistic and inhibition effects of switchgrass mixed with sub-bituminous coal and fluid coke during CO 2 gasification, Energy and Fuels. 27 (2013) 494–500. https://doi.org/10.1021/ef301567h.

[376] M.S. Masnadi, J.R. Grace, X.T. Bi, C.J. Lim, N. Ellis, Y.H. Li, A.P. Watkinson, Single-fuel steam gasification of switchgrass and coal in a bubbling fluidized bed: A comprehensive parametric reference for co-gasification study, Energy. 80 (2015) 133–147. https://doi.org/10.1016/j.energy.2014.11.054.

[377] J. Cardoso, V. Silva, D. Eusébio, Techno-economic analysis of a biomass gasification power plant dealing with forestry residues blends for electricity production in Portugal, J. Clean. Prod. 212 (2019) 741–753. https://doi.org/10.1016/j.jclepro.2018.12.054.

[378] P.R. Bhoi, R.L. Huhnke, A. Kumar, N. Indrawan, S. Thapa, Co-gasification of municipal solid waste and biomass in a commercial scale downdraft gasifier, Energy. 163 (2018) 513–518. https://doi.org/10.1016/j.energy.2018.08.151.

[379] M.P. Aznar, M.A. Caballero, J.A. Sancho, E. Francés, Plastic waste elimination by co-gasification with coal and biomass in fluidized bed with air in pilot plant, Fuel Process. Technol. 87 (2006) 409–420. https://doi.org/10.1016/j.fuproc.2005.09.006.

[380] M.L. Mastellone, L. Zaccariello, U. Arena, Co-gasification of coal, plastic waste and wood in a bubbling fluidized bed reactor, Fuel. 89 (2010) 2991–3000. https://doi.org/10.1016/j.fuel.2010.05.019.

[381] M. Narobe, J. Golob, D. Klinar, V. Francetič, B. Likozar, Co-gasification of biomass and plastics: Pyrolysis kinetics studies, experiments on 100kW dual fluidized bed pilot plant and development of thermodynamic equilibrium model and balances, Bioresour. Technol. 162 (2014) 21–29. https://doi.org/10.1016/j.biortech.2014.03.121.

[382] I.I. Ahmed, N. Nipattummakul, A.K. Gupta, Characteristics of syngas from co-gasification of polyethylene and woodchips, Appl. Energy. 88 (2011) 165–174. https://doi.org/10.1016/j.apenergy.2010.07.007.

[383] A. Borgogna, A. Salladini, L. Spadacini, A. Pitrelli, M.C. Annesini, G. Iaquaniello, Methanol production from Refuse Derived Fuel: Influence of feedstock composition on process yield through gasification analysis, J. Clean. Prod. 235 (2019) 1080–1089. https://doi.org/10.1016/j.jclepro.2019.06.185.

[384] Enerkem, Clean Fuels & Green Chemicals Green; Technology Companies, (2018). https://enerkem.com/about-us/company-profile/ (accessed July 29, 2019).

[385] G. Lopez, M. Artetxe, M. Amutio, J. Alvarez, J. Bilbao, M. Olazar, Recent advances in the gasification of waste plastics. A critical overview, Renew. Sustain. Energy Rev. 82 (2018) 576–596. https://doi.org/10.1016/j.rser.2017.09.032.

[386] F. Pinto, C. Franco, R.N. André, C. Tavares, M. Dias, I. Gulyurtlu, I. Cabrita, Effect of experimental conditions on co-gasification of coal, biomass and plastics wastes with air/steam mixtures in a fluidized bed system, Fuel. 82 (2003) 1967–1976. https://doi.org/10.1016/S0016-2361(03)00160-1.

[387] R. Xiao, B. Jin, H. Zhou, Z. Zhong, M. Zhang, Air gasification of polypropylene plastic waste in fluidized bed gasifier, Energy Convers. Manag. 48 (2007) 778–786. https://doi.org/10.1016/j.enconman.2006.09.004.

[388] J.P. Ciferno, J.J. Marano, Benchmarking biomass gasification technologies for fuels, chemicals and hydrogen production, report prepared for U.S. Department of Energy and National Energy Technology Laboratory, (2002) 58.

http://citeseerx.ist.psu.edu/viewdoc/download?doi=10.1.1.140.8405&rep=rep1&type=pdf.

[389] A. Ponzio, S. Kalisz, W. Blasiak, Effect of operating conditions on tar and gas composition in high temperature air/steam gasification (HTAG) of plastic containing waste, Fuel Process. Technol. 87 (2006) 223–233. https://doi.org/10.1016/j.fuproc.2005.08.002.

[390] L. Fagbemi, L. Khezami, R. Capart, Pyrolysis products from different biomasses: Application to the thermal cracking of tar, Appl. Energy. (2001). https://doi.org/10.1016/S0306-2619(01)00013-7.

[391] P. Morf, P. Hasler, T. Nussbaumer, Mechanisms and kinetics of homogeneous secondary reactions of tar from continuous pyrolysis of wood chips, Fuel. (2002). https://doi.org/10.1016/S0016-2361(01)00216-2.

[392] C. Brage, Q. Yu, K. Sjöström, Characteristics of evolution of tar from wood pyrolysis in a fixed-bed reactor, Fuel. (1996). https://doi.org/10.1016/0016-2361(95)00260-X.

[393] C. Berrueco, D. Montané, B. Matas Güell, G. del Alamo, Effect of temperature and dolomite on tar formation during gasification of torrefied biomass in a pressurized fluidized bed, Energy. 66 (2014) 849–859. https://doi.org/10.1016/j.energy.2013.12.035.

[394] R.A. Knight, Experience with raw gas analysis from pressurized gasification of biomass, Biomass and Bioenergy. (2000). https://doi.org/10.1016/S0961-9534(99)00070-7.

[395] C.M. Kinoshita, Y. Wang, J. Zhou, Tar formation under different biomass gasification conditions, J. Anal. Appl. Pyrolysis. (1994). https://doi.org/10.1016/0165-2370(94)00796-9.

[396] S. Wang, B. Ru, G. Dai, Z. Shi, J. Zhou, Z. Luo, M. Ni, K. Cen, Mechanism study on the pyrolysis of a synthetic β-O-4 dimer as lignin model compound, Proc. Combust. Inst. (2017). https://doi.org/10.1016/j.proci.2016.07.129.

[397] Y.H. Qin, A. Campen, T. Wiltowski, J. Feng, W. Li, The influence of different chemical compositions in biomass on gasification tar formation, Biomass and Bioenergy. 83 (2015) 77–84. https://doi.org/10.1016/j.biombioe.2015.09.001.

[398] H. Yu, Z. Zhang, Z. Li, D. Chen, Characteristics of tar formation during cellulose, hemicellulose and lignin gasification, Fuel. 118 (2014) 250–256. https://doi.org/10.1016/j.fuel.2013.10.080.

[399] T. Hosoya, H. Kawamoto, S. Saka, Pyrolysis gasification reactivities of primary tar and char fractions from cellulose and lignin as studied with a closed ampoule reactor, J. Anal. Appl. Pyrolysis. (2008). https://doi.org/10.1016/j.jaap.2008.06.002.

[400] B. Zhou, A. Dichiara, Y. Zhang, Q. Zhang, J. Zhou, Tar formation and evolution during biomass gasification: An experimental and theoretical study, Fuel. 234 (2018) 944–953. https://doi.org/10.1016/j.fuel.2018.07.105.

[401] Q. Wang, T. Endo, P. Aparu, H. Kurogawa, Study on biomass tar reduction by ash and fluidizing medium in a heterogeneous reaction, Int. J. Sustain. Dev. Plan. 9 (2014) 669–679. https://doi.org/10.2495/SDP-V9-N5-669-679.

[402] D.T. Pio, L.A.C. Tarelho, P.C.R. Pinto, Gasification-based biorefinery integration in the pulp and paper industry: A critical review, Renew. Sustain. Energy Rev. 133 (2020) 110210. https://doi.org/10.1016/j.rser.2020.110210.

[403] P. Cross, A. Kulkarni, H. Nam, S. Adhikari, O. Fasina, Bubbling fluidized bed gasification of short rotation Eucalyptus: Effect of harvesting age and bark, Biomass and Bioenergy. 110 (2018) 98–104. https://doi.org/10.1016/j.biombioe.2018.01.014.

[404] F. Pinto, J. Gominho, R.N. André, D. Gonçalves, M. Miranda, F. Varela, D. Neves, J. Santos, A. Lourenço, H. Pereira, Improvement of gasification performance of Eucalyptus globulus

stumps with torrefaction and densification pre-treatments, Fuel. 206 (2017) 289–299. https://doi.org/10.1016/j.fuel.2017.06.008.

[405] L. Jiang, S. Hu, Y. Wang, S. Su, L. Sun, B. Xu, L. He, J. Xiang, Catalytic effects of inherent alkali and alkaline earth metallic species on steam gasification of biomass, Int. J. Hydrogen Energy. 40 (2015) 15460–15469. https://doi.org/10.1016/j.ijhydene.2015.08.111.

[406] V. Skoulou, E. Kantarelis, S. Arvelakis, W. Yang, A. Zabaniotou, Effect of biomass leaching on H2 production, ash and tar behavior during high temperature steam gasification (HTSG) process, Int. J. Hydrogen Energy. 34 (2009) 5666–5673. https://doi.org/10.1016/j.ijhydene.2009.05.117.

[407] K. Hakouk, M. Klotz, E. Di Geronimo, V. Ranieri, J.A.Z. Pieterse, G. Aranda Almansa, A.M. Steele, S. Thorpe, Implementation of novel ice-templated materials for conversion of tars from gasification product gas, Fuel Process. Technol. 181 (2018) 340–351. https://doi.org/10.1016/j.fuproc.2018.10.009.

[408] K. Umeki, A. Moilanen, A. Gómez-Barea, J. Konttinen, A model of biomass char gasification describing the change in catalytic activity of ash, Chem. Eng. J. 207–208 (2012) 616–624. https://doi.org/10.1016/j.cej.2012.07.025.

[409] Y.A. Lenis, J.F. Pérez, A. Melgar, Fixed bed gasification of Jacaranda Copaia wood: Effect of packing factor and oxygen enriched air, Ind. Crops Prod. 84 (2016) 166–175. https://doi.org/10.1016/j.indcrop.2016.01.053.

[410] V. Nemanova, K. Engvall, Tar variability in the producer gas in a bubbling fluidized bed gasification system, Energy and Fuels. 28 (2014) 7494–7500. https://doi.org/10.1021/ef5015617.

[411] T. Phuphuakrat, N. Nipattummakul, T. Namioka, S. Kerdsuwan, K. Yoshikawa, Characterization of tar content in the syngas produced in a downdraft type fixed bed gasification system from dried sewage sludge, Fuel. 89 (2010) 2278–2284. https://doi.org/10.1016/j.fuel.2010.01.015.

[412] D.N. Bangala, N. Abatzoglou, J.P. Martin, E. Chornet, Catalytic Gas Conditioning: Application to Biomass and Waste Gasification, Ind. Eng. Chem. Res. 36 (1997) 4184–4192. https://doi.org/10.1021/ie960785a.

[413] J.J. Hernández, R. Ballesteros, G. Aranda, Characterisation of tars from biomass gasification: Effect of the operating conditions, Energy. 50 (2013) 333–342. https://doi.org/10.1016/j.energy.2012.12.005.

[414] M. Neubert, S. Reil, M. Wolff, D. Pöcher, H. Stork, C. Ultsch, M. Meiler, J. Messer, L. Kinzler, M. Dillig, S. Beer, J. Karl, Experimental comparison of solid phase adsorption (SPA), activated carbon test tubes and tar protocol (DIN CEN/TS 15439) for tar analysis of biomass derived syngas, Biomass and Bioenergy. 105 (2017) 443–452. https://doi.org/10.1016/j.biombioe.2017.08.006.

[415] K. Maniatis, A.A.C.M. Beenackers, Tar Protocols. IEA Bioenergy Gasification Task: Introduction, Biomass and Bioenergy. 18 (2000) 1–4. https://doi.org/10.1016/S0961-9534(99)00072-0.

[416] T. Yang, K. Jia, X. Kai, Y. Sun, Y. Li, R. Li, A study on the migration behavior of K, Na, and Cl during biomass gasification, BioResources. 11 (2016) 7133–7144. https://doi.org/10.15376/biores.11.3.7133-7144.

[417] D.T. Pio, L.A.C. Tarelho, T.F.V. Nunes, M.F. Baptista, M.A.A. Matos, Co-combustion of residual forest biomass and sludge in a pilot-scale bubbling fluidized bed, J. Clean. Prod. 249 (2020) 119309. https://doi.org/10.1016/j.jclepro.2019.119309.

[418] J. Udomsirichakorn, P.A. Salam, Review of hydrogen-enriched gas production from steam gasification of biomass: The prospect of CaO-based chemical looping gasification, Renew. Sustain. Energy Rev. 30 (2014) 565–579. https://doi.org/10.1016/j.rser.2013.10.013.

[419] K.Y. Chiang, Y.S. Chen, W.S. Tsai, C.H. Lu, K.L. Chien, Effect of calcium based catalyst on production of synthesis gas in gasification of waste bamboo chopsticks, Int. J. Hydrogen Energy. 37 (2012) 13737–13745. https://doi.org/10.1016/j.ijhydene.2012.03.042.

[420] C. Zhou, T. Stuermer, R. Gunarathne, W. Yang, W. Blasiak, Effect of calcium oxide on high-temperature steam gasification of municipal solid waste, Fuel. 122 (2014) 36–46. https://doi.org/10.1016/j.fuel.2014.01.029.

[421] M.A. Hamad, A.M. Radwan, D.A. Heggo, T. Moustafa, Hydrogen rich gas production from catalytic gasification of biomass, Renew. Energy. 85 (2016) 1290–1300. https://doi.org/10.1016/j.renene.2015.07.082.

[422] H. Nam, S. Wang, K.C. Sanjeev, M.W. Seo, S. Adhikari, R. Shakya, D. Lee, S.R. Shanmugam, Enriched hydrogen production over air and air-steam fluidized bed gasification in a bubbling fluidized bed reactor with CaO: Effects of biomass and bed material catalyst, Energy Convers. Manag. 225 (2020) 113408. https://doi.org/10.1016/j.enconman.2020.113408.

[423] T. Dahou, F. Defoort, B. Khiari, M. Labaki, C. Dupont, M. Jeguirim, Role of inorganics on the biomass char gasification reactivity: A review involving reaction mechanisms and kinetics models, Renew. Sustain. Energy Rev. 135 (2021) 110136. https://doi.org/10.1016/j.rser.2020.110136.

[424] T. Dahou, F. Defoort, M. Jeguirim, C. Dupont, Towards understanding the role of K during biomass steam gasification, Fuel. 282 (2020) 118806. https://doi.org/10.1016/j.fuel.2020.118806.

[425] F. Guo, X. Li, Y. Liu, K. Peng, C. Guo, Z. Rao, Catalytic cracking of biomass pyrolysis tar over char-supported catalysts, Energy Convers. Manag. 167 (2018) 81–90. https://doi.org/10.1016/j.enconman.2018.04.094.

[426] A. V. Bridgwater, The technical and economic feasibility of biomass gasification for power generation, Fuel. 74 (1995) 631–653. https://doi.org/10.1016/0016-2361(95)00001-L.

[427] S. Fürnsinn, H. Hofbauer, Health, Safety and Environment in Biomass Gasification, IEA Bioenergy Task 33/ Therm. Gasif. Biomass Int. Work. (2005) 153.

[428] J. Ahrenfeldt, T.P. Thomsen, U. Henriksen, L.R. Clausen, Biomass gasification cogeneration - A review of state of the art technology and near future perspectives, Appl. Therm. Eng. 50 (2013) 1407–1417. https://doi.org/10.1016/j.applthermaleng.2011.12.040.

[429] M. Simone, E. Guerrazzi, E. Biagini, C. Nicolella, L. Tognotti, Technological barriers of biomass gasification, Int. J. Heat Technol. 27 (2009) 127–132. https://www.mendeley.com/research-papers/technological-barriers-biomass-gasification/?utm_source=desktop&utm_medium=1.17.6&utm_campaign=open_catalog&userDocumentId=%7B32ba9c0f-a96a-46a5-a2ab-21a5a85dbf7c%7D (accessed October 1, 2018).

[430] D. Bonalumi, Preliminary Study of Pyrolysis and Gasification of Biomass and Thermosetting Resins for Energy Production, Energy Procedia. 101 (2016) 432–439. https://doi.org/10.1016/j.egypro.2016.11.055.

[431] B.K. Das, S.M.N. Hoque, Assessment of the Potential of Biomass Gasification for Electricity Generation in Bangladesh, J. Renew. Energy. 2014 (2014) 1–10. https://doi.org/10.1155/2014/429518.

[432] A. Mustafa, R.K. Calay, M.Y. Mustafa, A Techno-economic Study of a Biomass Gasification Plant for the Production of Transport Biofuel for Small Communities, Energy Procedia. 112 (2017) 529–536. https://doi.org/10.1016/j.egypro.2017.03.1111.

[433] J.P. Makwana, A.K. Joshi, G. Athawale, D. Singh, P. Mohanty, Air gasification of rice husk in bubbling fluidized bed reactor with bed heating by conventional charcoal, Bioresour. Technol. 178 (2015) 45–52. https://doi.org/10.1016/j.biortech.2014.09.111.

[434] K.R. Craig, M.K. Mann, Cost and Performance Analysis of Biomass-Based Integrated Gasification Combined-Cycle (BIGCC) Power Systems Cost and Performance Analysis of Biomass-Based Integrated Gasification Combined-Cycle (BIGCC) Power Systems, 1996.

[435] G.A. Ekama, Using bioprocess stoichiometry to build a plant-wide mass balance based steady-state WWTP model, Water Res. 43 (2009) 2101–2120. https://doi.org/10.1016/j.watres.2009.01.036.

[436] J.A. Daniels, Advances in Environmental Research. Volume 4, Nova Science Publishers, 2010. https://books.google.pt/books?id=BAsy2dy75PMC&source=gbs_slider_cls_metadata_0_mylibrary (accessed September 8, 2017).

[437] EEA, EU bioenergy potential from a resource-efficiency perspective, 2013. https://doi.org/10.2800/92247.

[438] B. Elbersen, I. Startisky, G. Hengeveld, M.-J. Schelhaas, H. Naeff, Atlas of EU biomass potentials, Biomass Futur. (2012). https://ec.europa.eu/energy/intelligent/projects/sites/iee-projects/files/projects/documents/biomass_futures_atlas_of_technical_and_economic_biomass_potential_en.pdf.

[439] U. Mantau, U. Saal, K. Prins, F. Steierer, M. Lindner, H. Verkerk, J. Eggers, N. Leek, J. Oldenburger, A. Asikainen, P. Anttila, EUwood - Real potential for changes in growth and use of EU forests. Final report., EUwood. (2010) 106p. https://doi.org/TREN/D2/491-2008.

[440] E.M.W. Smeets, A.P.C. Faaij, I.M. Lewandowski, W.C. Turkenburg, A bottom-up assessment and review of global bio-energy potentials to 2050, Prog. Energy Combust. Sci. 33 (2007) 56–106. https://doi.org/10.1016/j.pecs.2006.08.001.

[441] S. Ferreira, N.A. Moreira, E. Monteiro, Bioenergy overview for Portugal, Biomass and Bioenergy. 33 (2009) 1567–1576. https://doi.org/10.1016/j.biombioe.2009.07.020.

[442] J.L. Easterly, M. Burnham, Overview of biomass and waste fuel resources for power production, Biomass and Bioenergy. 10 (1996) 79–92. https://doi.org/10.1016/0961-9534(95)00063-1.

[443] Z.A.B.Z. Alauddin, P. Lahijani, M. Mohammadi, A.R. Mohamed, Gasification of lignocellulosic biomass in fluidized beds for renewable energy development: A review, Renew. Sustain. Energy Rev. 14 (2010) 2852–2862. https://doi.org/10.1016/j.rser.2010.07.026.

[444] I.E.A. Bioenergy, Contribution of Bioenergy to the World ' s Future Energy, IEA Bioenergy. (2007) 12. http://www.idahoforests.org/img/pdf/PotentialContribution.pdf.

[445] P. McKendry, Energy production from biomass (part 2): Conversion technologies, Bioresour. Technol. 83 (2002) 47–54. https://doi.org/10.1016/S0960-8524(01)00119-5.

[446] X. Zhang, A.O. Oyedun, A. Kumar, D. Oestreich, U. Arnold, J. Sauer, An optimized process design for oxymethylene ether production from woody-biomass-derived syngas, Biomass and Bioenergy. 90 (2016) 7–14. https://doi.org/10.1016/j.biombioe.2016.03.032.

[447] J. Chang, Y. Fu, Z. Luo, Experimental study for dimethyl ether production from biomass

gasification and simulation on dimethyl ether production, Biomass and Bioenergy. 39 (2012) 67–72. https://doi.org/10.1016/j.biombioe.2011.01.044.

[448] N. Mahbub, A.O. Oyedun, A. Kumar, D. Oestreich, U. Arnold, J. Sauer, A life cycle assessment of oxymethylene ether synthesis from biomass-derived syngas as a diesel additive, J. Clean. Prod. 165 (2017) 1249–1262. https://doi.org/10.1016/j.jclepro.2017.07.178.

[449] H. Li, D. Mehmood, E. Thorin, Z. Yu, Biomethane Production Via Anaerobic Digestion and Biomass Gasification, Energy Procedia. 105 (2017) 1172–1177. https://doi.org/10.1016/j.egypro.2017.03.490.

[450] Z. Bai, Q. Liu, J. Lei, H. Hong, H. Jin, New solar-biomass power generation system integrated a two-stage gasifier, Appl. Energy. 194 (2017) 310–319. https://doi.org/10.1016/j.apenergy.2016.06.081.

[451] J.L. Zheng, Y.H. Zhu, M.Q. Zhu, H.T. Wu, R.C. Sun, Bio-oil gasification using air - Steam as gasifying agents in an entrained flow gasifier, Energy. 142 (2018) 426–435. https://doi.org/10.1016/j.energy.2017.10.031.

[452] W. Zhang, Automotive fuels from biomass via gasification, Fuel Process. Technol. 91 (2010) 866–876. https://doi.org/10.1016/j.fuproc.2009.07.010.

[453] H. Hellsmark, S. Jacobsson, Realising the potential of gasified biomass in the European Union-Policy challenges in moving from demonstration plants to a larger scale diffusion, Energy Policy. 41 (2012) 507–518. https://doi.org/10.1016/j.enpol.2011.11.011.

[454] F.T. Princiotta, Global climate change - The technology challenge, Springer Science & Business Media, 2007. https://doi.org/10.2495/AIR070531.

[455] F. Lettner, P. Haselbacher, H. Timmerer, M. Seebacher, Deliverable D17: State of The Art from Case Studies and Good Design Principles, (n.d.) 1–16.

[456] Y.H. Qin, J. Feng, W.Y. Li, Formation of tar and its characterization during air-steam gasification of sawdust in a fluidized bed reactor, Fuel. 89 (2010) 1344–1347. https://doi.org/10.1016/j.fuel.2009.08.009.

[457] L. Duc, K. Morishita, T. Takar, Catalytic Decomposition of Biomass Tars at Low-Temperature, Biomass Now - Sustain. Growth Use. (2013). https://doi.org/10.5772/55356.

[458] J. Ken, T. Drylov, L. Neudert, V. Lukas, Cereal Canopy Structure – Its Assessment and Use in Efficient Crop Management, in: Biomass Now - Sustain. Growth Use, InTech, 2013: pp. 1–21. https://doi.org/10.5772/54528.

[459] S. Heidenreich, M. Müller, P.U. Foscolo, Advanced Biomass Gasification: New Concepts for Efficiency Increase and Product Flexibility, 2016.

[460] D. Świerczyński, C. Courson, L. Bedel, A. Kiennemann, S. Vilminot, Oxidation reduction behavior of iron-bearing olivines (Fe xMg1-x)2SiO4 used as catalysts for biomass gasification, Chem. Mater. 18 (2006) 897–905. https://doi.org/10.1021/cm051433+.

[461] R.C.E. Modolo, L.A.C. Tarelho, E.R. Teixeira, V.M. Ferreira, J.A. Labrincha, Treatment and use of bottom bed waste in biomass fluidized bed combustors, Fuel Process. Technol. 125 (2014) 170–181. https://doi.org/10.1016/j.fuproc.2014.03.040.

[462] L.A.C. Tarelho, E.R. Teixeira, D.F.R. Silva, R.C.E. Modolo, J.A. Labrincha, F. Rocha, Characteristics of distinct ash flows in a biomass thermal power plant with bubbling fluidised bed combustor, Energy. 90 (2015) 387–402. https://doi.org/10.1016/j.energy.2015.07.036.

[463] J. Filipe, Diagramas de Potencial Químico como Guias para a Estabilidade e Reactividade em Cimentos, Universidade de Aveiro, 2009.

[464] H. Yokokawa, N. Sakai, T. Kawada, M. Dokiya, Thermodynamic stability of perovskites and

related compounds in some alkaline earth-transition metal-oxygen systems, J. Solid State Chem. 94 (1991) 106–120. https://doi.org/10.1016/0022-4596(91)90225-7.

[465] R.G. Pinto, Synthesis of Fayalite Fe2SiO4 as a Tar Removal Catalyst for Biomass Gasification, (2017).

[466] L.D. Poulikakos, C. Papadaskalopoulou, B. Hofko, F. Gschösser, A. Cannone Falchetto, M. Bueno, M. Arraigada, J. Sousa, R. Ruiz, C. Petit, M. Loizidou, M.N. Partl, Harvesting the unexplored potential of European waste materials for road construction, Resour. Conserv. Recycl. 116 (2017) 32–44. https://doi.org/10.1016/j.resconrec.2016.09.008.

[467] M. Chen, L. Lu, S. Wang, P. Zhao, W. Zhang, S. Zhang, Investigation on the formation of tobermorite in calcium silicate board and its influence factors under autoclaved curing, Constr. Build. Mater. 143 (2017) 280–288. https://doi.org/10.1016/j.conbuildmat.2017.03.143.

[468] A. Yan, K.R. Wu, D. Zhang, W. Yao, Influence of concrete composition on the characterization of fracture surface, Cem. Concr. Compos. 25 (2003) 153–157. https://doi.org/10.1016/S0958-9465(02)00004-5.

[469] J. Udomsirichakorn, P. Basu, P.A. Salam, B. Acharya, Effect of CaO on tar reforming to hydrogen-enriched gas with in-process CO2 capture in a bubbling fluidized bed biomass steam gasifier, Int. J. Hydrogen Energy. 38 (2013) 14495–14504. https://doi.org/10.1016/j.ijhydene.2013.09.055.

[470] C.A. Jordan, G. Akay, Effect of CaO on tar production and dew point depression during gasification of fuel cane bagasse in a novel downdraft gasifier, Fuel Process. Technol. 106 (2013) 654–660. https://doi.org/10.1016/j.fuproc.2012.09.061.

[471] M. Azhar Uddin, H. Tsuda, S. Wu, E. Sasaoka, Catalytic decomposition of biomass tars with iron oxide catalysts, Fuel. 87 (2008) 451–459. https://doi.org/10.1016/j.fuel.2007.06.021.

[472] F. Lind, M. Seemann, H. Thunman, Continuous catalytic tar reforming of biomass derived raw gas with simultaneous catalyst regeneration, Ind. Eng. Chem. Res. 50 (2011) 11553–11562. https://doi.org/10.1021/ie200645s.

[473] F. Lind, N. Berguerand, M. Seemann, H. Thunman, Ilmenite and nickel as catalysts for upgrading of raw gas derived from biomass gasification, Energy and Fuels. 27 (2013) 997–1007. https://doi.org/10.1021/ef302091w.

[474] Z. Min, M. Asadullah, P. Yimsiri, S. Zhang, H. Wu, C.Z. Li, Catalytic reforming of tar during gasification. Part I. Steam reforming of biomass tar using ilmenite as a catalyst, Fuel. 90 (2011) 1847–1854. https://doi.org/10.1016/j.fuel.2010.12.039.

[475] N. Clausen, L. R., Elmegaard, B., & Houbak, Design of novel DME/methanol synthesis plants based on gasification of biomass, 2011.

[476] Z. Hao, B. Yang, D. Jahng, Combustion characteristics of biodried sewage sludge, Waste Manag. 72 (2018) 296–305. https://doi.org/10.1016/j.wasman.2017.11.008.

[477] J.H. Sung, S.K. Back, B.M. Jeong, J.H. Kim, H.S. Choi, H.N. Jang, Y.C. Seo, Oxy-fuel co-combustion of sewage sludge and wood pellets with flue gas recirculation in a circulating fluidized bed, Fuel Process. Technol. 172 (2018) 79–85. https://doi.org/10.1016/j.fuproc.2017.12.005.

[478] T. Meyer, P. Amin, D.G. Allen, H. Tran, Dewatering of pulp and paper mill biosludge and primary sludge, J. Environ. Chem. Eng. 6 (2018) 6317–6321. https://doi.org/10.1016/j.jece.2018.09.037.

[479] Z. Zhao, R. Wang, J. Wu, Q. Yin, C. Wang, Bottom ash characteristics and pollutant emission

during the co-combustion of pulverized coal with high mass-percentage sewage sludge, Energy. 171 (2019) 809–818. https://doi.org/10.1016/j.energy.2019.01.082.

[480] A. Kijo-Kleczkowska, K. Środa, M. Kosowska-Golachowska, T. Musiał, K. Wolski, Experimental research of sewage sludge with coal and biomass co-combustion, in pellet form, Waste Manag. 53 (2016) 165–181. https://doi.org/10.1016/j.wasman.2016.04.021.

[481] T. Chen, C. Lei, B. Yan, L. li Li, Analysis of heavy metals fixation and associated energy consumption during sewage sludge combustion: Bench scale and pilot test, J. Clean. Prod. 229 (2019) 1243–1250. https://doi.org/10.1016/j.jclepro.2019.04.358.

[482] M. Aho, J. Silvennoinen, Preventing chlorine deposition on heat transfer surfaces with aluminium-silicon rich biomass residue and additive, Fuel. 83 (2004) 1299–1305. https://doi.org/10.1016/j.fuel.2004.01.011.

[483] L.E. Åmand, B. Leckner, D. Eskilsson, C. Tullin, Deposits on heat transfer tubes during co-combustion of biofuels and sewage sludge, Fuel. 85 (2006) 1313–1322. https://doi.org/10.1016/j.fuel.2006.01.001.

[484] M. Aho, P. Yrjas, R. Taipale, M. Hupa, J. Silvennoinen, Reduction of superheater corrosion by co-firing risky biomass with sewage sludge, Fuel. 89 (2010) 2376–2386. https://doi.org/10.1016/j.fuel.2010.01.023.

[485] L.E. Åmand, B. Leckner, Metal emissions from co-combustion of sewage sludge and coal/wood in fluidized bed, Fuel. 83 (2004) 1803–1821. https://doi.org/10.1016/j.fuel.2004.01.014.

[486] B. Strömberg, F. Zintl, Release of Chlorine from Biomass and Model Compounds at Pyrolysis and Gasification Conditions, Prog. Thermochem. Biomass Convers. 11 (2008) 1234–1245. https://doi.org/10.1002/9780470694954.ch102.

[487] Z. Xie, X. Ma, HCl emission characteristics during the combustion of eucalyptus bark, Energy and Fuels. 28 (2014) 5826–5833. https://doi.org/10.1021/ef5009242.

[488] J.G. Olsson, U. Jäglid, J.B.C. Pettersson, P. Hald, Alkali metal emission during pyrolysis of biomass, Energy and Fuels. 11 (1997) 779–784. https://doi.org/10.1021/ef960096b.

[489] P.A. Jensen, F.J. Frandsen, K. Dam-Johansen, B. Sander, Experimental Investigation of the Transformation and Release to Gas Phase of Potassium and Chlorine during Straw Pyrolysis, Energy and Fuels. 14 (2000) 1280–1285. https://doi.org/10.1021/ef000104v.

[490] S.S. Lokare, A Mechanistic Investigation Of Ash Depostion in Pulverized-Coal and Biomass Combustion, ProQuest, 2008. https://books.google.com/books?id=mG6eWzZ-DzsC&pgis=1 (accessed April 21, 2016).

[491] P. Viklund, Superheater corrosion in biomass and waste fired boilers Characterisation , causes and prevention of chlorine-induced corrosion, 2013.

[492] M. Hupa, Ash-related issues in fluidized-bed combustion of biomasses: Recent research highlights, Energy and Fuels. 26 (2012) 4–14. https://doi.org/10.1021/ef201169k.

[493] H.P. Nielsen, F.J. Frandsen, K. Dam-Johansen, L.L. Baxter, Implications of chlorine-associated corrosion on the operation of biomass-fired boilers, Prog. Energy Combust. Sci. 26 (2000) 283–298. https://doi.org/10.1016/S0360-1285(00)00003-4.

[494] J.M. Johansen, J.G. Jakobsen, F.J. Frandsen, P. Glarborg, Release of K, Cl, and S during pyrolysis and combustion of high-chlorine biomass, Energy and Fuels. 25 (2011) 4961–4971. https://doi.org/10.1021/ef201098n.

[495] S.C. Van Lith, P.A. Jensen, F.J. Frandsen, P. Glarborg, Release of Inorganic Elements During Wood Combustion, Prepr. Pap.-Am. Chem. Soc., Div. Fuel Chem. 49 (2004) 87–88.

[496] M. Díaz-Ramírez, F.J. Frandsen, P. Glarborg, F. Sebastián, J. Royo, Partitioning of K, Cl, S and P during combustion of poplar and brassica energy crops, Fuel. 134 (2014) 209–219. https://doi.org/10.1016/j.fuel.2014.05.056.

[497] J.N. Knudsen, P.A. Jensen, K. Dam-Johansen, Transformation and release to the gas phase of Cl, K, and S during combustion of annual biomass, Energy and Fuels. 18 (2004) 1385–1399. https://doi.org/10.1021/ef049944q.

[498] S.C. van Lith, V. Alonso-Ramírez, P.A. Jensen, F.J. Frandsen, P. Glarborg, Release to the gas phase of inorganic elements during wood combustion. Part 1: Development and evaluation of quantification methods, Energy and Fuels. 20 (2006) 964–978. https://doi.org/10.1021/ef050131r.

[499] E. Vainio, P. Yrjas, M. Zevenhoven, A. Brink, T. Laurén, M. Hupa, T. Kajolinna, H. Vesala, The fate of chlorine, sulfur, and potassium during co-combustion of bark, sludge, and solid recovered fuel in an industrial scale BFB boiler, Fuel Process. Technol. 105 (2013) 59–68. https://doi.org/10.1016/j.fuproc.2011.08.021.

[500] A.I. Calvo, L.A.C. Tarelho, E.R. Teixeira, C. Alves, T. Nunes, M. Duarte, E. Coz, D. Custodio, A. Castro, B. Artiñano, R. Fraile, Particulate emissions from the co-combustion of forest biomass and sewage sludge in a bubbling fluidised bed reactor, Fuel Process. Technol. 114 (2013) 58–68. https://doi.org/10.1016/j.fuproc.2013.03.021.

[501] L.A.C. Tarelho, D.S.F. Neves, M.A.A. Matos, Forest biomass waste combustion in a pilot-scale bubbling fluidised bed combustor, Biomass and Bioenergy. 35 (2011) 1511–1523. https://doi.org/10.1016/j.biombioe.2010.12.052.

[502] L. Thierry, J.F. Ferrería de laFuente, F. Neuwahl, M. Canova, A. Pinasseau, I. Jankov, T. Brinkmann, S. Roudier, L.D. Sancho, BAT Reference Document for Large Combustion Plants. Industrial Emissions Directive 2010/75/EU (Integrated PollutionPrevention and Control)., 2016. http://eippcb.jrc.ec.europa.eu/reference/BREF/LCP_FinalDraft_06_2016.pdf.

[503] Diário da República, Decreto-Lei nº 119/2009, 23 de Junho, Diário Da República, 1.ª Série — N.º 119 — 23 Junho 2009. (2009) 4112–4116. https://data.dre.pt/eli/port/677/2009/06/23/p/dre/pt/html.

[504] Governo de Portugal, Portaria n.º 190-B/2018, (2018) 4–9.

[505] O. Sippula, Fine Particle Formation and Emissions in Biomass Combustion, 2010. http://www.atm.helsinki.fi/FAAR/reportseries/rs-108.pdf.

[506] J. Partanen, P. Backman, R. Backman, M. Hupa, Absorption of HCl by limestone in hot flue gases. Part I: The effects of temperature, gas atmosphere and absorbent quality, Fuel. 84 (2005) 1664–1673. https://doi.org/10.1016/j.fuel.2005.02.011.

[507] K.O. Davidsson, L.E. Åmand, B. Leckner, B. Kovacevik, M. Svane, M. Hagström, J.B.C. Pettersson, J. Petterson, H. Asteman, J.E. Svensson, L.G. Johansson, Potassium, chlorine, and sulfur in ash, particles, deposits, and corrosion during wood combustion in a circulating fluidized-bed boiler, Energy and Fuels. 21 (2007) 71–81. https://doi.org/10.1021/ef060306c.

[508] European Commission, 2050 long-term strategy | Climate Action, 2050 Long-Term Strateg. (2018). https://ec.europa.eu/clima/policies/strategies/2050_en (accessed May 10, 2020).

[509] M. Wang, R. Dewil, K. Maniatis, J. Wheeldon, T. Tan, J. Baeyens, Y. Fang, Biomass-derived aviation fuels: Challenges and perspective, Prog. Energy Combust. Sci. 74 (2019) 31–49. https://doi.org/10.1016/j.pecs.2019.04.004.

[510] S. Wang, G. Dai, H. Yang, Z. Luo, Lignocellulosic biomass pyrolysis mechanism: A state-of-the-art review, Prog. Energy Combust. Sci. 62 (2017) 33–86.

https://doi.org/10.1016/j.pecs.2017.05.004.

[511] M. Palmeros Parada, P. Osseweijer, J.A. Posada Duque, Sustainable biorefineries, an analysis of practices for incorporating sustainability in biorefinery design, Ind. Crops Prod. 106 (2017) 105–123. https://doi.org/10.1016/j.indcrop.2016.08.052.

[512] M.P. González-Vázquez, R. García, M. V. Gil, C. Pevida, F. Rubiera, Comparison of the gasification performance of multiple biomass types in a bubbling fluidized bed, Energy Convers. Manag. 176 (2018) 309–323. https://doi.org/10.1016/j.enconman.2018.09.020.

[513] H.C. Frey, Y. Zhu, Techno-economic analysis of combined cycle systems, in: Comb. Cycle Syst. Near-Zero Emiss. Power Gener., Elsevier, 2012: pp. 306–328. https://doi.org/10.1533/9780857096180.306.

[514] H. Viana, W.B. Cohen, D. Lopes, J. Aranha, Assessment of forest biomass for use as energy. GIS-based analysis of geographical availability and locations of wood-fired power plants in Portugal, Appl. Energy. 87 (2010) 2551–2560. https://doi.org/10.1016/j.apenergy.2010.02.007.

[515] J. Cardoso, V. Silva, D. Eusébio, Techno-economic analysis of a biomass gasification power plant dealing with forestry residues blends for electricity production in Portugal, J. Clean. Prod. 212 (2019) 741–753. https://doi.org/10.1016/j.jclepro.2018.12.054.

[516] Y. Richardson, J. Blin, A. Julbe, A short overview on purification and conditioning of syngas produced by biomass gasification: Catalytic strategies, process intensification and new concepts, Prog. Energy Combust. Sci. 38 (2012) 765–781. https://doi.org/10.1016/j.pecs.2011.12.001.

[517] N. Abdoulmoumine, S. Adhikari, A. Kulkarni, S. Chattanathan, A review on biomass gasification syngas cleanup, Appl. Energy. 155 (2015) 294–307. https://doi.org/10.1016/j.apenergy.2015.05.095.

[518] C. Courson, K. Gallucci, Gas cleaning for waste applications (syngas cleaning for catalytic synthetic natural gas synthesis), in: M. Materazzi, P.U. Foscolo (Eds.), Substit. Nat. Gas from Waste, Elsevier Inc., 2019: pp. 161–220. https://doi.org/10.1016/b978-0-12-815554-7.00008-8.

[519] C.M. Meijden, Development of the MILENA gasification technology for the production of Bio-SNG. PhD. Thesis., ECN Energy Res. Netherlands. (2010) 206.

[520] P. Nicolaou, Removal Utilization/Separation of Tars from Syngas, (2016) 106. https://doi.org/uuid:a8597980-a9d0-4137-a6ca-09bd796c7c3a.

[521] R.W.R. Zwart, Gas cleaning downstream biomass gasification, ECN-E. 1 (2009) 65.

[522] C.. Villela, J.L. Silveira, Ecological efficiency in thermoelectric power plants., Appl. Therm. Eng. 27 (2007) 840–847.

[523] J. Kotowicz, M. Brzęczek, M. Job, The thermodynamic and economic characteristics of the modern combined cycle power plant with gas turbine steam cooling, Energy. 164 (2018) 359–376. https://doi.org/10.1016/j.energy.2018.08.076.

[524] Gas Turbine World 2014-2015 Handbook, Project Planning, Engineering, Construction and Operation, 2014.

[525] D. Barisano, G. Canneto, F. Nanna, E. Alvino, G. Pinto, A. Villone, M. Carnevale, V. Valerio, A. Battafarano, G. Braccio, Steam/oxygen biomass gasification at pilot scale in an internally circulating bubbling fluidized bed reactor, Fuel Process. Technol. 141 (2016) 74–81. https://doi.org/10.1016/j.fuproc.2015.06.008.

[526] Z. Ghaffarpour, M. Mahmoudi, A.H. Mosaffa, L. Garousi Farshi, Thermoeconomic

assessment of a novel integrated biomass based power generation system including gas turbine cycle, solid oxide fuel cell and Rankine cycle, Energy Convers. Manag. 161 (2018) 1–12. https://doi.org/10.1016/j.enconman.2018.01.071.

[527] L.R.A. Ferreira, R.B. Otto, F.P. Silva, S.N.M. De Souza, S.S. De Souza, O.H. Ando Junior, Review of the energy potential of the residual biomass for the distributed generation in Brazil, Renew. Sustain. Energy Rev. 94 (2018) 440–455. https://doi.org/10.1016/j.rser.2018.06.034.

[528] Y.-H. Kiang, Chapter 4 - Database and analysis of fuel properties, fossil fuel, biomass, refuse-derived fuel, waste, biosludge and biocarbon, in: Fuel Prop. Estim. Combust. Process Charact., 2018: p. 103. https://doi.org/10.1016/B978-0-12-813473-3.00004-0.

[529] Z. Abu El-Rub, E.A. Bramer, G. Brem, Experimental comparison of biomass chars with other catalysts for tar reduction, Fuel. 87 (2008) 2243–2252. https://doi.org/10.1016/j.fuel.2008.01.004.

[530] G. Guan, M. Kaewpanha, X. Hao, A. Abudula, Catalytic steam reforming of biomass tar: Prospects and challenges, Renew. Sustain. Energy Rev. 58 (2016) 450–461. https://doi.org/10.1016/j.rser.2015.12.316.

[531] R.D. Treloar, Gas Installation Technology, Blackwell Publishing Ltd Library, Oxford, UK, 2005.

[532] D.T. Pedroso, E.B. Machin, N. Proenza Pérez, L.B. Braga, J.L. Silveira, N.P. Proenza, L.B. Braga, J.L. Silveira, N. Proenza Pérez, L.B. Braga, J.L. Silveira, Technical assessment of the Biomass Integrated Gasification / Gas Turbine Combined Cycle (BIG / GTCC) incorporation in the sugarcane industry, Renew. Energy. 114 (2017) 464–479. https://doi.org/10.1016/j.renene.2017.07.038.

[533] Brooks, J. F., GE Gas Turbine Performance Characteristics, Schenectady, NY, 2014.

[534] C. Ghenai, Combustion of syngas fuel in gas turbine can combustor, Adv. Mech. Eng. 2010 (2010). https://doi.org/10.1155/2010/342357.

[535] M. Renzi, C. Riolfi, M. Baratieri, Influence of the Syngas Feed on the Combustion Process and Performance of a Micro Gas Turbine with Steam Injection, Energy Procedia. 105 (2017) 1665–1670. https://doi.org/10.1016/j.egypro.2017.03.543.

[536] S. Park, G.M. Choi, M. Tanahashi, Combustion characteristics of syngas on scaled gas turbine combustor in pressurized condition: Pressure, H2/CO ratio, and N2 dilution of fuel, Fuel Process. Technol. 175 (2018) 104–112. https://doi.org/10.1016/j.fuproc.2018.03.039.

[537] D.A. Granados, F. Chejne, J.M. Mejía, Oxy-fuel combustion as an alternative for increasing lime production in rotary kilns, Appl. Energy. 158 (2015) 107–117. https://doi.org/10.1016/j.apenergy.2015.07.075.

[538] A.P. Watkinson, J.K. Brimacombe, Limestone calcination in a rotary kiln, Metall. Trans. B. 13 (1982) 369–378. https://doi.org/10.1007/BF02667752.

[539] A.A. Boateng, Rotary Kiln Minerals Process Applications, in: Rotary Kilns, 2016: pp. 231–264. https://doi.org/10.1016/b978-0-12-803780-5.00010-1.

[540] W. Elsner, M. Wysocki, P. Niegodajew, R. Borecki, Experimental and economic study of small-scale CHP installation equipped with downdraft gasifier and internal combustion engine, Appl. Energy. 202 (2017) 213–227. https://doi.org/10.1016/j.apenergy.2017.05.148.

[541] M.H. Taheri, A.H. Mosaffa, L.G. Farshi, Energy , exergy and economic assessments of a novel integrated biomass based multigeneration energy system with hydrogen production and LNG regasi fi cation cycle, Energy. 125 (2017) 162–177. https://doi.org/10.1016/j.energy.2017.02.124.

[542] D. Roy, S. Samanta, S. Ghosh, Thermo - economic assessment of biomass gasification - based power generation system consists of solid oxide fuel cell , supercritical carbon dioxide cycle and indirectly heated air turbine, Clean Technol. Environ. Policy. 21 (2019) 827–845. https://doi.org/10.1007/s10098-019-01671-7.

[543] Entidade Reguladora dos Serviços Energéticos, Tarifas e Preços para a Energia Elétrica e Outros Serviços 2020, Lisbon, 2020.

[544] Portadata, Taxas de juro sobre novas operações de empréstimos (média anual) a empresas: total e por escalão de crédito, 2020.

[545] Entidade Reguladora Dos Serviços Energéticos, Proveitos permitidos e ajustamentos para 2016 das empresas reguladas do setor elétrico, 2020.

[546] SendeCO2, Precios CO2 - Sendeco2, (2020). https://www.sendeco2.com/es/precios-co2 (accessed December 6, 2020).

[547] WaccExpert, WACC Expert - calculate your WACC!, (2020).

[548] Inflation.eu, Harmonised inflation Portugal 2019 – HICP inflation Portugal 2019, (n.d.).

[549] World Bank Group, Converting Biomass to Energy. A Guide for Developers and Investors, Washington, D.C., US, 2017. https://doi.org/10.1111/j.1574-6968.2010.02203.x.

[550] W.C. Lyons, G.J. Plisga, Michael D. Lorenz, Petroleum Economic Evaluation, in: Stand. Handb. Pet. Nat. Gas Eng., 2016: pp. 7-1-7–55. https://doi.org/10.1016/b978-0-12-383846-9.00007-2.

[551] Investopedia, Corporate Finance & Accounting, (2019) 2.

[552] Diário da República, Decreto Regulamentar n.º 25/2009 de 14 de Setembro. Diário da República, 1.ª série — N.º 178 — 11 de setembro de 2015, Lisboa, Portugal, 2009.

[553] P. Lamers, M.S. Roni, J.S. Tumuluru, J.J. Jacobson, K.G. Cafferty, J.K. Hansen, K. Kenney, F. Teymouri, B. Bals, Techno-economic analysis of decentralized biomass processing depots, Bioresour. Technol. 194 (2015) 205–213. https://doi.org/10.1016/j.biortech.2015.07.009.

[554] C.J.P. Freitas, Central Termoeléctrica a Biomassa Florestal, 2009.